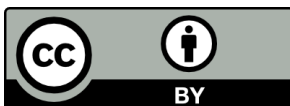


MANAGING THE IMPACTS OF EXTREME
CLIMATIC EVENTS RELATED TO INPUTS OF
ORGANIC MATTER ON THE ECOSYSTEM
SERVICES PROVIDED BY WATER SUPPLY
RESERVOIRS

Elias Msongolera Munthali



<http://creativecommons.org/licenses/by/4.0/deed.ca>

Aquesta obra està subjecta a una llicència Creative Commons Reconeixement

Esta obra está bajo una licencia Creative Commons Reconocimiento

This work is licensed under a Creative Commons Attribution licence

Universitat
de Girona



WAGENINGEN
UNIVERSITY & RESEARCH

DOCTORAL THESIS

*Managing the impacts of extreme climatic events related to inputs of organic matter on the ecosystem services
provided by water supply reservoirs.*

Elias Msongolera Munthali

2024



DOCTORAL THESIS

Managing the impacts of extreme climatic events related to inputs of organic matter on the ecosystem services provided by water supply reservoirs.

Elias Msongolera Munthali

2024

Doctorate in Water Science and Technology

Supervisor: Dr. Rafael Marcé (Blanes Centre for Advanced Studies, Spanish National Research Council, Spain).

Co-Supervisor: Professor Dr. Lisette de Senerpont Domis (Netherlands Institute of Ecology, Netherlands).

Tutor: Professor Sergi Sabater (Universitat de Girona).

Promotor: Dr. Miquel Lürling (Wageningen University and Research).

This research was conducted under the auspices of the Graduate School of the University of Girona, Spain and the Wageningen Institute for Environment and Climate Research Graduate School (WIMEK), The Netherlands, and as part of the joint PhD Programme MANTEL.

Thesis submitted to Universitat de Girona and Wageningen University and Research for the (double) degree of Doctor.

Universitat
de Girona



Dr Rafael Marcé, of Blanes Centre for Advanced Studies, Spanish National Research Council, and Professor Dr. Lisette de Senerpont Domis of The Netherlands Institute of Ecology,

ATTEST:

That the thesis title **“Managing the impacts of extreme climatic events related to inputs of organic matter on the ecosystem services provided by water supply reservoirs”**, presented by **Elias Msongolera Munthali** to obtain a double doctoral degree, has been completed under our supervision. For all intents and purposes, we hereby sign this document.

Dr Rafael Marcé (Girona):

Professor Dr. Lisette de Senerpont Domis (Wageningen):

Dedicated to:

My parents, Sabela & (late) John

and siblings

Inspiring quote:

“Only a life lived for others is a life worthwhile.”

Albert Einstein.

This thesis comprises the following open access authored publications:

- i. **Munthali, E.**; de Senerpont Domis, L. N.; Marcé, R. Drastic Reduction of Nutrient Loading to a Reservoir Alters Its Resistance to Impacts of Extreme Climatic Events. *Environ. Res. Lett.* 2022, 17 (8), 084007. <https://doi.org/10.1088/1748-9326/ac7df2>. **Impact Factor = 6.947**; Rank = Q1 in Environmental Science (all).
- ii. Sanchís, J.; Jaén-Gil, A.; Gago-Ferrero, P.; **Munthali, E.**; Farré, M. J. Characterization of Organic Matter by HRMS in Surface Waters: Effects of Chlorination on Molecular Fingerprints and Correlation with DBP Formation Potential. *Water Res.* 2020, 176. <https://doi.org/10.1016/j.watres.2020.115743>. **Impact Factor = 13.4**; Rank = Q1 in Water Science and Technology & Environmental Engineering.
- iii. **Munthali, E.**; Marcé, R.; Farré, M. J. Drivers of Variability in Disinfection By-Product Formation Potential in a Chain of Thermally Stratified Drinking Water Reservoirs. *Env. Sci Water Res Technol* 2022, 8 (5), 968–980. <https://doi.org/10.1039/D1EW00788B>. **Impact Factor = 5.819**; Rank = Q1 in Water Science and Technology & Environmental Engineering

Other publications and manuscripts I co-authored but are not part of this thesis:

- i. Armstrong, M., Zhan, Q., **Munthali, E.**, Jin, H., Teurlincx, S., Peters, P., Lüring, M., De Senerpont Domis, L.N., 2023. Stressors in a bottle: A microcosm study on phytoplankton assemblage response to extreme precipitation events under climate warming. *Freshw. Biol.* fwb.14109. <https://doi.org/10.1111/fwb.14109>
- ii. Cianci-Gaskill, J. A.; Klug, J. L.; Merrell, K. C.; Millar, E. E.; Wain, D. J.; Kramer, L.; van Wijk, D.; Paule-Mercado, M. C. A.; Finlay, K.; Glines, M. R.; **Munthali, E. M.**; Teurlincx, S.; Borre, L.; Yan, N. D. A Lake Management Framework for Global Application: Monitoring, Restoring, and Protecting Lakes through Community Engagement. *Lake Reserv. Manag.* 2024, 1–27. <https://doi.org/10.1080/10402381.2023.2299868>.
- iii. Wander, H. L.; Farruggia, M. J.; La Fuente, S.; Korver, M. C.; Chapina, R. J.; Robinson, J.; Bah, A.; **Munthali, E.**; Ghosh, R.; Stachelek, J.; Khandelwal, A.; Hanson, P. C.; Weathers, K. C. Using Knowledge-Guided Machine Learning To Assess Patterns of Areal Change in Waterbodies across the Contiguous United States. *Environ. Sci. Technol.* 2024, acs.est.3c05784. <https://doi.org/10.1021/acs.est.3c05784>.
- iv. Impacts of climate-induced drought on lake and reservoir biodiversity and ecosystem services: a systematic literature review. *Authors:* Sun, X., Armstrong, M., Moradi, A., Bhattacharya, R., Antão-Geraldes, A.M., **Munthali, E.**, Grossart, HP., Matsuzaki, S.S., Kangur, K., Dunalska, J.A., Stockwell, J.D., & Borre, L. **Status:** Submitted to *AMBIO Journal* (Springer).

ACRONYMS

AI	Aromaticity index.
AOX	Absorbable Organic Halides.
BCAN	Bromochloroacetonitrile.
BDCM	Bromodichloromethane.
BIX	Biological index.
CRAM	Carboxyl-rich alicyclic molecules.
CTD	Conductivity, temperature and depth.
CYd	Cao dissimilarity index.
DBCM	Dibromochloromethane.
DBE	Double bond equivalent.
DBPs	Disinfection by-products.
DCAN	Dichloroacetonitrile.
DCP	Dichloropropanone.
DO	Dissolved oxygen.
DOC	Dissolved organic carbon.
DOM	Dissolved organic matter.
d_s	Standardized median difference.
DWTP	Drinking water treatment plant.
ECEs	Extreme climatic events.
Epi	Epilimnion.
ESI	Electron spray ionization.
FI	Fluorescence index.

FP	Formation potential.
FTICR-MS	Fourier Transform Ion Cyclotron Resonance MS.
GF/F	Glass fibre filter.
g_s	Effect size metric.
HAAs	Haloacetic acids.
HANs	Haloacetonitriles.
HIX	Humification index.
HNO ₃	Nitric acid.
HRMS	High resolution mass spectrometry.
HRT	Hydraulic residence time.
HWMID	Heatwave magnitude index daily.
Hypo	Hypolimnion.
IPCC	Intergovernmental Panel on Climate Change.
J	Distance measure statistic for assessing Granger causality in quantiles.
KH ₂ PO ₄	Potassium dihydrogen phosphate.
KM	Kendrick mass.
KMD	Kendrick mass defect.
LC	Liquid chromatography.
metaB	Bottom of metalimnion depth.
metaT	Top of metalimnion depth.
MS	Mass spectrometry.
MTBE	Methyl tert-butyl ether.
NaClO	Sodium hypochlorite.

NaOH	Sodium hydroxide.
Na ₂ SO ₄	Sodium sulphate.
Na ₂ SO ₃	Sodium sulphite.
η_c	Uncorrelated white noise of the complete model.
NDMA	N-nitrosodimethylamine.
NH ₃	Ammonia.
NH ₄ ⁺	Ammonium.
NO ₃ ⁻	Nitrate.
NO ₂ ⁻	Nitrite.
η_r	Uncorrelated white noise of the restricted model.
nSSFI	Non-parametric standardized streamflow index.
nSLI	Non-parametric standardized water level index.
nSPI	Non-parametric standardized precipitation index.
PARAFAC	Parallel Factor Analysis.
PC	Principal component.
PCA	Principal component analysis.
PO ₄ ³⁻	Phosphate.
POT	Peak over threshold.
QA/QC	Quality control/Quality assurance.
SPE	Solid phase extraction.
SUVA ₂₅₄	Specific ultraviolet absorbance at $\lambda = 254$ nm.
TBM	Tribromomethane.
TCAN	Trichloroacetonitrile.

TCM	Trichloromethane.
TCP	Trichloropropanone.
TCNM	Trichloronitromethane.
THMs	Trihalomethanes.
TKN	Total kjeldahl nitrogen.
T _{max}	Maximum air temperature.
TN	Total nitrogen.
TOC	Total Organic Carbon.
TP/PT	Total phosphorus.
T [*] THMs	Total trihalomethanes.
T _w	Water temperature.
UHRMS	Ultrahigh resolution mass spectrometry.
UN	United Nations.
UVA ₂₅₄	Ultraviolet absorbance at $\lambda = 254$ nm.
VK	Van Krevelen.
WWTPs	Wastewater treatment plants.
X _t	Predictor variable timeseries.
Y _t	Response variable timeseries.

List of Figures

Figure 1. Schematic of a conventional water treatment process. SFBW = spent filter backwash. Image adapted from Li et al., 2018.	18
Figure 2. DOM sources in lakes. Image adapted from He et al., 2016. ¹ DOM* = singlet DOM, ³ DOM* = triplet DOM, ROS = reactive oxygen species, PrROS = precursors of ROS, AOC = anthropogenic organic contaminants, and M ⁿ⁺ = metal ions with positive charge of n.	47
Figure 3. DOM reactivity in lakes. Image adapted from He et al., 2016.	50
Figure 4. The segmentation of the 2D van Krevelen diagram. Image adapted from Antony et al., 2017.	63
Figure 5. Kendrick plot. Image adapted from Pikovskoi and Kosyakov, 2023.	64
Figure 6. The Ter Watershed Map. Paper I is based on location 2. Papers II and III are based on all locations (1-4)	83
Figure 7. Tier One analysis - Derivation of hydroclimatic extremes indices. Max = maximum, HWMId = Heatwave Magnitude Index daily, nSPI = non-parametric Standardized Precipitation Index, nSSFI = non-parametric Standardized Streamflow Flow Index and nSLI = non-parametric Standardized reservoir Level Index.	85
Figure 8. Aggregation of depth profiles of reservoir water quality into epilimnion and hypolimnion timeseries. WatT = Water temperature, DO = Dissolved oxygen, NO ₃ ⁻ = Nitrate, NH ₄ ⁺ = Ammonium, TP = Total phosphorus, Epi = Epilimnion, Hypo = Hypolimnion and WQ = Water quality.	86
Figure 9. Tier two analysis-causal inference modeling. Epi = Epilimnion, Hypo = Hypolimnion, WatT = Water temperature, DO = Dissolved oxygen, NO ₃ ⁻ = Nitrate, NH ₄ ⁺ = Ammonium, TP = Total phosphorus, Max = Maximum, WQ = Water quality and J = non-parametric causality-in-quantile test statistic.	87
Figure 10. Tier three analysis - Extreme events impact analysis. HWMId = Heatwave Magnitude Index daily, nSPI = non-parametric Standardized Precipitation Index, nSSFI = non-parametric Standardized Streamflow Flow Index and nSLI = non-parametric Standardized reservoir Level Index, Epi = Epilimnion, Hypo = Hypolimnion, WQ = Water quality, WatT = Water temperature, DO = Dissolved oxygen, NO ₃ ⁻ = Nitrate, NH ₄ ⁺ = Ammonium, TP = Total phosphorus, POT = Peak Over Threshold, WQ = Water quality and P = p-value.	88
Figure 11. Analytical pipeline for the determination of C- and N-DBP formation potential. NDMA = N-nitrosodimethylamine, LLE = Liquid-Liquid Extraction, LLME = Liquid-Liquid Micro Extraction, DBPs = Disinfection by-products, SPE = Solid Phase Extraction, MS = Mass Spectrometer, THMs = Trihalomethanes and HANs = Haloacetonitriles.	89
Figure 12. Dissolved organic matter molecular fingerprinting process. DOM = Dissolved organic matter, CDOM = Chromophoric dissolved organic matter, UV ₂₅₄ = Ultraviolet absorbance at 254 nm, 3D EEMs = 3 – dimensional Excitation-Emission Matrices, NO ₃ ⁻ = Nitrate, NH ₄ ⁺ = Ammonium, TN = Total Nitrogen, TP = Total phosphorus, PPL = Bond Elut Priority PolLutant Catridge, DOC = Dissolved Organic Carbon, BIX = Biological Index and HIX = Humification Index.	91

List of Tables

Table 1. Typical contaminants found in drinking water sources.	16
Table 2. A summary of commonly used climate indices for defining heatwaves (and their counterpart coldwaves).	29
Table 3. Changes and impacts promoted by heatwaves in aquatic ecosystems.	31
Table 4. A summary of drought indices commonly found in literature.	33
Table 5. Changes, mechanisms and impacts promoted by droughts in aquatic ecosystems.	35
Table 6. Changes and impacts promoted by rainstorms in aquatic ecosystems.	38
Table 7. Common DOM measurement methods.	54
Table 8. Typical DOM Fluorescence Peaks reported in literature.	57
Table 9. DOM Fluorescence indices commonly found in literature.	59
Table 10. Summary of molecular methods for the characterization of DOM.	61
Table 11. A summary of disinfection by-products commonly found in literature.	66
Table 12. A summary of nitrogenous DBP classes and their precursors.	72
Table 13. DBP regulatory thresholds across countries.	74
Table 14. A summary of common DBP predictive modeling approaches.	77
Table 15. A summary of statistical tests applied in the thesis.	93

Table of Contents

1	Introduction.....	13
1.1	Water as a driver of human civilization	13
1.2	Eutrophication of lakes and how it impacts water bodies and their associated ecosystem services.....	14
1.3	Municipal water treatment as an enabler of the provisioning ecosystem service of drinking water supply.....	15
1.3.1	Sources of contaminants in water sources	15
1.3.2	Conventional water treatment technology	18
1.4	Climatic extreme events and how they impact lakes and the ecosystem service of drinking water supply.....	27
1.4.1	Heatwaves	28
1.4.2	Droughts	32
1.4.3	Rainstorms	37
1.5	Ecosystem stability in the context of climate extremes and eutrophication	41
1.6	Exploring cause-effect relationships in environmental time-series	43
1.7	The allied effect of climate extreme and eutrophication on the ecosystem service of water supply	44
1.8	Dissolved Organic Matter (DOM).....	46
1.8.1	Nature and Sources.....	46
1.8.2	DOM functionality in aquatic ecosystems	48
1.8.3	Fate of DOM in Aquatic ecosystems.....	49
1.8.4	Drivers of DOM dynamics in watersheds.....	51
1.8.5	Controls on DOM loads to aquatic systems.....	52
1.8.6	DOM Measurement.....	53
1.9	Disinfection by-product formation in drinking water.....	65
1.9.1	Exposure, human health outcomes and regulation.....	73
1.9.2	Environmental factors modulating organic precursor dynamics.....	75
1.9.3	DBP surrogates and predictive modeling.....	76
2	Objectives and Hypotheses	81
2.1	General objective	81
2.2	Specific Objectives.....	81
2.3	Hypotheses.....	82
3	Methodology.....	83
3.1	Study Site.....	83
3.2	Methods.....	84

3.3	Statistical techniques.....	92
4	Results and discussion.....	94
4.1	Drastic reduction of nutrient loading to a reservoir alters its resistance to impacts of extreme climatic events.....	94
4.2	Characterization of organic matter by HRMS in surface waters: Effects of chlorination on molecular fingerprints and correlation with DBP formation potential.....	106
4.3	Drivers of variability in disinfection by-product formation potential in a chain of thermally stratified drinking water reservoirs.....	117
4.4	Discussion of hypotheses	131
4.5	DOM molecular regions affected by chlorination.	142
4.6	Potential surrogates for the prediction of DBP formation potential.....	142
4.7	Climate change impacts on the Ter Watershed and its implications for the management of the river - reservoirs system.....	145
4.8	Unresolved scientific questions requiring further research.....	148
5	Conclusions.....	150
6	Annexes.....	152
6.1	Drastic reduction of nutrient loading to a reservoir alters its resistance to impacts of extreme climatic events.....	152
6.2	Characterization of organic matter by HRMS in surface waters: Effects of chlorination on molecular fingerprints and correlation with DBP formation potential.....	183
6.3	Drivers of variability in disinfection by-product formation potential in a chain of thermally stratified drinking water reservoirs.....	227
7	References.....	270
8	Acknowledgements.....	318

Abstract in English

Water supply, one of the key ecosystem services provided by water bodies (rivers, reservoirs and lakes), is under threat due to climate change. Climate change mediated extreme events are already impacting water sources and are projected to increase in variability, magnitude and frequency. The provision of safe drinking water to the public plays a fundamental role in the sustainability of human civilization through the safeguarding of human health. Climate mediated extreme events are reported to impair source water quality in various ways, leading to increased treatment costs or water contamination as a result of treatment failure, with adverse effects on human health.

The formation of disinfection by-products (DBPs) in drinking water is one of the emerging concerns in the protection of human health because of the health-related outcomes such as cancer, respiratory problems and reproductive health defects associated with their formation. DBPs emerge from the unintended reactions between chemical disinfectants, inorganic compounds and dissolved organic matter (DOM) found in source waters. The occurrence of extreme events has the potential to exacerbate DOM concentration in source water, resulting in the provision of unsafe water to the public, which not only endangers human health but also undermines regulatory compliance, attracting a barrage of costs in form of litigations and non-compliance penalties. Consequently, understanding how extreme events impact water quality, in general and the formation of DBPs in particular, is of paramount importance to utility managers, water supply regulatory authorities and the public.

This thesis generally aims at providing insights on how source waters in lakes could be managed to ameliorate effects of DOM mediated by extreme events, in order to preserve the provision of the ecosystem service of drinking water supply. Particularly, we demonstrate 1) how extreme events are coupled with generic source water quality in causal relationships; 2) how molecular signatures of DOM change during drinking water chlorination; and 3) the role of water age, seasonality and thermal stratification in modulating the formation of DBPs in source waters. We achieve our overarching goal through a combination of various approaches. First, we apply advanced statistical techniques of non-linear dynamics and extreme value theory to a long term (55 years), low frequency dataset, generated from the Sau Reservoir (North East Spain), to establish causal links between the occurrence of extreme climate events and the concomitant response of

Abstract in English

reservoir water quality variables. In the causal inference analysis, hydrometeorological variables of maximum air temperature, streamflow, precipitation and reservoir water level, were used as predictor variables, whereas reservoir water quality parameters such as dissolved oxygen, nitrate, ammonium, total phosphorus and water temperature were used as response variables. On the other hand, assessing impacts of extreme climatic events was achieved by comparing medians of water quality variables in extreme versus non-extreme cases, using extreme event indices derived from hydrometeorological variables. Second, we sampled from a river-reservoir interconnected system of Ter-Sau-Susqueda-Pasteral, in autumn, winter and summer, for two purposes. The primary purpose was to profile how water age, thermal stratification and seasonality influence the formation of DBPs, by sampling at different depths from the river-reservoir interconnected system and carrying out DBP formation potential experiments. The other purpose was to gain insights into how water chlorination changes the molecular signatures of DOM in water, identify appropriate surrogates for the prediction of trihalomethanes (THMs) and Haloacetonitriles (HANs) classes of DBPs, through the use of non-targeted application of High Resolution Mass Spectrometry (HRMS) and DBP formation potential experiments.

Main results of this thesis are presented as three scientific articles. Causal inference and extreme events impact analyses, reported in **Paper I**, suggest that reservoir water quality variables were mostly affected by hydrological extremes, where droughts generally decreased dissolved oxygen concentration and increased ammonium concentration and temperature. On the other hand, extreme wetness increased concentration of dissolved oxygen and nitrate, while lowering concentration of ammonium and total phosphorus. The results also show a gradient, in which adverse effects were mostly being felt in the deeper water layers of the reservoir, as well as a trend of when the reservoir was eutrophic, suggesting that impacts of extreme events were modulated by reservoir trophic state, particularly in deeper water layers. On the other hand, the same gradient suggests dominance of more rapid processes in the upper water layers that dwarf the signal of extreme events in a low-frequency data (i.e., monthly) dataset.

Overall, results reported in **Paper II** indicate that chlorination altered DOM by decreasing the number and intensity of peaks in the lignin-like and lipid-like regions, while creating new halogenated and non-halogenated signals in the same regions and produced new highly oxidized molecules in the tannin-like region. In particular, chlorination significantly altered DOM by

Abstract in English

producing molecular features with smaller m/z , lower Kendrick Mass Defect (KMD) and a higher number of halogenated compounds. Specifically, chlorination altered the lignin-like/carboxyl-rich alicyclic molecules (CRAM), soil humic substances and the fatty acid-like region, in which several signals disappeared. Also, chlorination altered the condensed hydrocarbon region, where several new halogenated and non-halogenated features appeared, and the tannin-like region where several new oxidized features appeared. Additionally, two regions in the lignin-like region were identified with features that strongly correlated with THMs and HANs formation potential, making them suitable surrogates for prediction.

Paper III reports that when the three factors of water age, thermal stratification and seasonality were considered in isolation, total THMs formation potential exhibited a gradient of increasing from Ter River to Pastoral, whereas the formation of nitrogenous DBPs decreased across the same spatial continuum. This result highlights the important role played by water age in reservoirs in shaping the DBP formation patterns. However, if all factors were considered together, seasonality was the main driver that shaped DBP formation. Trends were observed in which the formation potential of trichloromethane (TCM), bromodichloromethane (BDCM) and Dichloroacetonitrile (DCAN) generally peaked in autumn, followed by summer and were lowest in winter. On the other hand, the formation potential N-nitrosodimethylamine (NDMA) peaked in summer and winter but was lowest in autumn, in major reservoirs of the system. There was no significant gradient in DBPs formation by reservoir depth. Although the maxima for TCM formation was still within regulatory threshold, the results suggest that storm events, that often occur in autumn, have the potential to tip total THM formation potential over the regulatory threshold, requiring either preventive or reparative measures. The results also indicate that seasonality might affect, differently, the formation of constituents of the same class of DBPs, as observed in the disparity between the formations of DCAN and NDMA.

Overall, what we learn from this thesis is that hydroclimatic extremes are intense in the Ter Watershed, they are negatively impacting most water quality variables, but that such impacts are modulated by reservoir trophic state. Relentlessly reducing eutrophication through nutrient reductions in the watershed has the potential to minimize adverse impacts of climate extremes on lakes. Regarding the ecosystem service of drinking water supply, we learn that trophic state improvements can also reduce the formation potential of DBPs in source waters that are used for

Abstract in English

drinking water supply, through reduced endogenous DOM production. We also learn that climate is the main driver of variability in DBP formation, overshadowing other factors such as water age. As such, refining our mechanistic understanding of how weather variables drive DBP formation and developing seasonally driven predictive frameworks, that can reliably capture DBP formation dynamics, would go a long way in helping water supply managers to cope with risks occasioned by uncertainties of the changing climate.

Abstract in Catalan

El subministrament d'aigua, un dels principals serveis ecosistèmics proporcionats pels cossos d'aigua dolça (rius, embassaments i llacs), està amenaçat a causa del canvi climàtic. Els esdeveniments extrems mediat pel canvi climàtic ja estan afectant les fonts d'aigua i es preveu que augmentaran en variabilitat, magnitud i freqüència. La provisió d'aigua potable segura per al públic juga un paper fonamental en la sostenibilitat de la civilització humana mitjançant la salvaguarda de la salut humana. Es sap que els esdeveniments climàtics extrems afecten la qualitat de l'aigua de diverses maneres, el que porta a un augment dels costos de tractament o la contaminació de l'aigua com a resultat de fallades en el tractament, amb efectes adversos sobre la salut humana.

La formació de subproductes de desinfecció (DBPs, per les seves sigles en anglès) a l'aigua potable és una de les preocupacions emergents en la protecció de la salut humana a causa dels resultats relacionats amb la salut associats amb la seva formació, com el càncer, problemes respiratoris i defectes en la salut reproductiva. Els DBPs provenen de les reaccions no desitjades entre desinfectants químics, compostos inorgànics i matèria orgànica dissolta (DOM) de les aigües naturals. L'ocurrència d'esdeveniments extrems té el potencial d'augmentar la concentració de DOM a l'aigua natural, amb el resultat de proveir aigua no segura per al públic, la qual cosa no només posa en perill la salut humana, sinó que també mina el compliment normatiu, a més d'una sèrie de costos en forma de litigis i multes per incompliments. En conseqüència, comprendre com els esdeveniments extrems afecten la qualitat de l'aigua en general i la formació de DBPs en particular és de suma importància per als gestors de serveis públics, les autoritats reguladores del subministrament d'aigua i el públic en general.

Aquesta tesi té com a objectiu proporcionar informació sobre com podrien gestionar-se les aigües naturals als llacs per mitigar els efectes del DOM mediat per esdeveniments extrems, amb la finalitat de preservar la provisió del servei ecosistèmic de subministrament d'aigua potable. En particular, demostrem 1) com els esdeveniments extrems estan relacionats amb la qualitat genèrica de l'aigua natural mitjançant relacions causals; 2) com canvien les signatures moleculars del DOM durant la cloració de l'aigua potable; i 3) el paper de l'edat de l'aigua, la estacionalitat i l'estratificació tèrmica en modular la formació de DBPs a les aigües naturals. Assolim el nostre objectiu general mitjançant una combinació de diversos enfocaments. En primer lloc, apliquem tècniques

Abstract in Catalan

estadístiques avançades de dinàmica no lineal i teoria de valors extrems a un conjunt de dades a llarg termini (55 anys), de baixa freqüència, mostrejats a l'embassament de Sau (nord-est d'Espanya), per establir vincles causals entre l'ocurrència d'esdeveniments climàtics extrems i la resposta concomitant de les variables de qualitat de l'aigua de l'embassament. En l'anàlisi d'inferència causal, les variables hidrometeorològiques de temperatura màxima de l'aire, cabal, precipitació i nivell de l'aigua de l'embassament es van utilitzar com a variables predictores, mentre que els paràmetres de qualitat de l'aigua de l'embassament, com ara oxigen dissolt, nitrats, amoni, fòsfor total i temperatura de l'aigua, es van utilitzar com a variables resposta. D'altra banda, l'avaluació dels impactes dels esdeveniments climàtics extrems es va aconseguir comparant les mitjanes de les variables de qualitat de l'aigua en casos extrems versus no extrems, utilitzant índexs d'esdeveniments extrems derivats de variables hidrometeorològiques. En segon lloc, vam mostrejar el sistema interconnectat riu-embassaments Ter-Sau-Suqueda-Pasteral, a la tardor, hivern i estiu, amb dos propòsits. El propòsit principal era entendre com l'edat de l'aigua dins del sistema d'embassaments, la estratificació tèrmica i la estacionalitat influeixen en la formació de DBPs, mitjançant mostreig a diferents profunditats del sistema riu-embassament i realitzant experiments de potencial de formació de DBP. L'altre propòsit era obtenir informació sobre com la cloració de l'aigua canvia les signatures moleculars del DOM a l'aigua, identificar variables substitutòries adequades per a la predicció de trihalometans (THMs) i haloacetunitrils (HANs) mitjançant l'aplicació de l'espectrometria de masses d'alta resolució (HRMS) i experiments de potencial de formació de DBP.

Els principals resultats d'aquesta tesi es presenten en tres articles científics. Els anàlisis d'inferència causal i impacte d'esdeveniments extrems, reportats a l'Article I, suggereixen que les variables de qualitat de l'aigua de l'embassament van ser principalment afectades pels extrems hidrològics, amb l'excepció del fòsfor total que va ser generalment sense resposta, suggerint que la seva dinàmica estava controlada pels cicles interns. Els resultats també mostren patrons clars d'efectes adversos que es sentien principalment a les capes més profundes de l'aigua de l'embassament i en el període en què l'embassament era descrit com a eutròfic, suggerint que els impactes dels esdeveniments extrems estan modulats per l'estat tròfic de l'embassament. D'altra banda, el patró observat a les capes superiors de l'aigua suggereix la dominància de processos més ràpids que amagen la senyal dels esdeveniments extrems en un conjunt de dades de baixa freqüència (és a dir, mensual).

Abstract in Catalan

Els resultats informats a l'Article II indiquen que la cloració va alterar el DOM al disminuir el nombre i intensitat de pics a les regions similars a la lignina i lípids, mentre creava noves senyals halogenades i no halogenades a les mateixes regions i produïa noves molècules altament oxidades a la regió similar a la tànica. En particular, la cloració va alterar significativament el DOM al produir característiques moleculars amb m/z més petits, menor defecte de massa de Kendrick (KMD) i un major nombre de compostos halogenats. Específicament, la cloració va alterar les molècules similars a la lignina/carboxil-rich alicyclic (CRAM), les substàncies húmiques del sòl i la regió similar als àcids grassos, en què diverses senyals van desaparèixer. A més, la cloració va alterar la regió d'hidrocarburs condensats, on van aparèixer diverses característiques noves halogenades i no halogenades, i la regió similar a la tànica on van aparèixer diverses característiques noves oxidades. A més, es van identificar dues regions a la regió similar a la lignina amb característiques que es correlacionaven fortament amb el potencial de formació de THMs i HANs, fent-los substituïts adequats per a la predicció.

L'Article III informa que, quan els tres factors d'edat de l'aigua, estratificació tèrmica i estacionalitat es van considerar de manera aïllada, el potencial de formació total de THMs va augmentar des del riu Ter fins a Pasteral, mentre que la tendència oposada, de disminuir en el mateix continu espacial, es va observar per a la formació de DBPs nitrogenats. Aquest resultat destaca el paper important jugat per l'edat de l'aigua en els embassaments en la configuració dels patrons de formació de DBPs. Tanmateix, si es consideraven tots els factors junts, la estacionalitat era el principal impulsor que configurava el patró de formació, en el qual el potencial de formació de triclorometà (TCM) i bromodiclorometà (BDCM), i dicloroacetunitrilo (DCAN) generalment assolien el seu punt àlgid a la tardor, seguit de l'estiu i eren més baixos a l'hivern. D'altra banda, el potencial de formació de N-nitrosodimetilamina (NDMA) assolia el seu punt àlgid a l'estiu i l'hivern, però era més baix a la tardor, als embassaments principals del sistema. La profunditat a l'embassament no va semblar influir significativament en la variabilitat de la formació de DBPs. Tot i que els màxims per a la formació de TCM encara estaven dins del llinar reglamentari, els resultats suggereixen que els esdeveniments de tempesta, que sovint ocorren a la tardor, tenen el potencial de superar el llinar reglamentari de formació total de THM, cosa que requereix mesures preventives o reparadores. Els resultats també indiquen que la estacionalitat podria afectar de manera diferent la formació de constituents de la mateixa classe de DBPs, com es veu en la disparitat entre les formacions de DCAN i NDMA.

Abstract in Catalan

En general, el que aprenem d'aquesta tesi és que els extrems hidroclimàtics són intensos a la conca del riu Ter, afecten negativament la majoria de les variables de qualitat de l'aigua, però que aquests impactes estan modulats per l'estat tròfic de l'embassament. Reduir l'eutrofització mitjançant la reducció de nutrients a la conca té el potencial de minimitzar els impactes adversos dels extrems climàtics als llacs. Pel que fa al servei ecosistèmic de subministrament d'aigua potable, aprenem que les millores en l'estat tròfic també poden reduir el potencial de formació de DBPs a les aigües naturals utilitzades per al subministrament d'aigua potable, mitjançant la reducció de la producció endògena de DOM. També aprenem que el clima és el principal impulsor de la variabilitat en la formació de DBPs, eclipsant altres factors com l'edat de l'aigua. Com a tal, perfeccionar la nostra comprensió mecanicista de com les variables climàtiques impulsen la formació de DBPs i desenvolupar marcs predictius que puguin capturar de manera fiable les dinàmiques de formació de DBPs, seria de gran ajuda per als gestors del subministrament d'aigua per fer front als riscos causats per les incerteses del canvi climàtic en curs.

Abstract in Spanish

El suministro de agua, uno de los principales servicios ecosistémicos proporcionados por los cuerpos de agua dulce (ríos, embalses y lagos), está bajo amenaza debido al cambio climático. Los eventos climáticos extremos mediados por el cambio climático ya están afectando las fuentes de agua y se proyecta que aumentarán en variabilidad, magnitud y frecuencia. La provisión de agua potable segura para el público juega un papel fundamental en la sostenibilidad de la civilización humana a través de la protección de la salud humana. Se sabe que los eventos climáticos extremos afectan la calidad del agua de diversas maneras, lo que lleva a un aumento en los costos de tratamiento o la contaminación del agua como resultado de fallos en el tratamiento, con efectos adversos en la salud humana.

La formación de subproductos de desinfección (DBPs, por sus siglas en inglés) en el agua potable es una de las preocupaciones emergentes en la protección de la salud humana debido a los resultados relacionados con la salud asociados con su formación, como el cáncer, problemas respiratorios y defectos en la salud reproductiva. Los DBPs surgen de las reacciones no deseadas entre desinfectantes químicos, compuestos inorgánicos y materia orgánica disuelta (DOM) de las aguas naturales. La ocurrencia de eventos extremos tiene el potencial de aumentar la concentración de DOM en el agua natural, dando como resultado la provisión de agua no segura para el público, lo que no solo pone en peligro la salud humana, sino que también socava el cumplimiento normativo, implicando una serie de costos en forma de litigios y multas por incumplimientos. En consecuencia, comprender cómo los eventos extremos afectan la calidad del agua en general y la formación de DBPs en particular es de suma importancia para los gestores de servicios públicos, las autoridades regulatorias del suministro de agua y el público en general.

Esta tesis tiene como objetivo proporcionar información sobre cómo podrían gestionarse las aguas naturales en lagos para mitigar los efectos del DOM mediado por eventos extremos, con el fin de preservar la provisión del servicio ecosistémico de suministro de agua potable. En particular, demostramos 1) cómo los eventos extremos están relacionados con la calidad genérica del agua natural usando relaciones causales; 2) cómo cambian las firmas moleculares del DOM durante la cloración del agua potable; y 3) el papel de la edad del agua, la estacionalidad y la estratificación térmica en modular la formación de DBPs en aguas naturales. Logramos nuestro objetivo general

Abstract in Spanish

mediante una combinación de varios enfoques. Primero, aplicamos técnicas estadísticas avanzadas de dinámica no lineal y teoría de valores extremos a un conjunto de datos a largo plazo (55 años), de baja frecuencia, muestreados en el embalse de Sau (noreste de España), para establecer vínculos causales entre la ocurrencia de eventos climáticos extremos y la respuesta concomitante de las variables de calidad del agua del embalse. En el análisis de inferencia causal, las variables hidrometeorológicas de temperatura máxima del aire, caudal, precipitación y nivel del agua del embalse se utilizaron como variables predictoras, mientras que los parámetros de calidad del agua del embalse, como oxígeno disuelto, nitrato, amonio, fósforo total y temperatura del agua, se utilizaron como variables respuesta. Por otro lado, la evaluación de los impactos de eventos climáticos extremos se logró comparando las medianas de las variables de calidad del agua en casos extremos versus no extremos, utilizando índices de eventos extremos derivados de variables hidrometeorológicas. En segundo lugar, muestreamos el sistema interconectado río-embalses Ter-Sau-Suqueda-Pasteral, en otoño, invierno y verano, con dos propósitos. El propósito principal era entender cómo la edad del agua dentro del sistema de embalses, la estratificación térmica y la estacionalidad influyen en la formación de DBPs, mediante muestreo a diferentes profundidades del sistema río-embalse y llevando a cabo experimentos de potencial de formación de DBP. El otro propósito era obtener información sobre cómo la cloración del agua cambia las firmas moleculares del DOM en el agua, identificar variables sustitutivas apropiadas para la predicción de trihalomethanes (THMs) y Haloacetoneitriles (HANs) mediante la aplicación de espectrometría de masas de alta resolución (HRMS) y experimentos de potencial de formación de DBP.

Los principales resultados de esta tesis se presentan en tres artículos científicos. Los análisis de inferencia causal e impacto de eventos extremos, reportados en el Artículo I, sugieren que las variables de calidad del agua del embalse fueron principalmente afectadas por extremos hidrológicos, con la excepción del fósforo total que fue generalmente no afectado, sugiriendo que su dinámica estaba controlada por ciclos internos. Los resultados también muestran patrones claros de efectos adversos que se sienten principalmente en las capas más profundas del agua del embalse y en el período en que se describía al embalse como eutrófico, sugiriendo que los impactos de eventos extremos están modulados por el estado trófico del embalse. Por otro lado, el patrón observado en las capas superiores del agua sugiere la dominancia de procesos más rápidos que eclipsan la señal de eventos extremos en un conjunto de datos de baja frecuencia (es decir, mensual).

Abstract in Spanish

Los resultados informados en el Artículo II indican que la cloración alteró el DOM al disminuir el número e intensidad de picos en las regiones similares a la lignina y lípidos, mientras creaba nuevas señales halogenadas y no halogenadas en las mismas regiones y producía nuevas moléculas altamente oxidadas en la región similar a la tanina. En particular, la cloración alteró significativamente el DOM al producir características moleculares con m/z más pequeñas, menor defecto de masa de Kendrick (KMD) y un mayor número de compuestos halogenados. Específicamente, la cloración alteró las moléculas similares a la lignina/carboxil-rich alicyclic (CRAM), las sustancias húmicas del suelo y la región similar a los ácidos grasos, en la que varias señales desaparecieron. Además, la cloración alteró la región de hidrocarburos condensados, donde aparecieron varias características nuevas halogenadas y no halogenadas, y la región similar a la tanina donde aparecieron varias características nuevas oxidadas. Además, se identificaron dos regiones en la región similar a la lignina con características que se correlacionaban fuertemente con el potencial de formación de THMs y HANs, haciéndolos sustitutos adecuados para la predicción.

El Artículo III informa que cuando se consideraron de forma aislada los tres factores de edad del agua, estratificación térmica y estacionalidad, el potencial de formación total de THMs aumentó desde el río Ter hasta Pasteral, mientras que se observó la tendencia opuesta, de disminuir en el mismo continuo espacial, para la formación de DBPs nitrogenados. Este resultado destaca el papel importante desempeñado por la edad del agua en

los embalses en la configuración de los patrones de formación de DBPs. Sin embargo, si se consideraban todos los factores juntos, la estacionalidad era el principal impulsor que configuraba el patrón de formación, en el que el potencial de formación de triclorometano (TCM) y bromodiclorometano (BDCM), y dicloroacetoneitrilo (DCAN) generalmente alcanzaban su punto máximo en otoño, seguido de verano y eran más bajos en invierno. Por otro lado, el potencial de formación de N-nitrosodimetilamina (NDMA) alcanzó su punto máximo en verano e invierno pero fue más bajo en otoño, en los embalses principales del sistema. La profundidad en el embalse no pareció influir significativamente en la variabilidad de la formación de DBPs. Aunque los máximos para la formación de TCM aún estaban dentro del umbral reglamentario, los resultados sugieren que los eventos de tormenta, que a menudo ocurren en otoño, tienen el potencial de

Abstract in Spanish

superar el umbral reglamentario de formación total de THM, lo que requiere medidas preventivas o reparadoras. Los resultados también indican que la estacionalidad podría afectar de manera diferente la formación de constituyentes de la misma clase de DBPs, como se observa en la disparidad entre las formaciones de DCAN y NDMA.

En general, lo que aprendemos de esta tesis es que los extremos hidroclimáticos son intensos en la cuenca del río Ter, afectan negativamente a la mayoría de las variables de calidad del agua, pero que tales impactos son modulados por el estado trófico del embalse. Reducir la eutrofización mediante la reducción de nutrientes en la cuenca tiene el potencial de minimizar los impactos adversos de los extremos climáticos en los lagos. En cuanto al servicio ecosistémico de suministro de agua potable, sugerimos que las mejoras en el estado trófico también pueden reducir el potencial de formación de DBPs en aguas fuente que se utilizan para el suministro de agua potable, mediante la reducción de la producción endógena de DOM. También aprendimos que el clima es el principal impulsor de la variabilidad en la formación de DBPs, eclipsando otros factores como la edad del agua.

Como tal, perfeccionar nuestra comprensión mecanicista de cómo las variables climáticas impulsan la formación de DBPs y desarrollar marcos predictivos que puedan capturar de manera confiable las dinámicas de formación de DBPs, sería de gran ayuda para que los gestores de suministro de agua enfrenten los riesgos ocasionados por las incertidumbres del cambio climático en curso.

Introduction

1 Introduction.

1.1 Water as a driver of human civilization.

From the ancient to modern human civilizations, water sources have played a key role in advancement of human civilizations (Wang and He, 2022), as have other factors such as soil (Minami, 2009; Savory, 1994) and energy (Islam and Hasanuzzaman, 2020; Price, 1995), among others. Water sources provide benefits such as water for the sustenance of human health, energy generation, irrigation, source of food, transportation of goods and advancement of cultural practices (Pietz and Zeisler-Vralsted, 2021). These benefits may explain the pattern of establishment and flourishing of human settlements in proximity with rivers and lakes. A number of civilizations are reported to have collapsed, in the past, as an aftermath of climate related perturbations to the hydrological cycle. These civilizations include the Maya civilization, which collapsed due to prolonged droughts in Yucatan, Mexico (Haug et al., 2003; Smyth et al., 2017), the Terramara society in Italy, which collapsed due to extended drought periods (Cremaschi et al., 2006) and the Andean Civilization in Peru and Bolivia, which collapsed due to reduced levels of lake Titicaca (Binford et al., 1997).

Although water is so central to the sustainability of humans, scientific research output on water as a subject matter remains low, at an average of under 10 % of the total research output of top countries that are publishing, in relation to other research fields (Mehmood, 2019). This low statistic implies that water does not receive the attention it deserves, hence there is a need to intensify research outputs on the water domain.

Introduction

1.2 Eutrophication of lakes and how it impacts water bodies and their associated ecosystem services.

Eutrophication is the enrichment of water bodies with excessive nutrients, particularly phosphorus and nitrogen, which can disturb the natural functioning of aquatic ecosystems (Lüring et al., 2016). The loading of water bodies with nutrients is directly driven by factors such as wastewater discharges, intensive raising of livestock, application of fertilizers, consumption of fossil fuels as energy sources, land use change and, indirectly, influenced by population growth, economic growth and changes in agricultural methods (Khan and Mohammad, 2014). All these factors can generate massive pollutant loads of nitrogen and phosphorus in the catchment, which will eventually end up in the water bodies through hydrological connectivity. At ecosystem scale, human induced nutrient enrichment generally alters the natural functioning of the system, leading to a curtailment of its associated ecosystem services (Smith et al., 1999). Eutrophication impairs aquatic ecosystems through various mechanisms, among them: **inducement of succession**, where a macrophyte dominated system gets replaced by a phytoplankton dominated system (Qin et al., 2013); **proliferation of phytoplankton** forming algal mats, whose death and decomposition causes foul smell on the beach; **production of cyanotoxins** which can be lethal to fish, animals and humans (Yang et al., 2008); **evolutionary changes** in aquatic ecosystem species through adaptation, weakened sexual selection, gene flow and homogenization of genetic diversity (Alexander et al., 2017); **depletion of dissolved oxygen** in the water column (Qin et al., 2013) which may result in massive death of aquatic animals (Yang et al., 2008); and **decreased biodiversity** (Qin et al., 2013) which may impact stability of the ecosystem. Furthermore, eutrophication may also cause lake ecosystems to be net emitters of carbon dioxide (Morales-Williams et al., 2021) and methane (Beaulieu et al., 2019), which are potent greenhouse gases. By impairing the ecological integrity i.e. composition, structure and processes (Fu et al., 2013) of aquatic ecosystems, eutrophication can negatively impact the systems' capability to provide benefits for the well-being of mankind. Such benefits that human beings obtain from ecosystems, for the improvement of their well-being, are termed as ecosystem services (Fisher et al., 2009; Fu et al., 2013). These services, which are generally anchored on the well-functioning of biodiversity (Walters and Scholes, 2017), are distinctly classified into four categories of provisioning (i.e. water supply and fisheries), regulating (i.e. flood control and soil erosion control), cultural (i.e. recreation

Introduction

and spiritual benefits) and supporting (i.e. pollination and nutrient cycling) (Brauman et al., 2007; Walters and Scholes, 2017).

1.3 Municipal water treatment as an enabler of the provisioning ecosystem service of drinking water supply.

1.3.1 Sources of contaminants in water sources.

In its raw form, water may contain physical, chemical and biological constituents in quantities that are unsuitable or even toxic for human consumption. These constituents may be naturally present in water based on the source i.e. oxides of nitrogen, heavy metals, hydrocarbons and radioactive substances, or they may be a result of anthropogenic pollution through various economic activities pursued by humans such as agriculture and industry i.e. pesticides, petrochemicals, heavy metals and radionuclides. Water contaminants are broadly categorized into inorganics, organics, microbial, radiological, suspended solids, and thermal pollution (Pooja et al., 2020). Table 1 summarizes contaminants commonly found in drinking water sources.

Introduction

Table 1. Typical contaminants found in drinking water sources.

Contaminant Group	Example	Source	Human health outcome	Reference
Inorganics	Heavy metal i.e. Cadmium, Chromium, Mercury, Manganese, Iron, Zinc and Fluoride.	Fluoride-Geological, pharmaceutical products, toothpaste, fertilisers and insecticides. Arsenic-Natural deposits, agricultural and industrial sources. Mercury-Agricultural runoff, landfills and factories. Lead-Municipal water supply pipes.	Arsenic causes arsenicosis, blindness, paralysis and cancer. Fluoride causes dental and skeletal fluorosis. Mercury-brain disorders, abortions and disruption of endocrine system. Lead-high blood pressure and kidney damage.	Sharma and Bhattacharya, 2017.
Organics	Pesticides i.e. Glyphosate, Dioxin, Methoxychlor, Toxaphene and Simazine. Volatile Organic Compounds (VOCs) i.e. Toluene, Benzene, Styrene and Vinyl chloride. Dyes. Persistent organic pollutants.	Agricultural and personal hygiene.	Pesticides damage liver and nervous system. VOCs cause cancer, damage liver and kidneys, cause reproductive disorders and birth defects.	Sharma and Bhattacharya, 2017.
Biological	Algae, protozoa, bacteria and viruses.	Algae-Nutrient pollution, Bacteria, Protozoa and Viruses-Wastewater.	Algae cause taste and odour problems and may produce toxins that can damage the liver and nervous system. Bacteria can cause cholera, dysentery and typhoid. Protozoa causes nausea, headache, diarrhea and dehydration. Viruses cause hepatitis and polio.	Sharma and Bhattacharya, 2017.
Radiological	Radiation i.e. alpha and beta, uranium, radon, polonium, thorium.	Soils, rocks and industrial waste.	Can cause cancer.	Pooja et al., 2020.

Introduction

In order to make it suitable for human consumption and avoid adversely affecting human health, water must undergo treatment using different processes and technologies. The concern of impacts on human health has compelled almost all national governments worldwide to establish and enforce regulations on drinking water quality and quantity, in form of standards, that service providers are supposed to adhere to in totality and at all times. To meet national prescribed standards, water supply utilities have to select processes and technologies based mostly on quality of source water, (Pakharuddin et al., 2021) and other criteria such as competence in the operation and management of a treatment technology (Melo et al., 2019), efficiency capabilities, reliability, capital costs, energy requirements and consumer economic conditions (Fuchs et al., 2015). Within the European Union economic area, common technologies used for treating surface water include: no treatment; conventional treatment (i.e. coagulation, sedimentation, filtration and chlorine disinfection); advanced treatment (i.e. carbon filtration, advanced oxidation processes, membranes and desalination); and conventional + advanced treatment (Hofman-Caris and Hofman, 2017; Van Der Hoek et al., 2014). In some cases, conventional methods include the activated carbon adsorption process (Villanueva et al., 2021). A recent scientometric study indicates that conventional water treatment technology ranks second to advanced oxidation processes (Valdiviezo Gonzales et al., 2021), whereas one Europe-wide survey indicated that conventional technology also ranked second to serial combinations of conventional and advanced oxidation process (Van Der Hoek et al., 2014), which attests to the continued relevance of conventional methods globally.

Introduction

1.3.2 Conventional water treatment technology.

This technology comprises both physical (i.e. screening, sedimentation, flocculation and filtration) and chemical (i.e. coagulation and disinfection) contaminant removal processes, arranged in a train of screening, followed by coagulation, flocculation, sedimentation, filtration and disinfection (Gerba, 2009). An overview of conventional water treatment processes is summarized in Figure 1.

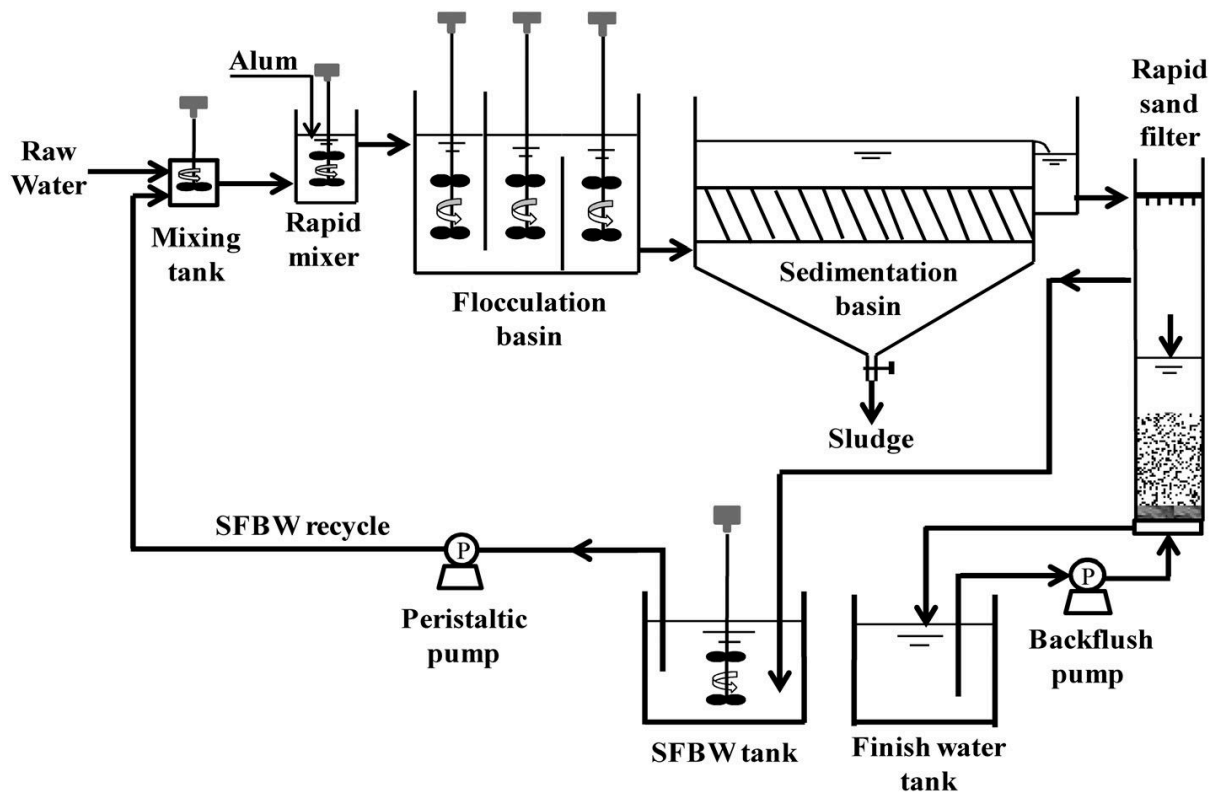


Figure 1. Schematic of a conventional water treatment process. SFBW = spent filter backwash. Image adapted from Li et al., 2018.

Introduction

1.3.2.1 Source.

Typical sources for municipal water abstraction are surface sources such as lakes, rivers or reservoirs which are impoundments on rivers. Also, groundwater is a reliable source of water for municipal water supply. Since both surface and groundwater are susceptible to contamination from pollutants (Schwarzenbach et al., 2010) presented in Table 1, it is mandatory for utilities to subject the water to some level of treatment in order to minimize contaminants to levels that are harmless to human health. The level of treatment required depends on the nature and concentrations of the contaminants. Nevertheless, conventional treatment suffices in many cases where the objective is to remove turbidity, natural organic matter and pathogenic microorganisms. Conventional processes are summarily explained in the sections below.

1.3.2.2 Coagulation.

This is a chemical process designed to aid the separation of dissolved and suspended particles from the water phase by sedimentation and filtration processes (Gerba, 2009). These particles include turbidity, dissolved organic matter and cyanobacteria. Chemicals added to raw water are called coagulants, which function by providing a surface onto which suspended particles agglomerate, become dense and are separated from the liquid phase. Typical coagulants used are often inorganic salts of either aluminium $\text{Al}_2(\text{SO}_4)_3 \cdot 14\text{H}_2\text{O}$ or iron i.e. ferric sulphate $\text{Fe}_2(\text{SO}_4)_3$ or ferric chloride (FeCl_3). In some cases, charged organic molecules called polyelectrolytes such as polyacrylamides, dimethyldiallyl-ammonium chloride, polyamines and starch, are added to water to enhance coagulation and filtration (Gerba, 2009). In recent years, plant based organic coagulants have been trialed and registered potential for industrial use, but their general uptake is low (Ang and Mohammad, 2020), except for tannin based coagulants that are commercially available (Saleem and Bachmann, 2019). Organic matter removal is achieved through precipitation reaction between the coagulant metal salts and organic matter or through adsorption onto flocs of aluminium hydroxide or ferric hydroxide (Gerba, 2009). Some of the main mechanisms by which coagulants function include charge neutralization, in which metal salts in coagulants hydrolyze and neutralize the negatively charged colloids, resulting into agglomeration of the colloidal impurities; adsorption on metal surfaces, in which metal salts from coagulants acts as surfaces onto which the negatively

Introduction

charged impurities adsorb; and sweep enmeshment, in which metal hydroxides precipitate at neutral pH and the impurities get enmeshed into the precipitates hence get removed from water. The effectiveness of this process depends on factors such as coagulant type and dose, water pH and the presence of interfering impurities (Pivokonsky et al., 2024).

1.3.2.3 Flocculation.

This is a physical process in which coagulated water is gently stirred in order to promote the formation of flocs by allowing collisions between the suspended particles in order to form bigger particles that can settle by sedimentation. Microbes are removed by adsorbing or getting entrapped into these particles (Gerba, 2009). Key mechanisms governing flocculation are fluid shear from mechanical mixing, differential particle settling by gravity and Brownian motion (Alansari and Amburgey, 2020).

1.3.2.4 Sedimentation.

In this physical process, the goal is to remove settleable particles from suspension with or without the aid of coagulants. Plain sedimentation occurs under circumstances where particles settle out of solution by gravity, without prior addition of chemicals at the coagulation stage. The converse is sedimentation following coagulation and flocculation, which requires a shorter time of between 2 and 4 hours to achieve the removal of flocculated particles, and is capable of reducing turbidity, color and bacteria (Shammas et al., 2005).

1.3.2.5 Filtration.

In this physical process, water from the sedimentation tank is passed through granular filters, generally made up of coarse silica, quartz sand and gravel or anthracite. The filters may be slow sand filters or rapid sand filters depending on hydraulic loading rates. In slow sand filters, the filter medium is largely sand (coarse and fine sand), supported by gravel and stone pebbles. Typical hydraulic loading rates, which are a measure of the particle contact with the filter bed, range between 0.1 to 0.3 m/hr., but best performances are achieved at lower loading rates. Slow sand filters remove contaminants from water through physical, chemical and biological processes.

Introduction

Biological processes degrade contaminants in the upper filter layer i.e. bacteria are removed through adsorption and predation by protozoa, whereas viruses are lysed by enzymes and grazing by bacteria and other higher organisms. Organic matter is removed together with nitrate and other organic contaminants by the slimy layer developed on top of the sand, called the schmutzdecke. Slow sand filters are also efficient in the removal of turbidity and recalcitrant organic compounds such as pharmaceuticals and herbicides (Verma et al., 2017). Contaminant removal in slow sand filters extends beyond the schmutzdecke into the autotrophic and heterotrophic zones that extends about 300mm into the filter column (Brandt et al., 2017). The efficiency of contaminant removal is limited by temperature because biological degradation is the key mechanism, such that performance is greatly reduced in low temperatures. Also, slow sand filters are limited in that they function well in low turbidity of under 10 NTU, otherwise, higher turbidities would require pre-treatment (Brandt et al., 2017). On the other hand, rapid gravity filters are designed for higher filtration rates, in the range of 6-7.5 m/hr., with some slight variations depending on application. Rapid gravity filters also use sand as the main medium of removing impurities. Although the medium could be monograde, most applications used graded sand i.e. fine to coarse sand, gravel and pebbles, in the top-to-bottom direction of flow (Brandt et al., 2017). Rapid gravity filters can remove inorganic contaminants such as iron, manganese arsenic and other toxic metals through oxidation on the filter media surface or oxidation in the supernatant water. The ability to remove heavy metals can be enhanced by adding to the sand oxides of iron and manganese and polyaniline, which increase adsorption surface area, leading to improved performance in the removal of more heavy metals including lead and chromium (Hoslett et al., 2018). Other than turbidity, sand filtration is effective in removing protozoan parasites such as *Giardia* and *Cryptosporidium*, but ineffective in the removal of bacteria and viruses. Over time, the filter media get clogged up by suspended particles, leading to increasing head loss or deteriorating filtrate quality, hence needs regular backwashing (Gerba, 2009; Gray, 2014). Rapid gravity filters are typically designed with an optimal filter run time of 24 hrs. but could be extended to under 48 hrs. without requiring backwashing. When the filter run time is reached, filters are taken offline to implement a backwash sequence, which comprises of agitating the filter media with compressed air to break up and loosen scum, followed by a flow of water in reverse of operational (filtration) mode. After washing, the filters are brought back online, beginning with filtering to waste in the first 15-60 minutes to correct high turbidity, before resuming normal filter operations (Brandt et al., 2017).

Introduction

1.3.2.6 Disinfection.

1.3.2.6.1 Historical perspective.

The advent of drinking water disinfection is considered as one of the best technological advancements ever developed for the safeguarding of public health (Ngwenya et al., 2013). Water disinfection involves applying physical or chemical agents to drinking water with the purpose of inactivating or destroying disease causing pathogens. Water disinfection began in Louisville, Kentucky, the USA, in 1896, followed by Europe, in Middelkerke, Belgium, in 1902, using chlorinated bleach, calcium hypochlorite and liquefied chlorine gas (Ngwenya et al., 2013). Over time, public health benefits of water disinfection have been appreciated worldwide and led to the expanded use of chlorination through other forms such as sodium hypochlorite, chloramine, chlorine dioxide and gaseous chlorine. Chloramine was first applied in Canada in 1916, followed by the USA in 1917 and 1926, as a measure of reducing the formation of DBPs. On the other hand, chlorine dioxide was first applied in Niagara Falls, New York, USA, in 1944, followed by Brussels, Belgium in 1956. The same early years saw inventions of other disinfection techniques such as ozonation, which was first applied at Oudshoorn, Netherlands in 1893, followed by France and the USA in 1906, for purposes of taste and odor control. Also, ultraviolet light, which is effective in destroying protozoan parasites such as giardia and cryptosporidium, and potassium permanganate, were developed around the same time (Ngwenya et al., 2013).

Introduction

1.3.2.6.2 Disinfection methods and mechanisms.

Among many chemical compounds, chlorine is the most preferred disinfectant because of its easiness to handle, strong oxidative power even in low concentrations, low price and its ability to provide a residual effect to counter re-contamination (Manasfi, 2021; Ngwenya et al., 2013). It is for these reasons that water chlorination is still the most widely used disinfection method worldwide, with a few exceptions such as the Netherlands where disinfection by using ultraviolet light (Ngwenya et al., 2013) is preferred instead of chlorination. Drinking water chlorination uses either gaseous chlorine (chlorine gas and chlorine dioxide), liquid chlorine (sodium hypochlorite), solid powder (calcium hypochlorite) or chloramines. The dissociation of gaseous, liquid and solid forms of chlorine in water yields hypochlorous and hypochlorite ions, which are potent disinfecting agents (Yang et al., 2018).

When chlorine dioxide is used to inactivate pathogens, pathogen inactivation is achieved through damage to the outer membrane, leading to leakage of proteins and oligosaccharides, and damage to the cytoplasmic membrane, resulting into denaturing of enzymes (Ofori et al., 2018, 2017), as well as causing damage to DNA and glutathione (Cai et al., 2021).

The germicidal action of calcium hypochlorite on bacteria such as *E.coli* is achieved by damaging cell membrane, enzymatic processes and nucleic acids (Sossou et al., 2016).

The popularity of chlorination as a disinfectant is, however, marred by taste and odor problems experienced at high doses, and its ineffectiveness against protozoa and helminth eggs (Pichel et al., 2019; Wolfe, 1990). Furthermore, the efficiency of chlorination significantly decreases when turbidity and dissolved organic matter are high (Chu et al., 2019). Besides, in the presence of dissolved organic carbon, drinking water chlorination produces chemical compounds that are potent carcinogens to consumers and, thus, their formation must be minimized through reduction in precursor compounds or through manipulation of disinfection conditions. Concerns surrounding the aesthetic shortfalls of water and the formation of DBPs from chlorination (Cai et

Introduction

al., 2021) have led to the exploration of other disinfection methods. These alternative disinfection methods include solar radiation, membrane technology (microfiltration, ultrafiltration and reverse osmosis) (Reid et al., 2023), metal disinfectants (potassium, silver and copper), ultrasonic disinfection, the use of halogens (iodine and bromine) and application of nanomaterials (chitosan, silver, nanosorbents, and nanofilters) (Ngwenya et al., 2013).

Ozonation, the second most used method of disinfection after chlorination (Pichel et al., 2019), has been applied as a pre-treatment measure to remove taste and odor compounds such as sulphides, iron and manganese (Manasfi, 2021). Also, ozone can be applied towards the end of the treatment train to achieve water disinfection through the germicidal action of the ozone itself (Von Gunten, 2003) or through the production of hydroxyl radicals that damage both the cell and DNA structures of pathogens (Ding et al., 2019; Von Gunten, 2003). The hydroxyl radicals cause denaturation of nucleic acids and depolymerization of proteins (Cai et al., 2021). Ozone disinfection is quite versatile across a wide range of pathogens (Cai et al., 2021) such as bacteria, viruses and is the only method which is very effective against giardia and cryptosporidium cysts (Pichel et al., 2019). However, ozone is less preferred due to the lack of a residual effect in the distribution system (Ding et al., 2019) and because it also forms DBPs (Cai et al., 2021) such as bromate, aldehydes, ketones, nitrosamines (in wastewater impacted source waters) and carboxylic acids (Manasfi, 2021). In addition, ozonation is deemed expensive in terms of capital and operational costs, requiring skilled maintenance and high energy requirements (Pichel et al., 2019).

Ultraviolet light inactivates pathogens by halting pathogen replication through the making of dimers from base pairs of microbial RNA and DNA (Reid et al., 2023), particularly by UV-B (280-320 nm), and destroying DNA, proteins, lipids and cell membranes by UV-C (200-280 nm) (Cai et al., 2021). On the other hand, UV-A (320-400 nm) inactivates pathogens by producing reactive oxygen species which damage pathogens by oxidizing proteins and lipids (Cai et al., 2021). However, UV irradiation does not kill pathogens (Gray, 2014). In particular, UV-C is effective in the destruction of microbes (Meulemans, 1987), with 254 nm as the optimum germicidal wavelength (Gray, 2014), where nucleic acids maximally absorb UV light (Augsburger et al., 2021).

Introduction

While effective against a wide range of pathogens such as spores, cysts and viruses, ultraviolet light disinfection does not provide a residual effect in the distribution system hence requires coupling with a secondary disinfectant such as chlorine (Wolfe, 1990). In addition, the application of UV light in water disinfection is marred by reduced efficiency overtime, from both the design perspective and when the lamp surfaces are fouled by the chemical and biological constituents of water (Pichel et al., 2019; Wolfe, 1990). Also, the manufacturing and operation of UV lamps is energy intensive, hence has high costs, particularly that they have a short life span, requiring replacement on a yearly basis (Pichel et al., 2019). Waste from the used UV lamps are an environmental concern because of the mercury they contain, which is a well-known environmental hazard (Pichel et al., 2019).

Other countries such as the Netherlands, Germany, Austria and Switzerland have significantly reduced or totally abandoned chlorination in favor of other strategies. These alternatives include prioritizing the best water source (uncontaminated groundwater), focusing on physical treatment processes such as sedimentation, filtration and UV disinfection and proofing the distribution mains against ingress. Additional strategies include preventing microbial re-growth in the distribution by producing and supplying biologically stable water, use of biostable materials and intensifying monitoring to timely detect system failures (Reid et al., 2023; Smeets et al., 2009).

Although technologies such as membrane filtration are resource intensive due to capital and operational expenditure (Reid et al., 2023), they immensely help in meeting regulatory compliance related to DBPs formation in potable water supplies.

This overview on common drinking water disinfection techniques highlights the unsuitability of chlorination alternatives in providing assurance of continued protection of distribution water against re-contamination. Continued large-scale application of chlorine suggests that perhaps water utilities rank the risk of microbial contamination, with instantaneous health outcomes, higher than the long-term cumulative risk of DBP toxicity. This summary implies that whichever primary disinfection technique is preferred by a utility, chlorination will still remain the default choice for secondary disinfection, hence the risk of toxicity from exposure to DBPs will be unrelenting in supplies that are still overly dependent on chemical disinfection. Thus, research that probes into DBP formation mechanisms and the extrinsic modulating factors, such as Papers II and III of this

Introduction

thesis, remains fundamental in refining the existing knowledge and may aid in decision making on the minimization of DBP formation in water utilities. It is in that respect that this thesis is largely devoted to the study of formation potential of disinfection by-products in source waters that are also greatly impacted by climate extremes, in order to understand how climate variables modulate DBP formation.

Water supply is a provisioning service that is operationally sensitive to eutrophication of aquatic ecosystems and generally leads to strains in financial resources required to avoid or treat physical and chemical constituents elevated by eutrophication. Such constituents include taste and odor, caused by cyanobacterial metabolites such as geosmin and 2-methylisoborneol (Olsen et al., 2016; Westerhoff et al., 2005); disinfection by-products caused by chlorination of dissolved organic carbon from phytoplankton biomass and metabolites (Palmstrom et al., 1988) and macrophyte (Cooke and Kennedy, 2001). Other constituents are sediment-based iron and manganese (Cooke and Kennedy, 2001) mobilized into the water column by anoxia; toxins produced by certain species of cyanobacteria and diatoms (Painter et al., 2022); and nitrate (Pretty et al., 2003). Also, high pH caused by primary production may increase chlorine demand during disinfection and enhance the formation of certain classes of disinfection by-products (Cooke and Kennedy, 2001; Tomlinson et al., 2016). While wealthier nations may meet the financial burden brought about by eutrophication, least developed nations may not cope, which may lead to the supply of unsafe water to the public.

Introduction

1.4 Climatic extreme events and how they impact lakes and the ecosystem service of drinking water supply.

There exist numerous domain specific definitions of climatic extreme events (van de Pol et al., 2017). In this thesis, we adopt Smith's definition of climatic extreme events (hereafter referred to as climate extremes) that includes rarity of both the climatological variables and ecosystem structure and function. As such, a climate extreme is defined as an occurrence in which a statistically rare climatic period alters ecosystem structure and function beyond the bounds that can be considered as normal variability (Smith, 2011). Rarity could take the form of either crossing a certain threshold in the probability distribution of the variable of interest, or variability in the entire distribution of the parameter of interest (resulting in a higher standard deviation), or both (Jahn, 2015). In that regard, climate extremes of relevance to the aquatic environment include both short term (occurring over less than 3 days) events such as wind or storms (tornados, heavy precipitation, hurricanes), and long term (occurring over more than 3 days) episodes such as cold waves, heatwaves, drought, or wildfire (Clarke et al., 2022; Sillmann et al., 2017; Wang et al., 2022; Zou et al., 2023). In both cases, climate extremes have been observed to increase in magnitude, frequency, intensity and duration due to climate change (Bertani et al., 2016; Ummenhofer and Meehl, 2017). Therefore, it is imperative to understand their nature and occurrence to improve the predictability and management of their impacts on people, ecosystems and the economy. Impacts of climate extremes on a particular system can either be positive, negative, or neutral (Maxwell et al., 2019), however, it is the negative impacts that are of concern for ecosystem managers and policy makers. The degree to which aquatic ecosystems get impacted by climate extremes depends on a diversity of factors such as exposure of the system to perturbation, resistance and resilience of the system (Jahn, 2015), geographical location (Sadro and Melack, 2012), size of the system (Bertani et al., 2016), morphometry (Klug et al., 2012; Zwart et al., 2017), frequency of perturbation (Kohzu et al., 2023), the magnitude (Jennings et al., 2012; Ogutu-Ohwayo et al., 2016), timing of the perturbation, and antecedent conditions of the system prior to arrival of the perturbation (Stockwell et al., 2020). This dependence on multiple factors challenges generalizability of responses, warranting for system specific understanding.

Introduction

1.4.1 Heatwaves.

Amongst the numerous definitions of heatwaves that appear in literature (Barriopedro et al., 2023), one approach defines a heatwave event as five or more consecutive days of extended heat, in which daily maximum air temperature exceeds the average maximum temperature by a margin of 5°C or more (Polazzo et al., 2022). The magnitude of temperature extremes is expressed in the form of indices recommended by the World Meteorological Organization CCI/CLIVAR Expert Team on Climate Change Detection Monitoring and Indices, which are grouped into four categories summarized in Table 2. This thesis adopted the Heatwave Magnitude Index daily, HWMId.

Introduction

Table 2. A summary of commonly used climate indices for defining heatwaves (and their counterpart coldwaves).

Index category	Index	Description	Reference
Absolute	TXx	Monthly maximum value of daily maximum air temperature.	Van Der Walt and Fitchett, 2022.
	TNx	Monthly maximum value of daily minimum air temperature.	
	TXn	Monthly minimum value of daily maximum air temperature.	
	TNn	Monthly minimum value of daily minimum air temperature.	
Threshold	Summer days, SU25	Count of days where TX > 25 °C.	
	Frost Days, FD	Annual number of days when TN < 0 °C.	
Percentile	TX90p	Count of days when TX > 90th percentile.	
	TN90p	Count of days when TN > 90th percentile.	
	TX10p	Count of days when TX < 10th percentile.	
	TN10p	Count of days when TN < 10th percentile.	
Duration	Warm Spell Duration Indicator, WSDI	Count of days in a span of at least 6 days where TX > 90th percentile.	Van Der Walt and Fitchett, 2022.
	Cold Spell Duration Indicator, CDSI	Count of days in a span of at least 6 days where TN < 10th percentile.	
	Heatwave Magnitude Index daily, HWMId	Annual maximum heatwave magnitude-cumulative normalized TX exceedances.	Barriopedro et al., 2023; Russo et al., 2015.

Introduction

Apart from the widely reported adverse human health outcomes occasioned by heatwaves i.e. mortality and morbidity (Campbell et al., 2018), aquatic ecosystems are also vulnerable and can be impacted by heatwaves, through changes in the physical, chemical and biological constituents in lakes, leading to losses of ecosystem structure and function. Table 3 summarizes changes and impacts on aquatic ecosystems associated with heatwaves.

Introduction

Table 3. Changes and impacts promoted by heatwaves in aquatic ecosystems.

Change	Impact	References
Enhanced evaporative water losses.	Lowering of lake levels, inducing ecosystem state change into a macrophyte dominated system.	Bertani et al., 2016; Woolway et al., 2022.
Enhanced density stratification.	Barrier (thermocline) for nutrient exchanges between the upper and lower water layers, lowering primary production.	Grimm et al., 2013.
Increased water temperature.	Higher microbial biomass and degradation rates. Reduction of biomass and diversity of thermally intolerant species across the food web. Alteration of sexual and mobility patterns in vertebrate predators.	Polazzo et al., 2022.
Increased water temperature and stratification.	Growth of cyanobacteria, some of which produce toxins as well as metabolites such as geosmin and methyl-isoborneol that cause taste and odor.	Polazzo et al., 2022; Westerhoff et al., 2005.
Reduced oxygen solubility and concentration.	Hypolimnetic anoxia and dissolution of sediment bound iron, manganese, nutrients and heavy metals into the water column, leading to the proliferation of algal blooms. Fish infection events and fish kills.	Blagrave et al., 2022; Jane et al., 2021; Polazzo et al., 2022; Tye et al., 2022.
Shortening of the ice cover season.	Replacement of cool water fish species by smaller (invasive) warm water fish species.	Woolway et al., 2022.

Introduction

Consequently, compromised functionality of lakes by heatwaves can adversely impact the ecosystem service of drinking water supply in various ways. First, solubilization of sediment bound metals such as iron and manganese (Cooke and Kennedy, 2001) may necessitate additional treatment costs to achieve regulatory compliance. Second, taste and odor compounds and toxins produced by algal blooms benefiting from anoxia driven internal nutrient cycling (Woolway et al., 2022), higher temperatures and stratification, may require advanced technologies to treat in order to produce aesthetically acceptable water for public supply. Lastly, excessive phytoplankton growth (Free et al., 2022; Jöhnk et al., 2008) increases precursor compounds that form toxic DBPs, hence additional treatment costs may be incurred to minimize their formation.

1.4.2 Droughts.

There are numerous definitions of droughts, which largely depend on the sector and the variable used to describe their occurrence, but almost all of them point to abnormal dry weather spells, caused by precipitation deficits, which are long enough to upset the hydrological balance (Mishra and Singh, 2010). Droughts are broadly classified into four categories as below:

- Meteorological i.e. precipitation deficits.
- Agricultural i.e. soil moisture deficit leading to crop failure.
- Hydrological i.e. stream flow, lake levels or groundwater level deficits (Field et al., 2012).
- Socio-economic i.e. failure of water resource systems to meet water demand as an economic good (Mishra and Singh, 2010).

The effects of droughts on a system are evaluated through various drought indices, as summarized in Table 4, which are derived either singly from precipitation or from combinations of precipitation with other hydrometeorological variables such as temperature and soil moisture (Mishra and Singh, 2010).

Introduction

Table 4. A summary of drought indices commonly found in literature.

Index	Description	Category	Reference
SPI	Standardized precipitation index.	Meteorological	Mishra and Singh, 2010; Zargar et al., 2011.
SPEI	Standardized precipitation and evapotranspiration index.	Meteorological	Zargar et al., 2011.
PDSI	Palmer drought severity index.	Hydrological	Mishra and Singh, 2010; Zargar et al., 2011.
CMI	Crop moisture index.	Agricultural	Mishra and Singh, 2010; Zargar et al., 2011.
RDI	Reconnaissance drought index.	Meteorological	Zargar et al., 2011.
SWSI	Surface water supply index.	Hydrological	Han and Singh, 2023; Mishra and Singh, 2010.
VCI	Vegetation condition index.	Agricultural	Han and Singh, 2023; Mishra and Singh, 2010.
RAI	Rainfall anomaly index.	Meteorological	Mishra and Singh, 2010; Zargar et al., 2011.
BMDI	Bhalme and Mooly drought index.	Agricultural	Mishra and Singh, 2010; Zargar et al., 2011.
NRI	National rainfall index.	Meteorological	Mishra and Singh, 2010.
RDI	Reclamation drought index.	Hydrological	Mishra and Singh, 2010.
SMDI	Soil moisture deficit index.	Agricultural	Mishra and Singh, 2010; Zargar et al., 2011.
SDI	Soybean drought index.	Agricultural	Mishra and Singh, 2010.
EP	Effective precipitation.	Meteorological	Mishra and Singh, 2010.
ETDI	Evapotranspiration deficit index.	Agricultural	Mishra and Singh, 2010.
SRI	Standardized runoff index.	Hydrological	Han and Singh, 2023; Mishra and Singh, 2010.
NDWI	Normalized difference water index.	Agricultural	Mishra and Singh, 2010.
CDI	Corn drought index.	Agricultural	Mishra and Singh, 2010.

Introduction

Droughts are a concern to ecologists because of their impacts on the structure and functioning of lake ecosystems, which are summarized in Table 5.

Introduction

Table 5. Changes, mechanisms and impacts promoted by droughts in aquatic ecosystems.

Change	Mechanism	Impact	References
Declined amphibian species diversity. Decline of invertebrates' community.	Droughts led to desiccation of eggs and larvae and increased toxicity to larvae from evapoconcentrated contaminants in amphibians. Droughts caused declines in invertebrate community due to mortality caused by desiccation and increased predation from reduced habitat size.	Disturbance of food web structure.	Carey and Alexander, 2003; Gerard, 2001; Mac Nally et al., 2017; Maxwell et al., 2019.
Lake terrestrialization in peatland catchments.	Peatland plants colonize margins of lakes forming buoyant vegetation mats. Peat vegetation accumulates, leading to shrinking of lakes. Droughts lower water levels, exposing lake sediments to roots of the colonizing plants. When levels build up, vegetation gets detached and spreads across the entire lake, causing a floating mat. Subsequent droughts lead to expansion of vegetation mats until the entire lake is colonized by the plants.	Reduced primary productivity, deterioration of fish communities and increased accumulation of carbon.	Ireland et al., 2012.
Increased ambient water temperatures.	Reduced water volumes during droughts are warmed more by same intensity of sun's radiation compared to periods of wet season.	Depletion of dissolved oxygen and reduced species biomass and diversity.	Mosley, 2015; Ahmadi et al., 2019; Brasil et al., 2016; Wlostowski et al., 2022.
Increased concentration of wastewater derived contaminants.	Droughts decrease water volumes in waterbodies, which reduces dilution of point source pollutants in wastewater impacted sources, resulting in increased concentration.	Increased water treatment costs.	Raseman et al., 2017; Wang et al., 2022.
Increased concentration of nutrients.	Droughts promote stratification in waterbodies, leading to increased concentration	Elevated risk of algal blooms which are toxic to fish, livestock and domestic animals.	Bond et al., 2008; Raseman et al., 2017.

Introduction

Change	Mechanism	Impact	References
	of nutrients and increasing the chance of algal bloom development.		
Increasing DOC.	Caused by evapoconcentration due decreased water levels during drought.	Reduced gross primary production and ecosystem respiration, driving lakes into autotrophy.	Aldridge, 2011; Chiu et al., 2020.
Algal bloom formation and promotion of toxin producing cyanobacteria.	Droughts reduce water volumes leading to reduced dilution capacity, increased residence time and absence of flushing. As a result, nutrients build up and algal blooms persist in a water body.	Adversely affect other aquatic life through the production of toxins.	Vanderley et al., 2021.
Anoxia.	Droughts cause increased heat and low dissolved oxygen. Also, droughts promote phytoplankton growth, leading to more biomass with high oxygen demand on biodegradation.	Large scale summer fish kills.	Lennox et al., 2019; Olds et al., 2011.
Impaired primary productivity.	Droughts may cause desiccation of aquatic plants and animals, habitat loss, decreased input of terrestrial nutrients and reduced photic zone, all of which affect benthic biota which is food for fish.	Decreased growth rate in fish (i.e. Golden perch).	Morrongiello et al., 2011.
Induced regime shifts in lakes, from macrophyte to cyanobacteria dominated state.	Low water level led to increased nutrient concentrations and hydraulic residence time, resulting in cyanobacteria growth.	Alterations of biotic and abiotic lake variables and biodiversity loss from persistence of invasive species.	Jeppesen et al., 2015; Zohary and Ostrovsky, 2011.

Introduction

Sustaining the ecosystem service of water supply, under drought conditions, is challenging because adherence to regulatory requirements requires investments to deal with drought-related challenges. Such challenges may range from water usage restrictions due to inadequate quantities (Grant et al., 2013; Hickey and Senevirathna, 2023), to anoxia (Yuntao Zhou et al., 2015) driven solubilization of metals such as iron and manganese in the water column (Banks et al., 2012; Christophoridis and Fytianos, 2006). In addition, algal blooms from concentrated nutrients (Li et al., 2017; Mosley et al., 2012) and hypolimnetic nutrients (Aldridge, 2011; Lehman, 2014), release taste and odor causing metabolites such as 2-methylisoborneol (2-MIB) (Su et al., 2017) and geosmin (Izaguirre and Taylor, 1995) that may require additional treatment. Also, droughts increase in-reservoir derived dissolved organic carbon (Lv et al., 2022) that can form DBPs (Summerhayes et al., 2011), which are potent carcinogens. Lastly, hydrological deficits can evapoconcentrate contaminants and solutes (Benotti et al., 2010; Braga et al., 2015) that may require additional treatment to reduce.

1.4.3 Rainstorms.

Rainstorms are associated with both positive and negative impacts on aquatic ecosystems. Positive impacts include improving oxygenation of the water column (Flaim et al., 2020; M. Liu et al., 2020) and increasing species richness in fish and invertebrates, due to increased availability of food (Maxwell et al., 2019). On the other hand, storms are largely destructive to aquatic ecosystems in several ways that are summarized in Table 6.

Introduction

Table 6. Changes and impacts promoted by rainstorms in aquatic ecosystems.

Change	Mechanism	Impact	References
Enhanced eutrophication.	Extreme rainfall deliver nutrient to lakes from industries, agricultural fields and urban areas.	Cyanobacterial bloom formation.	Blagrave et al., 2022; Woolway et al., 2022.
Excessive sediment loads.	Intense rainfall increased sediment loads into lakes, hence limiting light availability for primary producers. Light limitations reduce phytoplankton diversity by favoring only low light tolerant species.	Affects functionality of primary producers and decreases phytoplankton diversity.	Stockwell et al., 2020.
Enhances colored dissolved organic carbon loads.	Extreme rainfall exported increased amounts of terrestrial organic carbon loads, which lowered light availability to primary producers.	Reduces gross primary production.	Jennings et al., 2012; Sadro and Melack, 2012.
Shifts metabolism from autotrophy to heterotrophy.	Extreme precipitation events increased terrestrial dissolved organic carbon load into the lake leading to a short-term increase in respiration that consumed dissolved oxygen more than the rate it was being produced through autotrophy. Also, reduced temperature during extreme rainfall affected primary producers. Flushing out of primary producers during flooding also affected primary production.	Causes reductions in dissolved oxygen concentration and increased carbon dioxide and methane fluxes.	Jennings et al., 2012; Klug et al., 2012; Zwart et al., 2017.
Breaks thermal stratification.	Episodes of extreme precipitation led to destruction of thermal stratification in lakes, resulting into mixing of deoxygenated hypolimnetic water with surface water.	Decreased dissolved oxygen concentration in the epilimnion. Increased phytoplankton from hypolimnetic phosphorus being suspended back into the water column.	Jennings et al., 2012; Stockwell et al., 2020.

Introduction

Change	Mechanism	Impact	References
Flushing out primary producers.	Precipitation extremes caused diatoms to decline due to getting flushed out in temperate lakes.	Decrease of phytoplankton biomass.	Stockwell et al., 2020.
Causes surface water temperature to either decrease or increase.	Extreme precipitation increases sediment loads into lakes and suspended solids absorb heat, thereby increasing water temperature on the surface. In other cases, extreme rainfall, cooler than a lake, affected the surface heat budget of the lake hence lowering water temperature.	Enhancement of mixing or promotion of thermal stratification.	Rooney et al., 2018; Stockwell et al., 2020.

Introduction

Under precipitation extremes, municipal water supply is vulnerable to several challenges that can undermine continuity of supply as follows:

- Floods can bring gross pollution and destroy water treatment and supply infrastructure thereby curtailing supplies to consumers (Koks et al., 2022).
- Storms can export sediment loads from the catchment (Hickey and Senevirathna, 2023) and cause sediment resuspension in source waters (Levy et al., 2016), which may require additional chemicals to treat the high turbidity. If inadequately treated, high turbidity shields pathogenic microorganisms that can compromise the safety of supply (Chhetri et al., 2017; Graydon et al., 2022).
- Storms can cause the release of untreated wastewater, from the overwhelmed combined sewer systems (Burnet et al., 2019; Olds et al., 2018), that may overload water treatment systems with pollutants such as personal care products, pharmaceuticals, illicit drugs and hormones (Botturi et al., 2021), leading to the supply of poorly treated water which can endanger public health.
- High dissolved organic carbon loads from the catchment may require additional resources to treat in order to minimize the formation of hazardous DBPs during water chlorination (Doederer et al., 2018; Uzun et al., 2014).
- Run-off from extreme precipitation may export nutrients from the catchment which can result in excessive growth of phytoplankton (Shi et al., 2023; Yang et al., 2016). Excessive phytoplankton biomass may require additional treatment technologies to remove to minimize the formation of DBPs and reduce taste and odor causing metabolites.
- Storms can also de-stratify the water column (M. Liu et al., 2020), leading to mixing of nutrient rich hypolimnetic waters with the surface water, which can cause the proliferation of algal blooms.
- Pathogenic microorganisms, from high faecal loads in surface run-off, may overwhelm treatment systems and compromise water safety (Chhetri et al., 2017; Graydon et al., 2022).

Introduction

- Color spikes from high sediment loads and manganese (Hickey and Senevirathna, 2023) may require more chemicals to treat.
- Elevated concentrations of iron and manganese, released from sediment following thermal de-stratification (Zaw and Chiswell, 1999), may require additional treatment.

However, extreme precipitation may not be entirely negative for water supply. A recent simulation study suggests that run-off, from extreme rainfall, may inhibit algal blooms through limiting light access to primary producers caused by high inorganic turbidity and DOM and dilution effect on both nutrients and population of primary producers (Armstrong et al., 2023). The dilution effect of floods was also reported on Lake Sakadas' in Croatia, where both phytoplankton and chlorophyll concentrations decreased during high flows (Mihaljević et al., 2009).

1.5 Ecosystem stability in the context of climate extremes and eutrophication.

The ability of ecosystems to retain functionality and provide benefits to humans depends on their levels of ecological stability. Ecological stability bears both qualitative and quantitative definitions, whose understanding is fundamental to and imperative for the implementation of sound management practices to conserve functionality. Qualitatively, ecological stability refers to the ability of ecosystems to resist i.e. retain its functioning without changing internal structure (Parparov and Gal, 2017) or recover from perturbations such as environmental change (Parparov and Gal, 2017; Ross et al., 2021; Wang et al., 2017). Ecological stability is also defined by various quantitative metrics such as: **invariability**, which is the reciprocal of the squared coefficient of variation, and measures the magnitude of the ecosystem's response to environmental (Wang et al., 2017); **asymptotic resilience**, defined as the long term rate of return to the system's equilibrium (Arnoldi et al., 2016); **Holling's resilience**, defined as the amount of perturbation a dynamic system can absorb without changing state (Gunderson, 2000); **persistence**, which is length of time the system maintains the same state before changing in some defined manner (Donohue et al., 2016; Yang et al., 2019); the inverse of the Euclidean Distance between the current state of an ecological unit (i.e. state variables such water quality, Secchi depth, chlorophyll) and some predefined state (Parparov et al., 2015); **recovery**, defined as the ability to fully recover to reference conditions; **tolerance**, which is the ability of ecosystems to withstand perturbations (Van Meerbeek et al., 2021); and **resilience**, which is a measure of the ability of a system to contain

Introduction

perturbation while undergoing transformation, resulting in the retention of structure, function and identity. Furthermore, resilience comprises four layers of **resistance**, which measures the easiness of altering a system; **precariousness**, which measures the degree of closeness of the system to limits; **latitude**, which measures the maximum amount a system variable can be altered before losing its ability to recover (Walker et al., 2004); and **panarchy**, defined as the influence that the organizational state of a population has on its capabilities of enduring stress (Sommer et al., 2017). Perturbations that impact the ecological landscape of ecosystems can either be intrinsic, i.e. driven by variability in species interaction, or extrinsic, where environmental drivers external to the ecosystem, alter system properties (Ross et al., 2021). In addition, some studies report a “null” perturbation, in which there is no explicit driver, but rather variability is often occasioned by dynamical properties of the system under different conditions such as differences in species richness and environmental conditions (Kéfi et al., 2019). All perturbations possess four key properties of magnitude, duration, frequency and how they vary over time and space (Donohue et al., 2016). In terms of duration, the impact of perturbations on ecosystems can either be pulse i.e. short term, such as a chemical spill or press i.e. constant over long term, such as species extinction (Donohue et al., 2016), as long as the perturbation is present (Kéfi et al., 2019).

The loss of ecosystem services offered by a particular lake, under the hydroclimatic stressors highlighted in section 1.4, may depend on the extent to which the stability landscape of an aquatic ecosystem has been affected, i.e. whether the system has been driven beyond a recoverable tipping point by the perturbation. At ecosystem level, response to perturbations has been shown to depend on properties of the system (Ummenhofer and Meehl, 2017) like antecedent conditions i.e. trophic state (Lin et al., 2022), physicochemical lake conditions (Thayne et al., 2021) and morphometry (Vachon and Del Giorgio, 2014). Climate extremes, eutrophication of waterbodies and the interaction of these two stressors have been widely recognized as potent perturbations on the structure, functioning (Dokulil and Teubner, 2010) and ability of lakes to provide ecosystem benefits (Paerl and Paul, 2012). On the global scale, nearly 50% of water bodies in Asia, America and Europe are already being impacted by eutrophication (Herschy et al., 2012), whereas Africa trails at under 30% (Ansari et al., 2010). On the other hand, the prognosis of climate change attests to an outlook of increased frequency and magnitude (Thibault and Brown, 2008) of climate extremes, that may exacerbate adverse impacts of eutrophication (Meerhoff et al., 2022) in lakes used for drinking water supply. Understanding how intrinsic lake characteristics shape effects of hydroclimatic stressors is crucial in the projection and management of aquatic ecosystems in an

Introduction

era that is already being challenged by eutrophied water bodies and intensified climate extremes. However, knowledge on the role of individual traits of lakes in modulating impacts of climate extremes, as extrinsic stressors, remains limited. This deficiency may, partly, be due to limitations of relying on sampling extreme events (Doederer et al., 2018) and the use of high frequency data (Vachon and Del Giorgio, 2014) to capture dynamical effects of climate extremes on aquatic ecosystem, both of which might be impractical or expensive to implement. Thus, developing analytical approaches that can use routine low frequency monitoring data to track footprints of climate extremes in lakes, complementary to event-based sampling and insights from high frequency data analyses, would be worthwhile in safeguarding the ecological integrity of lakes in the face of multiple stressors. This thesis attempts to complement the existing methods by developing an innovative time series analysis using long term and low frequency water quality data, to track signatures of climate extremes in lakes.

1.6 Exploring cause-effect relationships in environmental time-series.

One of the biggest challenges when studying the impacts of climate extreme events on water quality in aquatic ecosystems is the unambiguous attribution of an observable variation in a water quality variable to a particular climatic event. Although event-based sampling and covariance patterns, observed between drivers and response variables, can provide a general sense of existence of causality, providing causal evidence between hydro-climatological variables and lake water quality requires establishing statistically valid causal relationships that exceed the otherwise superficial univariate correlation and regression-based analyses. Causal inference, based on time series analysis, is established conditional on three key assumptions. First, time-order, where cause needs to precede effect; second, causal sufficiency, where all direct drivers needed are observed; and third, the causal Markov condition, which states “that in a graphical model, a variable Y is independent of every other variable (not affected by Y), conditional on Y’s direct causes” (Runge et al., 2019). There are several causal frameworks that are mostly used in ecology in general and climate-aquatic systems in particular. One is the Granger Causality (GC), which is limited to lagged causal dependencies, in which the general idea is to test whether omitting previous time series values of driver X in a time series model including Y’s own and other drivers past values increases the prediction error of the next time step of Y. It would then be deemed that X causally influences Y. GC is mostly based on linear autoregressive models but, in recent times, non-linear dependencies have also been modeled. Another frequently used causality framework is the

Introduction

Nonlinear state-space models, such as the Convergent Cross Mapping (CCM), which assumes that interactions between drivers and response variables occur in a dynamical system (as opposed to stochastic processes). That is, causality between driver X and response Y can only be established if both variables belong to the same dynamical system, such that X is deemed to causally influence Y only if X can be predicted using the reconstructed system based on the time-delayed embedding of Y (Runge et al., 2019). The Causal network learning algorithms, such as the PC algorithm, starts with either a fully connected graphical model, followed by testing for the removal of links between variables, iteratively, based on preset conditions of growing cardinality or the “Greedy equivalence search” approach. It begins with an empty graphical model that gets iteratively populated by edges (links), in which edge addition or removal depends on criteria such as conditional independence test or score function that tests the likelihood of such a graphical structure given the available data. Finally, the Structural causal model (SCM) framework is also suitable for modeling contemporaneous dependencies in which the causal effect manifests itself instantaneously, hence it is likely going to be missed by time-lagged methods. Based on the “faithfulness” assumption, i.e. that all observed conditional independencies arise from causal structure, SCM advances the thought that when X is conditionally independent on Y given Z, graphical models $X \leftarrow Z \rightarrow Y$, $X \leftarrow Y \leftarrow Z$ and $X \rightarrow Y \rightarrow Z$, are all valid Markov equivalent, if there is no additional information on time-order (Runge et al., 2019). In this thesis, the nonlinear variant of the Granger Causality, called the non-parametric causality in quantiles (Balcilar et al., 2016), was adopted. This approach has been mostly used in econometric research (Bahramian and Saliminezhad, 2020; Balcilar et al., 2016; Shao et al., 2021) and our attempt to apply it in addressing causal relationships between hydroclimatology and lake water quality variability is, to the best of our knowledge, the first contribution in aquatic ecology research. Our interest was to observe causality unconstrained by linear dependencies, and also that captures lagged effects and across all quantiles, as opposed to causality in central tendencies only, hence the GC was the best fit for the purpose.

1.7 The allied effect of climate extremes and eutrophication on the ecosystem service of water supply.

Insights from Section 1.4 indicate that all the evaluated climatic extremes are associated with elevated dissolved organic carbon concentration, which is either endogenously generated, exported into lakes from watersheds, via enhanced hydrological connectivity in high flow conditions, or discharged into lakes through wastewater. Since this thesis focuses on the ecosystem service of

Introduction

drinking water supply, dissolved organic carbon is of paramount importance because of its role as a precursor for the formation of disinfection by-products during chlorination of drinking water supplies. Some of the DBPs are regulated in various countries across the globe, while other species are emerging and still under observation. The choice of zeroing in on DOC and DBP formation does not, in any way, undermine the relevance of other water supply related contaminants that are also caused by the same hydroclimatic stressors. However, these other contaminants are amenable to most conventional water treatment (Pichel et al., 2019) processes of coagulation, flocculation, filtration and chemical disinfection. On the other hand, the climate stressors under the consideration of this thesis can affect both the quantity and molecular properties of DOM (Zhou et al., 2020), rendering it untreatable by conventional methods, hence availing it to form the toxic halogenated compounds. Typical example is hydrophilic DOM that is recalcitrant to conventional treatment processes (Ignatev and Tuhkanen, 2019). Even in circumstances where technologies capable of treating recalcitrant DOM i.e. advanced oxidation and membrane filtration (Sun et al., 2023) may exist, their accessibility would likely be exclusive to wealthy utilities that can afford both the investment and operational costs, whereas most water utilities would be unable to make use of them. Thus, there is an urgent need to refine our understanding of the nature of precursors and DBP formation. At present, DBP research is one of the most dominating topics in the domain of drinking water research, evidenced by ranking first in Canada, and second overall across the globe, as reported in a recent bibliometric study (Weston et al., 2022). In the absence of a suitable alternative disinfectant to chlorination that can sustain residual disinfection in the distribution network (LeChevallier, 1999), the discourse on DBP formation and toxicity will continue to dominate drinking water research. Hence, devoting chapters of this thesis to study the fate and drivers of DOM, a DBP precursor, is an absolute necessity. The drinking water supply industry is often challenged by excessive DOM in source waters, in several ways outlined below:

- Aquatic DOM competes for adsorption sites on powdered activated carbon (Bruce et al., 2002; Newcombe and Cook, 2002) and granular activated carbon (Summers et al., 2013) with MIB and geosmin produced by cyanobacteria. Such competition interferes with the removal of these taste and odor causing compounds in water (Cerón-Vivas et al., 2023) during treatment, which affects the aesthetic acceptability of water and might require advanced treatment.

Introduction

- Excessive DOM causes color problems (Eikebrokk et al., 2004; Klante et al., 2021), which may increase treatment costs through increased coagulant demand, short filter run times and increased energy consumption. Also, treatment system upgrades may be necessary to deal with increased or altered character of DOM (Williamson et al., 2023).
- Algal-derived DOM increases concentration of assimilable organic carbon in water (Park et al., 2021), which may promote regrowth of pathogenic microorganisms in water distribution networks, resulting in taste and odor problems (Liu et al., 2013).
- Accumulation of algal-derived organic matter on membrane surfaces reduces permeate flux due to pore clogging of membrane filtration systems, which increases energy consumption (Ly et al., 2017).
- Excessive DOM undermines the efficacy of advanced oxidation processes, designed to degrade trace organic contaminants such as pharmaceuticals, personal care products, endocrine disrupting compounds, pesticides and algal toxins. DOM compromises such advanced oxidation processes by interfering with the formation of reactive species, scavenging the formed radicals and altering the transformation pathways of the trace organic contaminants (Yang et al., 2022).
- Excessive DOM may promote the release of trace metals such as iron, manganese and copper due to biodegradation of metal-organic matter complexes (Praise et al., 2020; Riise et al., 2023). Also, DOM mediated hypolimnetic anoxia may cause trace metal solubilization from sediments (Dent et al., 2014; Li et al., 2019).
- DOC is a precursor for the formation of toxic disinfection-byproducts during chlorination (Fernández-Pascual et al., 2023).

1.8 Dissolved Organic Matter (DOM).

1.8.1 Nature and Sources.

Some of the undesirable outcomes of singular or synergistic effects of eutrophication (Zhou et al., 2018) and climate extremes (Creed et al., 2018; Xenopoulos et al., 2021) in drinking water sources are elevated concentrations and altered molecular properties of DOM (Kaushal et al., 2014).

Introduction

Aquatic DOC is operationally defined as a complex mixture of both aromatic and aliphatic hydrocarbon structures (Leenheer, Jerry A. and Jean-Philippe Croué, 2003) that can pass through a 0.2-0.45 μm pore size filter (Tranvik and Von Wachenfeldt, 2014). Also, attached to the hydrocarbon structures are functional groups such as ketone, hydroxyl, amide and carboxyl (Leenheer, Jerry A. and Jean-Philippe Croué, 2003). The rest of material retained on the filter is called particulate organic carbon (POC), which, together with DOC, forms total organic carbon (TOC) (Zhang et al., 2021). Based on size and polarity, DOM can be generally classified as colloidal, hydrophobic, transphilic, or hydrophilic, of which each of the latter three can be either acidic, basic or neutral (Leenheer, Jerry A. and Jean-Philippe Croué, 2003). DOM can enter lakes via surface run-off and groundwater movement from the catchment (Solomon et al., 2015) or can be generated in-lakes through extracellular secretions by and degradation from phytoplankton (Liu et al., 2020), microorganisms, and macrophytes (Zhang et al., 2021). Figure 2 illustrates common DOM sources found in aquatic ecosystems.

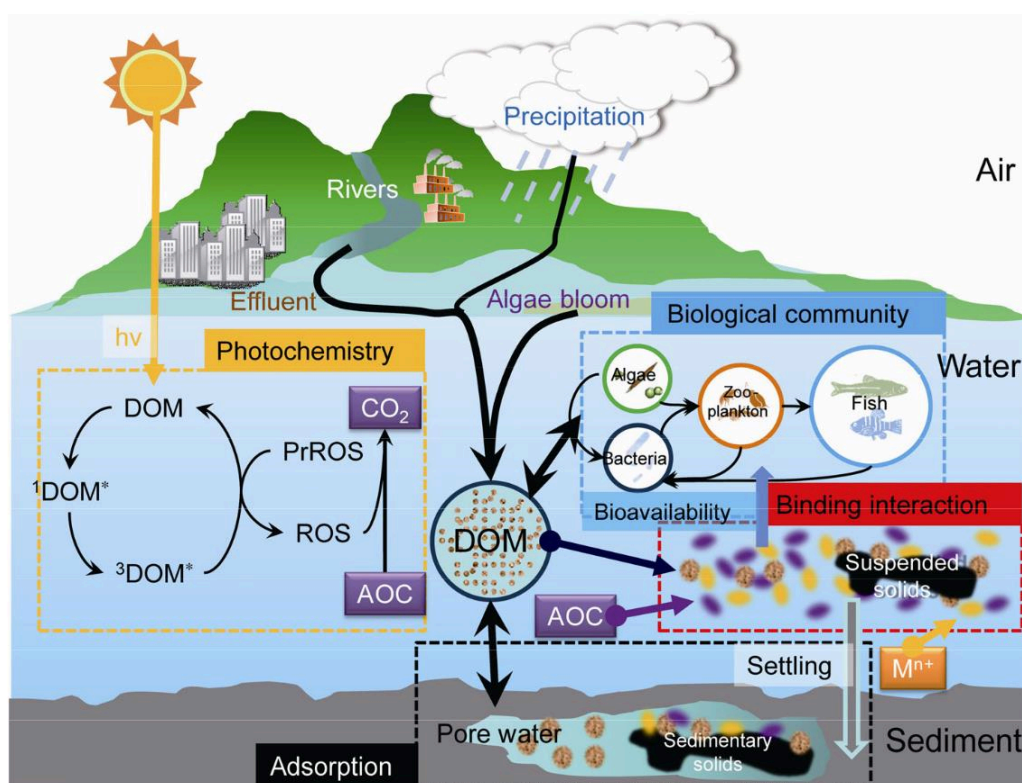


Figure 2. DOM sources in lakes. Image adapted from He et al., 2016. $^1\text{DOM}^*$ = singlet DOM, $^3\text{DOM}^*$ = triplet DOM, ROS = reactive oxygen species, PrROS = precursors of ROS, AOC = anthropogenic organic contaminants, and M^{n+} = metal ions with positive charge of n.

Introduction

Catchment derived (allochthonous) DOM forms the majority of DOM pools in inland waters. It is made up of high molecular weight phenolic compounds resulting from degradation of leaf litter and soil fulvic and humic compounds. Allochthonous DOM is poor in nutrient content (Mash et al., 2004), and typically made up of CHO group of molecules such as lignin, tannin (Maizel et al., 2017), quinones, carboxylic acids (Solomon et al., 2015) and pigments (Chow et al., 2005). However, a small portion of humic substances can also be generated within lakes (Tranvik and Von Wachenfeldt, 2014). Terrestrially derived DOM is more hydrophobic (Chow et al., 2005), more photoreactive (Hiriart-Baer et al., 2008), and as bio-labile as autochthonous DOM (Kellerman et al., 2015; Kothawala et al., 2012; Stadler et al., 2020) but bio-degrades at a slower rate than autochthonous DOM (Guillemette et al., 2013). On the other hand, in-lake derived (autochthonous) DOM is generally aliphatic, hydrophilic (Gondar et al., 2008) and transphilic (Chow et al., 2005) in polarity. Autochthonous DOM mostly consists of extracellular secretions and intracellular autolytic compounds produced by phytoplankton, macrophyte and microorganisms during primary production and cell death. Also, autochthonous DOM is composed of protein-like, peptides and amino acid compounds (Liu et al., 2022), and is rich in nutrient content (Mash et al., 2004). Anthropogenic activities are also recognized as a source of DOM through inputs of industrial wastewater, domestic sewage and agricultural run-off (Zhang et al., 2021).

Our study area, i.e. Sau Reservoir, has various sources of DOM such as terrestrial, in-reservoir generated and wastewater inputs, which imply varying character as well. In this thesis, DOM sources are tracked through the derivation of optical indices, to help in explaining the variability and speciation observed in DBP formation potential tests.

1.8.2 DOM functionality in aquatic ecosystems.

DOM dynamics are of ecological importance in lakes for several reasons. First, its concentration determines warming and stratification patterns of epilimnetic water, which may promote hypoxia in bottom water layers (Caplanne and Laurion, 2008). Second, its photo-reactivity generates hydrogen peroxide, organic peroxide and hydroxyl radicals that are instrumental in photodegradation of DOM itself, as well as other organic compounds in water (Mostofa et al., 2013). Third, light absorption in the ultraviolet and visible regions reduces the availability of

Introduction

photosynthetically active radiation in water, thereby reducing primary production (Mostofa et al., 2013). Lastly, its concentration in lakes drives methane emissions from lakes (Amaral et al., 2021; Zhou et al., 2018).

1.8.3 Fate of DOM in Aquatic ecosystems.

Within lakes, DOM can be mineralized via three mechanisms. One mechanism is bio-reactivity, where bacteria and fungi break down complex DOM structures as their source of energy. Photo-reactivity is another mechanism, where DOM is broken down by light and intermediate chemical species generated through absorption of shortwave radiation. The third mechanism is flocculation, where charged organic molecules aggregate with oppositely charged particles and metal ions, resulting in coalescence and eventual sedimentation (Berggren et al., 2022). However, most DOM is mineralized via bio-reactivity, resulting in the emission of greenhouse gasses such as carbon dioxide, methane, and nitrous oxide (Amaral et al., 2021; Liu et al., 2023), whereas photo-reactivity and flocculation play minor roles (Berggren et al., 2022). While DOM mineralization via bio-reactivity favors aliphatic structures, photo-reactivity degradation rates are highest in aromatic structures, whereas flocculation rates are high in DOM with anionic functional groups. In addition, these intrinsic molecular properties are modulated differently by extrinsic environmental variables of temperature, pH, nutrients, light, turbidity, salinity and metal ions, among others (Berggren et al., 2022). All the physical, chemical and biological processes capable of transforming various forms of organic matter in lakes are illustrated in Figure 3.

Introduction

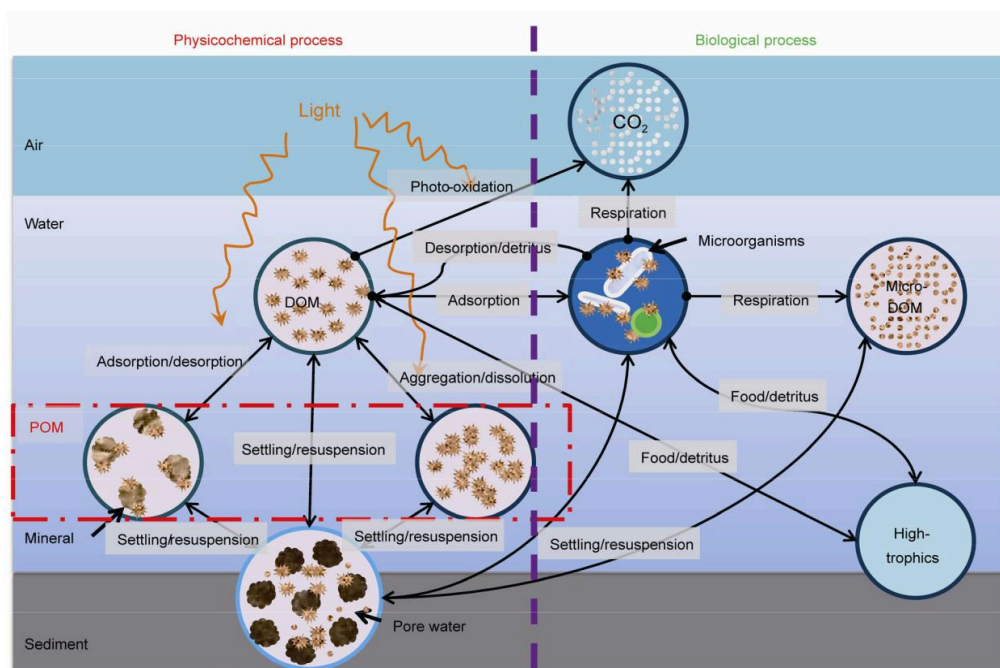


Figure 3. DOM reactivity in lakes. Image adapted from He et al., 2016.

In addition, there are several other reactions of environmental concern within the aquatic environment, in which DOM plays an important role. First, DOM is associated with the enhancement or reduction of methyl-mercury concentration in lakes (Ravichandran, 2004). Second, trace metal such as iron, can bind to DOM functional groups of carboxylates, thiols, amines and phenols (Aiken et al., 2011) available in humic acids, fulvic acids and protein-like components (Jie Zhang et al., 2023). Lastly, DOM can undergo sulfurization reactions with aqueous sulfide, leading to the enhancement of methyl-mercury production (Graham et al., 2017).

In **Papers II** and **III** of this thesis, optical and molecular techniques are applied to track mechanisms of DOM transformation along the river-reservoir continuum, to help in the interpretation of patterns observed in the formation potential of both N- and C-DBPs. Understanding the probable mechanisms is imperative for water resources management in that it helps to direct DOM pollution abatement interventions as well as water abstraction and treatment decisions.

Introduction

1.8.4 Drivers of DOM dynamics in watersheds.

Antecedent hydrological (droughts and precipitation) extremes and heatwaves drive the production and mobilization (Raymond et al., 2016) of allochthonous DOM into water bodies. In general, droughts decrease terrestrial DOM fluxes and concentration in water bodies due to severely reduced flow conditions which constrains DOM mobilization (Tiwari et al., 2022) and restrict microbial activity (Wu et al., 2023). On the other hand, extreme flow events such as storms raise DOM concentrations by orders of magnitude (Yoon and Raymond, 2012), due to enhanced hydrologic connectivity (Wu et al., 2023). However, other studies contend that extreme droughts increase the production of DOM due to a phenomenon called the “enzymatic latch”, in which enzymes that aid in the production of DOM by microbes, are triggered by droughts and never switch off thereafter (Worrall and Burt, 2004). On the other hand, heatwaves may enhance DOM export from the catchment by increasing soil respiration rates and biodegradation rates of plant organic material (Mostofa et al., 2013).

In-lake produced DOM depends on nutrients (Zhou et al., 2018) such as phosphorus, nitrogen and silica and access to photosynthetically active radiation (PAR) by primary producers (Stedmon and Markager, 2005). Aside from availability of nutrients and PAR, autochthonous DOM production is also modulated by meteorological variables of wind, temperature and precipitation. As a result, autochthonous DOM also responds to climate extremes of storms, wind events, heatwaves, and droughts. Storm events dilute or even flush out autochthonous DOM, but other studies have reported increased concentration of terrestrially derived DOM in Emerald Lake (Sadro and Melack, 2012) and Lake Taihu (Liu et al., 2021). Extreme wind events have been reported to increase DOM concentration of shallow lakes due to sediment resuspension from wind shear, which mobilizes sediment bound DOM (Wu et al., 2015). In some studies, heatwaves have been reported to increase DOM because of increased phytoplankton biomass (Pokrovsky et al., 2013), while, in other studies, warmer temperatures were associated with lower autochthonous DOM because of increased biodegradation rates (Zhou et al., 2018a). A modeling study in Canada (Wu and Yao, 2022) and observational studies in the Experimental Lake Area, also in Canada (Schindler et al., 1997) suggest that droughts cause lower DOM concentrations in lakes due to reduced flow conditions that limit export of terrestrially derived DOM.

Introduction

In this thesis, we study Sau Reservoir, a canyon shaped drinking water reservoir located in the middle stretch of the Ter River, inside the Ter Watershed, in the Mediterranean region of NE Spain. Its headwaters are located in the Pyrenees. The Sau Reservoir serves the ecosystem service of drinking water supply to the Barcelona Metropolitan City. Typical land uses within the watershed include urban settlement, agriculture (including pig farming) and industrial clusters, that are sources of nutrient pollution in Sau Reservoir (Marcé and Armengol, 2009). The Ter Watershed experiences both hydrological and meteorological extremes of droughts, precipitation extremes and heatwaves, which seem to have extrinsic effects on the concentration and character of dissolved organic matter, as exemplified in the reviewed literature. By extension, the same perturbations may drive dynamics of DBPs, whose formation is premised on DOC. Thus, a thorough understanding of how climate extremes affect DBP formation is of paramount importance because of the ecosystem service of drinking water supply that Sau Reservoir provides. Although DOM sampling did not coincide with the actual occurrence of these hydroclimatic perturbations, by sampling in almost all seasons, it was hoped that the extrinsic effect of season (a rough proxy for these climate extremes) on DOM would still be detectable because of their high probability of occurrence in the Mediterranean region.

1.8.5 Controls on DOM loads to aquatic systems.

Depending on source, DOM may be amenable to conventional water treatment process train of coagulation, flocculation, sedimentation, filtration and disinfection (Alver, 2019; Pakharuddin et al., 2021), particularly if it is terrestrially derived (Sanchez et al., 2013; Shi et al., 2021). On the other hand, low molecular weight autochthonous DOM, is poorly removed by conventional water treatment methods (Pan et al., 2023; Shutova et al., 2014) and may, therefore, form toxic DBPs upon chlor(am)ination.

Watershed management interventions such as reforestation (Mostofa et al., 2013a) are effective in reducing soil erosion that exports DBP precursor compounds into water bodies (Lin et al., 2021). In-lake derived DBP precursors may be minimized by reducing eutrophication of lakes, through limiting excessive fertilizer use, reducing disposal of untreated domestic and industrial wastewater and controlling animal breeding and aquaculture wastewater from reaching water sources (Lin et al., 2021).

Introduction

The modulation of DOM dynamics in lakes by climatological variables is an unavoidable phenomenon (Creed et al., 2018; K. Wang et al., 2023) and a constant source of concern for the water supply industry. As such, accepting their inevitable occurrence and impacts on aquatic DOM and devising appropriate management options that consider their inseparability with the business of drinking water supply, should be considered as the most pragmatic management approach. Such pragmatism may include anticipating climate extremes through predictive modeling for the solicitation of lead time to consider appropriate interventions in the face of impending water supply disruptive perturbation.

1.8.6 DOM Measurement.

1.8.6.1 Bulk DOC.

The bulk DOC can be accurately determined as carbon via chemical oxidation coupled to spectrophotometric detection methods (Kolka et al., 2008). On the other hand, molecular structure elucidation and resolution of such a complex mixture of organic compounds is nearly impossible at present. Bulk DOC concentration can also be reasonably estimated from various modeling such as combination of satellite technologies and artificial intelligence techniques. In addition, researchers have developed analytical techniques whose specific functions include elucidating DOC sources (i.e. stable and elemental isotopic composition), characterizing functional groups (i.e. UV-VIS absorption) and elucidating composition and source of DOC (i.e. fluorescence spectroscopy). Also, molecular characterization techniques, such as the Fourier Transform Infrared Spectroscopy (FTIR), Nuclear Magnetic Resonance Spectroscopy (NMR), and Fourier Transform Ion Cyclotron Resonance Mass Spectrometry (FT-ICR MS) have been developed by researchers, for different purposes. FTIR was developed for functional group determination, NMR for molecular formulae elucidation and FT-ICR MS for composition and molecular structure assignment (Zhang et al., 2021). DOC measurement techniques commonly reported in literature are summarized in Table 7.

Introduction

Table 7. Common DOM measurement methods.

Parameter	Targeted group	Techniques	Variables	Reference
DOC	Bulk	Oxidation and Spectrophotometry.		Kolka et al., 2008.
DOC	Bulk	Satellite technology and artificial intelligence prediction (Gaussian process Regression).	Green and red satellite bands, leaf area index-high vegetation and air temperature.	Harkort and Duan, 2023.
DOC	Bulk	Artificial intelligence prediction (Boosted Regression Trees).	Lake elevation, watershed area to volume ratio, surface solar radiation and precipitation.	Toming et al., 2020.
DOC	Bulk	Machine learning (Boosted Regression Trees).	Remotely sensed Chl-a, CDOM and Secchi depth.	Toming et al., 2016.
DOC	Bulk	Mass balance modeling.	Catchment area, total wetland area, upland area, DOC input, export and loading, runoff, lake discharge, DOC loss coefficients, DOC output, DOC load and water from upstream lakes.	O'Connor et al., 2009.
DOC	Bulk	Regression (Logistic) Modeling.	Proportion of wetland soil type, altitude, precipitation and catchment sensitivity to acid deposition.	Monteith et al., 2015.
DOC	Bulk	GIS and Multiple Regression modeling.	Watershed vegetation and 0-5% slope.	Winn et al., 2009.
DOC	CDOM	UV-VIS Spectroscopy.		Zhang et al., 2021.
DOC	FDOM	Fluorescence Spectroscopy.		Zhang et al., 2021.
DOC	Bulk	Fourier Transform Infrared Spectroscopy (IFTR), Nuclear Magnetic Resonance Spectroscopy (NMR) and Fourier Transform Ion Cyclotron Resonance Mass Spectrometry (FT-ICR MS).		Zhang et al., 2021.

Introduction

1.8.6.2 CDOM.

The bulk DOM consists of functional groups that are collectively known as chromophoric DOM (CDOM), with chemical properties that absorb light energy and re-emits it as fluorescence (Zhang et al., 2010). CDOM comprises humic substances, lignin phenols and aromatic amino acids, derived from both allochthonous and autochthonous sources (Zhang et al., 2021), or may be released from the lakebed following wind induced sediment resuspension (Yongqiang Zhou et al., 2015). In the natural environment, CDOM is largely composed of humics and is therefore mostly of allochthonous origin (Miao et al., 2019). CDOM absorbs light in the ultraviolet and blue regions of the electromagnetic spectrum, hence restricts transmittance of the harmful UV-B (280 nm-320 nm) into the water column (Zhang et al., 2009). CDOM is usually colored because it absorbs light energy in the visible region, although it also contains low molecular weight components such as acetate, formaldehyde and acetaldehyde that don't absorb in the visible region hence are not colored (Mostofa et al., 2013).

CDOM also contains groups of organic molecules (fluorophores), known as Fluorescent DOM (FDOM), whose electrons can absorb energy, get excited to higher energy levels and re-emit it as light or fluorescence on return to ground state, in which the absorption and emission wavelengths have molecular uniqueness (Fellman et al., 2010). Consequently, the characteristics, source, transformation, fate and dynamics of CDOM in lakes can easily and inexpensively be tracked through the application of absorption and fluorescence spectroscopic techniques (Hayakawa et al., 2016; Osburn et al., 2017; Wang et al., 2019). UV-VIS absorption is generally used to provide information on DOC concentration and composition. In particular, it has been observed that absorption at wavelengths such as 254 nm, 350 nm and 440 nm linearly correlates with DOC concentration especially in aquatic systems dominated by terrestrial DOM, which provides a rapid and inexpensive method to reasonably estimate DOC concentration in lakes in-situ. On the other hand, this linear relationship degrades in systems that are dominated by autochthonous DOM, anthropogenically impacted systems and in waters whose DOM has been extensively photodegraded (Minor et al., 2014). Also, advancements in remote sensing and satellite technologies have played a big role in the approximation of CDOM quantities in lakes covering a

Introduction

large spatial scale, a feat that would otherwise be tedious with laboratory based and in-situ site constrained measurements.

1.8.6.3 FDOM.

Fluorescence, measured by fluorometers, is also used for the quantification and characterization of DOM as FDOM. Fluorescence is generated from exciting CDOM in the UV range that averages around 370 nm, leading to emission in the blue region, ranging between 440 nm and 460 nm. Allochthonous DOM, whose constituents are lignin, tannins, polyphenols, melanins and quinones, generates the largest fluorescence intensity in natural waters (Fellman et al., 2010; Minor et al., 2014). During measurement, DOM fluorometers generate 3D Excitation-Emission matrices (EEMs) that can be processed by multivariate analyses such as principal component analysis (PCA), parallel factor (PARAFAC) analysis (Minor et al., 2014) and Kohonen's self-organizing maps (SOMs) (Cuss and Guéguen, 2016). Multivariate analyses are performed on EEMs to obtain insights into chemical composition of the DOM pool. In other cases, EEMs can be subjected to two-dimensional correlation spectroscopy (2D-COS), a data processing tool that improves spectral resolution of DOM absorbance data (Shang et al., 2022). Typical fluorophores that can be identified in the EEM-PARAFAC model are summarized in Table 8.

Introduction

Table 8. Typical DOM Fluorescence Peaks reported in literature.

Peak name	λ_{Ex} (nm)	λ_{Em} (nm)	Fluorofore name	Source	Reference
A	240-260	400-500	Humic and Fulvic Acids.	Allochthonous DOM.	Dubnick et al., 2010; Fellman et al., 2010; Vione et al., 2021.
B	270-275	304-312	Tyrosine-like.	Aquatic microorganisms.	Dubnick et al., 2010; Fellman et al., 2010; Vione et al., 2021.
C	300-400	400-500	Humic and Fulvic Acids.	Allochthonous DOM.	Dubnick et al., 2010; Fellman et al., 2010; Vione et al., 2021.
M		< 400	Marine humic acids.		Fellman et al., 2010; Vione et al., 2021.
T	270-280	330-368	Tryptophan-like.	Aquatic microorganisms.	Dubnick et al., 2010; Vione et al., 2021.
	350-450	650-700	Chlorophyll.	Microbial pigments.	Vione et al., 2021.
	330	400	Mycosporin-like amino acids.		Mostofa et al., 2013.
W	325-335	415-425	Fluorescent Whitening Agents.	Textile industry.	Mostofa et al., 2013; Vione et al., 2021.
	240	338	Protein-like.	Aquatic microorganisms	Vione et al., 2021.

Introduction

In addition to FDOM peaks, there are other derived optical DOM indices that provide insights into the nature, source and fate of fluorophores present in water samples. These indices include the fluorescence index, humification index and the biological index. Fluorescence Index (FI) is used to determine the source of DOM, either as microbially or terrestrially derived. The Humification Index (HIX) indicates the degree of humification, i.e. the breakdown of organic materials to form humus. The Freshness Index ($\beta:\alpha$), also known as the Biological Index (BIX), indicates the proportion of recently produced DOM from microbial sources (Begum et al., 2023). Respective index thresholds are summarized in Table 9.

Introduction

Table 9. DOM Fluorescence indices commonly found in literature.

Index	λ_{Ex} (nm)	λ_{Em} (nm)	Description	Thresholds	DOM Source	Reference
FI	370	ratio (470/520)	Fluorescence Index	High (~ 1.8)	Microbial	Bao et al., 2023; Fellman et al., 2010.
				Low (~ 1.2)	Terrestrial	
HIX	254	Peak area under (435-480)/peak area under ((300-345) + (435-480))	Humification index	Low (< 4)	Microbial	Bao et al., 2023; Fellman et al., 2010.
				Middle (4-10)	Mixture of both terrestrial and biological	
				High (> 16)	Terrestrial	
BIX ($\beta:\alpha$)	310	intensity at 380/(max. intensity at (420-435))	Biological index	High (0.8- 1)	Microbial	Bao et al., 2023; Fellman et al., 2010; Murphy et al., 2018.
				Low (< 0.6)	Terrestrial	

Introduction

A major caveat of CDOM spectroscopic techniques is that they apply to a small fraction of the DOM pool that is optically active in the UV and visible regions of the electromagnetic spectrum (Rosario-Ortiz and Korak, 2017), whereas the larger DOM pool is optically inactive. In addition, CDOM spectroscopic methods neither provide the molecular structure of the CDOM itself, nor that of the rest of the DOM pool (Zhang et al., 2021). However, the advent of molecular characterization techniques has been able to resolve some of the shortfalls of spectroscopic techniques. Specific details of such molecular methods have been summarized in Table 10.

Introduction

Table 10. Summary of molecular methods for the characterization of DOM

Technique	Description	Principle	Role	Reference
FTIR	Fourier transform infrared spectroscopy.	Infrared light absorption at particular wavelengths occurs due to vibration of functional groups. The intensity of absorption depends on the change in dipole moment of the vibrating molecule and concentration of the sample.	Identification of functional groups.	Minor et al., 2014.
NMR	Nuclear magnetic resonance spectroscopy.	Based on transitions in spin states of the nuclei of ^1H , ^{13}C , ^{15}N , and ^{31}P induced by radiation of specific radio frequencies, within a magnetic field.	Molecular structure elucidation; Shows linkages of functional groups.	Minor et al., 2014.
FT-ICR MS	Fourier transform ion cyclotron resonance mass spectrometry.	Based on cyclic oscillations of charged ions in a magnetic field, in which the oscillation frequency is related to the ion's m/z .	Chemical composition and molecular structure elucidation.	Geer Wallace and McCord, 2020; Zhang et al., 2021.

Introduction

Mass spectrometry analysis of bulk DOM generates molecular formulae in which C, H, O, N and S are the major elements that form distinct groups such CHO, CHON, CHOS and CHONS (Shang et al., 2022). The CHO class dominates the natural drinking water sources due to the increased abundance of biopolymers such as lignin (Shi et al., 2021). The empirical molecular formulae can also be used to generate indices such as the double bond equivalent (DBE) and modified aromaticity index (AI_{mod}), which indicate the degrees of unsaturation and aromaticity, respectively, in a molecule (Shi et al., 2021). DBE indicates the sum of double bonds and rings in a DOM molecule (Antony et al., 2017; Sleighter and Hatcher, 2007) excluding double bonds between C and heteroatoms such as O, N, S and P (Wagner et al., 2015). In addition, molecular formulae can also provide useful information on DOM compound classes through discretization of the aromaticity index and H:C elemental ratios. Such discrete regions are often projected on the two-dimensional (Hockaday et al., 2009) van Krevelen diagram, which graphically illustrates the elemental H:C molar ratios on the y-axis against O:C elemental molar ratios on the x-axis. The discretization of each DOM molecular formula on the VK diagram generates distinct groups such as combustion derived polycyclic aromatics ($AI > 0.66$), vascular plant derived polyphenols ($0.66 \leq AI < 0.50$), highly saturated and phenolic compounds ($0.50 \leq AI < 0.33$ and $H:C < 1.5$) and aliphatic compounds ($2.0 \leq H:C \leq 1.5$) (Feng et al., 2016; Sleighter and Hatcher, 2007). In addition, the segmentation of the 2D van Krevelen diagram into seven regions, based on the H:C, O:C and N:C elemental ratios, generates DOM groups of lipids, proteins, lignins/carboxyl-rich alicyclic compounds (CRAM), carbohydrates, unsaturated hydrocarbons, condensed aromatic structures and tannin (Feng et al., 2016; Liu et al., 2020; Shi et al., 2021). Such segments are illustrated in Figure 4.

Introduction

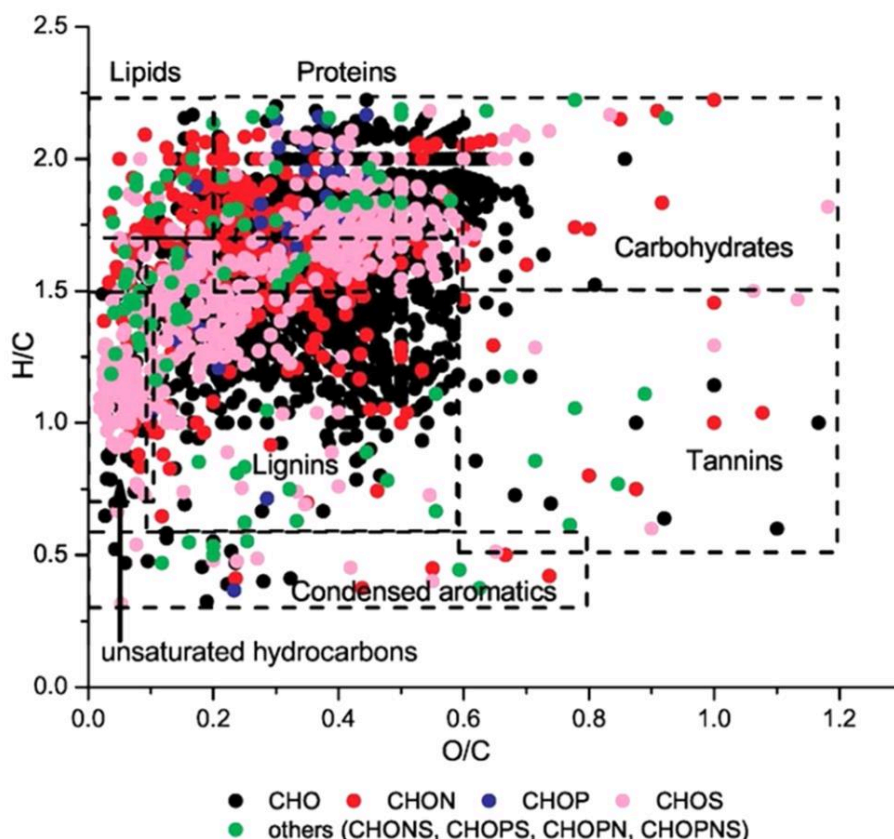


Figure 4. The segmentation of the 2D van Krevelen diagram. Image adapted from Antony *et al.*, 2017.

The degree of accuracy in molecular formulae assignment, from the realized mass spectra, determines levels of accuracy in computations of AI_{Mod} , DBE and segmentation of the van Krevelen diagram. An index, called the Kendrick Mass Defect (KMD), improves formula assignment in circumstances of higher m/z ratio, where there are more formulae exactly matching a single m/z value, which is typical of homologous series. Homologous series are a set of m/z compound values that have the same chemical backbone but only differ by integer multiples of functional groups such as CH_2 , CO , OCH_2 or $COOH$ (Mopper *et al.*, 2007; Sleighter and Hatcher, 2007). Thus, ions differing only by multiples of some functional group will have the same KMD. In circumstances where there exist multiple formulae for a single m/z value, the formula falling within a particular homologous series is chosen as the correct assignment (Sleighter and Hatcher, 2007). On the Kendrick plot (Hawkes and Kew, 2020), a graphical plot of KMD (y-axis) versus nominal Kendrick mass (x-axis), homologous series fall on the same horizontal line, as illustrated in Figure 5.

Introduction

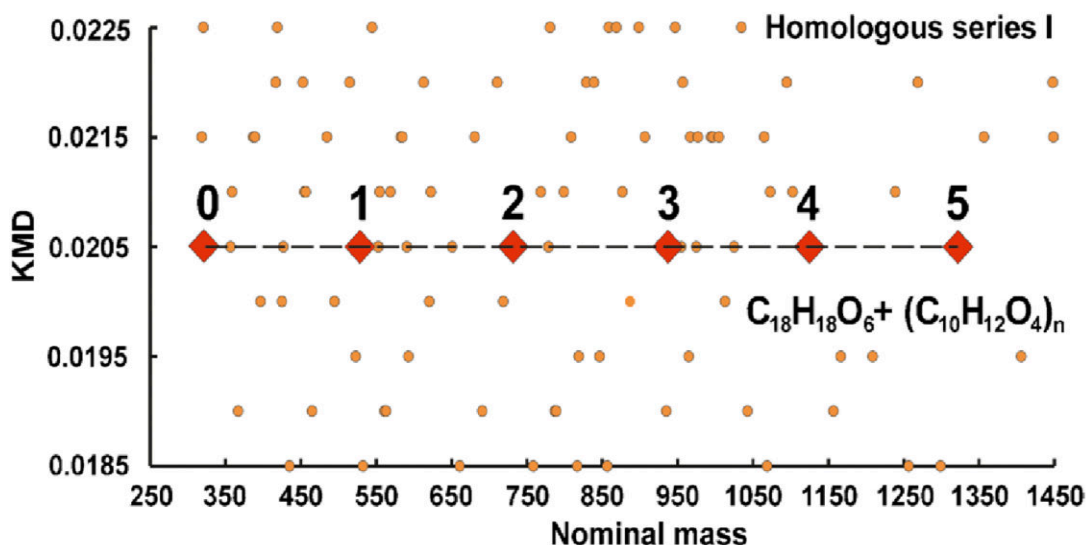


Figure 5. Kendrick plot. Image adapted from Pikovskoi and Kosyakov, 2023.

Useful as the technique is, mass spectrometry has some caveats that need consideration when interpreting and generalizing results. The first caveat is the inability to assign complete molecular structure of individual DOM components from the generated empirical formulae. The second caveat is difficulties in converting all the sample into ions for detection. The last caveat concerns signal suppression by analytes, interference from contaminants and analyte degradation in the ionization source (Minor et al., 2014). Overcoming these challenges calls for further research that will improve DOM characterization and management in aquatic ecosystems.

In **Paper II** of this thesis, various DOM characterization techniques were applied to gain insights useful in explaining core results on profiling changes on the molecular fingerprints of DOM following chlorination. Specifically, bulk DOC concentration, absorption, fluorescence and molecular structure indices were derived and used to interpret patterns of change in DOM functional groups because of chlorination and the formed DBPs. The end points of the analysis were some significant and novel contributions on DOM molecular regions that are transformed by chlorination and a discovery of potential surrogates for N-DBP formation. In **Paper III**, bulk DOC, absorption and fluorescence indices were measured to aid interpretation of DBP formation gradient along the river-reservoir chain and trends across seasons. At the end of the analysis, DOM

Introduction

fluorescence indices were quite instrumental in explaining the role of WRT and seasonality in modulating DBP formation potential.

1.9 Disinfection by-product formation in drinking water.

DBPs are organic compounds formed from the unintended reactions involving DOC (from natural, algal and wastewater), inorganic precursors (bromide and iodide) and chemical disinfectants (ozone, chlorine, chloramine and chlorine dioxide) (Krasner, 2009) during water treatment and distribution. DBPs are broadly categorized into two classes of carbonaceous and nitrogenous, based on whether the base organic precursor is either DOC or DON. Table 11 summarizes DBP classes, sub-classes and typical species that are commonly found in literature. Italicized names are the DBP species studied and hence reported in this thesis.

Introduction

Table 11. A summary of disinfection by-products commonly found in literature.

DBP Class	DBP Class	Sub-	DBP Acronym	DBP name	Reference
C-DBPs	THMs		TCM	<i>Trichloromethane.</i>	Culea et al., 2006; Kumari and Gupta, 2022.
			TBM	<i>Tribromomethane.</i>	
			BDCM	<i>Bromodichloromethane.</i>	
			DBCM	<i>Dibromochloromethane.</i>	
	HAAs		MCAA	Monochloroacetic acid.	Wang et al., 2020.
			MBAA	Monobromoacetic acid.	
			MIAA	Monoiodoacetic acid.	
			DCAA	Dichloroacetic acid.	
			DBAA	Dibromoacetic acid.	
			DIAA	Diiodoacetic acid.	
			BCAA	Bromochloroacetic acid.	
			CIAA	Chloroiodoacetic acid.	
			BIAA	Bromoiodoacetic acid.	
			TCAA	Trichloroacetic acid.	
			BDCAA	Bromodichloroacetic acid.	
			DBCAA	Dibromochloroacetic acid.	
			TBAA	Tribromoacetic acid.	
			DCIAA	Dichloroiodoacetic acid.	
			CDIAA	Chlorodiiodoacetic acid.	
			BCIAA	Bromochloroiodoacetic acid.	
	DBIAA	Dibromoiodoacetic acid.			

Introduction

DBP Class	DBP Class	Sub-	DBP Acronym	DBP name	Reference	
			BDIAA	Bromodiiodoacetic acid.		
			TIAA	Triiodoacetic acid.		
	HKs		DCP	<i>Dichloropropanone.</i>	Barceló, 2012; Kermani et al., 2013; Krasner et al., 2006.	
			TCP	<i>Trichloropropanone.</i>		
			TBP	Tribromopropanone.		
			CP	Chloropropanone.		
			DBP	Dibromopropanone.		
			BDCP	Bromodichloropropanone.		
			TetCP	Tetrachloropropanone.		
			TetBP	Tetrabromopropanone.		
			PentBP	Pentachloropropanone.		
			HexBP	Hexachloropropanone.		
	HALs		DCAL	Dichloroacetaldehyde.	Gao et al., 2019.	
			DBAL	Dibromoacetaldehyde.		
			BCAL	Bromochloroacetaldehyde.		
			TCAL	Trichloroacetaldehyde.		
			TBAL	Tribromoacetaldehyde.		
			BDCAL	Bromodichloroacetaldehyde.		
			DBCAL	Dibromochloroacetaldehyde.		
			CH	Chlorohydrate.		
	X-Furanones		MX	3-Chloro-4-(dichloromethyl)-5-hydroxy-2(5H)-furanone.		Diana et al., 2023; Krasner et al., 2006; Onstad and Weinberg, 2005.
			ZMX	(Z)-2-Chloro-3-(dichloromethyl)-4-oxobutenoic acid.		

Introduction

DBP Class	DBP Class	Sub-	DBP Acronym	DBP name	Reference
			EMX	(E)-2-Chloro-3-(dichloromethyl)-4-oxobutenoic acid.	
			red-MX	3-Chloro-4-(dichloromethyl)-2(5H)-furanone.	
			ox-MX	2-Chloro-3-(dichloromethyl)butenedioic acid.	
			BMX-1	3-Chloro-4-(bromochloromethyl)-5-hydroxy-2(5H)-furanone.	
			BEMX-1	(E)-2-Chloro-3-(bromochloromethyl)-4-oxobutenoic acid.	
			BMX-2	3-Chloro-4-(dibromomethyl)-5-hydroxy-2(5H)-furanone.	
			BEMX-2	(E)-2-Chloro-3-(dibromomethyl)-4-oxobutenoic acid.	
			BMX-3	3-Bromo-4-(dibromomethyl)-5-hydroxy-2(5H)-furanone.	
			BEMX-3	(E)-2-Bromo-3-(dibromomethyl)-4-oxobutenoic acid.	
			MCA ring	Mucochloric acid.	
			MCA open	2,3-Dichloro-4-oxobutenoic acid.	
			MoXC	Mixture of MX, ox-MX, ZMX, EMX, MCA ring and open.	
			BMX	Mixture of BMX-1, 2, 3, ring and open forms.	
			MXR	Methylated MX.	
	Iodinated THMs		IF	Iodoform.	Ioannou et al., 2016.
			DCIM	Dichloroiodomethane.	
			BCIM	Bromochloroiodomethane.	
			CDIM	Chlorodiiodomethane.	
			DBIM	Dibromoiodomethane.	
			BDIM	Bromodiiodomethane.	

Introduction

DBP Class	DBP Class	Sub-	DBP Acronym	DBP name	Reference
N-DBPs	NAs		NDMA	<i>N-nitrosodimethylamine.</i>	Boyd et al., 2011; Linge et al., 2017; Nawrocki and Andrzejewski, 2011.
			NPYR	<i>N-nitrosopyrrolidine.</i>	
			NMOR	<i>N-nitrosomorpholine.</i>	
			NPIP	<i>N-nitrosopiperidine.</i>	
			NDPA	<i>N-nitrosodi-n-propylamine.</i>	
			NDPhA	<i>N-nitrosodiphenylamine.</i>	
			NEMA	<i>N-nitrosoethylmethylamine.</i>	
			NDBA	<i>N-nitrosodibutylamine.</i>	
		NDEA	<i>N-nitrosodiethylamine.</i>		
	HANs		DCAN	<i>Dichloroacetonitrile.</i>	Huang et al., 2017.
			BCAN	<i>Bromochloroacetonitrile.</i>	
			TCAN	<i>Trichloroacetonitrile.</i>	
			DBAN	<i>Dibromoacetonitrile.</i>	
HAcAms		DCAcAm	Dichloroacetamide.	Ding et al., 2018; Huang et al., 2017; Liew et al., 2012.	
		TCAcAm	Trichloroacetamide.		
		BCAcAm	Bromochloroacetamide.		
		DBAcAm	Dibromoacetamide.		
		MBAcAm	Monobromoacetamide.		
		MCAcAm	Monochloroacetamide.		
		BDCAcAm	Bromodichloroacetamide.		
		TBAcAm	Tribromoacetamide.		
		CIAcAm	Chloroiodoacetamide.		
		BIAcAm	Bromoiodoacetamide.		
	DIAcAm	Diiodoacetamide.			

Introduction

DBP Class	DBP Class	Sub-	DBP Acronym	DBP name	Reference
			MIAcAm	Monoiodoacetamide.	
	HNMs		TCNM	<i>Trichloronitromethane.</i>	Hu et al., 2010.
			TBNM	Tribromonitromethane.	
			BDCNM	Bromodichlorochloronitromethane.	
			DBCNM	Dibromochloronitromethane.	
			CNM	Chloronitromethane.	
			DCNM	Dichloronitromethane.	
			BNM	Bromonitromethane.	
			DBNM	Dibromonitromethane.	
			BCNM	Bromochloronitromethane.	
		CNX		CNCl	
			CNBr	Cyanogen bromide.	

Introduction

Together, C- and N-DBPs form a small subset of over 600 DBP compounds that have, so far, been successfully identified (Shah and Mitch, 2012). C-DBP form from hydrophobic acids, bases and neutrals and hydrophilic compounds that are part of humic and fulvic acids, carboxylic acids, carbohydrates, (aromatic) amino acids and proteins, which, collectively, constitute NOM (Chang et al., 2001; Fu et al., 2017; Tak and Vellanki, 2018; Wang et al., 2015). In addition, C-DBPs also form substantially from algal organic matter and soluble microbial products (Tang et al., 2020).

Organic precursors that form N-DBPs are derived from dissolved organic nitrogen (DON), a nitrogen rich component of dissolved organic matter, comprising groups such as proteins, amino acids, amino sugars, amides, nitriles, pyrroles, purines and pyrimidines. DON is ubiquitous in wastewater effluent and algal impacted waters, although a small portion can be found in NOM (Bond, 2012). Within the nitrogenous family, N-DBP subclasses are generated from halogenation of various groups that constitute DON as summarized in Table 12.

Introduction

Table 12. A summary of nitrogenous DBP classes and their precursors

DBP Subclass	Organic precursor	Disinfection technique	Reference
HANs	Free amino acids, nucleic acids, proteinaceous materials and amino acids bound to humic substances.	Chlorination	Bond, 2012.
HAcAms	Hydrolysis of HANs but the majority of its precursors are unknown.	Chlorination	Bond, 2012.
HNMs	Nitrophenol, amino acids, amino sugars, primary amines and nucleic acids.	Ozonation combined with either chlorination or chloramination	Bond, 2012.
NAs	Dimethylamine, trimethylamine, ranitidine, tolylfluanid and diuron.	Chloramination	Bond, 2012.
CNX	Formaldehyde, glycine and amino acids.	Chlorination or chloramination	Bond, 2012.

Introduction

1.9.1 DBP exposure, human health outcomes and regulation.

Humans are exposed to DBPs through inhalation of volatile substances, dermal absorption and ingestion (Yang et al., 2018) of contaminated water, resulting in adverse health outcomes. First, exposure to THMs and HAAs could result in the development of tumors in livers and kidneys, loss of pregnancy, reduced sperm motility and reduced productive capacity in males, as observed in exposed rodents. Second, in humans, there exists evidence of exposure to chlorinated water and the prevalence of bladder, rectal and colon cancer, retarded prenatal development, reproductive defects, abortion, birth defects and still born babies (Mazhar et al., 2020). As a result of the aforementioned health risks associated with exposure to THMs and HAAs, C-DBPs are regulated in many countries across the world, a few of which are summarized in Table 13.

Introduction

Table 13. DBP regulatory thresholds across countries

DBP	Threshold	Country/Organization	Reference
TTHM	80 µg/L, 100 µg/L, 250 µg/L	USA, Canada and Australia.	Wang et al., 2015.
HAA ₅	60 µg/L	USA and Canada.	Wang et al., 2015.
TCM	60 µg/L, 100 µg/L	China and Europe.	Wang et al., 2015.
DCAA	50 µg/L	China.	Wang et al., 2015.
TCAA	100 µg/L	China.	Wang et al., 2015.
Bromate	10 µg/L	Europe.	Wang et al., 2015.
NDMA	40 ng/L, 100 ng/L, 100 ng/L	Canada, WHO and Australia.	Wang et al., 2015; Yang et al., 2018.
CNCl	70 µg/L, 40 µg/L	WHO and Australia.	Yang et al., 2018.
DBAN	70 µg/L	WHO.	Yang et al., 2018.
DCAN	20 µg/L	WHO.	Yang et al., 2018.

Introduction

In recent years, N-DBPs have attracted the attention of researchers, hence they are being regulated in a few countries and may be due for wide scale regulation soon, because subclasses such as HANs, HAoAm and HNMs are thought to be more carcinogenic, genotoxic or cytotoxic to humans, than the usually regulated C-DBPs (Shah and Mitch, 2012). Consequently, some countries have also begun regulating certain classes of N-DBPs that are deemed potentially toxic to humans (see Table 13).

The coherence between results of experimental exposure of model animals to DBPs and epidemiological studies linking human exposure to DBPs suggests the existence of real risks for these emerging and unconfirmed halogenated organic contaminants. As a result, it is imperative to increase research efforts in this domain, given that there hasn't been any replacement to chlorination suitable for maintaining a residual effect in water distribution networks, since the discovery of THMs formation during water chlorination in 1974 (Hrudey and Fawell, 2015).

1.9.2 Environmental factors modulating DBP organic precursor dynamics.

DBP precursors respond to the influence of hydroclimatic variables such as precipitation (Barry et al., 2016; Doederer et al., 2018) and air temperature (Raseman et al., 2017; Wright et al., 2013). Research on how summer temperatures and autumn-winter precipitation affect DBP formation potential of lake water suggests that responses are lake specific, but generally point to increased DBP formation potential in periods of extreme rainfall (Hur et al., 2014), high temperature (Beaudeau et al., 2011) and drought conditions (Wright et al., 2014). The sensitivity of DBP formation potential to climate variables bothers water supply managers, hence requires anticipation and preparedness, aided by modeling efforts (Bertone et al., 2016), to inform management and minimize water supply disruptions in episodes of climatic extremes. Existing scientific evidence alludes to the fact that impacts of climate extremes on DOC (a DBP formation potential precursor in lakes) are system specific due to modulation by other local variables such as lake size and morphometry (Soto Cárdenas et al., 2017). Consequently, it seems plausible to suggest that DBP formation potential in source waters will also respond to the same modulating factors. However, what is less known is the role of water residence time (WRT) in regulating the

Introduction

concentration and speciation of DBP formation, given that lakes are known to reduce terrestrial DOC concentration and alter its molecular properties (Kellerman et al., 2015; Minor and Stephens, 2008), depending on WRT (Zwart et al., 2017). Also, lakes act as nutrient traps (Williamson et al., 2008). Additionally, lakes that thermally stratify in summer also experience stratification of DOC (Gonsior et al., 2013; Wei et al., 2022) and nutrients (Noori et al., 2018; Wilhelm and Adrian, 2007; Yaseen and Bhat, 2021), which are known DBP precursors. However, whether thermal stratification also stratifies DBP formation potential is not sufficiently understood. Providing such insights, whether on a local (system), regional or global scale is of relevance to the water supply managers to better manage their systems in order to optimize quality of supply. **Paper III** of this thesis attempts to provide insights along these two highlighted conundrums.

1.9.3 DBP surrogates and predictive modeling.

Standard methods for detecting DBPs are time consuming, require complicated and expensive analytical equipment, and are unsuitable for the real time data generation (Sadiq and Rodriguez, 2004) necessary for quick decision making required in the municipal water supply industry. Hence, the need for alternative methods, with quick turnaround times, remains an unresolved quest for researchers that are actively working in this domain. Identifying suitable surrogates for the already existing and emerging DBPs and linking them to the occurrence, concentration and patterns of variability of DBPs, using mathematical models continues to attract the interest of researchers and water supply managers. So far, DBP predictive frameworks have been developed for purposes of understanding how operational parameters and water quality influence DBP formation, investigating reaction kinetics of their formation, or for predictive purposes complementary to bench-top monitoring (Sadiq and Rodriguez, 2004). Commonly applied models range from multiple linear regression, empirical kinetic and power functions models, Bayesian Network, to artificial intelligence-based models such as artificial neural networks (ANN) and principal component regression. Examples of DBP modeling studies and their respective predictive surrogates are summarized in Table 14.

Introduction

Table 14. A summary of common DBP predictive modeling approaches.

DBP	Modeling Framework	Surrogate	Reference
THMs.	Univariate linear correlations; Multiple regression models.	TOC/DOC, UV ₂₅₄ , pH, water temperature, bromide concentration, chlorine dose, and reaction time.	Sadiq and Rodriguez, 2004; Shahi et al., 2020.
THMs.	Empirical kinetic models.	Water temperature.	Sohn et al., 2004; Zhang et al., 2013.
DCAN, TCP and TCNM.	Multivariate linear regression.	Turbidity, temperature, DOC and conductivity.	Mian et al., 2020.
THMs and HAAs.	Regularized linear regression (lasso), boosted regression tree ensembles, principal components regression, supervised principal components, and fluorescent regional integration .	EEMs.	Trueman et al., 2016.
THMs and HAAs.	Empirical power functions.	DOC, Cl ₂ , pH, temperature, bromine and time.	Sohn et al., 2004.
THMs and HAAs.	ANN autoencoder.	raw 3D EEMs.	Peleato et al., 2018.
THMs and HAAs.	Deep convolutional neural networks (CNNs).	raw 3D EEMs.	Peleato, 2022.
HKs and THMs.	Radial basis function (RBF) – ANN.	Reaction temperature, water pH, DOC, UV ₂₅₄ , and concentrations of bromide, nitrite, ammonium and Cl ₂ .	Deng et al., 2021; Hong et al., 2020; Xu et al., 2022.
THMs.	Ensemble model LSBoost.	Chlorine dose, reaction time, DOC, temperature, pH, bromide concentration, UV ₂₅₄ and SUVA ₂₅₄ .	Sikder et al., 2023.
THM probabilities.	Multivariate Bayesian Network.	Disinfectant concentration, pH, TDS, nitrogen species and conductivity.	Li et al., 2021.
THMs.	Adaptive neuro-fuzzy inference system (ANFIS).	UVA ₂₅₄ , DOC, bromide, pH, temperature and residual chlorine.	Jianzhen Zhang et al., 2023.

Introduction

The superiority of artificial intelligence-based models lies in their capabilities to accurately capture nonlinear dependencies between DBPs and the easy to measure predictor variable groups of operational parameters, DOM optical and fluorescence spectroscopy and some selected water quality variables such as nutrients and bromide. However, there appears to be an element of site specificity on the model type, which suggests that perhaps predictive accuracy could be improved by applying an ensemble of models and selecting the best model from the results. Also, the above brief review of the surrogates used for DBP predictive modeling indicates that predictive capabilities of DOM molecular features have not been explored before. Thus, **Paper II** of this thesis attempts to contribute to this region of the scientific discourse by providing insights into how molecular features of DOM change during water chlorination and regions of the DOM pool that are promising DBPs predictive surrogates.

Although this thesis focusses mostly on understanding how climate extremes impact the formation potential of disinfection by-products in source waters, it should be highlighted that climate change also threatens other aspects of municipal water supply such as quantity as well as other dimensions of quality, that may specifically apply in the current context of the Ter Watershed. Since climate is a common modulator in both cases, there is a likelihood that efforts dedicated to ameliorating impacts of climate extremes on DBP formation may also address other climate related risks on drinking water supply operations. The Ter Watershed has been experiencing extreme droughts for decades, that have severely affected quantities of freshwater supply for potable use. Several policy instruments such as water reuse, construction of desalination plants (Navarro, 2018), inter-basin transfers (Molina and Melgarejo, 2016) and water use restrictions (González, 2011; Martin-Ortega et al., 2012), have been implemented to address water shortage. Besides water shortages, extreme temperatures are known to affect electricity supply, which may disrupt water treatment and supply operations. Also, extreme precipitation results in floods that damage water supply infrastructure such as pipes, hence disrupting water supply and increasing maintenance costs. Furthermore, extreme air temperature degrades water treatment and supply infrastructure such as motors and electronic components in pumps, corrodes metal pipes and degrades plastic underground pipes, resulting into increased maintenance costs (Lyle et al., 2023). In terms of source water quality, adverse impacts of climate change on the quality of water in rivers, lakes and reservoirs, have been extensively reported in scientific literature. However, the scarcity of studies that explicitly focus on impacts of climate change on drinking water supply operations of utilities that abstract from the Ter Watershed makes it difficult to comprehend a full spectrum of climatic risks threatening water

Introduction

supply operations in this watershed. On the other hand, that the Ter and other adjacent watersheds in Catalonia are experiencing trends of ever-increasing air temperatures, has been reported by numerous hydroclimatic studies, and such trends have been projected continue on the same trajectory in the medium to long term. The mismatch between the prevalence of hydroclimatic research and their limited impact analysis specific to the Ter watershed only leaves room for generalizations from other systems that have been sufficiently researched on. A few studies that have attempted to address causal impact of climate change on water quality in the Ter Watershed have addressed water quality from the perspective of river and reservoir ecological health, implying that we can only infer impacts on drinking water supply from either theory or similar studies from elsewhere. A few studies of climate change impact on drinking water quality in the Ter watershed indicate that increased air temperature concentrates nutrients (nitrogen and phosphorus) in the Ter River (Benítez-Gilabert et al., 2010), which may impact the available treatment technologies. Also, occasionally, the Ter Watershed experiences extreme precipitation (Llasat et al., 2021; Sanuy et al., 2021), which would be anticipated to enhance sediment export into reservoirs, hence impacting water treatment operations. However, some studies on the Ter and other rivers in Catalonia, have reported a lack of relationship between river discharge and sediment yields (Liquete et al., 2009). Also, yet other studies have reported a negative relationship, which was attributed to enhanced vegetative cover growing under increased average annual precipitation, which reduces sediment production and transport (Bachiller et al., 2019). In the absence of data on sediment loads in reservoirs of the Ter Watershed, it could be assumed that precipitations extremes would more likely raise suspended solids in source waters because vegetative cover is challenged by recurrent wildfire incidences (Francos et al., 2016) and the gradual change of land use from forestry to urbanization (Selkimäki and González-Olabarria, 2017). Both factors would increase sediment and organic carbon transport into water sources, which may increase coagulant demand and reduced filter run times (Slavik and Uhl, 2009) during water treatment operations. Occasional precipitation extremes occurring in the Ter watershed may cause increased microbial loads in source waters due to combined sewer overflows that introduce untreated wastewater into source waters (Boholm and Prutzer, 2017), which may endanger public health if water treatment is insufficient. Rising water temperature from climate warming, which is a reality in the Ter watershed, may lead to deterioration of disinfectant in water (Kimbrough, 2019) and growth of both pathogenic and non-pathogenic microorganisms (Boholm and Prutzer, 2017) in water systems with longer water age, particularly in utilities that use chloramine during disinfection. Also, increasing water temperature may enhance algal growth which causes taste and odor problems, resulting in customer dissatisfaction (de Loe and Plummer, 2010). When all these climate change

Introduction

related risks are considered together with DBP formation, which is the focus of this thesis, there is a strong case for intensifying research aimed at understanding how water utilities are coping with climate uncertainties and devising ways of their sustainability for a future dominated by the same climate phenomena.

2 Objectives and Hypotheses.

2.1 General objective.

The overarching objective of this thesis was to establish causal links between the occurrence of extreme climatic events in the Ter Watershed, the concomitant response of water quality of the Sau Reservoir in general, and the formation potential and evolution of disinfection by-products (DBPs) in particular. This thesis provides insights into the type of extreme events prevalent in the watershed, whether they are a potential threat to the ecosystem service of water supply, and probable management options that may ensure sustained provision of the ecosystem service of water supply.

2.2 Specific Objectives.

- i. Quantitatively track the occurrence of droughts, heat waves and storms in the Ter watershed and their footprints on reservoir water quality.
- ii. Assess the existence of resistance of water quality in the reservoir to such hydroclimatic perturbations and its dependence on the trophic state of the ecosystem.
- iii. Evaluate impacts of thermal stratification, seasonality and water residence time in shaping the concentrations and speciation of disinfection by-products formation potential in a reservoir and their implications towards reservoir abstraction management.
- iv. Provide insights into how water chlorination alters the molecular fingerprints of dissolved organic matter of reservoir water.
- v. Identify molecular features for use as surrogates for the predictive modeling of DBP formation.

Objectives and Hypotheses

2.3 Hypotheses.

- i. Hydroclimatic extremes are intense in the Ter Watershed; reservoir water quality responds negatively to the perturbations, but the response is shaped by trophic state.
- ii. Signatures of extreme climatic events can be detected in a coarse water quality time series with innovative statistical approaches, which should reduce reliance on high frequency data and its associated costly infrastructure.
- iii. Long water residence time (WRT) reduces the formation potential of both carbonaceous and nitrogenous disinfection by-products in reservoirs due to diminishing concentration of organic matter precursor compounds through mineralization.
- iv. Thermal stratification in deep reservoirs shapes speciation and stratification of disinfection by-products formation potential due to stratification of organic precursors.
- v. Seasonality drives speciation and formation potential of disinfection by-products in eutrophic systems, with higher formation potential occurring in summer.
- vi. DOM chlorination would reduce the number of features in both in-lake and terrestrially derived molecular groups and produce new halogenated features that correlate well with known carbonaceous and nitrogenous disinfection by-product formation potential.

3 Methodology.

3.1 Study Site.

This thesis comprises three papers, all based on the Sau Reservoir (41° 58' N; 2° 22' E) which is located on the Ter River, in North East Spain. Delineation of the Ter Watershed and the sampling locations are illustrated in Figure 6.

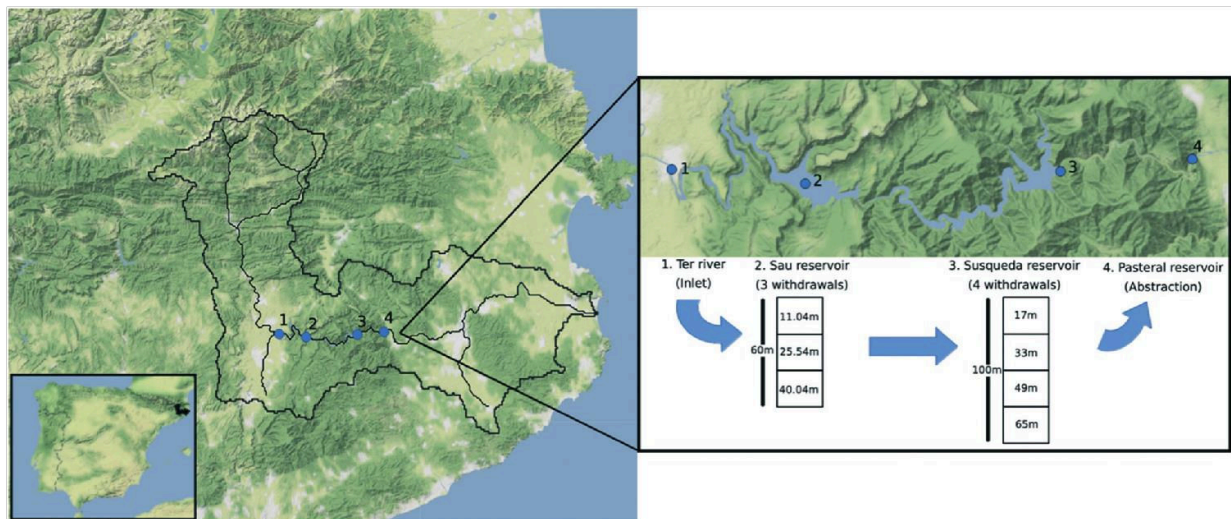


Figure 6. The Ter Watershed Map. **Paper I** is based on location 2. **Papers II and III** are based on all locations (1-4)

Land use within the Ter watershed includes forestry, arable farming and urbanization (López et al., 2011). Sau Reservoir was built in 1963 for hydropower and water supply to 4 million people in the Barcelona Metropolitan area (Ordóñez et al., 2010). Sau Reservoir lies downstream from a densely populated area where, between the years of 1991 and 1995, 16 wastewater treatment plants (WWTPs) were built to treat wastewater of the upstream population. The WWTPs were upgraded to secondary treatment during the early 2000s (Marcé et al., 2006), leading to substantial decreases in organic matter, nutrient loads and anoxia to the reservoir (Marcé et al., 2008).

Methodology

3.2 Methods.

Paper I is based on data analysis, where a combination of statistical methods is applied on reservoir water quality data and hydrometeorological variables to address various hypotheses expressed in section 2.3. First, climate extreme indices of drought and wetness were computed from precipitation, stream flow and reservoir water level data, resulting into the derivation of the non-parametric standardized precipitation index (nSPI), standardized streamflow index (nSSFI) and standardized reservoir level index (nSLI) (Hao and AghaKouchak, 2014). Also, a heat wave magnitude index daily (HWMId) (Russo et al., 2015) was derived from daily maximum air temperature time series. This Tier One analysis is illustrated in Figure 7.

Methodology

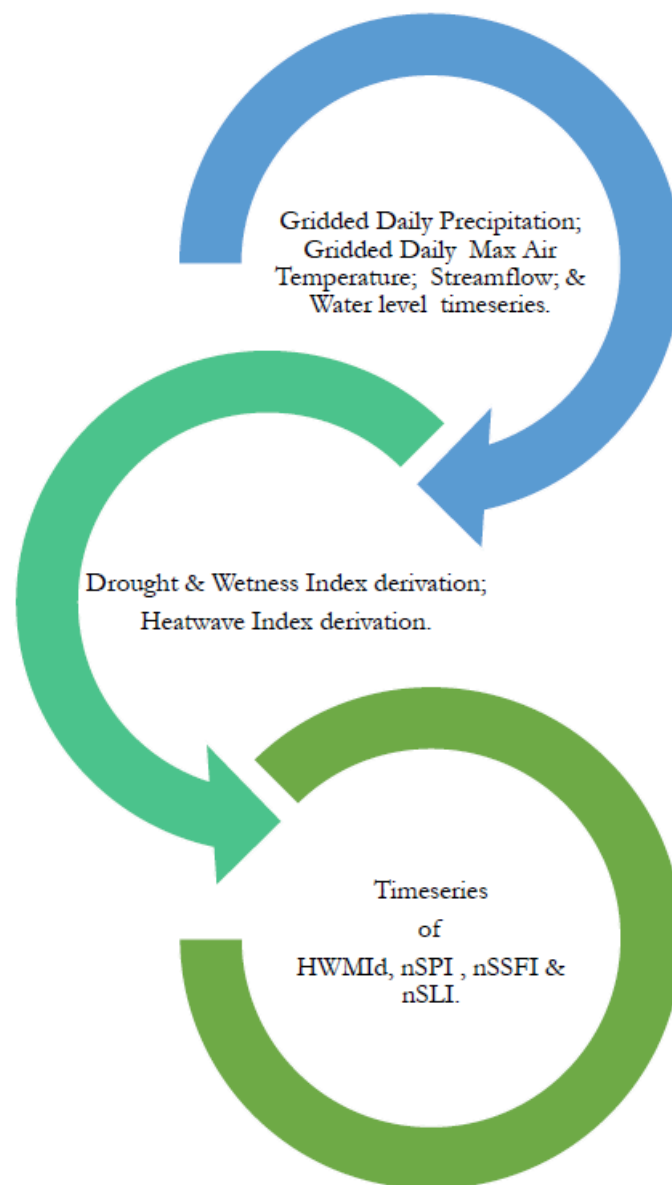


Figure 7. Tier One analysis - Derivation of hydroclimatic extremes indices. Max = maximum, HWMId = Heatwave Magnitude Index daily, nSPI = non-parametric Standardized Precipitation Index, nSSFI = non-parametric Standardized Streamflow Flow Index and nSLI = non-parametric Standardized reservoir Level Index.

Second, causal inference analysis was implemented, in which hydroclimatic time series were used to causally predict epilimnetic and hypolimnetic resolved reservoir water quality time series, in a non-parametric causality-in-quantile framework (Balcilar et al., 2017). This is a hypothesis testing method, where the main output is a test statistic (J), which is compared to a predetermined threshold value based on a chosen significance level, to infer causality. Figures 8 and 9 illustrate Tier Two analysis.

Methodology

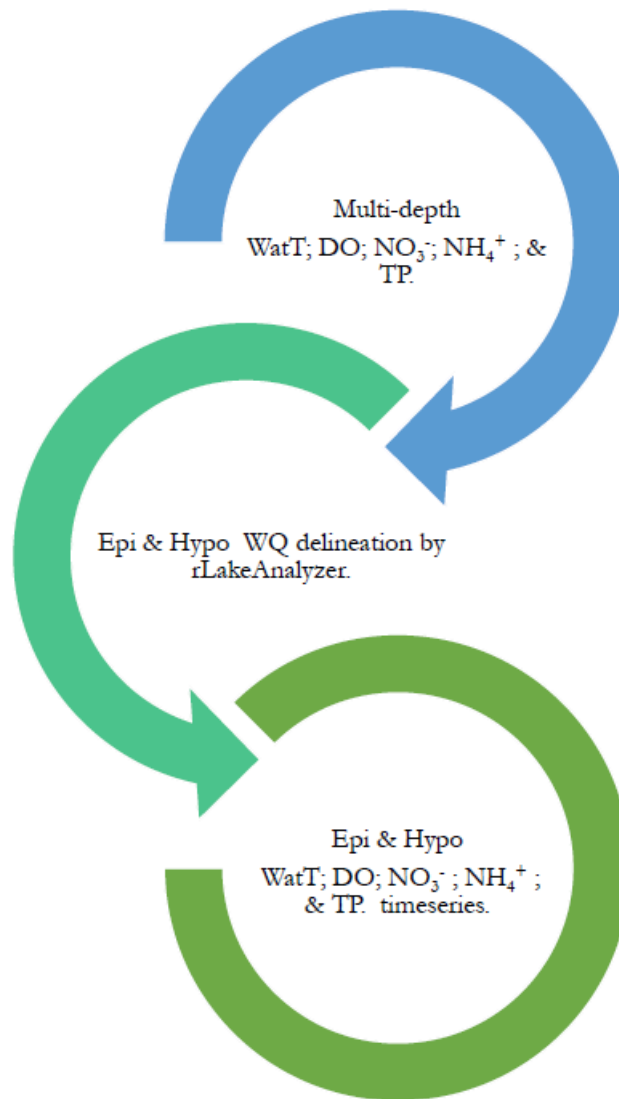


Figure 8. Aggregation of depth profiles of reservoir water quality into epilimnion and hypolimnion timeseries. *WatT* = Water temperature, *DO* = Dissolved oxygen, *NO₃⁻* = Nitrate, *NH₄⁺* = Ammonium, *TP* = Total phosphorus, *Epi* = Epilimnion, *Hypo* = Hypolimnion and *WQ* = Water quality.

Methodology

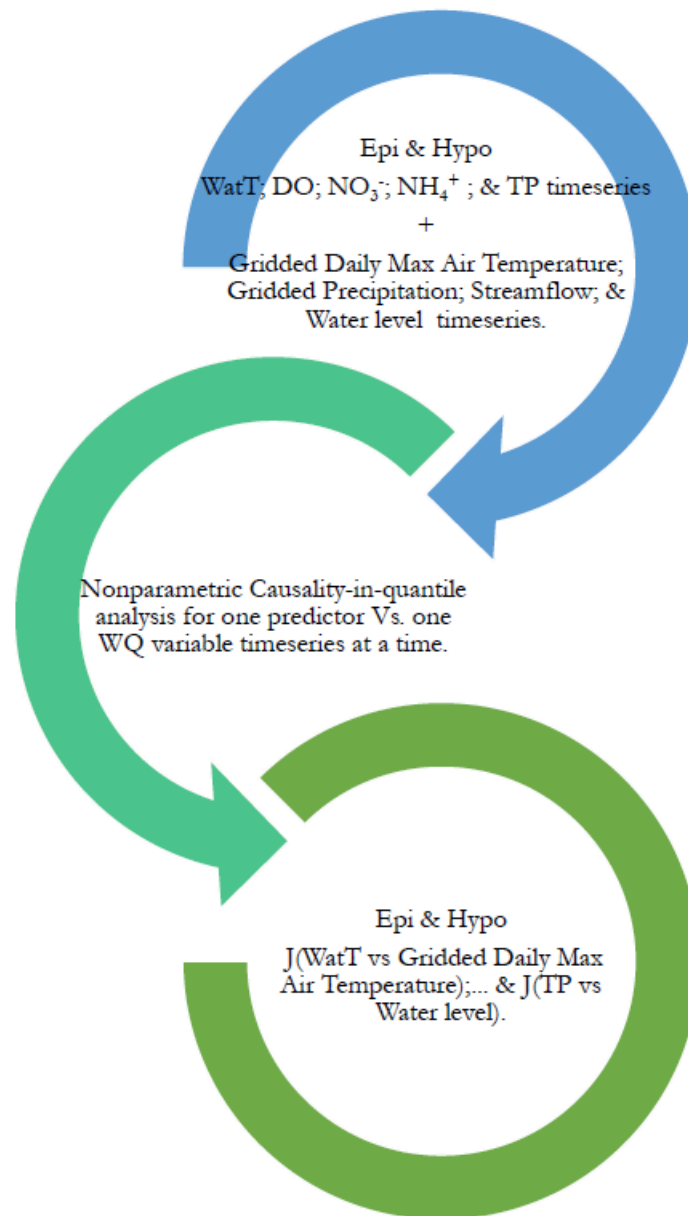


Figure 9. Tier two analysis-causal inference modeling. Epi = Epilimnion, Hypo = Hypolimnion, WatT = Water temperature, DO = Dissolved oxygen, NO₃ = Nitrate, NH₄⁺ = Ammonium, TP = Total phosphorus, Max = Maximum, WQ = Water quality and J = non-parametric causality-in-quantile test statistic.

Third, time series of climate extremes indices were used to partition epilimnetic and hypolimnetic reservoir water quality time series into extreme and non-extreme groups. Thereafter, water quality medians from extreme versus non-extreme groups were statistically compared, using the Welch's test (Zheng et al., 2013) to generated p-values that were compared with critical values based on the chosen confidence level. Also, outputs from the Welch's test were complemented by the effect size metric called the Hedges's g_s (Thompson, 2007), which denotes the effect size of the stressors (Lakens, 2013). Tier Three analysis is illustrated in Figure 10.

Methodology

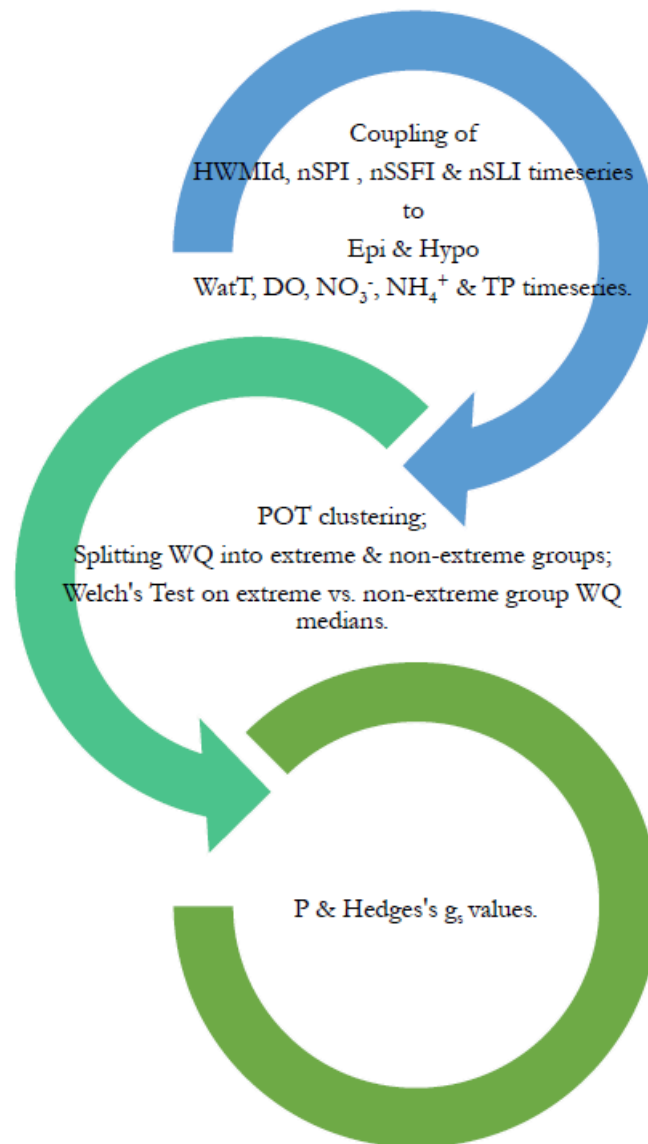


Figure 10. Tier three analysis - Extreme events impact analysis. HWMId = Heatwave Magnitude Index daily, nSPI = non-parametric Standardized Precipitation Index, nSSFi = non-parametric Standardized Streamflow Flow Index and nSLI = non-parametric Standardized reservoir Level Index, Epi = Epilimnion, Hypo = Hypolimnion, WQ = Water quality, WatT = Water temperature, DO = Dissolved oxygen, NO₃⁻ = Nitrate, NH₄⁺ = Ammonium, TP = Total phosphorus, POT = Peak Over Threshold, WQ = Water quality and P = *p*-value.

Papers II and III are based on seasonal field sampling campaigns conducted on the river-reservoir chain comprising the Ter, Sau, Susqueda and Pasteral systems, in which DOC and DBP formation potential were the main variables of interest, whereas nutrients and physical variables were complementary to aid the interpretation of the main data. In **Paper II**, key analyses of interest

Methodology

were the formation potential of DBPs and molecular profiling of DOM. All samples for volatile DBPs were processed following a method reported in (Liu et al., 2016). Figure 11 summarizes the analytical process for the determination of DBPs formation potential.

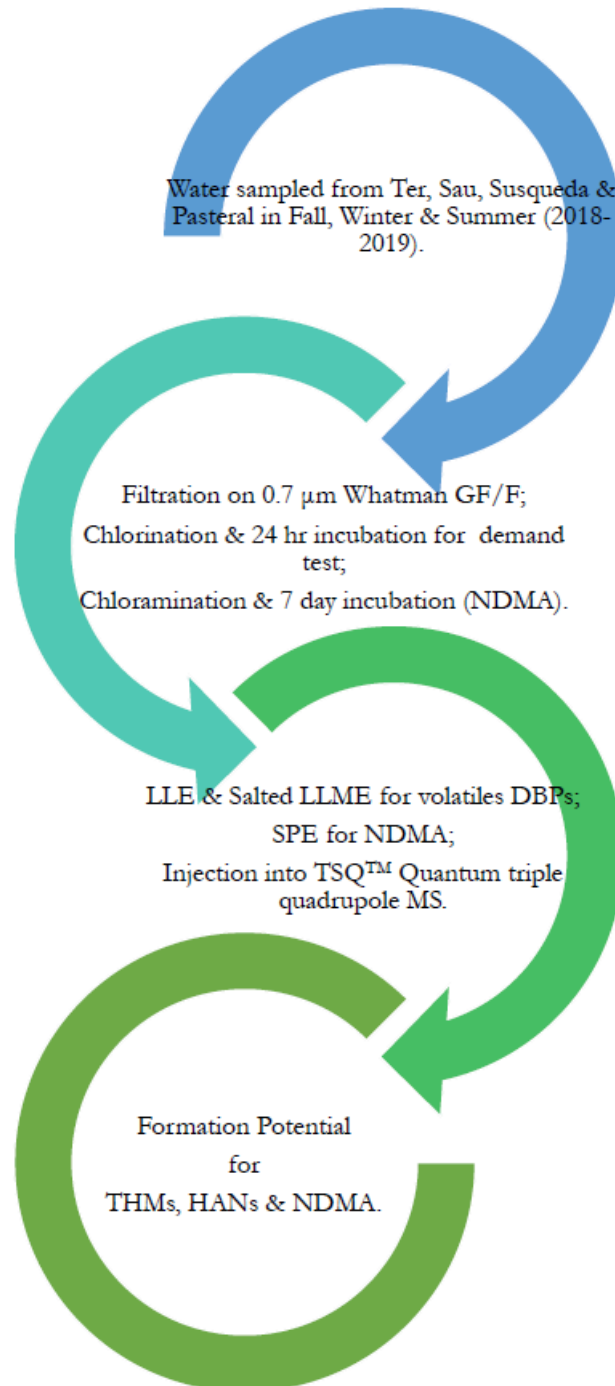


Figure 11. Analytical pipeline for the determination of C- and N-DBP formation potential. NDMA = N-nitrosodimethylamine, LLE = Liquid-Liquid Extraction, LLME = Liquid-Liquid Micro Extraction, DBPs = Disinfection by-products, SPE = Solid Phase Extraction, MS = Mass Spectrometer, THMs = Trihalomethanes and HANs = Haloacetonitriles.

Methodology

On the other hand, samples designated for molecular fingerprinting of DOM were extracted and analyzed on the LTQ Velos™ Orbitrap analyzer to yield sample spectra required in the computation of molecular indices such as DBE, AI_{Mod} and KMD. Molecular indices were used to assign DOM into regions of the van Krevelen diagram. In **Paper III**, DBP formation potential was the main focus of the analysis, supplemented by analyses of bulk DOC, optical indices, physical parameters and nutrients. Analysis of volatile DBP formation potential mirrored the same approach adopted in **Paper II**, with a slight difference in the extraction method (**Paper III** used LLE). On the other hand, determination of NDMA formation potential followed an analytical approach used by Sanchís et al., (2021). Additional parameters analyzed were bulk DOC, DOM optical indices of ultraviolet absorbance (UVA_{254}) and fluorescence (excitation-emission spectra), bromide and nutrients such total phosphorus, nitrate, nitrite, phosphate and ammonium. DOM 3D EEMs were further computationally processed to generate fluorescence indices of FI, BIX and HIX. All key processes in the profiling of DOM are illustrated in Figure 12.

Methodology

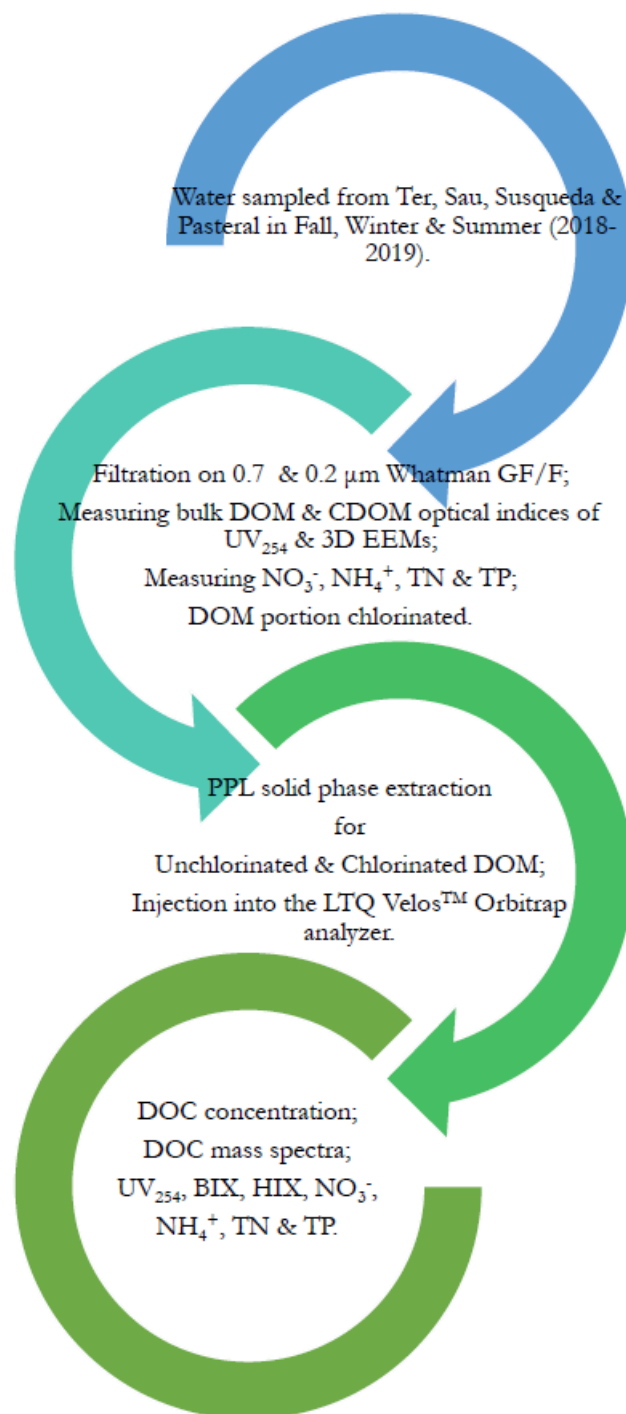


Figure 12. Dissolved organic matter molecular fingerprinting process. DOM = Dissolved organic matter, CDOM = Chromophoric dissolved organic matter, UV_{254} = Ultraviolet absorbance at 254 nm, 3D EEMs = 3 – dimensional Excitation-Emission Matrices, NO_3^- = Nitrate, NH_4^+ = Ammonium, TN = Total Nitrogen, TP = Total phosphorus, PPL = Bond Elut Priority PoLLutant Cartridge, DOC = Dissolved Organic Carbon, BIX = Biological Index and HIX = Humification Index.

Methodology

3.3 Statistical techniques.

A summary of all statistical methods applied across the three chapters of this thesis is presented in Table 15.

Methodology

Table 15. A summary of statistical tests applied in the thesis.

Method	Paper I	Paper II	Paper III	Reference
Descriptive (distribution summaries i.e. mean, median and standard deviation).	✓	✓	✓	Gudivada, 2017.
Brock, Dechert, and Scheinkman (BDS) Test.	✓			Matilla-García et al., 2004.
Non-parametric causality-in-quantiles.	✓			Balcilar et al., 2017; Fan and Li, 1999; Granger, 2008, 1988; Jeong et al., 2012; Silva et al., 2021.
Peak-over threshold (POT).	✓			Ghil et al., 2011; Ribatet, 2011.
Welch's test.	✓			Zheng et al., 2013.
Hedges's g_s .	✓			Lakens, 2013; Thompson, 2007.
Shapiro-Wilk.	✓	✓		King and Eckersley, 2019.
Student's t-tests.		✓		Hoffman, 2019.
Wilcoxon signed-ranks tests.	✓	✓		Scheff, 2016.
Bonferroni – Holm.		✓		Giocalone et al., 2018; McLaughlin and Sainani, 2014.
Principal component analysis.		✓	✓	Ringnér, 2008.
Spearman's correlation.		✓	✓	Puth et al., 2015.

Results and discussion

4 Results and discussion.

4.1 Drastic reduction of nutrient loading to a reservoir alters its resistance to impacts of extreme climatic events.

Munthali E, de Senerpont Domis LN, Marcé R. Drastic reduction of nutrient loading to a reservoir alters its resistance to impacts of extreme climatic events. *Environ Res Lett.* 2022 Aug 1;17(8):084007.

LETTER • OPEN ACCESS

Drastic reduction of nutrient loading to a reservoir alters its resistance to impacts of extreme climatic events

To cite this article: Elias Munthali *et al* 2022 *Environ. Res. Lett.* **17** 084007

View the [article online](#) for updates and enhancements.

You may also like

- [A retrospective study of the 2012–2016 California drought and its impacts on the power sector](#)
Jordan D Kern, Yufei Su and Joy Hill
- [Analysis The Influence of Hydrometeorological Disaster in Kera River Wajo Regency](#)
M R Pratama, F Maricar, R Kamma et al.
- [A compound event-oriented framework to tropical fire risk assessment in a changing climate](#)
Andreia F S Ribeiro, Paulo M Brando, Lucas Santos et al.



Breath Biopsy® OMNI®

The most advanced, complete solution for global breath biomarker analysis

TRANSFORM YOUR RESEARCH WORKFLOW



Expert Study Design & Management



Robust Breath Collection



Reliable Sample Processing & Analysis



In-depth Data Analysis



Specialist Data Interpretation

ENVIRONMENTAL RESEARCH
LETTERS

LETTER

Drastic reduction of nutrient loading to a reservoir alters its resistance to impacts of extreme climatic events

OPEN ACCESS

RECEIVED
18 February 2022REVISED
10 June 2022ACCEPTED FOR PUBLICATION
4 July 2022PUBLISHED
18 July 2022

Original content from this work may be used under the terms of the [Creative Commons Attribution 4.0 licence](#).

Any further distribution of this work must maintain attribution to the author(s) and the title of the work, journal citation and DOI.

Elias Munthali^{1,2,3,4,*} , Lisette N de Senerpont Domis^{3,5} and Rafael Marcé^{1,2}¹ Catalan Institute for Water Research (ICRA), Emili Grahit 101, 17003 Girona, Spain² University of Girona, Girona, Spain³ Netherlands Institute of Ecology (NIOO-KNAW), Droevendaalsesteeg 10, Wageningen, 6708 PB, The Netherlands⁴ Northern Region Water Board, Bloemwater Street, P/Bag 94, Mzuzu, Malawi⁵ Aquatic Ecology and Water Quality Management Group, Department of Environmental Sciences, Wageningen University, Droevendaalsesteeg 3a, 6708 PB, Wageningen, The Netherlands

* Author to whom any correspondence should be addressed.

E-mail: elias.munthali@gmail.com**Keywords:** causality-in-quantiles, drought, resilience, hydrometeorological variables, eutrophicationSupplementary material for this article is available [online](#)**Abstract**

By perturbing ecosystems, extreme climatic events (ECEs) can impair ecosystems' resistance and resilience to other pressures, leading to cascading effects on the continued provision of their ecosystem services. In aquatic ecology, most of the studies linking impacts of perturbations on ecosystems are based on controlled experiments and modeling, rather than real-world data. Using a 55 year dataset of hydrometeorological and reservoir water quality variables from the Ter catchment in Spain, we fill this gap by applying non-linear dynamics and extreme value theory concepts to test whether trophic state modulates reservoir ecosystem's response to ECEs. We show that both Granger causality between hydrometeorological and water quality variables and effects of ECEs on reservoir water quality diminish after drastic reduction in nutrient loading, supporting our hypothesis that the ecosystem's trophic state modulates its resistance to ECEs. Thus, by safeguarding reservoirs from nutrient pollution, water resources managers can ameliorate impacts of ECEs on ecosystem health.

1. Introduction

Eutrophication, i.e. the over enrichment of aquatic ecosystems with nutrients (Carpenter 2005), is one of the major challenges affecting the provision of aquatic ecosystem services. In its fifth global environment outlook report, the United Nations Environment Programme estimates that over 40% of the world's water bodies are experiencing moderate to heavy eutrophication (Xia *et al* 2016). Eutrophication increases drinking water treatment costs through increased organic matter from algal blooms (Foley *et al* 2012) or high iron and manganese concentrations (Munger *et al* 2019) promoted by anoxia (Carpenter 2005) and threatens water-based recreational activities from the proliferation of toxin producing cyanobacteria blooms (Padedda *et al* 2017).

Climate change might worsen eutrophication through increasing water temperature, intense or

reduced precipitation, changes in wind speed and direction and solar radiation (Xia *et al* 2016). As the climate is changing, so too are the occurrence, intensity, magnitude and variability of extreme climatic events (ECEs) such as heatwaves, droughts and heavy precipitation (IPCC 2014). In ecology, ECEs are episodes where unusual values of climate variables result in responses of an ecosystem that are outside the range of normal variability (Smith 2013). By perturbing lake ecosystems, ECEs may impede the provision of aquatic ecosystem services.

The resistance and resilience of lakes to impacts of ECEs may depend more on preceding lake conditions than on characteristics of the extreme events themselves (Thayne *et al* 2021). Resistance is how (in)susceptible the system is to perturbation (Mitra *et al* 2015, Nimmo *et al* 2015), whereas ecological resilience is the extent to which a system recovers (to its original or alternative state) after a perturbation

(Perfecto *et al* 2019, Thayne *et al* 2021), or the amount of disturbance a system can withstand without flipping into another state (Folke *et al* 2004).

The degree to which ECEs impact eutrophication related processes in water bodies varies with flow rate, morphology, geographical location and season, making the generalizations of responses impractical (Delpla *et al* 2009, Mosley 2015). For instance, while high air temperatures have been reported to increase stratification, leading to eutrophication in lakes from internal nutrient loading (Collins *et al* 2019), elsewhere, stratification is reported to have reduced nutrients in surface water layers (Xia *et al* 2016). Droughts have been reported to increase eutrophication and algal blooms in mesotrophic-eutrophic lakes (Lisi and Hein 2019), due to reduced lake volumes, which concentrates nutrients and promotes cyanobacteria blooms (Wright *et al* 2014); and increased frequency of water column mixing events (Soares *et al* 2019), which promotes internal nutrient loading, hence fuelling cyanobacterial blooms. Yet, in the Mediterranean region, lower water levels are reported to have prevented cyanobacteria blooms by promoting the abundance of macrophyte that out-competed the bloom causing cyanobacteria (Bakker and Hilt 2016). While intense rainfall has been reported to decrease algal blooms due to the reduction of light intensity through high turbidity and lake flushing (Xia *et al* 2016), in the floodplain lakes of the lower Dutch Rhine river, high rainfall intensity caused cyanobacterial blooms due to an influx of high nutrient river water through floods (Bakker and Hilt 2016). Also, floods are reported to have caused increased phytoplankton production in Gollinsee Lake due to anoxia-induced phosphorus release from the sediments (Brothers *et al* 2014). Furthermore, for shallow lakes, rising water levels inhibit light transmittance to lake bed macrophytes, leading to loss of their competitive advantage over phytoplankton and the subsequent dominance of cyanobacterial species (Bakker and Hilt 2016).

Such varied responses call for identifying modulators of lake responses to climate extremes, and we posit that lakes' trophic state might be one of the key factors.

The transient nature of most ECEs prompts researchers to rely on information, automatically collected at high frequency in lakes and rivers, to study their impacts on water quality (Marcé *et al* 2016). However, such a reliance on high frequency information is, to some extent, due to lack of appropriate methods to address these questions using low frequency (e.g. monthly) data, thereby side-lining the much more abundant long-term water quality records gathered from many aquatic ecosystems across the world. In addition, the majority of studies linking impacts of ECEs on ecosystems arise from highly controlled experiments (Veraart *et al* 2011) and modelling (Dakos *et al* 2012), hence are far

removed from real-world data (Veraart *et al* 2011). In this study, an innovative time-series approach is applied to long term monthly monitoring data, from a real-world system, to assess the role of the ecosystem's trophic state in modulating the resistance of water quality to impacts of ECEs. We took advantage of data from the long-term water quality monitoring program at Sau Reservoir (Spain) to unravel the behaviour of water quality under ECEs. During the last 55 years, Sau switched between two contrasting trophic states, following a drastic reduction in nutrient loading. We tested the hypothesis that the change in the trophic state of the reservoir significantly increased the resistance of the system's water quality to impacts of ECEs.

2. Data and methods

2.1. Study site

Sau Reservoir (41°58'N; 2°22'E, maximum depth 60 m, area 7.6 km², mean hydraulic retention time of 90 days) is located on the Ter River, in North East Spain. Its catchment area is 1790 km², with forestry (78%), arable farming (16%) and urbanization as the main land uses (López *et al* 2011). Sau Reservoir was built in 1963 for hydropower and water supply to 4 million people in the Barcelona Metropolitan area (Ordóñez *et al* 2010). Sau Reservoir lies downstream from a densely populated area where, between the years of 1991 and 1995, 16 wastewater treatment plants (WWTPs) were built, designed to treat waste water for 530 563 inhabitant-equivalents, representing 95% of the population upstream from the reservoir. The WWTPs were upgraded to secondary treatment during the early 2000s (Marcé *et al* 2006). The eutrophication process of Sau Reservoir is well described in the literature (Armengol *et al* 1986, Vidal and Om 1993, Armengol *et al* 1999, Marcé *et al* 2004, 2008b, 2010), showing an increase in nutrient loads from the 1960s to the early 1990s, accompanied by an increase in pigment concentrations and anoxia extent. From the late 1990s onwards, nutrient loads and anoxia have decreased substantially as a result of the WWTPs built upstream from the reservoir, which entailed a major reduction of organic matter and nutrient loads to the reservoir, with a sharp decrease of ammonium to nitrate molar ratio, from ~2.5 to 0.1 (Marcé *et al* 2008b). These changes improved the trophic status of the system, which previously experienced recurrent episodes of algal blooms and extended deep water anoxia (Ordóñez *et al* 2010).

2.2. Data

This study utilized (a) daily 20 km grid interpolated rainfall (Kg m⁻² s⁻¹) and air temperature (°C) of the Escenarios-PNACC dataset (Herrera *et al* 2012, 2016) from 1950 to 2015; (b) daily observations of hydrological time series of inflows (m³ s⁻¹) and reservoir water level (m.a.s.l) and monthly reservoir water

quality records of temperature (T_w , °C), dissolved oxygen (mg DO/l), nitrate (mg NO_3^- /l), ammonium (mg NH_4^+ /l) and total phosphorus (mg TP/l) from 1964 to 2019, sampled from several depths at the deepest part of the reservoir. The data was supplied by the Ens d'Abastament d'Aigua Ter-Llobregat. Further details on the water quality data are explained elsewhere in Marcé *et al* (2008b), López *et al* (2011) and Šimek *et al* (2011).

2.3. Data analysis

Hydrometeorological and reservoir water quality data were QC/QA checked and several climate indices were calculated before the main analyses were performed. First, the hydrometeorological variables were used as a set of predictors to infer causality, across quantiles, on the epilimnetic and hypolimnetic water quality variables (figure S19, stage 3), before (1963–1991) and after (1997–2015) the building and upgrading of WWTPs (hereafter referred to as before or after WWTPs). Second, climate indices of heatwaves, drought, and wet conditions were coupled to the epilimnetic and hypolimnetic timeseries to assess the behaviour of water quality during ECEs (figure S19, stage 4), before and after WWTPs.

2.3.1. Heatwave indices

Computation of heatwave indices applied the Heatwave Magnitude Index Daily (HWMID) framework (Russo *et al* 2015) by transforming the time series of daily maximum air temperature (T_{max}), from Escenarios-PNACC dataset, into an index. In this framework, a heatwave is defined as a period of 3 consecutive days in which the maximum temperature is above the 90th percentile of the daily maxima in the reference period of 1981–2010, centred on a 31 day window (text S2). HWMID calculations were implemented in the 'extRemes 2.0-0' package (Gilleland and Katz 2016).

2.3.2. Drought/wetness indices

Drought and wetness indices were derived from precipitation, streamflow and reservoir water level time series, using the non-parametric Standardized Drought Analysis Toolbox (Hao and AghaKouchak 2014, Farahmand and AghaKouchak 2015) (text S1), resulting into the non-parametric standardized streamflow index (nSSFI), the non-parametric standardized water level index (nSLI), and the non-parametric standardized precipitation index (nSPI).

2.3.3. Epilimnion and hypolimnion water quality time series

To simplify the analyses, multi-depth water quality time series of T_w , DO, NO_3^- , NH_4^+ , and TP were aggregated into an epilimnion and a hypolimnion time series. To achieve the aggregation, we supplied the LakeAnalyzer code (Read *et al* 2011) with a time series of water temperature and reservoir depth

profiles, from which the water temperature data was measured, for each day of the record. The code used such data to generate the top (metaT) and bottom (metaB) depths (m). The metaT is essentially the end of the epilimnion, whereas the metaB is the beginning of the hypolimnion. Thus, for water temperature and other reservoir water quality variables recorded at the same depth profiles supplied to the numerical code, the average value, on a particular day, was obtained by calculating the mean of all values at depths equal to and above metaT (for the epilimnion) and all values at depths equal to and below the metaB (for the hypolimnion). The output of this analysis was a single value of water quality variable for the epilimnion and hypolimnion for a particular day. Missing data in the monthly time series, for all water quality variables, were filled by interpolating small gaps of up to 3 months.

2.4. Statistical analyses

2.4.1. Granger-causality between hydrometeorological and reservoir water quality variables

This analysis aimed at establishing evidence of causality between the hydrometeorological and epilimnetic & hypolimnetic water quality timeseries, before and after WWTPs. The nonparametric Granger causality in quantiles method (Balcilar *et al* 2017), a non-linear variant of the Granger causality framework (Granger 2008), was applied to derive causal evidence. In the Granger framework, a causal model between two linear stationary time series X_t and Y_t is expressed as:

$$Y_t = \sum_{j=1}^m c_j X_{t-j} + \sum_{j=1}^m d_j Y_{t-j} + \eta_c \quad (1)$$

where η_c is an uncorrelated white-noise series in the complete model. In the model, X_t is assumed to cause Y_t only if it contains information in previous terms that improves the prediction of Y_t and that information is not present in any other predictor (Granger 1988). Based on a linear autoregressive model (Silva *et al* 2021), the bivariate Granger causality arises only if the independent variable in the complete model (equation (1)) brings predictability beyond the one provided by the autocorrelation of the dependent variable at lag 1 and beyond, in the restricted model:

$$Y_t = \sum_{j=1}^m d_j Y_{t-j} + \eta_r \quad (2)$$

where η_r is the uncorrelated white noise series of the restricted model.

Jeong *et al* (2012) extended the Granger framework to analysing causality in different quantiles of a time series, because other studies showed evidence of Granger-causality in tails of a variable distribution even when the mean or median did not show any evidence. They derived a 'distance measure' test statistic (J) for testing Granger causality in quantiles of

a dependent variable (Fan and Li 1999) based on the comparison of the quantiles in the prediction of Y_t with and without considering previous values of X_t .

In this study, the Jeong *et al* (2012) methodology was used to test for evidence of causality between hydrometeorological variables as predictors and epilimnetic and hypolimnetic reservoir water quality time series as response variables, using one predictor and one response variable at a time, before and after WWTPs. Granger causality was calculated at 15 discrete equidistant quantiles between 0 and 1. Significance was set at $p \sim 0.001$ for each analysis, running 1000 instances of the calculations with a random predictor, and comparing this outcome with the actual distribution of J values across quantiles (figure S2(a)). The J statistic, between the predictor and the response variable, is evaluated at 15 quantiles along the range of 0–1, and compared to the area occupied by results coming from 1000 realizations of the same calculation that uses a random predictor instead. We consider occurrence of Granger causality, in a given quantile, when the J statistic calculated with the observed predictor is higher than the maximum of the 1000 values obtained with the random predictor, in the same quantile (figure S2(a)).

In order to synthesize all the information generated by this analysis (1200 quantiles tested across layers, periods, predictors, and response variables), the J statistic was aggregated over three quantile groups (low quantiles: <0.25 ; central quantiles: $0.25\text{--}0.75$; high quantiles: >0.75). This was done by calculating the area in the J statistic plot (figure S2(b)), contained between the J statistic line of the predictor and the response variable and the maximum values of the 1000 realizations with the random predictor. Calculated over the three quantile ranges mentioned above, this procedure results in three areas, one for each quantile range (colored areas in figure S2(b)). These three areas were then normalized by dividing each area by the area under the line defined by the maximum values of the 1000 realizations obtained with the random predictors (grey area in figure S2(b)).

2.4.2. Impacts of ECEs on water quality before and after WWTPs

Impacts of ECEs on water quality were assessed by comparing median values of water quality variables in extreme and non-extreme conditions. The heatwave and drought/wetness indices (see sections 2.3.1 and 2.3.2) were used for the identification of ECEs. For the hydrometeorological events, first, nSSFI, nSLI, and nSPI index values considered beyond normal conditions (below or above zero), were clustered using the peaks-over-threshold (POT) approach (Ghil *et al* 2011), to remove autocorrelation. Then, the distribution of water quality values associated with the ECEs was split twice; first, into periods of before and after WWTPs and, second, corresponding

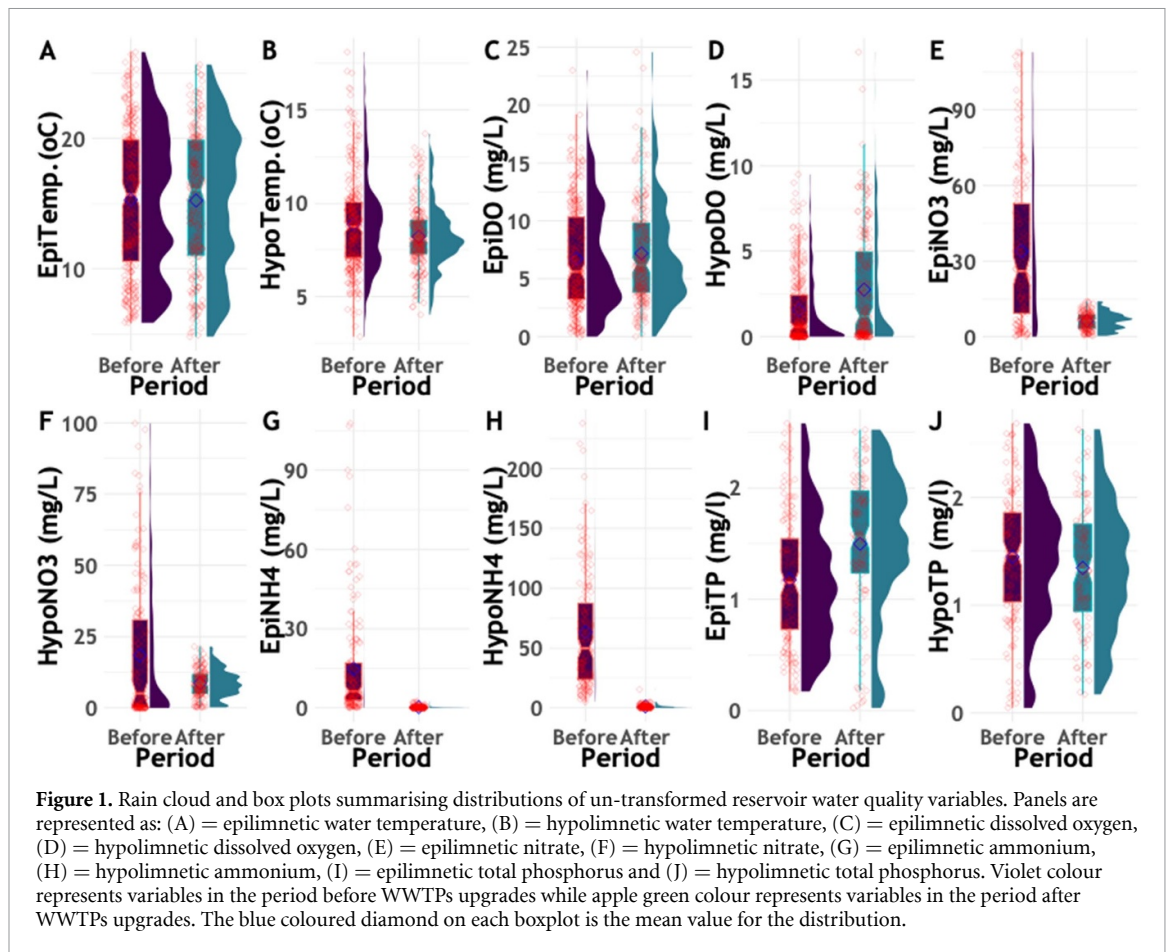
to events with indices beyond the threshold that could be considered extreme (<-1.3 & $>+1.3$) and the rest that could be considered beyond normal but not extreme ($>-1.3 <0$ & $>0 <1.3$). Thereafter, the value of the water quality variables in the epilimnion and hypolimnion, for each event, was calculated as the median of all data corresponding to that type of event. POT analysis was performed using the POT package, version 1.1-7 (Ribatet 2011). The medians of water quality variables, in extreme and non-extreme events, for each period, were compared using the Welch's test (Zheng *et al* 2013) on ranked values, which allows a robust comparison of non-normal distributions with different sample sizes and variances. The results of the Welch's test were reported as p-values, that were supplemented by the Hedges's g_s effect size metric (Lakens 2013). Hedges's g_s is a bias corrected standardized median difference (Cohen's d_s) measuring the degree to which sample results depart from anticipations expressed in the null hypothesis being tested from the data (Thompson 2007). The following Hedges's g_s thresholds for stating effect sizes were adopted: small ($g_s = 0.2$); medium ($g_s = 0.5$) and large ($g_s = 0.8$) (Thompson 2007, Lakens 2013). For heatwaves, the low number of events and their accumulation exclusively in summer months (June–August), required a different approach. A summer was considered to experience a heatwave if the HWMID value exceeded zero on any day during that summer. Thus, a maximum of one heatwave event could be defined for each year. Subsequently, every summer was assigned with values for the water quality variables. Assuming that a heatwave would have a long-lasting imprint on water quality during the summer period, the value of water quality variable in August was assigned. Thus, each summer either had or did not have a heatwave, and was paired with epilimnetic and hypolimnetic water quality data in August, after which, the analyses proceeded in the same way as the analyses examining the impacts of extreme drought and wet events.

All calculations and graphical illustrations were implemented in (R Core Team 2017).

3. Results

3.1. Historical changes in hydrometeorological and water quality variables

The period after WWTPs was characterized by lower medians of precipitation and inflow (Mann Whitney tests on pre-whitened series) than before WWTPs (figure S16, table S1). Interestingly, the frequency of extreme droughts, relative to total drought events, increased after WWTPs, from 5%–10% to 15%–16%, depending on the index (table S3(a)). Summers with heat waves also increased from 35% to 58% after WWTPs (table S3(c)). In contrast, the frequency of extreme wet events decreased after WWTPs,



from 9%–10% to 4%–5%, depending on the index (table S3(b)). Before WWTPs, the median of hypolimnetic DO was 105% lower than its corresponding median after WWTPs. On the other hand, the median of NH_4^+ was 98% higher than its corresponding median after WWTPs. Medians of NO_3^- , TP and T_w were statistically similar between the two periods (figure 1, table S2). In the epilimnion, the medians of NO_3^- and NH_4^+ were 75% and 98%, respectively, lower while the median of TP was 35% higher after WWTPs, compared with their respective medians before WWTPs (figure 1, table S2). Overall, the building and upgrading of WWTPs drastically reduced concentrations of nitrogen compounds in the reservoir, enhanced dissolved oxygen in the hypolimnetic water layers but did not seem to affect total phosphorus.

3.2. Causal relationships between hydrometeorological drivers and water quality variables

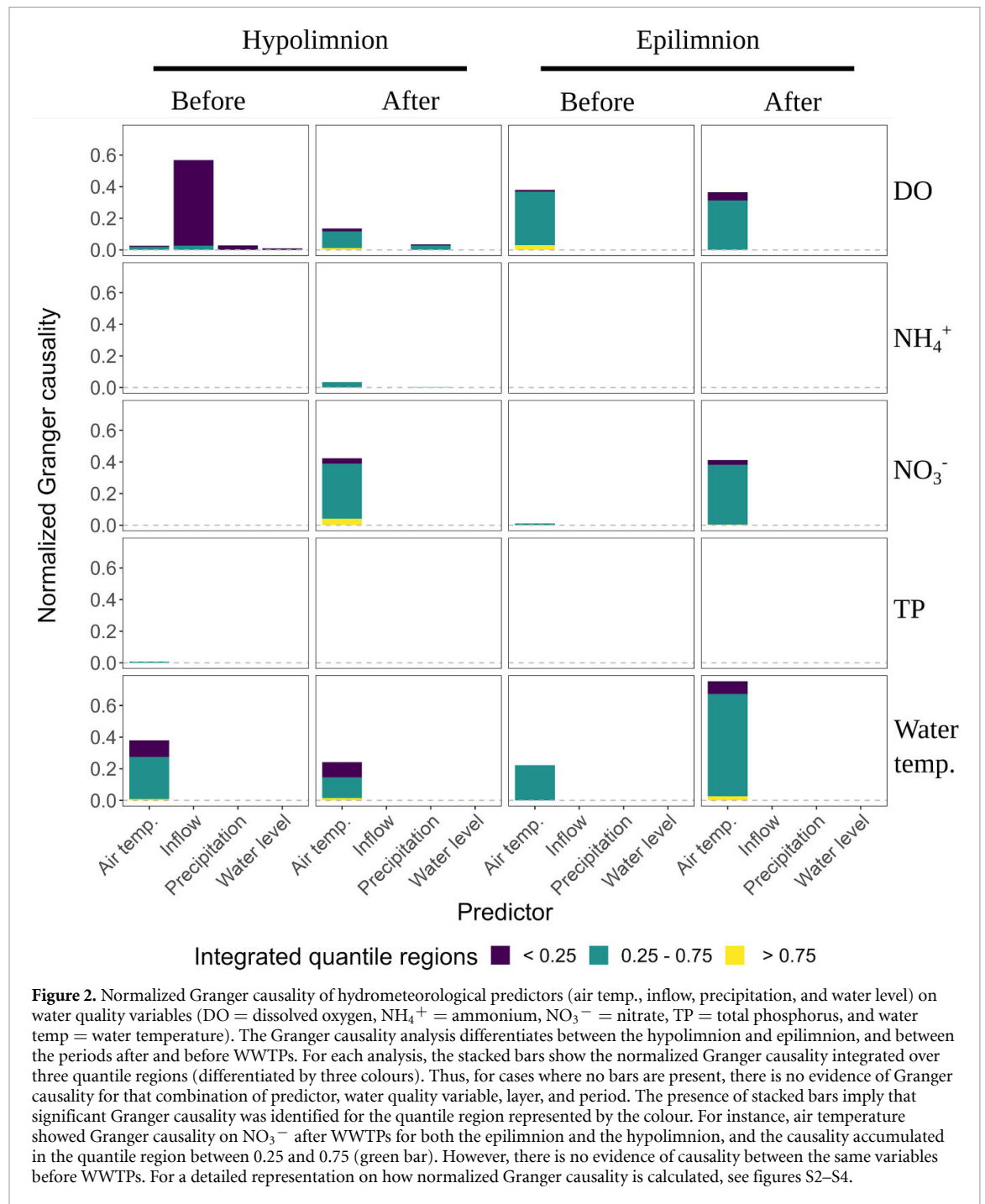
The building and upgrading of WWTPs affected the strength of Granger causality between hydrometeorology and water quality variables (figure 2, supplementary figures S3 and S4). The causal influence of inflow on hypolimnetic DO was particularly strong before WWTPs but disappeared after WWTPs

(figures 2 and S3). In contrast, Granger causality of inflow on DO was altogether absent in the epilimnion in both periods (figures 2 and S4). After WWTPs, hypolimnetic NO_3^- showed causality with T_{max} , covering the whole quantile range, and low to mid quantiles for epilimnetic NO_3^- and DO (figures 2, S3 and S4). TP was unresponsive to the four predictors, in both periods, except for a weak Granger causality with T_{max} before WWTPs (figures 2 and S3). Unsurprisingly, T_{max} showed a strong causality with T_w , which became even stronger in the epilimnion after WWTPs (figures 2, S3 and S4).

3.3. Impact of ECEs on water quality before and after WWTPs

Overall, the hypolimnion manifested a clear reduction of the impacts of ECEs after WWTPs, whereas the response in the epilimnion defied simple description and suggested a complex set of responses both before and after WWTPs (figure 3, tables S4–S8).

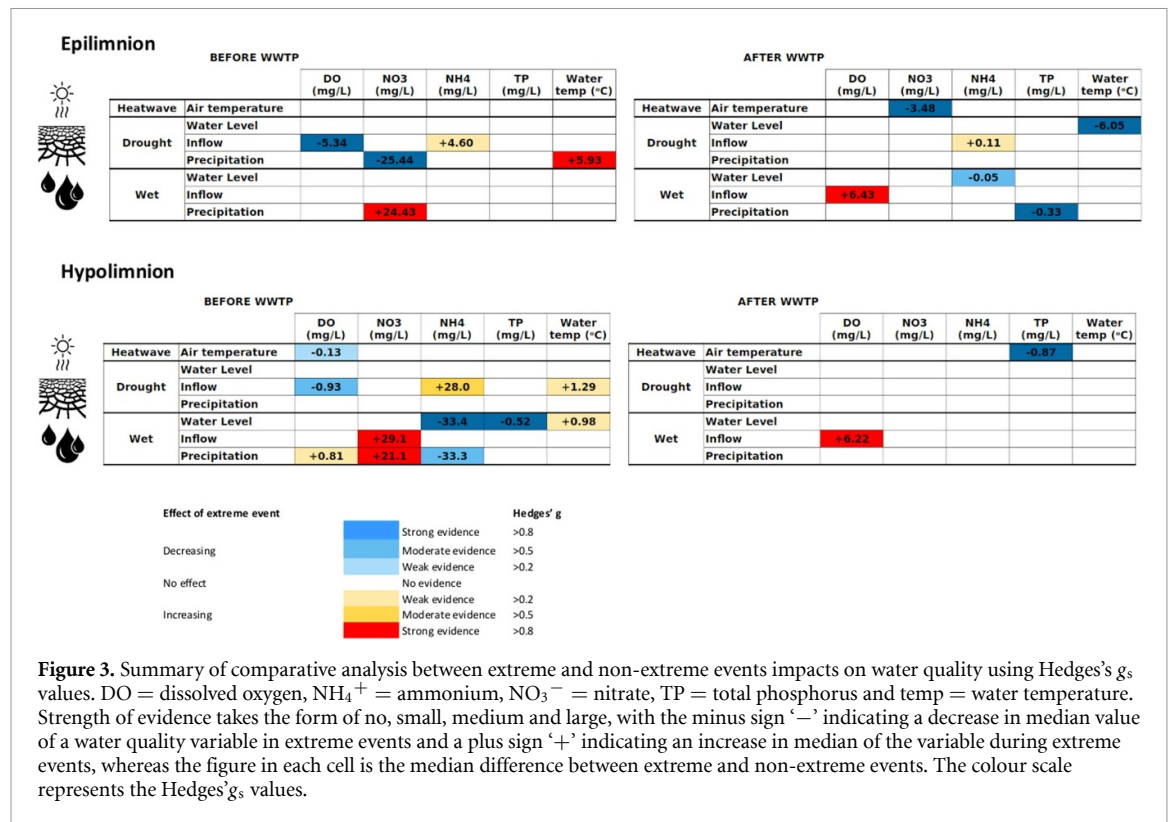
In the hypolimnion, extreme (streamflow) droughts were associated with a lower median of DO (moderate Hedges's g_s , figures 3 and S5, panel (C)) and higher medians for NH_4^+ (moderate Hedges's g_s , figures 3 and S7, panel (C)) and T_w (weak Hedges's g_s , figures 3 and S9, panel (C)) relative to non-extreme drought conditions, before WWTPs. However, after



WWTPs, none of the extreme drought conditions was associated with changes in any water quality variable. Extreme (inflow, water level & precipitation) wet events were associated with higher medians of DO (weak Hedges's g_s , figures 3 and S5, panel (M)), NO_3^- (strong Hedges's g_s , figures 3 and S6, panels (E), (M)) and T_w (weak Hedges's g_s , figures 3 and S9, panel (I)) and lower medians of NH_4^+ (strong & moderate Hedges's g_s , figures 3 and S7, panels (I), (M)) and TP (strong Hedges's g_s , figure 3 and table S7), relative to their respective non-extreme wet conditions, before WWTPs. While similar (streamflow) events were associated with a higher median value of DO (strong Hedges's g_s , figures 3 and S5, panel (F)),

the rest of water quality variables, however, were unaffected by extreme wet conditions after WWTPs. Before WWTPs, summers with heatwaves were associated with a lower median of DO (weak Hedges's g_s , figures 3 and S5, panel (A)) compared to summers without heatwaves, whereas the rest of the water quality variables were unresponsive to heatwaves. After WWTPs, summers with heatwaves were associated with a lower median of TP (strong Hedges's g_s , figure 3 and table S7) compared to summers without heatwaves, whereas no other water quality variable responded to heatwaves (figure 3, tables S4–S8).

In the epilimnion, extreme (inflow & precipitation) drought events were associated with lower



medians of DO (strong Hedges's g_s , figures 3 and S10, panel (C)) and NO_3^- (strong Hedges's g_s , figures 3 and S11, panel (K)) and higher medians of NH_4^+ (weak Hedges's g_s , figures 3 and S12, panel (C)) and T_w (strong Hedges's g_s , figures 3 and S14, panel (K)), relative to their respective non-extreme drought conditions, before WWTPs. Similar extreme (inflow & water level) droughts were not associated with any changes in DO but corresponded to a higher median of NH_4^+ (weak Hedges's g_s , figures 3 and S12, panel (D)) and a lower median of T_w (strong Hedges's g_s , figure 3 and table S8) after WWTPs. Extreme (precipitation) wet events were associated with a higher median of NO_3^- (strong Hedges's g_s , figures 3 and S11, panel (M)) relative to their non-extreme conditions before WWTPs. Similar extreme (precipitation) wet events were not associated with any change in NO_3^- but corresponded to a lower median of TP (strong Hedges's g_s , figure 3 and table S7), after WWTPs. Furthermore, extreme (water level and inflow) wet conditions were associated with a lower median of NH_4^+ (weak Hedges's g_s , figure 3 and table S6) and a higher median value of DO (strong Hedges's g_s , figures 3 and S10, panel (F)), respectively, after WWTPs. Summers with heat waves were associated with a decrease in the median of NO_3^- (strong Hedges's g_s , figures 3 and S11, panel (B)) relative to summers without heat waves after WWTPs, whereas no heat wave effect was observed on any water quality variable before WWTPs (tables S4–S8). After WWTPs, summers with heatwaves were associated with a lower median of TP (strong Hedges's g_s ,

figure 3 and table S7) compared to summers without heatwaves, whereas no any other water quality variable responded to heatwaves (figure 3, tables S4–S8).

4. Discussion

The hypothesis that a change in trophic state of the reservoir increased resistance of the system's water quality to impacts of ECEs, was supported by results from both the Granger causality in quantile (particularly on DO) and behaviour of water quality under ECEs analyses. Both analyses also suggested that the change in resistance of water quality to ECEs, before and after WWTPs, was particularly prominent in the hypolimnion, whereas the epilimnion retained a comparable sensitivity to ECEs. The absence of statistically significant differences in medians of almost all water quality variables (except for DO), between extreme and non-extreme hydrological events, in the hypolimnion, i.e. the absence of impacts of hydrological extreme events on water quality, after WWTPs, is interpreted as increased resistance, following the definitions provided for by Perfecto et al (2019), Thayne et al (2021) and Mitra et al (2015). Conversely, in the epilimnion, the presence of statistically significant differences in medians of water quality variables between extreme and non-extreme hydrological events, in both periods, implies the retention of sensitivity to impacts of those ECEs, hence interpreted as lack of or less resistance. The increased resistance of water quality to ECEs in the hypolimnion, after WWTPs, coincided with an

increased frequency of extreme droughts and heat-waves, making it unlikely that these observations were an artefact caused by a reduction in the number of ECEs.

The differences in behaviour between the epilimnion and hypolimnion suggest that reservoir biogeochemical processes play a fundamental role in defining the response of water quality to ECEs. We postulate that the observed differences in Granger causality and impacts of ECEs on DO concentrations are governed by (a) differing metabolic pathways of anabolism and catabolism dominating the epilimnion and hypolimnion respectively, and (b) stronger water-air coupling in the epilimnion making it susceptible to transient hydrometeorological conditions. The dominance of primary production in the epilimnion may have influenced the observed lack of causality between hydrometeorological variables and water quality (except T_{max}). Phytoplankton is a dynamic component of lake ecosystems, with a generation time in the order of days, whereas the monitoring program in Sau Reservoir was on a monthly basis. While a monthly sampling resolution can capture changes driven by eutrophication (Pomati *et al* 2012, Jochimsen *et al* 2013), it is insufficient to capture the short term dynamics of primary producers, operating on time scales of hours to days. Using monthly data may have limited the capability to predict water quality changes in the epilimnion.

Hypolimnetic water quality was more sensitive to ECEs probably due to the crucial role of organic matter degradation as a pathway for energy and matter flow in deep layers. Organic matter degradation in the hypolimnion is driven by the flow of organic materials from the river and the epilimnion, and the availability of electron acceptors (DO and NO_3^-). Degradation of organic matter does not show short-term oscillations typical of primary production processes (Bastviken *et al* 2004), which may explain our observed causality between inflow and DO.

High causality and the significant impacts of ECEs found in the hypolimnion, before WWTPs, could also be explained by background water quality conditions. Before the operationalization of the WWTPs, the hypolimnion was anoxic, with a very high NH_4^+ to NO_3^- molar ratio (Marcé *et al* 2008b). This scenario suggests a stronger role of organic matter degradation processes that keeps DO levels low. The high NH_4^+ to NO_3^- ratio originated from the fact that most dissolved nitrogen entered the reservoir as NH_4^+ and the presence of anoxia promoted denitrification (Hedin *et al* 1998, Burgin *et al* 2011). Thus, extreme drought conditions would exacerbate respiration processes, hence decreasing DO and increasing NH_4^+ concentrations. In contrast, extreme wet conditions would favour re-oxygenation, increase the NO_3^- load from non-point sources, and dilute NH_4^+ concentrations

from WWTPs. After WWTPs, only re-oxygenation during extreme wet events remained, suggesting a reduced role of respiration processes in the hypolimnion, which was no longer responding to extreme droughts through low DO and high NH_4^+ levels. Thus, the dramatic decrease in NH_4^+ concentration blurred the dilution effect of extreme wet events.

5. Conclusion

This study provides a novel approach to infer causality between hydrometeorological extreme events and reservoir water quality using low-frequency water quality time-series. The non-parametric causality-in-quantile approach to analysing a long term, low frequency dataset, gathered from a real and complex system, shows that trophic state modulates the resistance of reservoir water quality variables to effects of ECEs and that the deeper water layers are more strongly impacted by these events and hence their resistance is more dependent on trophic state. We hypothesise that by keeping reservoirs in good trophic state (mesotrophic to oligotrophic), their water quality becomes more resistant to impacts of extreme events, giving water resources managers some control in dealing with adverse effects of the climate extremes. We conclude that besides improving water quality (in order to achieve UN Sustainable Development Goal 6.3), having water uncompromised by nutrient pollution also ameliorates adverse effects of climate extremes on reservoir water quality.

Data availability statement

The data that support the findings of this study are available upon reasonable request from the authors.

Acknowledgments

This project has received funding from the European Union's Horizon 2020 research and innovation programme under the Marie Skłodowska-Curie Grant Agreement No. 722518.

The authors thank AEMET and University of Cantabria for the data provided for this work (Spain02 v5 dataset, available at www.meteo.unican.es/datasets/spain02). Authors also extend their appreciations to Syed Jawad Hussain Shahzad for providing the R codes through which the non-parametric causality in quantile computational framework was implemented.

ORCID iD

Elias Munthali  <https://orcid.org/0000-0001-6681-4371>

References

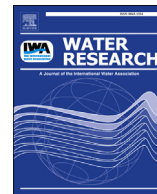
- Armengol J *et al* 1986 Phosphorus budgets and forms of phosphorus in the Sau reservoir sediment: an interpretation of the limnological record *Hydrobiologia* **143** 331–6
- Armengol J *et al* 1999 Longitudinal processes in canyon type reservoirs: the case of sau (N E Spain) eds J G Tundisi and M Straskraba *Theoretical Reservoir Ecology and Its Applications* (Rio de Janeiro: International Institute of Ecology, Brazilian Academy of Sciences and Backhuys Publishers) pp 313–45
- Bakker E S and Hilt S 2016 Impact of water-level fluctuations on cyanobacterial blooms: options for management *Aquat. Ecol.* **50** 485–98
- Balcilar M, Bekiros S and Gupta R 2017 The role of news-based uncertainty indices in predicting oil markets: a hybrid nonparametric quantile causality method *Empir. Econ.* **53** 879–89
- Bastviken D *et al* 2004 Degradation of dissolved organic matter in oxic and anoxic lake water *Limnol. Oceanogr.* **49** 109–16
- Brothers S *et al* 2014 A feedback loop links brownification and anoxia in a temperate, shallow lake *Limnol. Oceanogr.* **59** 1388–98
- Burgin A J *et al* 2011 Beyond carbon and nitrogen: how the microbial energy economy couples elemental cycles in diverse ecosystems *Front. Ecol. Environ.* **9** 44–52
- Carpenter S R 2005 Eutrophication of aquatic ecosystems: bistability and soil phosphorus *Proc. Natl Acad. Sci.* **102** 10002–5
- Collins S M *et al* 2019 Winter precipitation and summer temperature predict lake water quality at macroscales *Water Resour. Res.* **55** 2708–21
- Dakos V *et al* 2012 Methods for detecting early warnings of critical transitions in time series illustrated using simulated ecological data *PLoS One* **7** e41010
- Delpla I *et al* 2009 Impacts of climate change on surface water quality in relation to drinking water production *Environ. Int.* **35** 1225–33
- Fan Y and Li Q 1999 Central limit theorem for degenerate U-statistics of absolutely regular processes with applications to model specification testing *J. Nonparametr. Stat.* **10** 245–71
- Farahmand A and AghaKouchak A 2015 A generalized framework for deriving nonparametric standardized drought indicators *Adv. Water Resour.* **76** 140–5
- Foley B *et al* 2012 Long-term changes in oxygen depletion in a small temperate lake: effects of climate change and eutrophication: oxygen depletion in a small lake *Freshw. Biol.* **57** 278–89
- Folke C *et al* 2004 Regime shifts, resilience, and biodiversity in ecosystem management *Annu. Rev. Ecol. Evol. Syst.* **35** 557–81
- Ghil M *et al* 2011 Extreme events: dynamics, statistics and prediction *Nonlinear Process. Geophys.* **18** 295–350
- Gilleland E and Katz R W 2016 extRemes 2.0: an extreme value analysis package in R *J. Stat. Softw.* **72**
- Granger C W J 1988 Some recent development in a concept of causality *J. Econom.* **39** 199–211
- Granger C W J 2008 Investigating causal relations by econometric models and cross-spectral methods *Econometrica* **37** 424–38
- Hao Z and AghaKouchak A 2014 A nonparametric multivariate multi-index drought monitoring framework *J. Hydrometeorol.* **15** 89–101
- Hedin L O *et al* 1998 Thermodynamic constraints on nitrogen transformations and other biogeochemical processes at soil-stream interfaces *Ecology* **79** 684–703
- Herrera S *et al* 2012 Development and analysis of a 50-year high-resolution daily gridded precipitation dataset over Spain (Spain02): development and analysis of a 50-YEAR High-Resolution Daily Gridded Precipitation Dataset *Int. J. Climatol.* **32** 74–85
- Herrera S, Fernández J and Gutiérrez J M 2016 Update of the Spain02 gridded observational dataset for EURO-CORDEX evaluation: assessing the effect of the interpolation methodology: EURO-CORDEX compliant update of Spain02 *Int. J. Climatol.* **36** 900–8
- IPCC 2014 Climate change 2014 part A: global and sectoral aspects *Climate Change 2014: Impacts, Adaptation, and Vulnerability. Part A: Global and Sectoral Aspects. Contribution of Working Group II to the Fifth Assessment Report of the Intergovernmental Panel on Climate Change* ed C B Field *et al* (New York: Cambridge University Press) p 1132 (available at: papers2://publication/uuid/B8BF5043-C873-4AFD-97F9-A630782E590D)
- Jeong K, Härdle W K and Song S 2012 A consistent nonparametric test for causality in quantile *Econ. Theory* **28** 861–87
- Jochimsen M C, Kümmerlin R and Straile D 2013 Compensatory dynamics and the stability of phytoplankton biomass during four decades of eutrophication and oligotrophication *Ecol. Lett.* **16** 81–89
- Lakens D 2013 Calculating and reporting effect sizes to facilitate cumulative science: a practical primer for t-tests and ANOVAs *Front. Psychol.* **4**
- Lisi P J and Hein C L 2019 Eutrophication drives divergent water clarity responses to decadal variation in lake level *Limnol. Oceanogr.* **64** S49–59
- López P, Marcé R and Armengol J 2011 Net heterotrophy and CO₂ evasion from a productive calcareous reservoir: adding complexity to the metabolism-CO₂ evasion issue *J. Geophys. Res.* **116** 1–14
- Marcé R *et al* 2006 Nutrient fluxes through boundaries in the hypolimnion of Sau reservoir: Expected patterns and unanticipated processes *Limnetica* **25** 527–40
- Marcé R *et al* 2008a The role of allochthonous inputs of dissolved organic carbon on the hypolimnetic oxygen content of reservoirs *Ecosystems* **11** 1035–53
- Marcé R *et al* 2016 Automatic high frequency monitoring for improved lake and reservoir management *Environ. Sci. Technol.* **50** 10780–94
- Marcé R, Comerma M, García J C and Armengol J 2004 A neuro-fuzzy modeling tool to estimate fluvial nutrient loads in watersheds under time-varying human impact *Limnol. Oceanogr.* **2–11** 342–55
- Marcé R, Moreno-Ostos E and Armengol J 2008b The role of river inputs on the hypolimnetic chemistry of a productive reservoir: implications for management of anoxia and total phosphorus internal loading *Lake Reserv. Manage.* **24** 87–98
- Marcé R, Rodríguez-Arias M A, García J C and Armengol J 2010 El Niño Southern Oscillation and climate trends impact reservoir water quality *Glob. Change Biol.* **16** 2857–65
- Mitra C, Kurths J and Donner R V 2015 An integrative quantifier of multistability in complex systems based on ecological resilience *Sci. Rep.* **5** 16196
- Mosley L M 2015 Drought impacts on the water quality of freshwater systems; review and integration *Earth Sci. Rev.* **140** 203–14
- Munger Z W *et al* 2019 Oxygenation and hydrologic controls on iron and manganese mass budgets in a drinking-water reservoir *Lake Reserv. Manage.* **35** 277–91
- Nimmo D G *et al* 2015 Vive la résistance: reviving resistance for 21st century conservation *Trends Ecol. Evol.* **30** 516–23
- Ordóñez J *et al* 2010 On non-Eltonian methods of hunting Cladocera, or impacts of the introduction of planktivorous fish on zooplankton composition and clear-water phase occurrence in a Mediterranean reservoir *Hydrobiologia* **653** 119–29
- Padedda B M *et al* 2017 Consequences of eutrophication in the management of water resources in Mediterranean reservoirs: a case study of Lake Cedrino (Sardinia, Italy) *Glob. Ecol. Conserv.* **12** 21–35
- Perfecto I *et al* 2019 Response of coffee farms to hurricane maria: resistance and resilience from an extreme climatic event *Sci. Rep.* **9** 15668
- Pomati F *et al* 2012 Effects of re-oligotrophication and climate warming on plankton richness and community stability in a deep mesotrophic lake *Oikos* **121** 1317–27

- R Core Team 2017 R: a language and environment for statistical computing (available at: www.r-project.org/)
- Read J S et al 2011 Derivation of lake mixing and stratification indices from high-resolution lake buoy data *Environ. Model. Softw.* **26** 1325–36
- Ribatet M 2011 A user's guide to the pot package (version 1.4) an introduction to the EVT the univariate case pp 1–31
- Russo S, Sillmann J and Fischer E M 2015 Top ten European heatwaves since 1950 and their occurrence in the coming decades *Environ. Res. Lett.* **10** 124003
- Silva F N et al 2021 Detecting climate teleconnections with granger causality *Geophys. Res. Lett.* **48**
- Šimek K et al 2011 The effect of river water circulation on the distribution and functioning of reservoir microbial communities as determined by a relative distance approach *Ecosystems* **14** 1–14
- Smith M D 2013 Extreme climatic events *Climate Vulnerability: Understanding and Addressing Threats to Essential Resources* vol 4 (Cambridge, MA: Academic Press) pp 71–80
- Soares L M V et al 2019 Modelling drought impacts on the hydrodynamics of a tropical water supply reservoir *Inland Waters* **9** 422–37
- Thayne M W et al 2021 Antecedent lake conditions shape resistance and resilience of a shallow lake ecosystem following extreme wind storms *Limnol. Oceanogr.* **67** 1–20
- Thompson B 2007 Effect sizes, confidence intervals, and confidence intervals for effect sizes *Psychol. Sch.* **44** 423–32
- Veraart A J et al 2011 Recovery rates reflect distance to a tipping point in a living system *Nature* **481** 357–9
- Vidal A and Om J 1993 The eutrophication process in Sau Reservoir (NE Spain): a long term study *Int. Ver. Theor. Angew. Limnol.* **25** 1247–56
- Wright B et al 2014 Managing water quality impacts from drought on drinking water supplies *J. Water Supply: Res. Technol. AQUA* **63** 179–88
- Xia R et al 2016 The potential impacts of climate change factors on freshwater eutrophication: implications for research and countermeasures of water management in China *Sustainability* **8**
- Zheng L, Diamond J M and Denton D L 2013 Evaluation of whole effluent toxicity data characteristics and use of Welch's T-test in the test of significant toxicity analysis *Environ. Toxicol. Chem.* **32** 468–74

Results and discussion

4.2 Characterization of organic matter by HRMS in surface waters: Effects of chlorination on molecular fingerprints and correlation with DBP formation potential.

Sanchís J, Jaén-Gil A, Gago-Ferrero P, **Munthali E**, Farré MJ. Characterization of organic matter by HRMS in surface waters: Effects of chlorination on molecular fingerprints and correlation with DBP formation potential. *Water Res.* 2020;176.



Characterization of organic matter by HRMS in surface waters: Effects of chlorination on molecular fingerprints and correlation with DBP formation potential

Josep Sanchís ^{a, b, *}, Adrián Jaén-Gil ^{a, b}, Pablo Gago-Ferrero ^{a, b}, Elias Munthali ^{a, b},
 Maria José Farré ^{a, b, **}

^a Catalan Institute for Water Research (ICRA), Scientific and Technological Park of the University of Girona, H2O Building, C/Emili Grahit, 101, E17003, Girona, Spain

^b University of Girona, 17071, Girona, Spain

ARTICLE INFO

Article history:

Received 8 January 2020
 Received in revised form
 16 March 2020
 Accepted 20 March 2020
 Available online 25 March 2020

Keywords:

High resolution mass spectrometry
 Water chlorination
 Dissolved organic matter
 Disinfection by-products
 van krevelen diagram
 DBP formation Potential

ABSTRACT

In order to understand and minimize the formation of halogenated disinfection by-products (DBPs), it is important to investigate how dissolved organic matter (DOM) contributes to their generation. In the present study, we analysed the DOM profile of water samples from the Barcelona catchment area by high resolution mass spectrometry (HRMS) and we studied the changes after chlorination. Chlorination produced significant changes in the DOM, decreased the average m/z and Kendrick mass defect (KMD) of their spectra and decreased the number and abundance of lignin-like features. The Van Krevelen (VK) fingerprint exhibited several noticeable changes, including the appearance of highly oxidized peaks in the tannin-like region (average O/C, 0.78 ± 0.08), the appearance of features with low H/C and the disappearance of more than half of the lipids-like features. Up to 657 halogenated peaks were generated during sample chlorination, most of which in the condensed hydrocarbons-like and the lignin-like region of the VK diagram.

Around 200 features were found to be strongly correlated ($\rho \geq 0.795$) to the formation potential of trihalomethanes (THMs) and 5 were correlated with the formation potential of haloacetonitrile (HANs). They all were plotted in the lignin fraction of the VK diagram, but both groups of features exhibited different nitrogen content: those features related to HANs FP had at least one nitrogen atoms in their structures, whilst those related to THMs did not.

© 2020 The Authors. Published by Elsevier Ltd. This is an open access article under the CC BY-NC-ND license (<http://creativecommons.org/licenses/by-nc-nd/4.0/>).

1. Introduction

Water chlorination is an efficient and cost-effective method for removing pathogens related to waterborne diseases, such as typhoid fevers, cholera, botulism and dysentery. Its introduction in the early 20th century (EPA,US, 2000; Leal et al., 1909; Traube, 1894) is regarded as a major turning point in the history of water management. Notwithstanding the sanitary benefits of water

chlorination, the addition of disinfectants to water triggers the generation of a myriad of disinfection by-products (DBPs), some of which are carcinogenic and may cause several toxicological effects after chronic consumption, even at trace levels (Font-Ribera et al., 2018; Villanueva et al., 2015). Subsequently, the occurrence of halogenated DBPs derived from water chlorination is an emerging concern and several regulations have been enacted, at domestic and supranational level, to minimize the exposure of population to them (Chinese Department of Health, 2006; Commission, 1998; European Parliament, 2000; NHMRC and NRMCMC, 2011; US-EPA, 2006, 1998).

Brominated and chlorinated trihalomethanes (tribromo-, tri-chloro-, bromodichloro- and dibromochloromethane), also known as THMs, have attracted the most attention of both, academia and regulatory agencies, but the list of identified halogenated DBPs contains hundreds of molecules from families as diverse as

* Corresponding author. Catalan Institute for Water Research (ICRA), Scientific and Technological Park of the University of Girona, H2O Building, C/Emili Grahit, 101, E17003, Girona, Spain.

** Corresponding author. Catalan Institute for Water Research (ICRA), Scientific and Technological Park of the University of Girona, H2O Building, C/Emili Grahit, 101, E17003, Girona, Spain.

E-mail addresses: jsanchis@icra.cat (J. Sanchís), mjfarre@icra.cat (M.J. Farré).

haloacetic acids, haloacetonitriles, halo ketones, haloaldehydes, halonitromethanes, and haloacetamides, among others (Richardson et al., 2008). Recently, the use of non-target analyses has revealed the existence of a high number of previously unknown halogenated DBPs in drinking water (Richardson and Ternes, 2018). High resolution mass spectrometry (HRMS) and ultrahigh resolution mass spectrometry (UHRMS) analyses have contributed to determine their elemental composition through highly accurate m/z measurements (Zhang et al., 2014, 2012; Zhang and Yang, 2018).

Adsorbable Organic Halides (AOX) analyses often report the presence of a significant number of halogenated substances, the structures of which are yet to be elucidated. Hua and Reckhow observed that only ~45% of the total AOX could be explained by the presence of THMs, trihaloacetic acids and dihaloacetic acids (Hua and Reckhow, 2007); while Yeh et al. observed that the percentage of AOX that could be justified by the occurrence of targeted DBPs was rather variable (35–118%) in swimming pool water (Yeh et al., 2014). Finally, an unsettled amount of DBPs, halogenated or not, may be generated during water chlorination without being detectable by AOX or by conventional extraction and detection methods.

Direct measurements of target DBP are undoubtedly useful. However, the prediction of the DBP formation potential (FP) is equally important, particularly in those cases when adjusting the disinfection parameters is viable. In this regard, the characterization of dissolved organic matter (DOM) has proved to be a promising tool. Several DOM properties are closely related to the occurrence of DBP precursors (such as THMs), and/or can be used as descriptors for predicting their FPs. This includes DOM's spectroscopic properties (i.e., ultraviolet absorbance at $\lambda = 254$ nm or SUVA₂₅₄ (Hua et al., 2015) and fluorescent signal (Roccaro et al., 2009)), its composition (e.g., the presence of protein-like organic matter (Chu et al., 2010), aromatic moieties (Hua et al., 2015), and suspended particulate matter (Hou et al., 2018)), and the bulk concentration of DOM, which can be accounted as total organic carbon, TOC (Lee et al., 2009), or as dissolved organic carbon, DOC (Peng et al., 2016).

Commonly, predictive models are multi-parametrical and contemplate a wide range of physicochemical conditions (i.e. the concentrations of halide ions or the pH), as well as chlorination parameters (the reaction time, the temperature, the reagent dose, etc.) (Sohn et al., 2004). However, these models mostly rely on a reduced number of selected DBP. Target methods can hardly cover the quantitative analysis of the whole set of DBPs generated during water chlorination, because of (i) the large number of identified DBPs, (ii) the elevated costs of obtaining high purity standards for all of them, and (iii) the presence of unknown DBPs. Therefore, the risk of DBPs formation should be addressed using more holistic approaches, such as non-target analyses based on HRMS. The advances in mass spectrometry (MS) have allowed the identification of individual components of DOM, which is one of the most heterogeneous mixtures in the environment (Woods et al., 2009). High-field-strength Fourier Transform Ion Cyclotron Resonance MS (FTICR-MS) is capable of unravelling complex DOM mixtures across aquatic systems (Kellerman et al., 2014; Riedel et al., 2016), and Orbitrap-MS has proven to be a valid alternative, as it also is capable of detecting subtle changes in DOM profiles, despite of being able to assign fewer features due to its lower m/z resolution power (Farré et al., 2019; Hawkes et al., 2018, 2016; Patriarca et al., 2018; Yuthawong et al., 2019). The HRMS study of DOM is often complemented with graphical representations ("fingerprinting"), such as van Krevelen (VK) diagrams and Kendrick Mass Defect (KMD) plots, which assist in the visualization, interpretation and comparison of DOM profiles (Andersson et al., 2019; Kim et al., 2003; Lavonen et al., 2013).

The objective of the present study was to investigate the changes of the DOM after water chlorination from a multivariate analysis perspective and exploring the changes in their fingerprint, obtained with Orbitrap-MS, in order to (i) understand which regions of the fingerprints were more susceptible to changes during disinfection reactions and (ii) to identify surrogate features to help predicting DBP formation. To this aim, we extracted and analysed the DOM of ten surface water samples from Barcelona catchment area. DOM was isolated by solid-phase extraction (SPE) and analysed by HRMS. Instrumental analyses were conducted before and after lab scale chlorination tests, in order to track the changes in the DOM. The method was finally validated by investigating the correlation between m/z features and the concentrations of two families of halogenated DBPs: THMs and haloacetonitriles (HANs), chosen because of their relevance, hazardousness and representativeness in real drinking waters.

2. Methods and materials

2.1. Standards and reagents

HANs standards were obtained as a mix at 5.0 mg/mL in acetone (>95% purity) from Cluzeau (Sainte-Foy-la-Grande, France). THMs were purchased as a 1.0 mg/mL mix in methanol (TraceCERT® grade) from Sigma Aldrich. Deuterated 1,2-dibromopropane-d₆ (99.6 atom % D) was purchased from CDN isotopes (Quebec, Canada) and used as internal standard during DBP analyses (see details in the supporting information, Text S1).

Ultrapure water and methanol (Optima® LC/MS grade) were purchased from Fisher Chemical (Geel, BE, and Loughborough, UK, respectively). Methyl *tert*-butyl ether (MTBE, Chromasolv™ Plus), NaClO (6–14% active chlorine, Emplura® grade) and formic acid 98–100% (ACS/Reag. Ph Eur grades) were acquired from Merck (Darmstadt, Germany). Sulphuric acid 95–97% (Reag. Ph Eur grade) was obtained from Scharlau (Sentmenat, Spain).

Na₂SO₄ (≥99.0%, ACS grade) and anhydrous Na₂SO₃ (≥98.0%, BioUltra grade) were obtained from Sigma-Aldrich (ref. 239313). NaOH pellets (PA/ACS/ISO grades) were acquired from Panreac (Barcelona, Spain). KH₂PO₄ (ACS/ISO/Reag. Ph Eur grades) was obtained from Scharlau (Sentmenat, Spain). Nitrogen (99.995% purity) for extract drying was purchased from Abelló Linde (Barcelona, Spain).

Glass fibre filters (GF/F, 47 mm diameter, 0.7 μm mesh size) were obtained from Whatman (Little Chalfont, UK). Bond Elut PPL ("Priority PolLutant") cartridges (500 mg, 3 mL; reference 12105006) were purchased from Agilent Technologies (Santa Clara, CA, USA).

2.2. Sampling

The sampling was carried out in the Ter River Basin (NE of Spain, see Fig. 1) in February 2019. Samples were taken from the Ter River itself and from the three reservoirs Sau, Susqueda and Pasteral (169 hm³, 233 hm³ and 2 hm³, respectively). These reservoirs are relevant for the Barcelona metropolitan area, as they supply around 170 hm³ drinking water (Agència Catalana de l'Aigua, 2015)) through interbasin water transfer, and present certain differences in term of morphology, trophic state and residence time (with Sau being the most eutrophic water body of the reservoirs chain), all of which may have a potential impact in the nature and concentration of DBP precursors.

Samples were taken at the specified depth (see Table 1) in amber glass bottles letting no head-space. The bottles were immediately refrigerated and transported to the laboratory, where they were processed within 24 h following the general procedure



Fig. 1. Maps Location of the sampled waterbodies in Catalonia (a). The Ter River basin is highlighted in red (b and c), while the Sau, Susqueda and Pasteral reservoirs are highlighted in blue, black and green, respectively (c). Geodata obtained from Catalan Water Agencies website (Agència Catalana de l'Aigua, 2019). (For interpretation of the references to colour in this figure legend, the reader is referred to the Web version of this article.)

schematized in Fig. 2 and described in the following sections.

2.3. Batch chlorination experiments

The DBP FP was assessed following a modified version of the standard method (APHA, 2005) to obtain between 1 and 3 mg/L of residual free chlorine after 24 h of contact time as described in previous studies (De Vera et al., 2015; Doederer et al., 2014; Liu et al., 2016). Once determined, the specific chlorine dose was added to a 250 mL head-space free glass bottle. The bottle was capped and stored in an incubator, in the dark, at 25 °C, for 24 h. The residual chlorine was measured with a photometric cuvette test kit (LCK 310, Hach Lange GmbH, Düsseldorf, Germany). After measuring their chlorine content and quenching them with ascorbic acid, samples were extracted for DBP analysis (see Text S1 in the Supporting information) and for DOM characterization (see section 2.4).

2.4. Extraction of PPL-DOM

Raw and quenched chlorinated samples were processed following the same protocol. Aliquots of each sample were filtered through 0.7 µm mesh-size glass fibre filters and extracted by SPE according to the method described elsewhere (Dittmar and Koch, 2006) with minor modifications, as previously implemented in Farré et al. (2019). Briefly, 250 mL of filtered sample were acidified to pH 2.0 by adding formic acid drop by drop and were extracted with a PPL cartridge (500 mg, 3 mL). These cartridges contain a styrene-divinylbenzene polymeric phase, modified with a non-polar surface. Recent studies have shown that PPL-cartridges are found among the most efficient sorbents for DOM components, enabling a broad coverage of DOM constituents in one single collection while avoiding substantial leaching (Li et al., 2017), and

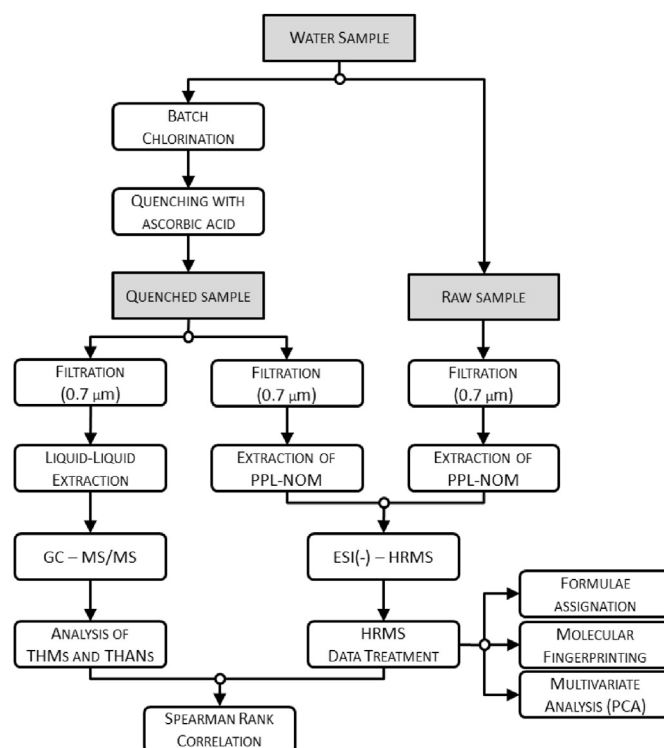


Fig. 2. Scheme of the experimental design.

Table 1
Summary of analysed samples.

Code	Water Body	Depth (m)	TOC (mg/L)	TN (mgN/L)	THMS FP (µg/L)	HANS FP (µg/L)
TER	Ter River	0	2.0	5.7	33.6	1.4
PAS	Pasteral Reservoir	0	3.7	2.7	55.8	3.1
SAU_0m	Sau Reservoir	0	2.7	4.2	38.5	2.9
SAU_13m	Sau Reservoir	13	2.9	4.2	48.1	3.1
SAU_30m	Sau Reservoir	30	2.7	4.8	56.9	5.1
SAU_42m	Sau Reservoir	42	2.7	5.0	44.7	4.5
SUS_0m	Susqueda Reservoir	0	3.3	2.7	57.8	3.6
SUS_8m	Susqueda Reservoir	8	3.3	2.7	57.5	3.9
SUS_35m	Susqueda Reservoir	35	3.4	2.7	73.6	4.8
SUS_80m	Susqueda Reservoir	80	3.4	2.7	75.9	5.1

they have been extensively applied to extract and characterize DOM from several water matrices (Arakawa et al., 2017; Farré et al., 2019; Li et al., 2016).

Prior to the extraction, cartridges were washed thrice with 1.0 mL of methanol and were soaked overnight with 1.0 mL of methanol. After being conditioned, the cartridges were washed with one volume of formic acid 0.1% v/v. Then, samples were loaded, under vacuum at approx. 2 mL/min. Salts were rinsed off with 3.0 mL of formic acid 0.1% v/v and cartridges were dried under vacuum for 15 min. Finally, the elution was carried out with 2.00 mL of methanol. The extracts were collected in previously tared liquid chromatography (LC) vials. 500 μ L of the methanolic extracts were diluted 1:1 with ultrapure water and stored at -20 °C until their instrumental analysis.

Procedural blanks consisting of 250 ± 1 mL of ultrapure water were filtered and extracted following the same protocol and in parallel with real samples analyses. Quenched chlorination blanks were also processed.

2.5. Instrumental analysis of organic matter

Analyses were carried out by HRMS using a LTQ Velos™ from Thermo Scientific (San José, CA, USA), using a hybrid Linear Ion Trap – Orbitrap analyser.

Extracts of blanks, raw samples and chlorinated samples were infused into the mass spectrometer at a flow of 8 μ L/min. The ionisation was performed with an electrospray ionisation (ESI) source operating in negative polarity. The instrumental parameters were set as follows: the capillary voltage was set at -3.1 kV; the capillary and the source heater temperatures were maintained at 275 °C and 45 °C, respectively; the sheath gas and the auxiliary gas flows were set at 28 and 5 a.u., while the sweep gas flow was turned off. 300 scans were acquired for every sample. Spectra were acquired in full-scan mode, with a resolution of 100,000 Da FWHM and a m/z range of 100–1000. The following signals were used as lock masses for internal calibration during spectra acquisition: m/z 369.08272 ($[\text{C}_{16}\text{H}_{17}\text{O}_{10}]^-$), m/z 397.11402 ($[\text{C}_{18}\text{H}_{21}\text{O}_{10}]^-$) and m/z 423.12967 ($[\text{C}_{20}\text{H}_{23}\text{O}_{10}]^-$).

2.6. Data treatment: determination of elemental compositions and fingerprinting

An averaged spectrum of each sample was obtained using the software Xcalibur™ 2.2 (Thermo Scientific). Spectra were exported as Excel Workbook format files and processed with a custom script in R (v. 3.5) using the RStudio environment (v. 1.1.463, R-Tools Technology).

The elemental compositions of the spectral signals were tentatively determined with functions from the R package MFAssignR (Schum et al., 2019). The workflow is fully described in the Supporting information (Text S2). Briefly, m/z signals were assigned to elemental formulae ($\text{CHON}_{0-5}\text{S}_{0-2}\text{Cl}_{0-2}\text{Br}_{0-2}$) using the function MFAssignR:MFAssign with the following restrictions: maximum tolerable m/z error: ± 1.0 ppm; m/z range: 100–1000; charge: only monocharged formulae were considered; range of O/C: 0–1.0; range of H/C: 0.3–2.5; range of DBEO: 1–10.

The presence of features with ^{32}S , ^{35}Cl or ^{79}Br atoms was double-checked by searching isotopologues containing ^{34}S , ^{37}Cl and ^{81}Br , respectively. The experimental $^{37}\text{Cl}/^{35}\text{Cl}$, $^{34}\text{S}/^{32}\text{S}$ and $^{81}\text{Br}/^{79}\text{Br}$ ratios were compared to natural isotopic ratios as detailed in Text S2.

The final list of formulae was represented in VK diagrams based on their O/C, H/C and N/C ratios. They were classified in predefined categories according to their location in the VK diagram. These classification criteria, detailed in Table S1, have been accepted in a multitude of recent DOM studies, although it should be noted that

they may not fully describe the structural diversity of the peaks that are contained in each compositional space, and it should be stressed that further structural elucidation should be performed to identify each substance and to unambiguously classify it (Schymanski et al., 2014).

The aromaticity index (AI) of each formula was calculated according to equation (1) (Koch and Dittmar, 2006):

$$AI = (1 + C - O - S - 0.5 \times H) / (C - O - S - N - P) \quad (1)$$

The double bond equivalent (DBE), normalized by the number of carbons, was calculated according to equation (2) (Melendez-Perez et al., 2016):

$$DBE / C = [1 + 0.5 \times (2 \times C - H + N)] / C \quad (2)$$

Masses were transformed to Kendrick mass (KM) values by normalizing their IUPAC (^{12}C based) mass by 1.0011178 ($\text{KM}_{\text{CH}_2} = 1.0000000$) (Kendrick, 1963). Then, KMD were calculated as in equation (3) (Hughey et al., 2001) and KMD plots were presented:

$$KMD = KM - [KM] \quad (3)$$

where KM and $[KM]$ stand for the Kendrick mass (KM) and the truncated Kendrick mass values, respectively.

2.7. Data treatment: descriptive statistics and multivariate analyses

Statistics and multivariate analyses were performed using the R packages *vegan* (Oksanen et al., 2019), *stats* (R Core Team, 2019) and *FactoMineR* (Lê et al., 2008), among others.

The data normality was checked using Shapiro–Wilk tests and the null hypothesis (H_0) was rejected when $p \leq 0.05$. Differences among raw samples and chlorinated samples were investigated using paired difference tests: Non-normally distributed data was assessed with Wilcoxon signed-ranks tests, while paired Student's t -tests were applied to normal datasets. In both cases, differences were considered significant at p values ≤ 0.05 . In multiple comparisons, p values were corrected using the Bonferroni–Holm method (p_{BH}).

A matrix was built containing the total set of formulae assigned in raw and chlorinated samples and their spectral abundances. Multivariate analyses (Principal Component Analysis, PCA) were carried out in order to elucidate trends among samples and to identify those features that better distinguished chlorinated from raw samples. Correlation among variables and principal components (PC) was quantified as the square cosine of their angle in the loading graph, which may range from 0 ($\alpha = 90^\circ$: orthogonal, totally uncorrelated) to 1 ($\alpha = 0^\circ$: parallel, perfectly correlated).

The dissimilarity among samples was explored using the function `vegdist` and represented with hierarchical clustering dendrograms (`stats:heatmap`).

The statistical dependence between THMs/HANs and the HRMS formulae were assessed in terms of Spearman's rank correlation. Only those formulae that had been detected in 70% of the samples were considered. Those pairs of variables that were correlated with Spearman's rank coefficients $\rho \geq 0.625$ and $\rho \geq 0.795$ were considered to be “statistically correlated” and “strongly correlated”, respectively. These thresholds imply correlations with statistical significances of, approximately, $p \leq 5.00 \times 10^{-2}$ and $p \leq 5.00 \times 10^{-3}$, respectively, according to equation (4):

$$t \approx \rho \sqrt{\frac{n-2}{1-\rho^2}}, \quad (4)$$

where n is the number of observations and t is the Student's T statistic, which is justified by the permutation argument (Kendall and Stuart, 1969).

2.8. Additional precautions and safety considerations

In order to avoid sample contamination, all the lab glassware employed in these experiments had been thoroughly cleaned as follows: (i) washed with detergent, (ii) immersed in nitric acid bath (HNO_3 10% v/v) overnight, (iii) rinsed with ultrapure water, (iv) rinsed with acetone and (v) thoroughly dried with nitrogen. Experiments were carried out under extraction fume.

3. Results and discussion

3.1. Data treatment and study of samples by hierarchical clustering analysis

Table 2 summarises the main characteristics of the infused spectra, distinguishing raw samples from chlorinated ones. As can be seen, the infusion of the raw extracts offered spectra with $\sim 85,000 \pm 3000$ peaks, most of which (approx. 90%) were found to be noise and low-intensity artefacts. Once cleaned up, spectra presented an average number of monoisotopic signals of $\sim 6800 \pm 200$. This value was relatively constant through the different samples and no significant trends were observed linking the number of signals and the sampling point or the depth of the water column.

Peaks were tentatively assigned to empirical formulae using a custom R script (Text S2). A matrix was built containing the detected features and their respective abundance in each sample. Samples were classified according to their dissimilarity by measuring their "Cao dissimilarity index" (CYd) (Cao et al., 1997). The resulting dendrogram (Fig. S1) satisfactorily grouped samples according to their two main characteristics: matrix (river or reservoir water) and water body (Ter River, Sau, Susqueda and Pasteral). Once the chlorinated samples were introduced into the model (Fig. S2), the type of treatment (raw or chlorinated sample) became the primary factor that drove the clustering. This highlights that water chlorination had a decisive impact in the elemental composition of DOM.

Table 2

Comparison of data obtained in raw and chlorinated samples. Normally distributed data are highlighted with a dagger ([†]), and those groups of data that are statistically different ($p < 0.0500$) are highlighted with an asterisk (*).

	Raw samples (average \pm st.dev)	Chlorinated (average \pm st.dev)	Ratio of averages	Comparison
No. of peaks (including noise)	85,530 \pm 3013	88,430 \pm 1675	1.04	$p = 0.0124$ *
Noise threshold (a.u.)	65 \pm 12 [†]	59 \pm 11 [†]	0.90	$p = 0.1931$
Number of signals ($S/N > 3$)	8475 \pm 297 [†]	9559 \pm 721 [†]	1.13	$p = 0.0003$ *
Intensity (a.u.)	6017 \pm 1,188 [†]	4288 \pm 837 [†]	0.71	$p = 0.0003$ *
m/z	394.2714 \pm 14.3346	357.9249 \pm 8.4016 [†]	0.91	$p = 0.0051$ *
Intensity-weighted m/z	360.9601 \pm 9.2478	344.5953 \pm 14.8454	0.95	$p = 0.0051$ *
KMD	0.3263 \pm 0.0155	0.2983 \pm 0.0110 [†]	0.91	$p = 0.0051$ *
Intensity-weighted KMD	0.2983 \pm 0.0110	0.2773 \pm 0.0078	0.97	$p = 0.0093$ *
O/C	0.4264 \pm 0.0139 [†]	0.4290 \pm 0.0120	1.01	$p = 0.5093$
Intensity-weighted O/C	0.4291 \pm 0.0182 [†]	0.4321 \pm 0.0172	1.01	$p = 0.5093$
H/C	1.0589 \pm 0.0248 [†]	1.0480 \pm 0.0254	0.99	$p = 0.2846$
Intensity-weighted H/C	1.1774 \pm 0.0197 [†]	1.1703 \pm 0.0121	0.99	$p = 0.2846$
N/C	0.0438 \pm 0.0058	0.0457 \pm 0.0079	1.04	$p = 0.3576$
Intensity-weighted N/C	0.0080 \pm 0.0070	0.0089 \pm 0.0084	1.12	$p = 0.1676$

3.2. Effects of chlorination to organic matter spectra and its KMD

As can be seen in Table 2, the number of signals detected by ESI(−) significantly increased after chlorination ($p = 0.0003$), from 8475 ± 297 to 9559 ± 721 . Accordingly, the number of peaks corresponding to monocharged molecules/fragments with exclusively ^{12}C atoms increased from 6832 ± 235 to 8418 ± 247 ($p < 10^{-4}$).

In parallel, the average intensity of these peaks decreased significantly (ratio, 0.71; $p = 0.0003$). More precisely, their average m/z , weighted by intensity, decreased from $m/z \sim 361 \pm 9$ to $\sim 345 \pm 15$ ($p = 0.0051$). These changes imply the breakage of larger molecules to create smaller, less intense, transformation products, which can be attributed to miscellaneous oxidative degradation reactions of DOM.

KMD plots corroborated a decrease in the average molecular mass of the spectra after chlorination. The number of peaks with $m/z > 600$ was lower after chlorination, as it is exemplified in Fig. 3, which shows the KMD plots of the Pasteral extracts, and the dataset was compressed in a narrower m/z window. This behaviour was observed in the whole set of KMD plots (which are collected in Fig. S3 in the Supporting Information).

In parallel, the average KMD and the intensity-averaged KMD decreased significantly ($p = 0.0051$ and $p = 0.0093$) after chlorination. As a general rule, low KMD values can be related to hydrogen-poorer molecules (e.g. aromatic compounds to the detriment of aliphatic molecules) (Nikolic, 2011) and more oxidized molecules (see Table S2). From a mechanistic point of view, this can be justified by the oxidation of hydroxyls to carbonyls, which produces aldehydes and ketones from primary and secondary alcohols, respectively (Deborde and Von Gunten, 2008; Hu et al., 2003). KMD can also decrease as a result of the hydrolysis of ketones, which produces highly oxidized molecules, such as monohydroxyl acetone, dihydroxyl acetone and, ultimately, lactate. Finally, a decrease in the KMD can be justified because of the introduction of halogens to the molecular structure.

3.3. Determination of elemental composition and effects of chlorination on the VK regions

The DOM profiles of every sample were fingerprinted building VK diagrams based on the O/C and H/C ratios of each identified formulae. Fig. S4, in the Supplementary Information, collects the whole set of VK diagrams, detailing the intensity and m/z of each feature with the size and colour of the scattered points. VK diagrams were used to automatically classify the detected features in VK compositional spaces defined by their O/C and H/C ratios. Fig. 3 shows a VK diagram of Pasteral's surface water (raw and

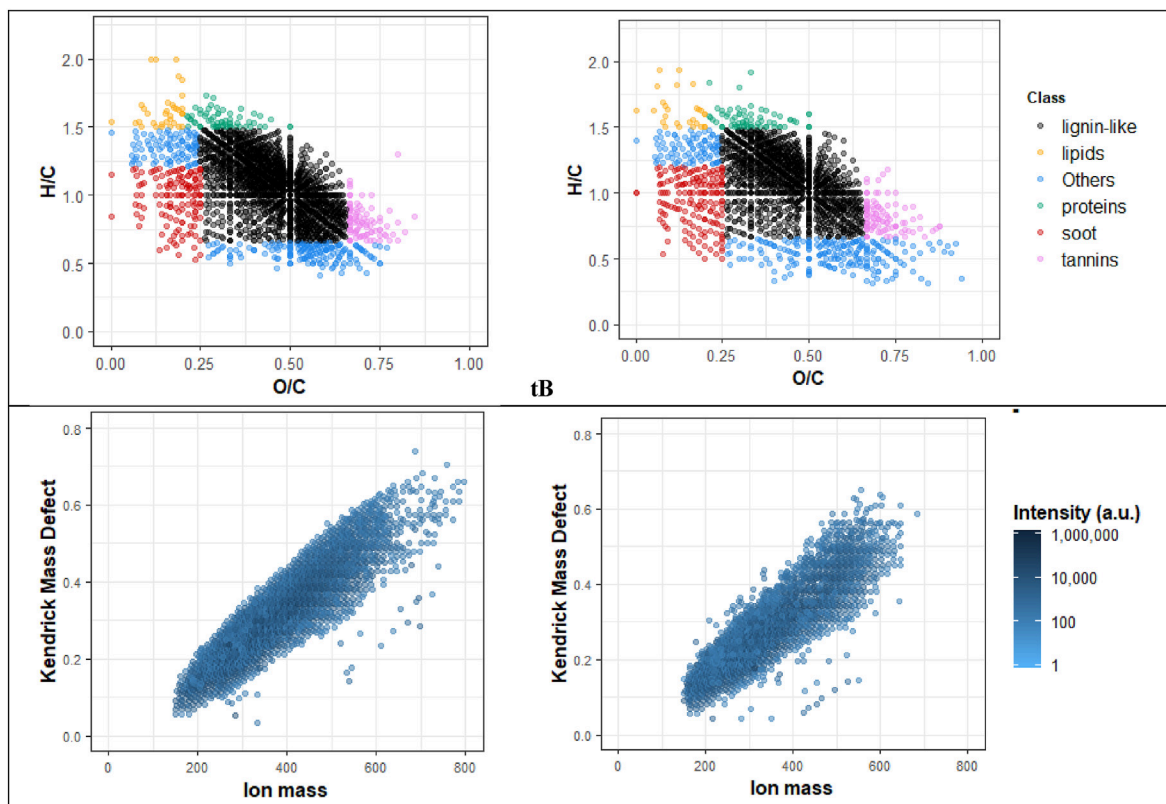


Fig. 3. VK diagrams (above) and KMD plots (above) of Pastoral reservoir, analysed before (left) and after (right) chlorination.

Table 3
Behaviour of features during chlorination according to their compositional space in the VK diagrams. Those values highlighted in bold font belong to the predominant trend in their corresponding VK region.

Subset of m/z	Main VK regions	Number of signals that ...					TOTAL
		... disappeared	... decreased	... didn't change	... increased	... appeared	
Full dataset	Lignin-like	1225 (34.7%)	1005 (28.5%)	606 (17.2%)	91 (2.58%)	605 (17.1%)	3532
	Tannin-like	59 (18.1%)	11 (3.37%)	108 (33.1%)	18 (5.52%)	130 (39.9%)	326
	Condensed hydrocarbon-like	203 (33.7%)	15 (2.49%)	188 (31.2%)	54 (8.96%)	143 (23.7%)	603
	Lipids-like	69 (56.6%)	13 (10.7%)	18 (14.8%)	0 (0%)	22 (18.0%)	122
	Protein-like	55 (23.7%)	40 (17.2%)	50 (21.6%)	12 (5.17%)	75 (32.3%)	232
Subset of halogenated signals	Lignin-like	129 (21.29%)	0 (0%)	16 (2.64%)	1 (0.17%)	460 (75.91%)	606
	Tannin-like	0 (0%)	0 (0%)	0 (0%)	0 (0%)	31 (100%)	31
	Condensed hydrocarbon-like	138 (49.11%)	1 (0.36%)	37 (13.17%)	2 (0.71%)	103 (36.65%)	281
	Lipids-like	43 (63.24%)	0 (0%)	8 (11.76%)	0 (0%)	17 (25%)	68
	Protein-like	27 (36%)	0 (0%)	2 (2.67%)	0 (0%)	46 (61.33%)	75

chlorinated extracts, on the left and right respectively), with their compositional spaces clearly delimited.

Table 3 summarises the relative abundances and behaviour of the features according to their location in the VK diagram. The group of features placed in the “lignin-like features” region was the most abundant in the analysed samples: 3532 peaks belonged to this compositional space, equivalent to ~73% of the total number of signals, which can be expected in common natural surface waters with no significant anthropogenic pressure. In freshwater DOM’s VK diagram, this compositional space is shared by lignin-related molecules (and ESI fragments), and signals related to carboxyl-rich alicyclic molecules (CRAM) (Lam et al., 2007), among other organic substances with the same compositional characteristics.

The number of features assigned to this region decreased both, in absolute and in relative terms, after chlorination. 1005 signals corresponding to lignin-like signals decreased their intensity

according to Wilcoxon signed-rank tests or paired Student’s *t* tests ($p < 0.05$) and 1225 signals disappeared completely. The abundances of 606 lignin-like features were unaltered. Only 91 features increased their concentrations and, finally, 665 new lignin-like peaks appeared after chlorination. Among the latter, 460 were assigned to halogenated formulae.

While the lignin-like region decreased in terms of intensity and number of peaks, it is no less true that it accumulated the highest number of new signals, highlighting the complex behaviour of the lignin fraction during water chlorination. Lignin is composed of complex mixtures of polymers based on phenol moieties (guaiacyl, syringyl, and *p*-hydroxyphenylpropane aromatic moieties) (National Research Council (US) Safe Drinking Water Committee, 1979), the chlorination of which is an importance source of halogenated DBPs (Chuang et al., 2015).

Lyon et al. (2014) also observed that fluorescent organic matter

corresponding to the Parallel Factor Analysis (PARAFAC) component C3 showed the highest reactivity to chlorination. This component is associated with terrestrial humic-like features, which include lignin breakdown products, degraded lignin and other aromatic intricate molecules. In the present work, the number of peaks tentatively related to soil-derived humics (defined in Šantl-Temkiv et al. (2013) as $H/C < 1.5$ and $A.I. \leq 0.5$) also decreased from 2088 ± 133 to 1768 ± 157 ($p = 0.0001$) and their average intensity decreased by 65%.

On another note, the number of peaks assigned as “lipids-like features” and “condensed hydrocarbon-like features” also decreased: Most lipids-like signals that had been detected in the original samples (56.6%) disappeared after chlorination and 11.0% significantly decreased their abundance ($p < 0.05$). Similarly, 203 condensed hydrocarbon-like features disappeared during the treatment. A total number of 143 new features appeared in the condensed hydrocarbon-like compositional compartment (103 of which, halogenated) and 22 new signals (17 of which halogenated) appeared in the lipid-like compartment after chlorination.

Chlorination caused the appearance of several new highly-oxidized molecules, with O/C ratios >0.75 (see, for example, the VK diagram in Fig. 3), a significant part of which belonged to the “tannin-like” region. The average O/C ratio of those new formulae was 0.767 ± 0.080 , significantly higher ($p < 10^{-4}$) than the O/C ratio of the other registered tannin-like m/z (0.717 ± 0.054). In parallel, the appearance of features with low H/C ratios ($H/C < 0.5$) was also observed.

In the present work, up to 1061 halogenated formulae were determined (Table 3). Naturally occurring halogenated features were mainly detected in the condensed hydrocarbon-like and the lignin-like regions (178 and 146 features, respectively). The number of halogenated features increased, as expected, after chlorination, particularly in the lignin-like region (460 new halogenated features). Up to 657 new halogenated features were identified. These halogenated signals are highlighted in the individual VK diagrams of each sample (Fig. S5 and Fig. S6 for chlorinated and brominated features, respectively). As it can be seen, most of the halogenated features occurring in natural water samples presented an O/C ratio lower than 0.5, while a large fraction of the new formulae was significantly more oxidized ($O/C > 0.5$).

The analytical method that was employed in the present work, involving SPE under vacuum and ESI-HRMS analysis, is not able to efficiently capture and detect commonly targeted DBPs because of their physicochemical properties (i.e., their typically high vapour pressures and low molecular masses). Therefore, those peaks assigned as halogenated features in the present study likely were related to semivolatiles/non-volatile components/fragments of halogenated DOM, which can occur by progressive halogenations of the α -carbon of carbonyl groups (for example, the haloform reaction (Morris, 1975)), the addition of halogens to double bonds (Ghanbari et al., 1983) and the additions to phenol rings (Gallard and von Gunten, 2002).

3.4. Classification of samples by PCA

In order to better understand the factors that differentiated raw and chlorinated samples, a PCA model was performed. The first two principal components, PC1 and PC2, explained 70.9% of the data variance (see the main PCs' eigenvalues in Fig. S7). The separation of chlorinated and untreated samples was clear in the score graphs of PC1 vs. PC2 (Fig. 4): chlorinated samples were related to low values of PC1 while untreated samples were related to high values of PC1.

PC1 was, therefore, closely related to samples chlorination. This PC was correlated with the concentrations of certain substances

with the general formula $C_xH_yO_z$. Table S3 lists those formulae the abundances of which were more closely correlated to PC1. As can be observed, their H/C ratios were compressed between 0.75 and 1.14 and their O/C ratios ranged from 0.37 to 0.52. This is in agreement with Zhang et al. (2012), where it was observed that “compounds with low degree of oxidation are more reactive toward free chlorine” in surface water from Shanghai and Beijing catchment areas. These features, located in the lignin-like region of the VK-diagram, presented negligible nitrogen content, a DBE/C that ranged from 0.50 to 0.69 and an $A.I. \leq 0.38$. Their DBE/C ratio suggests the prevalence of aromatic structures ($0.66 > DBE/C > 0.5$) and, according to their H/C ratio and A.I., they can be tentatively related to “soil-derived humics” ($H/C < 1.5$ and $A.I. \leq 0.5$), as discussed by Šantl-Temkiv et al. (2013). However, further instrumental analyses should be carried out to unambiguously identify their structure.

These tentatively identified humic-derived lignin-like features were highly intercorrelated (see Fig. S8) and sample chlorination decreased their intensity in a statistically significant manner (p_{BH} values from 0.0009 to 0.0020). The Ter sample exhibited a particularly low abundance of these lignin-like features, with concentrations of the same order than chlorinated samples, which probably justified its clustering in the dendrogram (Fig. S2).

3.5. Disinfection by-products formation potentials and correlation with HRMS features

The THMs and HANs FPs are detailed in Table 1. THMs FP ranged from 33.6 to 75.9 $\mu\text{g/L}$ ($54 \pm 14 \mu\text{g/L}$) and HANs FP ranged between 1.4 and 5.1 $\mu\text{g/L}$ ($3.8 \pm 1.2 \mu\text{g/L}$). The concentrations of THMs were, as expected, significantly higher than those of HANs and followed a relatively close trend: THMs FP and HANs FP correlated with a Pearson correlation coefficient of $r = 0.59$ and a Spearman's rank correlation coefficient of $\rho = 0.74$.

TOC was a satisfactory predictor of THMs FP ($R^2 = 0.60$ and $\rho = 0.77$) but it was a poor predictor of HANs FP ($R^2 = 0.24$ and $\rho = 0.37$). Similarly, total nitrogen (TN) inversely correlated with THMs FP ($R^2 = 0.58$ and $\rho = -0.63$) but was inadequately correlated with HANs FP ($R^2 = 0.14$ and $\rho = -0.09$). These results highlight the need to find more specific descriptors to understand the behaviour of a wider range of halogenated DBPs.

THMs FP and HANs FP were compared to the intensities of those features that had been detected in, at least, 7 of the 10 analysed samples. A total of 516 peaks were found to be correlated to THMs FP ($\rho \geq 0.625$) and 208 of them were “strongly correlated” ($\rho \geq 0.795$). Fig. 5 shows the VK diagram with signals being represented as a function of ρ : As can be seen, the strongly correlated signals were mostly lignin-like and/or CRAM features (H/C ranging from 0.71 to 1.6 and O/C ratios ranging from 0.06 to 0.52). These features also presented a very low nitrogen content (average $N/C = 0.005$). Interestingly, the formulae in Fig. 5, strongly correlated to THMs FP, are similar to those peaks (listed in Table S3) that, in the multivariate analyses, were good descriptors of chlorinated/raw samples differentiation. However, while both sets of peaks are similar in composition ($C_xH_yO_z$), in H/C ratio and in O/C ratio, only four particular features ($C_{13}H_{18}O_3$, $C_{15}H_{14}O_5$, $C_{15}H_{16}O_5$ and $C_{15}H_{20}O_3$) were members of both lists, corroborating that the formation of THMs is just one of the multiple reactions that affect DOM during water chlorination.

Similar to our results, Hua et al. (2015) also observed that the formation of THMs and trihaloacetic acids during water chlorination was correlated with $SUVA_{254}$, which is related to the presence of UV-absorbing molecules containing labile double bonds and aromatic rings. Also Beauchamp et al. (2018) found that differential UV absorbance and THMs concentrations were correlated with $0.62 \leq R^2 \leq 0.99$. Our results suggest that these compounds were

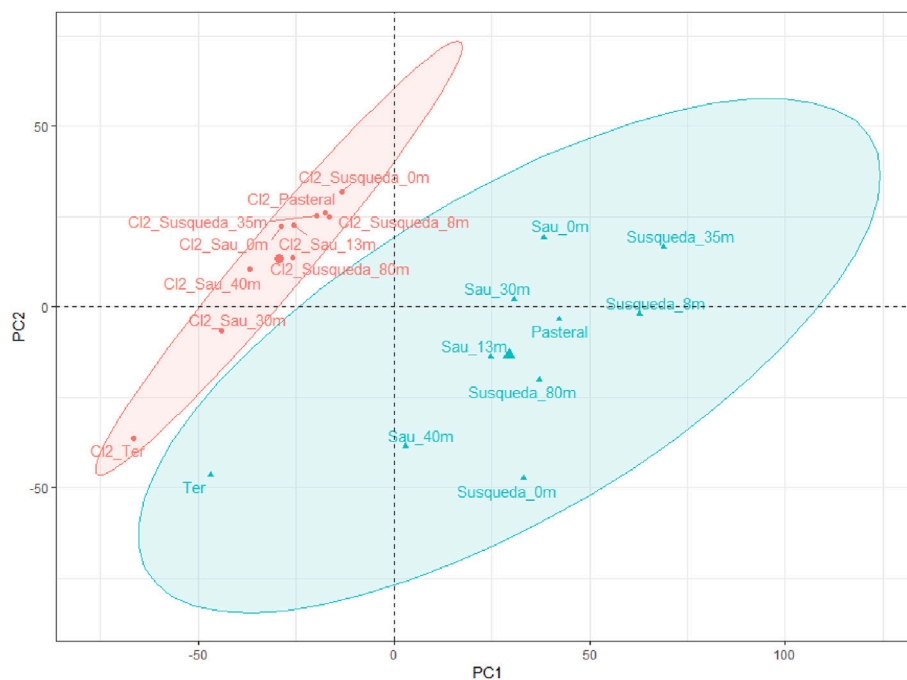


Fig. 4. Score plot of PCA with scaled data, representing samples in PC1 and PC2 axis. Chlorinated samples are presented in red while untreated samples are displayed in blue. The two ellipses were generated automatically highlighting an area with a 95% of possibility to containing samples of their kind. (For interpretation of the references to colour in this figure legend, the reader is referred to the Web version of this article.)

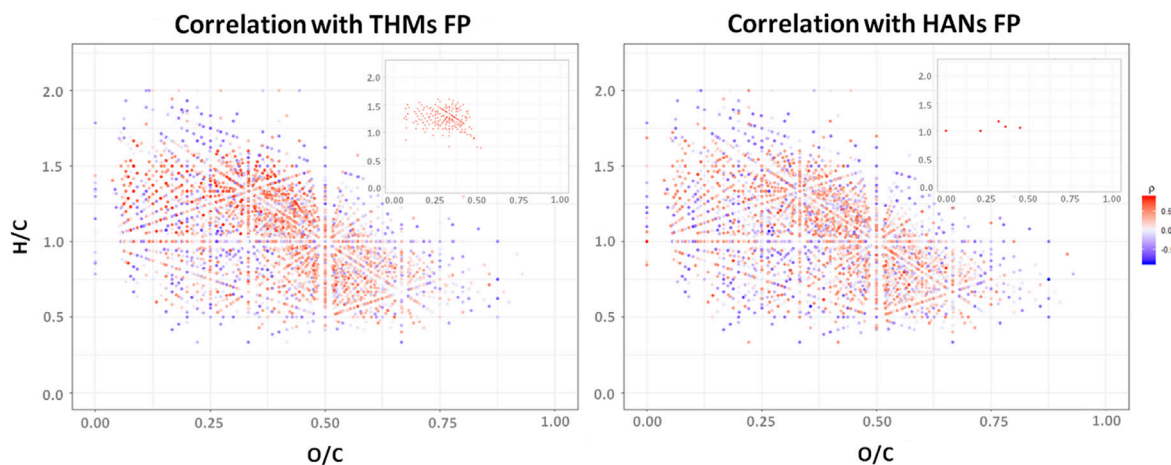


Fig. 5. VK diagram showing the Spearman correlation of THMs (left) and HANs (right) the formulae that were found in 70% of the samples. The miniature diagrams located the up-right corners content only those features that were strongly ($\rho \geq 0.795$) correlated to THMs and HANs FP, respectively.

particularly located in the lignin-like compositional space of the van Krevelen's DOM.

On another note, the number of features that correlated with HANs FP was smaller: 60 features were correlated with statistical significance ($\rho \geq 0.625$) and only 5 could be labelled as "strongly correlated" ($\rho \geq 0.795$). These features are good candidates to be used as predictors of HANs FP. These peaks were plotted in the lignin-like region, in a relatively narrow H/C vs O/C window (H/C ranging from 1.0 to 1.2 and O/C ranging from 0.19 to 0.49). Their nitrogen content was significantly high (average N/C = 0.49), which is expected considering that HANs are N-containing DBPs. The ternary VK diagrams illustrate the differences in the N/C ratios of those features related to THMs FP (Fig. S9) and those related to HANs FP (Fig. S10).

4. Conclusions

The primary object of this study was to better understand how water chlorination modified the DOM fingerprint obtained with HRMS. Our results obtained from 10 different surface water samples showed that water chlorination indeed produced significant changes in the composition of DOM and, subsequently, in their HRMS spectra. Chlorinated samples exhibited signals with smaller m/z, lower KMD and, as expected, a higher number of halogenated features. These changes were studied at fingerprinting level and from a multivariate analyses perspective.

Significant changes were observed in the regions of the lignin-like/CRAM, the soil humics, and that of the fatty acids-like features, where several signals disappeared during chlorination, as

well as in the condensed hydrocarbon region, where several new features, halogenated and non-halogenated, were detected. In the tannin-like region, several new features, primarily corresponding to highly oxidized formulae, were also detected. Overall, these changes sufficed to successfully classifying the analysed samples according to their treatment status (raw/chlorinated) and origin, via hierarchical clustering analyses and PCA scores.

In PCA it was concluded that sample chlorination (related to PC1) primarily involved a decrease in the concentration of non-nitrogenized lignin-like features. Up to 28 signals were found to be highly correlated ($\cos^2(\alpha) > 0.95$) to sample chlorination, all of them with $C_xH_yO_z$ formulae and elemental ratios (H/C & O/C) characteristic from the ligning-like/CRAM compositional space.

Finally, we identified two regions of the VK diagram, located within the lignin-like features, that were strongly correlated ($\rho \geq 0.795$) to THMs and HANs FP. To the best of our knowledge, the present work is the first to identify surrogates of HAN generation during chlorination of surface waters.

Recently, Williams et al. (2019) described how removing certain portions of the DOM pool, in real plant scale, significantly decrease the formation potential of individual chlorinated and brominated DBPs. Our study is a promising step towards identifying appropriate surrogates capable of anticipating the risk that chlorination DBPs may pose for the final consumer, offering a higher selectivity than unspecific techniques, such as TOC and SUVA₂₅₄ measurements. Moreover, this approach may be applied to other relevant families of DBPs. However, with the current results, it is not possible to unambiguously affirm that these features correspond to direct precursors of THMs and HANs. Further studies should be conducted (e.g. using liquid chromatography coupled to HRMS, curated libraries and standards) to univocally identify compounds and individually test their DBPs FP. However, our results clearly indicate that these two regions of the VK diagram play a crucial role in the formation of the analysed DBPs.

Declaration of competing interest

The authors declare that they have no known competing financial interests or personal relationships that could have appeared to influence the work reported in this paper.

Acknowledgements

This project was funded by the Spanish Ministry of Science, Innovation and Universities, AEI-MICIU, and the European Fund for Regional Development under the National Program for Research Aimed at the Challenges of Society, through the project NDMA_Predict (CTM 2017-85335-R); and by the European Union's Horizon 2020 Research and Innovation Programme, through the MANTELITN Project (Grant No: 722518). The authors thank Generalitat de Catalunya through Consolidated Research Group ENV 2017 SGR 1124 and Tech 2017 SGR 1318. ICRA researchers thank funding from CERCA program. MJF acknowledges her Ramón y Cajal fellowship (RyC-2015-17108), from the AEI-MICIU; AJG acknowledges his PhD scholarship from AGAUR (2019FI_B2_00202), from the Government of Catalonia; PGF acknowledges SmartWorkflow, which has received funding from the European Union's Horizon 2020 R&I program under grant 791235. The authors would like to thank the staff of the Scientific and Technical Services of the Catalan Institute of Water Research for their invaluable assistance.

Appendix A. Supplementary data

Supplementary data to this article can be found online at <https://doi.org/10.1016/j.watres.2020.115743>.

References

- Agència Catalana de l'Aigua, 2019. Agència Catalana de l'Aigua Website: Generalitat de Catalunya [WWW Document]. <http://aca.gencat.cat/ca/laigua/consulta-dades/geoserveis/>. accessed 10.15.19.
- Agència Catalana de l'Aigua, 2015. Pla de gestió del districte de conca fluvial de Catalunya 2016-2021.
- Andersson, A., Harir, M., Gonsior, M., Hertkorn, N., Schmitt-Kopplin, P., Kylin, H., Karlsson, S., Ashiq, M.J., Lavonen, E., Nilsson, K., 2019. Waterworks-specific composition of drinking water disinfection by-products. *Environ. Sci. Water Res. Technol.* 5, 861–872.
- APHA, PHA, 2005. AWWA and WPCF Standard Methods for the Examination of Waters and Waste Waters.
- Arakawa, N., Aluwihare, L.I., Simpson, A.J., Soong, R., Stephens, B.M., Lane-Coplen, D., 2017. Carotenoids are the likely precursor of a significant fraction of marine dissolved organic matter. *Sci. Adv.* 3, e1602976.
- Beauchamp, N., Lafamme, O., Simard, S., Dorea, C., Pelletier, G., Bouchard, C., Rodriguez, M., 2018. Relationships between DBP concentrations and differential UV absorbance in full-scale conditions. *Water Res.* 131, 110–121.
- Cao, Y., Williams, W.P., Bark, A.W., 1997. Similarity measure bias in river benthic Aufwuchs community analysis. *Water Environ. Res.* 69, 95–106.
- Chinese Department of Health, 2006. GB5749-2006. P.R. China Standards for Drinking Water Quality.
- Chu, W.-H., Gao, N.-Y., Deng, Y., Krasner, S.W., 2010. Precursors of dichloroacetamide, an emerging nitrogenous DBP formed during chlorination or chloramination. *Environ. Sci. Technol.* 44, 3908–3912.
- Chuang, Y.-H., McCurry, D.L., Tung, H., Mitch, W.A., 2015. Formation pathways and trade-offs between haloacetamides and haloacetaldehydes during combined chlorination and chloramination of lignin phenols and natural waters. *Environ. Sci. Technol.* 49, 14432–14440.
- Commission, E., 1998. Council Directive 98/83/EC of 3 November 1998 on the quality of water intended for human consumption. *Off. J. Eur. communities* 41, 32–54.
- De Vera, G.A., Stalter, D., Gernjak, W., Weinberg, H.S., Keller, J., Farré, M.J., 2015. Towards reducing DBP formation potential of drinking water by favouring direct ozone over hydroxyl radical reactions during ozonation. *Water Res.* 87, 49–58.
- Deborde, M., Von Gunten, U.R.S., 2008. Reactions of chlorine with inorganic and organic compounds during water treatment—kinetics and mechanisms: a critical review. *Water Res.* 42, 13–51.
- Dittmar, T., Koch, B.P., 2006. Thermogenic organic matter dissolved in the abyssal ocean. *Mar. Chem.* 102, 208–217.
- Doederer, K., Gernjak, W., Weinberg, H.S., Farré, M.J., 2014. Factors affecting the formation of disinfection by-products during chlorination and chloramination of secondary effluent for the production of high quality recycled water. *Water Res.* 48, 218–228.
- EPA., U.S., 2000. The History of Drinking Water Treatment.
- European Parliament, 2000. Directive 2000/60/EC of the European Parliament and of the Council of 23 October 2000 establishing a framework for Community action in the field of water policy. *Off. J. Eur. Parliam.* L327, 1–82.
- Farré, M.J., Jaén-Gil, A., Hawkes, J., Petrovic, M., Catalán, N., 2019. Orbitrap molecular fingerprint of dissolved organic matter in natural waters and its relationship with NDMA formation potential. *Sci. Total Environ.* 670, 1019–1027.
- Font-Ribera, L., Gràcia-Lavedan, E., Aragonés, N., Pérez-Gómez, B., Pollán, M., Amiano, P., Jiménez-Zabala, A., Castaño-Vinyals, G., Roca-Barceló, A., Ardanaz, E., 2018. Long-term exposure to trihalomethanes in drinking water and breast cancer in the Spanish multicase-control study on cancer (MCC-Spain). *Environ. Int.* 112, 227–234.
- Gallard, H., von Gunten, U., 2002. Chlorination of phenols: kinetics and formation of chloroform. *Environ. Sci. Technol.* 36, 884–890.
- Ghanbari, H.A., Wheeler, W.B., Kirk, J.R., 1983. Reactions of chlorine and chlorine dioxide with free fatty acids, fatty acid esters, and triglycerides. *Water Chlorination Environ. Impact Heal. Eff.* 4.
- Hawkes, J.A., Dittmar, T., Patriarca, C., Tranvik, L., Bergquist, J., 2016. Evaluation of the Orbitrap mass spectrometer for the molecular fingerprinting analysis of natural dissolved organic matter. *Anal. Chem.* 88, 7698–7704.
- Hawkes, J.A., Radoman, N., Bergquist, J., Wallin, M.B., Tranvik, L.J., Löfgren, S., 2018. Regional diversity of complex dissolved organic matter across forested hemiboreal headwater streams. *Sci. Rep.* 8, 16060.
- Hou, M., Chu, W., Wang, F., Deng, Y., Gao, N., Zhang, D., 2018. The contribution of atmospheric particulate matter to the formation of CX3R-type disinfection by-products in rainwater during chlorination. *Water Res.* 145, 531–540.
- Hu, J., Cheng, S., Aizawa, T., Terao, Y., Kunikane, S., 2003. Products of aqueous chlorination of 17 β -estradiol and their estrogenic activities. *Environ. Sci. Technol.* 37, 5665–5670.
- Hua, G., Reckhow, D.A., 2007. Comparison of disinfection byproduct formation from chlorine and alternative disinfectants. *Water Res.* 41, 1667–1678.
- Hua, G., Reckhow, D.A., Abusallout, I., 2015. Correlation between SUVA and DBP formation during chlorination and chloramination of NOM fractions from different sources. *Chemosphere* 130, 82–89.
- Hughey, C.A., Hendrickson, C.L., Rodgers, R.P., Marshall, A.G., Qian, K., 2001. Kendrick mass defect spectrum: a compact visual analysis for ultrahigh-resolution broadband mass spectra. *Anal. Chem.* 73, 4676–4681.
- Kellerman, A.M., Dittmar, T., Kothawala, D.N., Tranvik, L.J., 2014. Chemodiversity of

- dissolved organic matter in lakes driven by climate and hydrology. *Nat. Commun.* 5, 3804.
- Kendall, M.G., Stuart, A., 1969. Inference and Relationship (Hafner).
- Kendrick, E., 1963. A mass scale based on CH₂= 14.0000 for high resolution mass spectrometry of organic compounds. *Anal. Chem.* 35, 2146–2154.
- Kim, S., Kramer, R.W., Hatcher, P.G., 2003. Graphical method for analysis of ultrahigh-resolution broadband mass spectra of natural organic matter, the van Krevelen diagram. *Anal. Chem.* 75, 5336–5344.
- Koch, B.P., Dittmar, T., 2006. From mass to structure: an aromaticity index for high-resolution mass data of natural organic matter. *Rapid Commun. Mass Spectrom.* 20, 926–932.
- Lam, B., Baer, A., Alaei, M., Lefebvre, B., Moser, A., Williams, A., Simpson, A.J., 2007. Major structural components in freshwater dissolved organic matter. *Environ. Sci. Technol.* 41 (24), 8240–8247. <https://doi.org/10.1021/es0713072>.
- Lavonen, E.E., Gonsior, M., Tranvik, L.J., Schmitt-Kopplin, P., Köhler, S.J., 2013. Selective chlorination of natural organic matter: identification of previously unknown disinfection byproducts. *Environ. Sci. Technol.* 47, 2264–2271.
- Lê, S., Josse, J., Husson, F., 2008. FactoMineR: an R package for multivariate analysis. *J. Stat. Software* 25, 1–18.
- Leal, J.L., Fuller, G.W., Johnson, G.A., 1909. The Sterilization Plant of the Jersey City Water Supply Company at Boonton. *Amer. Water Works Assoc. NJ*.
- Lee, J., Ha, K.-T., Zoh, K.-D., 2009. Characteristics of trihalomethane (THM) production and associated health risk assessment in swimming pool waters treated with different disinfection methods. *Sci. Total Environ.* 407, 1990–1997.
- Li, Y., Harir, M., Lucio, M., Kanawati, B., Smirnov, K., Flerus, R., Koch, B.P., Schmitt-Kopplin, P., Hertkorn, N., 2016. Proposed guidelines for solid phase extraction of Suwannee River dissolved organic matter. *Anal. Chem.* 88, 6680–6688.
- Li, Y., Harir, M., Uhl, J., Kanawati, B., Lucio, M., Smirnov, K.S., Koch, B.P., Schmitt-Kopplin, P., Hertkorn, N., 2017. How representative are dissolved organic matter (DOM) extracts? A comprehensive study of sorbent selectivity for DOM isolation. *Water Res.* 116, 316–323.
- Liu, P., Farré, M.J., Keller, J., Gernjak, W., 2016. Reducing natural organic matter and disinfection by-product precursors by alternating oxic and anoxic conditions during engineered short residence time riverbank filtration: a laboratory-scale column study. *Sci. Total Environ.* 565, 616–625.
- Lyon, Bonnie A., Corey, Rose M., Weinberg, Howard S., 2014. Changes in dissolved organic matter fluorescence and disinfection byproduct formation from UV and subsequent chlorination/chloramination. *J. Hazard Mater.* 264, 411–419. <https://doi.org/10.1016/j.jhazmat.2013.10.065>.
- Melendez-Perez, J.J., Martínez-Mejía, M.J., Eberlin, M.N., 2016. A reformulated aromaticity index equation under consideration for non-aromatic and non-condensed aromatic cyclic carbonyl compounds. *Org. Geochem.* 95, 29–33.
- Morris, J.C., 1975. Formation of Halogenated Organics by Chlorination of Water Supplies: a Review. Office of Research and Development, US Environmental Protection Agency.
- National Research Council (US) Safe Drinking Water Committee, 1979. The Chemistry of Disinfectants in Water: Reactions and Products. Environmental Protection Agency, Office of Drinking Water.
- NHMRC, NRMCC, 2011. Australian Drinking Water Guidelines Paper 6 National Water Quality Management Strategy. National Health and Medical Research Council, National Resource Management Ministerial Council, Commonwealth of Australia, Canberra. ISBN: 1864965118. Downloaded from. <https://www.nhmrc.gov.au/about-us/publications/australian-drinking-water-guidelines#block-views-block-file-attachments-content-block-1>.
- Nikolic, G., 2011. Fourier Transforms: Approach to Scientific Principles. BoD—Books on Demand.
- Oksanen, J., Blanchet, F.G., Friendly, M., Kindt, R., Legendre, P., McGinn, D., Minchin, P.R., O'Hara, R.B., Simpson, G.L., Solymos, P., Stevens, M.H.H., Szoecs, E., Wagner, H., 2019. *Vegan: Community Ecology Package*. R Package Version 1.17-4. <https://CRAN.R-project.org/package=vegan>.
- Patriarca, C., Bergquist, J., Sjöberg, P.J.R., Tranvik, L., Hawkes, J.A., 2018. Online HPLC-ESI-HRMS method for the analysis and comparison of different dissolved organic matter samples. *Environ. Sci. Technol.* 52, 2091–2099.
- Peng, D., Saravia, F., Abbt-Braun, G., Horn, H., 2016. Occurrence and simulation of trihalomethanes in swimming pool water: a simple prediction method based on DOC and mass balance. *Water Res.* 88, 634–642.
- R Core Team, 2019. *A Language and Environment for Statistical Computing*. R Foundation for Statistical Computing, Vienna, Austria, 2012. <https://www.R-project.org>.
- Richardson, S.D., Ternes, T.A., 2018. Water analysis: emerging contaminants and current issues. *Anal. Chem.* 90, 398–428.
- Richardson, S.D., Thruston Jr., A.D., Krasner, S.W., Weinberg, H.S., Miltner, R.J., Schenck, K.M., Narotsky, M.G., McKague, A.B., Simmons, J.E., 2008. Integrated disinfection by-products mixtures research: comprehensive characterization of water concentrates prepared from chlorinated and ozonated/postchlorinated drinking water. *J. Toxicol. Environ. Health Part A* 71, 1165–1186.
- Riedel, T., Zark, M., Vähätalo, A.V., Niggemann, J., Spencer, R.G.M., Hernes, P.J., Dittmar, T., 2016. Molecular signatures of biogeochemical transformations in dissolved organic matter from ten world rivers. *Front. Earth Sci.* 4, 85.
- Roccaro, P., Vagliasindi, F.G.A., Korshin, G.V., 2009. Changes in NOM fluorescence caused by chlorination and their associations with disinfection by-products formation. *Environ. Sci. Technol.* 43, 724–729.
- Santl, Temkiv, T., Finster, K., Dittmar, T., Hansen, B.M., Thyraug, R., Nielsen, N.W., Karlson, U.G., 2013. Hailstones: a window into the microbial and chemical inventory of a storm cloud. *PLoS One* 8, e53550.
- Schum, S., Mazzoleni, L., Brown, L., 2019. MFAssignR: Molecular Formula Assignment Using CHOFIT Algorithm. R package version 0.0.5.
- Schymanski, E.L., Jeon, J., Gulde, R., Fenner, K., Ruff, M., Singer, H.P., Hollender, J., 2014. Identifying Small Molecules via High Resolution Mass Spectrometry: Communicating Confidence.
- Sohn, J., Amy, G., Cho, J., Lee, Y., Yoon, Y., 2004. Disinfectant decay and disinfection by-products formation model development: chlorination and ozonation by-products. *Water Res.* 38, 2461–2478.
- Traube, M., 1894. Einfaches Verfahren Wasser in grossen Mengen keimfrei zu machen. *Med. Microbiol. Immunol.* 16, 149–150.
- US-EPA, 2006. Stage 2 Disinfectants and Disinfection Byproducts Rule (Stage 2 DBPR) 71 FR 388.
- US-EPA, 1998. Stage 1 Disinfectants and Disinfection Byproducts Rule (Stage 1 DBPR) 63 FR 69390.
- Villanueva, C.M., Cordier, S., Font-Ribera, L., Salas, L.A., Levallois, P., 2015. Overview of disinfection by-products and associated health effects. *Curr. Environ. Heal. reports* 2, 107–115.
- Williams, C.J., Conrad, D., Kothawala, D.N., Baulch, H.M., 2019. Selective removal of dissolved organic matter affects the production and speciation of disinfection byproducts. *Sci. Total Environ.* 652, 75–84.
- Woods, G.C., Simpson, M.J., Kelleher, B.P., McCaul, M., Kingery, W.L., Simpson, A.J., 2009. Online high-performance size exclusion chromatography– nuclear magnetic resonance for the characterization of dissolved organic matter. *Environ. Sci. Technol.* 44, 624–630.
- Yeh, R.Y.L., Farré, M.J., Stalter, D., Tang, J.Y.M., Molendijk, J., Escher, B.I., 2014. Bio-analytical and chemical evaluation of disinfection by-products in swimming pool water. *Water Res.* 59, 172–184.
- Yuthawong, V., Kasuga, I., Kurisu, F., Furumai, H., 2019. Molecular-level changes in dissolved organic matter compositions in lake inba water during KMnO₄ oxidation: assessment by Orbitrap mass spectrometry. *J. Water Environ. Technol.* 17, 27–39.
- Zhang, H., Yang, M., 2018. Characterization of brominated disinfection byproducts formed during chloramination of fulvic acid in the presence of bromide. *Sci. Total Environ.* 627, 118–124.
- Zhang, H., Zhang, Y., Shi, Q., Hu, J., Chu, M., Yu, J., Yang, M., 2012. Study on transformation of natural organic matter in source water during chlorination and its chlorinated products using ultrahigh resolution mass spectrometry. *Environ. Sci. Technol.* 46, 4396–4402. <https://doi.org/10.1021/es203587q>.
- Zhang, H., Zhang, Y., Shi, Q., Zheng, H., Yang, M., 2014. Characterization of unknown brominated disinfection byproducts during chlorination using ultrahigh resolution mass spectrometry. *Environ. Sci. Technol.* 48, 3112–3119.

Result and discussion

4.3 Drivers of variability in disinfection by-product formation potential in a chain of thermally stratified drinking water reservoirs.

Munthali E, Marcé R, Farré MJ. Drivers of variability in disinfection by-product formation potential in a chain of thermally stratified drinking water reservoirs. *Env Sci Water Res Technol.* 2022;8(5):968–80.



Cite this: *Environ. Sci.: Water Res. Technol.*, 2022, 8, 968

Drivers of variability in disinfection by-product formation potential in a chain of thermally stratified drinking water reservoirs†

Elias Munthali, *abcd Rafael Marcé^{ab} and Maria José Farré *ab

Eutrophication, run-off and wastewater inputs to lakes have been identified as significant sources of disinfection by-product (DBPs) precursors, which are suspected carcinogens, in chlor(am)inated water. However, studies addressing the impacts of reservoirs and thermal stratification on DBP precursors are scarce. We conducted a seasonal study along a river-reservoir interconnected system, to investigate the effects of hydraulic residence time (HRT), thermal stratification, and seasonality on the levels and speciation of carbonaceous and nitrogenous DBP formation potential (FP) in source waters. Formation of 4 trihalomethanes (THMs), 4 haloacetonitriles (HANs), 2 halo ketones and *N*-nitrosodimethylamine (NDMA) was measured on filtered lake water. Total THMs (TTHMs) FP was below $93 \mu\text{g L}^{-1}$, of which 59–87% of it was trichloromethane (TCM). Formation of dichloroacetonitrile (DCAN), 1,1,1-trichloropropanone (TCP), and NDMA was under $12 \mu\text{g L}^{-1}$, $13 \mu\text{g L}^{-1}$ and 73ng L^{-1} , respectively. The FP of the remaining DBPs was under $2 \mu\text{g L}^{-1}$. While the effect of depth on DBP FP was insignificant, inter-system and seasonal effects were conspicuous. The most significant variable affecting DBP formation was season, where carbonaceous DBP FP was higher in autumn and summer than in winter. TTHM FP ranged from a 160% median increase in the river upstream of the reservoirs, to a 31% median increase in the last reservoir of the system, from winter to summer. On the contrary, NDMA FP ranged from a 145% median decrease in the river upstream of the reservoirs to an 11% median decrease in the middle reservoir, from winter to summer. TTHMs FP increased from the river upstream of the reservoirs to the last reservoir of the system (40.6% median increase), whereas the opposite trend was also observed for NDMA FP (63% median decrease).

Received 27th October 2021,
Accepted 25th February 2022

DOI: 10.1039/d1ew00788b

rsc.li/es-water

Water impact

This research presents the spatial and seasonal effects on DBP formation potential of an interconnected river-reservoir natural system. Results show that while spatial variability including depth is insignificant, seasonality is the main driver of the observed variability. In particular, carbonaceous DBP FP was higher in autumn and summer than in winter, while the opposite was observed for nitrogen containing DBPs such as NDMA.

1 Introduction

Chlorinating drinking water generates disinfection by-products (DBPs) that are suspected to cause cancer,¹ reproductive defects,² and respiratory problems.³ These compounds are formed from unintended reactions between

disinfectants, natural dissolved organic matter (DOM) compounds such as humic and fulvic acids⁴ and algal organic matter,⁵ anthropogenic DOM from wastewater discharge^{6,7} and inorganic ions present in water.

In surface waters, DOM is affected by natural factors such as precipitation, droughts, microbial and photolytic processes, as well as anthropogenic factors such as land use, wastewater inputs and global warming,⁸ making it challenging to manage. While it is possible to control land use and wastewater discharge into drinking water sources, meteorological variables institute seasonal variability in DOM speciation and concentrations, which affects DBP formation potential (FP),⁹ hence it is challenging to manage.

Seasonality effects on DBP precursor compounds in lakes and reservoirs have been extensively studied and mostly allude to increased concentration of DBP FP when lakes

^a Catalan Institute for Water Research (ICRA), Carrer Emili Grahit, 101, 17003 Girona, Spain. E-mail: elias.munthali@gmail.com, mjfarre@icra.cat

^b University of Girona, Girona, Spain

^c Netherlands Institute of Ecology (NIOO-KNAW), Droevendaalsesteeg 10, 6708 PB Wageningen, NL, Netherlands

^d Northern Region Water Board (NRWB), Bloemwater Street, P/Bag 94, Mzuzu, Malawi

† Electronic supplementary information (ESI) available. See DOI: 10.1039/d1ew00788b



begin warming up. For instance, a study in three reservoirs in Turkey reported an increase in dissolved organic carbon (DOC) and carbonaceous DBP reactivity in fall, with the lowest values in winter;¹⁰ a year-long study in Córdoba (Spain) reported a six fold increase in DBP FP in raw water, from spring to summer, for both carbonaceous and nitrogenous DBPs;¹¹ In Quebec, Canada, a study reported increased FP of haloacetonitriles (HANs) and halo ketones from spring to summer, followed by a drop in winter.¹² Effects of summer thermal stratification on DBP FP have been reported in some studies, although far much less than studies on seasonal effects, but the results are inconclusive. For example, Bukaveckas and co-authors reported that trihalomethane (THM) FP in waters of Taylorsville was highest in the hypolimnion, in summer, compared to the epilimnion and other months, which was attributed to production of precursors from microbial degradation of organic matter.¹³ Similarly, a study in the Horseshoe–Bartlett reservoir in Arizona by Nguyen and co-authors reported that haloacetic acids (HAAs) FP increased with depth from summer to fall, which was attributed to photodegradation of DOC.¹⁴ Yet, a study by Kraus and co-authors on San Luis reservoir in California did not observe any trend with depth on the FP of THMs and HAAs in any season.¹⁵ Such reported variability suggests that effects of thermal stratification on DBP FP may be location-specific and thus requires system-specific studies to fully comprehend its implications.

Effects of hydraulic residence time (HRT) on DBP FP have not received much attention yet, but are necessary to be understood, given that nutrients and DOM may be retained and undergo physico-chemical and microbial transformation processes in lakes, which might influence speciation and concentration of DBP FP. Depending on HRT and in-lake processes, reservoirs may act as sources or sinks of both nutrients^{16,17} and organic matter,¹⁸ resulting in varied implications on downstream water uses. Hence, the main objective of this study was to investigate effects of HRT, stratification, and seasonality on the levels and speciation of DBP FP in a chain of three interconnected reservoirs in Catalunya (Spain), to understand the main drivers of DBP FP variability. With this aim, we carried out seasonal sampling campaigns in autumn, winter and summer, in the Ter River and three reservoirs (Sau, Susqueda and Pasteral) to investigate, at the laboratory scale, the FP of a suite of both carbonaceous and nitrogenous DBPs.

The initial hypotheses were (i) nitrogenous DBP FP would be higher in surface than in deep water layers due to higher density of phytoplankton in the euphotic zone in summer, (ii) DBP FP would decrease longitudinally (*i.e.* Ter > Sau > Susqueda > Pasteral) due to decreasing eutrophication and longer HRT, and (iii) DBP FP would be highest in summer than in other seasons as a result of increased DOM concentration from accelerated microbial activity and algal growth.

2 Methods

2.1 Study sites

Samples were collected in November 2018, February 2019 and July 2019, from Ter River (41°58'48.43" N, 2°18'32.79" E), Sau (41°58'27.11" N, 2°23'3.45" E), Susqueda (41°58'45.12" N, 2°31'37.99" E) and Pasteral (41°59'3.95" N, 2°36'4.28" E) reservoirs, which lie in the middle stretch of the 200 km long Ter River that originates from the Pyrenees mountain ranges and drains into the Mediterranean Sea (Fig. 1). There was no sampling performed in the spring season (April 2019). From Sau reservoir, water can be withdrawn from any of three available withdrawal depths and transferred to Susqueda reservoir. On the other hand, Susqueda has four withdrawal depths, from which water is alternately drawn and transferred to Pasteral reservoir for eventual abstraction, treatment, and supply to the Barcelona Metropolitan area, that serves over 4 million people. Alternate withdrawal of water from different depths is a well-known practice in reservoir management, carried out to optimize water quality by countering seasonal changes in water quality parameters at different depths.

Sau and Susqueda reservoirs are deep systems, in which the average depth of Susqueda is twice that of Sau, but both systems have comparable HRT of approximately 3 months. In contrast, Pasteral is shallow, with a mean depth that is five times smaller than Sau and ten times shallower than Susqueda, and an HRT of 0.04 months (Table 1, Fig. 1).

2.2 Sampling procedure and preservation

Surface water samples were taken from Ter River and Pasteral reservoir by walking to the sites and collecting a grab sample, while samples from Sau and Susqueda were taken by boating to the deepest point of each reservoir to collect four samples from different depths of the water column. Ter River and Pasteral reservoir are too shallow to provide samples from different depths, hence, only surface water could be sampled. All samples for DOM and DBP FP tests were collected in 2.5 L amber glass bottles (prewashed with nitric acid, rinsed and dried in the oven), fully filled with water sample to avoid headspace at the top. On the other hand, samples for nutrients were collected in 50 ml-conical bottom polypropylene tubes (Deltalab, Spain), in sets of filtered and unfiltered samples. The tubes were rinsed with the filtered water sample (0.7 µm Whatman GF/F filter) twice before filling the tubes with samples. All surface water samples were collected by immersing bottles at about 0.5 m from the surface. Sampling depths in Sau and Susqueda reservoirs were determined by targeting locations with sharp changes in temperature, conductivity or turbidity profiles, measured by the SBE 19 plus conductivity, temperature and depth (CTD) profiler (Sea Bird Electronics, USA), resulting into a total of 4 samples collected from each reservoir. Details of depths from which samples were collected, for all the sampling events, are contained in Table 2. Sub-surface samples were collected by using a 5 L depth sampler (UWITEC, Austria), which was



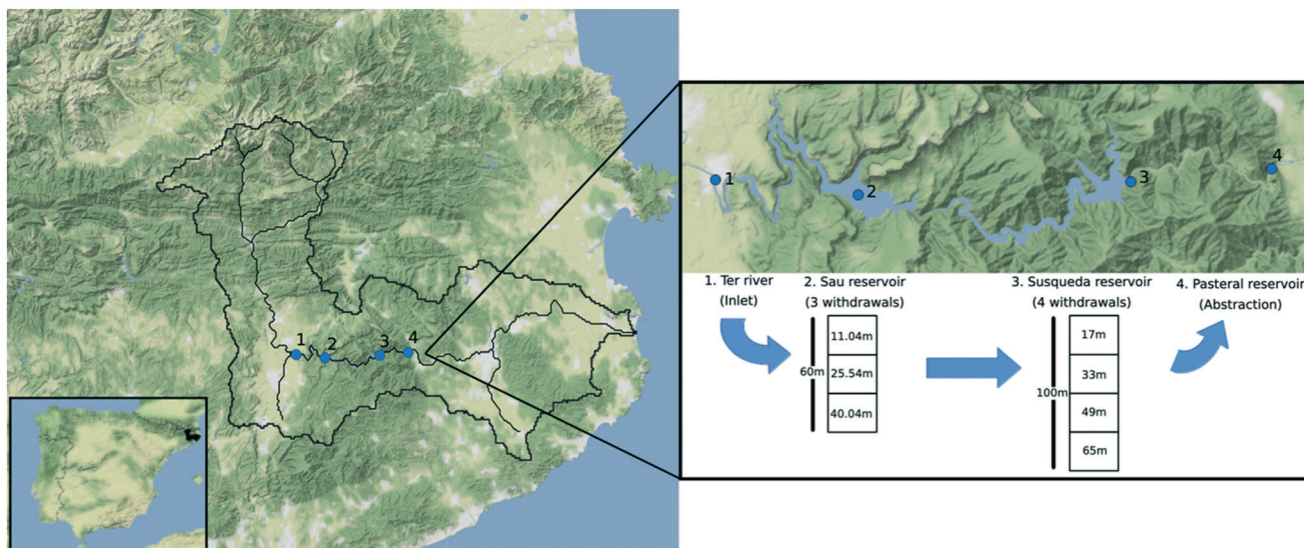


Fig. 1 Map illustrating position of the Ter catchment in Spain, the four sampling locations (Ter River, Sau, Susqueda and Pastoral reservoirs) and water abstraction depths for Sau and Susqueda.

rinsed with one sample wash volume before collecting the final sample at each depth. To collect a sample, the sampler was lowered into the water column with the lid open until the desired depth was reached, after which the lid was automatically closed by pulling the rope. The samples were transferred to the laboratory and kept at 4 °C until the day of analysis, which was not later than two days after sampling.

2.3 Nutrient analysis

Prior to analysis, samples for nitrate, nitrite, ammonium and bromine were filtered through a Whatman 0.2 µm GFF/F filter. Bromide, nitrate, nitrite, phosphate and ammonium were analysed by ionic chromatography, on a DIONEX ICS-5000 ion chromatography system (Thermo Fisher Scientific, USA). DOC was analysed by catalytic oxidation, on a TOC-V CSH analyzer (Shimadzu, Japan). Total phosphorus samples were pre-digested, followed by colorimetric analysis¹⁹ on a UV-1800 scanning spectrophotometer (Shimadzu, Japan). Total Kjeldahl nitrogen (TKN) was analysed using the macro-Kjeldahl approach of acid digestion, distillation and eventual quantification.²⁰

2.4 Dissolved organic matter optical properties

DOM absorbance (ultraviolet absorbance, UVA_{254}) was measured on the 8453 UV-vis diode array spectrophotometer

(Agilent Technologies, USA) and, thereafter, using the same cuvette (1 cm path length quartz) and sample, fluorescence excitation-emission spectra were measured on the F-7000 fluorescence spectrophotometer (Hitachi, Japan). Excitation wavelength ranged from 200 nm to 449 nm, spaced at 3 nm intervals, whereas emission wavelength ranged from 250 nm to 598 nm, also spaced at 3 nm intervals. Excitation and emission slit widths were set at 5 nm. The resultant absorbances, excitation and emission spectra were processed using an in-house Octave²¹ code to produce organic matter optical indices such as the humification index (HIX), biological index (BIX) and fluorescence index (FI), which shed light on the sources of DOM present in water. HIX, a measure of DOM maturation (indicated by the extent of aromaticity),²² is calculated as the ratio of peak areas in the emission wavelength ranges of 435–480 nm and 300–345 nm, respectively, both excited at 254 nm. Low HIX values of <4 indicate that DOM is of microbial origin; the middle range of 4–10 indicates a mixture of both humic and biological sources; whereas high values of >16 indicate that DOM is of terrestrial origin.²³ On the other hand, BIX, representing the extent of in-reservoir produced DOM, is defined by fluorescence intensity ratios of emissions at 380 nm and 430 nm respectively, both excited at 310 nm.²³ High BIX values of >1 suggest that DOM is, predominantly, of microbial origin, whereas low values (≤ 0.7) indicate low autochthonous DOM

Table 1 Morphometric features of Sau, Susqueda and Pastoral reservoirs

	Max volume (hm ³)	Max depth (m)	Surface area (ha)	Mean water residence time (months)	Mean depth (m)	Altitude (masl)
Sau	168.5	65	570	3.6	25.2	425
Susqueda	233	110	466	3.3	50.3	351
Pastoral	2	5.7	35	0.04	5.7	185

Data sources: ref. 79–82.



Table 2 Details of depth locations from which samples were collected across all systems and sampling events

Date	Depth code	System/actual depth (m)			
		Ter	Sau	Susqueda	Pasteral
2018-11-05	1	0.5	0.5	0.5	0.5
2019-02-04	1	0.5	0.5	0.5	0.5
2019-07-12	1	0.5	0.5	0.5	0.5
2018-11-05	2	0.5	15	20	0.5
2019-02-04	2	0.5	13	8	0.5
2019-07-12	2	0.5	5	4.5	0.5
2018-11-05	3	0.5	30	40	0.5
2019-02-04	3	0.5	30	35	0.5
2019-07-12	3	0.5	15	23	0.5
2018-11-05	4	0.5	40	70	0.5
2019-02-04	4	0.5	42	80	0.5
2019-07-12	4	0.5	30	80	0.5

production.²³ Fluorescence index, which indicates the relative contribution of allochthonous and autochthonous sources to the total DOM pool, is defined by the ratio of emissions at wavelengths of 470 nm and 520 nm respectively, both excited at 370 nm.²⁴ Low FI values of ≤ 1.4 indicate that DOM is of terrestrial origin, whereas high values of ≥ 1.9 indicate that DOM is microbially derived.²⁶ Milli-Q blanks, freshly produced just before analyses, were ran at the beginning and after every 10 samples, and subtracted from each sample spectra to correct for Raman scattering,^{25,27} and inner filter effects were corrected by subtracting UV-visible absorbance spectra from each EEM spectra.^{23,26,28} Specific ultraviolet absorbance ($SUVA_{254}$), an indicator of DOM aromaticity,²⁹ was obtained by dividing ultraviolet absorbance data with its corresponding DOC values.

2.5 Disinfection by-product FP tests

Formation of volatile DBPs such as trichloromethane (TCM), bromodichloromethane (BDCM), 1,1-dichloropropanone (DCP), dibromochloromethane (DBCM), 1,1,1-trichloropropanone, tribromomethane (TBM), trichloroacetonitrile (TCAN), trichloronitromethane (TCNM), dichloroacetonitrile and bromochloroacetonitrile (BCAN) was performed following a standard method previously applied by Liu and co-authors³⁰ whereas the *N*-nitrosodimethylamine (NDMA) FP test followed a standard procedure previously published by Mitch and co-authors.³¹ A summary of analytical procedure for both classes of DBPs is provided in the ESI† Text S1.

2.6 Statistical analysis

Descriptive statistics. The nature of systems sampled (e.g. river for which only one sample per date was collected and reservoirs where sampling at several depths was possible) implied an unbalanced sampling design in terms of the number of samples available from each system. As such, data distribution summary statistics of mean, median and standard deviation were used to describe the observed spatial trends in DBP FP and their respective yield.

Principal component analysis (PCA). In order to explore the potential drivers of variability in DBP FP and nutrients from the measured factors of system (a proxy for HRT), depth and season, PCA was applied to a (27 × 19) data matrix comprising of 27 samples collected from Sau, Susqueda and Pasteral reservoirs and measured for nutrients, DOM optical indices, and DBP FP, across the three seasons and four different depths. The goal was to generate a two-dimensional space from a linear combination of all the measured water quality variables, where sample identities could be projected to observe the clustering pattern of DBP FP, nutrients and a combination of both nutrients and DBP FP.

Correlation analyses among the measured parameters.

Linear associations amongst nutrients, DOM optical indices, and DBP FP results were explored by applying the Spearman rank correlation coefficient test, at type I error rates of $\alpha = 0.05$, $\alpha = 0.01$, $\alpha = 0.001$ and $\alpha = 0.0001$, in order to determine if some nutrients and DOM optical indices could be used as predictive surrogates for DBP FP. To obtain the correlation coefficients and their statistical significance, the “corstars” *R* function (written by Guillaume T. Vallet) was applied to the standardized data. The resultant correlation coefficients were classified as either none (0), poor (0.1–0.2), fair (0.3–0.5), moderate (0.6–0.7), very strong (0.8–0.9) or perfect (1).³²

All calculations and graphical illustrations were implemented in R³³ version 4.40.

3 Results and discussion

3.1 General disinfection by-product FP trends

Formation potential (FP) tests were performed in all samples collected from the four systems. In general, of the six carbonaceous DBPs formed above the limit of detection, TCM formed in largest quantities (maximum of 80 $\mu\text{g L}^{-1}$), followed by BDCM (maximum of 12.9 $\mu\text{g L}^{-1}$) and 1,1,1-TCP (maximum of 13.0 $\mu\text{g L}^{-1}$), while DBCM formed up to 2.5 $\mu\text{g L}^{-1}$ (ESI† Fig. S1 and S2, Tables S1, S3, S5 and S7). Maximum FP of 1,1-DCP and TBM were 0.8 $\mu\text{g L}^{-1}$ for both species. TCM FP recorded a maximum of about 80 $\mu\text{g L}^{-1}$, which is similar to concentrations found in other studies in Yuqiao³⁴ and Qingyuan reservoirs^{35,36} from China, and other reservoirs in Japan,³⁷ wherein TCM FP also dominated the FP of the carbonaceous DBPs investigated. Within the nitrogen containing DBP family, DCAN FP was the dominating species, measured at a maximum concentration of 11.9 $\mu\text{g L}^{-1}$, which is consistent with similar results reported by Wang and co-authors³⁶ (ESI† Fig. S1 and S2, Tables S1, S3, S5 and S7). BCAN, TCAN and TCNM formed at maximum quantities of 1.5 $\mu\text{g L}^{-1}$, 0.2 $\mu\text{g L}^{-1}$ and 2.0 $\mu\text{g L}^{-1}$, respectively (above the 0.1 $\mu\text{g L}^{-1}$ detection limit, ESI† Tables S1, S3, S5 and S7). NDMA, which could be quantified in the low ng L^{-1} range, formed at a maximum of 72 ng L^{-1} (ESI† Fig. S1 and S2, Tables S1, S3, S5 and S7). In all the four systems, DCAN FP was measured between 7 and 10 times lower than TCM FP (ESI† Fig. S2, Tables S1, S3, S5 and S7), suggesting that



precursor compounds responsible for the formation of carbonaceous DBPs (DOC) were in majority, compared to nitrogenous species (DON). Even though the ranges of spectroscopic indices of HIX ($>3 \leq 15$), BIX (≤ 0.9) and FI (1.56–1.85) (ESI† Fig. S6 and S7, Tables S9–S12), suggest that DOM across the four systems was a mixture of both humic-like and microbial derived, the maxima of HIX, BIX and FI indicate that a larger proportion of DOM was humic in nature,^{23,38,39} that preferentially forms carbonaceous DBPs.⁴⁰

3.2 Effect of the system on disinfection by-product FP

Contrary to the initial hypotheses, the median values of TTHM FP increased across the river-reservoirs chain (Fig. 1), ranging from $33 \mu\text{g L}^{-1}$ to $90 \mu\text{g L}^{-1}$. Specific TTHM also increased across the same river-reservoir continuum, particularly between Ter and Susqueda (ESI† Fig. S5). The opposite trend was hypothesized because reservoirs act as organic matter¹⁸ and nutrients^{16,17} traps, which would imply a reduction in concentration of DBP precursor compounds across the systems. Instead, the results suggested that increasing HRT, particularly in Sau and Susqueda reservoirs, led to the production of more carbonaceous DBP precursors. The increment in precursor concentration was probably not largely a result of additional in-reservoir production (both BIX and FI are below the minimums of 1 and 1.9 respectively, ESI† Fig. S6 and S7, Tables S9–S12) but probably from the biodegradation of terrestrial organic matter,⁴¹ with increased aromaticity and molecular weight^{42,43} that have a higher propensity to form carbonaceous DBPs.⁴⁴ These observations were supported by an increasing trend observed in medians of UVA₂₅₄, SUVA₂₅₄ and HIX (ESI† Fig. S7) and suggests the vital role of HRT in promoting the microbial transformation of complex allochthonous organic matter into more simpler compounds⁴¹ which have enhanced reactivity with chlorine. On the other hand, results showed an inverse trend for nitrogenous DBP FP, particularly NDMA, that decreased from a maximum 72 ng L^{-1} in Ter River to a maximum of 34 ng L^{-1} in Pasteral (Fig. 2 and S1†). The yield of NDMA also showed similar decreasing trends (ESI† Fig. S5). This finding was consistent with the hypothesis that DBP precursors would decrease from the Ter River to Pasteral reservoir, given that eutrophication decreases across the systems, as nutrients are trapped and mineralized in reservoirs.⁴⁵ Additionally, wastewater, which is a major precursor source for NDMA⁴⁶ and HANs⁴⁷ formation, is discharged into Ter River first and its impact is reduced along the way as the river drains into the reservoir chain. However, results showed a lack of systemic gradient for DCAN FP (median values were roughly similar, Fig. 2), suggesting DCAN precursors (free amino acids and peptides^{48,49}) were recalcitrant, which contradicts other experimental findings,^{50,51} which reported that solar irradiation and biodegradation, respectively, were effective in degrading both amino acid model compounds and DCAN FP. The difference could be due to the high organic and inorganic turbidity of the investigated systems,

which would undermine the effectiveness of solar irradiance. NDMA FP median values were significantly different between Ter and Sau only (median values in Sau, Susqueda and Pasteral reservoirs were roughly similar around 20 ng L^{-1} , Fig. 2), suggesting occurrence of biodegradation of NDMA precursors⁵¹ such as secondary, tertiary and quaternary amines,⁵² which was also demonstrated in a microcosm experiment of Woods and co-authors.⁵³ The sharp drop in NDMA FP between Ter River and Sau reservoir, again, highlighted the role of HRT in NDMA precursor attenuation along the same continuum. Sanchís and co-authors⁵⁴ investigated NDMA FP along the Llobregat river (Spain) and found that NDMA precursors decreased probably because of natural attenuation. Nevertheless, the current disinfection practice employed at the water works abstracting water from this system is chlorination, that, although is associated with increased carbonaceous DBP formation,⁵⁵ does not generate NDMA, compared to chloramination.⁵⁶ Monitoring the formation of DBPs at the drinking water treatment plant (DWTP) was beyond the scope of the study, however, roughly around the winter sampling event (February 2019), Godo-Pla and co-authors investigated the formation of THMs at the same DWTP, with other scientific objectives, and found that TTHMs FP at the output of the DWTP was always below $50 \mu\text{g L}^{-1}$.⁵⁷

3.3 Effect of reservoir depth on disinfection by-product FP

Of the four measured THMs FP, TCM and BDCM and their respective yield, showed marginal trends of increasing FP with increasing depth, mostly in winter, both in Sau and Susqueda reservoirs (ESI† Fig. S1 and S2), whereas the FP was either similar or randomly varied with increasing depth in other seasons (ESI† Fig. S1 and S2). TCP FP and its yield were mostly constant with increasing depth (ESI† Fig. S1 and S2). These findings were unexpected as the initial hypothesis, which is supported by depth trends observed in DOC, UVA₂₅₄ and HIX (ESI† Fig. S6), predicted a gradient of increasing FP with increasing depth in summer, probably due to photodegradation of precursors in the euphotic zone, and anoxic biodegradation of complex organic matter in the deeper layers in stratified periods^{13,58} but not in winter when the reservoirs are fully mixed. For nitrogenous species, DCAN FP and its yield increased with increasing depth in autumn, in both reservoirs; remained roughly the same in winter; and decreased with increasing depth in summer (ESI† Fig. S1 and S2), in Sau reservoir only, which was supported by the depth trends observed in BIX in winter and summer (ESI† Fig. S6). Also, in Sau reservoir, NDMA FP decreased from the surface to the metalimnion and remained constant up to the bottom layers in autumn; remained roughly constant in winter; and increased with increasing depth in summer (ESI† Fig. S1), which was supported by SUVA₂₅₄ (autumn) and BIX depth trends in autumn and winter only (ESI† Fig. S6). On the other hand, in Susqueda reservoir, NDMA FP remained constant with increasing depth in autumn and winter but decreased



from the surface to the metalimnion and remained constant up to the bottom water layers in summer (ESI† Fig. S1), which was supported by the BIX depth trend (ESI† Fig. S6), whereas its yield was constant in both reservoirs and across all seasons (ESI† Fig. S2). The initial hypothesis had anticipated a decreasing FP of both DCAN and NDMA, in both reservoirs, with increasing depth in autumn and summer because of the proliferation of phytoplankton in the euphotic zone, which could have contributed more precursors in the upper water layers, as suggested by depth trend observed in BIX (ESI† Fig. S6). Elsewhere in California, Gerecke and Sedlak reported higher NDMA FP in the epilimnion than the hypolimnion of the San Pablo and San Leandro reservoirs, during stratification, which was suspected to originate from atmospheric deposition or photo-transformation of organic matter from the feeding streams.⁵⁹ The reverse summer trend observed in Sau, in this study, might be due to increased concentration of precursor from anoxic degradation of the sinking particulate organic matter from phytoplankton in the euphotic zone. Overall, the observed marginal depth trends are, in our opinion, minor to have meaningful implications for depth withdrawal management, since the effect of depth on DBP formation was small and not statistically significant.

3.4 Effect of season on disinfection by-product FP

As expected, the FP of TCM and BDCM and their associated yield, were highest in autumn and summer and lowest in winter in all reservoirs (ESI† Fig. S1–S4, Tables S3–S8). The observed autumn increase in carbonaceous DBP FP may be a result of increased DOC concentrations from precipitation mediated terrestrially derived DOM,¹⁰ and the increase of DBP FP in summer might be due to higher concentration of organic matter compounds from augmented microbial activity in warmer environments⁶⁰ and some contribution from autochthonous derived precursor compounds,^{49,61} both of which are supported by the measured trends in DOC and SUVA₂₅₄ (autumn, ESI† Fig. S7). On the other hand, TCP FP and its yield did not show any seasonal differences (ESI† Fig. S1–S4, Tables S3–S8). Considering nitrogenous DBPs, the FP and yield for DCAN was also highest in autumn and summer, and lowest in winter, in all the four systems (Fig. 2 and S1–S4†), which could be attributed to increased input of wastewater derived precursors (in autumn high flows), contribution from algal sources in summer,⁶² as supported by the summer BIX trends and SUVA₂₅₄ (autumn) trend (Sau and Susqueda, ESI† Fig. S6 and S7) and some contribution from terrestrially derived DOM.^{63,64} NDMA FP was highest in summer followed by winter and lowest in autumn in both Sau and Susqueda reservoirs (supported by BIX trend in ESI† Fig. S6 and S7); highest in winter and lowest in summer in the Ter River; and highest in autumn, lowest in winter and summer in Pastoral reservoir (Fig. 2 and S1†). In contrast, the yield of NDMA was constant across all seasons, in almost all the systems, except in

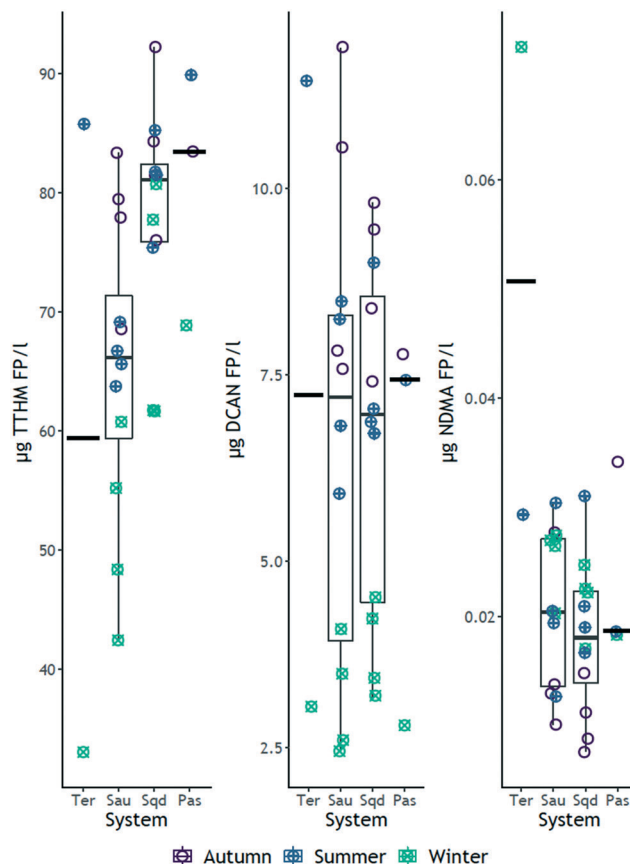


Fig. 2 Box and jitter plots for DBP FPs of TTHMs, DCAN and NDMA, grouped by system and season. The green colored dots are the formation potential values in winter, the blue dots are formation potential values in summer and the violet dots represent formation potential values in autumn. The circles are the actual formation potential data. The horizontal bar on each of the four systems represents the median value for all data of that particular system.

Pastoral where it was highest in autumn and lowest in winter (ESI† Fig. S2 and S4). The absence of seasonal variations in the yield of NDMA in most of the systems might be due to a lack of relationship between DOC and NDMA. Initial hypotheses had anticipated highest carbonaceous DBP FP in all the systems in autumn due to mobilization of precursors from the catchment (supported by trends in TCM and BDCM FP, ESI† Fig. S1 and S2), as was also reported elsewhere,⁶⁵ and the highest nitrogenous DBP FP in summer (due to phytoplankton growth⁶⁶) and autumn (due to increased wastewater inputs⁶⁷), followed by the lowest FP in winter (due to reservoir turn-over). DCAN FP (in all systems) and, to some extent, NDMA FP (Sau and Susqueda, in summer only) confirmed our expectations (ESI† Fig. S1 and S2). However, high NDMA FP in winter in the Ter, Sau and Susqueda, and lowest values recorded in autumn were unexpected, even though, elsewhere in Korea and Japan, similar findings were reported,^{68,69} which was attributed to lower biological and photodegradation of precursor compounds due to reduced microbial activity and temperature in winter. Elsewhere in China, Zhou and co-



When the Ter sample was included in the PCAs, seasonality patterns were retained in both the FP and yield data (ESI† Fig. S10 and S11), but depth patterns were marginally visible in the FP PCA only, particularly on Sau reservoir data (ESI† Fig. S10) and not in the yield PCA (Fig. S11†).

3.6 Correlation analyses between evaluated parameters

TCM FP and its yield showed positive correlation with UVA₂₅₄ (fair & fair, $r = 0.53$, $r = 0.56$), DOC (fair, $r = 0.37$) and PO₄³⁻ (fair & fair, $r = 0.40$, $r = 0.58$), whereas the rest of nutrients and other DOM optical indices negatively correlated with TCM as: TN (fair & fair, $r = -0.56$, $r = -0.59$) and NO₃⁻ (fair & fair, $r = -0.59$, $r = -0.57$) (Tables 3 and S13†). In addition, the yield of TCM positively correlated with SUVA₂₅₄ (moderate, $r = 0.60$) and TP (fair, $r = 0.48$), and negatively correlated with BIX (fair, $r = -0.59$) and FI (fair, $r =$

-0.52) (ESI† Table S13). The significant correlation observed between UVA₂₅₄ and TCM FP agreed with other findings,^{77,78} although, in their studies, the correlations were stronger ($r = 0.91$, $p < 0.01$), and $r = 0.897$, $p < 0.001$, respectively). On the other hand, BDCM FP positively correlated with DOC (fair, $r = 0.54$), NO₂⁻ (moderate $r = 0.68$), TKN (fair, $r = 0.38$) and BIX (fair, $r = 0.45$) and negatively with PO₄³⁻ (fair, $r = -0.49$), TP (fair, $r = -0.49$), SUVA₂₅₄ (fair, $r = -0.54$) and NH₄⁺ (fair, $r = -0.52$) (Table 3). In addition, the yield of BDCM positively correlated with NO₂⁻ (fair $r = 0.48$) and negatively correlated with DOC (fair, $r = -0.44$) and HIX (fair, $r = -0.46$). Correlations with DOC also agreed with findings of Watson and co-authors,⁷⁸ although, in their study, the correlation was very strong ($r = 0.86$, $p < 0.01$). However, the lack of significant correlation between BDCM FP and UVA₂₅₄, and the negative correlation with SUVA₂₅₄ were contrary to the findings of Watson and co-authors⁷⁸ who reported very strong associations ($r = 0.90$, $r = 0.80$, $p < 0.01$, respectively).

Table 3 Nutrients-DOM optical indices-DBP FP Spearman rank correlation matrix

	mgN_NH ₄ ⁺	mgC_DOC	mgN_TN	mgN_TKN	mgP_PO ₄ ³⁻	mgP_PT	mgN_NO ₃ ⁻	mgN_NO ₂ ⁻	UVA ₂₅₄	SUVA ₂₅₄	FI
mgN_NH ₄ ⁺	1										
mgC_DOC	-0.54**	1									
mgN_TN	0.27	-0.12	1								
mgN_TKN	-0.38*	0.16	-0.35	1							
mgP_PO ₄ ³⁻	0.43*	-0.21	-0.39*	-0.28	1						
mgP_PT	0.51**	-0.24	-0.36	-0.18	0.87****	1					
mgN_NO ₃ ⁻	0.27	-0.17	0.97****	-0.35	-0.37*	-0.32	1				
mgN_NO ₂ ⁻	-0.12	0.26	0.2	0.32	-0.62***	-0.35	0.13	1			
UVA ₂₅₄	0.23	0.06	-0.3	-0.3	0.87****	0.61***	-0.3	-0.64***	1		
SUVA ₂₅₄	0.55**	-0.18	-0.15	-0.42*	0.79****	0.61***	-0.16	-0.57**	0.79****	1	
FI	-0.03	0.14	0.49**	-0.1	-0.53**	-0.33	0.49**	0.38*	-0.54**	-0.41*	1
BIX	-0.26	0.04	0.2	0.43*	-0.66****	-0.52**	0.16	0.57**	-0.74****	-0.71****	0.17
HIX	-0.06	0.11	0.37*	-0.31	-0.03	-0.09	0.40*	-0.28	0.16	0.13	0.34
μgTCM	-0.22	0.37*	-0.56**	0.16	0.40*	0.28	-0.59***	-0.11	0.53**	0.19	-0.3
μgBDCM	-0.52**	0.54**	-0.07	0.38*	-0.49**	-0.49**	-0.16	0.68****	-0.31	-0.54**	0.09
μgDCAN	-0.1	0.41*	-0.57**	0.28	0.3	0.29	-0.67****	0.26	0.31	0.1	-0.37*
μgDBCM	-0.1	0.02	0.58****	0.15	-0.87****	-0.67****	0.56**	0.72****	-0.88****	-0.70****	0.60***
μgTCP	-0.14	-0.05	0.2	-0.01	-0.45*	-0.25	0.3	0.09	-0.50**	-0.33	0.33
μgNDMA	-0.01	-0.31	0.36	0.09	-0.37*	-0.26	0.36	0.18	-0.44*	-0.37*	0.40*

	BIX	HIX	μgTCM	μgBDCM	μgDCAN	μgDBCM	μgTCP	μgNDMA
mgN_NH ₄ ⁺								
mgC_DOC								
mgN_TN								
mgN_TKN								
mgP_PO ₄ ³⁻								
mgP_PT								
mgN_NO ₃ ⁻								
mgN_NO ₂ ⁻								
UVA ₂₅₄								
SUVA ₂₅₄								
FI								
BIX	1							
HIX	-0.58**	1						
μgTCM	-0.35	-0.06	1					
μgBDCM	0.45*	-0.24	0.41*	1				
μgDCAN	0.02	-0.50**	0.74****	0.54**	1			
μgDBCM	0.69****	-0.03	-0.54**	0.40*	-0.33	1		
μgTCP	0.19	0.33	-0.41*	-0.19	-0.56**	0.42*	1	
μgNDMA	0.35	0	-0.25	-0.02	-0.43*	0.49**	0.32	1

Note: **** = $p < 0.0001$, *** = $p < 0.001$, ** = $p < 0.01$, * = $p < 0.05$.



Probably, the differences might relate to the fact that they were dealing with a one-off analysis of synthetic water, whereas the presently investigated samples were collected from natural systems, over a couple of seasons. TCP FP negatively correlated with PO_4^{3-} (fair, $r = -0.45$) and UVA_{254} (fair, $r = -0.50$), whereas its yield positively correlated with NO_3^- (fair, $r = 0.45$) and negatively correlated with DOC (fair, $r = -0.59$) and UVA_{254} (fair, $r = -0.49$) (ESI† Table S13). Overall, the observed correlations between carbonaceous DBP FP, its associated yield and nutrients appeared less strong to consider nutrients as predictive surrogates for the FP of TCM, BDCM and TCP.

For nitrogenous DBP FP, DCAN FP and its yield positively correlated with DOC (fair, $r = 0.41$) and negatively correlated with TN (fair & fair, $r = -0.57$, $r = -0.48$), NO_3^- (moderate & fair, $r = -0.67$, $r = -0.58$), FI (fair & fair, $r = -0.37$, $r = -0.39$) and HIX (fair & moderate, $r = -0.50$, $r = -0.66$) (Tables 3 and S13†), implying that none of the measured nutrients and other DOM optical indices could be used as acceptable surrogates to predict DCAN FP. The observed correlation of DCAN FP with DOC agreed with findings of Watson and co-authors⁷⁸ although their study reported a very strong association ($r = 0.80$, $p < 0.01$) plus other strong associations with UVA_{254} ($r = 0.90$, $p < 0.01$) and SUVA_{254} ($r = 0.83$, $p < 0.01$), both of which were absent in this study. On the other hand, NDMA FP positively correlated with the DOM optical index of FI (fair, $r = 0.40$) and negatively correlated with PO_4^{3-} (fair, $r = -0.37$), UVA_{254} (fair, $r = -0.44$) and SUVA_{254} (fair, $r = -0.37$) (Table 3). In addition, the yield of NDMA positively correlated with NO_3^- (fair, $r = 0.45$) and TN (fair, $r = 0.44$) and negatively correlated with DOC (fair, $r = -0.55$) and UVA_{254} (fair, $r = -0.39$). While the present study did not find significant correlations between NDMA FP and DOC, in a USA study, Yang and co-authors⁷⁷ reported fair and positive correlations for both DOC ($r = 0.535$, $p < 0.001$) and UVA_{254} ($r = 0.417$, $p < 0.001$). Instead, in the present study, NDMA FP negatively correlated with UVA_{254} (fair, $r = -0.44$) and SUVA_{254} (fair, $r = -0.37$), whereas its yield negatively correlated with DOC (fair, $r = -0.55$) and UVA_{254} (fair, $r = -0.39$) (ESI† Table S13). The difference might relate to differences in sampling seasons, as they did not sample in winter.

Associations amongst DBP FP were also explored to identify which species could be used as surrogates for other DBP FP. Results indicated that BDCM FP positively correlated with TCM FP (fair, $r = 0.41$) (Table 3), which agrees with findings of Watson and co-authors⁷⁸ ($r = 0.92$, $p < 0.01$); TCP FP negatively correlated with DCAN FP (fair, $r = -0.56$) and TCM FP (fair, $r = -0.41$) (Table 3). DCAN FP positively correlated with both TCM FP (moderate, $r = 0.74$) (Table 2), agreeing with findings of Watson and co-authors⁷⁸ ($r = 0.96$, $p < 0.01$) and BDCM (fair, $r = 0.54$), which also agrees with findings of Watson and co-authors⁷⁸ ($r = 0.89$, $p < 0.01$). NDMA FP negatively correlated with DCAN FP (fair, $r = -0.43$) (Table 3). The yield of TCM positively correlated with the yield of DCAN (fair, $r = 0.57$), as did the yield of BDCM (fair, r

$= 0.54$) (ESI† Table S13). The yield of TCP positively correlated with the yield of NDMA (moderate, $r = 0.67$). The yield of DCAN negatively correlated with the yields of TCP (moderate, $r = -0.59$) and NDMA (fair, $r = -0.43$) (ESI† Table S13). These associations suggest that DCAN FP can be expected when THM FP is present but can't be considered suitable proxies for each other.

4 Conclusions

The effect of HRT, depth and season on concentration and speciation of carbonaceous DBP and nitrogenous DBP FP in stratified lakes was investigated. When the three studied factors were considered in isolation, the FP of carbonaceous DBPs increased from Ter across to Pasteral reservoir, while FP of the nitrogenous DBPs (particularly NDMA) decreased across the same spatial scale. However, when the Ter sample (which behaved as an outlier) was not considered, spatial variability was insignificant, as the results seemed to cluster by season, meaning seasonality was the main driver of the observed variability. In particular, carbonaceous DBP FP was higher in autumn and summer than in winter, while the opposite was observed for nitrogen containing DBPs such as NDMA. Additionally, depth was not a significant driver of variability in the FP of DBPs studied.

This study adds a dimension of HRT, depth, and stratification effects on speciation of DBP formation potential, which have been less studied and extends the knowledge base of a few studies that have tackled the influence of seasonality on DBP FP in lakes and reservoirs.

Conflicts of interest

There are no conflicts to declare.

Acknowledgements

This project has received funding from the European Union's Horizon 2020 research and Innovation Programme under the Marie Skłodowska-Curie grant agreement No 722518. The authors thank Generalitat de Catalunya through Consolidated Research Groups ICRA_ENV 2017SGR1124 and ICRA_Tech 2017SGR1318. ICRA researchers thank funding from the CERCA program. MJF acknowledges her Ramón y Cajal fellowship (RyC-2015-17108), from the AEI-MICIU. The authors also wish to acknowledge the invaluable support rendered to them by the laboratory staff at Catalan Institute for Water Research, during the sampling and processing of the samples that culminated into this article.

References

- I. Evlampidou, L. Font-Ribera, D. Rojas-Rueda, E. Gracia-Lavedan, N. Costet, N. Pearce, P. Vineis, J. J. K. Jaakkola, F. Delloye, K. C. Makris, E. G. Stephanou, S. Kargaki, F.



- Kozisek, T. Sigsgaard, B. Hansen, J. Schullehner, R. Nahkur, C. Galey, C. Zwiener, M. Vargha, E. Righi, G. Aggazzotti, G. Kalnina, R. Grazuleviciene, K. Polanska, D. Gubkova, K. Bitenc, E. H. Goslan, M. Kogevinas and C. M. Villanueva, Trihalomethanes in Drinking Water and Bladder Cancer Burden in the European Union, *Environ. Health Perspect.*, 2020, **128**, 017001.
- 2 J. A. Kaufman, J. M. Wright, A. Evans, Z. Rivera-Núñez, A. Meyer and M. G. Narotsky, Associations Between Disinfection By-Product Exposures and Craniofacial Birth Defects, *J. Occup. Environ. Med.*, 2018, **60**, 109–119.
 - 3 A. Florentin, A. Hautemanière and P. Hartemann, Health effects of disinfection by-products in chlorinated swimming pools, *Int. J. Hyg. Environ. Health*, 2011, **214**, 461–469.
 - 4 M. Sillanpää, M. C. Ncibi, A. Matilainen and M. Vepsäläinen, Removal of natural organic matter in drinking water treatment by coagulation: A comprehensive review, *Chemosphere*, 2018, **190**, 54–71.
 - 5 Y. Tang, X. Long, M. Wu, S. Yang, N. Gao, B. Xu and S. Dutta, Bibliometric review of research trends on disinfection by-products in drinking water during 1975–2018, *Sep. Purif. Technol.*, 2020, **241**, 116741.
 - 6 C. Postigo and S. D. Richardson, Transformation of pharmaceuticals during oxidation/disinfection processes in drinking water treatment, *J. Hazard. Mater.*, 2014, **279**, 461–475.
 - 7 C. Postigo, R. Gil-Solsona, M. F. Herrera-Batista, P. Gago-Ferrero, N. Alygizakis, L. Ahrens and K. Wiberg, A step forward in the detection of byproducts of anthropogenic organic micropollutants in chlorinated water, *Trends Environ. Anal. Chem.*, 2021, **32**, e00148.
 - 8 N. B. Weston, W. P. Porubsky, V. A. Samarkin, M. Erickson, S. E. Macavoy and S. B. Joye, Porewater Stoichiometry of Terminal Metabolic Products, Sulfate, and Dissolved Organic Carbon and Nitrogen in Estuarine Intertidal Creek-bank Sediments, *Biogeochemistry*, 2006, **77**, 375–408.
 - 9 M. Valdivia-Garcia, P. Weir, Z. Frogbrook, D. W. Graham and D. Werner, Climatic, Geographic and Operational Determinants of Trihalomethanes (THMs) in Drinking Water Systems, *Sci. Rep.*, 2016, **6**, 35027.
 - 10 V. Uyak, K. Ozdemir and I. Toroz, Seasonal variations of disinfection by-product precursors profile and their removal through surface water treatment plants, *Sci. Total Environ.*, 2008, **390**, 417–424.
 - 11 M. Serrano, I. Montesinos, M. J. Cardador, M. Silva and M. Gallego, Seasonal evaluation of the presence of 46 disinfection by-products throughout a drinking water treatment plant, *Sci. Total Environ.*, 2015, **517**, 246–258.
 - 12 G. Chhipi-Shrestha, M. Rodriguez and R. Sadiq, Unregulated disinfection By-products in drinking water in Quebec: A meta analysis, *J. Environ. Manage.*, 2018, **223**, 984–1000.
 - 13 P. A. Bukaveckas, D. McGaha, J. M. Shostell, R. Schultz and J. D. Jack, Internal and external sources of THM precursors in a midwestern reservoir, *J. – Am. Water Works Assoc.*, 2007, **99**, 127–136.
 - 14 M. L. Nguyen, L. A. Baker and P. Westerhoff, DOC and DBP precursors in western US watersheds and reservoirs, *J. – Am. Water Works Assoc.*, 2002, **94**, 98–112.
 - 15 T. E. C. Kraus, B. A. Bergamaschi, P. J. Hernes, D. Doctor, C. Kendall, B. D. Downing and R. F. Losee, How reservoirs alter drinking water quality: Organic matter sources, sinks, and transformations, *Lake Reservoir Manage.*, 2011, **27**, 205–219.
 - 16 X. Ran, A. F. Bouwman, Z. Yu and J. Liu, Implications of eutrophication for biogeochemical processes in the Three Gorges Reservoir, China, *Reg. Environ. Change*, 2019, **19**, 55–63.
 - 17 C. Teodoru and B. Wehrli, Retention of sediments and nutrients in the Iron Gate I Reservoir on the Danube River, *Biogeochemistry*, 2005, **76**, 539–565.
 - 18 S. J. Parks and L. A. Baker, Sources and transport of organic carbon in an Arizona river-reservoir system, *Water Res.*, 1997, **31**, 1751–1759.
 - 19 S. H. Jenkins, Standard Methods for the Examination of Water and Wastewater, *Water Res.*, 1982, **16**, 1495–1496.
 - 20 R. Baird and L. Bridgewater, *Standard methods for the examination of water and wastewater*, American Public Health Association, Washington, D.C., 23rd edn, 2017.
 - 21 J. W. Eaton, D. Bateman, S. Hauberg and R. Wehring, *GNU Octave version 3.8.1 manual: a high-level interactive language for numerical computations*, CreateSpace Independent Publishing Platform, 2014, ISBN 1441413006, URL <http://www.gnu.org/software/octave/doc/interpreter/>.
 - 22 M. Tedetti, P. Cuet, C. Guigue and M. Goutx, Characterization of dissolved organic matter in a coral reef ecosystem subjected to anthropogenic pressures (La Réunion Island, Indian Ocean) using multi-dimensional fluorescence spectroscopy, *Sci. Total Environ.*, 2011, **409**, 2198–2210.
 - 23 A. Huguet, L. Vacher, S. Relexans, S. Saubusse, J. M. Froidefond and E. Parlanti, Properties of fluorescent dissolved organic matter in the Gironde Estuary, *Org. Geochem.*, 2009, **40**, 706–719.
 - 24 J. P. Casas-Ruiz, J. Tittel, D. von Schiller, N. Catalán, B. Obrador, L. Gómez-Gener, E. Zwirnmann, S. Sabater and R. Marcé, Drought-induced discontinuities in the source and degradation of dissolved organic matter in a Mediterranean river, *Biogeochemistry*, 2016, **127**, 125–139.
 - 25 A. M. Hansen, T. E. C. Kraus, B. A. Pellerin, J. A. Fleck, B. D. Downing and B. A. Bergamaschi, *Optical properties of dissolved organic matter (DOM): Effects of biological and photolytic degradation*, 2016, pp. 1015–1032.
 - 26 J. E. Birdwell and A. S. Engel, Characterization of dissolved organic matter in cave and spring waters using UV-Vis absorbance and fluorescence spectroscopy, *Org. Geochem.*, 2010, **41**, 270–280.
 - 27 C. A. Stedmon and R. Bro, *Oceanography: Methods Characterizing dissolved organic matter fluorescence with parallel factor analysis: a tutorial*, 2008, pp. 572–579.
 - 28 D. N. Kothawala, K. R. Murphy, C. A. Stedmon, G. A. Weyhenmeyer and L. J. Tranvik, Inner filter correction of



- dissolved organic matter fluorescence, *Limnol. Oceanogr.: Methods*, 2013, **11**, 616–630.
- 29 S. S. Marais, E. J. Ncube, T. A. M. Msagati, B. B. Mamba and T. T. I. Nkambule, Assessment of trihalomethane (THM) precursors using specific ultraviolet absorbance (SUVA) and molecular size distribution (MSD), *J. Water Process. Eng.*, 2019, **27**, 143–151.
- 30 P. Liu, M. J. Farré, J. Keller and W. Gernjak, Reducing natural organic matter and disinfection by-product precursors by alternating oxic and anoxic conditions during engineered short residence time riverbank filtration: A laboratory-scale column study, *Sci. Total Environ.*, 2016, **565**, 616–625.
- 31 W. A. Mitch, A. C. Gerecke and D. L. Sedlak, A N-Nitrosodimethylamine (NDMA) precursor analysis for chlorination of water and wastewater, *Water Res.*, 2003, **37**, 3733–3741.
- 32 H. Akoglu, User's guide to correlation coefficients, *Turk. J. Emerg. Med.*, 2018, **18**, 91–93.
- 33 R. CoreTeam, *R: A Language and Environment for Statistical Computing*, 2017, vol. 2.
- 34 H. Y. Zhai, X. Z. He, Y. Zhang, T. T. Du, A. S. Adeleye and Y. Li, Disinfection byproduct formation in drinking water sources: A case study of Yuqiao reservoir, *Chemosphere*, 2017, **181**, 224–231.
- 35 F. Wang, B. Gao, D. Ma, Q. Yue, R. Li and Q. Wang, Reduction of disinfection by-product precursors in reservoir water by coagulation and ultrafiltration, *Environ. Sci. Pollut. Res.*, 2016, **23**, 22914–22923.
- 36 F. Wang, B. Y. Gao, Q. Y. Yue, F. Bu and X. Shen, Effects of ozonation, powdered activated carbon adsorption, and coagulation on the removal of disinfection by-product precursors in reservoir water, *Environ. Sci. Pollut. Res.*, 2017, **24**, 17945–17954.
- 37 H. Sakai, S. Tokuhara, M. Murakami, K. Kosaka, K. Oguma and S. Takizawa, Comparison of chlorination and chloramination in carbonaceous and nitrogenous disinfection byproduct formation potentials with prolonged contact time, *Water Res.*, 2016, **88**, 661–670.
- 38 S. Inamdar, N. Finger, S. Singh, M. Mitchell, D. Levia, H. Bais, D. Scott and P. McHale, Dissolved organic matter (DOM) concentration and quality in a forested mid-Atlantic watershed, USA, *Biogeochemistry*, 2012, **108**, 55–76.
- 39 J. Zhang, T. Maqbool, Y. Qiu, Y. Qin, M. B. Asif, C. Chen and Z. Zhang, Determining the leading sources of N-nitrosamines and dissolved organic matter in four reservoirs in Southern China, *Sci. Total Environ.*, 2021, **771**, 145409–145409.
- 40 C. Fang, X. Yang, S. Ding, X. Luan, R. Xiao, Z. Du, P. Wang, W. An and W. Chu, Characterization of Dissolved Organic Matter and Its Derived Disinfection Byproduct Formation along the Yangtze River, *Environ. Sci. Technol.*, 2021, **55**, 12326–12336.
- 41 A. T. Chow, A. T. O'Geen, R. A. Dahlgren, F. J. Diaz, K.-H. Wong and P.-K. Wong, Reactivity of Litter Leachates from California Oak Woodlands in the Formation of Disinfection By-Products, *J. Environ. Qual.*, 2011, **40**, 1607–1616.
- 42 J. F. Hunt and T. Ohno, Characterization of fresh and decomposed dissolved organic matter using excitation-emission matrix fluorescence spectroscopy and multiway analysis, *J. Agric. Food Chem.*, 2007, **55**, 2121–2128.
- 43 Q. Li, X. Guo, L. Chen, Y. Li, D. Yuan, B. Dai and S. Wang, Investigating the spectral characteristic and humification degree of dissolved organic matter in saline-alkali soil using spectroscopic techniques, *Front. Earth Sci.*, 2017, **11**, 76–84.
- 44 C. Y. Hu, H. Z. Zhu, Y. L. Lin, T. Y. Zhang, F. Zhang and B. Xu, Dissolved organic matter fractions and disinfection by-product formation potential from major raw waters in the water-receiving areas of south-to-north water diversion project, China, *Desalin. Water Treat.*, 2015, **56**, 1689–1697.
- 45 G. Jossette, B. Leporcq, N. Sanchez and X. Philippon, Biogeochemical mass-balances (C, N, P, Si) in three large reservoirs of the Seine Basin (France), *Biogeochemistry*, 1999, **47**, 119–146.
- 46 S. W. Krasner, The formation and control of emerging disinfection by-products of health concern, *Philos. Trans. R. Soc., A*, 2009, **367**, 4077–4095.
- 47 T. Bond, Precursors of nitrogenous disinfection by-products in drinking water—A critical review and analysis, *J. Hazard. Mater.*, 2012, **16**.
- 48 W. Chu, N. Gao, Y. Deng and X. Li, in *Recent Advances in Disinfection by-Products*, ed. T. Karanfil, B. Mitch, P. Westerhoff and Y. Xie, Amer Chemical Soc, Washington, 2015, vol. 1190, pp. 307–339.
- 49 W. Chu, D. Yao, Y. Deng, M. Sui and N. Gao, Production of trihalomethanes, haloacetaldehydes and haloacetonitriles during chlorination of microcystin-LR and impacts of pre-oxidation on their formation, *J. Hazard. Mater.*, 2017, **327**, 153–160.
- 50 W. Qian-Yuan, L. Chao, D. Ye, W. Wen-Long, H. Huang and H. Hong-Ying, Elimination of disinfection byproduct formation potential in reclaimed water during solar light irradiation, *Water Res.*, 2016, **95**, 260–267.
- 51 R. Zhang, F. Wang, W. Chu, C. Fang, H. Wang, M. Hou, R. Xiao and G. Ji, Microbial degradation of typical amino acids and its impact on the formation of trihalomethanes, haloacetonitriles and haloacetamides during chlor(am)ination, *Water Res.*, 2019, **159**, 55–64.
- 52 S. W. Krasner, W. A. Mitch, D. L. McCurry, D. Hanigan and P. Westerhoff, Formation, precursors, control, and occurrence of nitrosamines in drinking water: A review, *Water Res.*, 2013, **47**, 4433–4450.
- 53 G. C. Woods and E. R. V. Dickenson, Natural attenuation of NDMA precursors in an urban, wastewater-dominated wash, *Water Res.*, 2016, **89**, 293–300.
- 54 J. Sanchís, W. Gernjak, A. Munné, N. Catalán, M. Petrovic and M. J. Farré, Fate of N-nitrosodimethylamine and its precursors during a wastewater reuse trial in the Llobregat River (Spain), *J. Hazard. Mater.*, 2021, **4075**, 124346.
- 55 E. H. Goslan, S. W. Krasner, M. Bower, S. A. Rocks, P. Holmes, L. S. Levy and S. A. Parsons, A comparison of disinfection by-products found in chlorinated and



- chloraminated drinking waters in Scotland, *Water Res.*, 2009, **43**, 4698–4706.
- 56 J. W. A. Charrois, J. M. Boyd, K. L. Froese and S. E. Hrudey, Occurrence of N-nitrosamines in Alberta public drinking-water distribution systems, *J. Environ. Eng. Sci.*, 2007, **6**, 103–114.
- 57 L. Godo-Pla, J. J. Rodríguez, J. Suquet, P. Emiliano, F. Valero, M. Poch and H. Monclús, Control of primary disinfection in a drinking water treatment plant based on a fuzzy inference system, *Process Saf. Environ. Prot.*, 2021, **145**, 63–70.
- 58 C. Stepczuk, E. M. Owens, S. W. Effler, M. T. Auer and J. A. Bloomfield, A modeling analysis of THM precursors for a eutrophic reservoir, *Lake Reservoir Manage.*, 1998, **14**, 367–378.
- 59 A. C. Gerecke and D. L. Sedlak, Precursors of N-nitrosodimethylamine in natural waters, *Environ. Sci. Technol.*, 2003, **37**, 1331–1336.
- 60 X. R. Zhou, Y. L. Lin, T. Y. Zhang, B. Xu, W. H. Chu, T. C. Cao and W. Q. Zhu, Speciation and seasonal variation of various disinfection by-products in a full-scale drinking water treatment plant in East China, *Water Sci. Technol.: Water Supply*, 2019, **19**, 1579–1586.
- 61 E. H. Goslan, C. Seigle, D. Purcell, R. Henderson, S. A. Parsons, B. Jefferson and S. J. Judd, Carbonaceous and nitrogenous disinfection by-product formation from algal organic matter, *Chemosphere*, 2017, **170**, 1–9.
- 62 T. Bond, J. Huang, M. R. Templeton and N. Graham, Occurrence and control of nitrogenous disinfection by-products in drinking water – A review, *Water Res.*, 2011, **45**, 4341–4354.
- 63 A. T. Chow, S.-T. Lee, A. T. O'Geen, T. Orozco, D. Beaudette, P.-K. Wong, P. J. Hernes, K. W. Tate and R. A. Dahlgren, Litter Contributions to Dissolved Organic Matter and Disinfection Byproduct Precursors in California Oak Woodland Watersheds, *J. Environ. Qual.*, 2009, **38**, 2334–2343.
- 64 Q. Zhang, W. F. Kuang, L. Y. Liu, K. Li, K. H. Wong, A. T. Chow and P. K. Wong, Trihalomethane, haloacetonitrile, and chloral hydrate formation potentials of organic carbon fractions from sub-tropical forest soils, *J. Hazard. Mater.*, 2009, **172**, 880–887.
- 65 E. H. Goslan, D. A. Fearing, J. Banks, D. Wilson, P. Hills, A. T. Campbell and S. A. Parsons, Seasonal variations in the disinfection by-product precursor profile of a reservoir water, *J. Water Supply: Res. Technol.-AQUA*, 2002, **51**, 475–482.
- 66 J. Fang, J. Ma, X. Yang and C. Shang, Formation of carbonaceous and nitrogenous disinfection by-products from the chlorination of *Microcystis aeruginosa*, *Water Res.*, 2010, **44**, 1934–1940.
- 67 S. W. Krasner, P. Westerhoff, B. Chen, B. E. Rittmann and G. Amy, Occurrence of Disinfection Byproducts in United States Wastewater Treatment Plant Effluents, *Environ. Sci. Technol.*, 2009, **43**, 8320–8325.
- 68 S. Park, S. Jung and H. Kim, Regional and seasonal distributions of N-nitrosodimethylamine (NDMA) concentrations in chlorinated drinkingwater distribution systems in Korea, *Water*, 2019, **11**, 2645.
- 69 B. Zhao, N. Nakada, S. Itai, S. Hanamoto, K. Okumura and H. Tanaka, Diurnal patterns of N-nitrosodimethylamine and formaldehyde behaviors in different seasons in surface water influenced by effluent from sewage treatment plants, *J. Hazard. Mater.*, 2020, **383**, 121155.
- 70 N. Yang, C. Zhang, L. Wang, Y. Li, W. Zhang, L. Niu, H. Zhang and L. Wang, Nitrogen cycling processes and the role of multi-trophic microbiota in dam-induced river-reservoir systems, *Water Res.*, 2021, **206**, 117730.
- 71 M. Lürling, F. Eshetu, E. J. Faassen, S. Kosten and V. L. M. Huszar, Comparison of cyanobacterial and green algal growth rates at different temperatures: Temperature and phytoplankton growth rates, *Freshwater Biol.*, 2013, **58**, 552–559.
- 72 Y. Du, F. Chen, K. Xiao, C. Song, H. He, Q. Zhang, Y. Zhou, K. Jang, Y. Zhang, P. Xing, Z. Liu, Y. Zhang and Y. Lu, Water Residence Time and Temperature Drive the Dynamics of Dissolved Organic Matter in Alpine Lakes in the Tibetan Plateau, *Global Biogeochem. Cycles*, 2021, **35**, e2020GB006908.
- 73 E. Asmala, R. Autio, H. Kaartokallio, C. A. Stedmon and D. N. Thomas, Processing of humic-rich riverine dissolved organic matter by estuarine bacteria: effects of predegradation and inorganic nutrients, *Aquat. Sci.*, 2014, **76**, 451–463.
- 74 I. Reche, M. L. Pace and J. J. Cole, Interactions of Photobleaching and Inorganic Nutrients in Determining Bacterial Growth on Colored Dissolved Organic Carbon, *Microb. Ecol.*, 1998, **36**, 270–280.
- 75 X. Li, N. R. H. Rao, K. L. Linge, C. A. Joll, S. Khan and R. K. Henderson, Formation of algal-derived nitrogenous disinfection by-products during chlorination and chloramination, *Water Res.*, 2020, **183**, 116047.
- 76 J. C. Watson, Establishing Evidence for Internal Structure Using Exploratory Factor Analysis, *Meas. Eval. Couns. Dev.*, 2017, **50**, 232–238.
- 77 L. Yang, D. Kim, H. Uzun, T. Karanfil and J. Hur, Assessing trihalomethanes (THMs) and N-nitrosodimethylamine (NDMA) formation potentials in drinking water treatment plants using fluorescence spectroscopy and parallel factor analysis, *Chemosphere*, 2015, **121**, 84–91.
- 78 K. Watson, M. J. Farré, F. D. L. Leusch and N. Knight, Using fluorescence-parallel factor analysis for assessing disinfection by-product formation and natural organic matter removal efficiency in secondary treated synthetic drinking waters, *Sci. Total Environ.*, 2018, **640–641**, 31–40.
- 79 M. A. Puig, J. Armengol, G. Gonzalez, J. Peñuelas, S. Sabater and F. Sabater, Chemical and Biological Changes in the Ter River Induced by a Series of Reservoirs, Regul. Streams, 1987, 373–382.
- 80 J. Carol, L. Benejam, C. Alcaraz, L. Zamora and E. Navarro, The effects of limnological features on fish assemblages of 14 Spanish reservoirs, 2006, 66–77.



- 81 A. Vila-Gispert, M. G. Fox, L. Zamora and R. Moreno-Amich, Morphological variation in pumpkinseed *Lepomis gibbosus* introduced into Iberian lakes and reservoirs; adaptations to habitat type and diet?, *J. Fish Biol.*, 2007, **71**, 163–181.
- 82 V. Moschini-Carlos, M. Pompêo, P. Y. Nishimura and J. Armengol, Phytoplankton as trophic descriptors of a series of Mediterranean reservoirs (Catalonia, Spain), *Fundam. Appl. Limnol.*, 2018, **191**, 37–52.



Results and discussion

4.4 Discussion of hypotheses.

Hypothesis i: Hydroclimatic extremes are intense in the Ter Watershed, reservoir water quality responds negatively to the perturbations, but the response is shaped by trophic state.

In this thesis, we put forward a proposition that healthy (less eutrophic) aquatic ecosystems may be more resistant to impacts of climate extremes. In authenticating this proposition, we interrogated a long-term dataset of hydroclimatic time series using two approaches. The first approach involved establishing causal links between hydroclimatic variables, as predictors of reservoir water quality. With this method, we were able to observe the range of quantiles of response variables that causally responded to predictor variables. However, this approach could not specifically ascertain if the observed causal effects were a result of hydroclimatic extremes values. This uncertainty necessitated implementation of an additional (second) layer of analysis, in which we derived climate extreme indices from hydroclimatic variables, coupled them to reservoir water quality time series and assessed the occurrence of differences in medians of water quality in extreme versus non-extreme conditions. In summary, results reported in **Paper I** suggest that hydroclimatic perturbations, that negatively impacted aquatic ecosystems, were mostly droughts, extreme precipitation and, to a lesser extent, heatwaves. These perturbations were associated with decreased dissolved oxygen concentration and increased ammonium concentration (during droughts), increased nitrate concentration (during extreme flows) and decreased dissolved oxygen concentration (during droughts and heatwaves). Nutrient and organic matter abatement interventions implemented in the watershed substantially improved the trophic state of the reservoir, which seems to have improved hypolimnetic oxygenation conditions the most by reducing organic matter concentration, hence oxygen demand required for organic matter biodegradation. Thus, droughts and heatwaves, whose magnitude inversely varies with dissolved oxygen concentration, could only manifest their imprints in the hypolimnion, as the epilimnion was often well oxygenated by primary production, as well as wind mediated oxygen dissolution. Also, the same stressors could only affect the hypolimnion before building of WWTPs, as it had high oxygen demand for the degradation of high phytoplankton biomass. On the other hand, trophic state improvements meant less phytoplankton biomass after the building of WWTPs, hence reduced oxygen demand for respiration. As such, the relevance of droughts and heatwaves as perturbations on dissolved oxygen and increased NH_4^+ concentration diminished. Watershed

Results and discussion

management programs that led to reduction of nitrate loads into the reservoir relegated the relevance of extreme precipitation mediated run-off on nitrate concentrations to the period before implementation of the interventions only. It also explains why extreme precipitation was no longer relevant on nitrate concentration, in both the epilimnion and hypolimnion, following the construction and upgrading of WWTPs. Also, it should be emphasized that in the epilimnion, most of the aforementioned negative imprints of perturbations on water quality disappear after implementation of nutrient abatement interventions, except for high NH_4^+ concentration which persists post the building of WWTPs. The mechanisms behind the persistence of NH_4^+ in the epilimnion, are not, at present, well understood but evapoconcentration may be speculated to be one of the mechanisms. The scenario where the same magnitudes of hydroclimatic perturbations impact water quality only before construction of WWTPs and that no such effects are felt afterwards, is interpreted as resistance (Nimmo et al., 2015; Thayne et al., 2021). The aquatic ecosystem is deemed resistant because water quality no longer responded to the same magnitude and perturbations (i.e. resisted change). The observed resistance can, plausibly, be attributed to improvement of the reservoir trophic state following the implementation of nutrient reduction strategies in the watershed.

The improvement in trophic state reported in **Paper I** mostly benefited dissolved oxygen dynamics, which has also been reported in other previous studies in the same watershed, that attributed improvements in trophic state to building of tertiary WWTPs (Marcé et al., 2008; Ordóñez et al., 2010). Tertiary WWTPs are specially adapted for nutrient removal (Zhou et al., 2022), whereas dissolved organic matter is efficiently removed by secondary wastewater treatment processes (Marcé et al., 2008). Such improved dissolved oxygen conditions could result from decreased oxygen demand for the biodegradation of both terrestrial, in-reservoir derived organic matter (Le Moal et al., 2019), wastewater effluent (Xue et al., 2017) and oxidation of sediment bound reduced substances (Müller et al., 2012). The epilimnion is usually unaffected by eutrophication induced dissolved oxygen depletion because it is well aerated by the mechanical action of wind and waves and oxygenation from primary production, so much so that oxygen demand by ecosystem respiration is often exceeded by the available supply. On the other hand, the hypolimnion is usually isolated from aeration during stratification periods and primary production is usually non-existent, hence oxygen demand for ecosystem respiration exceeds available supply, leading to hypoxia (Brusseau et al., 2019). However, in some cases, the entire water column can become irreversibly anoxic after turn-over events that mix anoxic hypolimnetic waters with oxic epilimnetic waters, as reported by a study on Lake Vechten, which was attributed to the existence of alternative stable states (Bush et al., 2017).

Results and discussion

Autochthonous DOC concentration linearly correlates with lake trophic state (Wen, 2022), hence reduced eutrophication likely resulted in less in-reservoir DOM production. Also, terrestrial DOM export may decline because of reduced microbial degradation of DOM and disrupted hydrologic connectivity (Szkokan-Emilson et al., 2017; Wu et al., 2023) due to increased drought frequency in the Ter watershed after construction of WWTPs. In addition, dominant ammonium load before the construction of WWTPs may have increased oxygen demand during nitrification, whereas such oxygen demand probably declined after WWTPs were built in the watershed, due to diminished ammonium. Furthermore, the construction of WWTPs decreases DOM during the primary and secondary stages of treatment (Xue et al., 2017), hence effluent DOM was reduced. Thus, all four factors may result in reduced oxygen demand, hence improvements in concentrations of dissolved oxygen in the period following the building and upgrading of WWTPs.

Although results reported in **Paper I** excluded dissolved organic matter, due to insufficient time series, the dynamics of dissolved oxygen under perturbations of droughts, extreme precipitation and heat waves, suggest dissolved organic matter could have been causally responsive to the same variables. Consequently, elevated concentrations of dissolved organic matter could be anticipated under the influence of the same perturbations that can potentially form both carbonaceous and nitrogenous disinfection by-products. Thus, nutrient abatement initiatives that result in decreased dissolved organic carbon loads in the reservoir, could also reduce the formation potential of DBPs. Unraveling patterns of dissolved organic matter variability under the same stressors would be a worthwhile research direction to inform water supply management.

Results and discussion

Hypothesis ii: Signatures of extreme climatic events can be detected in a coarse water quality time series with innovative statistical approaches, which should reduce reliance on high frequency data and its associated costly infrastructure.

Climate extremes have, for long, been recognized to adversely impact aquatic ecosystems, consequently threatening ecosystem health and its associated benefits to society. To date, ecologists have relied on either event-based sampling or deployment of platforms on lakes that have capabilities of sensing both weather and a suite of water quality variables, with high frequency and in real time, to detect instantaneous or lagged coupling between lake water quality and intensification of climate variables. While both approaches can establish causal links reasonably well, event-based sampling may be challenged with technicalities of implementations in cases where it becomes too risky for humans and equipment, to implement, for instance, in ravaging storm events such as tornadoes. Also, deployment of high frequency sensing equipment comes with a huge infrastructure cost that may be prohibitive for resource constrained laboratories, institutions or nations, most of which are the most vulnerable to adverse impacts of climate extremes on lake ecosystems. This thesis advances a proposition that, apart from the aforementioned traditional methods, establishing causal links between climate extremes and lake water quality can also be achieved in an innovative way that involves being adept at the choice and application of statistical methods. Innovatively applying statistical techniques can mine footprints of climate extremes in the low frequency water quality data that is routinely monitored in many lakes across the globe. In **Paper I** of this thesis, we report causal effects of both hydroclimatic variables and their derived indices on a long term, routinely generated low frequency reservoir water quality. Such causal effects were established through a careful application of statistical techniques. Outcomes of this analysis are discussed under the first hypothesis of the discussion section. The fact that mechanisms identified by our innovative approach agree with what is often identified by and reported using the traditional methods of event based sampling and high frequency sensing, suggests the plausibility of our proposition. We are not suggesting this innovative approach to replace traditional methods, rather, we view it as complementary to the existing methods and an alternative for entities that are incapable of investing in high frequency weather and water quality sensing infrastructure.

Results and discussion

Hypothesis iii: Long water residence time (WRT) reduces the formation potential of both carbonaceous and nitrogenous disinfection by-products in reservoirs due to diminishing concentration of organic matter precursor compounds through mineralization.

Generally, there is a paucity of studies evaluating effects of water age in lakes (let alone on eutrophic systems) on the formation potential of either C- or N- DBPs or both. Instead, similar existing research on the impact of water age on DBPs, concerns the dynamics of chlorinated water in the distribution networks, in which THMs concentrations have been observed to increase with longer residence times. Longer WRT in the distribution increases reaction times between precursors and disinfectants (Simard et al., 2011), particularly when some level of disinfectant is maintained, otherwise THMs deteriorate with increasing water age in the absence of sustained reactivity with NOM (Ratpukdi et al., 2019). In the same distribution, HANs have been reported to decrease in concentration with increasing water age, due to hydrolysis and biodegradation (Ratpukdi et al., 2019). Although time is the common variable of interest in both cases, its impact in the distribution networks differs from the context of water sources such as lakes. In lakes, depending on trophic state, water age might increase or decrease the formation potential of DBPs, based on whether precursors are continuously being degraded without in-reservoir production or otherwise. Thus, it would be anticipated that in the absence of in-reservoir generation of precursor compounds, the formation potential of DBPs would degrade with increasing water age due to mineralization of precursors. Conversely, in eutrophic systems with substantial generation of in-reservoir DOM, the formation potential is expected to increase. However, **Paper III** of this thesis reports intriguing results for the formation potential of THMs. The combined WRT from Sau to Pastoral is nearly 200 days, and eutrophication wanes along the river-reservoir chain. **Paper III** reports an increase in the formation potential of TTHMs, along the river-reservoir chain, while in-reservoir production of DOM is minor (both BIX and FI were less than minimums of 1 and 1.9, respectively, (Casas-Ruiz et al., 2016; Huguet et al., 2009) in both major reservoirs of the system. Thus, we can plausibly suggest that the observed increase in the formation potential of THMs is due to the role played by WRT in providing microorganisms with time to biodegrade complex terrestrially derived organic matter into simpler organic compounds. These biodegradation products, with increased aromaticity, readily react with chlorine to form C-DBPs (Chow et al., 2011). We consider this finding novel, as well as the contribution on the role of HRT in

Results and discussion

trihalomethane formation potential, significant, given that there is paucity of such kinds of studies in the scientific literature.

The decrease in NDMA formation potential from the Ter River to Pastoral Reservoir, reported in **Paper III**, suggests a decrease in precursor concentrations along the river-reservoir chain. This decrease is probably due to biodegradation and photolysis (Sanchís et al., 2021; Woods and Dickenson, 2016), also exemplifying the crucial role of WRT in the attenuation of precursor compounds such as secondary, tertiary (Bond et al., 2017) and quaternary amines (dimethylamine, diethanolamine and triethanolamine) (Alaba et al., 2017). Although algal and agricultural runoff impacted waters are plausible precursor sources (Sgroi et al., 2018; Zeng et al., 2016), the likely origin of NDMA precursors is the wastewater (Krasner et al., 2018; Wang et al., 2014) discharged in the Ter River. Thus, precursors in the wastewater may have been degrading along the river-reservoir chain, since in-reservoir DOM production seemed insignificant. On the other hand, the formation potential of DCAN leveled off at median values that were roughly the same, suggesting that their precursors were largely recalcitrant to any form of degradation over the entire WRT of circa 200 days. This finding was surprising, since amino acids are reported to be easily biodegradable (Tang et al., 2012; Zhang et al., 2019) and are also susceptible to photodegradation (Xu et al., 2020). In this river-reservoir system, possible DCAN organic precursor sources may be wastewater (Li et al., 2019; Peng et al., 2022; Tang et al., 2012), terrestrially derived DOM (Chen et al., 2019; Chow et al., 2009) and, to a lesser extent, in-lake derived DOM (Goslan et al., 2017; Wang et al., 2023; Zhang et al., 2016). If the precursor source was largely exogenous DOM, WRT effects could as well have manifested themselves out, generating a gradient of increasing formation potential across the river-reservoir system, similar to THMs. On the other hand, if DCAN largely formed from wastewater, a gradient of decreasing formation potential along the river-reservoir system could also have been visible, as effects of wastewater decrease with increasing WRT. The absence of these two anticipated patterns point to the existence of precursors that are invariant in the time domain, which are, at present, unknown and, therefore, warrant further studies. Although dissolved amino acids such as tryptophan, tyrosine, aspartic acid, asparagine, cysteine, methionine and glutamic acid are known precursors capable of forming DCAN during chlorination (Jia et al., 2016), their concentration in the natural environment is low. Instead, dihaloacetonitriles are thought to substantially form from amino nitrogen present in proteinaceous material or bound to humic acids (Reckhow et al., 2001) and fulvic acids (Xu et al., 2020).

Results and discussion

From the perspective of the regulated C-DBPs, the gradient of TTHMs formation suggests that abstracting water from Sau perhaps is the best option, as, being the first reservoir in the chain, the formation potential is lower and therefore would need less treatment. However, formation potential experiments are amplified both in terms of time of reactivity between the disinfectant and precursors and quantities of the disinfectants used, likely resulting in inflated formation potential levels that are not a reflection of typical waterworks operational conditions. **Paper III** of this thesis reports a raw water TTHMs formation potential of under 93 $\mu\text{g}/\text{L}$, which is already below the EU regulatory threshold of 100 $\mu\text{g}/\text{L}$ for treated drinking water. In reality, the recorded formation potential will be further reduced due to operational processes that are designed to reduce precursor concentrations such as coagulation (Sillanpää et al., 2018) and activated carbon adsorption (Zhang et al., 2015). As such, the costs that may be incurred in changing the abstraction location may not justify the minor gains of reducing the formation potential. Furthermore, although currently unregulated, the gradient in NDMA formation potential indicates that the current abstraction point at Pasteral is the best option due to its lowest formation potential. When this result is considered with TTHMs formation potential, it can be argued that maintaining the current abstraction strategy remains the best option.

Hypothesis iv: Thermal stratification in deep reservoirs shapes speciation and stratification of disinfection by-products formation potential due to stratification of organic precursors.

Studies examining gradients in the variability of DBPs formation potential by depth, in deep lakes, are uncommon. As such, our results reported in **Paper III** of this thesis, are a significant contribution in this research domain. Overall, gradients of variability in DBP formation potential by depth appear to be driven by season. The observed gradient of increasing THM formation potential with depth in both Sau and Susqueda reservoirs, in winter, came as a surprise because both reservoirs turn over in winter, which should result in equilibration of precursors and the formation potential. Instead, a trend of THM formation potential stratifying in summer, was anticipated because thermal stratification also stratifies precursor compounds (Li et al., 2008; Stepczuk et al., 1998). A trend of decreasing THM formation in summer, along a gradient of increasing depth, was anticipated due to the prevalence of primary productivity within the euphotic zone, which can generate precursor compounds, as was also reported in other eutrophic systems (Stepczuk et al., 1998). The usual THM formation potential predictive surrogates such as DOC,

Results and discussion

UV₂₅₄ and HIX exhibited a gradient of increasing with depth in summer, which would suggest increased generation of precursors from biodegradation of both exogenic and endogenic organic matter in the hypolimnion, but there was no concomitant gradient of increasing THM formation potential, with increasing depth in summer. In fact, one study on Taylorsville Lake reported a gradient in the formation potential of THM as being highest in the hypolimnion in summer, which was attributed to release of precursors from biodegradation of largely terrestrial organic matter (Bukaveckas et al., 2007). Thus, the gradient reported in **Paper III**, suggests that the generation of THMs from autochthonous precursors dominated the influence of precursors from biodegradation of terrestrial and decaying phytoplankton biomass in the hypolimnion. In summary, thermal stratification affected the formation of C-DBPs and in a surprising way for winter, in that reservoir turn-over didn't seem to evenly distribute precursor compounds.

For N-DBP formation, it was expected that their major precursor sources were wastewater, which should have been evenly distributed across the water column, and that stratification of formation potential would then be driven by additional precursors from either terrestrial or in-reservoir DOM sources. If such was the case, there would have been a gradient in the formation potential of DCAN and NDMA, both of which would have been higher in the euphotic zone, due to thriving of algal derived precursors (Stepczuk et al., 1998). Both compounds would then exhibit a gradient of decreasing with increasing depth from summer to probably early autumn but get evenly distributed across the water column in winter due to reservoir turnover equilibrating precursors. While the trend for DCAN formation in winter and summer, as reported in **Paper III**, agrees with the anticipated patterns, its gradient of increasing formation with increasing depth in autumn suggests that more precursors may have been generated in the hypolimnion, probably from biodegradation of allochthonous DOM, which is known to contain DCAN precursors (Zhang et al., 2009). On the other hand, the formation potential of NDMA in Susqueda agreed with the anticipated trends of late autumn, winter and summer, suggesting that algal-derived precursors in the euphotic zone may have contributed to the observed gradient. In Sau, the trend for NDMA formation in winter was as expected, but the summer trend suggests that the degradation rate of NDMA precursors in the euphotic zone exceeded the production rate, leading to a net decrease in the formation potential. Such a gradient of increasing NDMA formation by depth might be speculated to be due to either photolysis, (Pehlivanoglu-Mantas and Sedlak, 2006; Woods and Dickenson, 2016) or aerobic biodegradation (Na-Phatthalung et al., 2019; Sharp et al., 2005) of organic precursors enhanced by high surface water temperature (Zhao et al., 2020). Also, the gradient of decreasing NDMA formation potential with increasing depth, observed in Sau in autumn, suggests generation of precursors in the surface water layers, probably from algal primary

Results and discussion

production. In general, DBP formation potential gradients by depth reported in **Paper III**, for both carbonaceous and nitrogenous species, are subtle and irregular, hence are less likely to have meaningful management implications, particularly considering that formation potential experiments are conducted at amplified reaction times and oxidant concentrations. In fact, a few previous studies that have examined DBP formation, under stratification conditions in deep lakes, reported contrasting results, with some studies reporting no significant gradient in THM formation (Kraus et al., 2011), whereas others reported substantial gradient of increases in THM formation potential with increasing depth (Hobson et al., 2010). Thus, whether selective water withdrawal from different depths, a common practice in the water supply industry, which is implemented to optimize water quality for subsequent treatment operations (Ma, 2004; Song et al., 2023; Weber et al., 2017), benefits DBP formation potential control and management, remains system specific and definitively unresolved, although it could be reasonably deemed inconsequential in the cases of Sau and Susqueda Reservoirs.

Hypothesis v: Seasonality drives speciation and formation potential of disinfection by-products in eutrophic systems, with higher formation potential occurring in summer.

Trends in the variability of THM formation showed an increase in autumn, probably because of rainfall and its associated run-off, that exported terrestrial DOM into key reservoirs of the system (Sau and Susqueda), which increased precursor compounds (humic and fulvic acids) and hence, the formation potential (Uyak et al., 2008). Furthermore, the observed trend of increased formation potential in summer suggests the role of higher temperature in enhancing microbial degradation rates of complex allochthonous DOM (Zhou et al., 2019) into smaller compounds that can readily react with chlorine to form THMs. While the same summer temperature may have played some role in the production of in-reservoir DOM, which is a potent DCAN precursor (Bond et al., 2011), spectroscopic indices of BIX and FI suggest that autochthonous DOM production was insignificant. Trends in DCAN formation potential mimicked the pattern of THMs formation, perhaps due to the common factor of precipitation, which may have increased the volumes of wastewater inputs into the reservoirs, whose DON has the propensity to form DCAN and other N-DBPs. Also, portions of terrestrially derived DOM contain DON that has been reported to form DCAN and other HANs (Zhang et al., 2009), which may explain the trend of higher formation potential in autumn. Furthermore, the increased formation potential may have

Results and discussion

been due to increased concentration of wastewater DON, because of decreased dilution in summer low base flow conditions (Khorasani et al., 2021).

The trend of increased NDMA formation potential in Sau and Susqueda in summer was anticipated, as it may relate to increased precursor compounds production from temperature mediated algal productivity (Li et al., 2012; Zeng et al., 2016) and perhaps increased proportion of wastewater relative to base flow volume in summer (Khorasani et al., 2021). However, the trend of decreased NDMA formation in autumn was unexpected, as volumes of wastewater, a major source of NDMA precursors (Aydin et al., 2012), increase due to intense precipitation, which should have increased NDMA formation. Instead, results reported in **Paper III**, suggest that high autumn flows may have diluted NDMA precursors in the wastewater, as was also reported by a study in anthropogenically less impacted systems. Even more surprising is the trend of increased formation potential in winter, in Ter, Sau and Susqueda, when reservoirs turnover. However, elsewhere, similar trends of increased NDMA formation potential in winter and reduced formation in summer were speculated to have risen from reduced precursor biodegradation rates in winter due to low temperatures, hence availing a full range of precursors for formation potential tests. For instance, in the Yudo River basin in Japan, NDMA precursors in rivers degraded by mechanisms of photolysis and temperature mediated microbial degradation, and that attenuation of NDMA precursors was low and unexpected in winter (Zhao et al., 2020). The same mechanism may explain the trend of higher formation potential recorded in Ter, Sau and Susqueda in winter. Zhao's study may also explain the trend of low NDMA formation potential observed in the Ter River in summer, whereas a reversed trend was observed in Sau and Susqueda. Such trends suggest that photolysis of NDMA precursors may have been more effective in Ter River, whereas Sau and Susqueda may experience organic turbidity in summer due to algal blooms, which makes photodegradation ineffective. Similar trends of increasing NDMA formation potential in winter and a decrease in summer have also been reported in a mountain lake in Denver, the USA (Woods et al., 2015) and a reservoir in Andalusia, Spain (Jurado-Sánchez et al., 2012), in which the high formation potential values were attributed to ineffective chemical pre-oxidation in low temperatures of winter.

Evaluating each of the three variables of system (proxy for WRT), season and reservoir depth (proxy for thermal stratification) influence on DBP formation potential, reveals that seasonality plays an important role in driving the observed patterns. Consequently, it is no surprise that

Results and discussion

pooling together all these factors also isolates seasonality as the overall driver of the observed variability in the DBP formation potential results. Seasons are driven by meteorological factors, as such a concerted effort in the understanding and prediction of impacts of weather events on DBP formation potential would be a worthwhile undertaking for water resources managers, particularly in the present and future eras of climate variability.

Hypothesis vi: DOM chlorination would reduce the number of features in both in-lake and terrestrially derived molecular groups and produce new halogenated features that correlate strongly with known carbonaceous and nitrogenous disinfection by-product formation potential.

Aquatic DOM has been shown to be chemodiverse because of its complexity in the type and amounts of chemical groups that constitute its bulk composition. Within the DOM pool, the similarity of groups is determined by DOM sources i.e. whether it is terrestrially, in-lake, wastewater, urban run-off derived or of agricultural fields and industrial sources. Consequently, individual molecular groups within the DOM pool will respond differently to chemical disinfection methods such as chlorination, chloramination and ozonation. At the study design stage of **Paper II**, it was anticipated that some groups of the DOM pool would be affected by chlorination, while others would generally resist. For the groups that would be susceptible to chlorination, the number of molecular features corresponding to a particular group was expected to decline after chlorination, while also giving rise to new halogenated molecular features lying within the same molecular groups. It was further anticipated that the newly created halogenated molecular features would strongly correlate with the formation potential of DBPs that have been identified by previous research, to originate from the same molecular regions affected by chlorination in the present study. HRMS results of DOM profiling reported in **Paper II**, indicate that chlorination altered molecular regions of lignin-like, tannin-like, CRAM and lipid-like, by reducing their intensity and the number of features and creating new halogenated and highly oxidized features that belonged to the same affected regions. In lieu of structure verification, the new features identified by HRMS could only be assumed as semi-volatile or non-volatile DBP formation. Thus, the DOM regions anticipated to be affected by chlorination were altered and generated new features. A detailed account on the changes occasioned by chlorination of DOM is provided in the sections below:

Results and discussion

4.5 DOM molecular regions affected by chlorination.

The observation reported in **Paper II**, that chlorination resulted in the decrease of average peak intensity and decreased KMD, alludes to cleavage of larger DOM molecules into smaller and less intense molecular fragments (Milstead and Remucal, 2021). This finding corroborates results of another study in a drinking water treatment plant in North Eastern China, which also reported that chlorination broke larger DOM molecules into smaller organic compounds with lower intensity (Xu et al., 2022). In addition, the same paper reports that chlorination decreased the number of features classified as lipid-like and condensed hydrocarbon-like. Similar results were also reported in another study on the Coal Creek River, USA, in which the affected regions were associated with formation of C-DBPs (Leonard et al., 2022). Also, the finding reported in the same paper that chlorination causes the appearance of highly oxidized features, with $O/C > 0.75$, mostly in the tannin-like and the lignin-like regions, was also corroborated by another study that sampled four water treatment plants in Sweden. This Swedish study reported that chlorination produced DOM features that were highly oxidized, with an O/C higher than what pre-existed before chlorination, which was suspected to belong to highly aromatic compounds substituted with an oxygen functional group (Lavonen et al., 2013). Even in lieu of direct attribution, it can reasonably be speculated that such oxygen-rich aromatic compounds may have belonged to the tannin-like or lignin-like groups of DOM.

4.6 Potential surrogates for the prediction of DBP formation potential.

DBP formation potential experiments are usually long, tedious, expensive and require high level analytical skills to undertake. In that regard, researchers are always looking for potential surrogates that could, instead, be easily measured by affordable and scalable instruments, with a quick turnaround time, and yet provide reliable estimates of the DBP species to help in decision making. Identification of such predictive surrogates was one of the side objectives of this thesis. To that aim, the observed positive correlations between TCM formation potential and UVA_{254} and DOC, as reported in **Paper III**, have also been reported by other researchers, and point to the fact that DOC is a well-known organic precursor responsible for the formation of TCM and other THMs (Chow et al., 2003; Musikavong and Wattanachira, 2013). Furthermore, correlations with UVA_{254} , alludes to the fact that aromatic high molecular weight and electron-rich compounds, preferentially

Results and discussion

form C-DBPs (Milstead and Remucal, 2021) such as TCM and HAAs. In **Paper III** of this thesis, both DOC and UVA₂₅₄ were ranked as fair surrogates (Akoglu, 2018), hence unconvincing for predictive purposes. Similarly, in a study on Beaver Lake, DOC and UVA₂₅₄ correlated poorly with TCM formation potential, under extreme precipitation (Pifer et al., 2014). On the other hand, in a study on University Lake and a nearby WWTP, great correlations were reported between TCM and UV₂₅₄, whereas there was no correlation with DOC (Jutaporn et al., 2019). In yet another study involving nutrient amended water from Beaver Lake Reservoir, strong correlations were reported between TCM formation potential with both DOC and UV₂₅₄ (Mash et al., 2014). In fact, **Paper II** of this thesis reports strong correlations between THM formation potential and molecular features in the lignin-like region of the van Krevelen diagram, which is plausible, as this region contains the lignin phenols derived from vascular plants, that known to generate C-DBPs (Kasuga et al., 2020; Pellerin et al., 2010) such as HAAs and THMs (Hua et al., 2014) upon chlorination. Thus, correlation results should be interpreted with caution, considering that different DOM sources have varied propensity to form DBPs, which drives the observed differences in correlations across the studies (Chow et al., 2008). The reported differences in correlation levels imply that the predictive quality of a particular surrogate might depend on other variables such as water source and season. Indeed, in **Paper II** of this thesis, TOC was deemed a satisfactory predictor of THM formation potential in the winter samples, whereas pooling all the data gathered across fall, winter and summer, as reported in **Paper III**, returned DOC as a fair predictor, suggesting that seasonality influenced correlation strengths.

Fair correlations between DCAN formation and DOC are an indicator that a portion of DCAN precursors originate from terrestrial DOM, as was also reported elsewhere (Zhang et al., 2009). **Paper II** of this thesis also reports a comparable Spearman's correlation coefficient between TOC and HANs formation potential, which was deemed poor. Also, **Paper II** of this thesis reports novel strong correlations between HANs FP and molecular features, with high nitrogen content (average N/C = 0.49) in the lignin-like region of the van Krevelen diagram, which puts them as potential HANs formation potential predictive surrogates. These molecular features may likely be the DON attached to humic and fulvic acid substances of terrestrial DOM, that has been reported in **Paper III** of this thesis as well as in many other studies (Chen et al., 2019; Jian et al., 2016; Zhang et al., 2009), to generate DCAN. Formation of HANs from lignin phenols was also reported in a study on model compounds that preferentially generated HAAs (Hua et al., 2014) and DCAN, which is considered as an intermediate product of HAAs formation (Yu and Reckhow, 2015).

Results and discussion

Negative association with FI suggests that DCAN's precursors may not have been from autochthonous sources. On the other hand, negative correlations between DCAN formation potential and nitrogen species was anticipated as inorganic nitrogen is not part of DON, a precursor that generates DCAN. Positive associations between NDMA formation potential and FI indicate that a portion of NDMA may have formed from endogenic algal derived precursors. UVA_{254} and $SUVA_{254}$ reflect the aromaticity and molecular weight distribution of DOM fractions, hence their negative association with NDMA was anticipated as DOC is not regarded as a precursor for NDMA formation. Overall, the associations observed in between N-DBPs and potential surrogates such as DOC and FI are weak and therefore inappropriate for predictive purposes in this system, the exception being the lignin-like region of the VK diagram, reported in **Paper II**, in which correlations are strong enough to be considered as predictive surrogates.

Positive associations between the formation potential of TCM and BDCM are plausible and indicate that both are derived from the same organic precursor (DOC) and could therefore be expected to form alongside each other, particularly in systems with some levels of bromide. In **Paper III** of this thesis, the formation potential of THMs (TCM+BDCM) positively correlated with DCAN FP, which could be attributed to the commonality of DOC as a precursor. The strong association between DCAN and TCM formation suggests that the likelihood of finding either of them in one system implies that the other species is also present. However, this relationship may not be universally valid because of variability of precursor sources across systems, i.e. while, in the present system, DCAN possibly formed from wastewater based and terrestrial DON, the DCAN-TCM FP relationship will likely vary in oligotrophic systems that are unaffected by anthropogenic pollution, or in systems where DOM source is either entirely terrestrial or autochthonous. Thus, universally using TCM formation potential as predictive surrogate for DCAN formation may underestimate toxicity risk from the more toxic N-DBPs, as was also argued by other authors (Furst et al., 2021), since the relationship between these species decouples in other systems.

An observation reported in **Paper II**, where molecular features rich in oxygen content correlated strongly with THM formation potential, agrees with a number of similar previous studies. For instance, a study conducted on 20 drinking water treatment plants, reported that TCM formation potential strongly correlated with features that had low H/C and high O/C ratios, implying that TCM formation favored molecular features that were unsaturated aliphatic, polycyclic aromatic and phenolic (Wang et al., 2017). Also, a study on Phong River in Thailand reported that

Results and discussion

disinfecting with chlorine and chlorine dioxide selectively targeted DOM functional groups that were rich in oxygen content (Prasert et al., 2023). Furthermore, in Wisconsin, the USA, a study of drinking water utilities reported strong positive correlations between THM and HANs and highly oxidized DOM (Milstead and Remucal, 2021).

Although molecular fingerprinting DOM is also a highly specialized domain, requiring advanced skills and sophisticated analytical equipment, information generated from the efforts on molecular features, that correlate with DBP formation potential might still be considered useful surrogates in the sense that there is still some savings on time, compared to additional efforts required in DBP formation potential experiments, particularly on incubation time and LLE procedures. With the on-going efforts directed at automating extraction techniques, such as online SPE (Farré et al., 2016; Helle et al., 2011), prospects are high that turn-around times will be greatly reduced in molecular fingerprinting, generating surrogate information in nearly real time, resulting in faster decision making.

4.7 Climate change impacts on the Ter Watershed and its implications for the management of the river - reservoirs system.

Climate change footprints on the Ter–Sau–Susqueda–Pasteral system have been subject of numerous studies in the past, attesting to the importance of this system in the provision of various ecosystem services. Some researchers have reported trends of declining precipitation, river discharge (Gallart et al., 2011; Liqueste et al., 2009), seasonal floods, as well as increasing trends in evapotranspiration, air temperature (Liqueste et al., 2009) and severe droughts, all of which are climate change phenomena. Consequently, hydrologic deficits have had numerous ramifications on the ecosystem service of water supply to the Barcelona Metropolitan City which is a major beneficiary of the Ter Watershed. Due to dwindling precipitation and recurrent droughts, there has been water use restrictions imposed on consumers as mitigation measure to cope with water supply deficits (March and Saurí, 2010; Mazo and Alcantud, 2012). From the perspective of water quality, some studies carried out in the Ter Watershed, have reported deteriorating quality such as development of hypolimnetic anoxia due to declining streamflow caused by El Niño Southern Oscillation (Marcé et al., 2010), a general increase in reservoir water temperature (Marcé and Armengol, 2009) and sporadic algal blooms (Becker et al., 2010). Results reported in this thesis are mostly in agreement with this previous research. For instance, Paper 1 reports increased drought

Results and discussion

frequency, decreased frequency extreme wet events, increased frequency of heatwave events, reduced dissolved oxygen under drought and heatwave conditions and increased water temperature under heatwave conditions, from the early 2000s, all of which agree with previous findings on the same watershed. Future (up to the middle of the 21st century) climate projections for the Ter Catchment also indicate that hydrologic deficits, evapotranspiration, and air temperature will continue to increase (Funes et al., 2021). Coupling these climate projections with findings reported in this thesis paints a bleak future for water supply in a number of possible ways. First, reduced stream flow, rising water temperature and decreased dissolved oxygen levels might lead to the recurrence of algal blooms that were characteristic of the system in the early 2000s (Becker et al., 2010; Takkouk and Casamitjana, 2016; Vidal et al., 2012), which will be very challenging to treat. Second, reduced streamflow will imply that the major proportion of inflow will be treated wastewater (Marcé et al., 2021), which may result in contaminant enrichment in the reservoir (Staben et al., 2015), that becomes expensive to treat (de Loe and Plummer, 2010). Third, decreased precipitation and streamflow will mean that the major source of organic matter would be autochthonous, which is recalcitrant to conventional water treatment methods and therefore requires advanced treatment processes that are expensive in terms of both capital investments and operational expenditure.

Through this thesis, we learn that Sau and Susqueda reservoirs are still eutrophic, although there have been significant improvements in trophic state since the construction and upgrading of WWTPs. We also demonstrate that climate extremes are intense within the Ter Watershed and the frequency of droughts and heatwaves has been increasing, whereas that of extreme wet events has been decreasing, from the early 2000s. Also, adverse impacts of climate extremes on reservoir water quality are ubiquitous and seem to depend on reservoir trophic state. Dissolved oxygen depletion due to biodegradation of both endogenous and exogenous DOM, mediated by high air temperature, seems to be a persistent occurrence in these reservoirs that requires addressing. At present, allochthonous DOM is the dominant source in both reservoirs, but with the on-going decreasing frequency of extreme precipitation events, autochthonous DOM sources may dominate the systems in future. While it is seemingly impossible to halt increasing drought and heatwave frequencies, which enhance dissolved oxygen depletion, minimizing eutrophication would improve oxygenation conditions through reduced oxygen demand for organic matter respiration. Nitrogen and phosphorus inputs from the agricultural activities in the watershed should be kept under control to minimize exports into the reservoirs. The obligation to keep eutrophication of waterbodies to low levels to ensure that lakes remain oxygenated, is applicable to many other lakes

Results and discussion

across the globe, whether they are currently eutrophied or not, for purposes of ensuring continuity of the benefits that lakes supply to the surrounding dependants.

Besides improving general oxygen conditions in lakes, trophic state improvement can also reduce DBP formation potential due to reductions in the production of in-lake algal organic matter, which is a precursor for the formation of both C- and N-DBPs. That trophic state improvement reduces organic matter loads in lakes, is, indirectly, exemplified in results of **Paper I** of this thesis, in which we demonstrate increased resistance of dissolved oxygen to stressors of droughts and heatwaves, across the entire water column. The key mechanism of oxygen depletion under droughts and heatwaves is enhanced (aerobic) degradation rates of dissolved organic matter, which was prominent prior to the construction of WWTPs. On the other hand, the same magnitude of droughts and heatwaves did not influence dissolved oxygen dynamics after the building of WWTPs, which could be attributed to reductions in organic matter loads in the reservoir. The dynamics of dissolved oxygen in the two periods of contrasting trophic state, reasonably suggest reductions in organic matter loads following the building of WWTPs. Consequently, even in the absence of actual DBP data, it is plausible to anticipate that improvements in trophic state of lakes can lead to declines in DBP formation potential due to reduced dissolved organic matter which is a precursor for DBP formation. Other than Sau reservoir, these dissolved oxygen and organic matter dynamics may be valid in eutrophic lakes where endogenous DOM dominates or where droughts and heatwaves are likely to intensify, hence disrupting hydrologic connectivity. On the other hand, in watersheds where heavy rainfall events are expected to be more frequent, impacted lakes are likely to be dominated by terrestrially dissolved organic matter, hence potential gains of trophic state improvement, are likely going to be dwarfed by the dominance of terrestrially derived organic matter.

Monitoring of DBPs formation potential has been integral in the water quality monitoring programmes implemented by the water supply authority that abstracts from the Ter catchment. To date, C-DBP formation has been the sole focus of monitoring, probably because of regulatory compliance requirements of the European Union. Monitoring the formation of N-DBPs has never been part of their operational water quality monitoring activities, yet there is a growing number of scientific publications that report increased toxicity of these nitrogenous species, compared to the traditionally monitored C-DBPs. By incorporating N-DBP formation in this thesis, we aimed at initiating a conversation on the need of extending monitoring to cover these nitrogenous by-products, in lieu of mandatory compliance monitoring. Although the formation potential of N-

Results and discussion

DBPs (DCAN and NDMA) at the abstraction spot is not very high, their significant formation should sound an alarm to water resource managers to consider investing in monitoring programmes and equipment, to track trends in their formation. These nitrogenous species form from DON, which is ubiquitous in wastewater that is routinely discharged in the Ter River. Thus, it is apparent that there is always a risk of increased N-DBP formation for the water that is currently being abstracted from this watershed. This risk of increased formation of N-DBPs may also arise from the fact that volumes and concentration of wastewater discharges might increase due to population growth and evapoconcentration, respectively, occasioned by the observed increases in the frequency of droughts and heatwaves. Already, several countries, where DBP formation research is established, are regulating some of these N-DBPs and it may not be long, from now, before the European Union pronounces mandatory monitoring of these nitrogenous species. By starting to generate data on the formation of N-DBPs now, the water utility abstracting from these sources will have some level of preparedness for regulatory compliance monitoring in terms of the required treatment process modifications, given that N-DBP precursors are poorly removed by conventional water treatment methods.

4.8 Unresolved scientific questions requiring further research.

In **Paper I**, we had hoped for establishing causality between climate extremes and dissolved organic matter, with an eventual aim of linking the dynamics to DBP formation. However, we couldn't find adequate DOC data for these high-level statistical analyses. Therefore, pursuing causality, but with a focus on the actual DBP formation potential data, from the routine monitoring implemented by the Ens d'Abastament d'Aigua Ter-Llobregat, a water utility that abstracts from this watershed, would be a worthwhile research exercise.

Developing a predictive framework that links seasonal climate predictions to the formation of DBPs at the waterworks, remains quite a crucial but un-attempted research area that can radically improve water supply operations by enhancing preparedness for the possible upcoming changes in precursor levels and subsequent formation potential mediated by the predicted climate variables. The framework would stand in the gap between uncertainties surrounding patterns of future climate variability and the associated anxiety experienced by water supply authorities due to their inability to control climate, its associated extremes and impacts on water supply operations.

Results and discussion

Consequently, this research gap is recommended for urgent attention. The potential for wide adoption of the framework would be high because of the commonality of climatic impacts on water supply operations.

Section 1.9.3 of this thesis (in the introduction) provides a literature-based overview of DBP formation potential prediction from a range of explanatory variables, using empirical statistical relationships. Empirical modeling is data intensive, yet resource, technical skills, equipment and time requirements in the generation of DBP data are enormous, hence restrictive on the amount of data that could be generated. Therefore, establishing mechanistic links between (DOM-based) precursors and DBP formation might allow process-based model prediction of DBP formation through coupling with other already existing watershed and lake hydrodynamic and biogeochemical models. Such an approach is attractive because it would not be too demanding in terms of the required amount of data. It is worth the effort because of its potential use in resource constrained circumstances, where DBP formation data is likely going to be a severe limitation.

Conclusions

5 Conclusions.

A thoughtful evaluation of scientific evidence presented in **Papers I, II and III** leads us to the following conclusions:

- i. The Ter Watershed experiences intense hydroclimatic extremes of droughts, rainstorms and heatwaves around Sau Reservoir and that the frequency of droughts and heatwaves increased from the early 2000s, whereas rainstorms decreased in their frequency in the same reference period.
- ii. Reservoir water quality mostly responds negatively to hydroclimatic extremes but that this response is largely shaped by trophic state, such that the reservoir becomes more resistant to adverse effects of climatic extremes in less eutrophic conditions.
- iii. Improvements in reservoir trophic state during the last decades benefited more hypolimnetic water layers, which recorded resistance to all adverse impacts of hydroclimatic extremes.
- iv. Increased resistance of reservoir water quality to adverse impacts of hydroclimatic extremes, due to trophic state improvements, manifested greatly in the dynamics of dissolved oxygen, suggesting that eutrophication control measures in the watershed led to significant reductions in dissolved organic matter loads in the reservoir.
- v. Footprints of hydroclimatic extremes were identifiable in coarse monthly reservoir water quality timeseries using an innovative sequence of statistical analyses, which, not only complements analyses from high frequency data, but also opens up alternatives for monitoring agencies with low purchasing power to afford the purchase of high frequency water quality logging infrastructure.
- vi. Chlorination of water coming from the Sau-Susqueda reservoir system cleaves large dissolved organic matter molecules into smaller compounds, leading to reduced peak intensity, alterations of the lipid-like, tannin-like and lignin-like regions of the DOM pools and formation of new halogenated organic compounds in the same regions.
- vii. Molecular features from the tannin-like region of the DOM pool were identified as strong surrogates for the prediction of the formation potential of both THM and DCAN, which broadens the ranges of currently available proxies.
- viii. Water age in the Sau-Susqueda reservoir system is an important factor in the dynamics of DBP precursor compounds but that its role is not always reductive in nature, as it may also

Conclusions

result in both increases and reductions in the formation potential of DBPs depending on class.

- ix. Seasonality is a major factor driving the dynamics of DBP formation after chlorination of water from the Sau-Susqueda reservoir system, but that the response of DBP formation potential depends on class, i.e. whether it is C- or N-DBP, as well as subclasses within each of these two classes. This observation implies that predictive efforts should target subclasses for accurate forecasting.
- x. Subtle depth stratifications in DBP formation potential are largely regulated by seasonality.

Annex 1

6 Annexes

6.1 Drastic reduction of nutrient loading to a reservoir alters its resistance to impacts of extreme climatic events.

SUPPLEMENTARY MATERIAL

Drastic reduction of nutrient loading to a reservoir alters its resistance to impacts of extreme climatic events

Text S1: Derivation of meteorological/hydrological drought indices

Drought/wetness indices were obtained by transforming precipitation, streamflow and reservoir water level data in a non-parametric Standardized Drought Analysis Toolbox (SDAT) framework (Farahmand and Aghakouchak, 2015). In the framework, firstly, marginal empirical probability of monthly accumulations of precipitation data are derived by applying the empirical Gringorten plotting position equation,

$$P(x_i) = (i - 0.44) / (n + 0.12), \quad \text{equation 1}$$

in which n = sample size, i = rank of non-zero precipitation data from smallest, $P(x_i)$ = empirical probability (Gringorten, 1963). Secondly, outputs from the above equation are transformed into a Standardized Index (SI) following the equation;

$$SI = \Phi^{-1}(p), \quad \text{equation 2}$$

where Φ is the standard normal distribution function and p is the probability. This results into a time series of indices to which thresholds can be applied to determine severity of drought and, contrastingly, wetness. The original SDAT code is in MATLAB but, in our analysis, was translated into R (CoreTeam, 2017a). The framework was also applied to

monthly average values of streamflow and reservoir level to generate additional drought indices complementary to precipitation indices.

Text S2: Derivation of heatwave indices

Computation of heatwave indices adopted the Heatwave Magnitude Index Daily (HWMID), as proposed by (Russo, Sillmann and Fischer, 2015) to transform a time series of daily maximum air temperature (T_{max}) data into a standardized index. In this method, a heatwave is defined as a period of 3 consecutive days in which the maximum temperature is above the 90th percentile of the daily maxima in the reference period of 1981-2010, centered on a 31 day window. The output is a time series of HWMID values, each of which is the sum of the consecutive days composing a heatwave. Components of each HWMID can be split into a daily magnitude by applying the formula:

$$M_d(T_d) = \{(T_d - T_{30y25p}) / (T_{30y75p} - T_{30y25p})\} \quad \text{equation 3}$$

if $T_d > T_{30y25p}$, or
 0 if $T_d \leq T_{30y25p}$, in which

T_d is temperature of the day, T_{30y25p} is the 25th percentile of T_{max} for 1981-2010 reference period and T_{30y75p} is the 75th percentile of T_{max} for the 1981-2010 reference period. In its original form, the method returns a maximum value of heatwaves in a year. Since we were interested in generating a time series of all heatwaves in a given year, we modified the code slightly to return all the heatwaves. A detailed description of the original method can be found in (Russo *et al.*, 2014) and (Schaller *et al.*, 2018). HWMID calculations were implemented in the “extRemes 2.0-0” R-package (Gilleland and Katz, 2016) using R (CoreTeam, 2017b) statistical software.

Table SI: ‘Before’ and ‘After’ comparison of pre-whitened medians of hydrometeorological variables

	N (Bef)	N (Aft)	Median (Bef)	Median (Aft)	P	g_s
Air Temperature (°C)	7300	6922	0.7616856	0.4769373	*2.17E-14	0.13
Precipitation (Kg/m²/s)	7302	6937	7.51E-09	0	*7.87E-06	0.00
Inflow (m³/s)	7300	6916	1.802401	1.555347	*2.12E-05	0.01
Water level (m.a.s.l)	7300	6933	0.846747	0.66527	*0	**0.55

† N = number of samples; Bef = The ‘Before’ period; Aft = The ‘After’ period; P = p-value; g_s = Bias corrected Cohen’s d_s. * = significant p (α=0.05). ★ = Weak g_s, ★★ = Moderate g_s, and ★★★ = Strong g_s.

Table S2: ‘Before’ and ‘After’ comparison of pre-whitened medians of reservoir water quality variables

Water Quality		N (Bef)	N (Aft)	Median (Bef)	Median (Aft)	P	g _s
NO3 (mg/l)	Epi	180	196	8.06	1.88	*6.36E-15	**0.58
	Hypo	165	195	2.31	2.31	6.59E-03	0.08
NH4 (mg/l)	Epi	174	152	0.16	0.02	8.38E-02	0.02
	Hypo	185	151	7.25	0.10	*8.16E-14	*0.35
DO (mg/l)	Epi	178	195	4.76	3.51	*6.12E-06	*0.45
	Hypo	196	203	0.18	1.29	*4.29E-13	**0.68
TP (µg/l)	Epi	176	114	841.35	605.03	*3.04E-06	*0.46
	Hypo	181	113	741.65	602.32	*0.004302942	*0.28
T (°C)	Epi	212	202	11.61	10.95	*2.45E-04	*0.37
	Hypo	212	190	5.50	3.03	*4.93E-43	***1.74

† N = number of samples; Bef = The ‘Before’ period; Aft = The ‘After’ period; P = p-value; g_s= Bias corrected Cohen’s d_s. * = significant p (α=0.05). * = Weak g_s, ** = Moderate g_s, and *** = Strong g_s.

Table S3a: Summary of drought events

Droughts										
Hydrometeorological Variable	Before					After				
	Total events	Count		%		Total events	Count		%	
		Extreme	Non-Extreme	Extreme	Non-Extreme		Extreme	Non-Extreme	Extreme	Non-Extreme
Streamflow	288	14	139	4.86	48.26	224	35	88	15.63	39.29
Water level	288	12	121	4.17	42.01	224	38	101	16.96	45.09
Precipitation	288	29	118	10.07	40.97	224	38	101	16.96	45.09

Table S3b: Summary of wet events

Wet Events										
Hydrometeorological Variable	Before					After				
	Total events	Count		%		Total events	Count		%	
		Extreme	Non-Extreme	Extreme	Non-Extreme		Extreme	Non-Extreme	Extreme	Non-Extreme
Streamflow	288	27	107	9.38	37.15	224	8	89	3.57	39.73
Water level	288	30	122	10.42	42.36	224	12	71	5.36	31.7
Precipitation	288	26	115	9.03	39.93	224	12	71	5.36	31.7

Table S3c: Summary of heatwave events

Heatwaves										
Hydrometeoro- logical Variable	Before					After				
	Total events	Count		%		Total events	Count		%	
		Extreme	Non-Ex- treme	Extreme	Non-Ex- treme		Extreme	Non-Ex- treme		
Air temperature	20	7	13	35	65	19	11	8	57.9	42.1

Table S4: Results for analysis of extreme events effects on dissolved oxygen

Climate Index			# of samples		Median (mg/l)		P	g _s
			Non-extreme	Extreme	Non-extreme	Extreme		
Heatwave	Epi	Before	13	7	4.3	6.5	0.099	0.68
		After	7	11	4.3	4.8	0.23	0.25
	Hypo	Before	13	7	0.17	0.04	*0.034	*0.31
		After	8	11	0.52	0.54	0.36	0.02
Drought (Precipitation)	Epi	Before	38	22	7.7	4.9	0.075	0.57
		After	10	24	6.6	6.5	0.37	0.014
	Hypo	Before	38	22	0.4	0.2	0.06	0.14
		After	12	24	1.1	2.2	0.45	0.43
Drought (Inflow)	Epi	Before	25	8	8.7	3.3	*0.002	1.024
		After	16	11	6	6.5	0.82	0.16
	Hypo	Before	25	8	0.93	0	*0.00000186	** 0.55
		After	18	11	2.4	1	0.19	0.6
Drought (Water level)	Epi	Before	10	4	9.4	6.2	0.09	1.22
		After	7	3	5.8	6.4	0.24	0.39
	Hypo	Before	10	4	1.1	0.6	0.29	0.84

		After	7	3	0.6	1.5	0.81	0.82
Wet (Precipitation)	Epi	Before	31	22	6.9	7	0.57	0.033
		After	23	7	5.8	6.2	0.11	0.11
	Hypo	Before	31	22	0.6	1.4	*0.013	*0.43
		After	25	8	1.9	1.6	0.57	0.11
Wet(Inflow)	Epi	Before	18	15	6.3	8.1	0.36	0.5
		After	15	8	4.5	11	*0.033	***
	Hypo	Before	18	15	1.1	1.7	0.21	1.6
		After	17	8	0.8	7	*0.0003	***
		Before	11	6	5.7	7.4	0.1137	2.5
		After	7	3	4.3	7.4	0.26	0.43
Wet(Water level)	Epi	Before	11	6	0.5	1.2	0.11	0.27
		After	7	3	1.2	2.7	0.24	0.66

† Epi = Epilimnion; Hypo = Hypolimnion; P = p-value; g_s = Bias corrected Cohen's d_s . * = significant p ($\alpha=0.05$). * = Weak g_s , ** = Moderate g_s , and *** = Strong g_s .

Table S5: Results for analysis of extreme events effects on nitrate

Climate Index			# of samples		Median (mg/l)		P	g _s
			Non-extreme	Extreme	Non-extreme	Extreme		
Heatwave	Epi	Before	5	6	3.9	12.8	0.0752	0.74
		After	7	10	5.2	1.7	*0.0021	*** 1.76
	Hypo	Before	5	6	1.3	1.7	0.37	0.035
		After	7	10	6.3	9.2	0.25	0.56
Drought (Precipitation)	Epi	Before	22	14	40.9	15.3	*0.0311	*** 0.97
		After	9	23	6.1	6.6	0.34	0.18
	Hypo	Before	22	14	7.6	4.7	0.24	0.12
		After	9	23	8.5	9.3	0.57	0.17
Drought (Inflow)	Epi	Before	12	7	23.1	22	0.57	0.031
		After	13	11	6.4	6.5	0.53	0.057
	Hypo	Before	12	7	14.7	6.7	0.35	0.47
		After	13	11	7.8	8.1	0.6	0.053
Drought (Water level)	Epi	Before	7	2	39.2	29.2	0.68	0.41
		After	6	3	4.4	6.3	0.21	0.75

	Hypo	Before	7	2	32.3	12.8	0.079	1.58
		After	6	3	13.2	6.1	0.28	1.62
Wet (Precipitation)	Epi	Before	19	12	24.7	49.2	*0.0241	***
		After	22	5	6.6	6.5	0.35	0.87
	Hypo	Before	19	12	4.2	25.4	*0.022	***
		After	22	5	7.7	7.7	0.36	1.15
								0.002
Wet (Inflow)	Epi	Before	10	7	18.3	28.3	0.073	0.39
		After	15	6	4.8	9.3	0.055	1.21
	Hypo	Before	10	7	5.7	34.8	*0.037	***
		After	15	6	7.2	10.8	0.086	1.63
								0.59
Wet (Water level)	Epi	Before	6	4	44.2	26	0.22	1.7
		After	7	3	5.3	7.4	0.11	0.78
	Hypo	Before	6	4	13.5	13.4	0.35	0.004
		After	7	3	13.4	12.8	0.31	0.16

† Epi = Epilimnion; Hypo = Hypolimnion; P = p-value; g_s = Bias corrected Cohen's d_s . * = significant p ($\alpha=0.05$). * = Weak g_s , ** = Moderate g_s , and *** = Strong g_s .

Table S6: Results for analysis of extreme events effects on ammonium

Climate Index			# of samples		Median (mg/l)		P	g _s
			Non-extreme	Extreme	Non-extreme	Extreme		
Heatwave	Epi	Before	5	6	7.2	7.5	0.5	0.015
		After	10	7	0.08	0.13	0.11	0.2
	Hypo	Before	5	6	55.9	54.2	0.63	0.024
		After	7	10	0.8	0.55	0.095	0.096
Drought (Precipitation)	Epi	Before	22	14	7.6	9.3	0.241	0.06
		After	9	23	0.1	0.1	0.57	0.005
	Hypo	Before	22	14	56	77.3	0.4	0.34
		After	9	23	0.96	0.74	0.75	0.19
Drought (Inflow)	Epi	Before	12	7	5.7	10.3	*0.046	*0.215
		After	13	11	0.06	0.17	*0.0052	*0.31
	Hypo	Before	12	7	38	66.1	*0.032	**0.61
		After	13	11	0.67	0.96	0.14	0.25
Drought (Water level)	Epi	Before	7	2	3.9	28.6	0.2	2.09
		After	6	3	0.1	0.18	0.069	0.53

	Hypo	Before	7	2	31.6	79.6	0.44	1.16
		After	6	3	0.22	0.83	0.12	0.77
Wet (Precipitation)	Epi	Before	19	12	13.6	5.9	0.05	0.35
		After	22	5	0.1	0.09	0.38	0.0174
	Hypo	Before	19	12	73	39.7	*0.0034	**0.66
		After	22	5	0.5	0.4	0.47	0.023
Wet (Inflow)	Epi	Before	10	7	10.9	4.3	0.06	0.44
		After	15	6	0.09	0.12	0.61	0.06
	Hypo	Before	10	7	53.6	36.9	0.16	0.4
		After	15	6	0.4	0.78	0.47	0.23
Wet (Water level)	Epi	Before	6	4	8.9	4.8	0.19	0.74
		After	7	3	0.08	0.03	*0.0006	*0.3
	Hypo	Before	6	4	58.4	25	*0.022	***
		After	7	3	0.6	0.12	0.056	1.63 0.89

† Epi = Epilimnion; Hypo = Hypolimnion; P = p-value; g_s = Bias corrected Cohen's d_s . * = significant p ($\alpha=0.05$). * = Weak g_s , ** = Moderate g_s , and *** = Strong g_s .

Table S7: Results for analysis of extreme events effects on total phosphorus

Climate Index			# of samples		Median ($\mu\text{g/l}$)		P	g _s
			Non-extreme	Extreme	Non-extreme	Extreme		
Heatwave	Epi	Before	5	6	1608.8	1085.9	0.26	0.76
		After	5	7	1218.4	1573	0.191	0.69
	Hypo	Before	5	6	1605.4	1707.6	0.57	0.16
		After	5	7	1857.3	985.7	*0.032	***
							1.63	
Drought (Precipitation)	Epi	Before	22	14	1154.9	1130.7	0.23	0.055
		After	6	16	1773.8	1572.3	0.31	0.36
	Hypo	Before	22	14	1658.4	1684.4	0.29	0.041
		After	6	16	1545.2	1290.9	0.081	0.46
Drought (Inflow)	Epi	Before	12	7	1047	1343.8	0.43	0.47
		After	11	9	1260.5	1676.9	0.054	0.73
	Hypo	Before	12	7	1316.9	1699.6	0.09	0.673
		After	11	9	1291.3	1319.8	0.45	0.07
Drought (Water level)	Epi	Before	7	2	1723	1588	0.5	0.28
		After	5	3	1583.9	1790.3	0.13	0.47

	Hypo	Before	7	2	1329	1423.6	0.32	0.22
		After	5	3	1291.3	1107.4	0.23	0.95
Wet (Precipitation)	Epi	Before	19	12	1344.9	1087	0.12	0.49
		After	16	4	1722.4	1388.4	*0.03162	***
								1.11
	Hypo	Before	19	12	1541.7	1315.5	0.27	0.36
		After	16	4	1077	1380.4	0.29	1.21
Wet (Inflow)	Epi	Before	10	7	970	1195.1	0.17	0.39
		After	13	5	1583.9	1382.5	0.086	0.11
	Hypo	Before	10	7	1529.6	1096.1	0.057	0.96
		After	13	5	990.7	1668.3	0.059	0.35
Wet (Water level)	Epi	Before	6	4	760.1	1065.9	0.16	1.76
		After	5	2	1716.7	1332.1	0.068	1.31
	Hypo	Before	6	4	1699.6	1176.9	*0.034	***2.1
		After	5	2	1186.7	1005.3	0.41	0.57

† Epi=Epilimnion; Hypo=Hypolimnion; P=p-value; g_s = Bias corrected Cohen's d_s . * = significant p ($\alpha=0.05$). * = Weak g_s , ** = Moderate g_s , and *** = Strong g_s .

Table S8: Results for analysis of extreme events effects on water temperature

Climate Index			# of samples		Median (°C)		P	g _s
			Non-extreme	Extreme	Non-extreme	Extreme		
Heatwave	Epi	Before	13	7	21.6	22.6	0.22	0.46
		After	7	11	21	21.7	0.0803	0.36
	Hypo	Before	13	7	9.7	11.8	0.36	0.65
		After	7	11	8.6	7.8	0.06	0.37
Drought (Precipitation)	Epi	Before	40	22	13.8	19.7	*0.009	***1.1
		After	10	24	13	15.5	0.36	0.48
	Hypo	Before	40	22	9.5	9.4	0.57	0.03
		After	10	24	7.8	7.6	0.56	0.002
Drought (Inflow)	Epi	Before	25	8	12.3	16.5	0.062	0.67
		After	17	11	15.2	15.2	0.27	0.0022
	Hypo	Before	25	8	8.2	9.5	*0.012	*0.49
		After	17	11	8.4	7.9	0.74	0.22
Drought (Water level)	Epi	Before	9	4	14.3	17.3	0.25	0.89
		After	7	3	20.1	14.1	*0.010	***2.2
	Hypo	Before	9	4	8.7	8.5	0.43	0.13

		After	7	3	8.2	8.2	0.33	0.3
Wetness (Precipitation)	Epi	Before	30	23	17	15	0.082	0.41
		After	24	7	13.2	14.4	0.62	0.21
	Hypo	Before	30	23	9.4	9.1	0.44	0.1
		After	24	7	8.2	7.9	0.29	0.18
Wetness (Inflow)	Epi	Before	18	15	13	14.6	0.23	0.32
		After	15	8	15.8	11.5	0.052	0.78
	Hypo	Before	18	15	8.4	9.4	0.16	0.41
		After	15	8	7.9	7.6	0.38	0.22
Wetness (Water level)	Epi	Before	11	6	16.8	16.3	0.27	0.096
		After	7	3	17.1	15.6	0.13	0.43
	Hypo	Before	11	6	8.8	9.8	*0.023	*0.45
		After	7	3	7.2	7.9	0.12	0.44

† Epi = Epilimnion; Hypo = Hypolimnion; P = p-value; g_s = Bias corrected Cohen's d_s . * = significant p ($\alpha=0.05$). * = Weak g_s , ** = Moderate g_s , and *** = Strong g_s

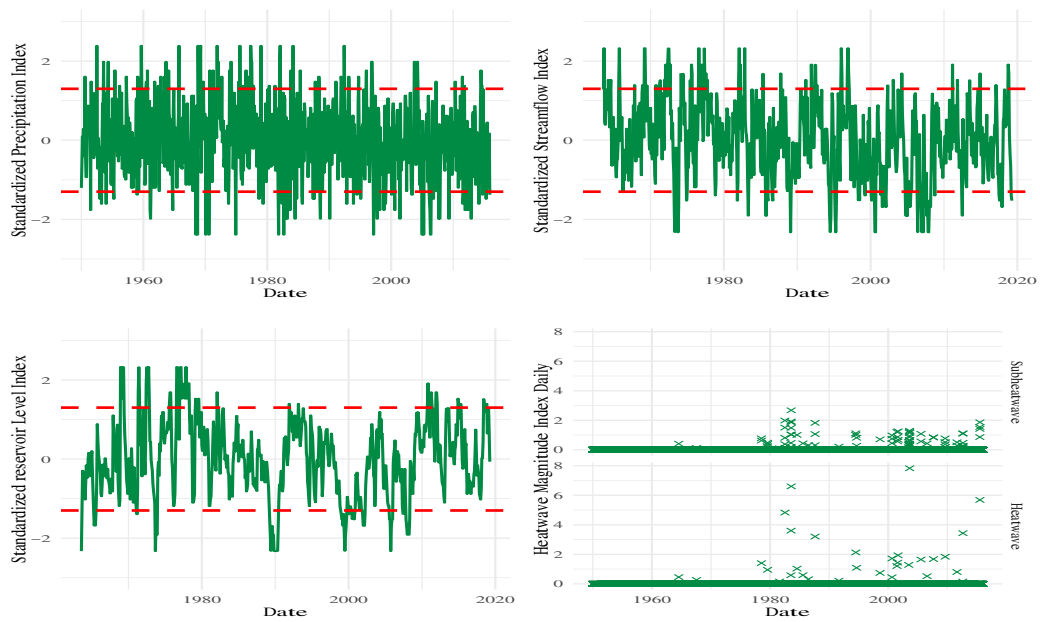


Figure S1: Extreme events indices of Standardized Precipitation Index(nSPI), Standardized Streamflow Index(nSSFI), Standardized reservoir Level Index (nSLI) and Heatwave Magnitude Index Daily (HWMID), derived from hydrometeorological timeseries of precipitation, streamflow, reservoir water level and daily maximum air temperature respectively. The red dashed lines represent a cut-off point (± 1.3) below or above which is the extreme event region, whereas the values in between represent normal and dry/wet events that are non-extreme.

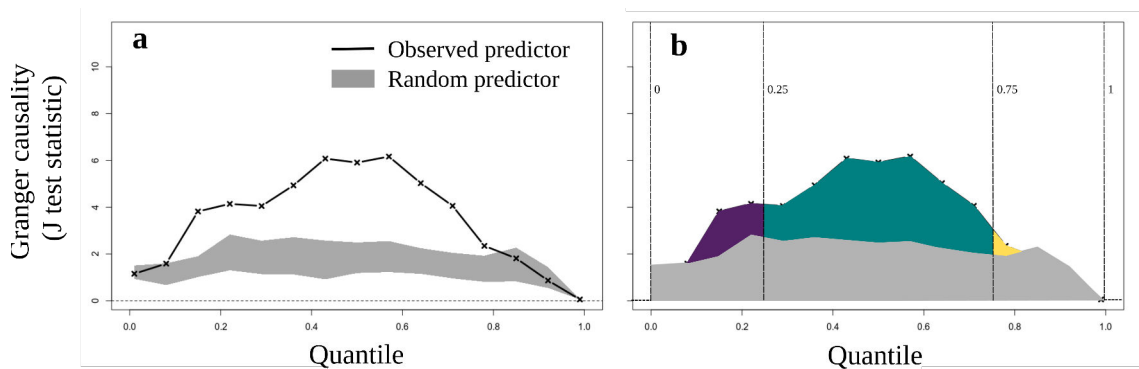


Figure S2. a) Example of a Granger causality analysis between a response variable and an observed predictor. The J statistic between the predictor and the response variable is evaluated at several quantiles along the range 0 to 1, and this is compared to the area occupied by results coming from 1000 realizations of the same calculation but using a random predictor instead. We consider Granger causality when the J statistic calculated with the observed predictor is higher than the maximum value obtained with the random predictors. In this example, most Granger causality accumulates in the central quantiles, with no Granger causality for quantiles > 0.8 . b) Graphical representation of the areas integrated to obtain Normalized Granger causalities aggregated for three quantile ranges (< 0.25 , between 0.25 and 0.75, > 0.75) for a result such the obtained in panel a. Each of the colored areas above the maximum value obtained with the random predictors are divided by the grey area to obtain the normalized value for the corresponding quantile range. Note that colors used in this panel are consistent with colors in Figure 2 in the main manuscript.

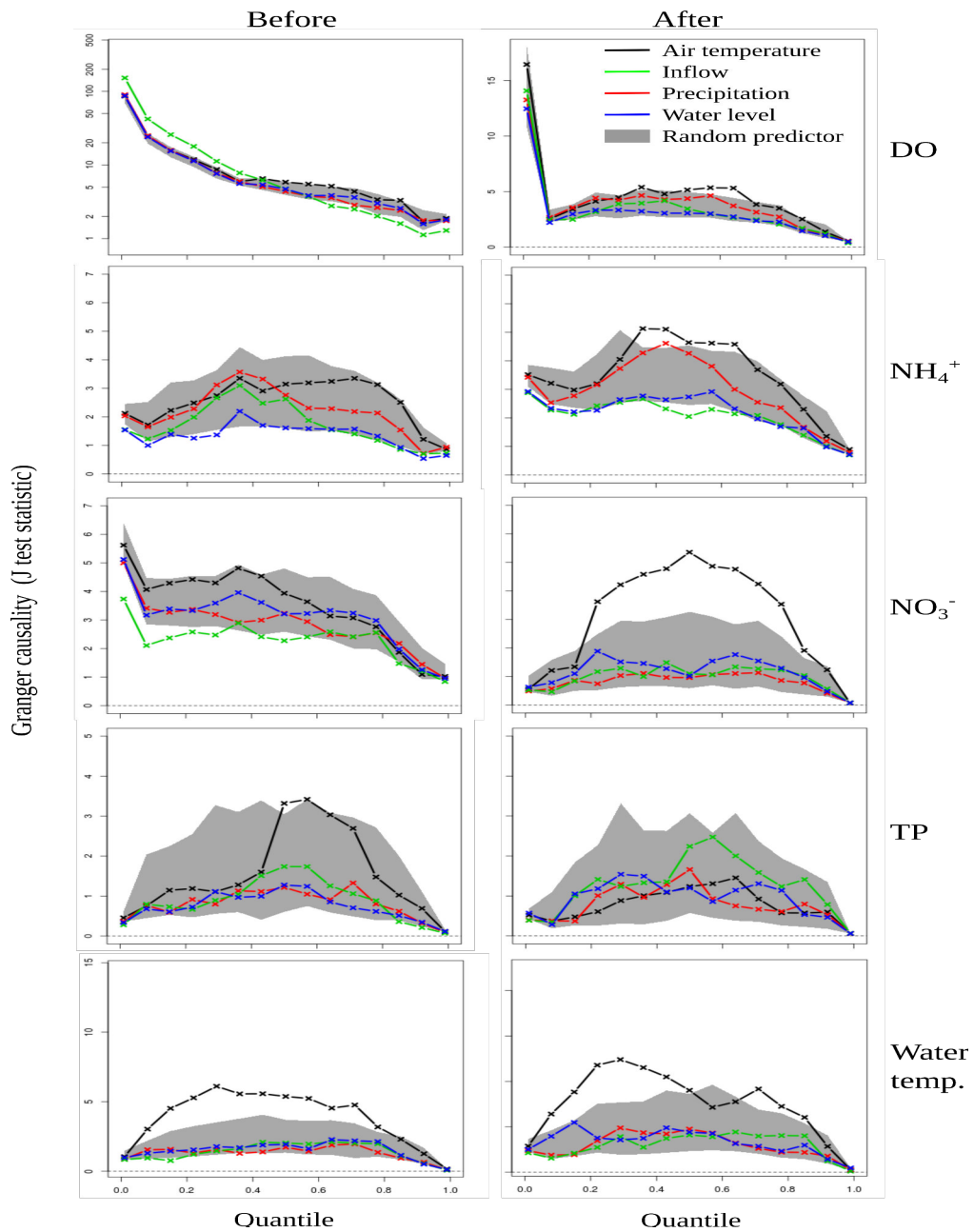


Figure S3. Granger causality analysis for the hypolimnion. Rows differentiate periods after and before WWTPs upgrade, while rows differentiate response variables (dissolved oxygen, ammonium, nitrate, total phosphorus, water temperature). The lines in each panel are for different predictors (air temperature, inflow, precipitation, water level). Grey areas contain the results for 1000 random predictors. Note the log scale in the topmost left panel.

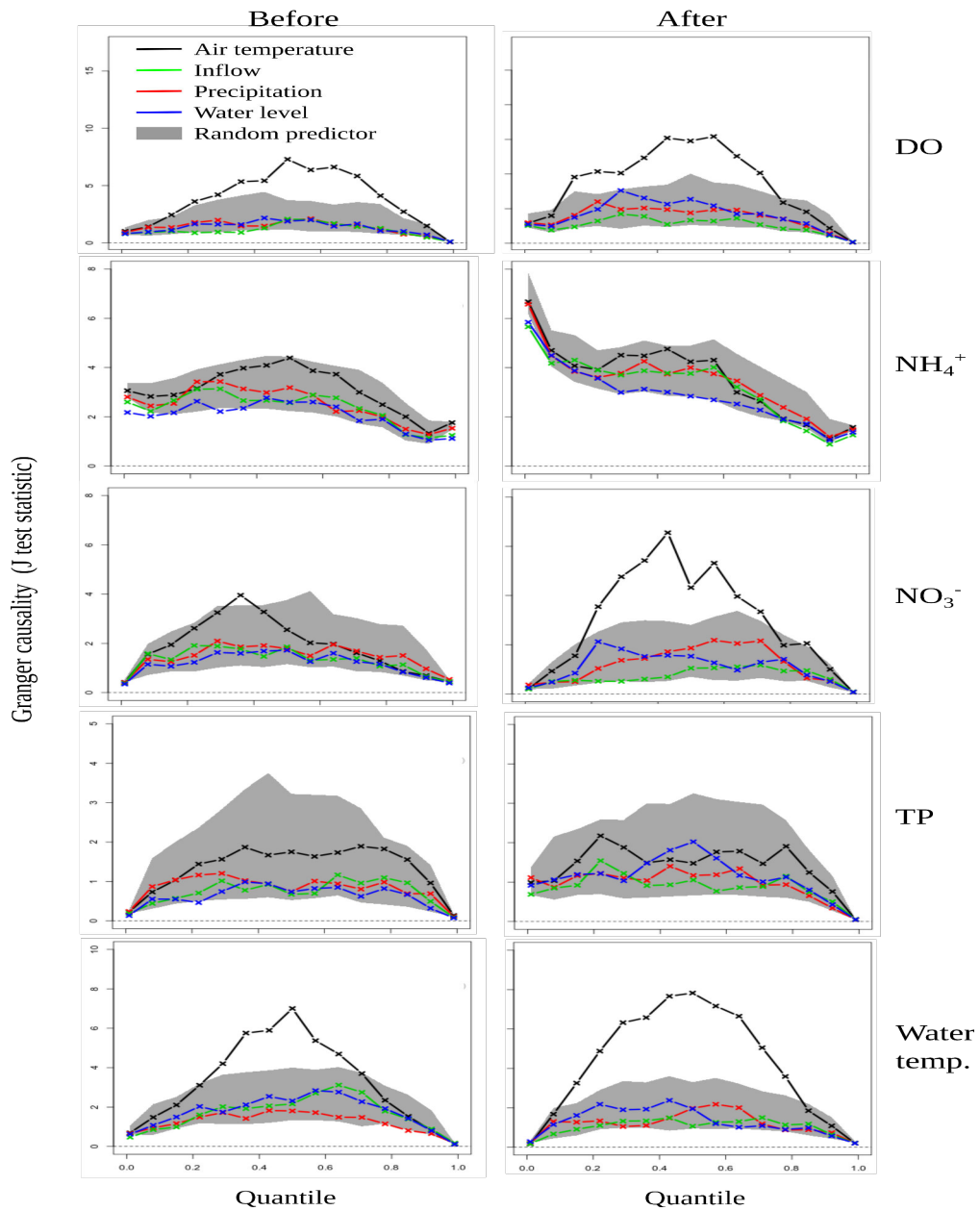


Figure S4. Granger causality analysis for the epilimnion. Rows differentiate periods before and after WWTPs upgrade, while rows differentiate response variables (dissolved oxygen, ammonium, nitrate, total phosphorus, water temperature). The lines in each panel are for different predictors (air temperature, inflow, precipitation, water level). Grey areas contain the results for 1000 random predictors.

Hypolimnetic Dissolved Oxygen

Classification ■ Extreme ■ Non_Extreme

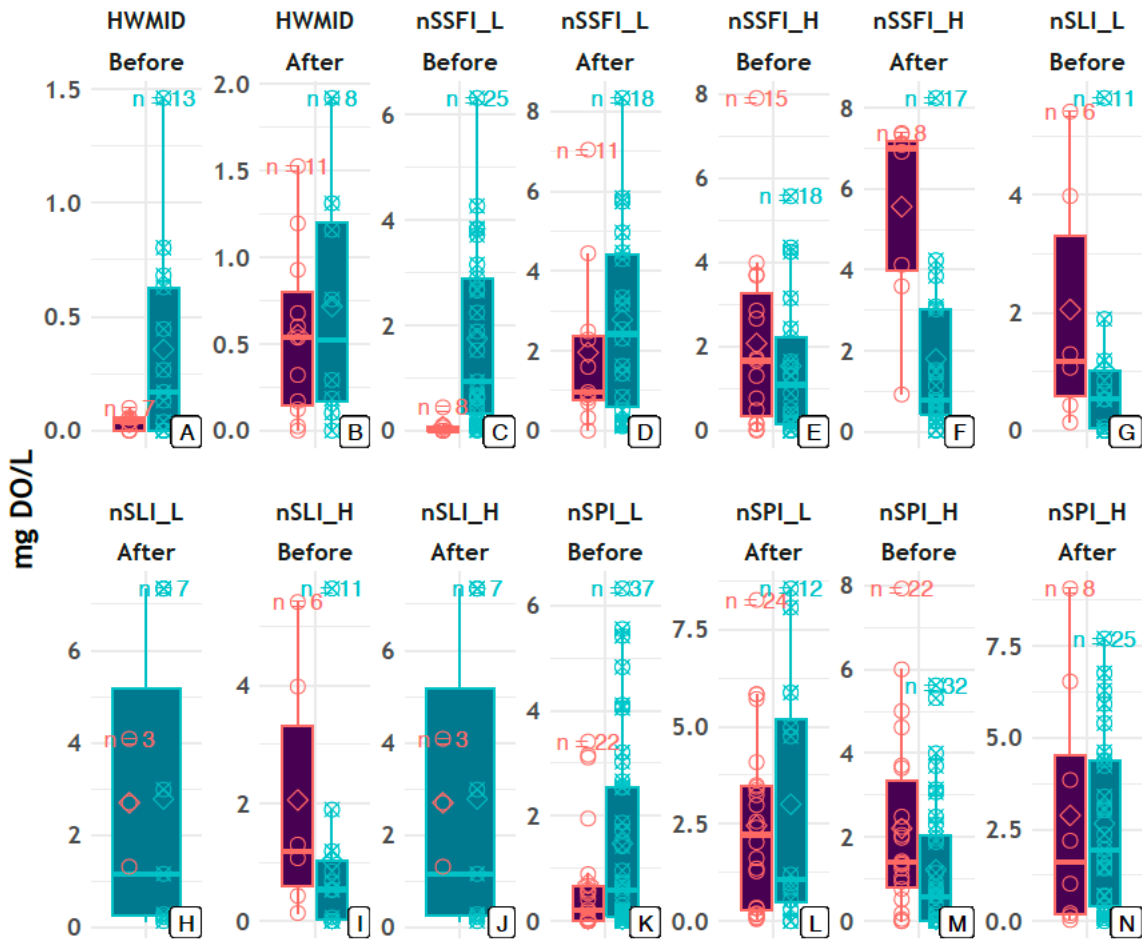


Figure S5: Box and jitter plots summarising distributions of hypolimnetic dissolved oxygen (DO) under extreme and non-extreme climatic conditions represented by indices, in the “Before” and “After” periods. Panels A- B represent DO under heatwave conditions, C-F represent DO under streamflow conditions, G-J represent DO under reservoir level conditions and K- N represent DO under precipitation conditions. Each panel also contains the number of samples (n) under comparison and a diamond symbol marking the position of the mean in the distribution.

Hypolimnetic Nitrate

Classification ■ Extreme ■ Non_Extreme

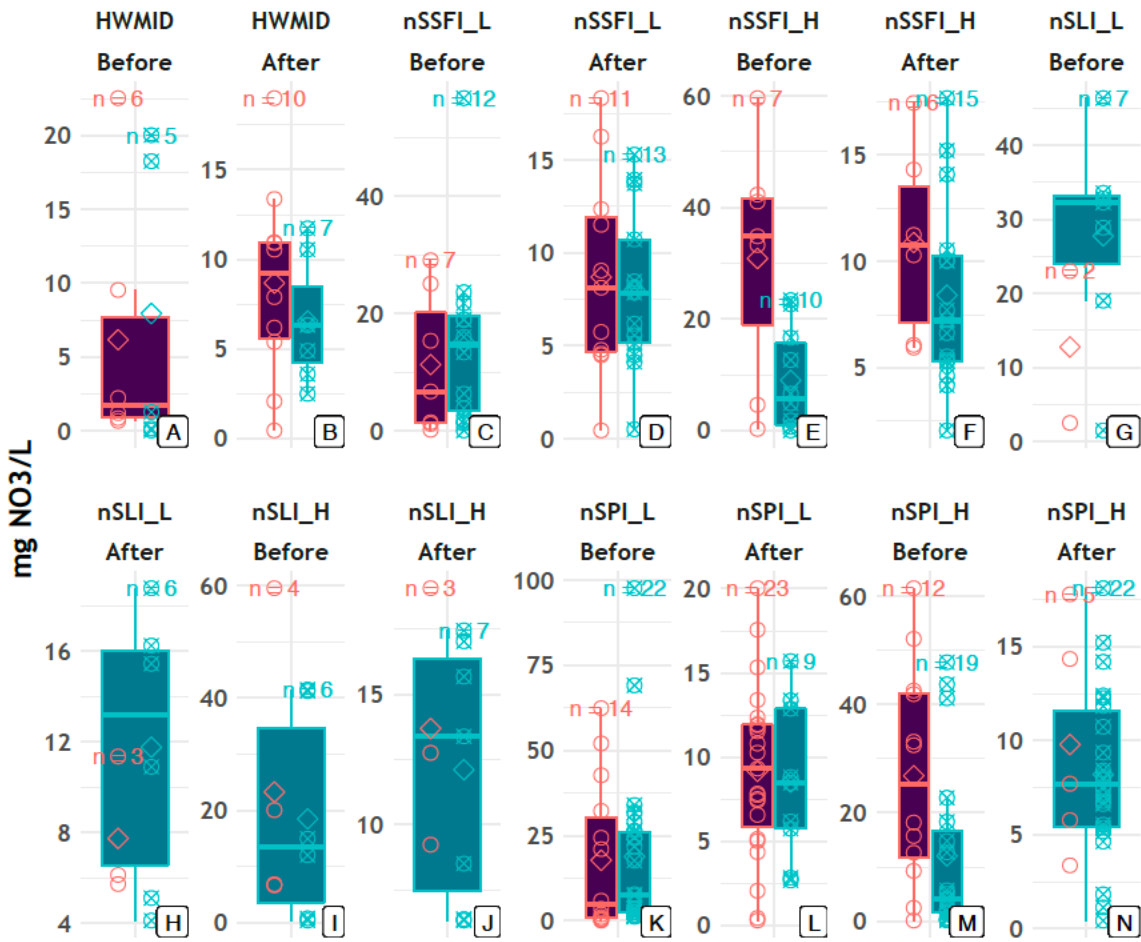


Figure S6: Box and jitter plots summarising distributions of hypolimnetic nitrate (NO_3^-) under extreme and non-extreme climatic conditions represented by indices, in the “Before” and “After” periods. Panels A- B represent NO_3^- under heatwave conditions, C-F represent NO_3^- under streamflow conditions, G-J represent NO_3^- under reservoir level conditions and K-N represent NO_3^- under precipitation conditions. Each panel also contains the number of samples (n) under comparison and a diamond symbol marking the position of the mean in the distribution.

Hypolimnetic Ammonium

Classification ⊠ Extreme ⊠ Non_Extreme

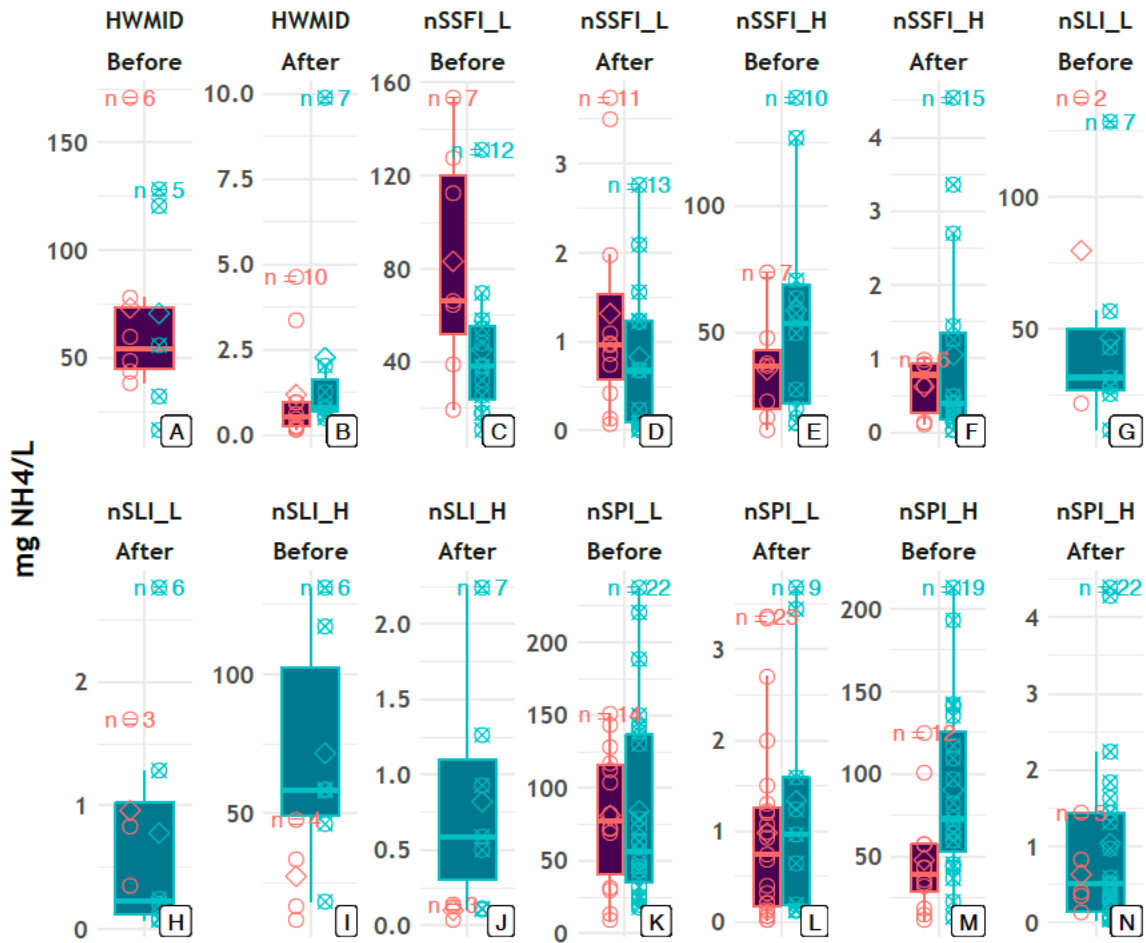


Figure S7: Box and jitter plots summarising distributions of hypolimnetic ammonium (NH_4^+) under extreme and non-extreme climatic conditions represented by indices, in the “Before” and “After” periods. Panels A- B represent NH_4^+ under heatwave conditions, C-F represent NH_4^+ under streamflow conditions, G-J represent NH_4^+ under reservoir level conditions and K-N represent NH_4^+ under precipitation conditions. Each panel also contains the number of samples (n) under comparison and a diamond symbol marking the position of the mean in the distribution.

Hypolimnetic Total Phosphorus

Classification ⊠ Extreme ⊠ Non_Extreme

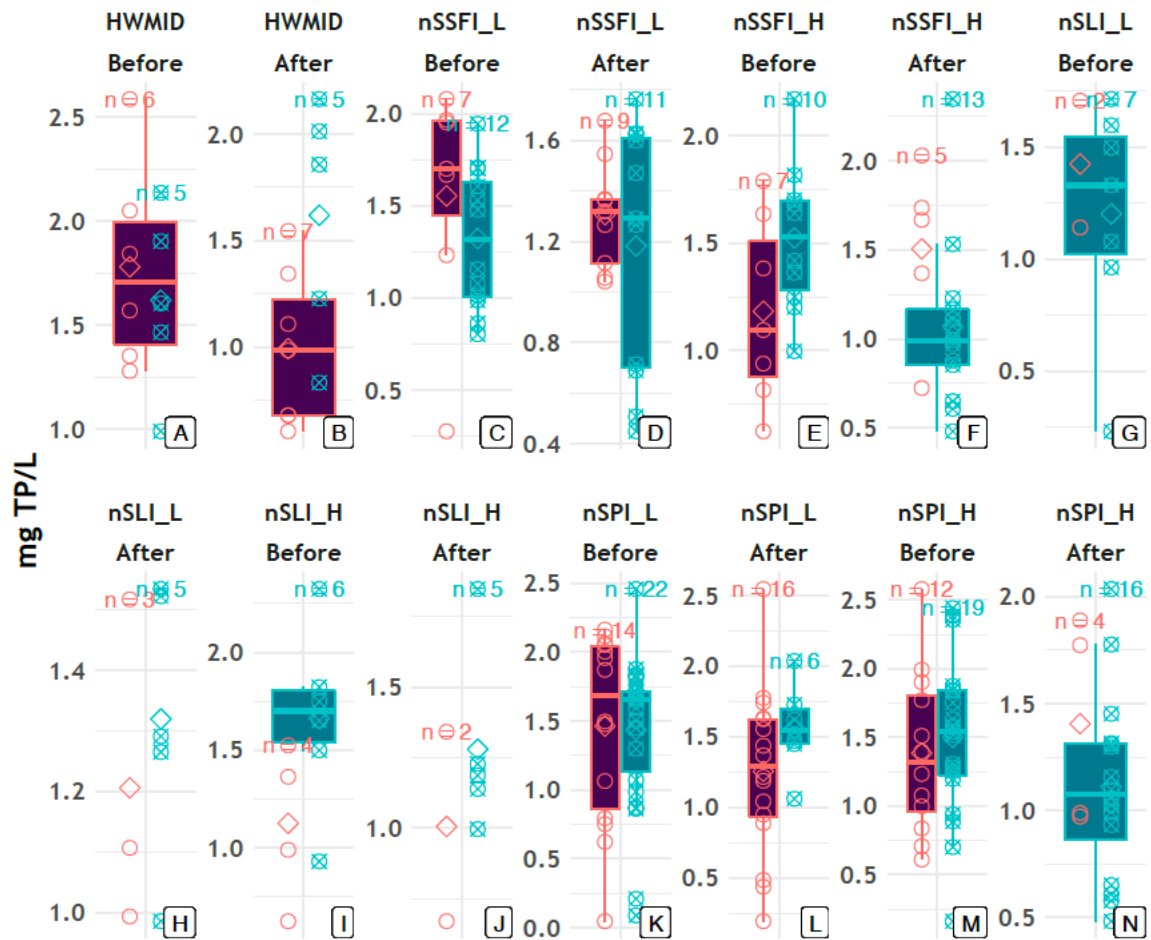


Figure S8: Box and jitter plots summarising distributions of hypolimnetic total phosphorus (TP) under extreme(-H) and non-extreme (-L) climatic conditions represented by indices, in the “Before” and “After” periods. Panels A- B represent TP under heatwave conditions, C-F represent TP under streamflow conditions, G-J represent TP under reservoir level conditions and K-N represent TP under precipitation conditions. Each panel also contains the number of samples (n) under comparison and a diamond symbol marking the position of the mean in the distribution.

Hypolimnetic Temperature

Classification ■ Extreme ■ Non_Extreme

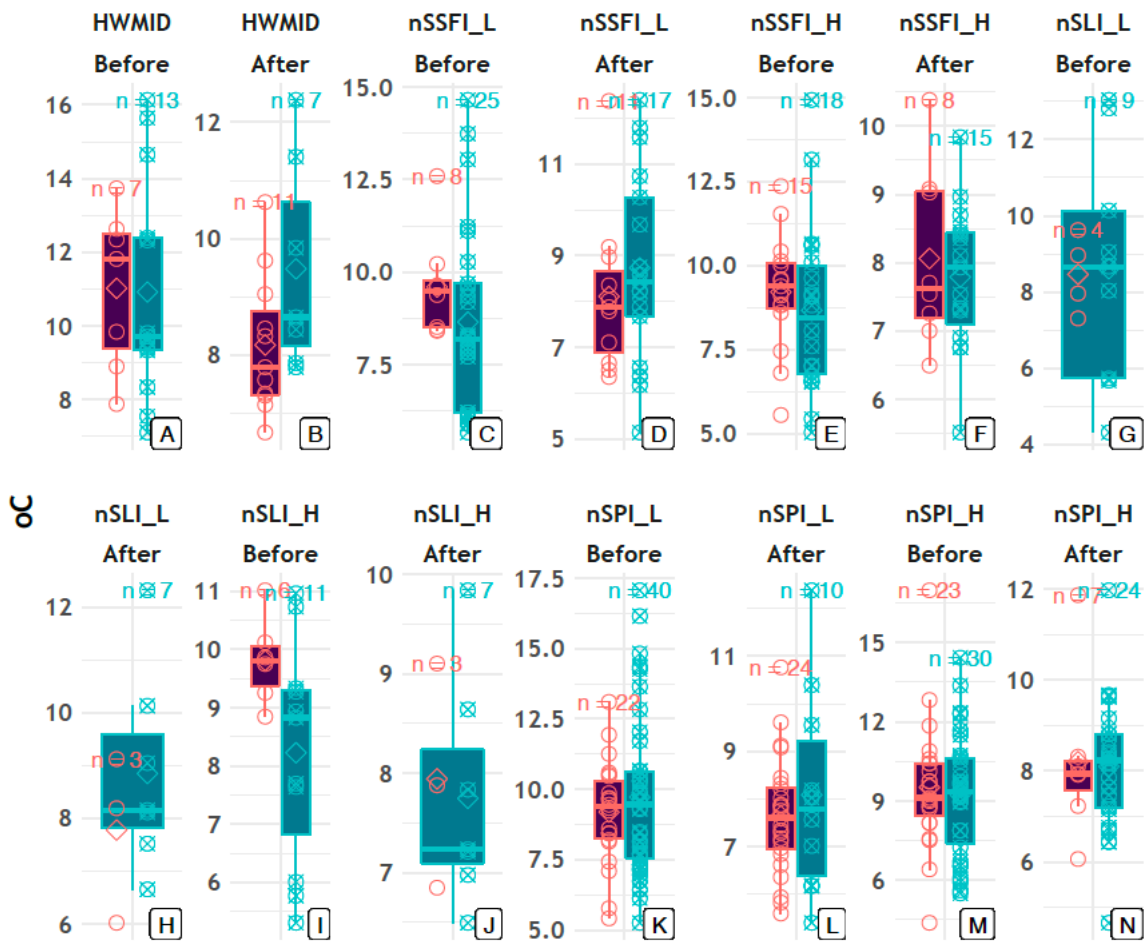


Figure S9: Box and jitter plots summarising distributions of hypolimnetic temperature (T_w) under extreme(-H) and non-extreme (-L) climatic conditions represented by indices, in the “Before” and “After” periods. Panels A- B represent T_w under heatwave conditions, C-F represent T_w under streamflow conditions, G-J represent T_w under reservoir level conditions and K-N represent T_w under precipitation conditions. Each panel also contains the number of samples (n) under comparison and a diamond symbol marking the position of the mean in the distribution.

Epilimnetic Dissolved Oxygen

Classification ■ Extreme ■ Non_Extreme

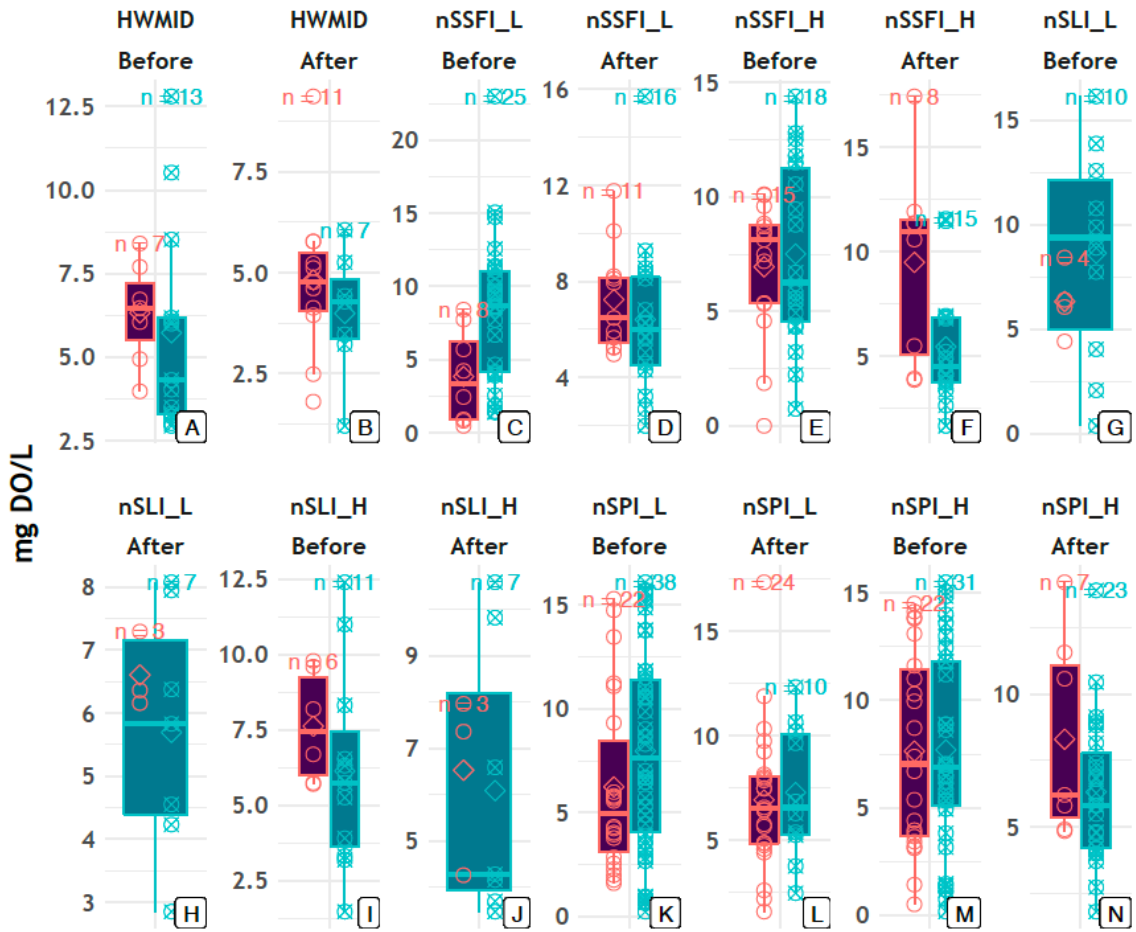


Figure S10: Box and jitter plots summarising distributions of epilimnetic dissolved oxygen (DO) under extreme and non-extreme climatic conditions represented by indices, in the “Before” and “After” periods. Panels A- B represent DO under heatwave conditions, C-F represent DO under streamflow conditions, G-J represent DO under reservoir level conditions and K-N represent DO under precipitation conditions. Each panel also contains the number of samples (n) under comparison and a diamond symbol marking the position of the mean in the distribution.

Epilimnetic Nitrate

Classification ⊠ Extreme ⊠ Non_Extreme

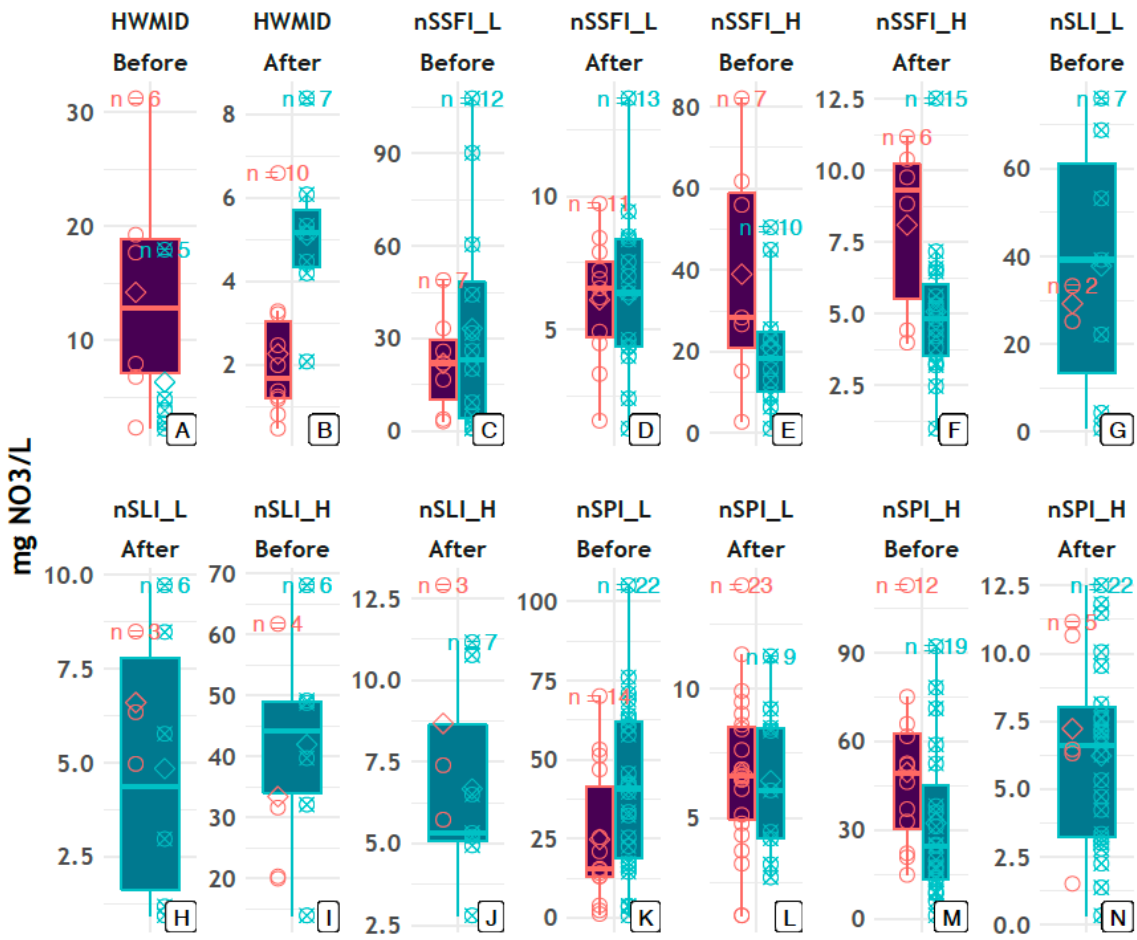


Figure S11: Box and jitter plots summarising distributions of epilimnetic nitrate (NO_3^-) under extreme and non-extreme climatic conditions represented by indices, in the “Before” and “After” periods. Panels A- B represent NO_3^- under heatwave conditions, C-F represent NO_3^- under streamflow conditions, G-J represent NO_3^- under reservoir level conditions and K-N represent NO_3^- under precipitation conditions. Each panel also contains the number of samples (n) under comparison and a diamond symbol marking the position of the mean in the distribution.

Epilimnetic Ammonium

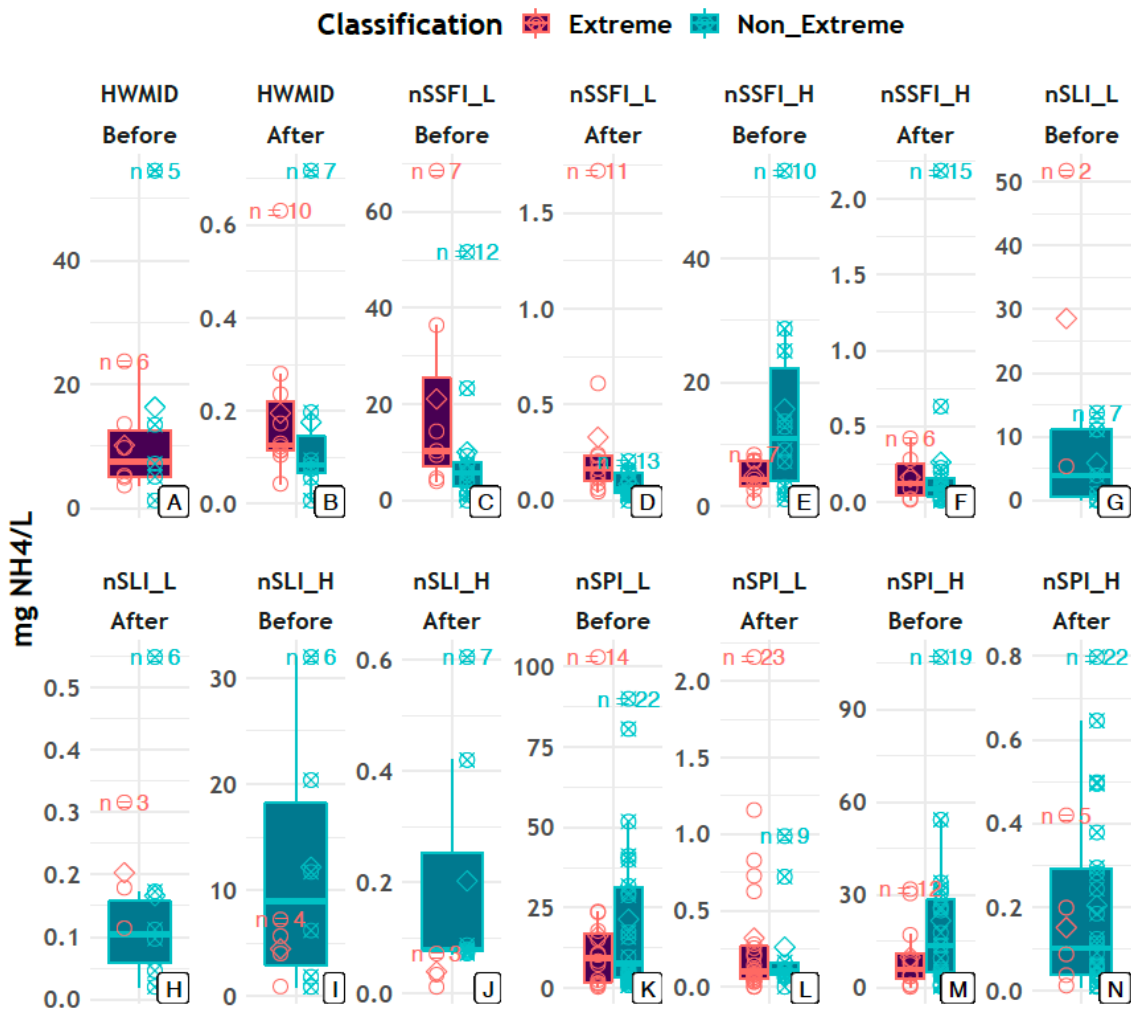


Figure S12: Box and jitter plots summarising distributions of epilimnetic ammonium (NH_4^+) under extreme and non-extreme climatic conditions represented by indices, in the “Before” and “After” periods. Panels A- B represent NH_4^+ under heatwave conditions, C-F represent NH_4^+ under streamflow conditions, G-J represent NH_4^+ under reservoir level conditions and K-N represent NH_4^+ under precipitation conditions. Each panel also contains the number of samples (n) under comparison and a diamond symbol marking the position of the mean in the distribution.

Epilimnetic Total Phosphorus

Classification ■ Extreme ■ Non_Extreme

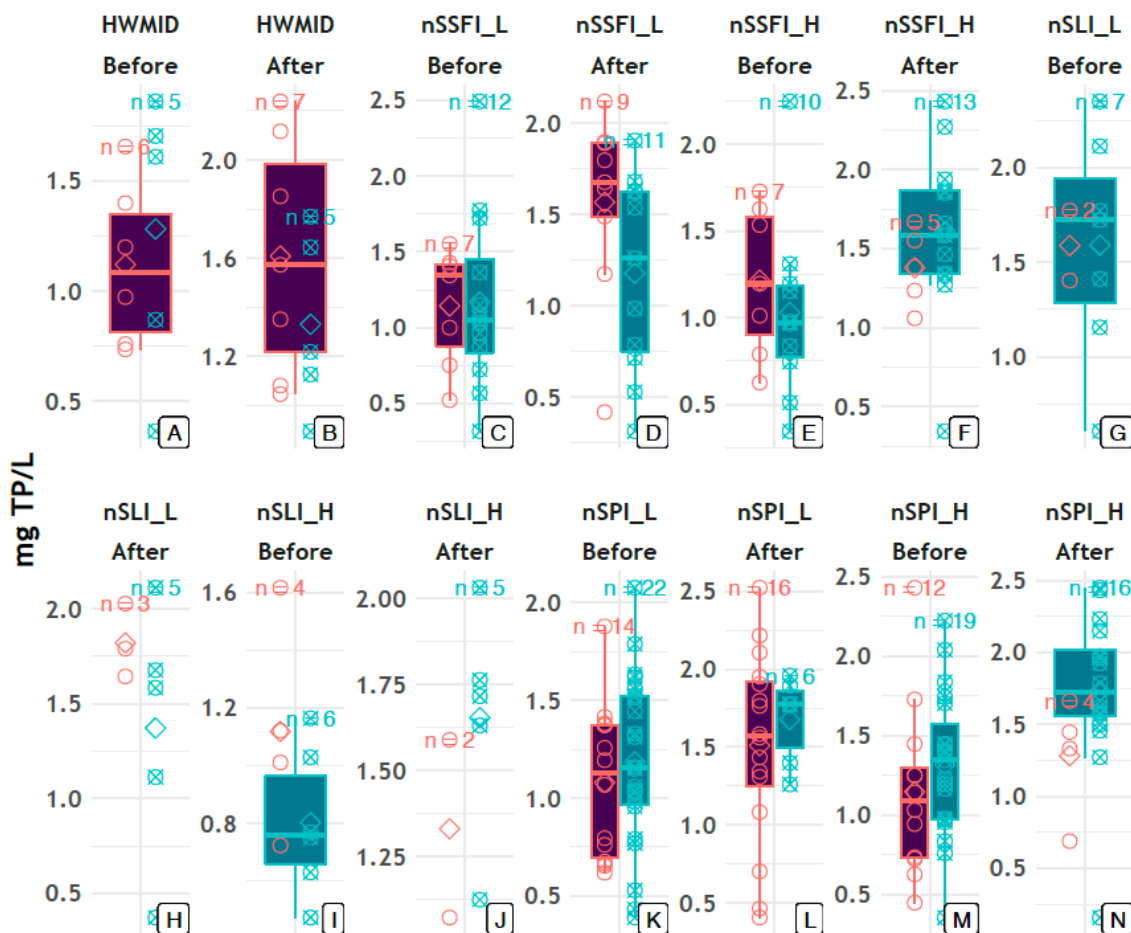


Figure S13: Box and jitter plots summarising distributions of epilimnetic total phosphorus (TP) under extreme and non-extreme climatic conditions represented by indices, in the “Before” and “After” periods. Panels A- B represent TP under heatwave conditions, C-F represent TP under streamflow conditions, G-J represent TP under reservoir level conditions and K-N represent TP under precipitation conditions. Each panel also contains the number of samples (n) under comparison and a diamond symbol marking the position of the mean in the distribution.

Epilimnetic Temperature

Classification ■ Extreme ■ Non_Extreme

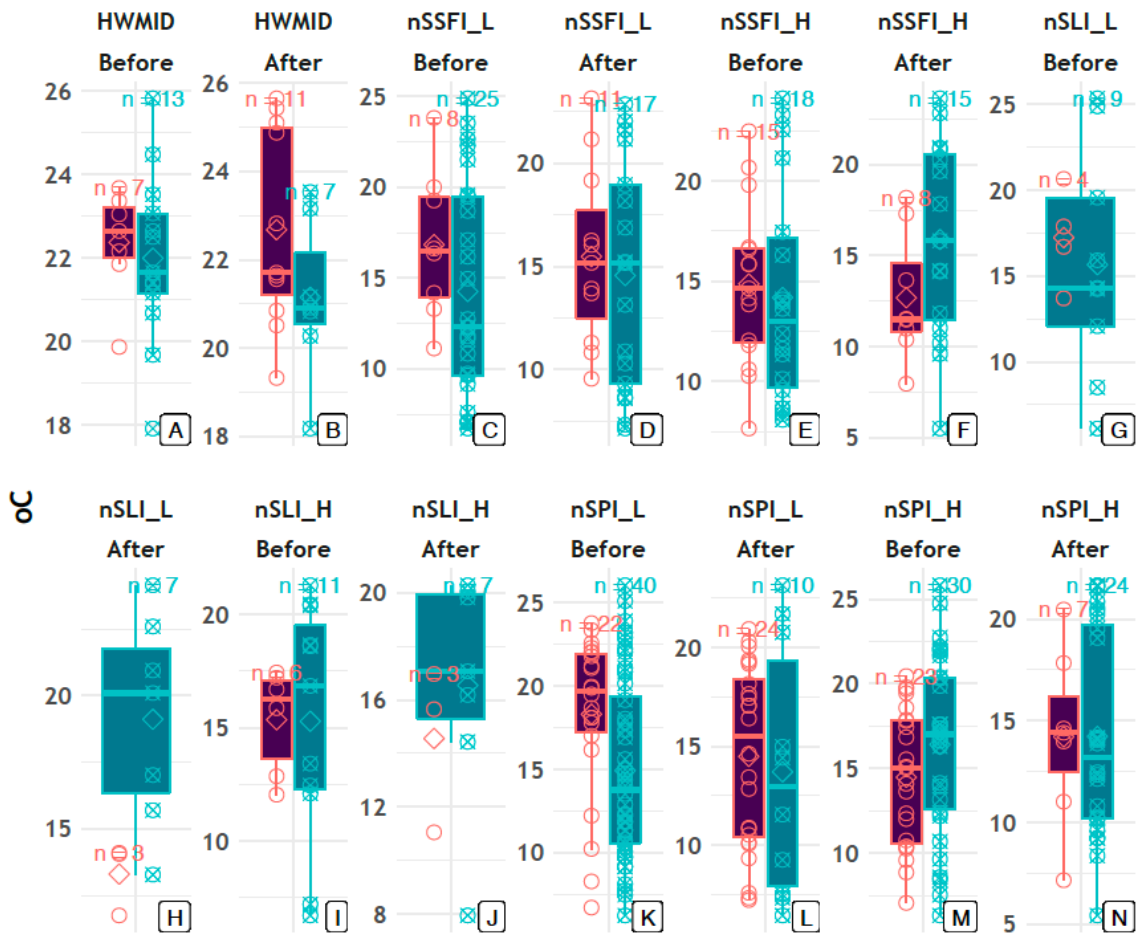


Figure S14: Box and jitter plots summarising distributions of epilimnetic temperature (T_w) under extreme(-H) and non-extreme (-L) climatic conditions represented by indices, in the “Before” and “After” periods. Panels A- B represent T_w under heatwave conditions, C-F represent T_w under streamflow conditions, G-J represent T_w under reservoir level conditions and K-N represent T_w under precipitation conditions. Each panel also contains the number of samples (n) under comparison and a diamond symbol marking the position of the mean in the distribution.

References

CoreTeam, R. (2017) *R: A Language and Environment for Statistical Computing*. Available at: <https://www.r-project.org/>.

Farahmand, A. and Aghakouchak, A. (2015) 'Advances in Water Resources A generalized framework for deriving nonparametric standardized drought indicators', *ADVANCES IN WATER RESOURCES*, 76, pp. 140–145. doi:10.1016/j.advwatres.2014.11.012.

Gilleland, E. and Katz, R.W. (2016) 'ExtRemes 2.0: An extreme value analysis package in R', *Journal of Statistical Software*, 72(8). doi:10.18637/jss.v072.i08.

Gringorten, I. (1963) 'A plotting rule for extreme probability paper', *Journal of Geophysical Research*, 68(3), pp. 813–814. doi:10.1029/JZ068i003p00813.

Russo, S. et al. (2014) 'Magnitude of extreme heat waves in present climate and their projection in a warming world', *Journal of Geophysical Research Atmospheres*, 119(22), pp. 12500–12512. doi:10.1002/2014JD022098.

Russo, S., Sillmann, J. and Fischer, E.M. (2015) 'Top ten European heatwaves since 1950 and their occurrence in the coming decades', *Environmental Research Letters*, 10(12). doi:10.1088/1748-9326/10/12/124003.

Schaller, N. et al. (2018) 'Influence of blocking on Northern European and Western Russian heatwaves in large climate model ensembles', *Environmental Research Letters*, 13(5). doi:10.1088/1748-9326/aaba55.

Annex 2

- 6.2 Characterization of organic matter by HRMS in surface waters: Effects of chlorination on molecular fingerprints and correlation with DBP formation potential.**

Supporting Information

Characterization of organic matter by HRMS in surface waters: Effects of chlorination on molecular fingerprints and correlation with DBP formation potential

Josep Sanchís^{1,2,*}, Adrián Jaén-Gil^{1,2}, Pablo Gago-Ferrero^{1,2}, Elias Munthali^{1,2}, Maria José Farre^{1,2,*}

¹ Catalan Institute for Water Research (ICRA), Scientific and Technological Park of the University of Girona, H2O Building, C/Emili Grahit, 101, E17003, Girona, Spain.

² University of Girona, 17071, Girona, Spain.

*Co-corresponding authors: jsanchis@icra.cat and mjfarre@icra.cat

Contents

Text S1	2
Text S2	3
Figure S1	5
Figure S2	6
Figure S3	7
Figure S4	17
Figure S5	27
Figure S6	31
Figure S7	35
Figure S8	36
Figure S9	37
Figure S10.....	38
Table S1	39
Table S2	40
Table S3	41
Table S4.....	42

Text S1. Analysis of target DBPs.

DBP analysis was performed by liquid-liquid salted microextraction and gas chromatography coupled to mass spectrometry (GC–MS), using a TSQ Quantum triple quadrupole mass spectrometer system (Thermo Fisher Scientific) equipped with a TriPlus™ autosampler.

Sample pH was adjusted to pH 3.5 with 0.2 N sulphuric acid, and extracted using 3 mL of MtBE containing 200 µg/L of d₆-1,2-dibromopropane as internal standard. After the addition of ~10 g of high purity sodium sulphate, the samples were vortexed for 1 minute and left to settle for 5 min. Finally, ~1.5 mL of MtBE extract was transferred into 2 mL vials for injection.

The injector was operated in splitless mode. Chromatographic separation was performed using a ZB1701 from Phenomenex (30m x 0.25mm x 0.25µm). The oven temperature program was as follows: 40°C for 25 min, ramp to 145°C at 5°C/min and held for 2 min and then ramp to 260°C at 20°C/min and held for 10 min. The inlet temperature was set at 200°C. The reporting limit of all the DBPs was 0.1 µg/L, and the recoveries were above 90%. Acquired data were processed by TracerFinder EFS 3.1 software and the monitored ions are described in **Table S4**.

Text S2. Description of the R script used for the annotation of DOM spectra.

Here, the R script that was employed for assigning empirical formulae to the DOM spectra is described. The workflow consisted in three main steps:

1. Noise removal: First, the KMD_{noise} of each sample were estimated using the function `KMDNoise`. This function builds the KMD plot of the spectrum and isolates the peaks contained in the region of the plot delimited by the lines:

$$KMD = 0.1132 \times m/z + b_1 \quad \text{equation S1}$$

$$KMD = 0.1132 \times m/z + b_2, \quad \text{equation S2}$$

with $b_1 = 0.05$ and $b_2 = 0.2$. This characteristic region is expected to mainly contain m/z artifacts (i.e. harmonics and aberrant signals), avoiding informative mono- and multicharged signals (Schum, 2019). The average intensity of the peaks contained in the said region is defined as the KMD_{noise} . The noise threshold was defined individually for each sample as three times its KMD_{noise} . Those peaks with intensities lower than this threshold were discarded.

2. ^{13}C isotope filter: those signals containing one or more ^{13}C atom were filtered out using the `IsoFiltR` function. Briefly, this function selects those peaks containing one or more ^{13}C atoms on basis of their isotopic pattern (Zheng et al., 2019). Only those signals corresponding to monocharged molecules/fragments with no ^{13}C atoms were further considered.

3. Determination of elemental composition: m/z signals were assigned to elemental formulae using the function `MFAssign` with the following restrictions: m/z range: 100–1000; charge: only monocharged formulae were considered; range of O/C: 0–1.0; range of H/C: 0.3–2.5; range of DBEO: -1–10; maximum tolerable m/z error: ± 1.0 ppm. Formulae were assigned following a multistep process:

- Assignment of $C_xH_yO_zN_{0-5}S_{0-2}$ and $C_xH_yO_zN_{0-5}Cl_{0-2}$: Two lists of formulae, which potentially contained ^{32}S and ^{35}Cl atoms, were obtained.
- Isotopic confirmation of Cl and S: The lists of formulae containing ^{32}S and ^{35}Cl was refined using a custom isotopic filter based on $^{34}S/^{32}S$ and $^{37}Cl/^{35}Cl$ mass defects (± 30 mDa tolerance) and natural isotopic ratios (1:0.044 \pm 0.018 and 1:0.324 \pm 0.113).
- Formulae $C_xH_yO_zN_{0-5}Br_{0-2}$: The `MFAssign` function does not allow to directly determining the presence of Br heteroatoms. To circumvent this, those m/z signals that had not been assigned and confirmed in the previous step were transformed by subtracting the exact m/z of a ^{79}Br atom and adding the exact m/z of a 1H atom (see equation 3). Formulae $C_xH_yO_zN_{0-5}$ were then assigned to the new set of signals. The resulting list of formulae was corrected back by subtracting a 1H atom and adding a ^{79}Br atom. Finally, this process was then repeated, now considering two Br atoms (see equation S4).

$$m/z_{new} = m/z_{original} - 78.9183 + 1.0078 \quad \text{equation S3}$$

$$m/z_{new}' = m/z_{new} - 78.9183 + 1.0078 \quad \text{equation S4}$$

- Isotopic confirmation of Br: The lists of formulae containing ^{79}Br was refined using a custom isotopic filter based on $^{79}\text{Br}/^{81}\text{Br}$ mass defect (± 30 mDa tolerance) and isotopic ratio ($1:0.973 \pm 0.243$).
- Assignment of formulae $\text{C}_x\text{H}_y\text{O}_z\text{N}_{0-5}$: The elemental compositions of those m/z that had not been assigned in the previous steps were tentatively assigned using the MFAssign function with no heteroatoms other than O and N.

Figure S1. Dendrogram showing the differences among samples according to their CYd.

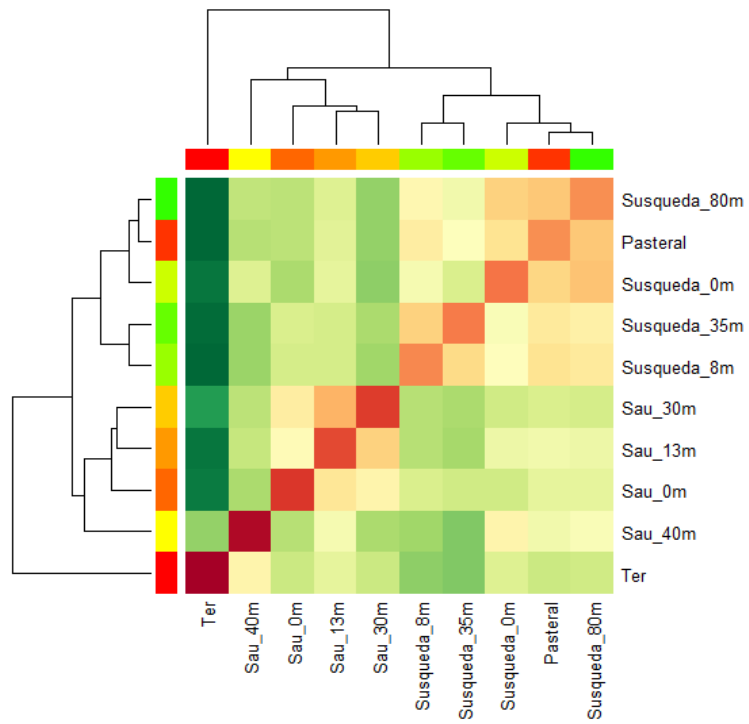


Figure S2. Dendrogram of raw and chlorinated samples, clustered according to their CYd.

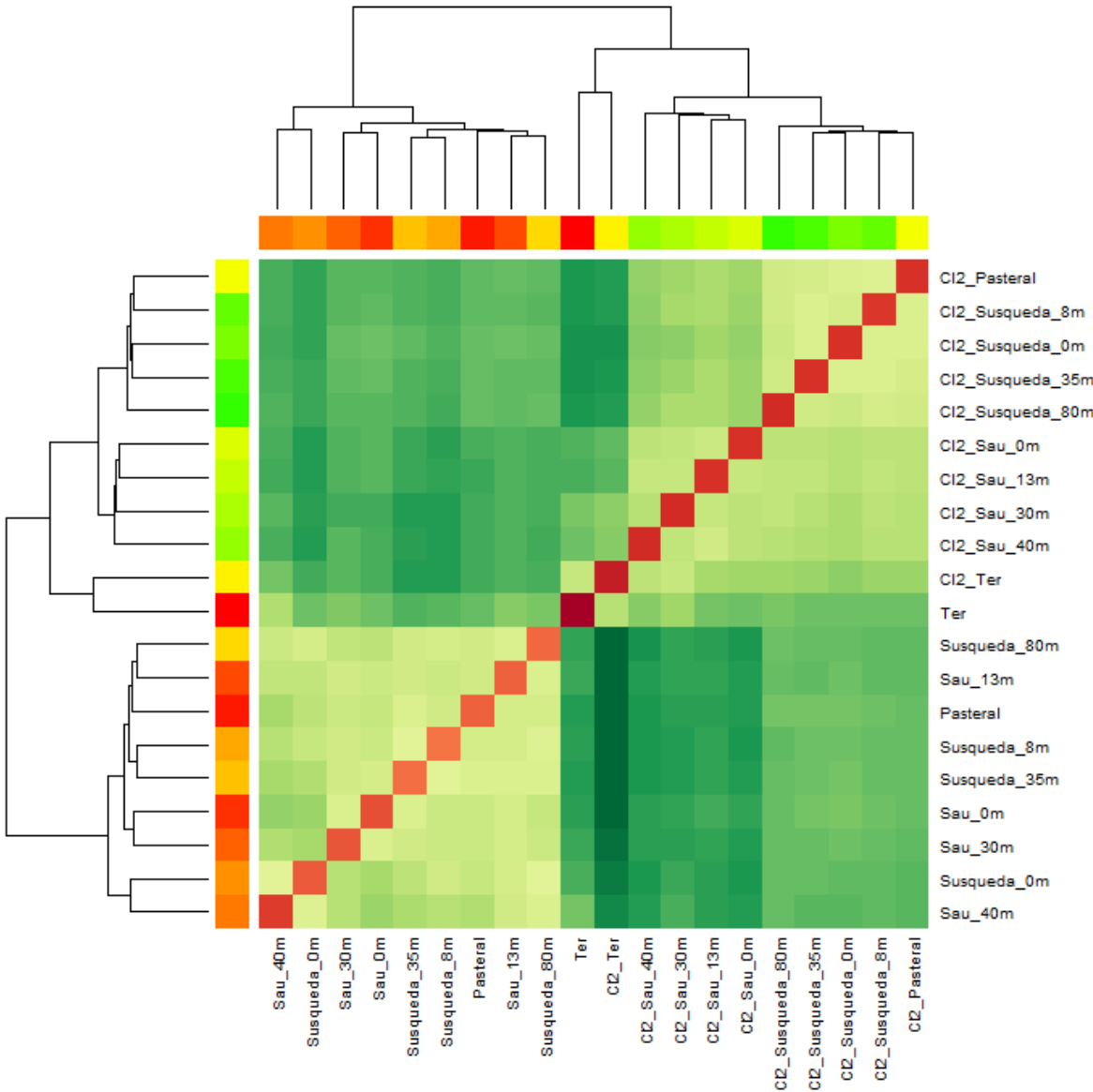


Figure S3a. KMD plots of the analysed samples.

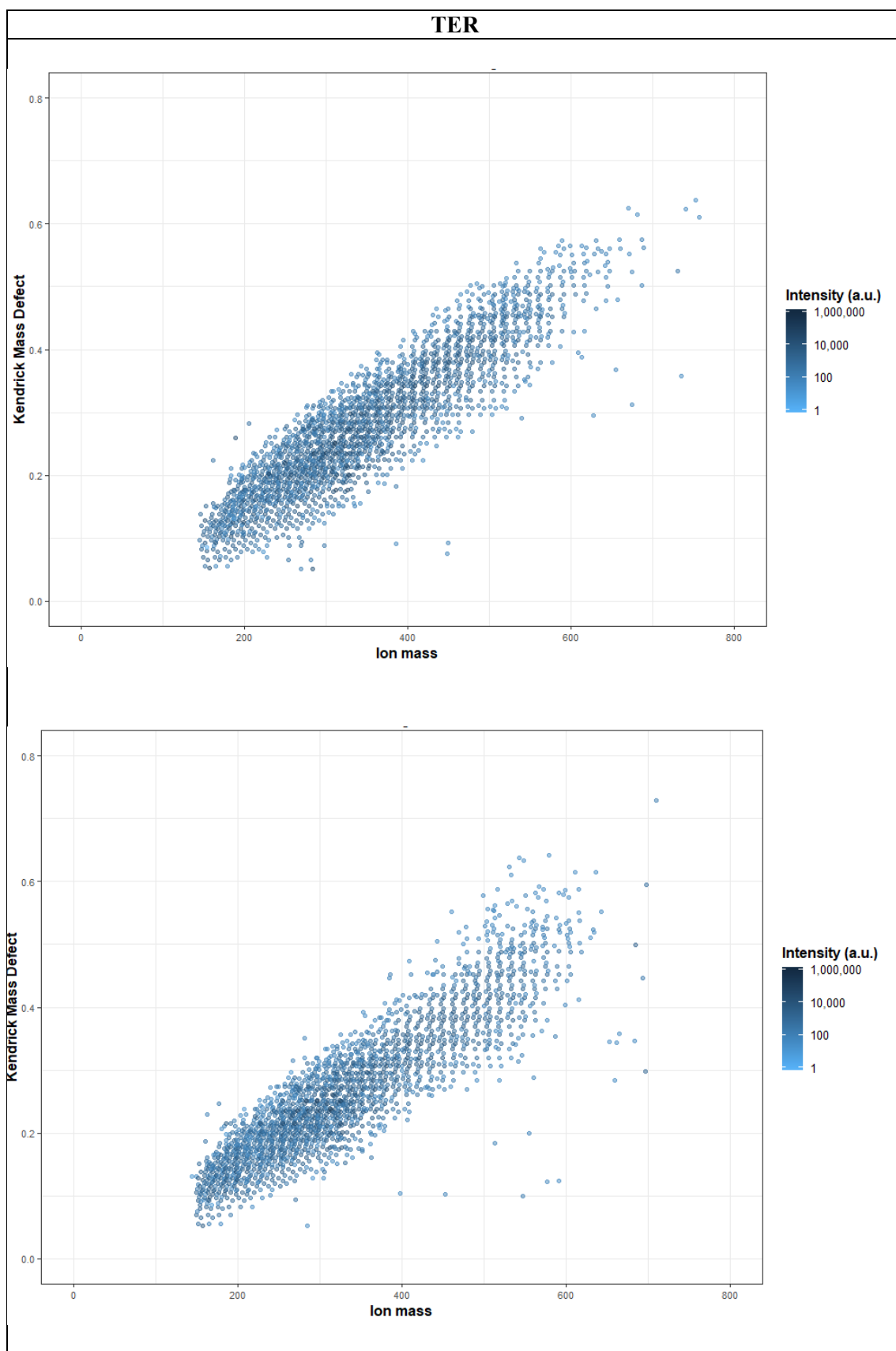


Figure S3b. KMD plots of the analysed samples.

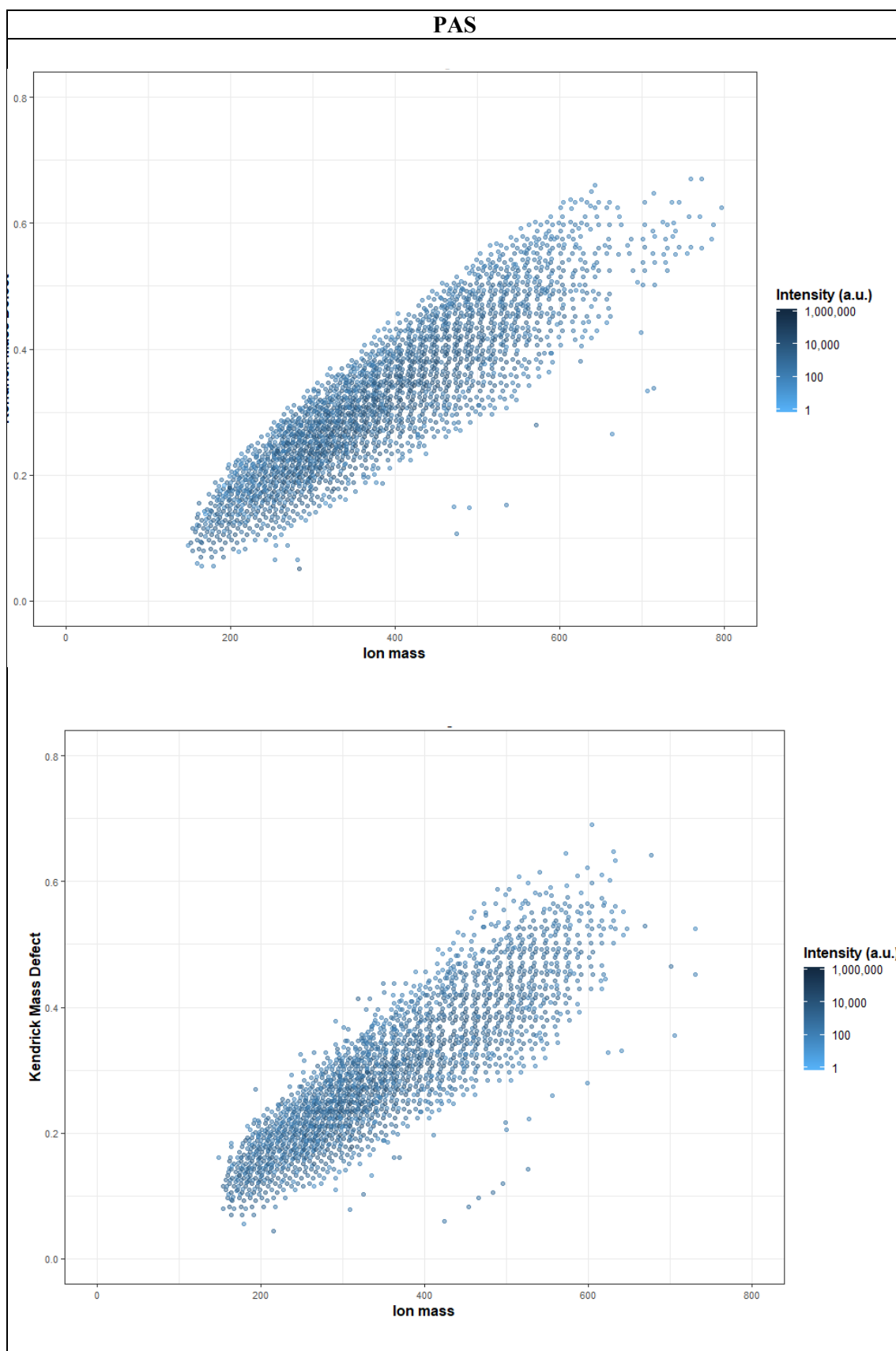


Figure S3c. KMD plots of the analysed samples.

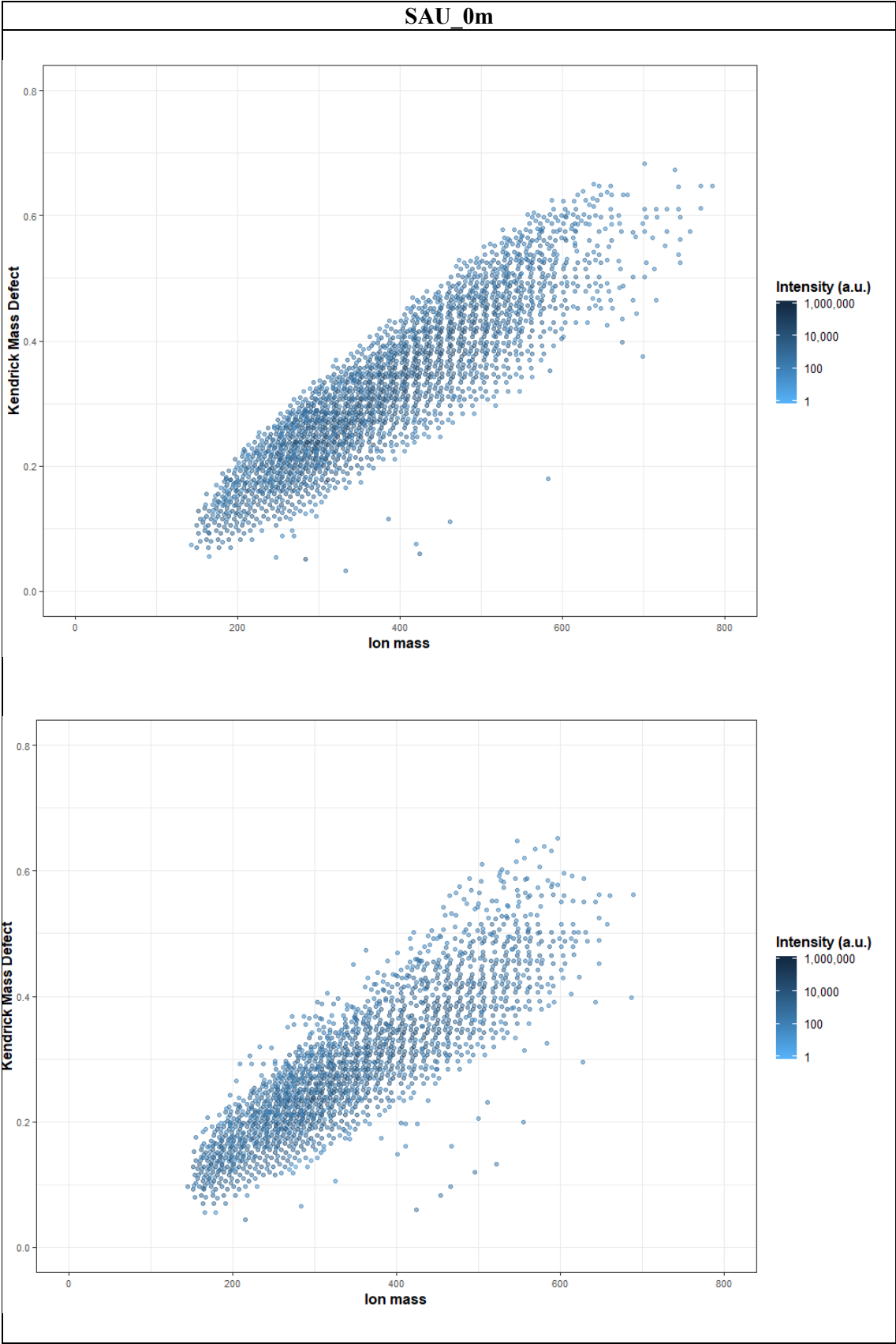


Figure S3d. KMD plots of the analysed samples.

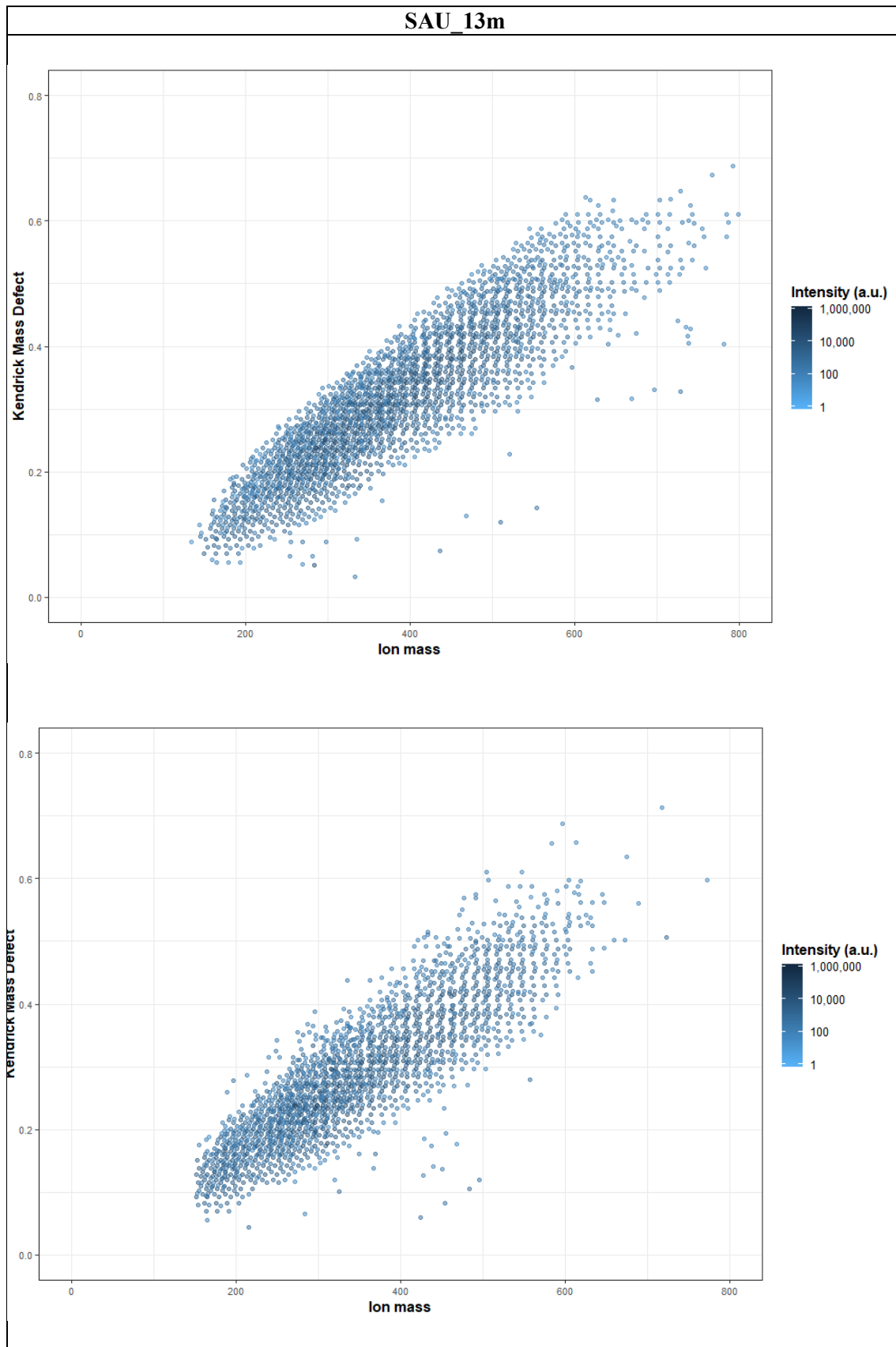


Figure S3e. KMD plots of the analysed samples.

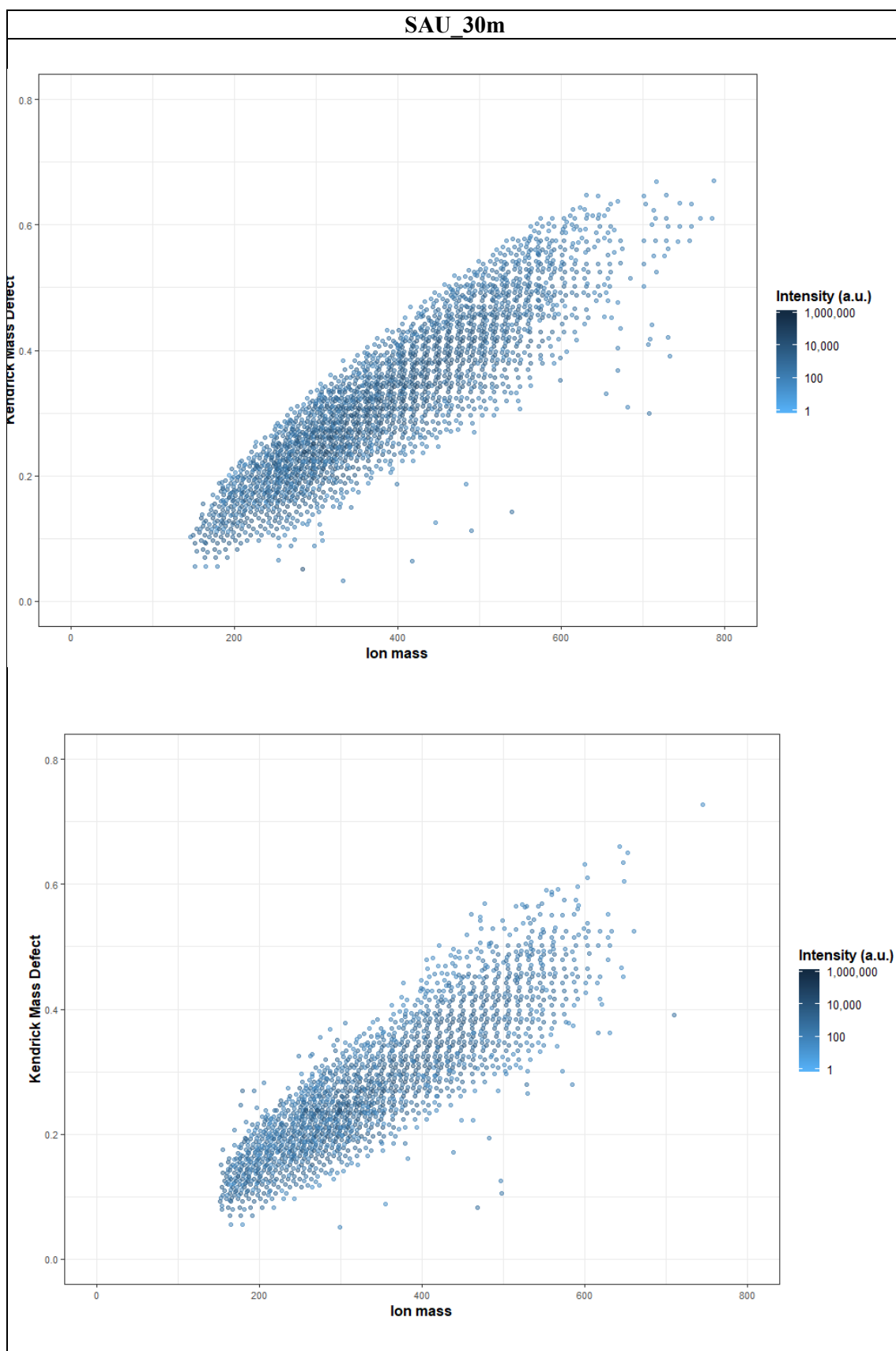


Figure S3f. KMD plots of the analysed samples.

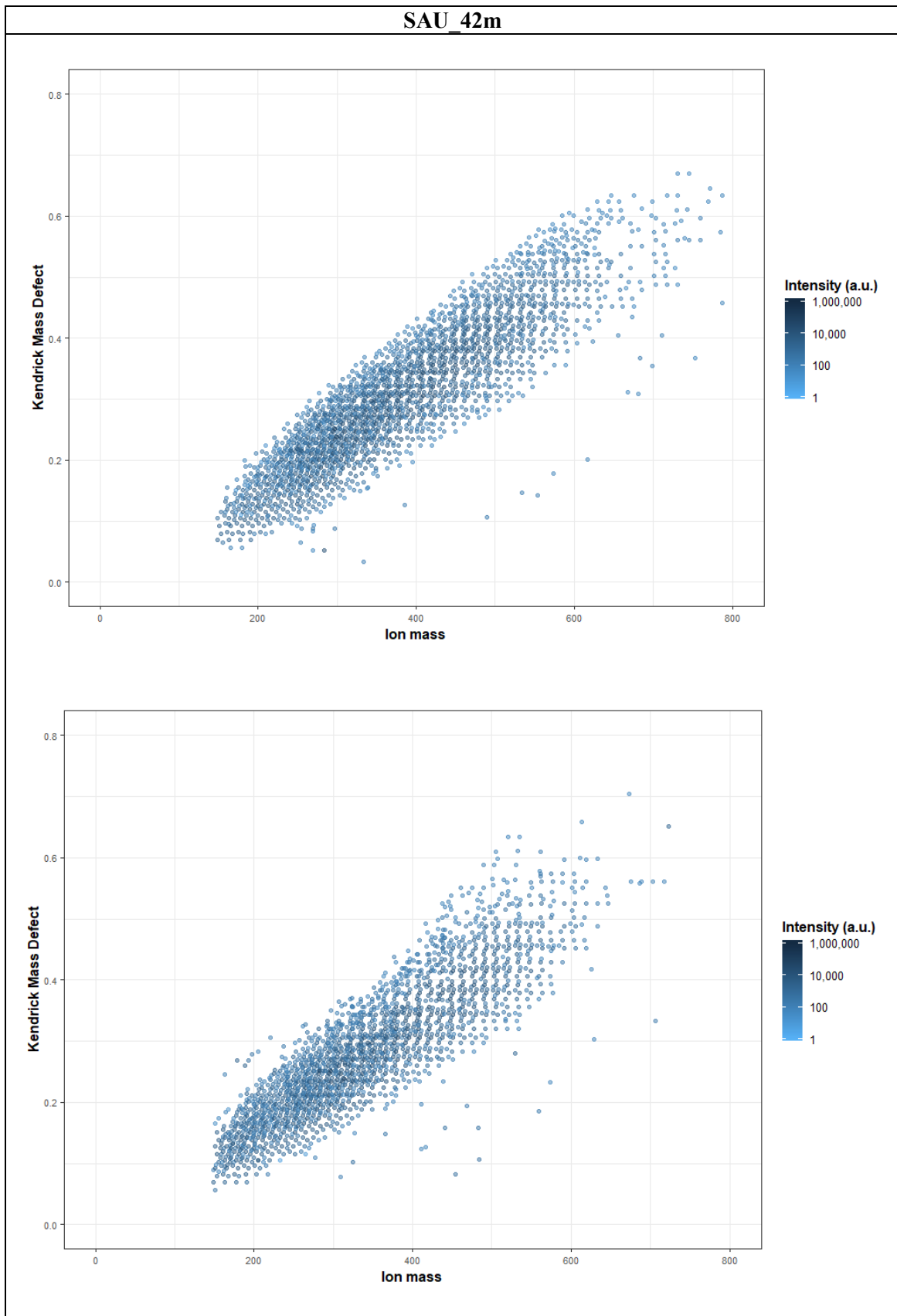


Figure S3g. KMD plots of the analysed samples.

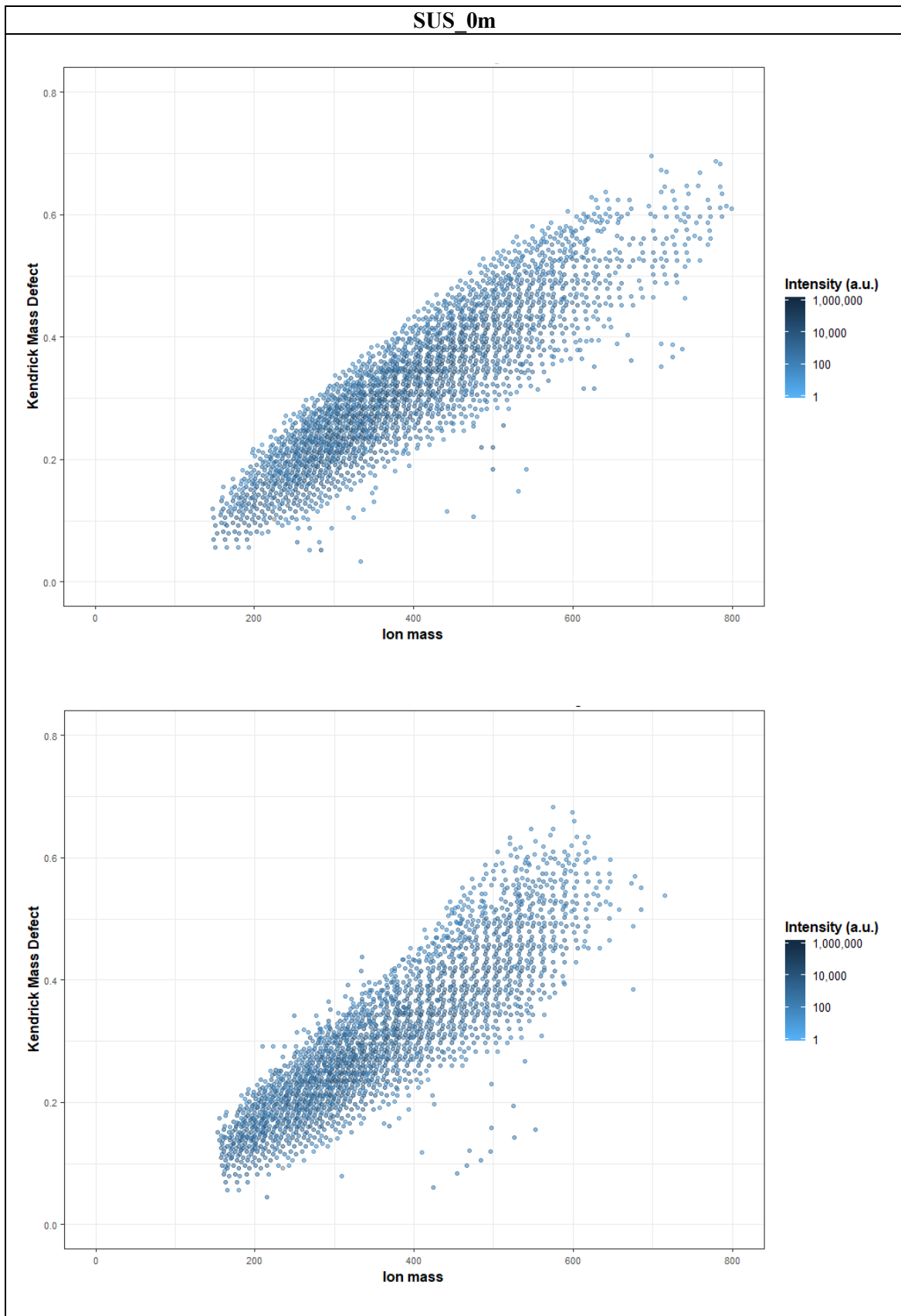


Figure S3h. KMD plots of the analysed samples.

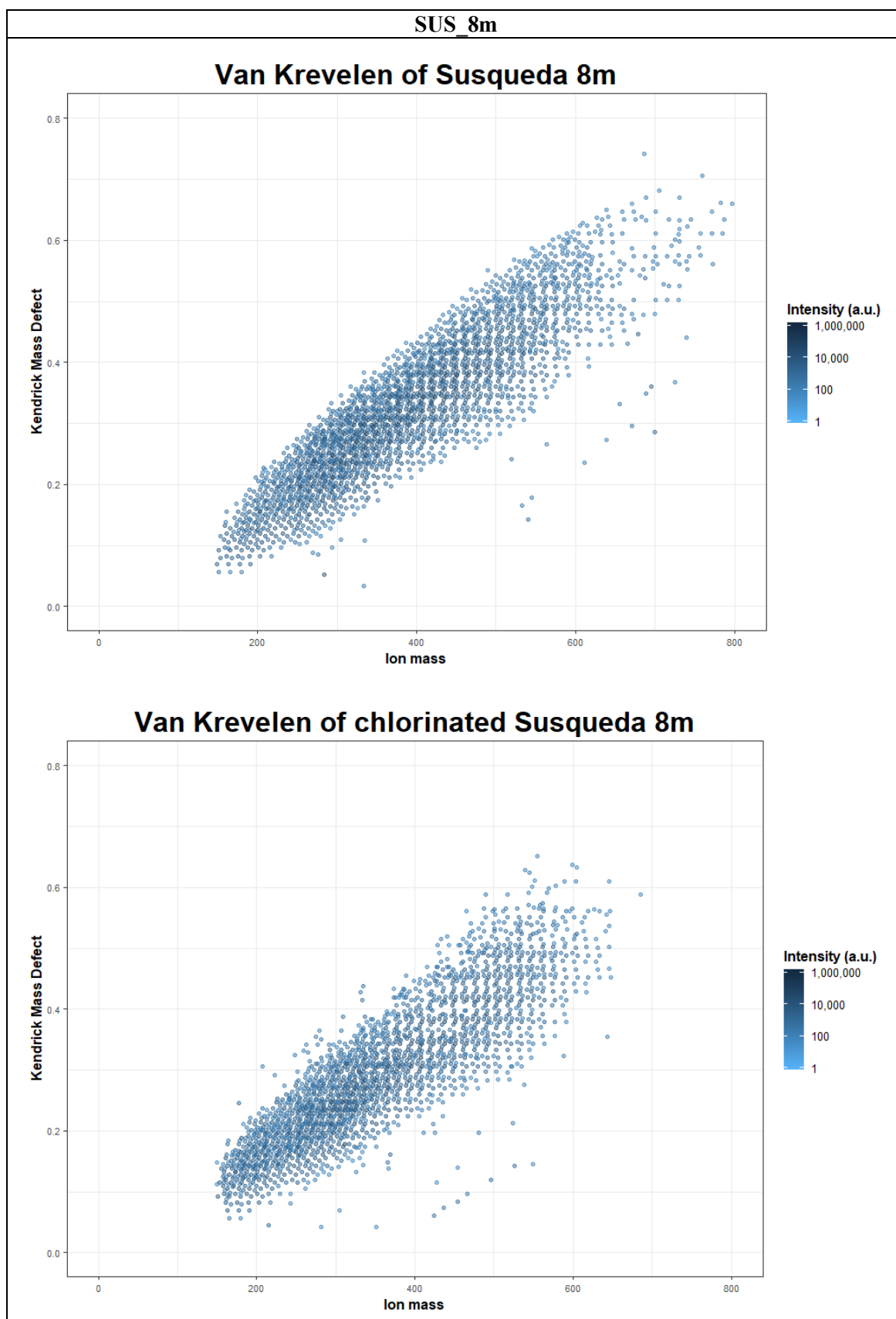


Figure S3i. KMD plots of the analysed samples.

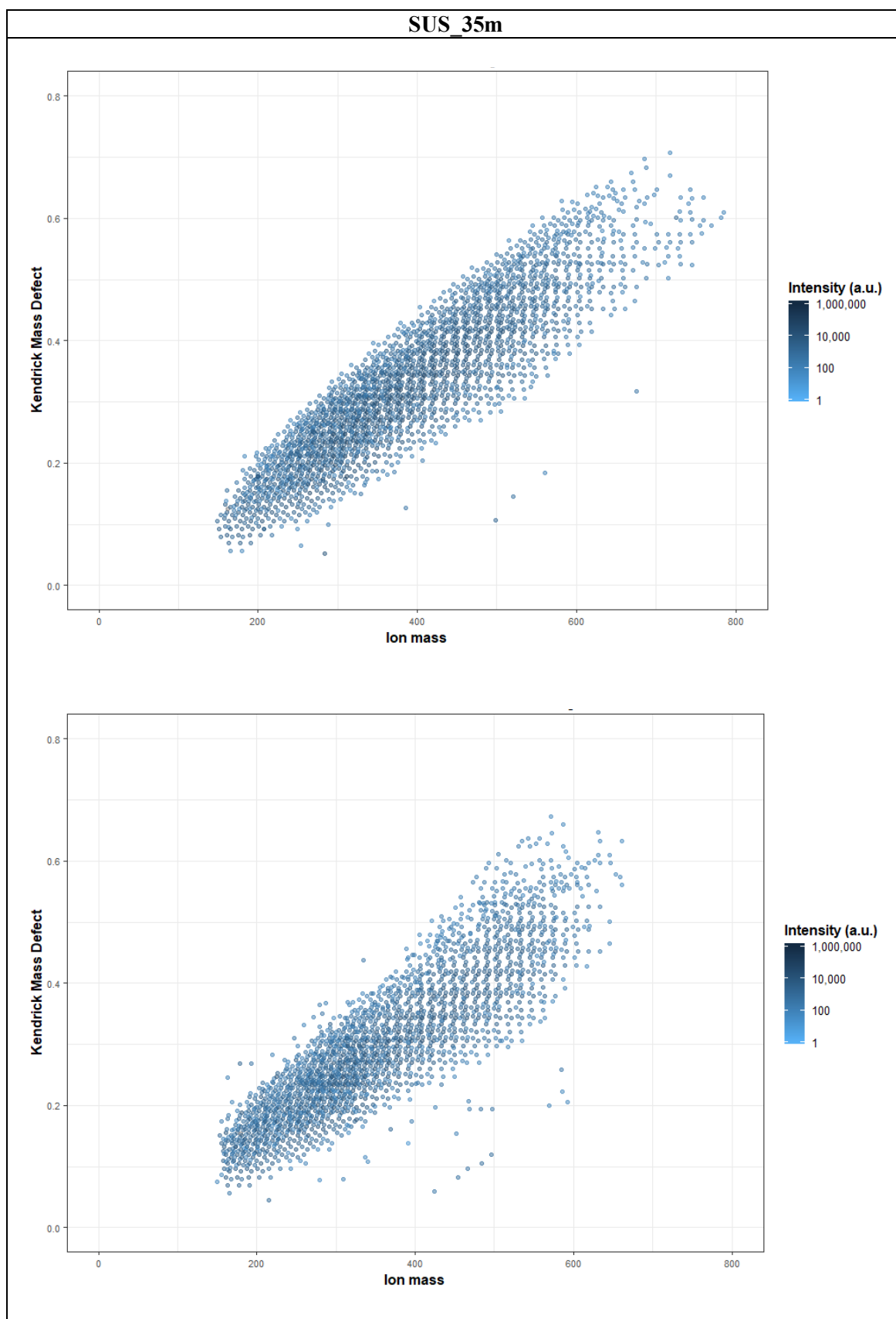


Figure S3j. KMD plots of the analysed samples.

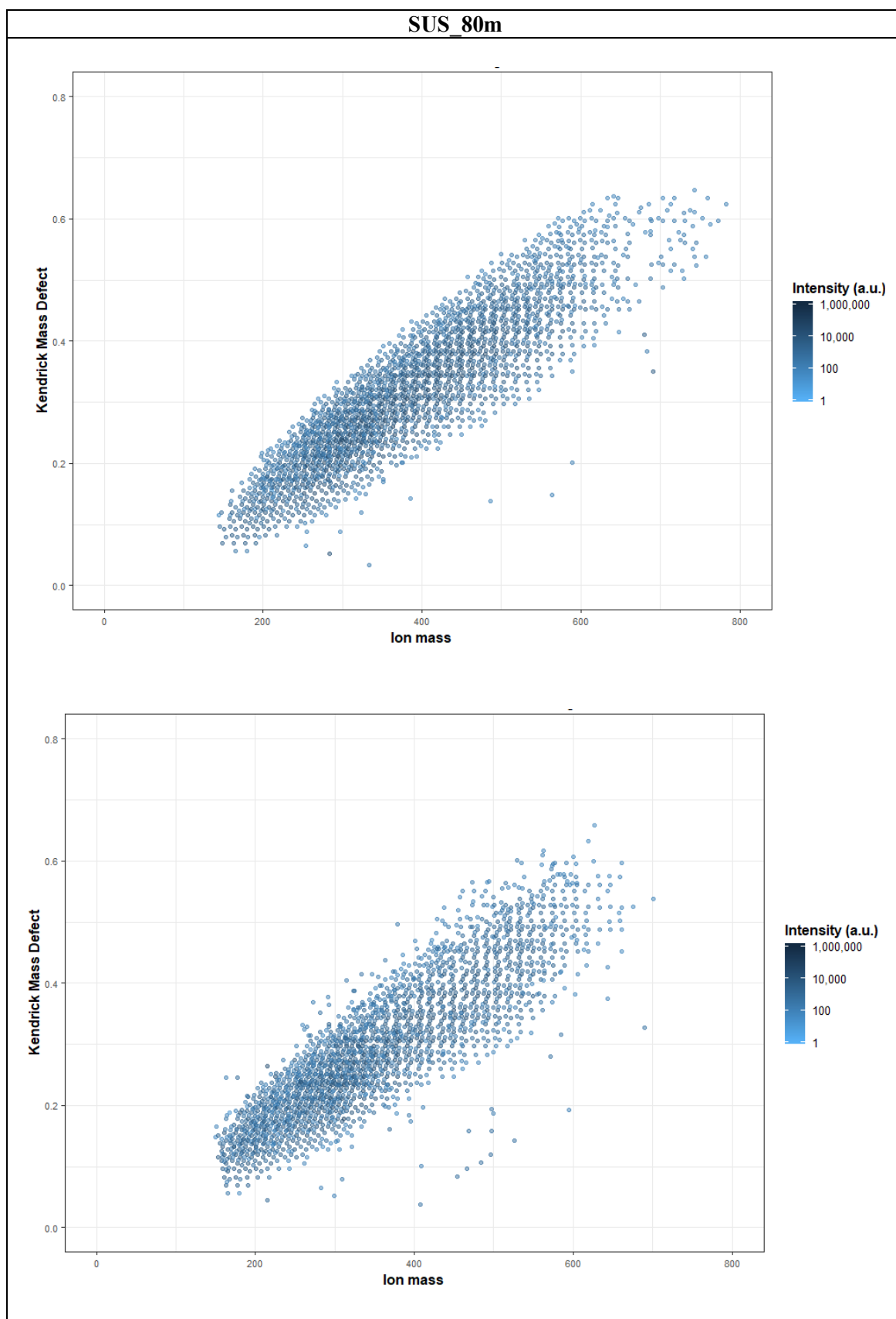


Figure S4a. VK diagrams of the analysed samples.

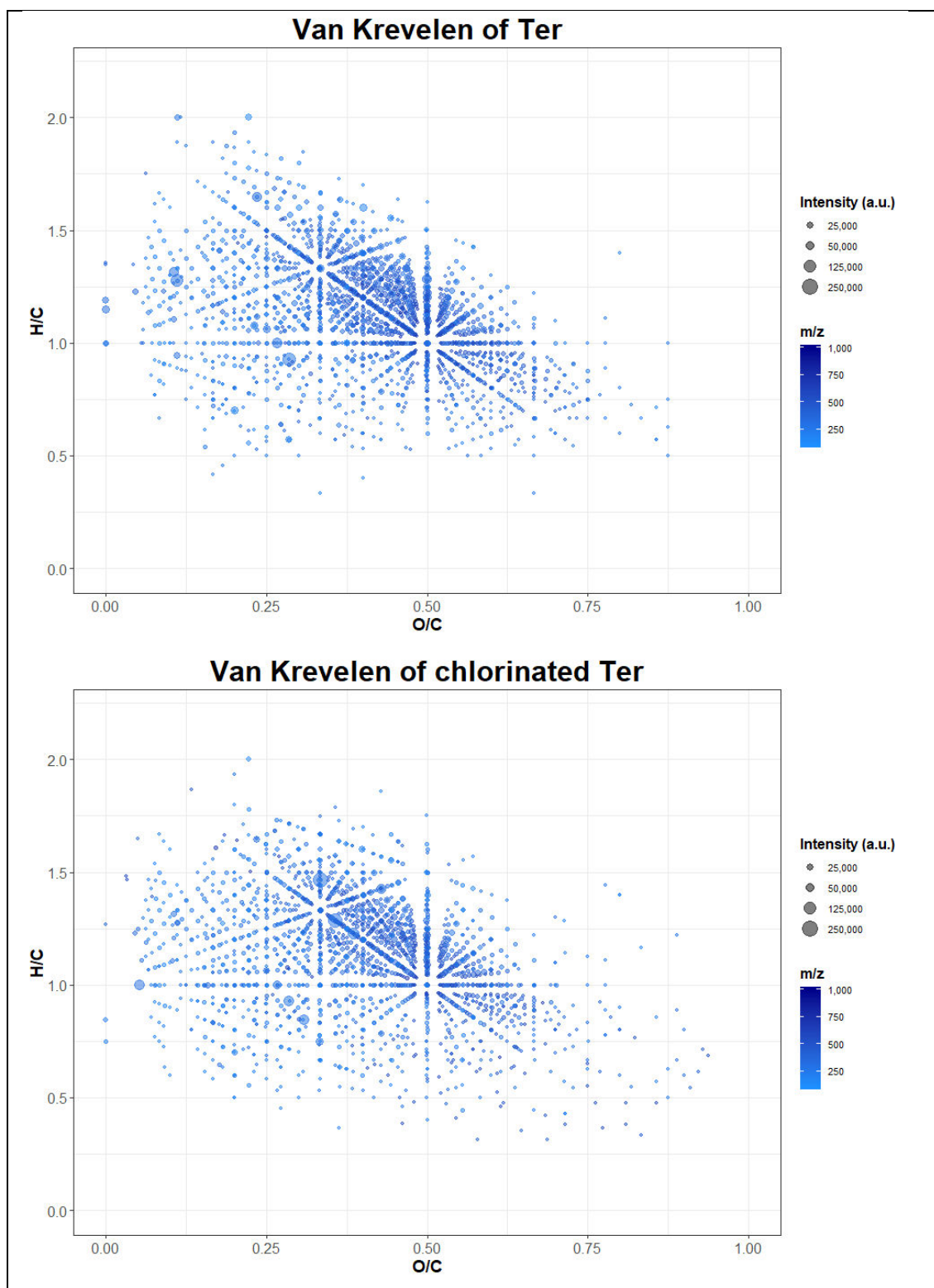


Figure S4b. VK diagrams of the analysed samples.

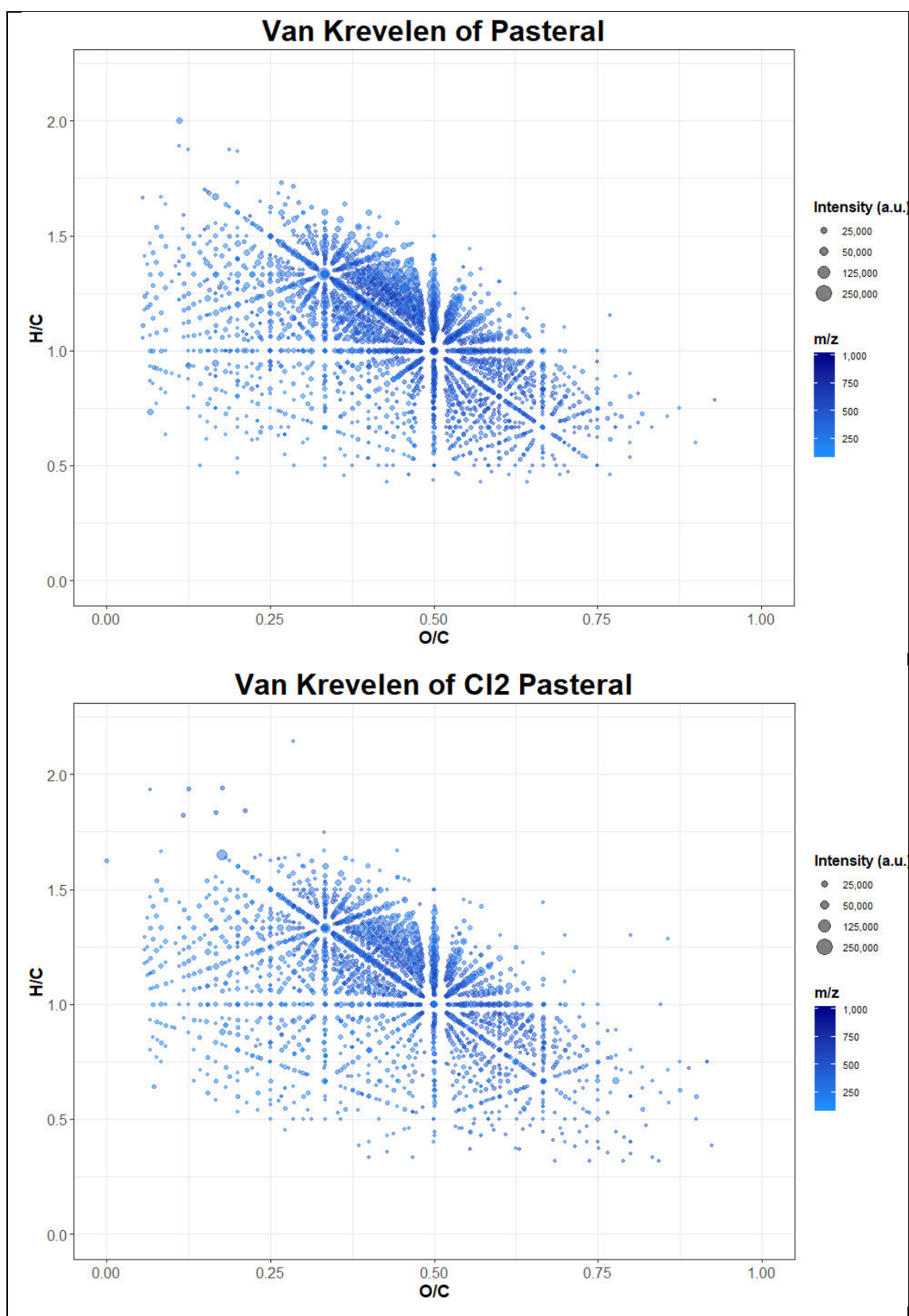


Figure S4c. VK diagrams of the analysed samples.

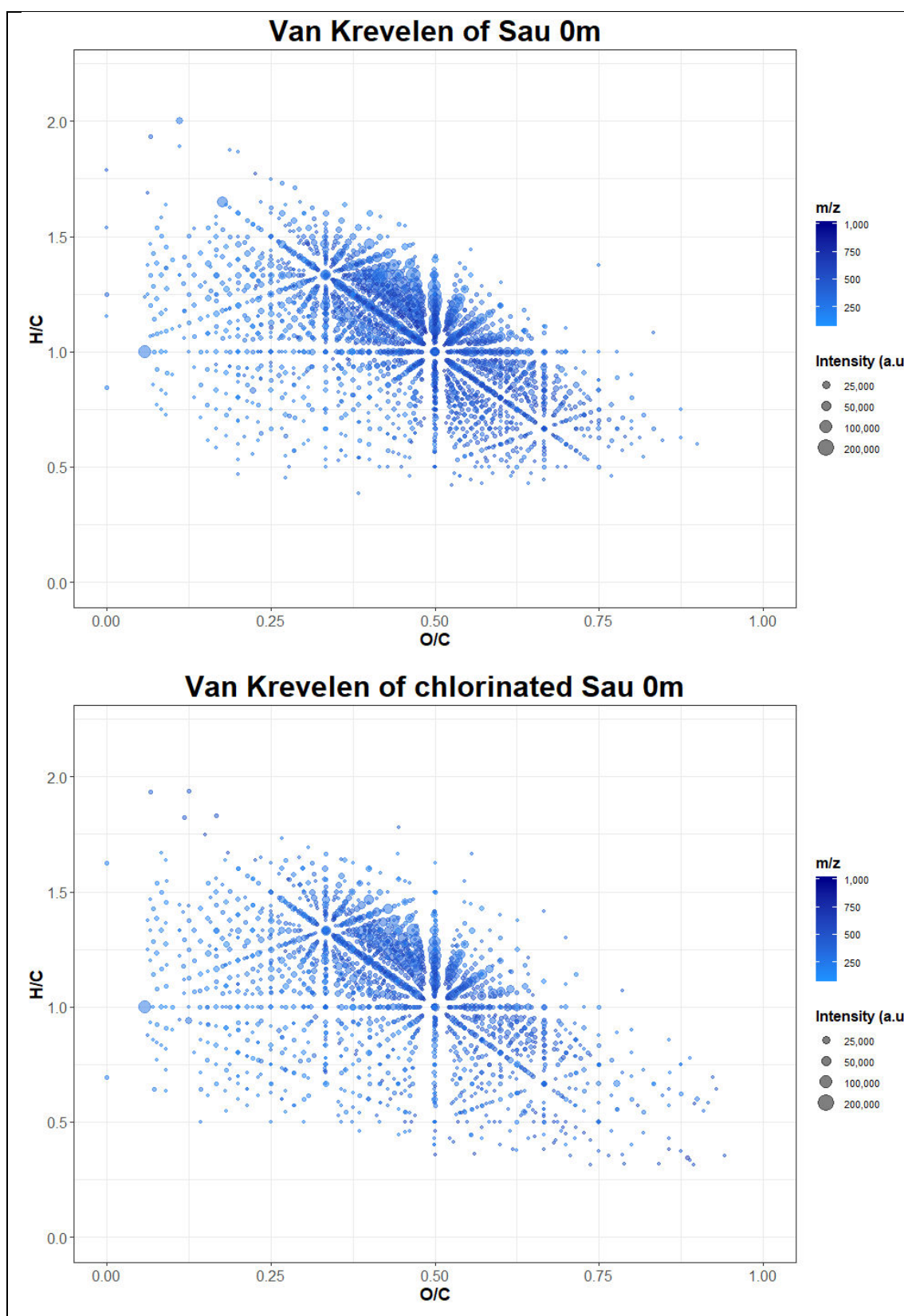


Figure S4d. VK diagrams of the analysed samples.

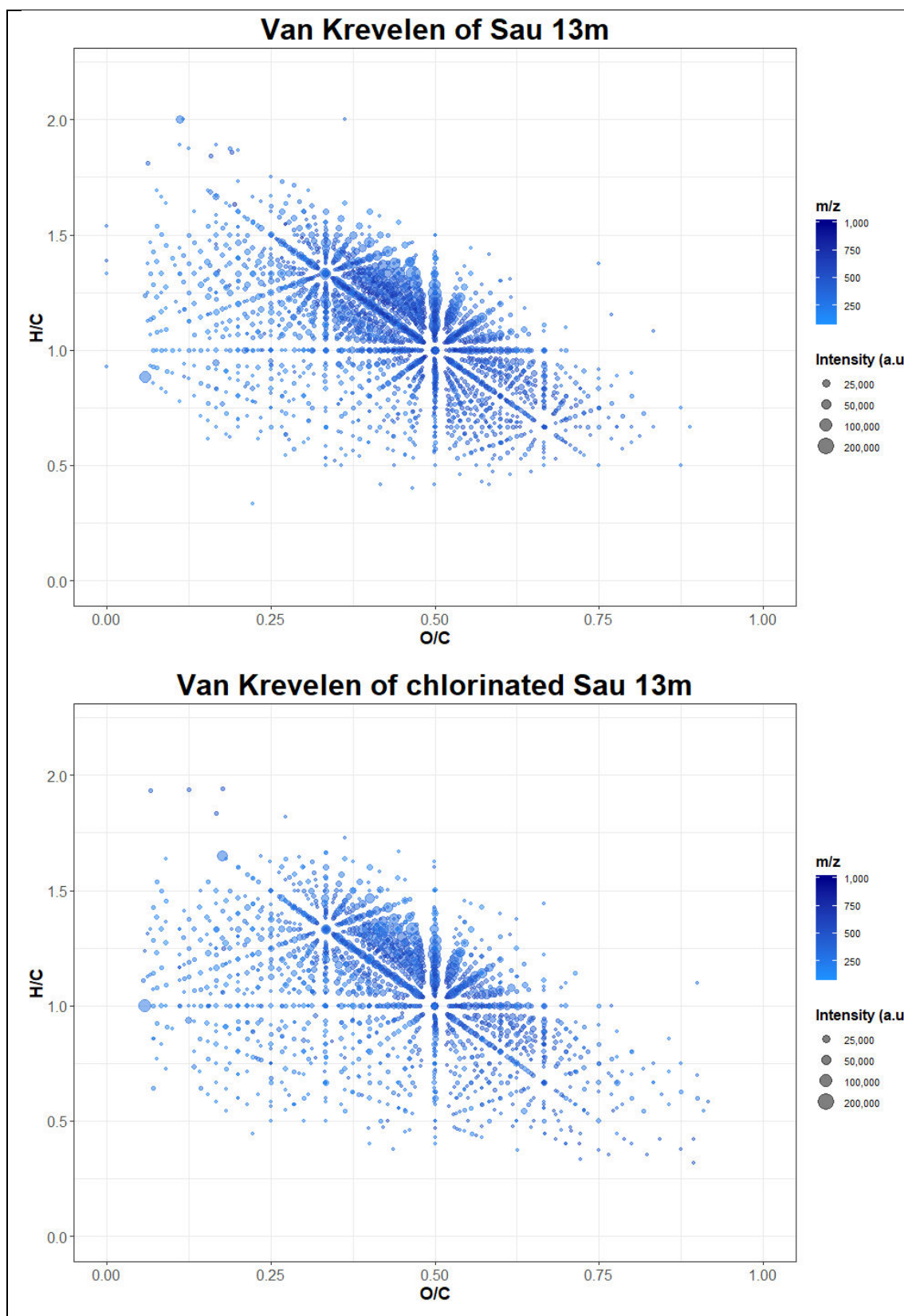


Figure S4e. VK diagrams of the analysed samples.

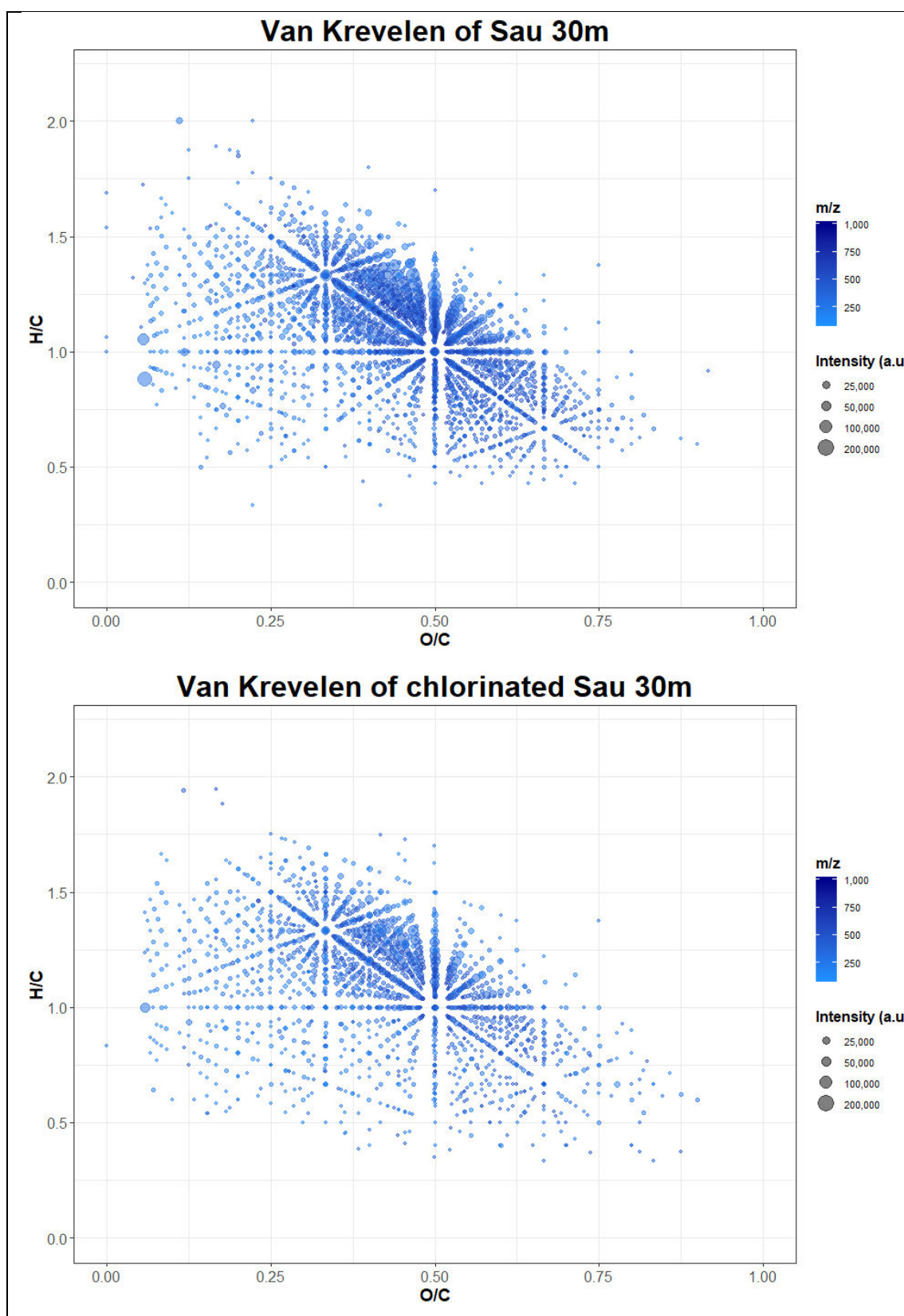


Figure S4f. VK diagrams of the analysed samples.

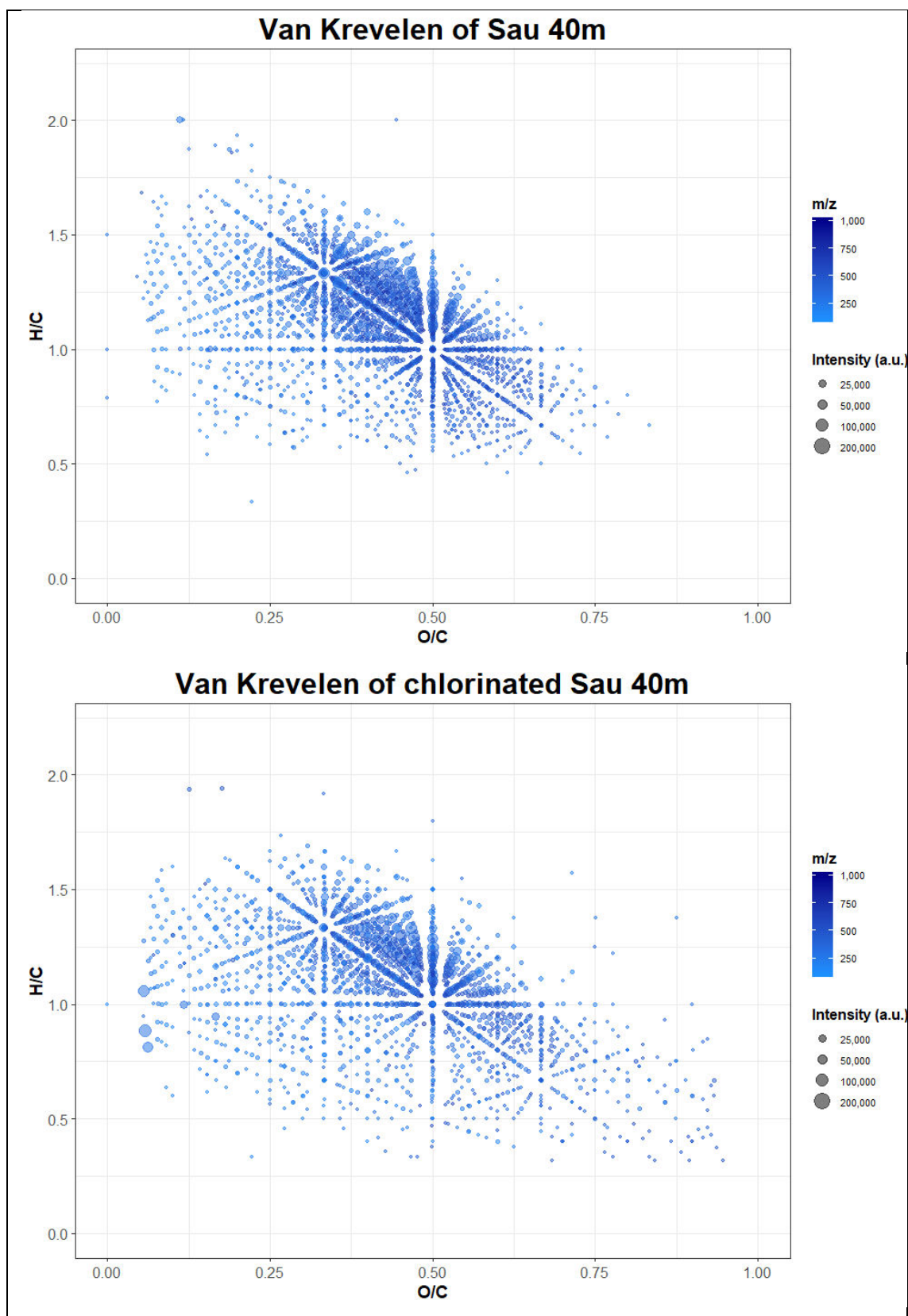


Figure S4g. VK diagrams of the analysed samples.

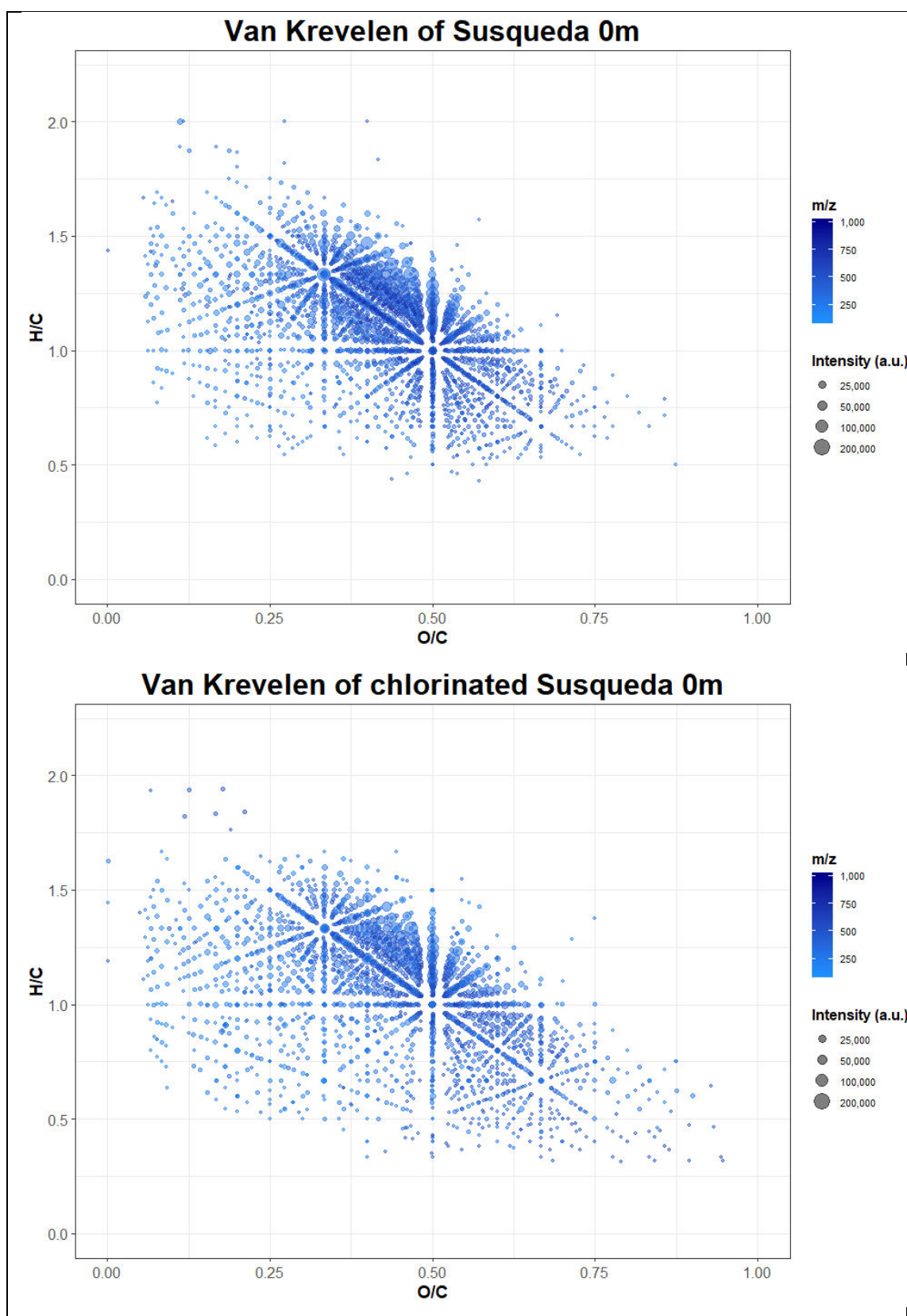


Figure S4h. VK diagrams of the analysed samples.

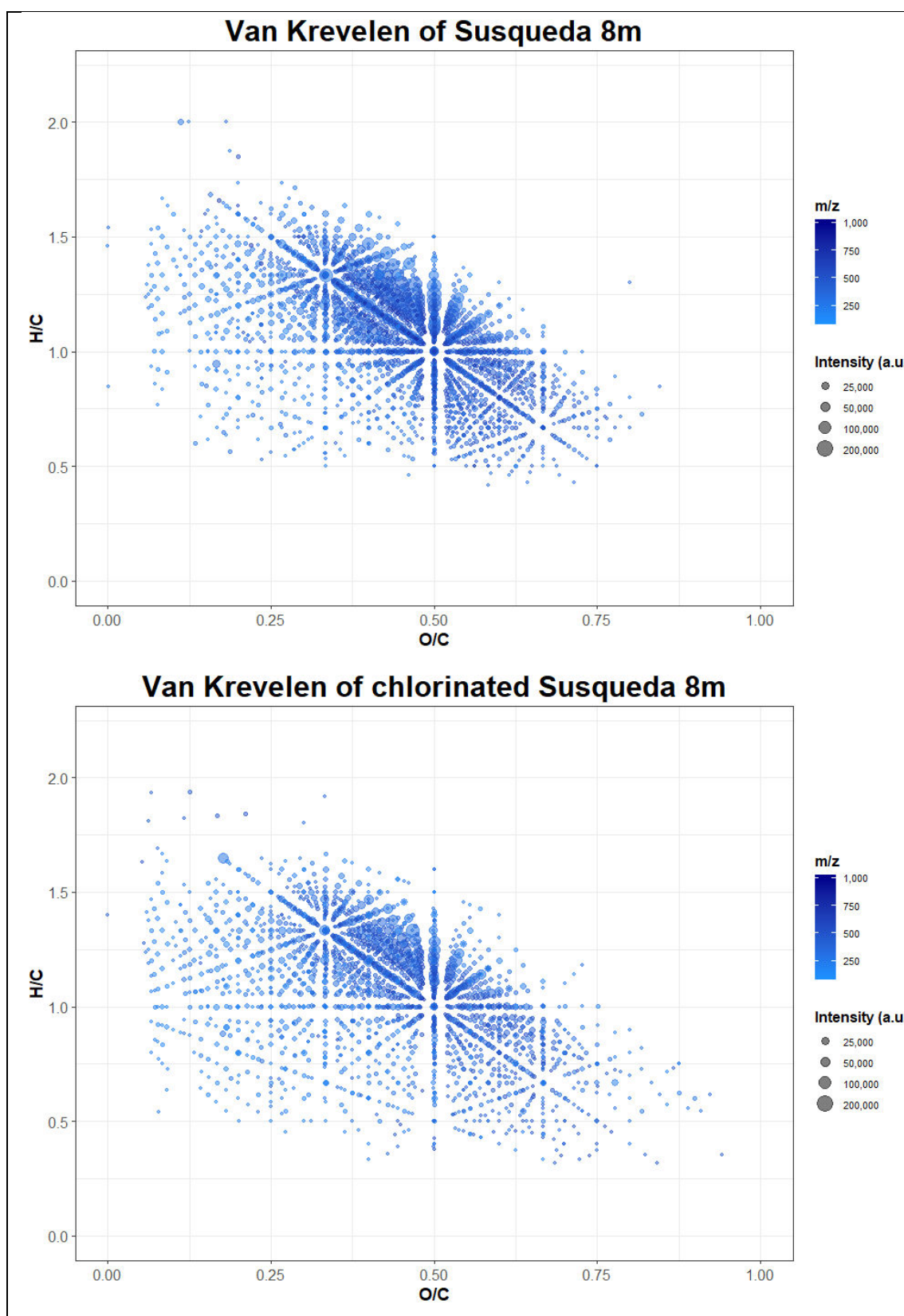


Figure S4i. VK diagrams of the analysed samples.

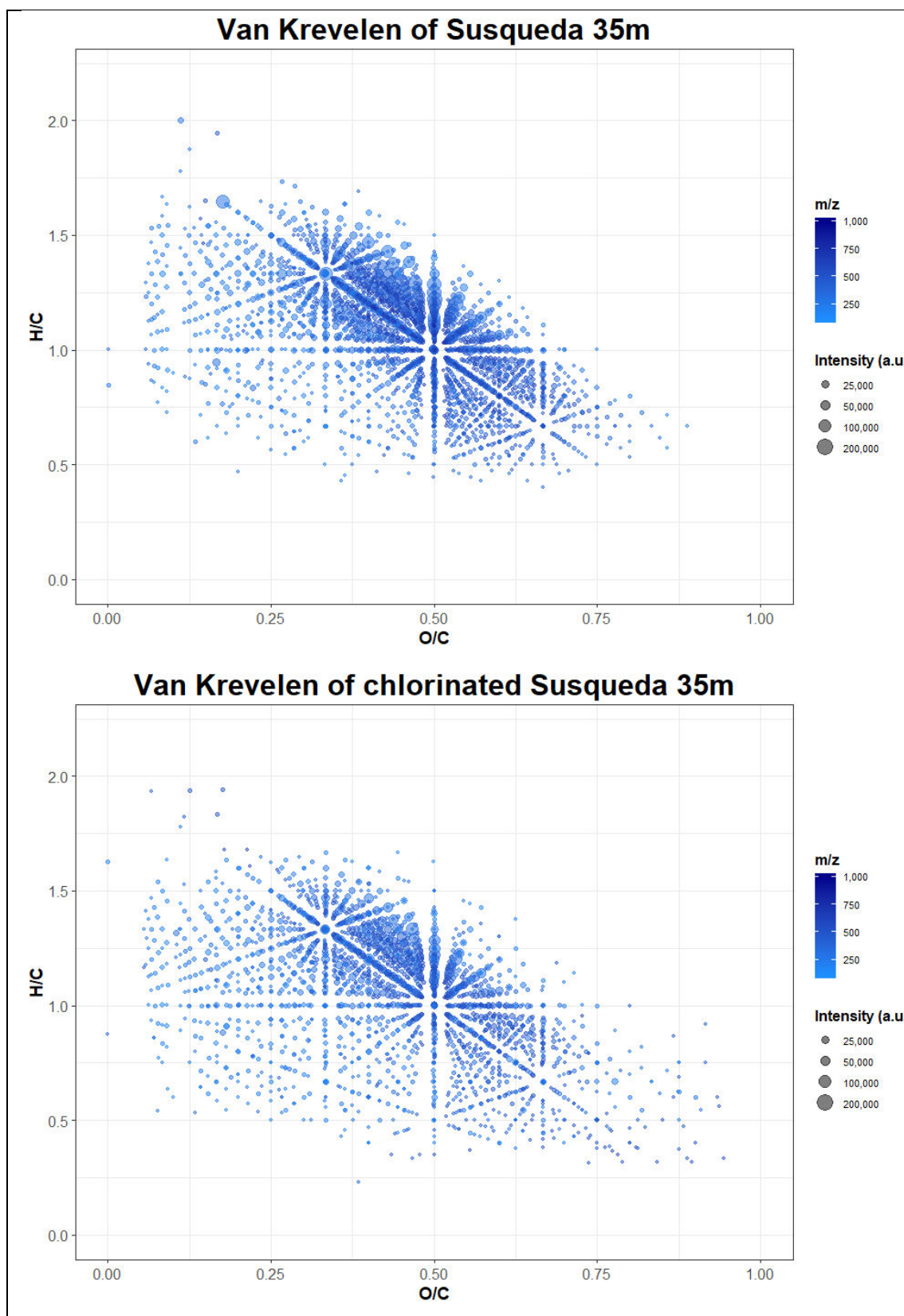


Figure S4j. VK diagrams of the analysed samples.

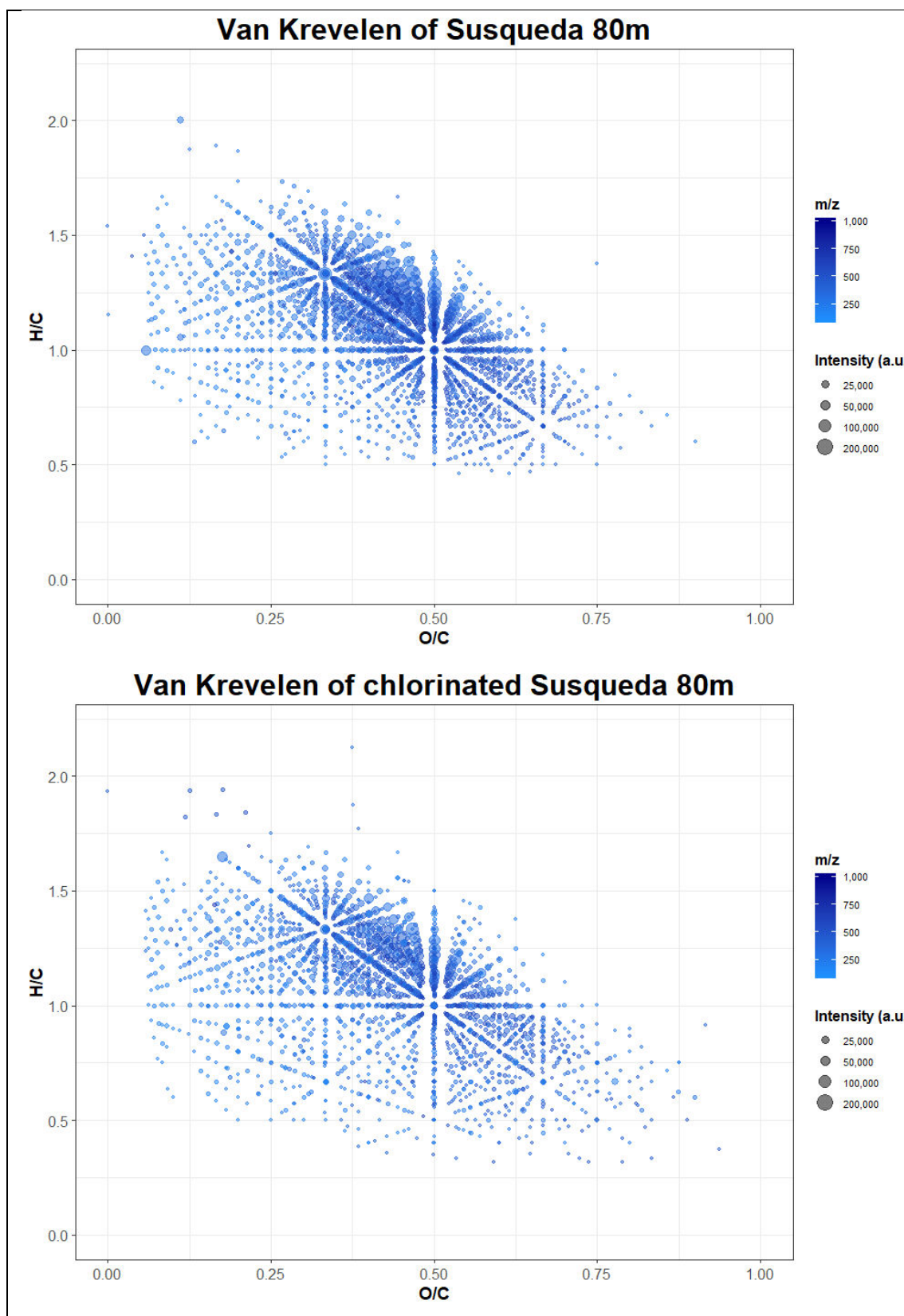


Figure S5a. Chlorinated features in VK diagrams. Red and blue dots indicate signals with one and two halogenated atoms, respectively.

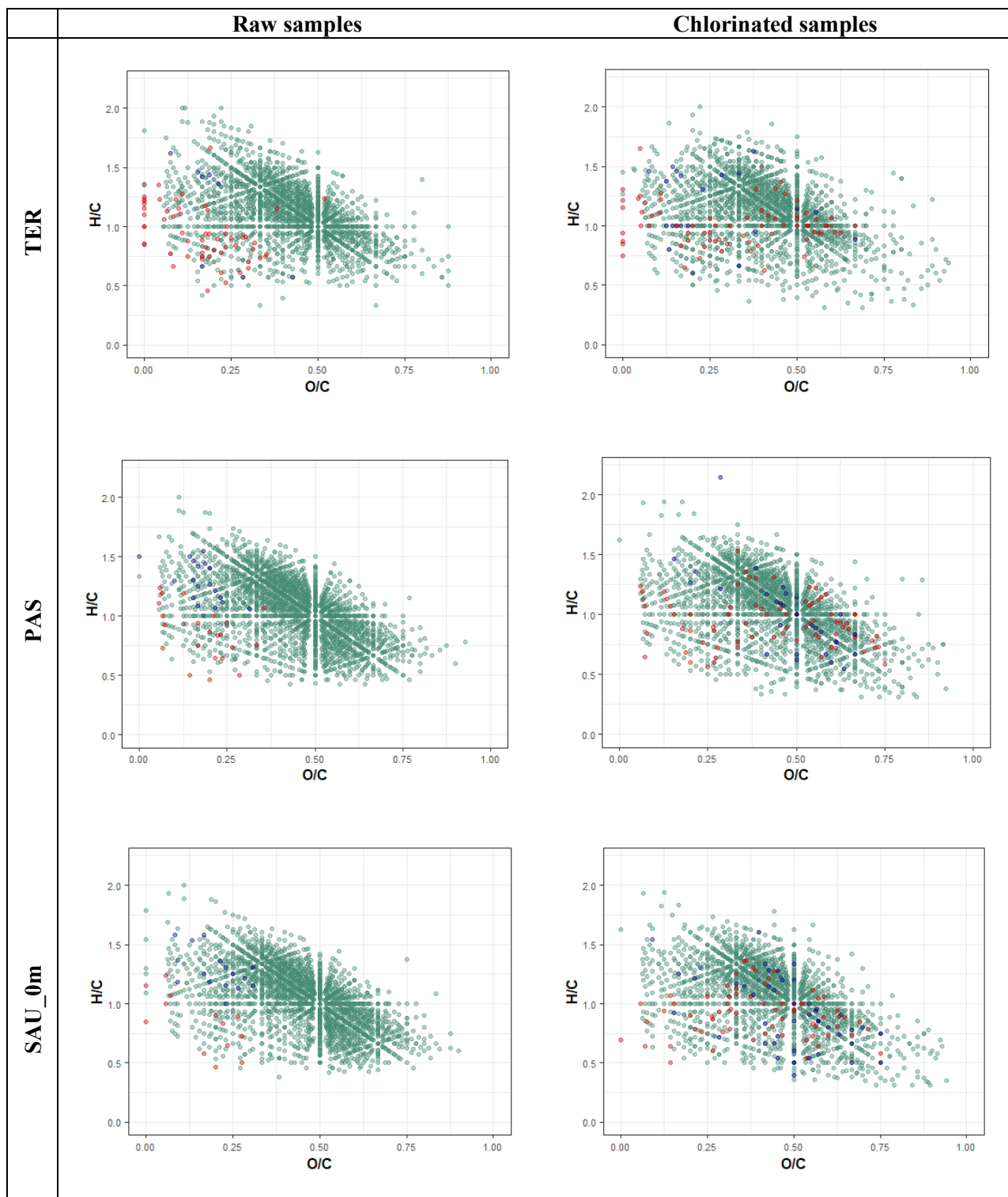


Figure S5b. Chlorinated features in VK diagrams. Red and blue dots indicate signals with one and two halogenated atoms, respectively.

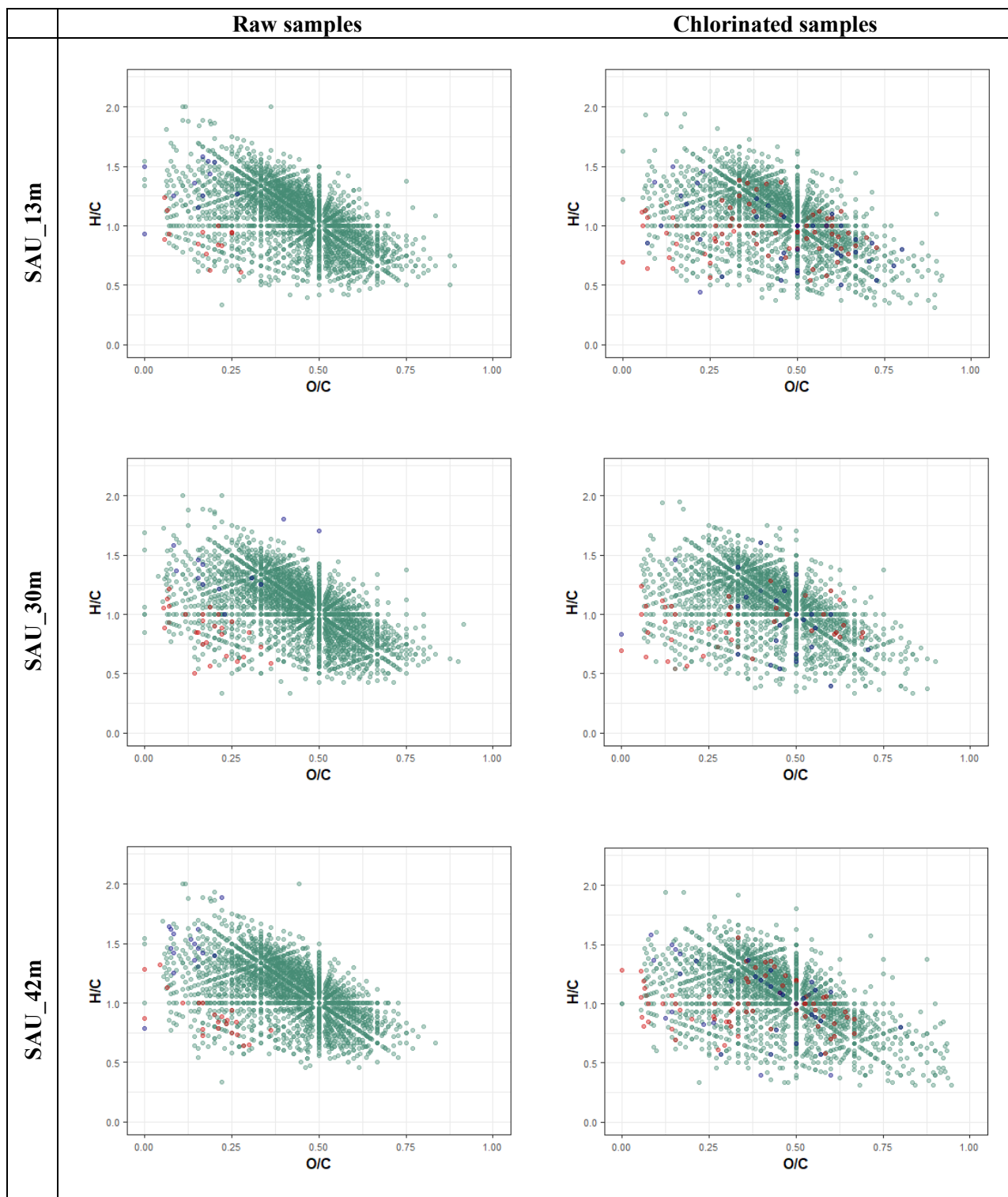


Figure S5c. Chlorinated features in VK diagrams. Red and blue dots indicate signals with one and two halogenated atoms, respectively.

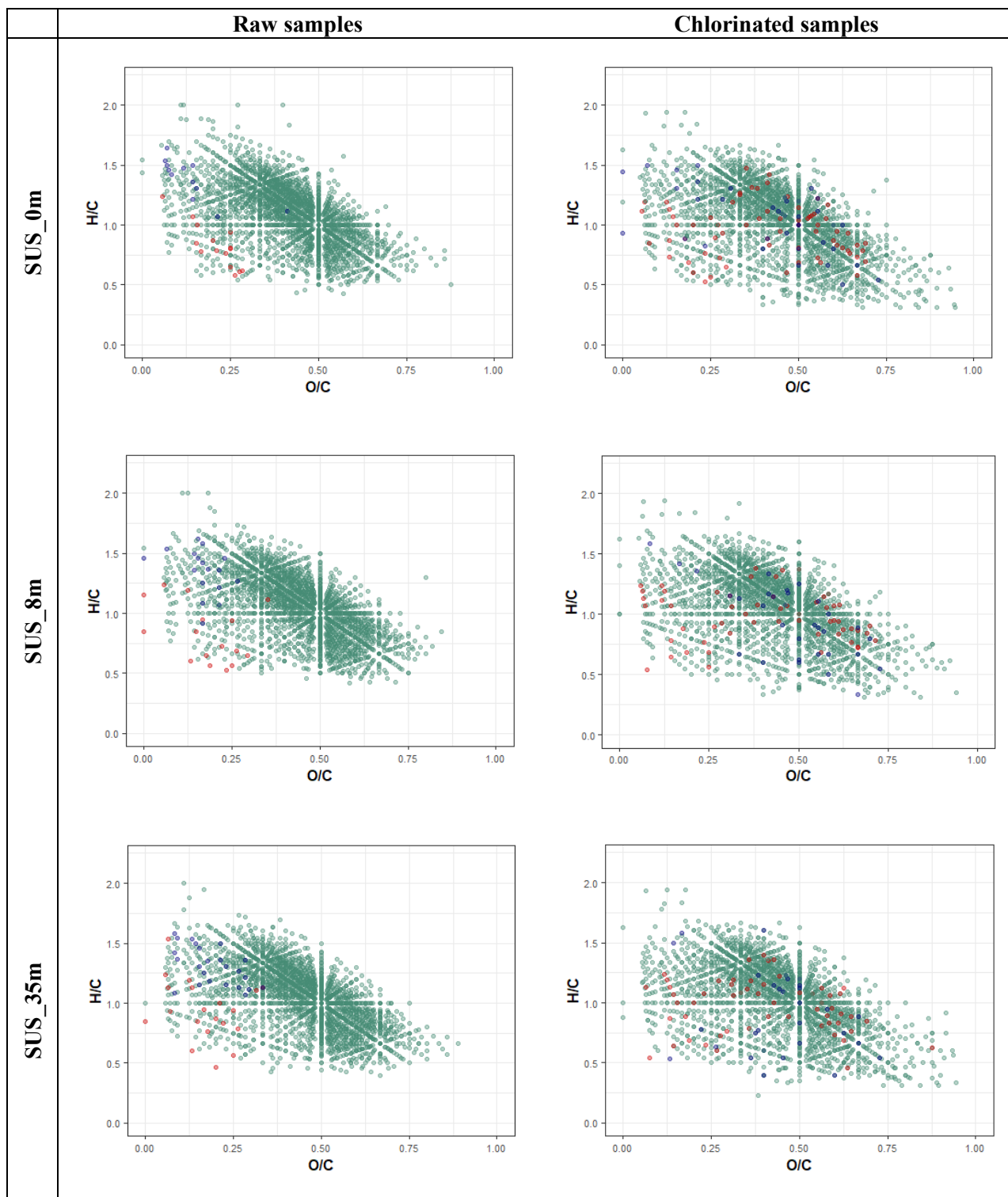


Figure S5d. Chlorinated features in VK diagrams. Red and blue dots indicate signals with one and two halogenated atoms, respectively.

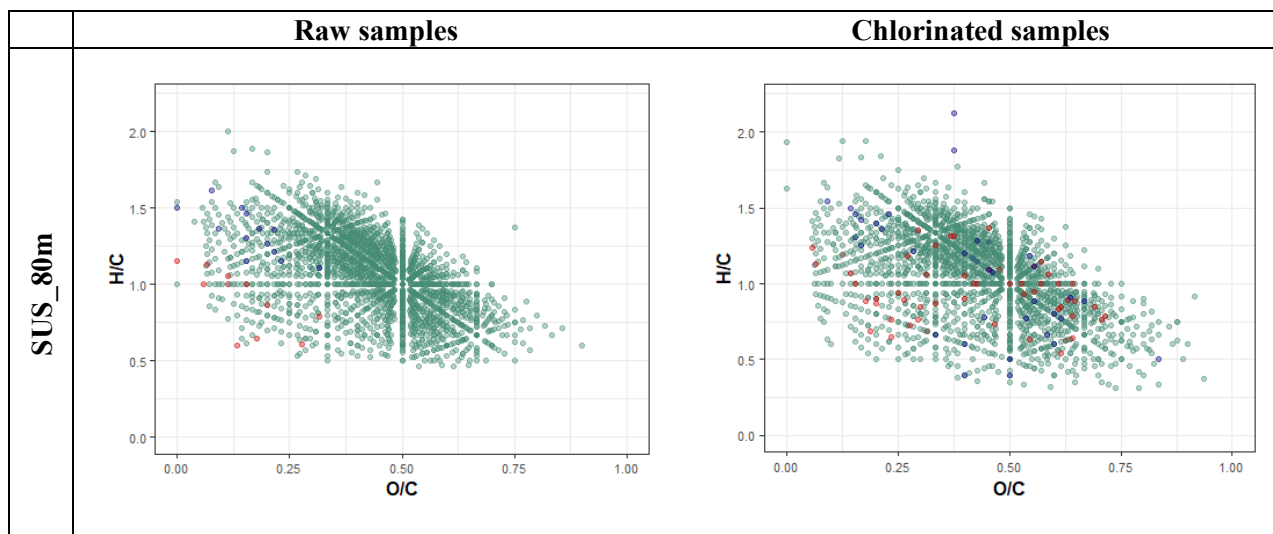


Figure S6a. Brominated features in VK diagrams. Red and blue dots indicate signals with one and two halogenated atoms, respectively.

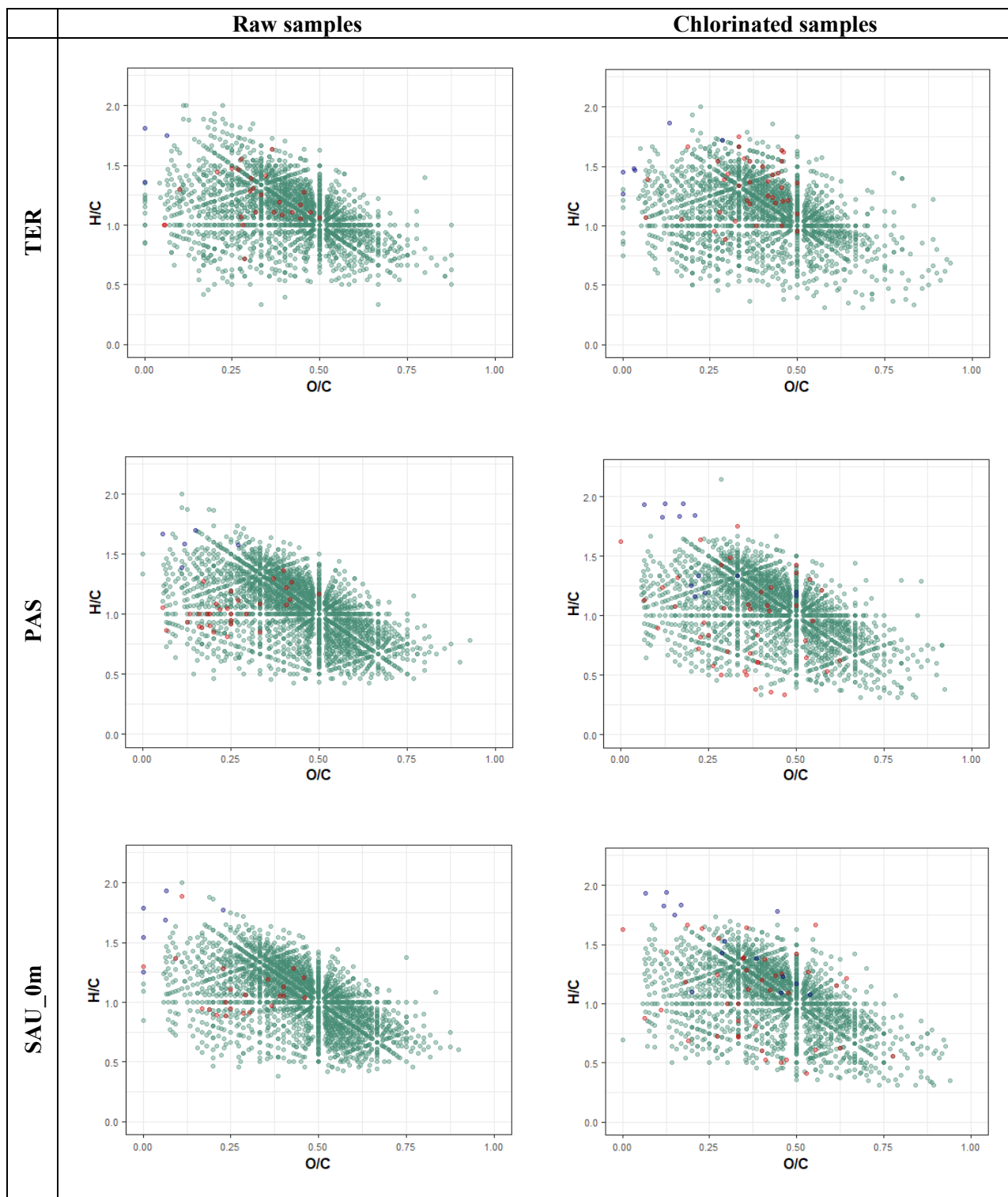


Figure S6b. Brominated features in VK diagrams. Red and blue dots indicate signals with one and two halogenated atoms, respectively.

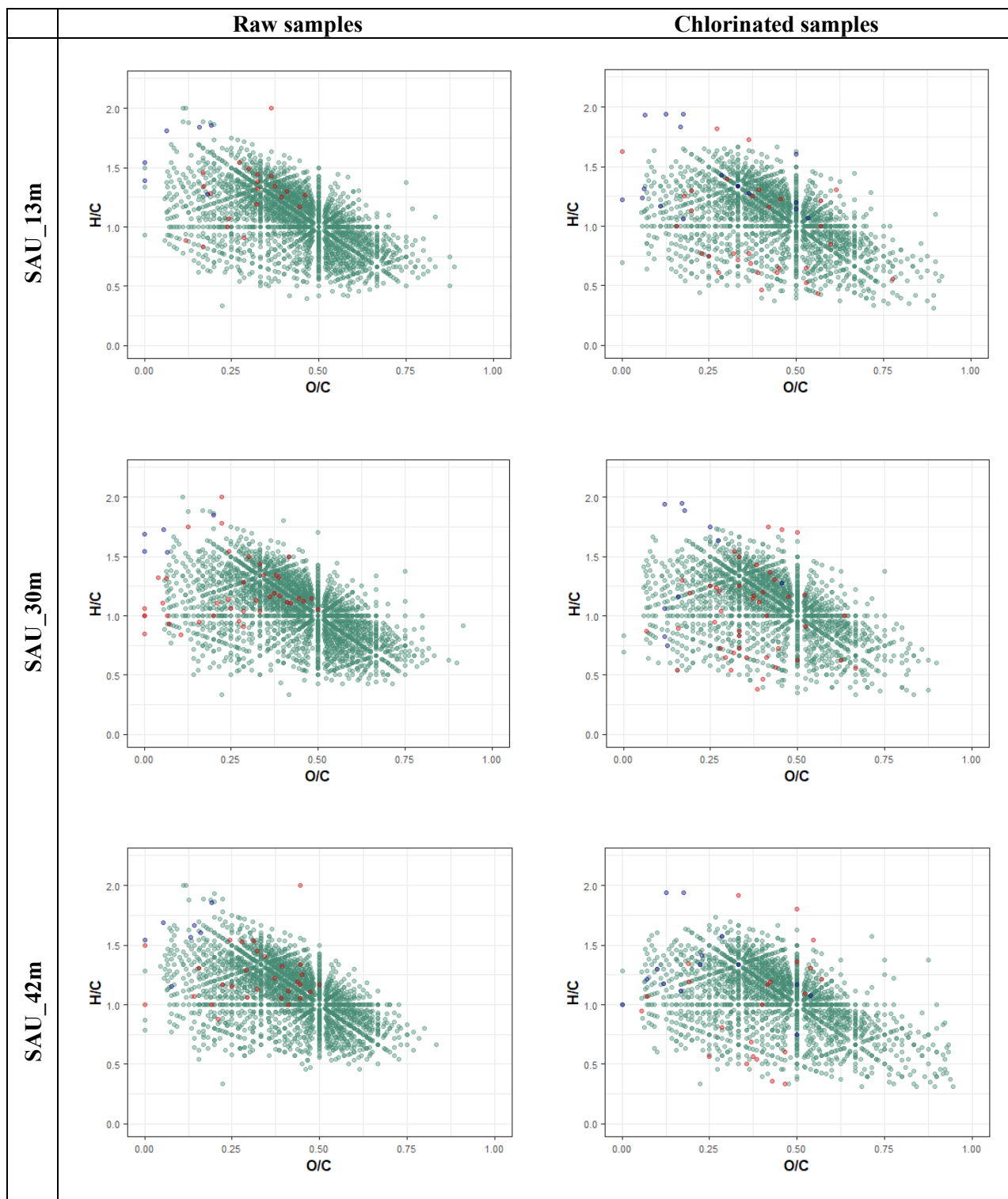


Figure S6c. Brominated features in VK diagrams. Red and blue dots indicate signals with one and two halogenated atoms, respectively.

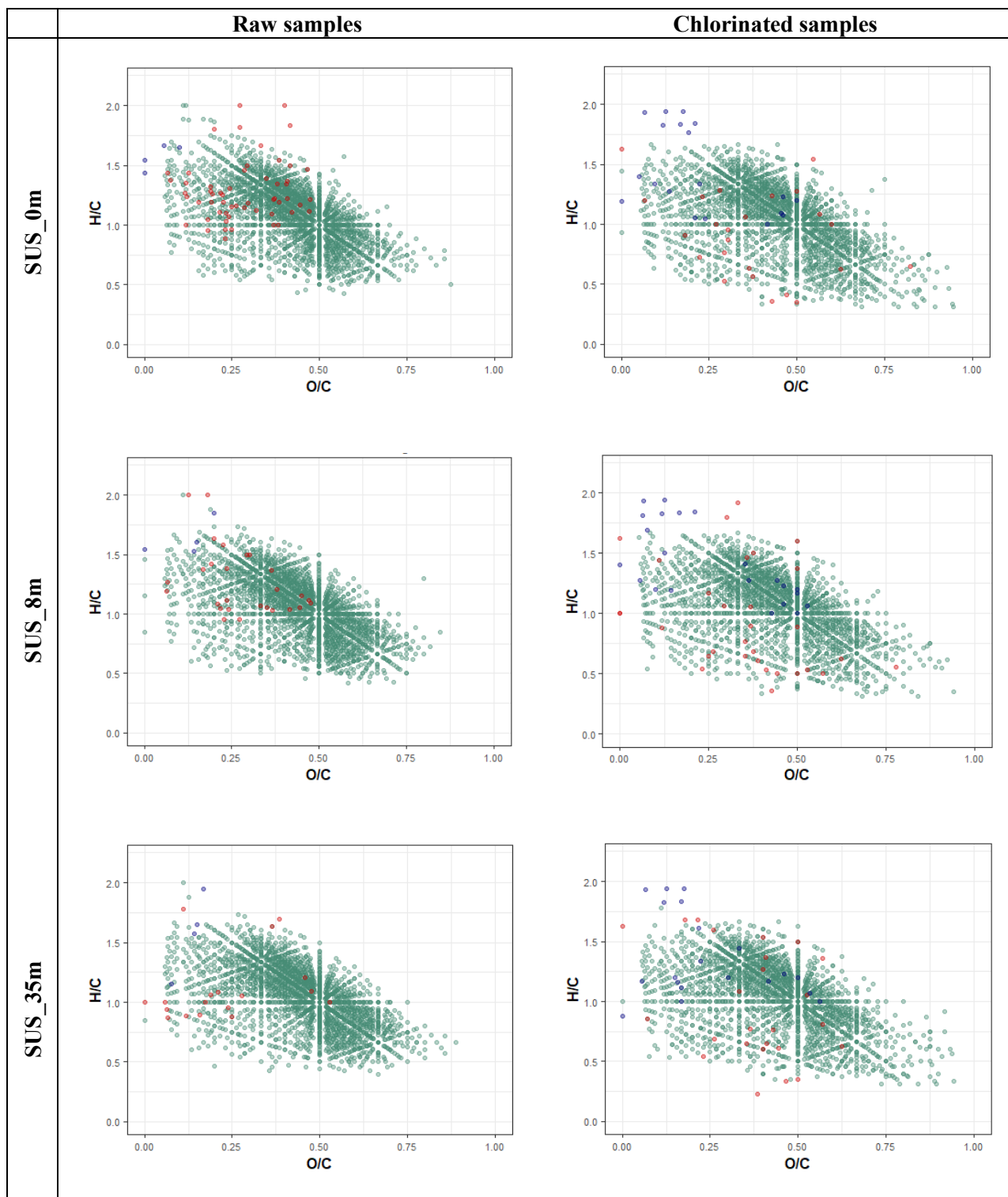


Figure S6d. Brominated features in VK diagrams. Red and blue dots indicate signals with one and two halogenated atoms, respectively.

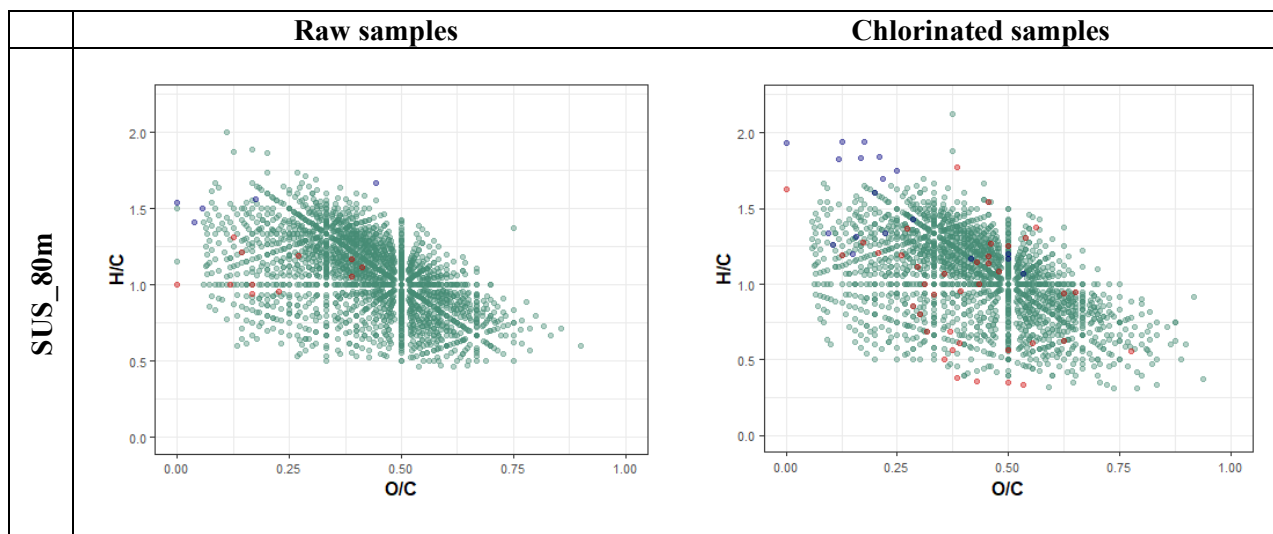


Figure S7. Contribution of the first seven PC to the overall variance of the PCA model

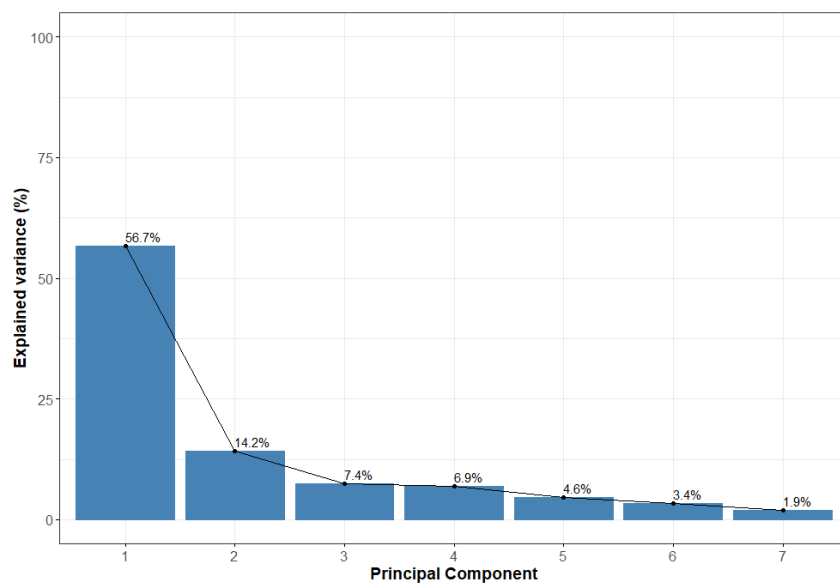


Figure S8. Correlation matrix of lignin-like substances that were related ($\cos^2\alpha \geq 0.95$) to PC1.

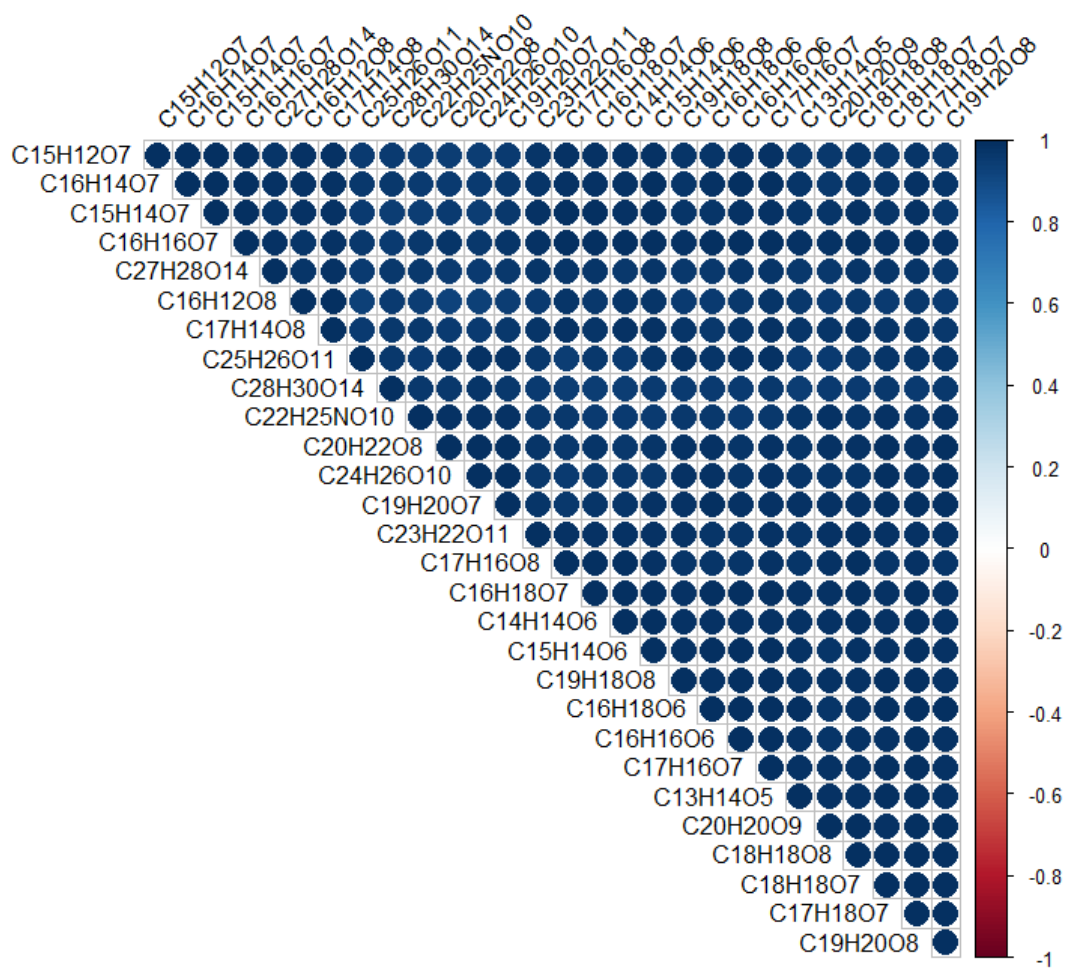


Figure S9. Ternary VK diagrams showing the correlation of detected features with THMs FP. The first diagram displays the whole set of features and the diagram below displays only those features that strongly correlated ($\rho \geq 0.795$) with THMs FP (below).

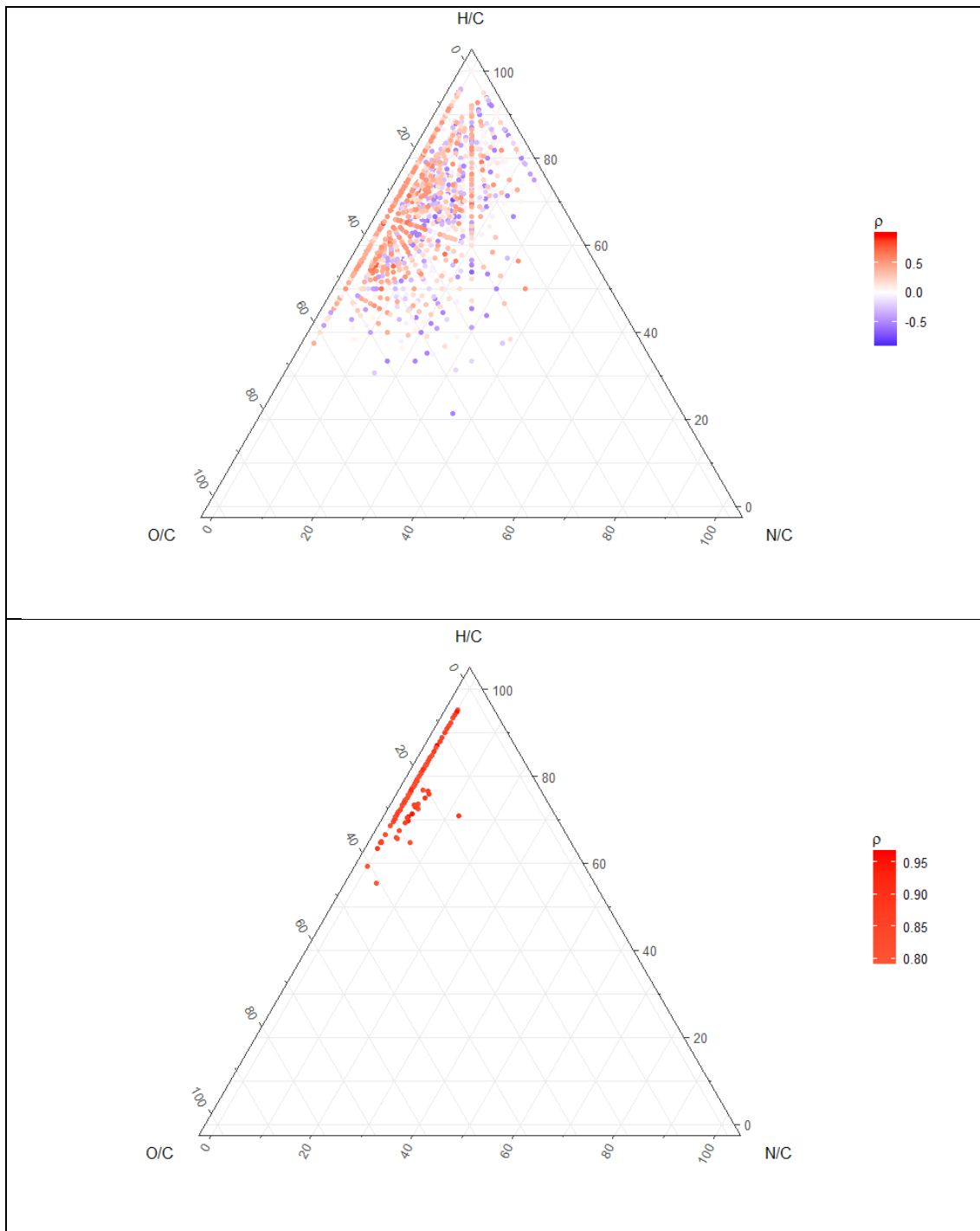


Figure S10. Ternary VK diagrams showing the correlation of detected features with HANs FP. The first diagram displays the whole set of features and the diagram below displays only those features that strongly correlated ($\rho \geq 0.795$) with HANs FP (below).

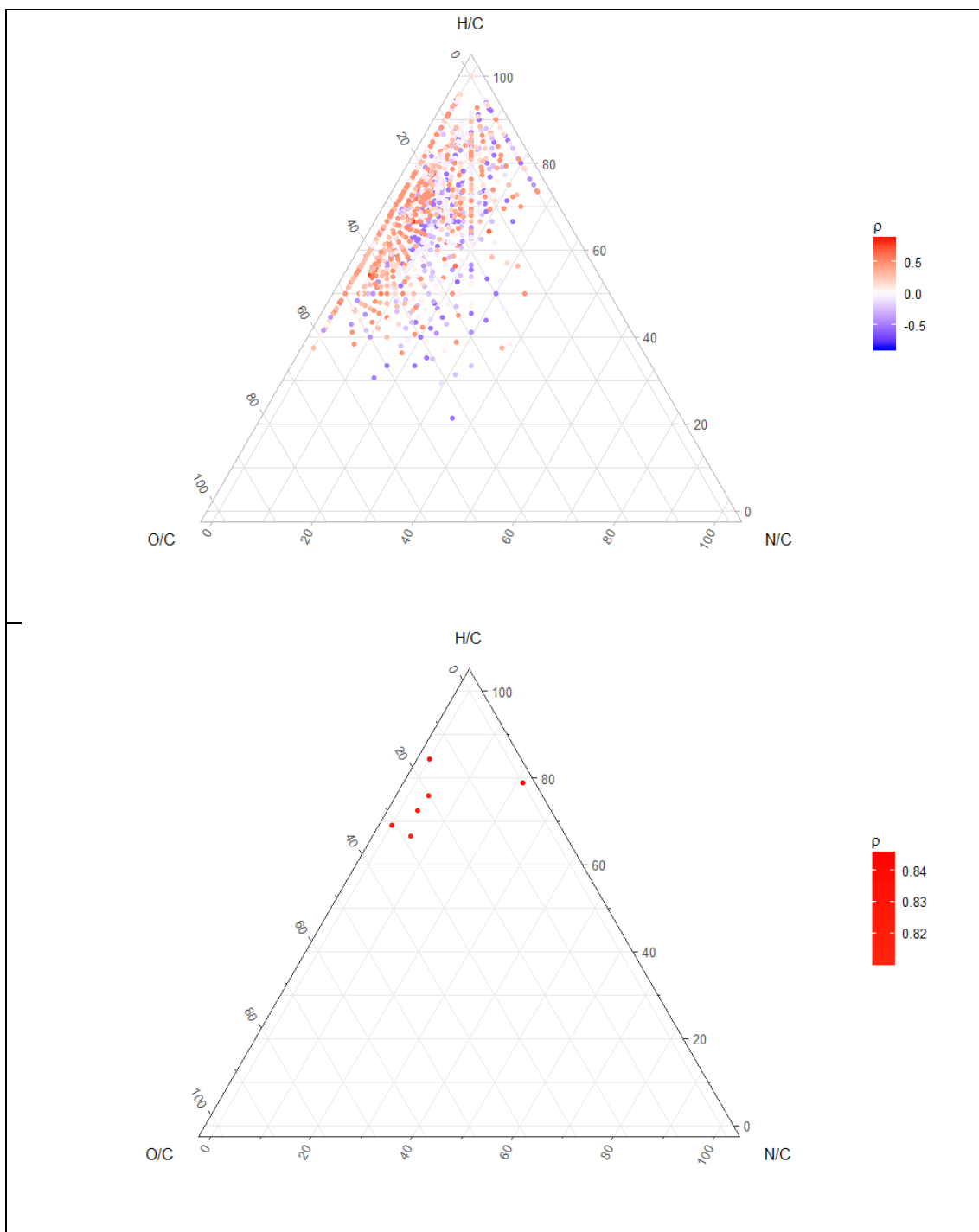


Table S1. Criteria for the classification of empirical formulae according to their location in the VK diagrams, adapted from Minor et al. (2014).

Class of features	H/C range	O/C range
Lipids-like features	$1.50 \leq \text{H/C} \leq 2.30$	$0.2 \leq \text{O/C}$
Peptides-like features	$1.50 \leq \text{H/C} \leq 2.25$	$0.2 < \text{O/C} \leq 0.5$
Aminosugars-like features	$1.50 \leq \text{H/C} \leq 2.25$	$0.5 < \text{O/C} \leq 0.7$
Carbohydrate-like features	$1.50 \leq \text{H/C} \leq 2.40$	$0.7 < \text{O/C}$
Soot-like features	$0.00 \leq \text{H/C} \leq 0.50$	$0.25 < \text{O/C}$
Condensed hydrocarbon-like features	$0.50 \leq \text{H/C} \leq 1.20$	$0.25 < \text{O/C}$
Lignin-like features	$0.66 \leq \text{H/C} \leq 1.50$	$0.25 \leq \text{O/C} \leq 0.66$
Tannin-like features	$0.66 \leq \text{H/C} \leq 1.33$	$0.66 < \text{O/C} \leq 0.95$

Table S2. KMD of selected groups of atoms. As can be seen, the KMD substantially decreases as protons are being progressively substituted by halogen atoms. Also, the hydroxylation of methylene groups and their further oxidation to carbonyls decreases the KMD of the molecule.

	-CH₂-CH₂-	-CH=CH-	-CH₂-CH³⁵Cl-
m/z	28.0313	26.0157	61.9923
KM	28.0000	25.9867	61.9231
 KM 	28	26	62
KMD	0.0000	-0.0133	-0.0769
	-CH³⁵Cl-CH³⁵Cl-	-CH₂-CH⁷⁹Br-	-CH⁷⁹Br-CH⁷⁹Br-
m/z	95.9534	105.9418	183.8523
KM	95.8462	105.8235	183.6470
 KM 	96	106	184
KMD	-0.1538	-0.1765	-0.3530
	-H	-³⁵Cl	-⁷⁹Br
m/z	1.0078	34.9689	78.9183
KM	1.0067	34.9298	78.8302
 KM 	1	35	79
KMD	0.0067	-0.0702	-0.1698
	-CH₂-	-CHOH-	-CO-
m/z	14.0157	30.0101	27.9949
KM	14.0000	29.9771	27.9637
 KM 	14	30	28
KMD	0.0000	-0.0229	-0.0363

Table S3. List of features that correlated with PC1 with a $\cos^2(\alpha) > 0.95$.

Formula	$\cos^2(\alpha)$	H/C	O/C	N/C	DBE/C	A.I.
C₁₇H₁₆O₇	0.983	0.94	0.41	0.00	0.59	0.30
C₁₇H₁₄O₈	0.978	0.82	0.47	0.00	0.65	0.33
C₁₉H₂₀O₇	0.973	1.05	0.37	0.00	0.53	0.25
C₁₈H₁₈O₇	0.972	1.00	0.39	0.00	0.56	0.27
C₁₆H₁₆O₇	0.970	1.00	0.44	0.00	0.56	0.22
C₁₉H₁₈O₈	0.969	0.95	0.42	0.00	0.58	0.27
C₁₉H₂₀O₈	0.967	1.05	0.42	0.00	0.53	0.18
C₁₇H₁₈O₇	0.966	1.06	0.41	0.00	0.53	0.20
C₁₅H₁₄O₆	0.966	0.93	0.40	0.00	0.60	0.33
C₂₈H₃₀O₁₄	0.965	1.07	0.50	0.00	0.50	0.00
C₁₈H₁₈O₈	0.965	1.00	0.44	0.00	0.56	0.20
C₁₆H₁₄O₇	0.964	0.88	0.44	0.00	0.63	0.33
C₁₆H₁₆O₆	0.963	1.00	0.38	0.00	0.56	0.30
C₂₄H₂₆O₁₀	0.963	1.08	0.42	0.00	0.50	0.14
C₁₆H₁₈O₆	0.961	1.13	0.38	0.00	0.50	0.20
C₁₅H₁₂O₇	0.960	0.80	0.47	0.00	0.67	0.38
C₁₆H₁₂O₈	0.960	0.75	0.50	0.00	0.69	0.38
C₂₂H₂₅NO₁₀	0.959	1.14	0.45	0.05	0.50	0.05
C₁₇H₁₆O₈	0.958	0.94	0.47	0.00	0.59	0.22
C₂₇H₂₈O₁₄	0.958	1.04	0.52	0.00	0.52	0.00
C₁₃H₁₄O₅	0.956	1.08	0.38	0.00	0.54	0.25
C₂₅H₂₆O₁₁	0.956	1.04	0.44	0.00	0.52	0.14
C₂₃H₂₂O₁₁	0.955	0.96	0.48	0.00	0.57	0.17
C₁₆H₁₈O₇	0.955	1.13	0.44	0.00	0.50	0.11
C₂₀H₂₀O₉	0.954	1.00	0.45	0.00	0.55	0.18
C₁₄H₁₄O₆	0.954	1.00	0.43	0.00	0.57	0.25
C₂₀H₂₂O₈	0.952	1.10	0.40	0.00	0.50	0.17
C₁₅H₁₄O₇	0.951	0.93	0.47	0.00	0.60	0.25
Range	0.951–0.983	0.75–1.14	0.37–0.52	0.00–0.05	0.50–0.69	0.00–0.38
Mean ± st.dev.	0.962 ± 0.008	0.997 ± 0.097	0.44 ± 0.04	0.00 ± 0.01	0.56 ± 0.05	0.21 ± 0.10

Table S4. Retention time (t_R) and selected ions monitored for the quantification of DBPs.

DBP	t_R (min)	SIM 1 (m/z)	SIM 2 (m/z)
Trichloromethane (TCM)	3.59	83	85
Trichloroacetonitrile (TCAN)	4.12	108	110
Bromodichloromethane (BDCM)	5.50	83	129
Dichloroacetonitrile (DCAN)	6.61	74	82
Dibromochloromethane (DBCM)	6.66	129	127
<i>Internal standard</i>	<i>7.06</i>	<i>127</i>	<i>129</i>
Tribromomethane (TBM)	7.77	173	171
Bromochloroacetonitrile (BCAN)	7.80	74	155
Dibromoacetonitrile (DBAN)	9.19	118	120

Annex 3

6.3 Drivers of variability in disinfection by-product formation potential in a chain of thermally stratified drinking water reservoirs.

1 Drivers of variability in disinfection by-
2 product formation potential in a chain of
3 thermally stratified drinking water
4 reservoirs

5
6
7 Elias Munthali^{a,b,c,d*}, Rafael Marcé^{a,b}, Maria José Farré^{a,b*}

8
9 ^aCatalan Institute for Water Research (ICRA), Emili Grahit 101, 17003 Girona, Spain

10 ^bUniversity of Girona, Girona, Spain

11 ^cNetherlands Institute of Ecology (NIOO-KNAW), Droevendaalsesteeg 10, 6708 PB
12 Wageningen NL.

13 ^dNorthern Region Water Board (NRWB), Bloemwater Street, P/Bag 94, Mzuzu, Malawi.

14
15 *Corresponding authors

16 Mr. Elias Munthali,

17 Northern Region Water Board,

18 Bloemwater Street,

19 P/Bag 94,

20 Mzuzu-Malawi.

21 Email address: elias.munthali@gmail.com

22
23 Dr. Maria José Farré

24 Carrer Emili Grahit, 101

25 Edifici H2O, Parc Científic i Tecnològic de la Universitat de Girona

26 E- 17003 Girona (Spain)

27 Email: mjfarre@icra.cat

28 **Text S1: Disinfection by-products (DBP) formation potential (FP) analytical**
29 **procedure**

30 **Reagents**

31 NDMA standard for GC-MS analysis (5000 µg/mL in methanol, Supelco) had a purity of > 99.9%.
32 Deuterated d6-NDMA (> 98% Cambridge Isotope Laboratories, Inc) and d14-NDPA (N-
33 nitrosodipropylamine, > 99% Restek) were used as surrogate and internal standard, respectively.
34 NH₄Cl (> 99.5%, Sigma-Aldrich), NaOH (ACS, ISO, Scharlau) and NaClO (reagent grade,
35 available chlorine ≥ 4%, Sigma-Aldrich) were used for the NDMA FP test. KH₂PO₄ (> 99%,
36 Sigma-Aldrich) and Na₂HPO₄ (> 99%, Sigma-Aldrich) were used to prepare pH buffer solutions.
37 Na₂SO₃ (> 98%, Sigma-Aldrich) was employed to quench residual disinfectant in the NDMA FP
38 tests. THMs were purchased as a 1.0 mg/mL mix in methanol (TraceCERT® grade) from Sigma
39 Aldrich. Deuterated 1,2-dibromopropane-d6 (99.6 atom % D) was purchased from CDN
40 isotopes and used as internal standard during DBP FP analyses. Methyl tert-butyl ether (MtBE,
41 Chromasolv™ Plus) and Na₂SO₄ (≥ 99.0 %, ACS grade) were obtained from Sigma Aldrich. The
42 remaining volatile DBPs were purchased from Cluzeau lab as a mix of 5.0 mg/mL in acetone (>
43 95 % purity).

44 Commercial DPD test kits (LCK310, Hach Lange) were used for the analysis of free and total
45 chlorine using a Hach DR2800 spectrophotometer. Ultrapure water and methanol (Optima®
46 LC/MS grade) were purchased from Fisher Chemical. Nitrogen (99.995% purity) for extract
47 drying was purchased from Abelló-Linde. Glass fibre filters (GF/F, 47 mm diameter, 0.7 µm mesh
48 size) were obtained from Whatman. Activated charcoal cartridges (6 mL, 2 g) optimized for
49 NDMA extraction were purchased from Resteck.

50 **Analytical methods**

51 All samples were filtered through 0.7 µm Glass fiber filters (GF/F, 47 mm diameter) prior to
52 performing DBP FP tests. NDMA FP test followed standard procedure previously published by

53 Mitch and co-authors ¹. In summary, phosphate buffered (10 mM) water samples were
54 chloraminated with a 140 ppm monochloramine solution and incubated at 25 °C for 7 days. A 7-
55 10 day incubation period for NDMA analysis is standard practice because monochloramine
56 reacts slowly with NDMA precursor compounds ²⁻⁴. To prepare a monochloramine solution,
57 free chlorine was added to an ammonium chloride solution at a 1.2:1 N:Cl molar ratio previously
58 adjusted to pH 8. Afterwards, the samples were quenched with sodium sulfite and extracted. In
59 extraction, 1-litre of each sample was spiked with 25 ng/L of d₆NDMA surrogate, passed through
60 coconut charcoal and eluted with dichloromethane. The extracted volume was concentrated
61 using a gentle stream of nitrogen gas until 1 ml was left, which was then spiked with a 25 µg/L
62 of d₁₄NDPA internal standard. GC-MS/MS analysis of NDMA was performed by a Trace GC
63 Ultra gas chromatograph equipped with a TriPlus™ autosampler coupled to a TSQ™ Quantum
64 triple quadrupole mass spectrometer system (Thermo Fisher Scientific). Chromatographic
65 separation was performed using a ZB 1701 column from Phenomenex (30 m x 0.25 mm x 0.25
66 µm). The injector temperature was 250 °C and was operated in splitless mode. The oven
67 temperature program was as follows: 40 °C held for 1 min, ramp to 65 °C at 5 °C /min, ramp to
68 110 °C at 10 °C /min held for 1 min and finally ramp to 240 °C at 25 °C /min and held for 1 min.
69 Mass spectrometric ionization was carried out in electron impact (EI) ionization mode (EI voltage
70 of 70 eV and a source temperature of 250 °C as described in Farré and co-authors ⁵ . The
71 method reporting limit was 1 ng/L, and the recoveries were above 70%.

72 On the other hand, volatile DBP FP analyses of trichloromethane, bromodichloromethane
73 (BDCM), 1,1-dichloropropanone (DCP), dibromochloromethane (DBCM), 1,1,1-
74 trichloropropanone, tribromomethane (TBM), trichloroacetonitrile (TCAN),
75 trichloronitromethane (TCNM), dichloroacetonitrile and bromochloroacetonitrile (BCAN)
76 were performed following a standard method as previously applied Liu and co-authors ⁶ . In

77 summary, multiples of each sample were put in 250 ml headspace free glass bottles and
78 chlorinated with 2, 5 and 10 ppm of sodium hypochlorite solution, capped and incubated in the
79 dark at 25 °C for 24 hrs. The 24 hour incubation time is standard practice in the analysis of
80 volatile DBPs because the reaction between hypochlorite and volatile DBPs is faster hence 24
81 hrs is deemed more realistic ^{7,8}. Afterwards, residual chlorine was measured with photometric
82 cuvette test kits (LCK 310, Hach Lange GmbH, Düsseldorf, Germany). For each sample, a glass
83 bottle with residual chlorine in the range of 1-3 ppm was retained and quenched with ascorbic
84 acid. Sample pH was adjusted to 3.5 with 0.2 N sulphuric acid in a 30 ml aliquot and extracted
85 using 3 ml of MtBE containing 200 µg/L of d6-1,2-dibromopropane as internal standard. After
86 the addition of ~10 g of high purity sodium sulphate, the samples were vortexed for 1 minute
87 and left to settle for 5 min. Finally, ~1.5 mL of MtBE extract was transferred into 2 ml vials for
88 injection into the GC/MS. The injector was operated in splitless mode. Chromatographic
89 separation was performed using a ZB1701 column from Phenomenex (30 m x 0.25 mm x 0.25
90 µm). The oven temperature program was as follows: 40 °C for 25 min, ramp to 145 °C at 5 °C
91 /min and held for 2 min and then ramp to 260 °C at 20 °C /min and held for 10 min as described
92 elsewhere ⁹. The limit of quantification for all volatile DBP FP was 0.1 µg/L, and the recoveries
93 were above 90 %.

Table S1: DBP FP (L⁻¹) data for Ter

Season	n	µgTCM	µgBDCM	µgTCAN	µgDCP	µgTCNM	µgDCAN	µgDBCM	µgTCP	µgTBM	µgBCAN	µgDBAN	µgNDMA
Winter	1	19.49	7.44	<LoQ	0.12	0.08	3.04	2.52	3.57	0.15	1.13	0.29	0.07
Summer	1	69.92	10.29	0.04	0.81	0.67	11.43	1.41	4.17	0.74	1.19	< LoQ	0.03

† LoQ = Limit of Quantification

Table S2: Specific DBP FP data for Ter

Season	n	µgTCM/m gDOC	µgBDCM/m gDOC	µgTCAN/m gDOC	µgDCP/m gDOC	µgTCNM/m gDOC	µgDCAN/m gDOC	µgDBCM/m gDOC	µgTCP/m gDOC	µgTBM/m gDOC	µgBCAN/m gDOC	µgDBAN/m gDOC	µgNDMA/m gDOC
Winter	1	9.66	3.69	0.00	0.06	0.04	1.51	1.25	1.77	0.08	0.56	0.14	0.04
Summer	1	14.81	2.18	0.01	0.17	0.14	2.42	0.30	0.88	0.16	0.25	0.00	0.01

Table S3: Summaries of DBP FP (L⁻¹) data for Sau

Season	n	Summary	µgTCM	µgBDCM	µgTCAN	µgDCP	µgTCNM	µgDCAN	µgDBCM	µgTCP	µgTBM	µgBCAN	µgDBAN	µgNDMA
Autumn	4	Min	57.66	8.37	< LoQ	< LoQ	1.46	7.59	0.37	2.07	< LoQ	0.77	< LoQ	0.01
		Max	70.45	10.07	< LoQ	< LoQ	1.68	11.89	0.55	2.41	< LoQ	1.31	< LoQ	0.03
		Mean	65.20	9.42	< LoQ	< LoQ	1.59	9.47	0.49	2.23	< LoQ	1.01	< LoQ	0.02
		Median	66.36	9.62	< LoQ	< LoQ	1.60	9.19	0.52	2.22	< LoQ	0.98	< LoQ	0.01
		Stdev	5.40	0.82	< LoQ	< LoQ	0.10	2.10	0.09	0.14	< LoQ	0.25	< LoQ	0.01
Winter	4	Min	31.20	5.92	< LoQ	0.20	0.16	2.44	1.29	3.75	0.06	0.42	0.06	0.02
		Max	44.87	10.04	< LoQ	0.38	0.41	4.09	1.89	7.13	0.09	0.92	0.14	0.03
		Mean	37.59	7.81	< LoQ	0.29	0.27	3.15	1.58	4.71	0.08	0.66	0.10	0.03
		Median	37.15	7.63	< LoQ	0.30	0.26	3.04	1.58	3.99	0.08	0.66	0.09	0.03
		Stdev	5.87	1.70	< LoQ	0.08	0.11	0.77	0.30	1.61	0.02	0.26	0.04	0.00
Summer	4	Min	48.98	10.13	0.00	0.37	0.60	5.91	1.54	3.02	0.74	0.73	0.00	0.01
		Max	50.85	12.94	0.13	0.49	1.10	8.48	2.20	4.07	0.79	1.45	0.04	0.03
		Mean	49.87	11.01	0.08	0.45	0.79	7.36	1.86	3.58	0.77	1.19	0.02	0.02
		Median	49.83	10.49	0.12	0.46	0.74	7.52	1.86	3.61	0.76	1.28	0.02	0.02
		Stdev	0.99	1.31	0.07	0.05	0.22	1.22	0.27	0.46	0.03	0.32	0.02	0.01

† LoQ = Limit of Quantification

Table S4: Specific DBP FP for Sau

Season	n	Summary	µgTCM/mgDOC	µgBDCM/mgDOC	µgTCAN/mgDOC	µgDCP/mgDOC	µgTCNM/mgDOC	µgDCAN/mgDOC	µgDBCm/mgDOC	µgTCP/mgDOC	µgTBM/mgDOC	µgBCAN/mgDOC	µgDBAN/mgDOC	µgNDMA/mgDOC
Autumn	4	Min	13.78	2.00	0.00	0.00	0.35	1.87	0.09	0.52	0.00	0.18	0.00	0.00
		Max	19.22	2.76	0.00	0.00	0.46	3.26	0.16	0.66	0.00	0.36	0.00	0.00
		Mean	17.10	2.48	0.00	0.00	0.42	2.73	0.13	0.58	0.00	0.29	0.00	0.00
		Median	18.29	2.67	0.00	0.00	0.46	3.08	0.15	0.57	0.00	0.32	0.00	0.00
		Stdev	2.91	0.41	0.00	0.00	0.06	0.75	0.04	0.07	0.00	0.09	0.00	0.00
Winter	4	Min	11.46	2.18	0.00	0.08	0.06	0.89	0.47	1.39	0.02	0.15	0.02	0.01
		Max	16.44	3.68	0.00	0.13	0.15	1.50	0.69	2.44	0.03	0.34	0.05	0.01
		Mean	13.59	2.83	0.00	0.11	0.10	1.14	0.57	1.69	0.03	0.24	0.04	0.01
		Median	13.22	2.72	0.00	0.11	0.09	1.09	0.57	1.46	0.03	0.24	0.03	0.01
		Stdev	2.08	0.64	0.00	0.03	0.04	0.30	0.12	0.50	0.01	0.10	0.01	0.00
Summer	4	Min	11.06	2.54	0.00	0.10	0.16	1.48	0.39	0.75	0.17	0.18	0.00	0.00
		Max	15.69	3.17	0.04	0.13	0.24	2.62	0.56	1.17	0.23	0.45	0.01	0.01
		Mean	12.96	2.83	0.02	0.11	0.20	1.94	0.48	0.93	0.20	0.31	0.00	0.01
		Median	12.55	2.81	0.02	0.12	0.21	1.82	0.49	0.91	0.20	0.31	0.00	0.01
		Stdev	1.96	0.26	0.02	0.01	0.04	0.55	0.07	0.21	0.02	0.11	0.01	0.00

Table S5: Summaries of DBP FP (L⁻¹) data for Susqueda

Season	n	Summary	µgTCM	µgBDCM	µgTCAN	µgDCP	µgTCNM	µgDCAN	µgDBCM	µgTCP	µgTBM	µgBCAN	µgDBAN	µgNDMA
Autumn	4	Min	63.97	9.13	< LoQ	< LoQ	1.25	7.40	0.44	2.10	< LoQ	0.87	< LoQ	0.01
		Max	79.44	9.78	< LoQ	< LoQ	1.97	9.81	0.48	2.58	< LoQ	0.97	< LoQ	0.01
		Mean	71.17	9.49	< LoQ	< LoQ	1.52	8.77	0.46	2.41	< LoQ	0.92	< LoQ	0.01
		Median	70.63	9.51	< LoQ	< LoQ	1.44	8.93	0.46	2.47	< LoQ	0.92	< LoQ	0.01
		Stdev	6.47	0.27	< LoQ	< LoQ	0.33	1.09	0.02	0.22	< LoQ	0.04	< LoQ	0.00
Winter	4	Min	49.77	6.48	< LoQ	0.30	0.32	3.18	1.09	3.87	0.06	0.36	0.06	0.02
		Max	66.21	8.43	< LoQ	0.45	0.51	4.52	1.20	4.91	0.06	0.52	0.06	0.02
		Mean	57.57	7.41	< LoQ	0.38	0.42	3.85	1.15	4.34	0.06	0.43	0.06	0.02
		Median	57.16	7.36	< LoQ	0.38	0.43	3.84	1.16	4.29	0.06	0.43	0.06	0.02
		Stdev	8.82	1.06	< LoQ	0.06	0.09	0.64	0.05	0.43	< LoQ	0.07	< LoQ	0.00
Summer	4	Min	58.11	11.23	< LoQ	0.44	0.70	6.72	1.44	3.71	0.75	0.74	< LoQ	0.02
		Max	68.41	12.29	0.20	0.66	1.04	8.99	1.86	4.17	0.79	1.03	< LoQ	0.03
		Mean	63.74	11.64	0.06	0.57	0.85	7.41	1.66	3.95	0.77	0.88	< LoQ	0.02
		Median	64.23	11.51	0.03	0.59	0.82	6.97	1.68	3.96	0.77	0.87	< LoQ	0.02
		Stdev	4.27	0.46	0.09	0.09	0.16	1.06	0.17	0.23	0.02	0.12	< LoQ	0.01

† LoQ = Limit of Quantification

Table S6: Specific DBPs FP for Susqueda

Season	n	Summary	µgTCM/mgDOC	µgBDCM/mgDOC	µgTCAN/mgDOC	µgDCP/mgDOC	µgTCNM/mgDOC	µgDCAN/mgDOC	µgDBCM/mgDOC	µgTCP/mgDOC	µgTBM/mgDOC	µgBCAN/mgDOC	µgDBAN/mgDOC	µgNDMA/mgDOC
Autumn	4	Min	20.14	2.83	0.00	0.00	0.37	2.33	0.13	0.63	0.00	0.26	0.00	0.00
		Max	23.11	2.88	0.00	0.00	0.59	2.93	0.15	0.76	0.00	0.28	0.00	0.00
		Mean	21.37	2.85	0.00	0.00	0.46	2.63	0.14	0.72	0.00	0.28	0.00	0.00
		Median	21.11	2.85	0.00	0.00	0.44	2.63	0.14	0.75	0.00	0.28	0.00	0.00
		Stdev	1.30	0.02	0.00	0.00	0.09	0.26	0.01	0.07	0.00	0.01	0.00	0.00
Winter	4	Min	15.22	1.98	0.00	0.09	0.10	0.98	0.34	1.19	0.02	0.11	0.02	0.01
		Max	19.44	2.48	0.00	0.13	0.15	1.33	0.35	1.44	0.02	0.15	0.02	0.01
		Mean	17.26	2.22	0.00	0.11	0.13	1.15	0.35	1.30	0.02	0.13	0.02	0.01
		Median	17.18	2.21	0.00	0.11	0.13	1.15	0.35	1.29	0.02	0.13	0.02	0.01
		Stdev	2.23	0.26	0.00	0.02	0.03	0.16	0.01	0.11	0.00	0.02	0.00	0.00
Summer	4	Min	13.04	2.33	0.00	0.09	0.16	1.38	0.33	0.75	0.15	0.15	0.00	0.00
		Max	20.55	4.05	0.06	0.20	0.26	2.53	0.61	1.46	0.28	0.31	0.00	0.01
		Mean	16.63	3.05	0.02	0.15	0.22	1.95	0.44	1.05	0.20	0.23	0.00	0.01
		Median	16.48	2.90	0.01	0.16	0.23	1.95	0.40	1.00	0.19	0.24	0.00	0.00
		Stdev	3.82	0.75	0.03	0.05	0.05	0.59	0.12	0.33	0.06	0.08	0.00	0.00

Table S7: DBP FP (L⁻¹) data for Pasteral

Season	n	µgTCM	µgBDCM	µgTCAN	µgDCP	µgTCNM	µgDCAN	µgDBCm	µgTCP	µgTBM	µgBCAN	µgDBAN	µgNDMA
Autumn	1	72.46	8.24	< LoQ	< LoQ	1.00	7.78	0.44	2.34	< LoQ	0.78	< LoQ	0.03
Winter	1	48.67	6.06	< LoQ	0.79	0.39	2.79	1.06	13.11	0.06	0.30	0.06	0.02
Summer	1	72.94	11.84	0.03	0.60	0.88	7.44	1.48	3.64	0.75	0.66	< LoQ	0.02

† LoQ = Limit of Quantification

Table S8: Specific DBP FP for Pasteral

Season	n	µgTCM/m gDOC	µgBDCM/m gDOC	µgTCAN/m gDOC	µgDCP/m gDOC	µgTCNM/m gDOC	µgDCAN/m gDOC	µgDBCm/m gDOC	µgTCP/m gDOC	µgTBM/m gDOC	µgBCAN/m gDOC	µgDBAN/m gDOC	µgNDMA/m gDOC
Autumn	1	21.37	2.43	0.00	0.00	0.30	2.30	0.13	0.69	0.00	0.23	0.00	0.01
Winter	1	13.20	1.64	0.00	0.21	0.11	0.76	0.29	3.55	0.02	0.08	0.02	0.01
Summer	1	13.61	2.21	0.01	0.11	0.17	1.39	0.28	0.68	0.14	0.12	0.00	0.00

Table S9: Nutrients (L⁻¹) and DOM optical indices for Ter

Season	n	mgN_NH4	mgC_DOC	mgN_TN	mgN_TKN	mgP_PO4 ³⁻	mgP_PT	mgN_NO3 ⁻	mgN_NO2 ⁻	Br ⁻	UVA ₂₅₄	SUVA ₂₅₄	FI	BIX	HIX
Winter	1	0.18	2.02	5.75	< LoQ	0.02	0.04	4.66	0.02	< LoQ	0.04	0.02	1.85	0.87	4.62
Summer	1	< LoQ	4.72	1.56	0.76	0.04	0.10	0.63	0.05	< LoQ	0.06	0.01	1.74	0.75	6.38

† LoQ = Limit of Quantification

Table S10: *Sau* nutrients (L⁻¹) and DOM optical indices

Season	n	Summary	mgN_NH4	mgC_DOC	mgN_TN	mgN_TKN	mgP_PO ₄ ³⁻	mgP_PT	mgN_NO ₃ ⁻	mgN_NO ₂ ⁻	Br ⁻	UVA ₂₅₄	SUVA ₂₅₄	FI	BIX	HIX
Autumn	4	Min	0.08	3.43	1.97	0.69	0.04	0.05	1.45	0.01	< LoQ	0.11	0.03	1.56	0.71	5.71
		Max	0.10	4.18	2.97	0.82	0.09	0.11	2.27	0.02	< LoQ	0.14	0.04	1.58	0.76	6.72
		Mean	0.09	3.76	2.48	0.76	0.07	0.08	1.88	0.01	< LoQ	0.13	0.04	1.57	0.73	6.15
		Median	0.09	3.65	2.49	0.76	0.06	0.08	1.90	0.01	< LoQ	0.13	0.04	1.57	0.73	6.09
		Stdev	0.02	0.39	0.48	0.09	0.02	0.03	0.40	0.01	< LoQ	0.01	0.01	0.01	0.02	0.45
Winter	4	Min	0.01	2.69	4.16	< LoQ	0.03	0.04	3.03	0.00	< LoQ	0.07	0.02	1.65	0.70	9.40
		Max	0.14	2.92	4.97	< LoQ	0.03	0.06	4.32	0.03	< LoQ	0.07	0.03	1.74	0.75	11.14
		Mean	0.06	2.77	4.54	< LoQ	0.03	0.05	3.77	0.02	< LoQ	0.07	0.03	1.69	0.72	10.40
		Median	0.05	2.73	4.52	< LoQ	0.03	0.05	3.86	0.02	< LoQ	0.07	0.03	1.69	0.72	10.53
		Stdev	0.06	0.11	0.41	< LoQ	0.00	0.01	0.58	0.01	< LoQ	0.00	0.00	0.04	0.02	0.82
Summer	4	Min	0.07	3.24	1.74	0.98	< LoQ	0.02	1.16	0.01	< LoQ	0.04	0.01	1.61	0.75	3.43
		Max	0.07	4.58	4.44	1.08	< LoQ	0.03	3.56	0.03	< LoQ	0.07	0.02	1.71	0.90	9.95
		Mean	0.07	3.91	2.73	1.03	< LoQ	0.02	2.01	0.03	< LoQ	0.05	0.01	1.67	0.83	6.81
		Median	0.07	3.91	2.37	1.03	< LoQ	0.02	1.66	0.03	< LoQ	0.05	0.01	1.68	0.83	6.93
		Stdev	N/A	0.55	1.21	0.05	< LoQ	0.01	1.09	0.01	< LoQ	0.01	0.00	0.05	0.08	3.27

† LoQ = Limit of Quantification

Table S11: Susquehanna nutrients (L^{-1}) and DOM optical indices

Season	n	Summary	mgN_NH4	mgC_DOC	mgN_TN	mgN_TKN	mgP_PO ₄ ³⁻	mgP_PT	mgN_NO ₃ ⁻	mgN_NO ₂ ⁻	Br ⁻	UV ₂₅₄	SUVA ₂₅₄	FI	BIX	HIX
Autumn	4	Min	0.01	3.18	1.58	< LoQ	0.05	0.05	1.06	0.01	< LoQ	0.12	0.04	1.61	0.64	8.95
		Max	0.04	3.44	1.93	< LoQ	0.06	0.07	1.33	0.01	< LoQ	0.13	0.04	1.65	0.65	9.60
		Mean	0.02	3.33	1.74	< LoQ	0.06	0.06	1.17	0.01	< LoQ	0.12	0.04	1.63	0.65	9.27
		Median	0.02	3.35	1.73	< LoQ	0.06	0.06	1.15	0.01	< LoQ	0.12	0.04	1.63	0.65	9.26
		Stdev	0.02	0.11	0.17	< LoQ	0.01	0.01	0.13	0.00	< LoQ	0.01	0.00	0.02	0.01	0.30
Winter	4	Min	0.00	3.25	2.65	1.66	0.04	0.05	2.11	< LoQ	< LoQ	0.08	0.02	1.62	0.68	13.07
		Max	0.02	3.41	2.71	1.66	0.04	0.06	2.34	< LoQ	< LoQ	0.09	0.03	1.67	0.69	14.03
		Mean	0.01	3.33	2.69	1.66	0.04	0.05	2.24	< LoQ	< LoQ	0.09	0.03	1.65	0.69	13.73
		Median	0.00	3.33	2.70	1.66	0.04	0.05	2.25	< LoQ	< LoQ	0.09	0.03	1.66	0.69	13.90
		Stdev	0.01	0.08	0.02	N/A	0.00	0.00	0.10	< LoQ	< LoQ	0.01	0.00	0.02	0.01	0.44
Summer	4	Min	< LoQ	2.83	2.49	0.57	< LoQ	0.01	1.98	0.02	< LoQ	0.05	0.01	1.56	0.69	5.48
		Max	< LoQ	4.98	3.44	1.19	< LoQ	0.03	2.92	0.03	< LoQ	0.08	0.02	1.69	0.88	15.10
		Mean	< LoQ	4.00	2.95	0.89	< LoQ	0.02	2.33	0.03	< LoQ	0.07	0.02	1.65	0.79	9.44
		Median	< LoQ	4.10	2.94	0.91	< LoQ	0.02	2.20	0.02	< LoQ	0.07	0.02	1.68	0.78	8.59
		Stdev	< LoQ	0.99	0.44	0.25	< LoQ	0.01	0.42	0.00	< LoQ	0.01	0.00	0.07	0.08	4.28

† LoQ = Limit of Quantification

Table S12: *Pastoral nutrients (L⁻¹) and DOM optical indices*

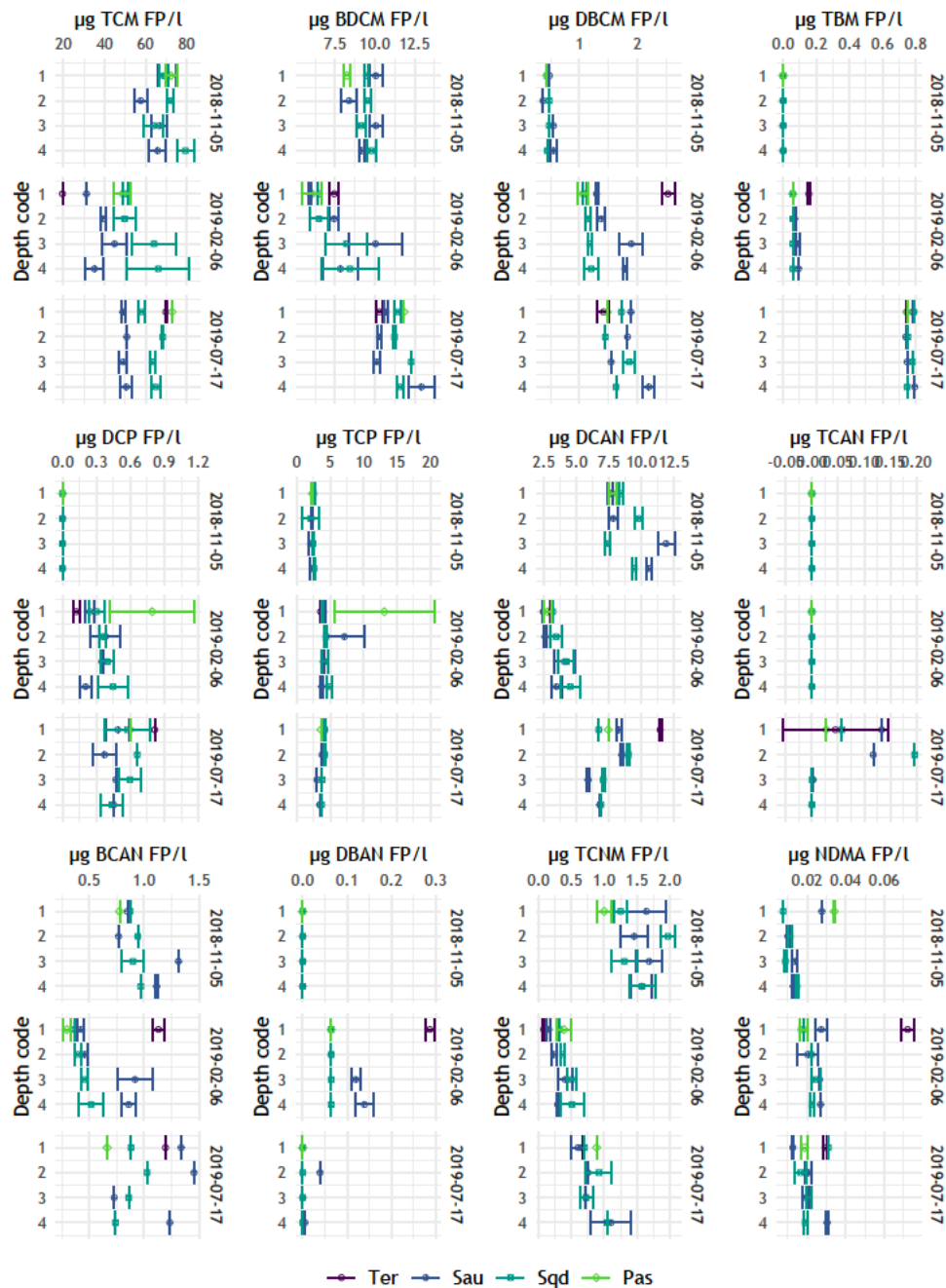
Season	n	mgN_NH4	mgC_TOC	mgN_TN	mgN_TKN	mgP_PO ₄ ³⁻	mgP_PT	mgN_NO ₃ ⁻	mgN_NO ₂ ⁻	Br ⁻	UVA ₂₅₄	SUVA ₂₅₄	FI	BIX	HIX
Autumn	1	0.01	3.39	1.58	1.75	0.05	0.05	1.00	< LoQ	< LoQ	0.13	0.04	1.62	0.68	8.60
Winter	1	0.01	3.69	2.66	< LoQ	0.04	0.05	2.24	< LoQ	< LoQ	0.10	0.03	1.66	0.73	8.80
Summer	1	< LoQ	5.36	3.17	< LoQ	< LoQ	0.01	2.54	0.02	< LoQ	0.08	0.02	1.70	0.72	12.48

† LoQ = Limit of Quantification

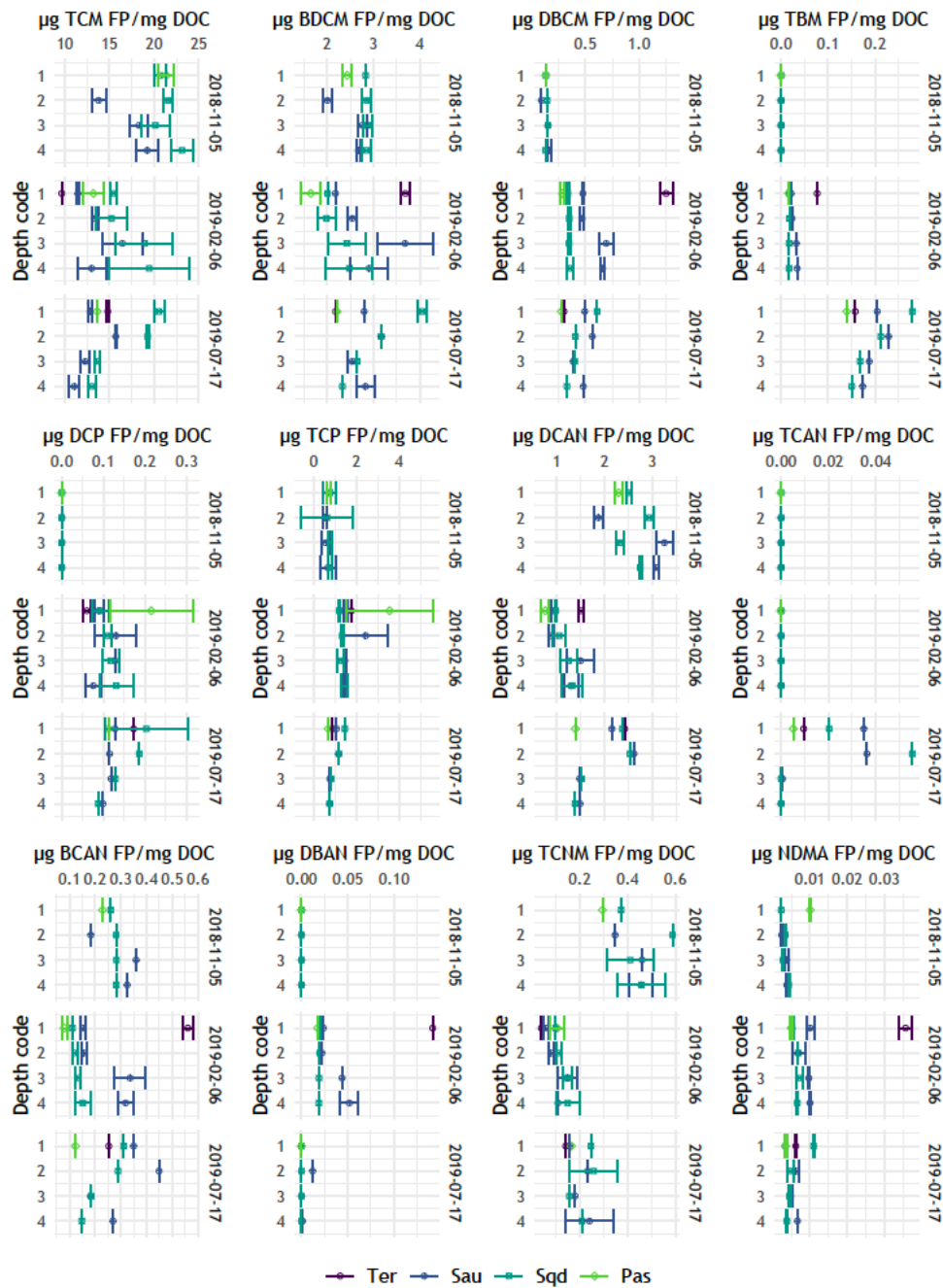
Table S13: Correlation matrix between measured nutrients and specific DBP

	SpTCM	SpBDCM	SpDCAN	SpTCP	SpNDMA	mgN_NH4	mgC_DOC	mgN_TN	mgN_TKN	mgP_PO4 ³⁻	mgP_PT	mgN_NO3 ⁻	mgN_NO2 ⁻	UVA ₂₅₄	SUVA ₂₅₄	FI	BIX	HIX	
SpTCM	1																		
SpBDCM	0.25	1																	
SpDCAN	0.57**	0.54**	1																
SpTCP	-0.27	0.08	-0.59***	1															
SpNDMA	-0.22	0.12	-0.43*	0.67****	1														
mgN_NH4	0.18	0.36	0.13	0.22	0.24	1													
mgC_DOC	-0.14	-0.44*	0.13	-0.59***	-0.55**	-0.65***	1												
mgN_TN	-0.59**	0.08	-0.48*	0.32	0.44*	0.25	-0.18	1											
mgN_TKN	0.06	0.05	0.24	-0.13	0.03	-0.37	0.2	-0.35	1										
mgP_PO4 ³⁻	0.58**	-0.19	0.28	-0.3	-0.28	0.48*	-0.17	-0.36	-0.31	1									
mgP_PT	0.48**	-0.09	0.27	-0.11	-0.14	0.54**	-0.24	-0.34	-0.21	0.87****	1								
mgN_NO3 ⁻	-0.57**	0.03	-0.58**	0.45*	0.45*	0.26	-0.24	0.96****	-0.35	-0.35	-0.31	1							
mgN_NO2 ⁻	-0.31	0.48*	0.3	-0.03	0.04	-0.16	0.21	0.18	0.35	-0.62***	-0.35	0.11	1						
UVA ₂₅₄	0.56**	-0.34	0.18	-0.49**	-0.39*	0.25	0.12	-0.26	-0.32	0.86****	0.61***	-0.28	-0.64***	1					
SUVA ₂₅₄	0.60***	-0.06	0.21	-0.22	-0.15	0.51**	-0.31	-0.21	-0.40*	0.89****	0.68****	-0.21	-0.69****	0.88****	1				
FI	-0.52**	0.04	-0.39*	0.3	0.37	-0.08	0.06	0.49**	-0.08	-0.51**	-0.31	0.50**	0.36	-0.52**	-0.53**	1			
BIX	-0.49**	0.28	0.11	0.23	0.23	-0.22	0.1	0.23	0.40*	-0.70****	-0.54**	0.2	0.62***	-0.77****	-0.71****	0.24	1		
HIX	-0.08	-0.46*	-0.66***	0.15	0.11	-0.12	0.03	0.35	-0.29	0	-0.09	0.39*	-0.34	0.2	0.05	0.29	-0.55**	1	

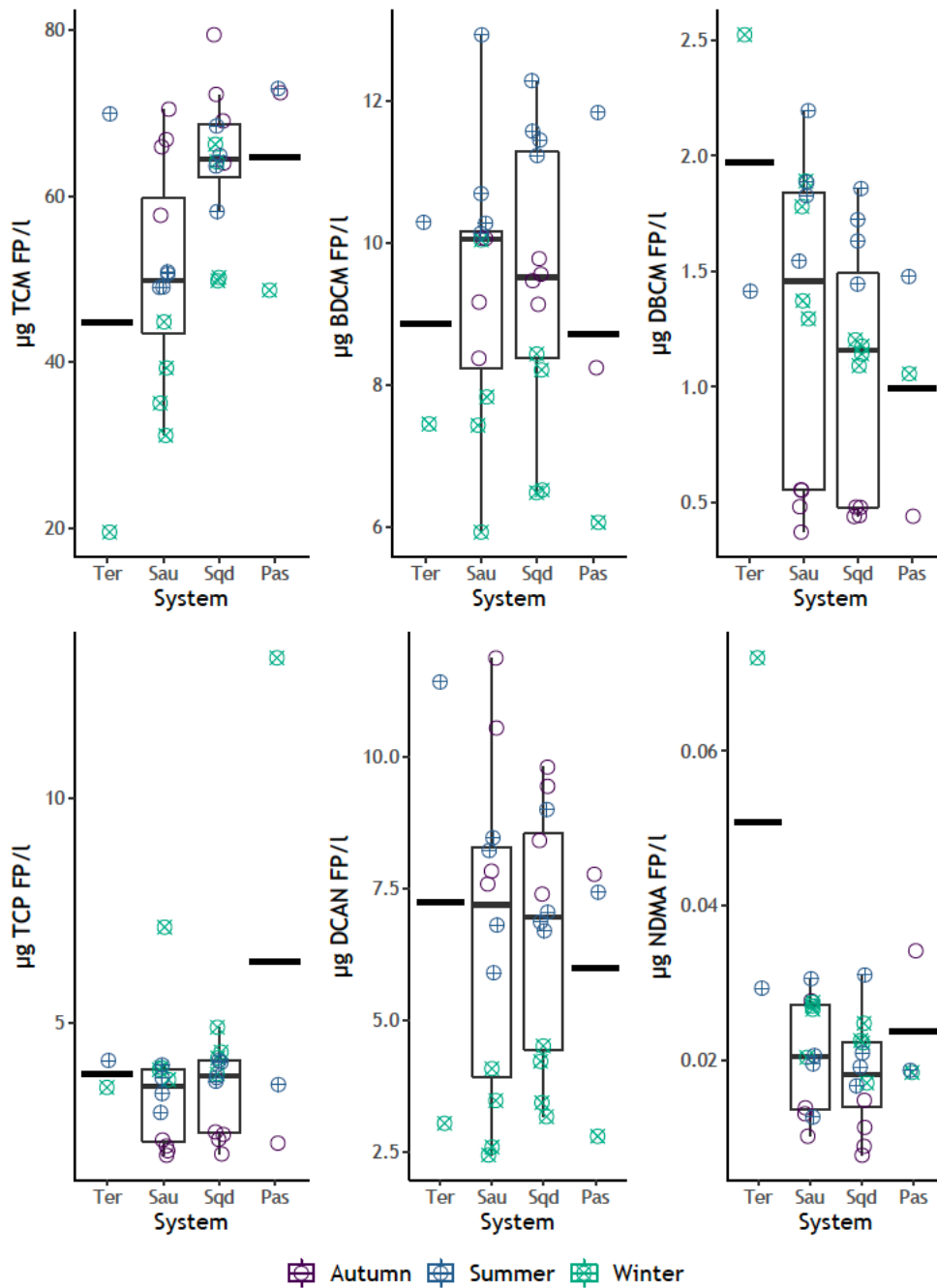
Note: **** = $p < 0.0001$, *** = $p < 0.001$, ** = $p < 0.01$, * = $p < 0.05$



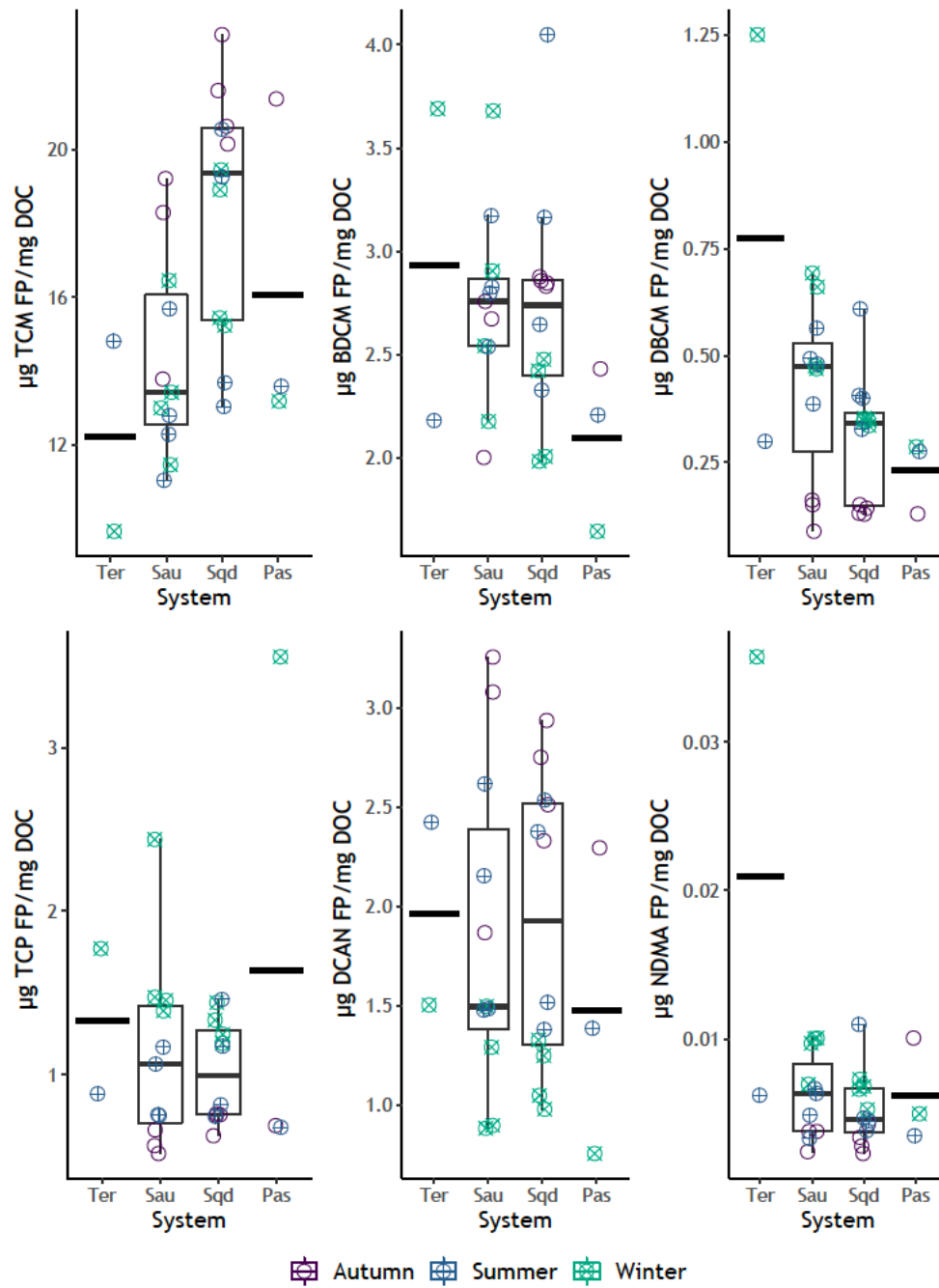
Supplementary Figure S1: Spatio-temporal variability of all DBP FP. The violet color represent samples from Ter River, the blue color represents samples from Sau Reservoir, the deep green color represents samples from Susqueda Reservoir whereas the bright green color represent samples from Pasteral Reservoir. Depth codes represent surface (1), thermocline (2), upper hypolimnion (3) and bottom hypolimnion (4).



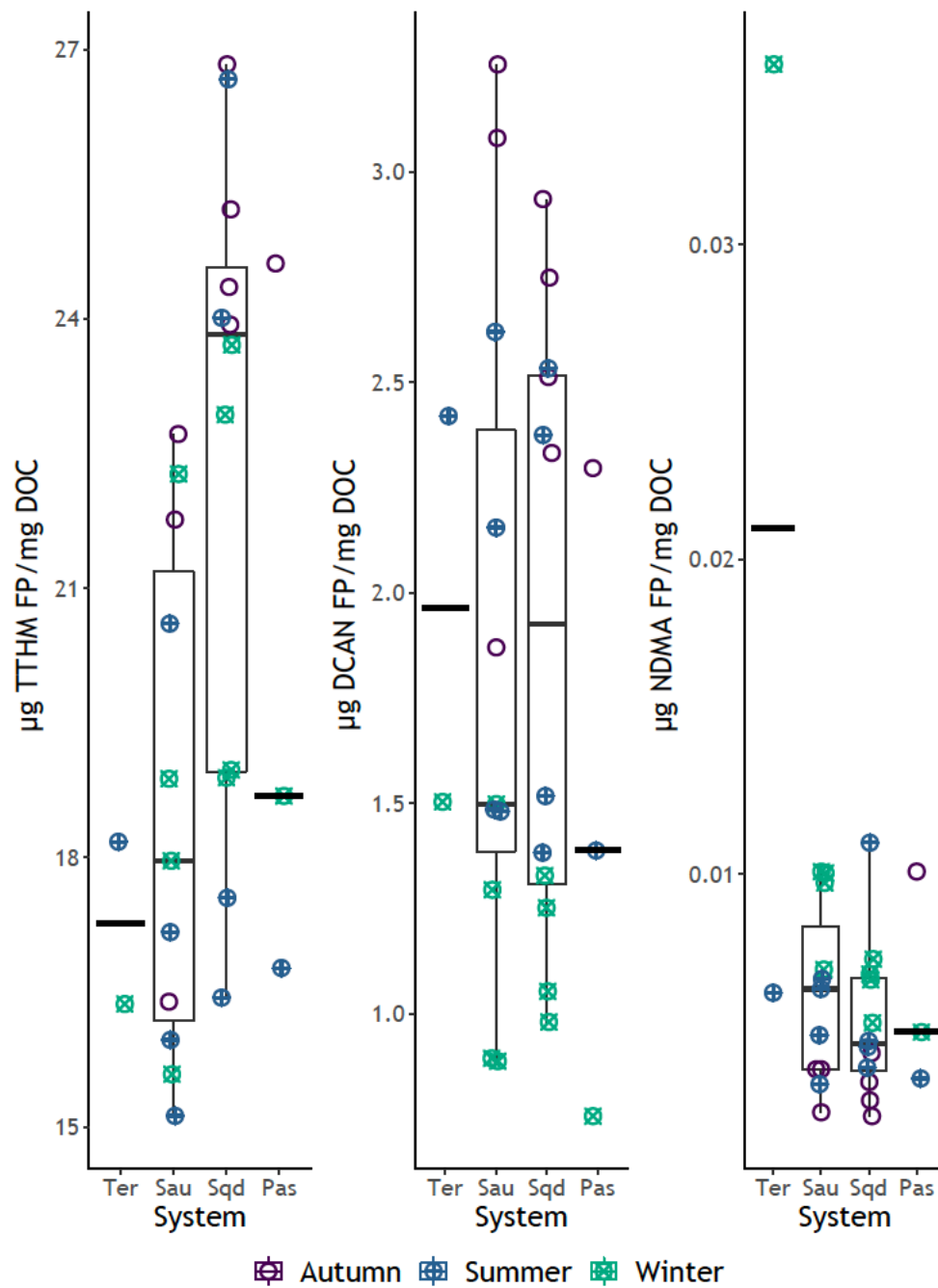
Supplementary Figure S2: Spatio-temporal variability of all yields of DBP. The violet color represent samples from Ter River, the blue color represents samples from Sau Reservoir, the deep green color represents samples from Susqueda Reservoir whereas the bright green color circles represent samples from Pasteral Reservoir. Depth codes represent surface (1), thermocline (2), upper hypolimnion (3) and bottom hypolimnion (4).



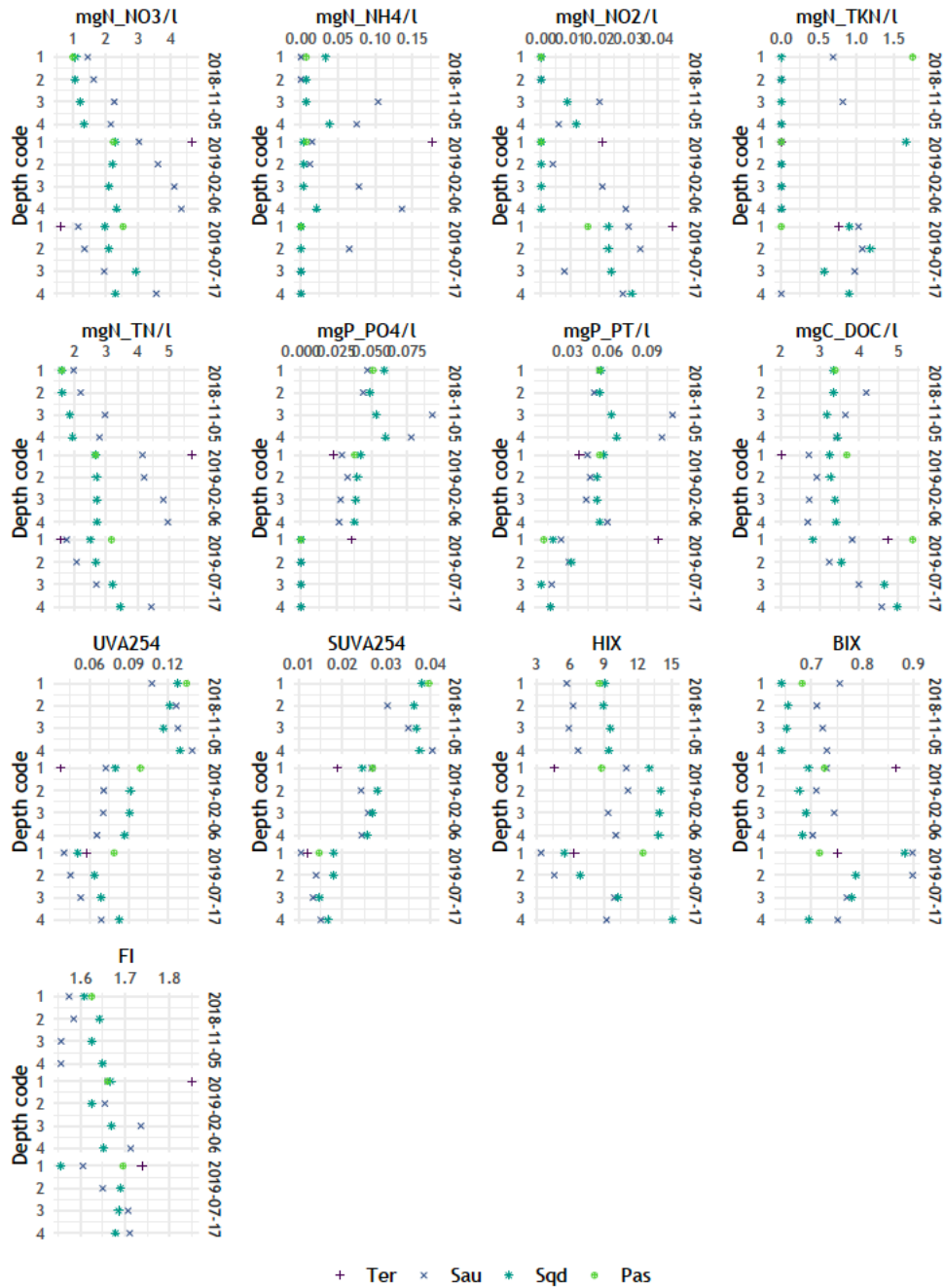
Supplementary Figure S3: Spatial variability of all significantly formed µg/L DBP. The green crossed circles represent winter values, the blue crossed circles represent summer values whereas the violet circles represent autumn values. The circles represent the actual formation potential data. The thick horizontal bar on each of the four systems represents the median value for all data of that particular system.



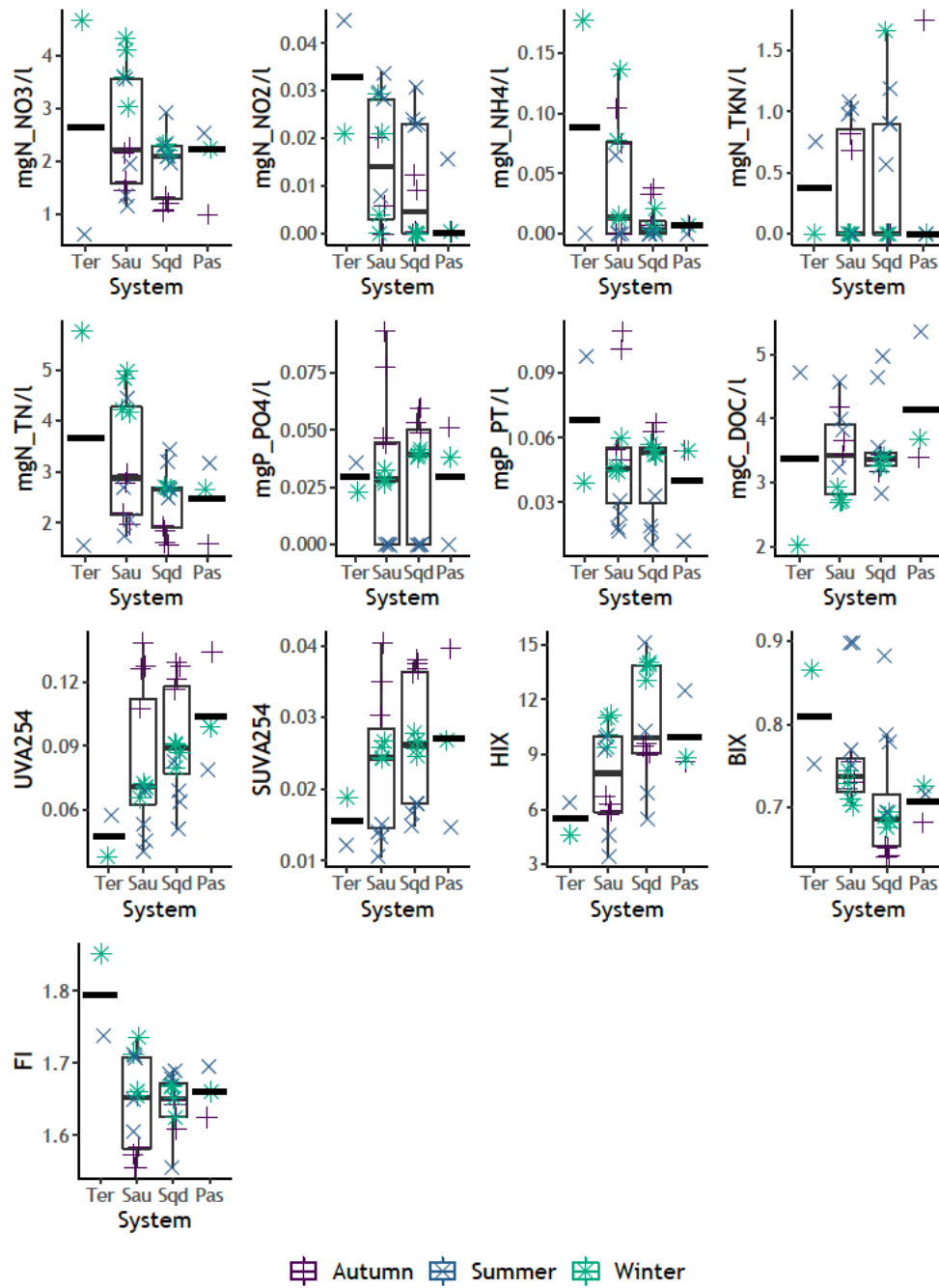
Supplementary Figure S4: Spatial variability of yields for all significantly formed DBP. The green crossed circles represent winter values, the blue crossed circles represent summer values whereas the violet circles represent autumn values. The thick horizontal bar on each of the four systems represents the median value for all data of that particular system.



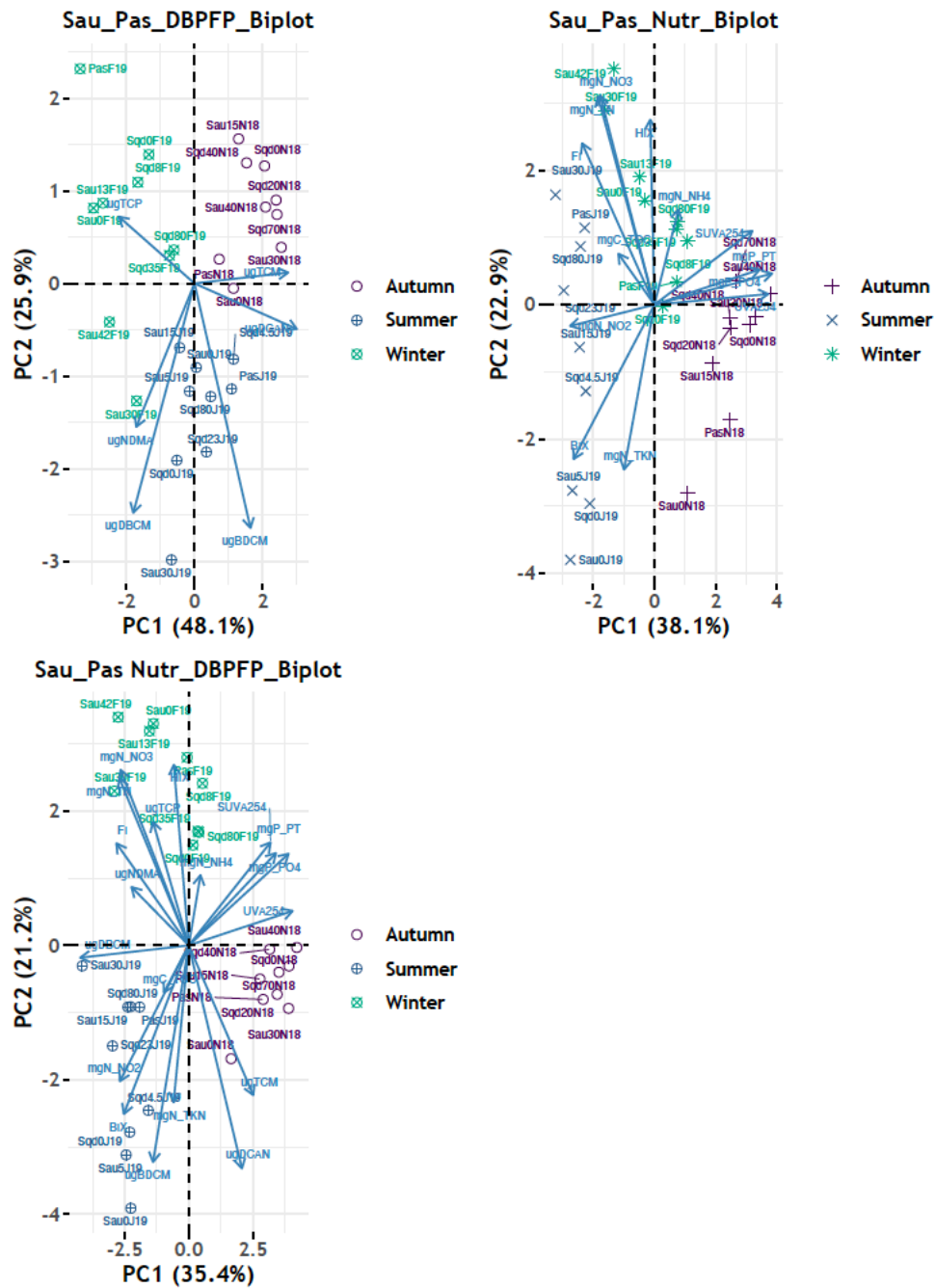
Supplementary Figure S5: Box and jitter plots for specific DBP FP of TTHMs, DCAN and NDMA, grouped by system and season. The green crossed circles represent formation potential values in winter, the blue crossed circles represent formation potential values in summer and the violet circles represent formation potential values in autumn. The circles represent the actual formation potential data. The thick horizontal bar on each of the four systems represents the median value for all data of that particular system.



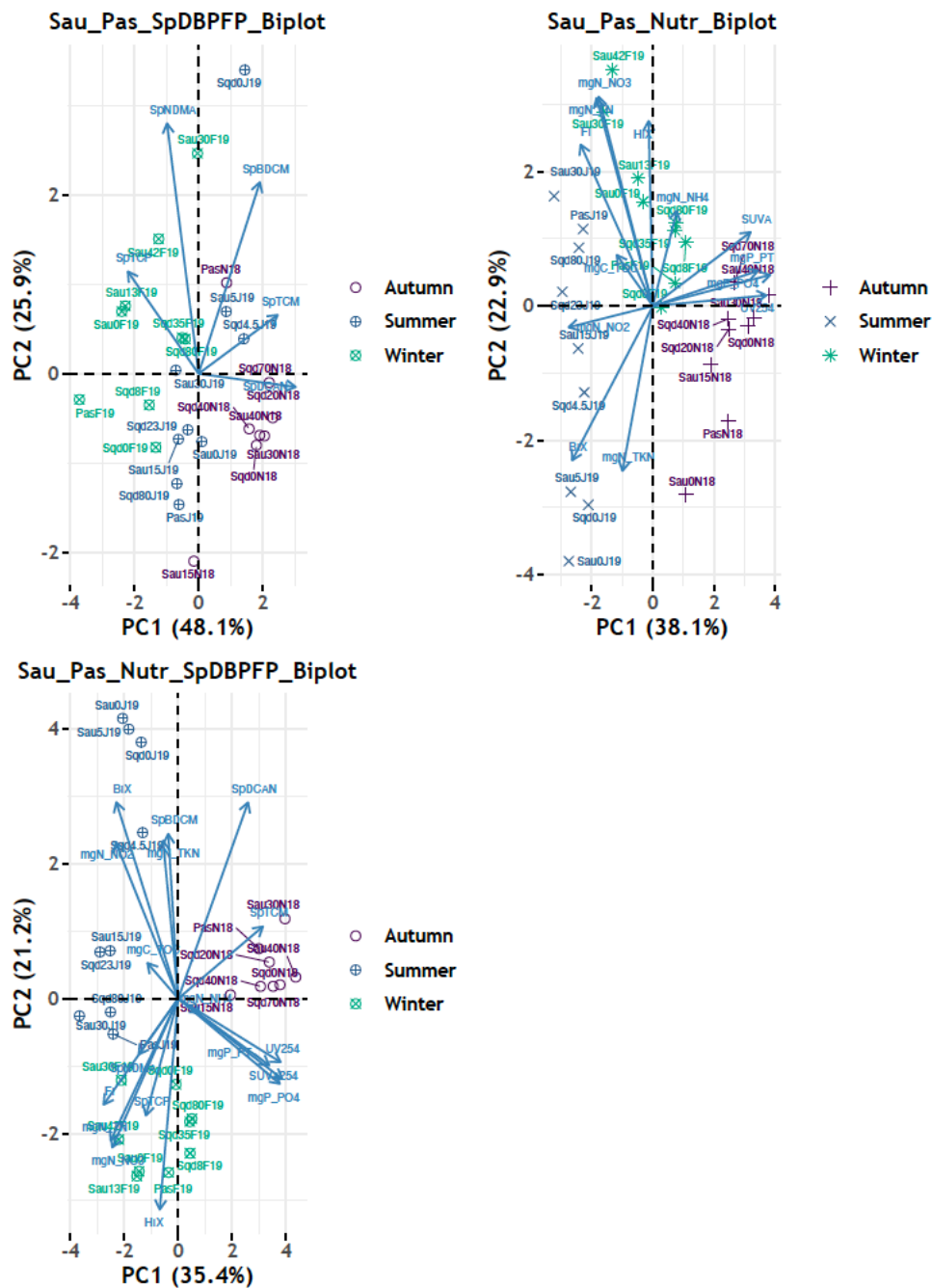
Supplementary Figure S6: Nutrients and DOM optical indices variability across depths. The brown crosses represent samples from Ter River, the blue crosses represent samples from Sau Reservoir, the deep green stars represent samples from Susqueda Reservoir whereas the bright green crossed circles represent samples from Pasteral Reservoir. Depth codes represent surface (1), thermocline (2), upper hypolimnion (3) and bottom (4).



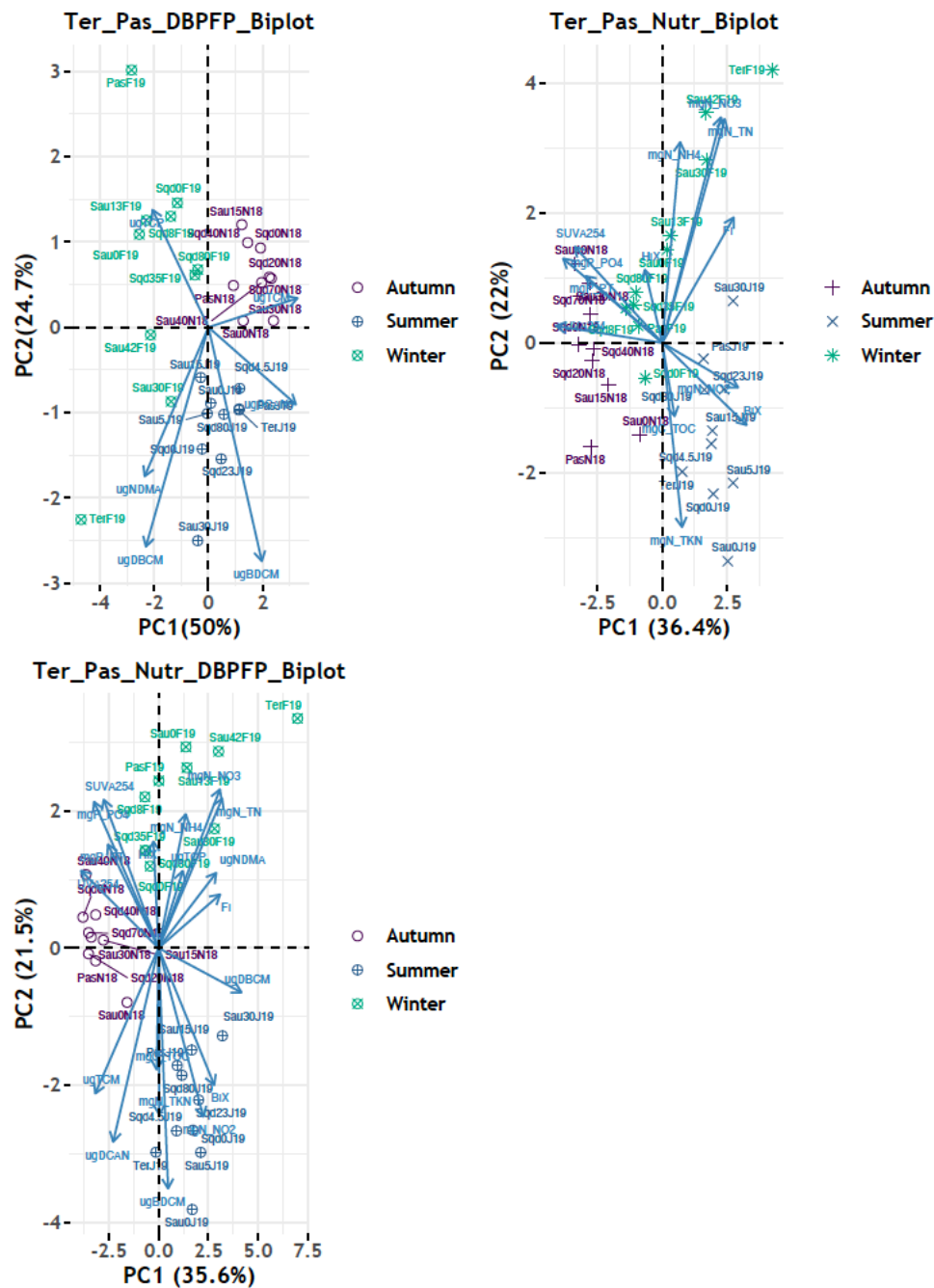
Supplementary Figure S7: Spatial-temporal distribution of nutrients and DOM optical indices across the Ter-Sau-Susqueda-Pastoral system. The green stars represent winter values, the blue crosses represent summer values whereas the violet crosses represent autumn values. The thick horizontal bar on each of the four systems represents the median value for all data of that particular system.



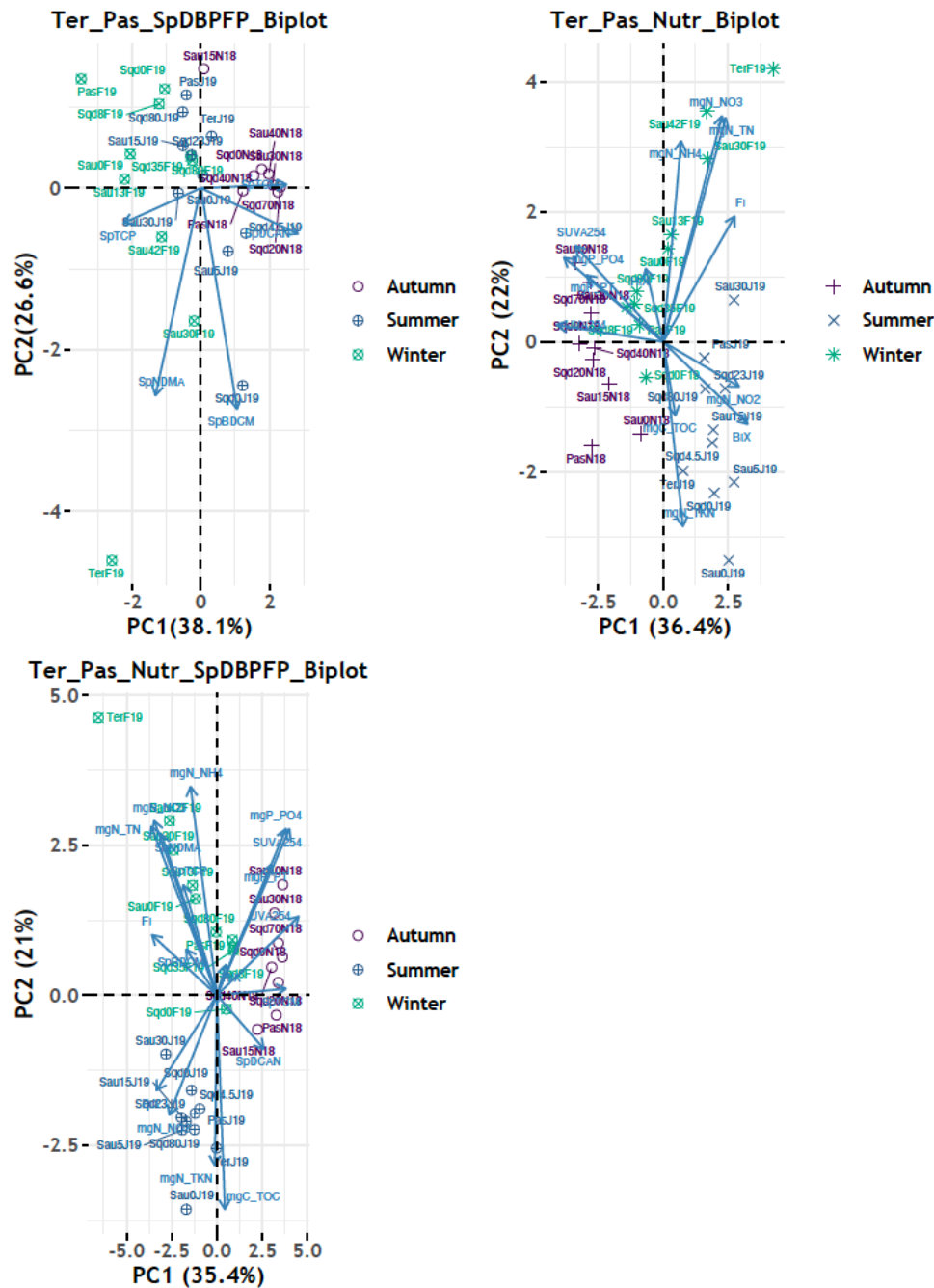
Supplementary Figure S8: PCA biplots for DBP FP, nutrients, and DBP FP + nutrients, excluding a Ter River sample, illustrating clustering by season. Violet circles represent samples collected in autumn, green crossed circles represent samples collected in winter, whereas blue crossed circles represent samples collected in summer. The blue labeled arrows represent the projection of the measured nutrients, DOM optical indices and DBP FPs on the two-dimensional plots. Samples were coded as: the first 3 letters are an abbreviation of the location (Ter = Ter, Sau = Sau, Sqd = Susqueda, Pas = Pasteral), followed by depth(m) from which the sample was collected (e.g. 0 = surface, 40m...80m) and, finally, an abbreviation of sampling month and year (e.g. N18 = November 2018, F19 = February 2019, J19 = July 2019).



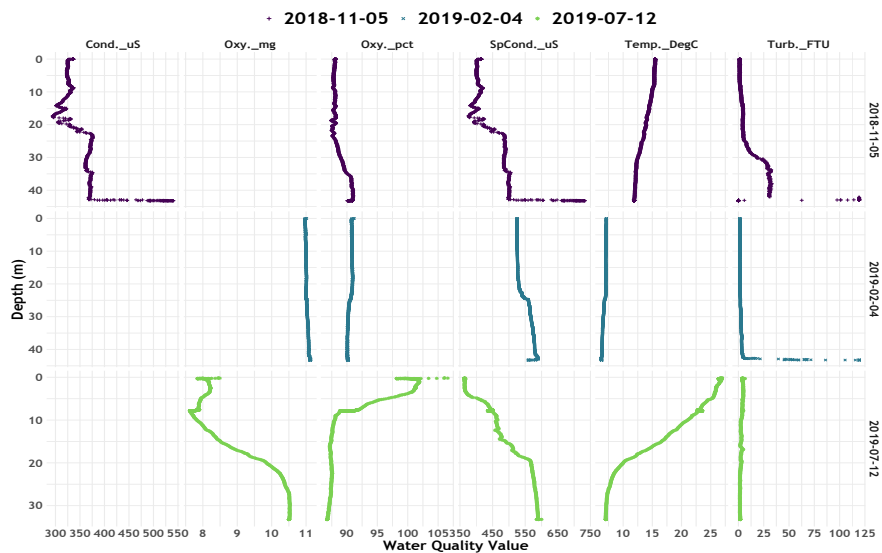
Supplementary Figure S9: PCA biplots for specific DBP FP, nutrients and specific DBP FP + nutrients, excluding a Ter River sample, illustrating clustering by season. Violet circles represent samples collected in autumn, green crossed circles represent samples collected in winter, whereas blue labeled arrows represent the projection of the measured nutrients, DOM optical indices and DBP FPs on the two-dimensional plots. Samples were coded as: the first 3 letters are an abbreviation of the location (Ter = Ter, Sau = Sau, Sqd = Susqueda, Pas = Pasteral), followed by depth(m) from which the sample was collected (e.g. 0 = surface, 40m...80m) and, finally, an abbreviation of sampling month and year (e.g. N18 = November 2018, F19 = February 2019, J19 = July 2019).



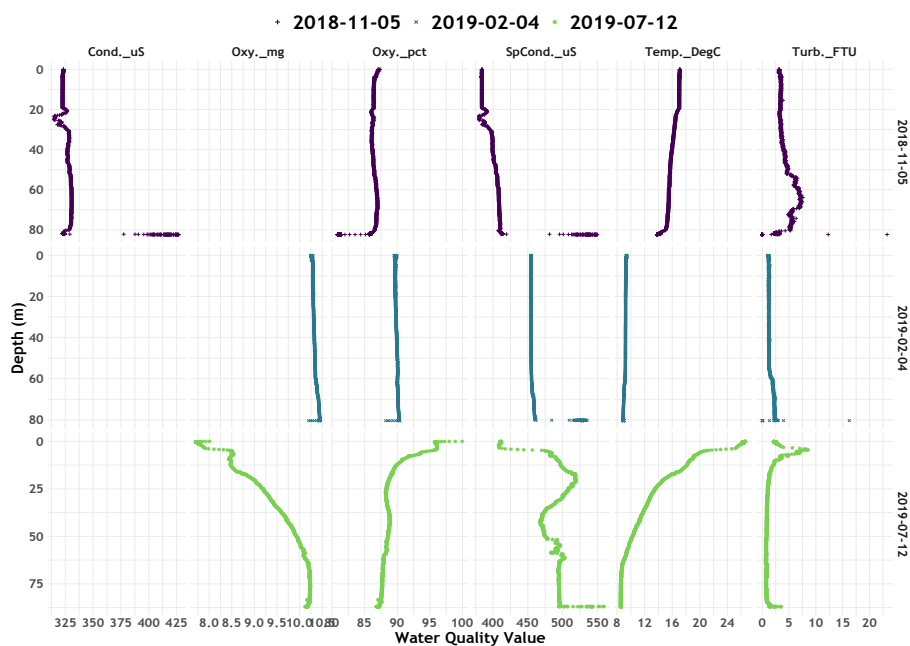
Supplementary Figure S10: PCA biplots for DBPs FP, nutrients and DBP FP + nutrients, including a Ter River sample, illustrating clustering by season. Violet circles and crosses represent samples collected in autumn, green crossed circles and stars represent samples collected in winter, whereas blue crossed circles and crosses represent samples collected in summer. The blue labeled arrows represent the projection of the measured nutrients, DOM optical indices and DBP FPs on the two-dimensional plots. Samples were coded as: the first 3 letters are an abbreviation of the location (Ter = Ter, Sau = Sau, Sqd = Susqueda, Pas = Pasteral), followed by depth(m) from which the sample was collected (e.g. 0 = surface, 40m...80m) and, finally, an abbreviation of sampling month and year (e.g. N18 = November 2018, F19 = February 2019, J19 = July 2019).



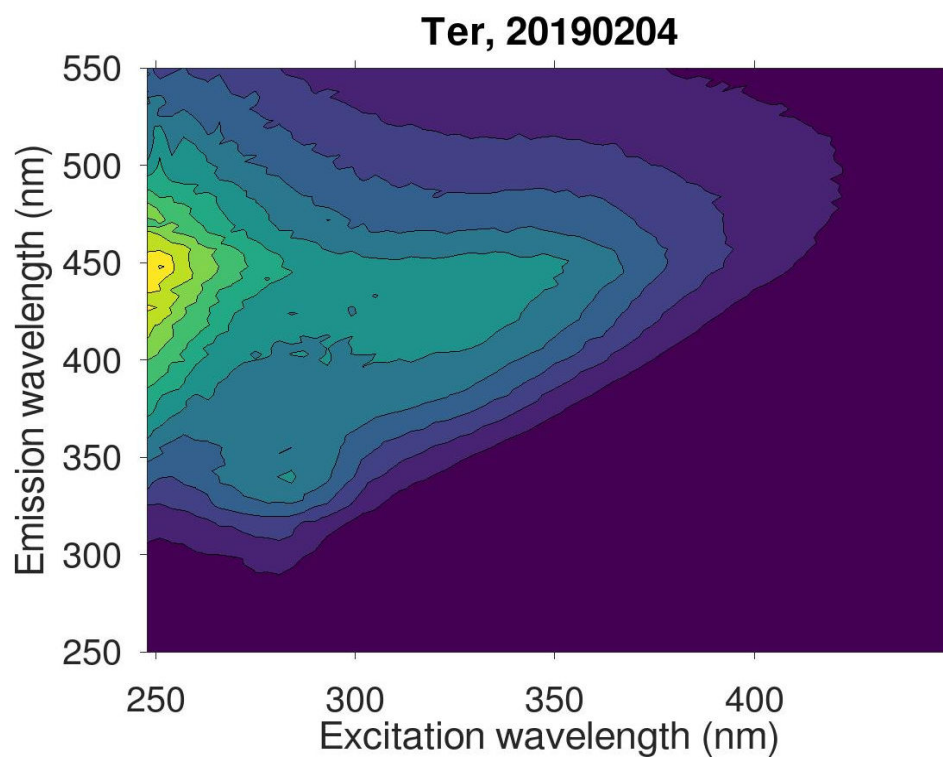
Supplementary Figure S11: PCA biplots for specific DBP FP, nutrients and specific DBP FP + nutrients, including a Ter River sample, illustrating clustering by season. Violet circles and crosses represent samples collected in autumn, green crossed circles and stars represent samples collected in winter, whereas blue crossed circles and crosses represent samples collected in summer. The blue labeled arrows represent the projection of the measured nutrients, DOM optical indices and DBP FPs on the two-dimensional plots. Samples were coded as: the first 3 letters are an abbreviation of the location (Ter = Ter, Sau = Sau, Sqd = Susqueda, Pas = Pasteral), followed by depth(m) from which the sample was collected (e.g. 0 = surface, 40m...80m) and, finally, an abbreviation of sampling month and year (e.g. N18 = November 2018, F19 = February 2019, J19 = July 2019).



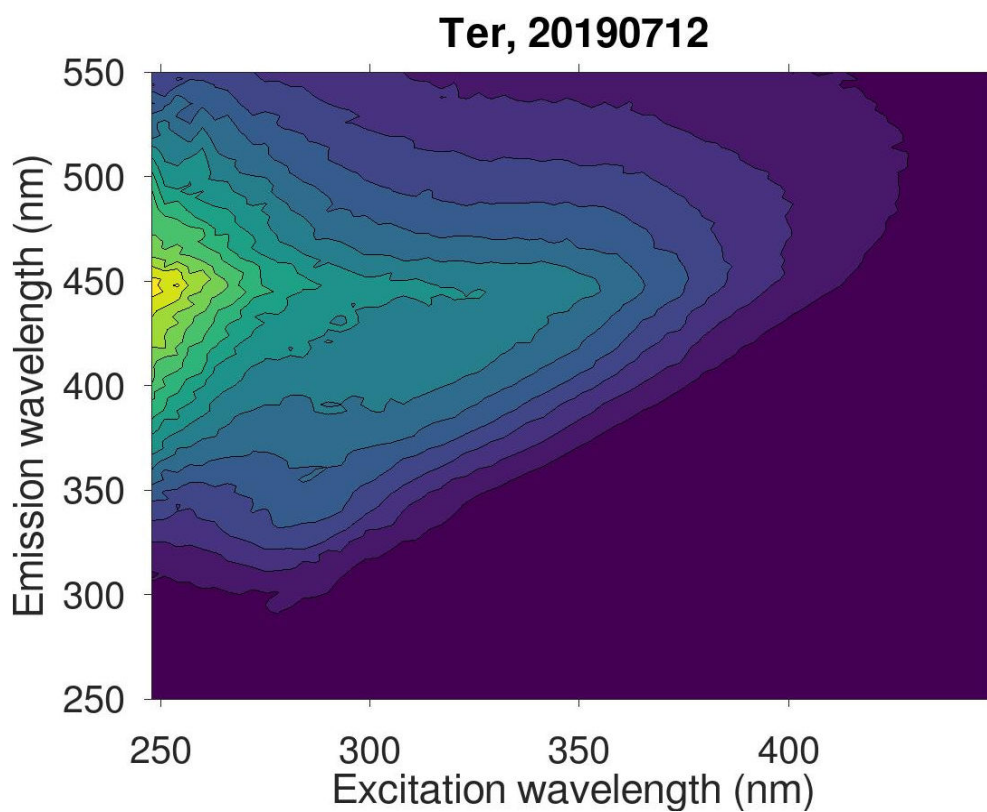
Supplementary Figure S12: Point plots for Sau CTD profile data for all the sampling events. Cond.uS = Conductivity ($\mu\text{S}/\text{cm}$); Oxy._mg = Oxygen (mg/l); Oxy._pct = Oxygen (%); SpCond._uS = Specific Conductance ($\mu\text{S}/\text{cm}$); Temp._DegC = Temperature ($^{\circ}\text{C}$) and Turb._FTU = Turbidity (FTU).



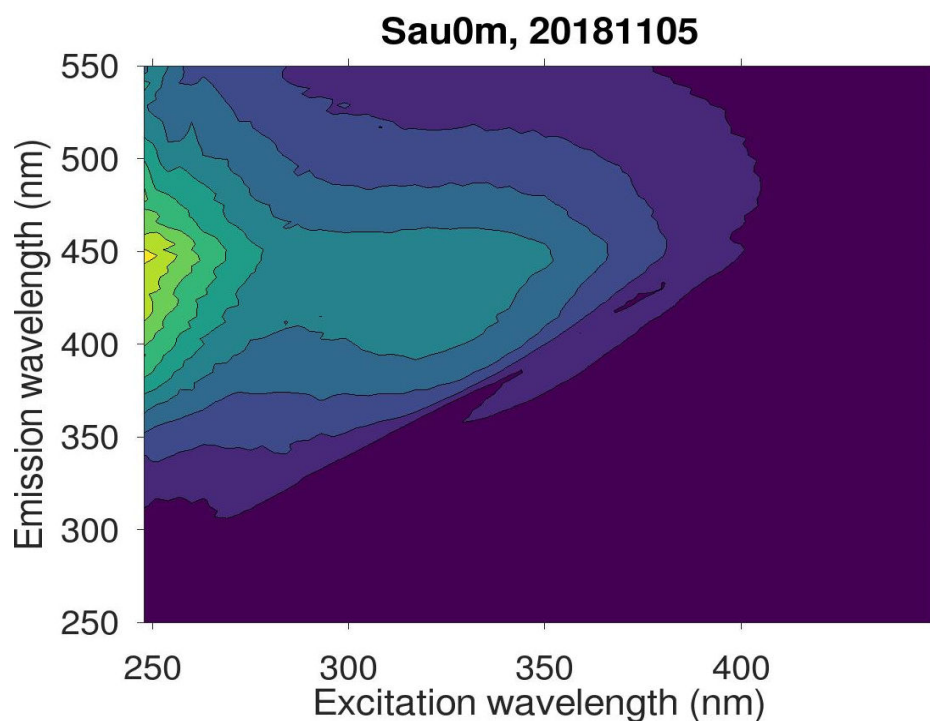
Supplementary Figure S13: Point plots for Susquehanna CTD profile data for all sampling events. Cond.uS = Conductivity ($\mu\text{S}/\text{cm}$); Oxy._mg = Oxygen (mg/l); Oxy._pct = Oxygen (%); SpCond._uS = Specific Conductance ($\mu\text{S}/\text{cm}$); Temp._DegC = Temperature ($^{\circ}\text{C}$) and Turb._FTU = Turbidity (FTU).



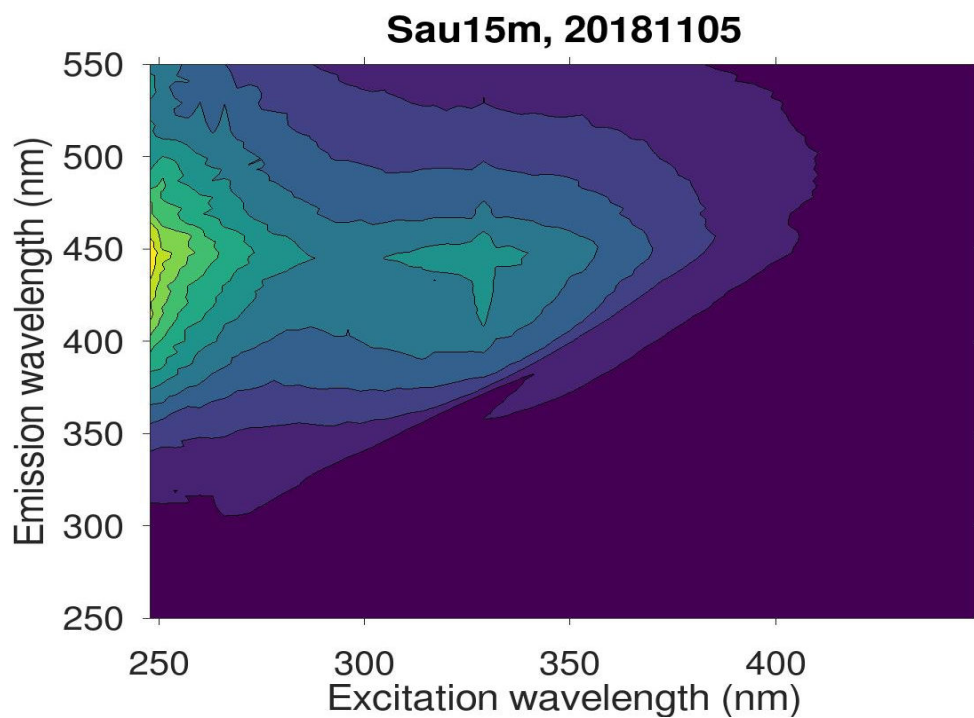
Supplementary Figure S14: Excitation-Emission matrix (EEM) for a sample collected from Ter River on 2019-02-04.



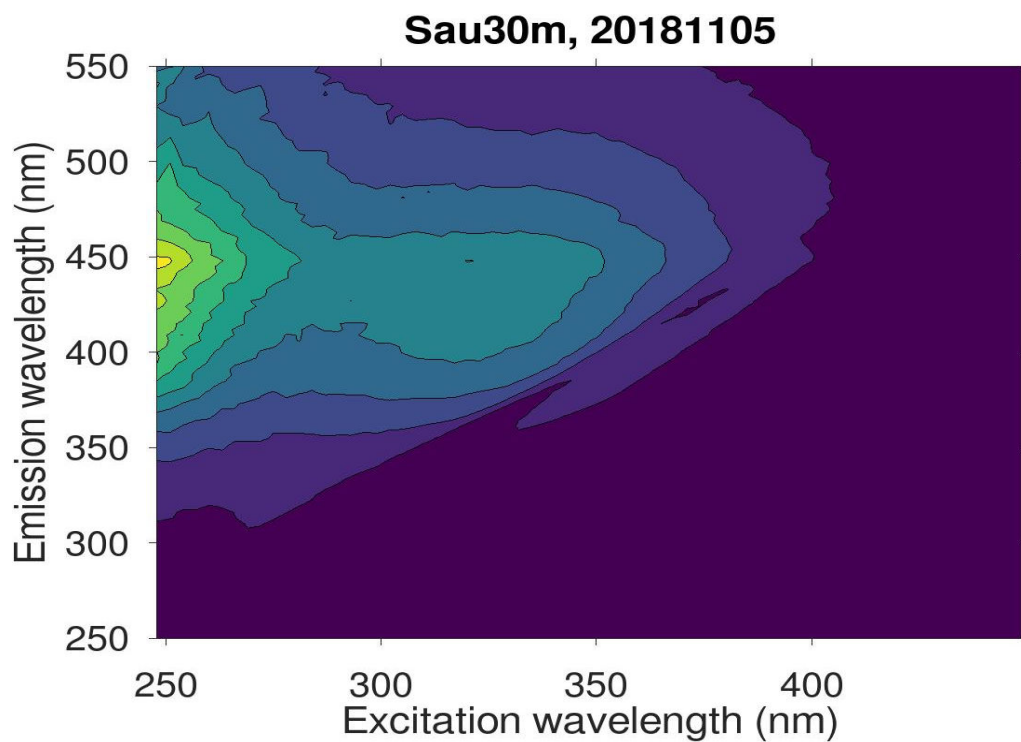
Supplementary Figure S15: Excitation-Emission matrix (EEM) for a sample collected from Ter River on 2019-07-12.



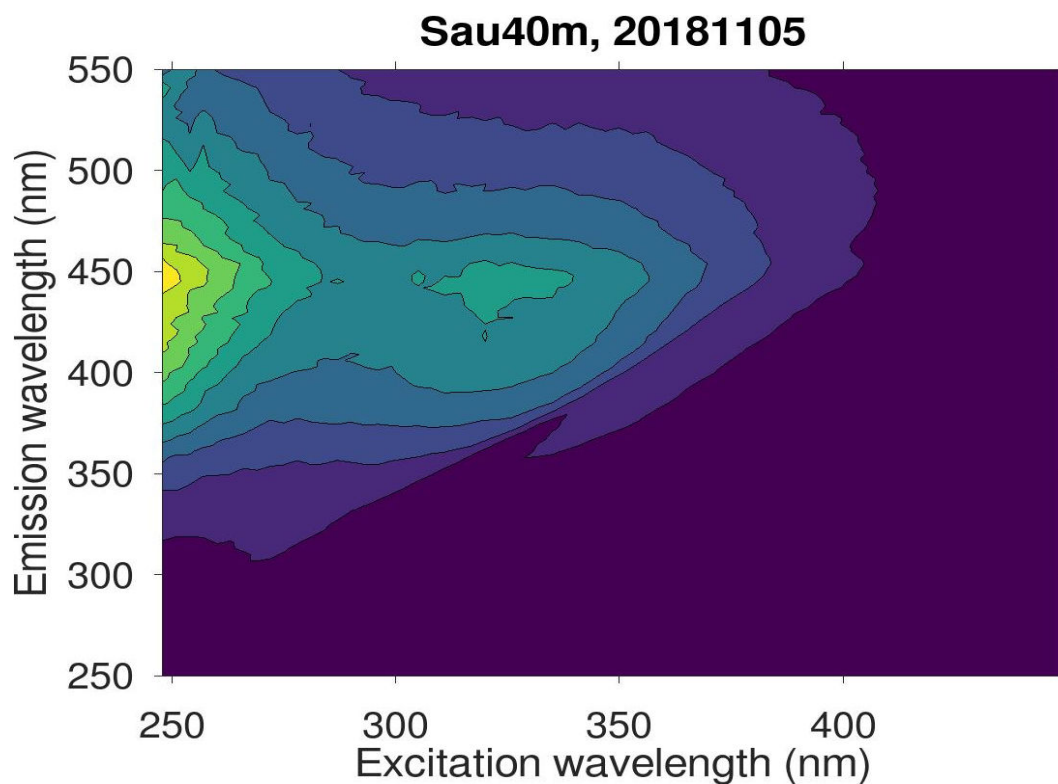
Supplementary Figure S16: Excitation-Emission matrix (EEM) for a sample collected from the surface of Sau Reservoir on 2018-11-05.



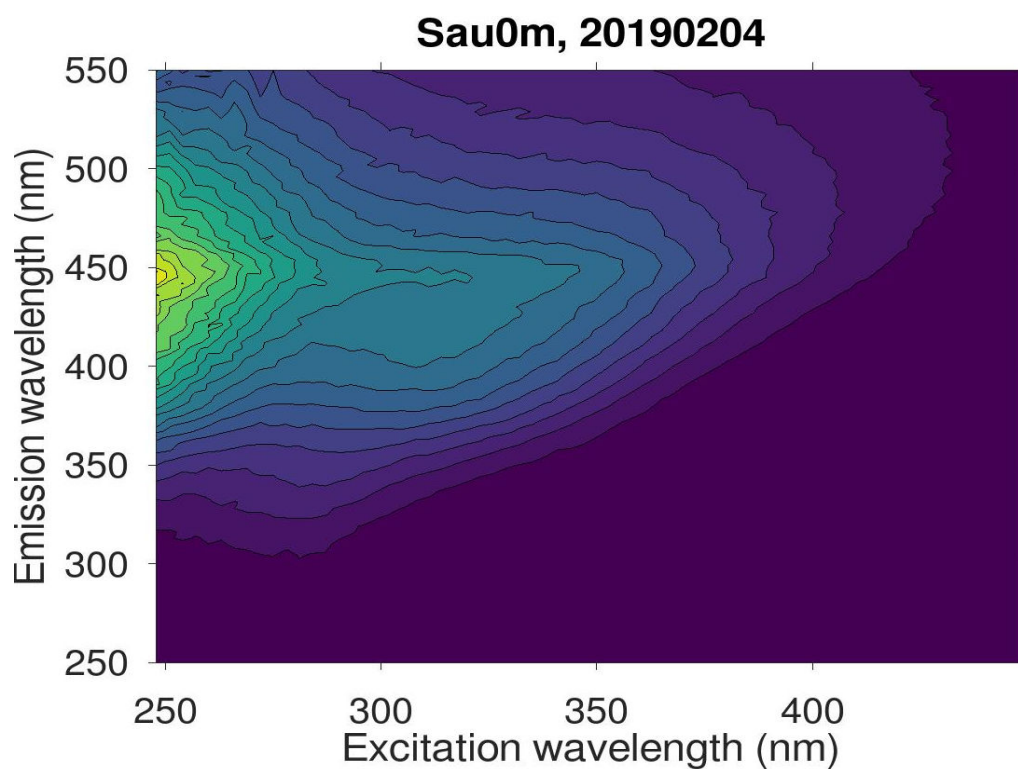
Supplementary Figure S17: Excitation-Emission matrix (EEM) for a sample collected at a depth of 15 m from the surface of Sau Reservoir on 2018-11-05.



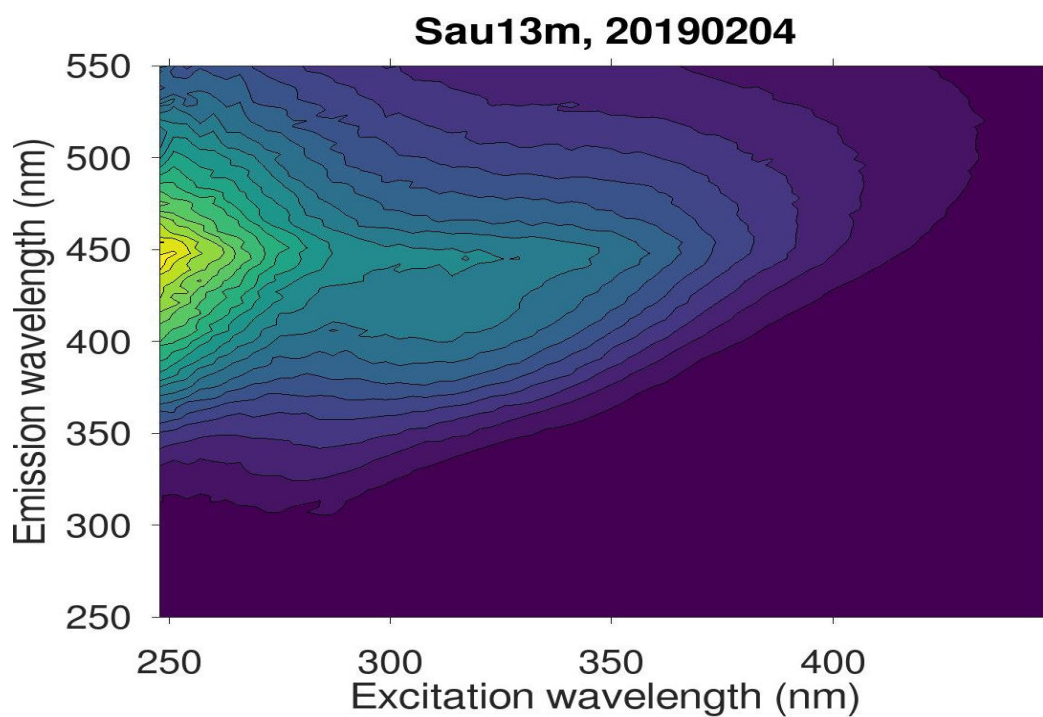
Supplementary Figure S18: Excitation-Emission matrix (EEM) for a sample collected at a depth of 30 m from the surface of Sau Reservoir on 2018-11-05.



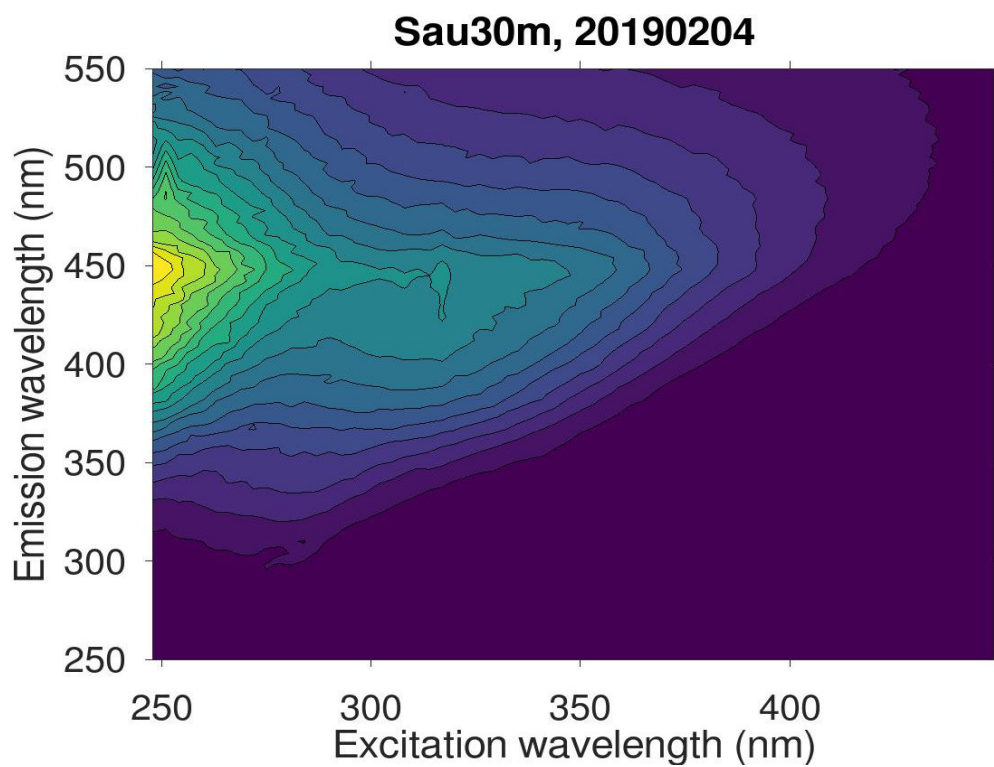
Supplementary Figure S19: Excitation-Emission matrix (EEM) for a sample collected at a depth of 40 m from the surface of Sau Reservoir on 2018-11-05.



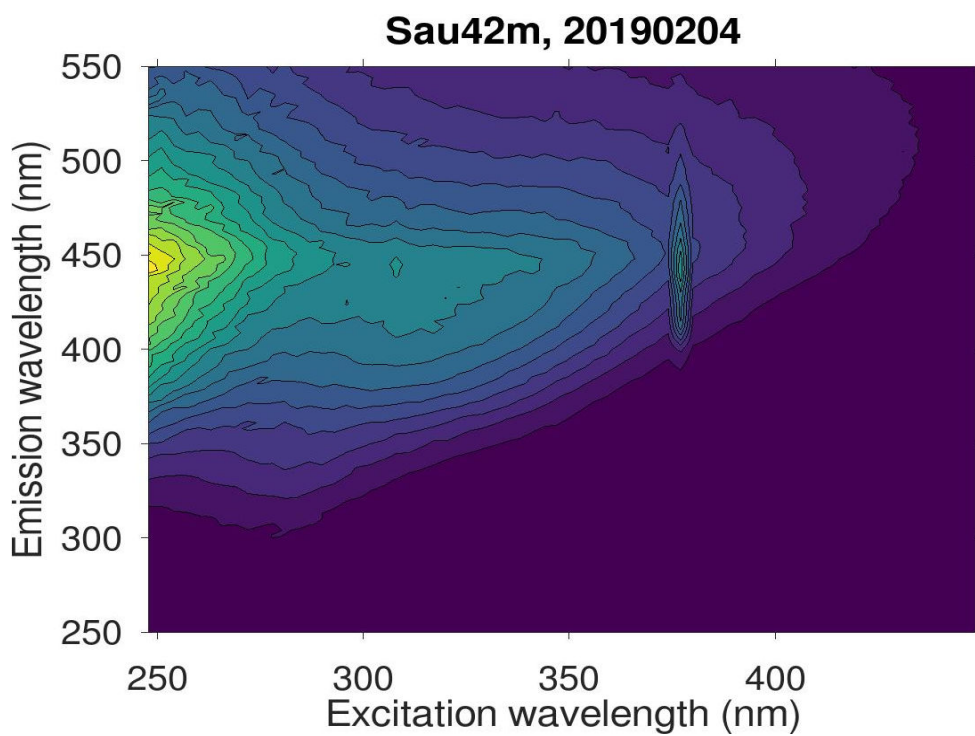
Supplementary Figure S20: Excitation-Emission matrix (EEM) for a sample collected from the surface of Sau Reservoir on 2019-02-04.



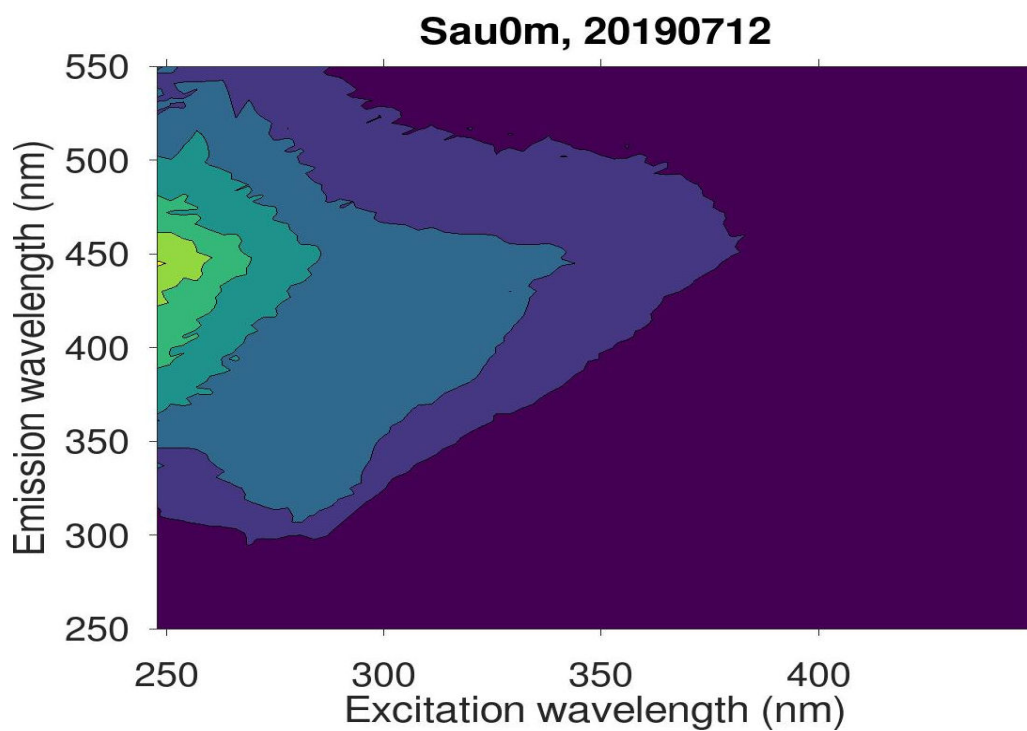
Supplementary Figure S21: Excitation-Emission matrix (EEM) for a sample collected at a depth of 13 m from the surface of Sau Reservoir on 2019-02-04.



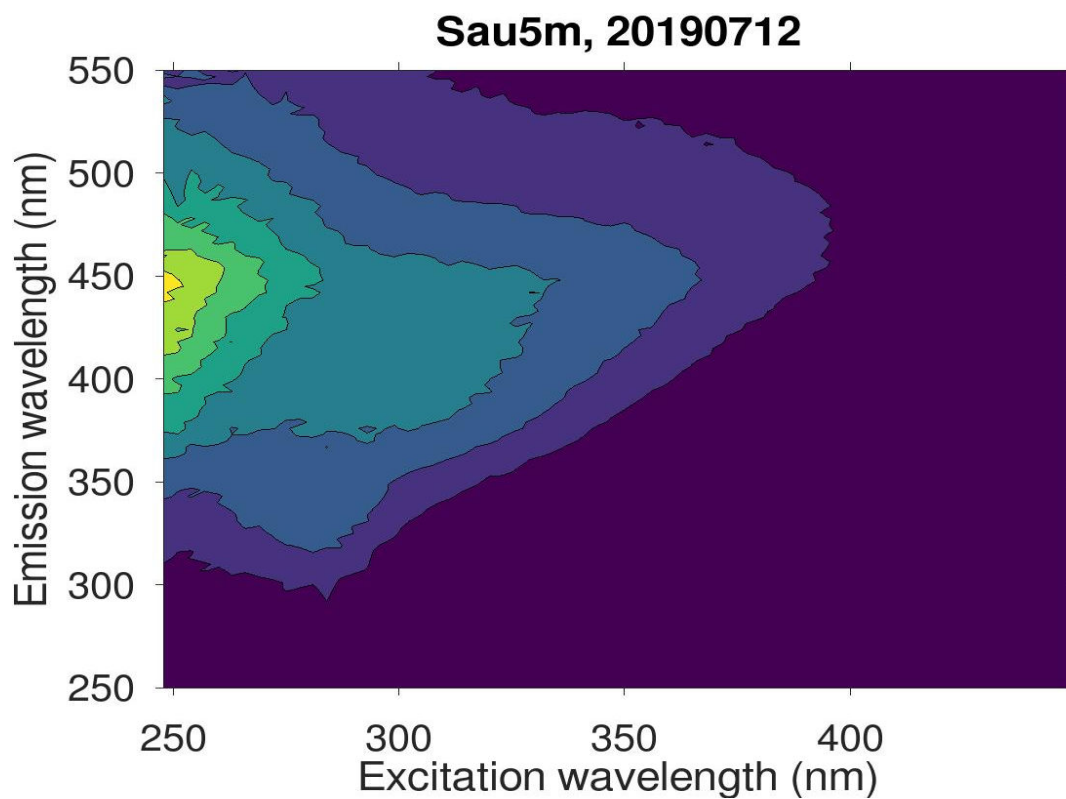
Supplementary Figure S22: Excitation-Emission matrix (EEM) for a sample collected at a depth of 30 m from the surface of Sau Reservoir on 2019-02-04.



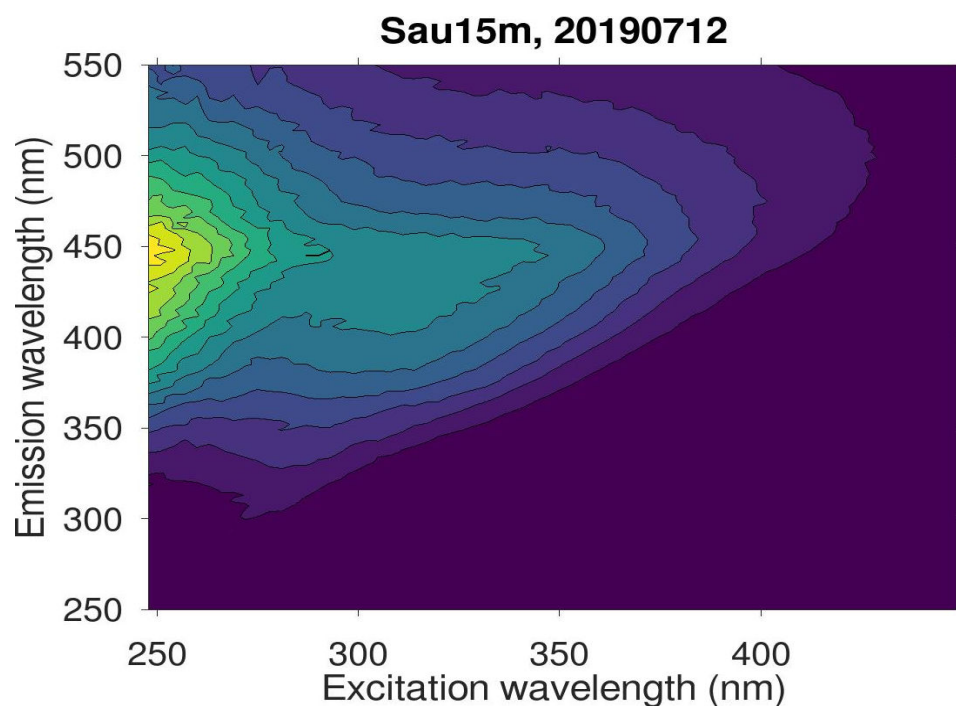
Supplementary Figure S23: Excitation-Emission matrix (EEM) for a sample collected at a depth of 42 m from the surface of Sau Reservoir on 2019-02-04.



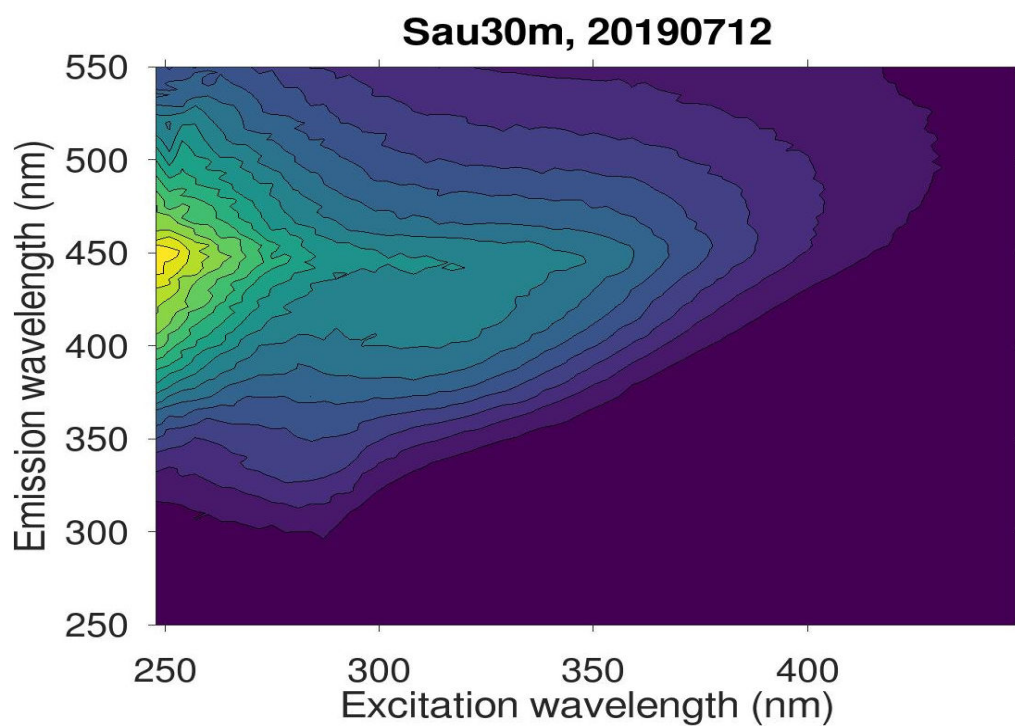
Supplementary Figure S24: Excitation-Emission matrix (EEM) for a sample collected from the surface of Sau Reservoir on 2019-07-12.



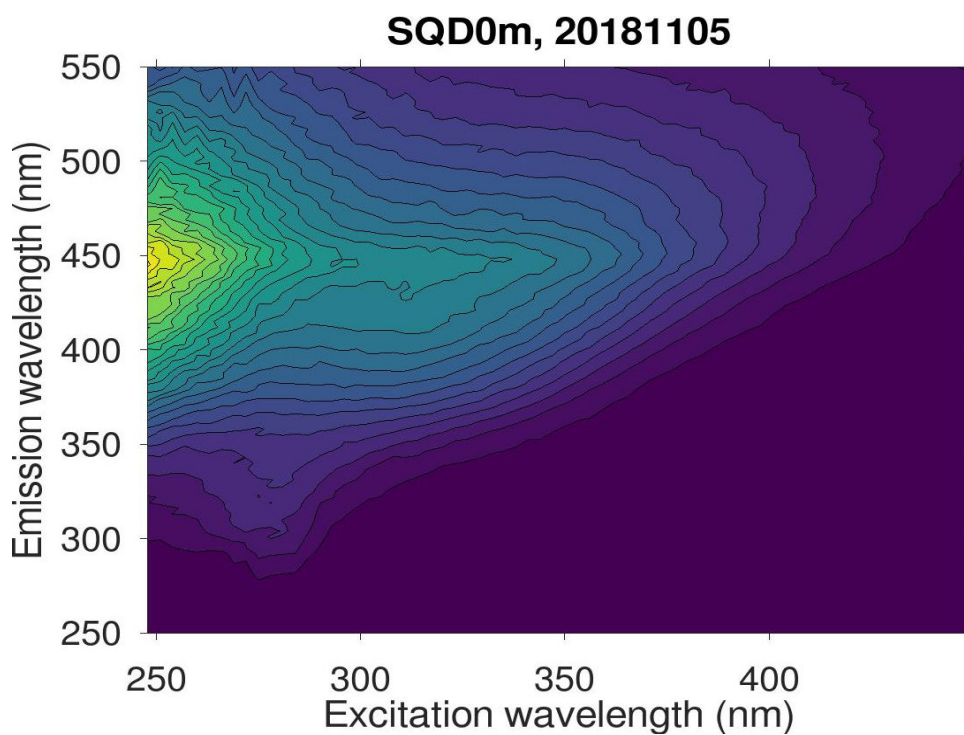
Supplementary Figure S25: Excitation-Emission matrix (EEM) for a sample collected at a depth of 5 m from the surface of Sau Reservoir on 2019-07-12.



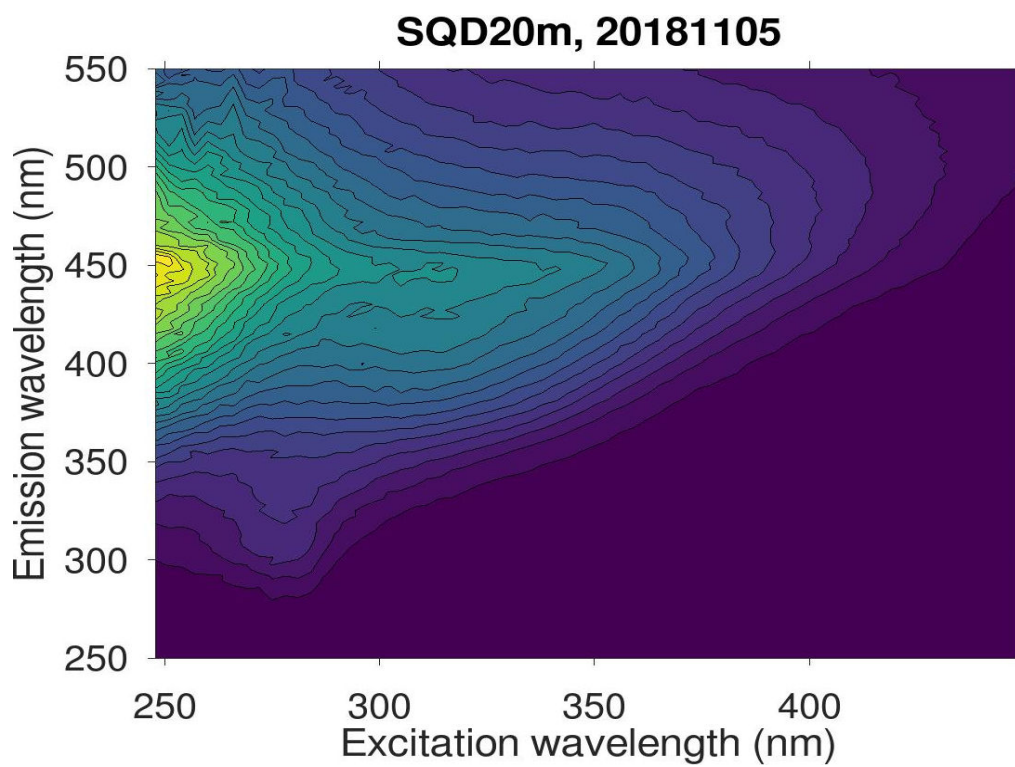
Supplementary Figure S26: Excitation-Emission matrix (EEM) for a sample collected at a depth of 15 m from the surface of Sau Reservoir on 2019-07-12.



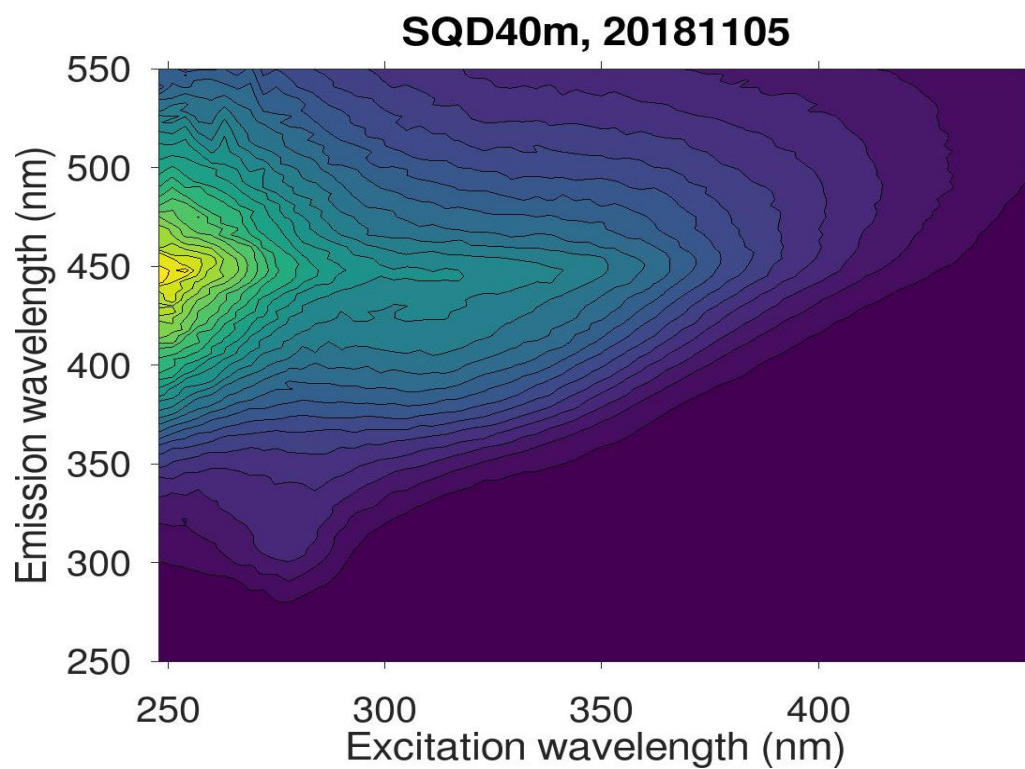
Supplementary Figure S27: Excitation-Emission matrix (EEM) for a sample collected at a depth of 15 m from the surface of Sau Reservoir on 2019-07-12.



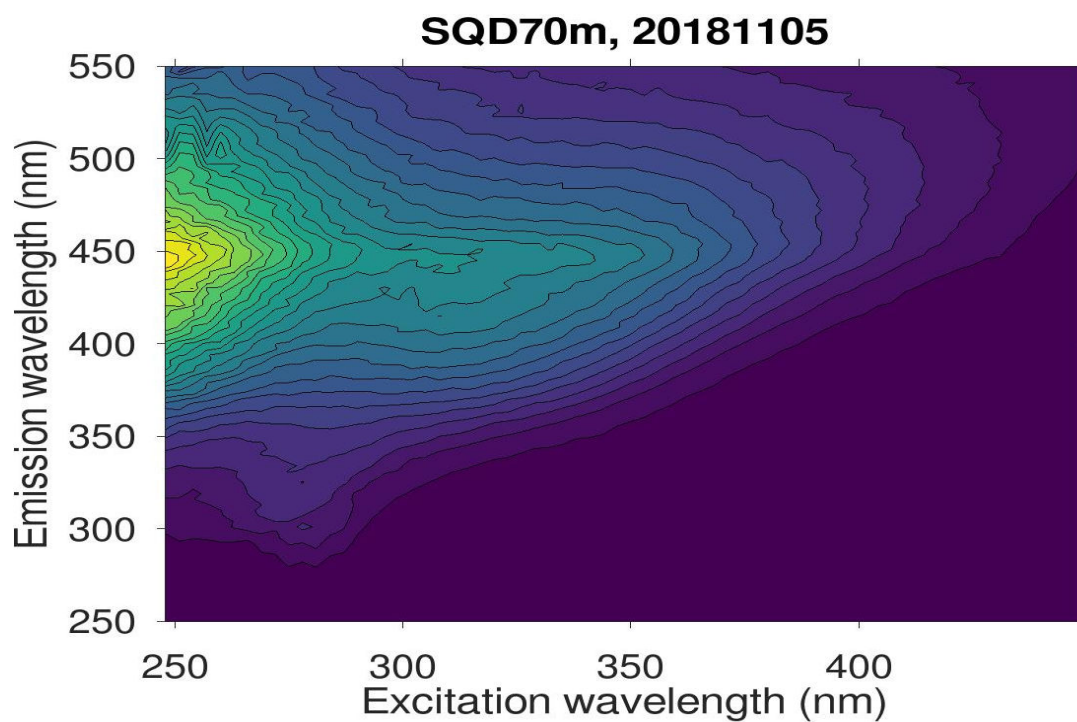
Supplementary Figure S28: Excitation-Emission matrix (EEM) for a sample collected from the surface of Susqueda Reservoir on 2018-11-05.



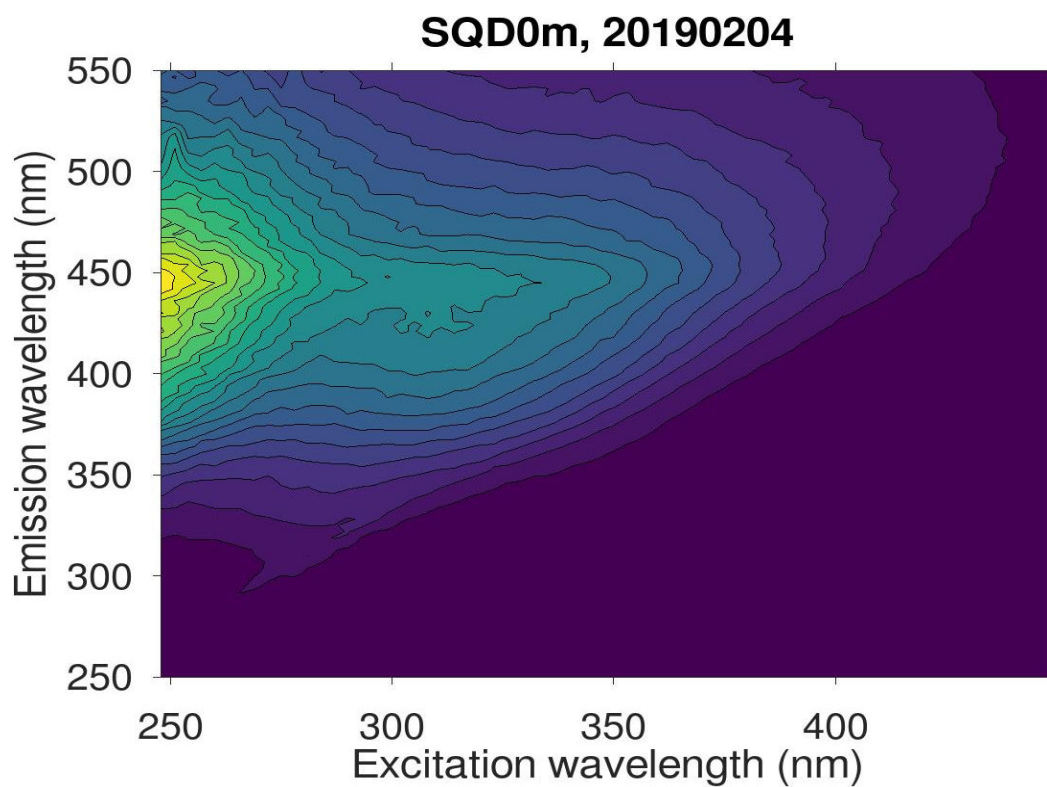
Supplementary Figure S29: Excitation-Emission matrix (EEM) for a sample collected at a depth of 20 m from the surface of Susqueda Reservoir on 2018-11-05.



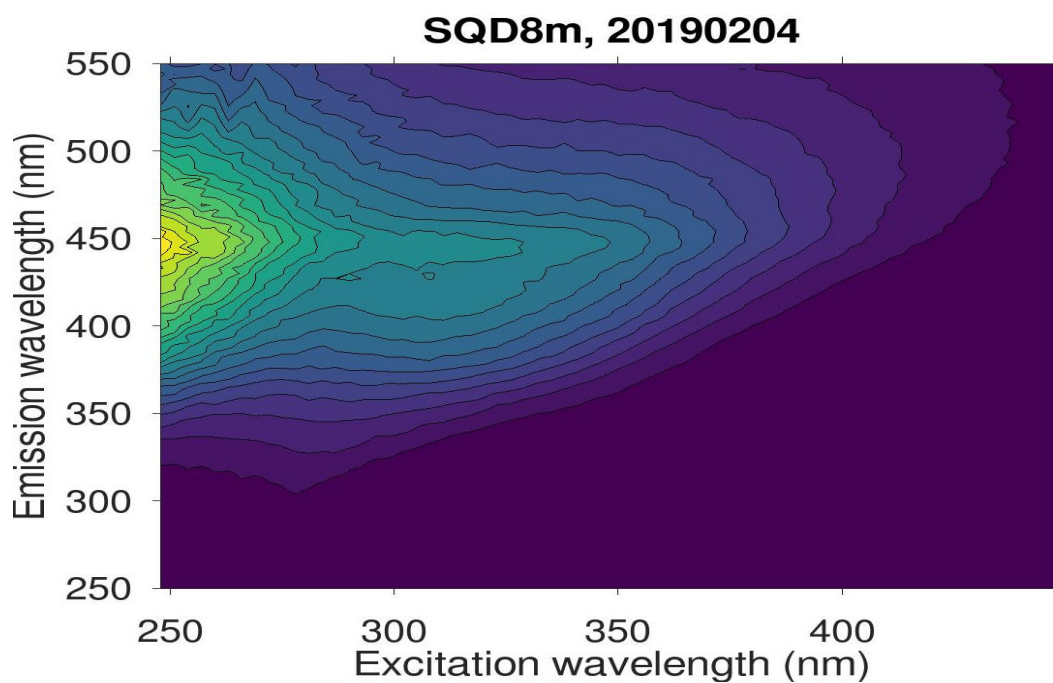
Supplementary Figure S30: Excitation-Emission matrix (EEM) for a sample collected at a depth of 40 m from the surface of Susqueda Reservoir on 2018-11-05.



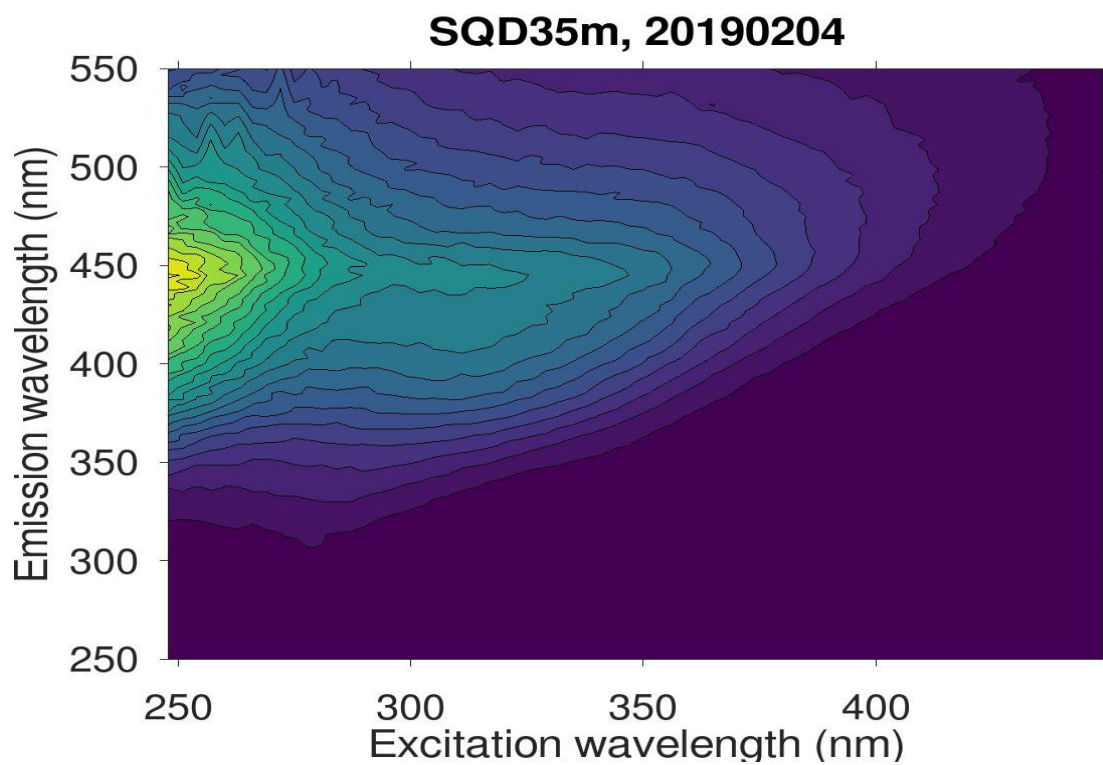
Supplementary Figure S31: Excitation-Emission matrix (EEM) for a sample collected at a depth of 70 m from the surface of Susqueda Reservoir on 2018-11-05.



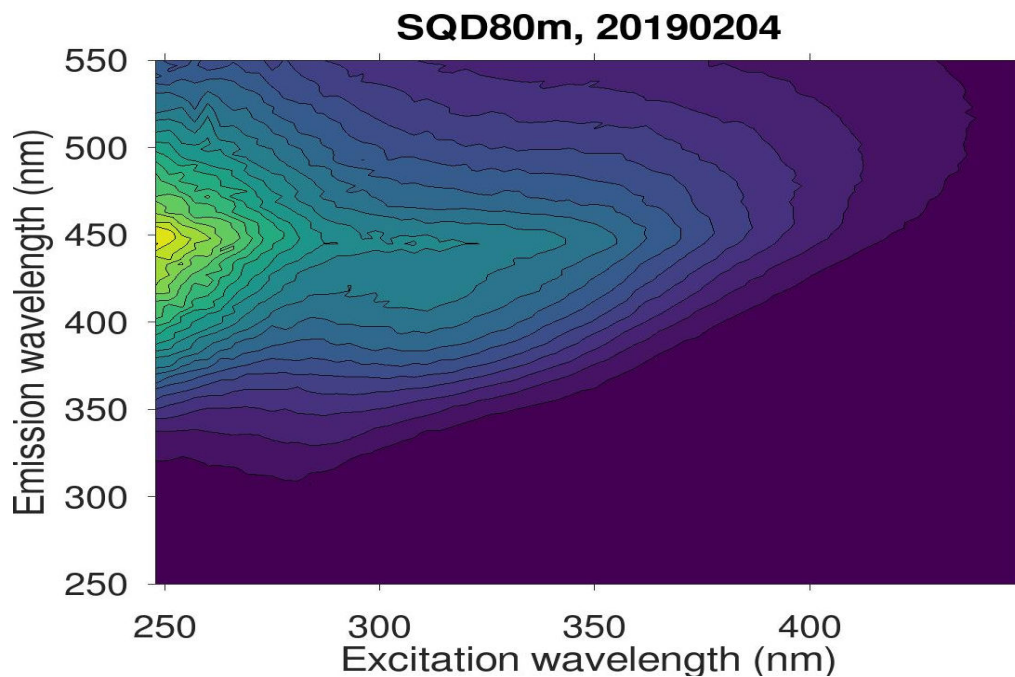
Supplementary Figure S32: Excitation-Emission matrix (EEM) for a sample collected from the surface of Susqueda Reservoir on 2019-02-04.



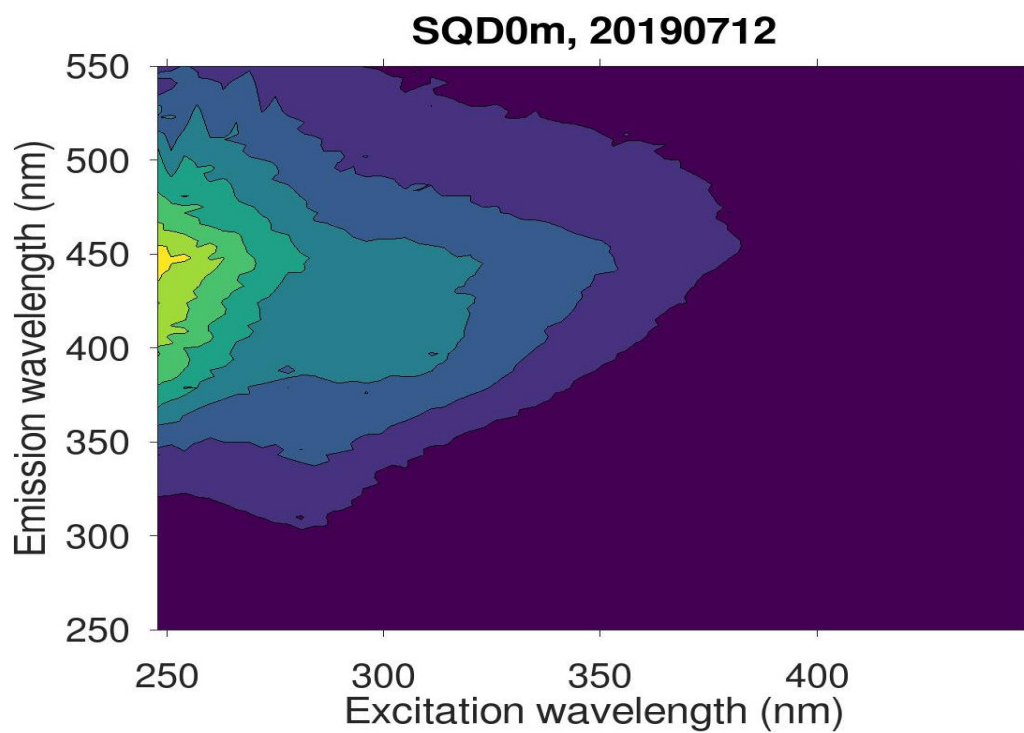
Supplementary Figure S33: Excitation-Emission matrix (EEM) for a sample collected at a depth of 8 m from the surface of Susqueda Reservoir on 2019-02-04.



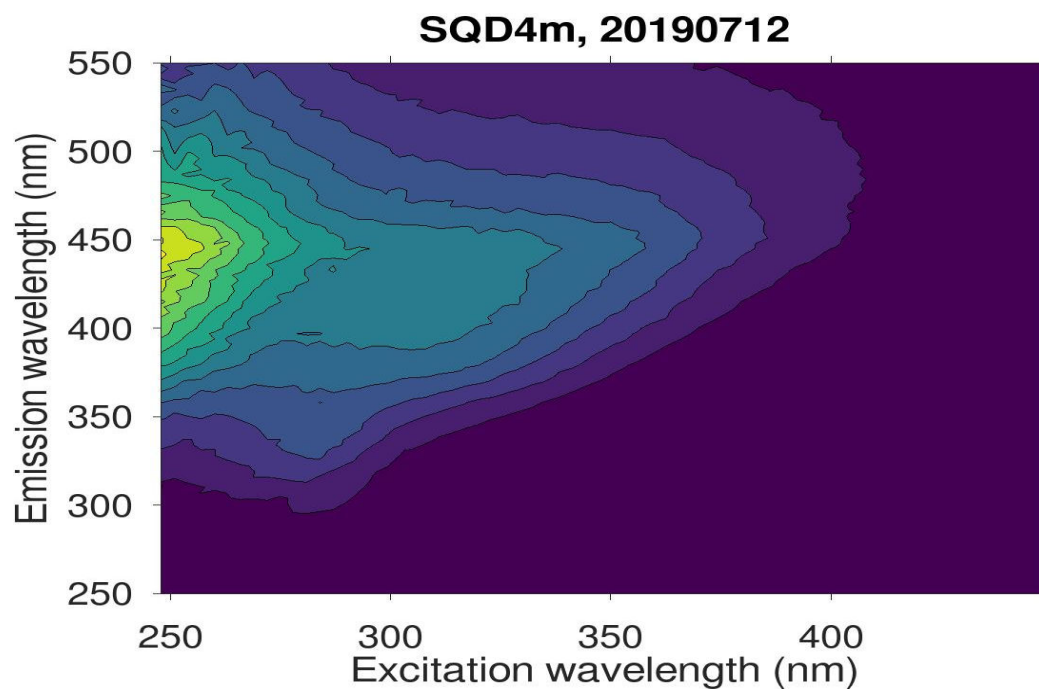
Supplementary Figure S34: Excitation-Emission matrix (EEM) for a sample collected at a depth of 35 m from the surface of Susqueda Reservoir on 2019-02-04.



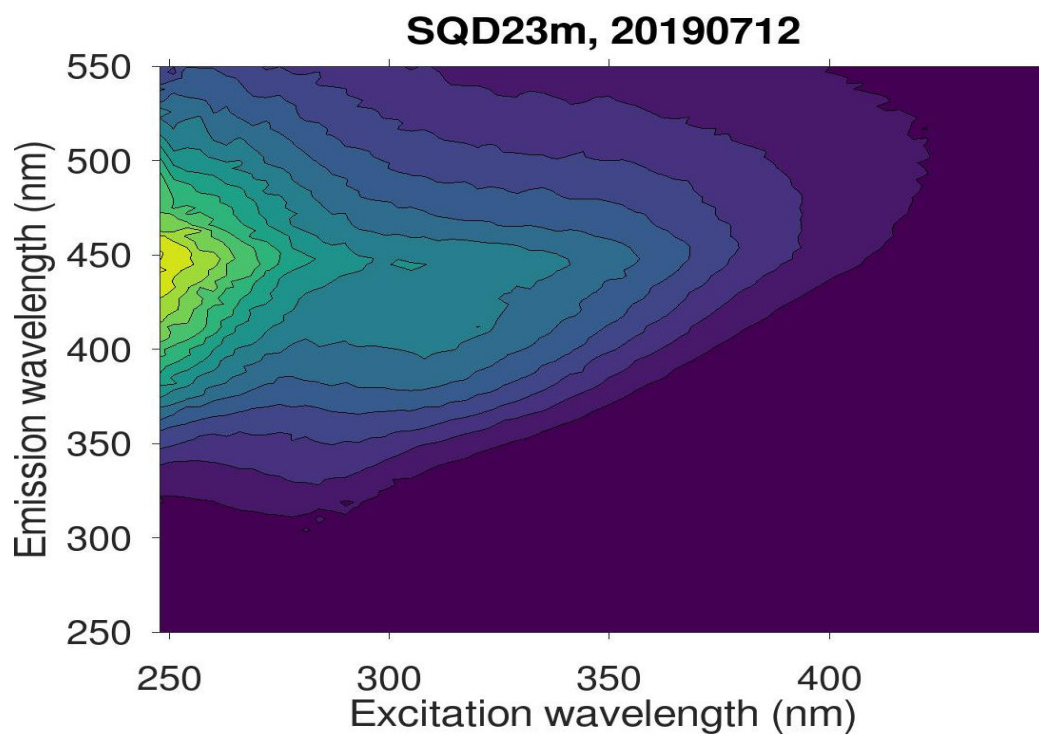
Supplementary Figure S35: Excitation-Emission matrix (EEM) for a sample collected at a depth of 80 m from the surface of Susqueda Reservoir on 2019-02-04.



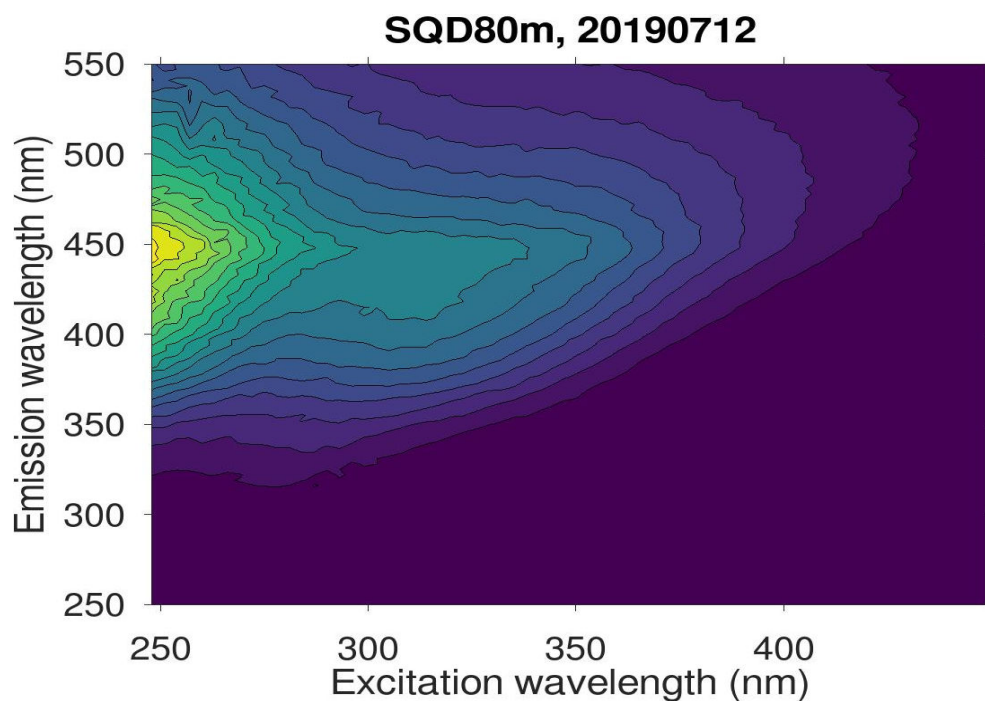
Supplementary Figure S36: Excitation-Emission matrix (EEM) for a sample collected from the surface of Susqueda Reservoir on 2019-07-12.



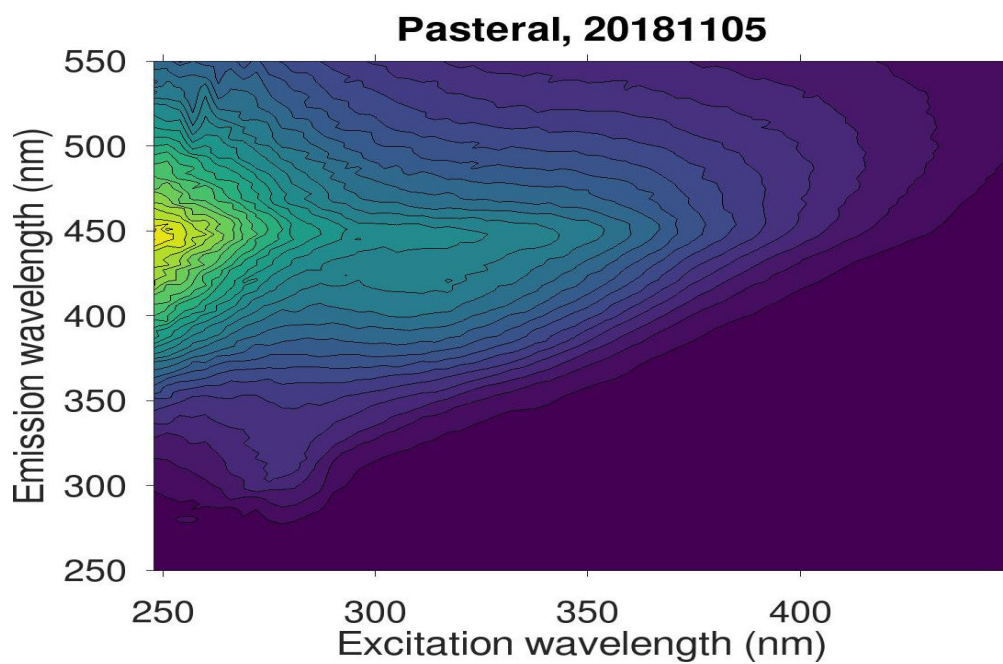
Supplementary Figure S37: Excitation-Emission matrix (EEM) for a sample collected at a depth of 4 m from the surface of Susqueda Reservoir on 2019-07-12.



Supplementary Figure S38: Excitation-Emission matrix (EEM) for a sample collected at a depth of 23 m from the surface of Susqueda Reservoir on 2019-07-12.

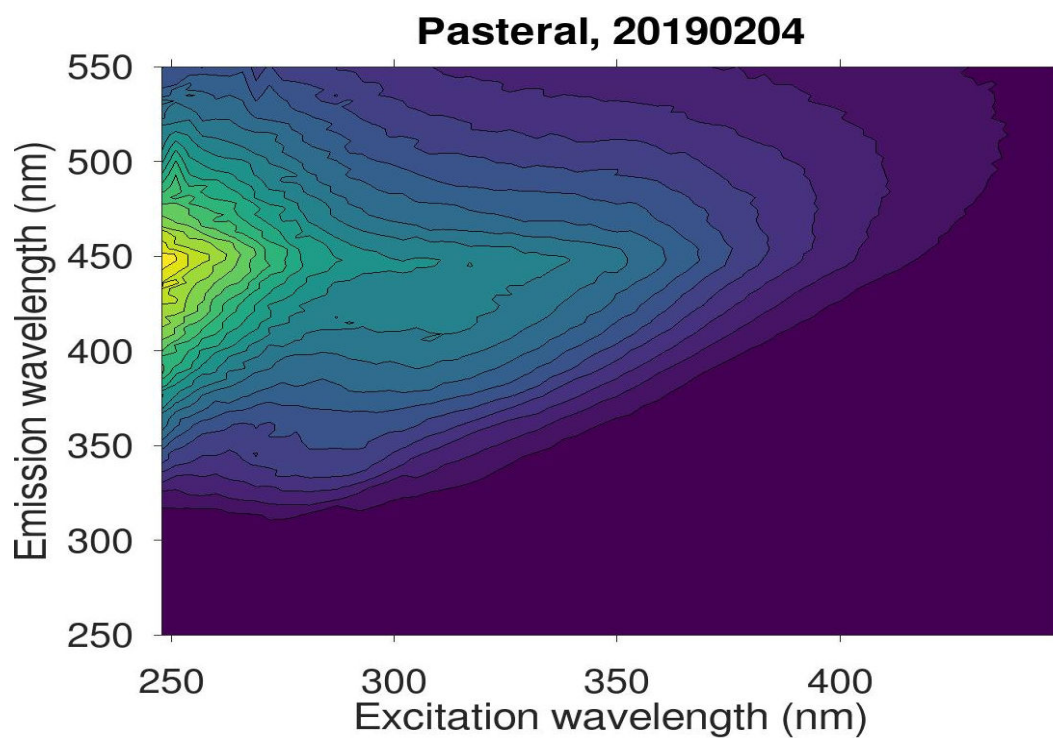


Supplementary Figure S39: Excitation-Emission matrix (EEM) for a sample collected at a depth of 80 m from the surface of Susqueda Reservoir on 2019-07-12.



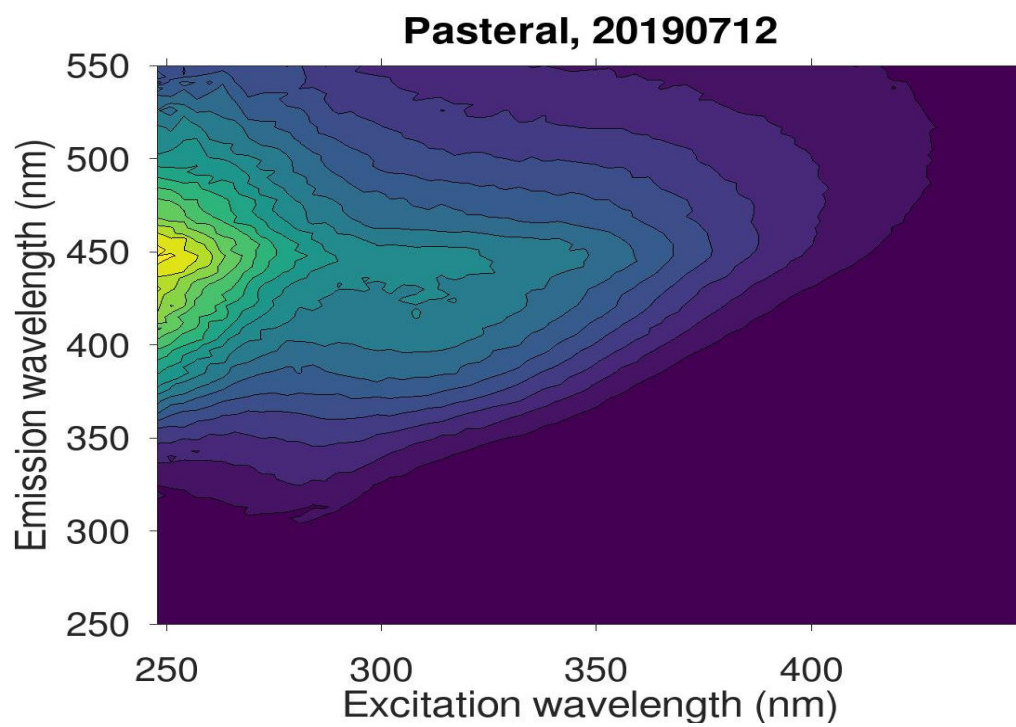
Supplementary Figure S40: Excitation-Emission matrix (EEM) for a sample collected from the surface of Pasteral

Reservoir on 2018-11-05.



Supplementary Figure S41: Excitation-Emission matrix (EEM) for a sample collected from the surface of Pasteral

Reservoir on 2019-02-04.



Supplementary Figure S42: Excitation-Emission matrix (EEM) for a sample collected from the surface of Pasteral Reservoir on 2019-07-12.

References

- 1 W. A. Mitch, A. C. Gerecke and D. L. Sedlak, A N-Nitrosodimethylamine (NDMA) precursor analysis for chlorination of water and wastewater, *Water Res.*, 2003, **37**, 3733–3741.
- 2 E. Bei, X. Li, F. Wu, S. Li, X. He, Y. Wang, Y. Qiu, Y. Wang, C. Wang, J. Wang, X. Zhang and C. Chen, Formation of N-nitrosodimethylamine precursors through the microbiological metabolism of nitrogenous substrates in water, *Water Res.*, 2020, **183**, 116055.
- 3 G. C. Woods and E. R. V. Dickenson, Natural attenuation of NDMA precursors in an urban, wastewater-dominated wash, *Water Res.*, 2016, **89**, 293–300.
- 4 E. Pehlivanoglu-Mantas and D. L. Sedlak, The fate of wastewater-derived NDMA precursors in the aquatic environment, *Water Res.*, 2006, **40**, 1287–1293.
- 5 M. J. Farré, S. Insa, J. Mamo and D. Barceló, Determination of ^{15}N - nitrosodimethylamine precursors in different water matrices by automated on-line solid- phase extraction ultra-high-performance-liquid chromatography tandem mass spectrometry, *J. Chromatogr. A*, , DOI:10.1016/j.chroma.2016.06.064.
- 6 P. Liu, M. J. Farré, J. Keller and W. Gernjak, Reducing natural organic matter and disinfection by-product precursors by alternating oxic and anoxic conditions during engineered short residence time riverbank filtration: A laboratory-scale column study, *Sci. Total Environ.*, 2016, **565**, 616–625.
- 7 A. Dotson and P. Westerhoff, Occurrence and removal of amino acids during drinking water treatment, *J. Am. Water Works Assoc.*, 2009, **101**, 101-+.
- 8 J. Sanchís, A. Jaén-Gil, P. Gago-Ferrero, E. Munthali and M. J. Farré, Characterization of organic matter by HRMS in surface waters: Effects of chlorination on molecular

References

7 References.

- Ahmadi, B., Ahmadalipour, A., Moradkhani, H., 2019. Hydrological drought persistence and recovery over the CONUS: A multi-stage framework considering water quantity and quality. *Water Res.* 150, 97–110. <https://doi.org/10.1016/j.watres.2018.11.052>
- Aiken, G.R., Hsu-Kim, H., Ryan, J.N., 2011. Influence of Dissolved Organic Matter on the Environmental Fate of Metals, Nanoparticles, and Colloids. *Environ. Sci. Technol.* 45, 3196–3201. <https://doi.org/10.1021/es103992s>
- Akoglu, H., 2018. User's guide to correlation coefficients. *Turk. J. Emerg. Med.* 18, 91–93. <https://doi.org/10.1016/j.tjem.2018.08.001>
- Alaba, P.A., Sani, Y.M., Olupinla, S.F., Daud, W.M.W., Mohammed, I.Y., Enweremadu, C.C., Ayodele, O.O., 2017. Toward N-nitrosamines free water: Formation, prevention, and removal. *Crit. Rev. Environ. Sci. Technol.* 47, 2448–2489. <https://doi.org/10.1080/10643389.2018.1430438>
- Alansari, A., Amburgey, J., 2020. Critical elements of flocculation in drinking water treatment. *AWWA Water Sci.* 2, e1213. <https://doi.org/10.1002/aws2.1213>
- Aldridge, K., 2011. Impact of a drought on nutrient concentrations in the Lower Lakes (Murray Darling Basin, Australia). *Inland Waters* 1, 159–176. <https://doi.org/10.5268/IW-1.3.409>
- Alexander, T.J., Vonlanthen, P., Seehausen, O., 2017. Does eutrophication-driven evolution change aquatic ecosystems? *Philos. Trans. R. Soc. B Biol. Sci.* 372, 20160041. <https://doi.org/10.1098/rstb.2016.0041>
- Alver, A., 2019. Evaluation of conventional drinking water treatment plant efficiency according to water quality index and health risk assessment. *Environ. Sci. Pollut. Res.* 26, 27225–27238. <https://doi.org/10.1007/s11356-019-05801-y>
- Amaral, V., Ortega, T., Romera-Castillo, C., Forja, J., 2021. Linkages between greenhouse gases (CO₂, CH₄, and N₂O) and dissolved organic matter composition in a shallow estuary. *Sci. Total Environ.* 788, 147863. <https://doi.org/10.1016/j.scitotenv.2021.147863>
- Ang, W.L., Mohammad, A.W., 2020. State of the art and sustainability of natural coagulants in water and wastewater treatment. *J. Clean. Prod.* 262, 121267. <https://doi.org/10.1016/j.jclepro.2020.121267>
- Ansari, A.A., Gill, S.S., Khan, F.A., 2010. Eutrophication: Threat to Aquatic Ecosystems, in: Ansari, A.A., Singh Gill, S., Lanza, G.R., Rast, W. (Eds.), *Eutrophication: Causes,*

References

- Consequences and Control. Springer Netherlands, Dordrecht, pp. 143–170. https://doi.org/10.1007/978-90-481-9625-8_7
- Antony, R., Willoughby, A.S., Grannas, A.M., Catanzano, V., Sleighter, R.L., Thamban, M., Hatcher, P.G., Nair, S., 2017. Molecular Insights on Dissolved Organic Matter Transformation by Supraglacial Microbial Communities. *Environ. Sci. Technol.* 51, 4328–4337. <https://doi.org/10.1021/acs.est.6b05780>
- Armstrong, M., Zhan, Q., Munthali, E., Jin, H., Teurlincx, S., Peters, P., Lüring, M., De Senerpont Domis, L.N., 2023. Stressors in a bottle: A microcosm study on phytoplankton assemblage response to extreme precipitation events under climate warming. *Freshw. Biol.* fwb.14109. <https://doi.org/10.1111/fwb.14109>
- Arnoldi, J.-F., Loreau, M., Haegeman, B., 2016. Resilience, reactivity and variability: A mathematical comparison of ecological stability measures. *J. Theor. Biol.* 389, 47–59. <https://doi.org/10.1016/j.jtbi.2015.10.012>
- Augsburger, N., Rachmadi, A.T., Zaouri, N., Lee, Y., Hong, P.-Y., 2021. Recent Update on UV Disinfection to Fulfill the Disinfection Credit Value for Enteric Viruses in Water. *Environ. Sci. Technol.* 55, 16283–16298. <https://doi.org/10.1021/acs.est.1c03092>
- Aydin, E., Yaman, F.B., Genceli, E.A., Topuz, E., Erdim, E., Gurel, M., Ipek, M., Pehlivanoglu-Mantas, E., 2012. Occurrence of THM and NDMA precursors in a watershed: Effect of seasons and anthropogenic pollution. *J. Hazard. Mater.* 221, 86–91. <https://doi.org/10.1016/j.jhazmat.2012.04.012>
- Bachiller, A.R., Rodríguez, J.L.G., Sánchez, J.C.R., Gómez, D.L., 2019. Specific sediment yield model for reservoirs with medium-sized basins in Spain: An empirical and statistical approach. *Sci. Total Environ.* 681, 82–101. <https://doi.org/10.1016/j.scitotenv.2019.05.029>
- Bahramian, P., Saliminezhad, A., 2020. On the relationship between export and economic growth: A nonparametric causality-in-quantiles approach for Turkey. *J. Int. Trade Econ. Dev.* 29, 131–145. <https://doi.org/10.1080/09638199.2019.1648537>
- Balcilar, M., Bekiros, S., Gupta, R., 2017a. The role of news-based uncertainty indices in predicting oil markets: a hybrid nonparametric quantile causality method. *Empir. Econ.* 53, 879–889. <https://doi.org/10.1007/s00181-016-1150-0>
- Balcilar, M., Gupta, R., Kyei, C., Wohar, M.E., 2016a. Does Economic Policy Uncertainty Predict Exchange Rate Returns and Volatility? Evidence from a Nonparametric Causality-in-Quantiles Test. *Open Econ. Rev.* 27, 229–250. <https://doi.org/10.1007/s11079-016-9388-x>

References

- Balcilar, M., Gupta, R., Pierdzioch, C., 2016b. Does uncertainty move the gold price? New evidence from a nonparametric causality-in-quantiles test. *Resour. Policy* 49, 74–80. <https://doi.org/10.1016/j.resourpol.2016.04.004>
- Balcilar, M., Gupta, R., Pierdzioch, C., Wohar, M.E., 2017b. Do terror attacks affect the dollar-pound exchange rate? A nonparametric causality-in-quantiles analysis. *North Am. J. Econ. Finance* 41, 44–56. <https://doi.org/10.1016/j.najef.2017.03.010>
- Banks, J.L., Ross, D.J., Keough, M.J., Eyre, B.D., Macleod, C.K., 2012. Measuring hypoxia induced metal release from highly contaminated estuarine sediments during a 40day laboratory incubation experiment. *Sci. Total Environ.* 420, 229–237. <https://doi.org/10.1016/j.scitotenv.2012.01.033>
- Bao, Y., Huang, T., Ning, C., Sun, T., Tao, P., Wang, J., Sun, Q., 2023. Changes of DOM and its correlation with internal nutrient release during cyanobacterial growth and decline in Lake Chaohu, China. *J. Environ. Sci.* 124, 769–781. <https://doi.org/10.1016/j.jes.2022.02.019>
- Barceló, D. (Ed.), 2012. *Emerging Organic Contaminants and Human Health, The Handbook of Environmental Chemistry*. Springer Berlin Heidelberg, Berlin, Heidelberg. <https://doi.org/10.1007/978-3-642-28132-7>
- Barriopedro, D., García-Herrera, R., Ordóñez, C., Miralles, D.G., Salcedo-Sanz, S., 2023. Heat Waves: Physical Understanding and Scientific Challenges. *Rev. Geophys.* 61, e2022RG000780. <https://doi.org/10.1029/2022RG000780>
- Barry, M., Chiu, C., Westerhoff, P., 2016. Severe Weather Effects on Water Quality in Central Arizona. *J. AWWA* 108. <https://doi.org/10.5942/jawwa.2016.108.0027>
- Beaudeau, P., Pascal, M., Mouly, D., Galey, C., Thomas, O., 2011. Health risks associated with drinking water in a context of climate change in France: a review of surveillance requirements. *J. Water Clim. Change* 2, 230–246. <https://doi.org/10.2166/wcc.2011.010>
- Beaulieu, J.J., DelSontro, T., Downing, J.A., 2019. Eutrophication will increase methane emissions from lakes and impoundments during the 21st century. *Nat. Commun.* 10, 1375. <https://doi.org/10.1038/s41467-019-09100-5>
- Becker, V., Caputo, L., Ordóñez, J., Marcé, R., Armengol, J., Crossetti, L.O., Huszar, V.L.M., 2010. Driving factors of the phytoplankton functional groups in a deep Mediterranean reservoir. *Water Res.* 44, 3345–3354. <https://doi.org/10.1016/j.watres.2010.03.018>
- Begum, M.S., Park, J.-H., Yang, L., Shin, K.H., Hur, J., 2023. Optical and molecular indices of dissolved organic matter for estimating biodegradability and resulting carbon dioxide

References

- production in inland waters: A review. *Water Res.* 228, 119362. <https://doi.org/10.1016/j.watres.2022.119362>
- Benítez-Gilabert, M., Alvarez-Cobelas, M., Angeler, D.G., 2010. Effects of climatic change on stream water quality in Spain. *Clim. Change* 103, 339–352. <https://doi.org/10.1007/s10584-009-9778-9>
- Benotti, M.J., Stanford, B.D., Snyder, S.A., 2010. Impact of Drought on Wastewater Contaminants in an Urban Water Supply. *J. Environ. Qual.* 39, 1196–1200. <https://doi.org/10.2134/jeq2009.0072>
- Berggren, M., Guillemette, F., Bieroza, M., Buffam, I., Deininger, A., Hawkes, J.A., Kothawala, D.N., LaBrie, R., Lapierre, J., Murphy, K.R., Al-Kharusi, E.S., Rulli, M.P.D., Hensgens, G., Younes, H., Wünsch, U.J., 2022. Unified understanding of intrinsic and extrinsic controls of dissolved organic carbon reactivity in aquatic ecosystems. *Ecology* 103. <https://doi.org/10.1002/ecy.3763>
- Bertani, I., Primicerio, R., Rossetti, G., 2016. Extreme Climatic Event Triggers a Lake Regime Shift that Propagates Across Multiple Trophic Levels. *Ecosystems* 19, 16–31. <https://doi.org/10.1007/s10021-015-9914-5>
- Bertone, E., Sahin, O., Richards, R., Roiko, A., 2016. Extreme events, water quality and health: A participatory Bayesian risk assessment tool for managers of reservoirs. *J. Clean. Prod.* 135, 657–667. <https://doi.org/10.1016/j.jclepro.2016.06.158>
- Binford, M.W., Kolata, A.L., Brenner, M., Janusek, J.W., Seddon, M.T., Abbott, M., Curtis, J.H., 1997. Climate Variation and the Rise and Fall of an Andean Civilization. *Quat. Res.* 47, 235–248. <https://doi.org/10.1006/qres.1997.1882>
- Blagrave, K., Moslenko, L., Khan, U.T., Benoit, N., Howell, T., Sharma, S., 2022. Heatwaves and storms contribute to degraded water quality conditions in the nearshore of Lake Ontario. *J. Gt. Lakes Res.* 48, 903–913. <https://doi.org/10.1016/j.jglr.2022.04.008>
- Boholm, Å., Prutzer, M., 2017. Experts' understandings of drinking water risk management in a climate change scenario. *Clim. Risk Manag.* 16, 133–144. <https://doi.org/10.1016/j.crm.2017.01.003>
- Bond, N.R., Lake, P.S., Arthington, A.H., 2008. The impacts of drought on freshwater ecosystems: an Australian perspective. *Hydrobiologia* 600, 3–16. <https://doi.org/10.1007/s10750-008-9326-z>
- Bond, T., 2012. Precursors of nitrogenous disinfection by-products in drinking water—A critical review and analysis. *J. Hazard. Mater.* 16.

References

- Bond, T., Huang, J., Templeton, M.R., Graham, N., 2011. Occurrence and control of nitrogenous disinfection by-products in drinking water – A review. *Water Res.* 45, 4341–4354. <https://doi.org/10.1016/j.watres.2011.05.034>
- Bond, T., Simperler, A., Graham, N., Ling, L., Gan, W., Yang, X., Templeton, M.R., 2017. Defining the molecular properties of N-nitrosodimethylamine (NDMA) precursors using computational chemistry. *Environ. Sci. Water Res. Technol.* 3, 502–512. <https://doi.org/10.1039/C7EW00068E>
- Botturi, A., Ozbayram, E.G., Tondera, K., Gilbert, N.I., Rouault, P., Caradot, N., Gutierrez, O., Daneshgar, S., Frison, N., Akyol, Ç., Foglia, A., Eusebi, A.L., Fatone, F., 2021. Combined sewer overflows: A critical review on best practice and innovative solutions to mitigate impacts on environment and human health. *Crit. Rev. Environ. Sci. Technol.* 51, 1585–1618. <https://doi.org/10.1080/10643389.2020.1757957>
- Boyd, J.M., Hruday, S.E., Li, X.-F., Richardson, S.D., 2011. Solid-phase extraction and high-performance liquid chromatography mass spectrometry analysis of nitrosamines in treated drinking water and wastewater. *TrAC Trends Anal. Chem.* 30, 1410–1421. <https://doi.org/10.1016/j.trac.2011.06.009>
- Braga, G.G., Becker, V., Oliveira, J.N.P.D., Mendonça Junior, J.R.D., Bezerra, A.F.D.M., Torres, L.M., Galvão, Â.M.F., Mattos, A., 2015. Influence of extended drought on water quality in tropical reservoirs in a semiarid region. *Acta Limnol. Bras.* 27, 15–23. <https://doi.org/10.1590/S2179-975X2214>
- Brandt, M.J., Johnson, K.M., Elphinston, A.J., Ratnayaka, D.D., 2017. Water Filtration, in: Twort's Water Supply. Elsevier, pp. 367–406. <https://doi.org/10.1016/B978-0-08-100025-0.00009-0>
- Brasil, J., Attayde, J.L., Vasconcelos, F.R., Dantas, D.D.F., Huszar, V.L.M., 2016. Drought-induced water-level reduction favors cyanobacteria blooms in tropical shallow lakes. *Hydrobiologia* 770, 145–164. <https://doi.org/10.1007/s10750-015-2578-5>
- Brauman, K.A., Daily, G.C., Duarte, T.K., Mooney, H.A., 2007. The Nature and Value of Ecosystem Services: An Overview Highlighting Hydrologic Services. *Annu. Rev. Environ. Resour.* 32, 67–98. <https://doi.org/10.1146/annurev.energy.32.031306.102758>
- Bruce, D., Westerhoff, P., Brawley-Chesworth, A., 2002. Removal of 2-methylisoborneol and geosmin in surface water treatment plants in Arizona. *J. Water Supply Res. Technol.-Aqua* 51, 183–198. <https://doi.org/10.2166/aqua.2002.0016>

References

- Brusseau, M.L., Walker, D.B., Fitzsimmons, K., 2019. Physical-Chemical Characteristics of Water, in: Environmental and Pollution Science. Elsevier, pp. 23–45. <https://doi.org/10.1016/B978-0-12-814719-1.00003-3>
- Bukaveckas, P.A., McGaha, D., Shostell, J.M., Schultz, R., Jack, J.D., 2007. Internal and external sources of THM precursors in a midwestern reservoir. *J. Am. Water Works Assoc.* 99, 127–136. <https://doi.org/10.1002/j.1551-8833.2007.tb07933.x>
- Burnet, J.-B., Sylvestre, É., Jalbert, J., Imbeault, S., Servais, P., Prévost, M., Dorner, S., 2019. Tracking the contribution of multiple raw and treated wastewater discharges at an urban drinking water supply using near real-time monitoring of β -d-glucuronidase activity. *Water Res.* 164, 114869. <https://doi.org/10.1016/j.watres.2019.114869>
- Bush, T., Diao, M., Allen, R.J., Sinnige, R., Muyzer, G., Huisman, J., 2017. Oxic-anoxic regime shifts mediated by feedbacks between biogeochemical processes and microbial community dynamics. *Nat. Commun.* 8, 789. <https://doi.org/10.1038/s41467-017-00912-x>
- Cai, Y., Sun, T., Li, G., An, T., 2021. Traditional and Emerging Water Disinfection Technologies Challenging the Control of Antibiotic-Resistant Bacteria and Antibiotic Resistance Genes. *ACS EST Eng.* 1, 1046–1064. <https://doi.org/10.1021/acsestengg.1c00110>
- Campbell, S., Remenyi, T.A., White, C.J., Johnston, F.H., 2018. Heatwave and health impact research: A global review. *Health Place* 53, 210–218. <https://doi.org/10.1016/j.healthplace.2018.08.017>
- Cancho, B., Ventura, F., Galceran, T., 2000. Simultaneous determination of cyanogen chloride and cyanogen bromide in treated water at sub-mg / L levels by a new solid-phase microextraction–gas chromatographic–electron-capture detection method. *J Chromatogr A*.
- Caplanne, S., Laurion, I., 2008. Effect of chromophoric dissolved organic matter on epilimnetic stratification in lakes. *Aquat. Sci.* 70, 123–133. <https://doi.org/10.1007/s00027-007-7006-0>
- Carey, C., Alexander, M.A., 2003. Climate change and amphibian declines: is there a link? *Divers. Distrib.* 9, 111–121. <https://doi.org/10.1046/j.1472-4642.2003.00011.x>
- Casas-Ruiz, J.P., Tittel, J., von Schiller, D., Catalán, N., Obrador, B., Gómez-Gener, L., Zwirnmann, E., Sabater, S., Marcé, R., 2016. Drought-induced discontinuities in the source and degradation of dissolved organic matter in a Mediterranean river. *Biogeochemistry* 127, 125–139. <https://doi.org/10.1007/s10533-015-0173-5>

References

- Cerón-Vivas, A., Villamizar León, M.P., Cajigas, Á.A., 2023. Geosmin and 2-methylisoborneol removal in drinking water treatment. *Water Pract. Technol.* 18, 159–167. <https://doi.org/10.2166/wpt.2022.167>
- Chang, E.E., Chiang, P.-C., Ko, Y.-W., Lan, W.-H., 2001. Characteristics of organic precursors and their relationship with disinfection by-products. *Chemosphere* 44, 1231–1236. [https://doi.org/10.1016/S0045-6535\(00\)00499-9](https://doi.org/10.1016/S0045-6535(00)00499-9)
- Chen, H., Tsai, K.-P., Su, Q., Chow, A.T., Wang, J.-J., 2019. Throughfall Dissolved Organic Matter as a Terrestrial Disinfection Byproduct Precursor. *ACS Earth Space Chem.* 3, 1603–1613. <https://doi.org/10.1021/acsearthspacechem.9b00088>
- Chhetri, B.K., Takaro, T.K., Balshaw, R., Otterstatter, M., Mak, S., Lem, M., Zubel, M., Lysyshyn, M., Clarkson, L., Edwards, J., Fleury, M.D., Henderson, S.B., Galanis, E., 2017. Associations between extreme precipitation and acute gastro-intestinal illness due to cryptosporidiosis and giardiasis in an urban Canadian drinking water system (1997–2009). *J. Water Health* 15, 898–907. <https://doi.org/10.2166/wh.2017.100>
- Chiu, C.-Y., Jones, J.R., Rusak, J.A., Lin, H.-C., Nakayama, K., Kratz, T.K., Liu, W.-C., Tang, S.-L., Tsai, J.-W., 2020. Terrestrial loads of dissolved organic matter drive inter-annual carbon flux in subtropical lakes during times of drought. *Sci. Total Environ.* 717, 137052. <https://doi.org/10.1016/j.scitotenv.2020.137052>
- Chow, A.T., Dahlgren, R.A., Zhang, Q., Wong, P.K., 2008. Relationships between specific ultraviolet absorbance and trihalomethane precursors of different carbon sources. *J. Water Supply Res. Technol.-Aqua* 57, 471–480. <https://doi.org/10.2166/aqua.2008.064>
- Chow, A.T., Gao, S., Dahlgren, R.A., 2005. Physical and chemical fractionation of dissolved organic matter and trihalomethane precursors: A review. *J. Water Supply Res. Technol.-Aqua* 54, 475–507.
- Chow, A.T., Lee, S.-T., O’Geen, A.T., Orozco, T., Beaudette, D., Wong, P.-K., Hernes, P.J., Tate, K.W., Dahlgren, R.A., 2009. Litter Contributions to Dissolved Organic Matter and Disinfection Byproduct Precursors in California Oak Woodland Watersheds. *J. Environ. Qual.* 38, 2334–2343. <https://doi.org/10.2134/jeq2008.0394>
- Chow, A.T., O’Geen, A.T., Dahlgren, R.A., Díaz, F.J., Wong, K.-H., Wong, P.-K., 2011. Reactivity of Litter Leachates from California Oak Woodlands in the Formation of Disinfection By-Products. *J. Environ. Qual.* 40, 1607–1616. <https://doi.org/10.2134/jeq2010.0488>
- Chow, A.T., Tanji, K.K., Gao, S., 2003. Production of dissolved organic carbon (DOC) and trihalomethane (THM) precursor from peat soils. *Water Res.* 37, 4475–4485. [https://doi.org/10.1016/S0043-1354\(03\)00437-8](https://doi.org/10.1016/S0043-1354(03)00437-8)

References

- Christophoridis, C., Fytianos, K., 2006. Conditions Affecting the Release of Phosphorus from Surface Lake Sediments. *J. Environ. Qual.* 35, 1181–1192. <https://doi.org/10.2134/jeq2005.0213>
- Chu, C., Ryberg, E.C., Loeb, S.K., Suh, M.-J., Kim, J.-H., 2019. Water Disinfection in Rural Areas Demands Unconventional Solar Technologies. *Acc. Chem. Res.* 52, 1187–1195. <https://doi.org/10.1021/acs.accounts.8b00578>
- Clarke, B., Otto, F., Stuart-Smith, R., Harrington, L., 2022. Extreme weather impacts of climate change: an attribution perspective. *Environ. Res. Clim.* 1, 012001. <https://doi.org/10.1088/2752-5295/ac6e7d>
- Cooke, G.D., Kennedy, R.H., 2001. Managing Drinking Water Supplies. *Lake Reserv. Manag.* 17, 157–174. <https://doi.org/10.1080/07438140109354128>
- Creed, I.F., Bergström, A.-K., Trick, C.G., Grimm, N.B., Hessen, D.O., Karlsson, J., Kidd, K.A., Kritzberg, E., McKnight, D.M., Freeman, E.C., Senar, O.E., Andersson, A., Ask, J., Berggren, M., Cherif, M., Giesler, R., Hotchkiss, E.R., Kortelainen, P., Palta, M.M., Vrede, T., Weyhenmeyer, G.A., 2018. Global change-driven effects on dissolved organic matter composition: Implications for food webs of northern lakes. *Glob. Change Biol.* 0–1. <https://doi.org/10.1111/gcb.14129>
- Cremaschi, M., Pizzi, C., Valsecchi, V., 2006. Water management and land use in the terramare and a possible climatic co-factor in their abandonment: The case study of the terramara of Poviglio Santa Rosa (northern Italy). *Quat. Int.* 151, 87–98. <https://doi.org/10.1016/j.quaint.2006.01.020>
- Culea, M., Cozar, O., Ristoiu, D., 2006. Methods validation for the determination of trihalomethanes in drinking water. *J. Mass Spectrom.* 41, 1594–1597. <https://doi.org/10.1002/jms.1149>
- Cuss, C.W., Guéguen, C., 2016. Analysis of dissolved organic matter fluorescence using self-organizing maps: mini-review and tutorial. *Anal. Methods* 8, 716–725. <https://doi.org/10.1039/C5AY02549D>
- Diana, M., Farré, M.J., Sanchís, J., Kanda, R., Felipe-Sotelo, M., Bond, T., 2023. The formation of furan-like disinfection byproducts from phenolic precursors. *Environ. Sci. Water Res. Technol.* 9, 419–432. <https://doi.org/10.1039/D2EW00803C>
- de Loe, R., Plummer, R., 2010. Climate Change, Adaptive Capacity, and Governance for Drinking Water in Canada. *Clim. Change*.

References

- Deng, Y., Zhou, X., Shen, J., Xiao, G., Hong, H., Lin, H., Wu, F., Liao, B.-Q., 2021. New methods based on back propagation (BP) and radial basis function (RBF) artificial neural networks (ANNs) for predicting the occurrence of halo ketones in tap water. *Sci. Total Environ.* 772, 145534. <https://doi.org/10.1016/j.scitotenv.2021.145534>
- Dent, S.R., Beutel, M.W., Gantzer, P., Moore, B.C., 2014. Response of methylmercury, total mercury, iron and manganese to oxygenation of an anoxic hypolimnion in North Twin Lake, Washington. *Lake Reserv. Manag.* 30, 119–130. <https://doi.org/10.1080/10402381.2014.898350>
- Ding, S., Chu, W., Krasner, S.W., Yu, Y., Fang, C., Xu, B., Gao, N., 2018. The stability of chlorinated, brominated, and iodinated haloacetamides in drinking water. *Water Res.* 142, 490–500. <https://doi.org/10.1016/j.watres.2018.06.024>
- Ding, W., Jin, W., Cao, S., Zhou, X., Wang, C., Jiang, Q., Huang, H., Tu, R., Han, S.-F., Wang, Q., 2019. Ozone disinfection of chlorine-resistant bacteria in drinking water. *Water Res.* 160, 339–349. <https://doi.org/10.1016/j.watres.2019.05.014>
- Dmitrienko, S.G., Apyari, V.V., Gorbunova, M.V., Tolmacheva, V.V., Zolotov, Yu.A., 2020. Homogeneous Liquid–Liquid Microextraction of Organic Compounds. *J. Anal. Chem.* 75, 1371–1383. <https://doi.org/10.1134/S1061934820110052>
- Doederer, K., Ilieva, Z., Keller, J., 2018. Impact of a severe rain event on C- and N-DBP precursor removal using IEX. *Water Supply* 18, 2092–2099. <https://doi.org/10.2166/ws.2018.033>
- Dokulil, M.T., Teubner, K., 2010. Eutrophication and Climate Change: Present Situation and Future Scenarios, in: Ansari, A.A., Singh Gill, S., Lanza, G.R., Rast, W. (Eds.), *Eutrophication: Causes, Consequences and Control*. Springer Netherlands, Dordrecht, pp. 1–16. https://doi.org/10.1007/978-90-481-9625-8_1
- Donohue, I., Hillebrand, H., Montoya, J.M., Petchey, O.L., Pimm, S.L., Fowler, M.S., Healy, K., Jackson, A.L., Lurgi, M., McClean, D., O'Connor, N.E., O'Gorman, E.J., Yang, Q., 2016. Navigating the complexity of ecological stability. *Ecol. Lett.* 19, 1172–1185. <https://doi.org/10.1111/ele.12648>
- Dubnick, A., Barker, J., Sharp, M., Wadham, J., Lis, G., Telling, J., Fitzsimons, S., Jackson, M., 2010. Characterization of dissolved organic matter (DOM) from glacial environments using total fluorescence spectroscopy and parallel factor analysis. *Ann. Glaciol.* 51, 111–122. <https://doi.org/10.3189/172756411795931912>
- Eikebrokk, B., Vogt, R.D., Liltved, H., 2004. NOM increase in Northern European source waters: discussion of possible causes and impacts on coagulation/contact filtration processes. *Water Supply* 4, 47–54. <https://doi.org/10.2166/ws.2004.0060>

References

- Fan, Y., Li, Q., 1999. Central limit theorem for degenerate U-statistics of absolutely regular processes with applications to model specification testing. *J. Nonparametric Stat.* 10, 245–271. <https://doi.org/10.1080/10485259908832762>
- Farré, M.J., Insa, S., Mamo, J., Barceló, D., 2016. Determination of ¹⁵N -nitrosodimethylamine precursors in different water matrices by automated on-line solid- phase extraction ultra-high-performance-liquid chromatography tandem mass spectrometry. *J. Chromatogr. A.* <https://doi.org/10.1016/j.chroma.2016.06.064>
- Fellman, J.B., Hood, E., Spencer, R.G.M., 2010. Fluorescence spectroscopy opens new windows into dissolved organic matter dynamics in freshwater ecosystems: A review. *Limnol. Oceanogr.* 55, 2452–2462. <https://doi.org/10.4319/lo.2010.55.6.2452>
- Feng, L., Xu, J., Kang, S., Li, X., Li, Y., Jiang, B., Shi, Q., 2016. Chemical Composition of Microbe-Derived Dissolved Organic Matter in Cryoconite in Tibetan Plateau Glaciers: Insights from Fourier Transform Ion Cyclotron Resonance Mass Spectrometry Analysis. *Environ. Sci. Technol.* 50, 13215–13223. <https://doi.org/10.1021/acs.est.6b03971>
- Fernández-Pascual, E., Droz, B., O'Dwyer, J., O'Driscoll, C., Goslan, E.H., Harrison, S., Weatherill, J., 2023. Fluorescent Dissolved Organic Matter Components as Surrogates for Disinfection Byproduct Formation in Drinking Water: A Critical Review. *ACS EST Water* 3, 1997–2008. <https://doi.org/10.1021/acsestwater.2c00583>
- Field, C.B., Barros, V., Stocker, T.F., Dahe, Q. (Eds.), 2012. *Managing the Risks of Extreme Events and Disasters to Advance Climate Change Adaptation: Special Report of the Intergovernmental Panel on Climate Change.* Cambridge University Press, Cambridge. <https://doi.org/10.1017/CBO9781139177245>
- Fisher, B., Turner, R.K., Morling, P., 2009. Defining and classifying ecosystem services for decision making. *Ecol. Econ.* 68, 643–653. <https://doi.org/10.1016/j.ecolecon.2008.09.014>
- Flaim, G., Andreis, D., Piccolroaz, S., Obertegger, U., 2020. Ice Cover and Extreme Events Determine Dissolved Oxygen in a Placid Mountain Lake. *Water Resour. Res.* 56. <https://doi.org/10.1029/2020WR027321>
- Francos, M., Pereira, P., Alcañiz, M., Mataix-Solera, J., Úbeda, X., 2016. Impact of an intense rainfall event on soil properties following a wildfire in a Mediterranean environment (North-East Spain). *Sci. Total Environ.* 572, 1353–1362. <https://doi.org/10.1016/j.scitotenv.2016.01.145>
- Free, G., Bresciani, M., Pinardi, M., Simis, S., Liu, X., Albergel, C., Giardino, C., 2022. Investigating lake chlorophyll-a responses to the 2019 European double heatwave using satellite remote sensing. *Ecol. Indic.* 142, 109217. <https://doi.org/10.1016/j.ecolind.2022.109217>

References

- Fu, B., Wang, S., Su, C., Forsius, M., 2013. Linking ecosystem processes and ecosystem services. *Curr. Opin. Environ. Sustain.* 5, 4–10. <https://doi.org/10.1016/j.cosust.2012.12.002>
- Fu, J., Lee, W.-N., Coleman, C., Nowack, K., Carter, J., Huang, C.-H., 2017. Removal of disinfection byproduct (DBP) precursors in water by two-stage biofiltration treatment. *Water Res.* 123, 224–235. <https://doi.org/10.1016/j.watres.2017.06.073>
- Fuchs, S., Silva, A., Anggraini, A.K., Mahdariza, F., 2015. Planning and installation of a drinking water treatment in Gunungkidul, Java, Indonesia. *Water Supply* 15, 42–49. <https://doi.org/10.2166/ws.2014.080>
- Funes, I., Savé, R., De Herralde, F., Biel, C., Pla, E., Pascual, D., Zabalza, J., Cantos, G., Borràs, G., Vayreda, J., Aranda, X., 2021. Modeling impacts of climate change on the water needs and growing cycle of crops in three Mediterranean basins. *Agric. Water Manag.* 249, 106797. <https://doi.org/10.1016/j.agwat.2021.106797>
- Furst, K.E., Bolorinos, J., Mitch, W.A., 2021. Use of trihalomethanes as a surrogate for haloacetonitrile exposure introduces misclassification bias. *Water Res.* X 11, 100089. <https://doi.org/10.1016/j.wroa.2021.100089>
- Gallart, F., Delgado, J., Beatson, S.J.V., Posner, H., Llorens, P., Marcé, R., 2011. Analysing the effect of global change on the historical trends of water resources in the headwaters of the Llobregat and Ter river basins (Catalonia, Spain). *Phys. Chem. Earth Parts ABC* 36, 655–661. <https://doi.org/10.1016/j.pce.2011.04.009>
- Gao, J., Proulx, F., Rodriguez, M.J., 2019. Occurrence and spatio-temporal variability of halogenated acetaldehydes in full-scale drinking water systems. *Sci. Total Environ.* 693, 133517. <https://doi.org/10.1016/j.scitotenv.2019.07.323>
- Geer Wallace, M.A., McCord, J.P., 2020. High-resolution mass spectrometry, in: *Breathborne Biomarkers and the Human Volatilome*. Elsevier, pp. 253–270. <https://doi.org/10.1016/B978-0-12-819967-1.00016-5>
- Gerard, C., 2001. Consequences of a drought on freshwater gastropod and trematode communities.
- Gerba, C.P., 2009. Drinking Water Treatment, in: *Environmental Microbiology*. Elsevier, pp. 531–538. <https://doi.org/10.1016/B978-0-12-370519-8.00025-0>
- Ghil, M., Yiou, P., Hallegatte, S., Malamud, B.D., Naveau, P., Soloviev, A., Friederichs, P., Keilis-Borok, V., Kondrashov, D., Kossobokov, V., Mestre, O., Nicolis, C., Rust, H.W., Shebalin, P., Vrac, M., Witt, A., Zaliapin, I., 2011. Extreme events: dynamics, statistics and prediction. *Nonlinear Process. Geophys.* 18, 295–350. <https://doi.org/10.5194/npg-18-295-2011>

References

- Giocalone, M., Agata, Z., Cozzucoli, P.C., Alibrandi, A., 2018. Bonferroni-Holm and permutation tests to compare health data: methodological and applicative issues. *BMC Med. Res. Methodol.* 18, 81. <https://doi.org/10.1186/s12874-018-0540-8>
- Gondar, D., Thacker, S.A., Tipping, E., Baker, A., 2008. Functional variability of dissolved organic matter from the surface water of a productive lake. *Water Res.* 42, 81–90. <https://doi.org/10.1016/j.watres.2007.07.006>
- Gonsior, M., Schmitt-Kopplin, P., Bastviken, D., 2013. Depth-dependent molecular composition and photo-reactivity of dissolved organic matter in a boreal lake under winter and summer conditions. *Biogeosciences* 10, 6945–6956. <https://doi.org/10.5194/bg-10-6945-2013>
- González, J.F., 2011. Assessing the Macroeconomic Impact of Water Supply Restrictions Through an Input–Output Analysis. *Water Resour. Manag.* 25, 2335–2347. <https://doi.org/10.1007/s11269-011-9811-4>
- Goslan, E.H., Seigle, C., Purcell, D., Henderson, R., Parsons, S.A., Jefferson, B., Judd, S.J., 2017. Carbonaceous and nitrogenous disinfection by-product formation from algal organic matter. *Chemosphere* 170, 1–9. <https://doi.org/10.1016/j.chemosphere.2016.11.148>
- Graham, A.M., Cameron-Burr, K.T., Hajic, H.A., Lee, C., Msekela, D., Gilmour, C.C., 2017. Sulfurization of Dissolved Organic Matter Increases Hg–Sulfide–Dissolved Organic Matter Bioavailability to a Hg-Methylating Bacterium. *Environ. Sci. Technol.* 51, 9080–9088. <https://doi.org/10.1021/acs.est.7b02781>
- Granger, C.W.J., 2008. Investigating Causal Relations by Econometric Models and Cross-Spectral Methods. *Essays Econom. Vol II Collect. Pap. Clive W J Granger* 37, 31–47. <https://doi.org/10.1017/ccol052179207x.002>
- Granger, C.W.J., 1988. Some recent development in a concept of causality. *J. Econom.* 39, 199–211. [https://doi.org/10.1016/0304-4076\(88\)90045-0](https://doi.org/10.1016/0304-4076(88)90045-0)
- Grant, S.B., Fletcher, T.D., Feldman, D., Saphores, J.-D., Cook, P.L.M., Stewardson, M., Low, K., Burry, K., Hamilton, A.J., 2013. Adapting Urban Water Systems to a Changing Climate: Lessons from the Millennium Drought in Southeast Australia. *Environ. Sci. Technol.* 47, 10727–10734. <https://doi.org/10.1021/es400618z>
- Gray, N.F., 2014. Filtration Methods, in: *Microbiology of Waterborne Diseases*. Elsevier, pp. 631–650. <https://doi.org/10.1016/B978-0-12-415846-7.00035-4>
- Gray, N.F., 2014. Ultraviolet Disinfection, in: *Microbiology of Waterborne Diseases*. Elsevier, pp. 617–630. <https://doi.org/10.1016/B978-0-12-415846-7.00034-2>
- Graydon, R.C., Mezzacapo, M., Boehme, J., Foldy, S., Edge, T.A., Brubacher, J., Chan, H.M., Dellinger, M., Faustman, E.M., Rose, J.B., Takaro, T.K., 2022. Associations between

References

- extreme precipitation, drinking water, and protozoan acute gastrointestinal illnesses in four North American Great Lakes cities (2009–2014). *J. Water Health* 20, 849–862. <https://doi.org/10.2166/wh.2022.018>
- Grimm, N.B., Chapin, F.S., Bierwagen, B., Gonzalez, P., Groffman, P.M., Luo, Y., Melton, F., Nadelhoffer, K., Pairis, A., Raymond, P.A., Schimel, J., Williamson, C.E., 2013. The impacts of climate change on ecosystem structure and function. *Front. Ecol. Environ.* 11, 474–482. <https://doi.org/10.1890/120282>
- Gudivada, V.N., 2017. Data Analytics, in: *Data Analytics for Intelligent Transportation Systems*. Elsevier, pp. 31–67. <https://doi.org/10.1016/B978-0-12-809715-1.00002-X>
- Guillemette, F., McCallister, S.L., Del Giorgio, P.A., 2013. Differentiating the degradation dynamics of algal and terrestrial carbon within complex natural dissolved organic carbon in temperate lakes. *J. Geophys. Res. Biogeosciences* 118, 963–973. <https://doi.org/10.1002/jgrg.20077>
- Gunderson, L.H., 2000. Ecological Resilience—In Theory and Application. *Annu. Rev. Ecol. Syst.* 31, 425–439. <https://doi.org/10.1146/annurev.ecolsys.31.1.425>
- Han, J., Singh, V.P., 2023. A review of widely used drought indices and the challenges of drought assessment under climate change. *Environ. Monit. Assess.* 195, 1438. <https://doi.org/10.1007/s10661-023-12062-3>
- Hao, Z., AghaKouchak, A., 2014. A Nonparametric Multivariate Multi-Index Drought Monitoring Framework. *J. Hydrometeorol.* 15, 89–101. <https://doi.org/10.1175/JHM-D-12-0160.1>
- Harkort, L., Duan, Z., 2023. Estimation of dissolved organic carbon from inland waters at a large scale using satellite data and machine learning methods. *Water Res.* 229, 119478. <https://doi.org/10.1016/j.watres.2022.119478>
- Haug, G.H., Gunther, D., Peterson, L.C., Sigman, D.M., Hughen, K.A., Aeschlimann, B., 2003. *Climate and the Collapse of Maya Civilization* 299.
- Hawkes, J.A., Kew, W., 2020. High-resolution mass spectrometry strategies for the investigation of dissolved organic matter, in: *Multidimensional Analytical Techniques in Environmental Research*. Elsevier, pp. 71–104. <https://doi.org/10.1016/B978-0-12-818896-5.00004-1>
- Hayakawa, K., Kojima, R., Wada, C., Suzuki, T., Sugiyama, Y., Kumagai, T., Takei, N., Bamba, D., 2016. Distribution and characteristics of ultraviolet absorption and fluorescence of dissolved organic matter in a large lake (Lake Biwa, Japan). *J. Gt. Lakes Res.* 42, 571–579. <https://doi.org/10.1016/j.jglr.2016.02.006>

References

- He, W., Bai, Z., Li, Y., Kong, X., Liu, W., Yang, C., Yang, B., Xu, F., 2016. Advances in environmental behaviors and effects of dissolved organic matter in aquatic ecosystems. *Sci. China Earth Sci.* 59, 746–759. <https://doi.org/10.1007/s11430-015-5248-6>
- Helle, N., Baden, M., Petersen, K., 2011. Automated Solid Phase Extraction, in: Zweigenbaum, J. (Ed.), *Mass Spectrometry in Food Safety, Methods in Molecular Biology*. Humana Press, Totowa, NJ, pp. 93–129. https://doi.org/10.1007/978-1-61779-136-9_5
- Herschy, R.W., Herschy, R.W., Wolanski, E., Andutta, F., Delhez, E., Fairbridge, R.W., Bengtsson, L., Farley, M., Sklar, F.H., Fontaine, T.D., 2012. Ecological Threat to Lakes and Reservoirs, in: Bengtsson, L., Herschy, R.W., Fairbridge, R.W. (Eds.), *Encyclopedia of Lakes and Reservoirs, Encyclopedia of Earth Sciences Series*. Springer Netherlands, Dordrecht, pp. 233–234. https://doi.org/10.1007/978-1-4020-4410-6_74
- Hickey, A., Senevirathna, L., 2023. Performance of regional water purification plants during extreme weather events: three case studies from New South Wales, Australia. *Environ. Sci. Pollut. Res.* <https://doi.org/10.1007/s11356-023-28101-y>
- Hiriart-Baer, V.P., Diep, N., Smith, R.E.H., 2008. Dissolved Organic Matter in the Great Lakes: Role and Nature of Allochthonous Material. *J. Gt. Lakes Res.* 34, 383–394. [https://doi.org/10.3394/0380-1330\(2008\)34\[383:DOMITG\]2.0.CO;2](https://doi.org/10.3394/0380-1330(2008)34[383:DOMITG]2.0.CO;2)
- Hobson, P., Fabris, R., Develter, E., Linden, L.G., Burch, M.D., Brookes, J.D., 2010. Reservoir Inflow Monitoring for Improved Management of Treated Water Quality—A South Australian Experience. *Water Resour. Manag.* 24, 4161–4174. <https://doi.org/10.1007/s11269-010-9651-7>
- Hockaday, W.C., Purcell, J.M., Marshall, A.G., Baldock, J.A., Hatcher, P.G., 2009. Electrospray and photoionization mass spectrometry for the characterization of organic matter in natural waters: a qualitative assessment: Characterization of organic matter in natural waters. *Limnol. Oceanogr. Methods* 7, 81–95. <https://doi.org/10.4319/lom.2009.7.81>
- Hoffman, J.I.E., 2019. Comparison of Two Groups: t-Tests and Nonparametric Tests, in: *Basic Biostatistics for Medical and Biomedical Practitioners*. Elsevier, pp. 341–366. <https://doi.org/10.1016/B978-0-12-817084-7.00022-X>
- Hofman-Caris, R., Hofman, J., 2017. Limitations of Conventional Drinking Water Technologies in Pollutant Removal, in: Gil, A., Galeano, L.A., Vicente, M.Á. (Eds.), *Applications of Advanced Oxidation Processes (AOPs) in Drinking Water Treatment, The Handbook of Environmental Chemistry*. Springer International Publishing, Cham, pp. 21–51. https://doi.org/10.1007/698_2017_83

References

- Hong, H., Zhang, Z., Guo, A., Shen, L., Sun, H., Liang, Y., Wu, F., Lin, H., 2020. Radial basis function artificial neural network (RBF ANN) as well as the hybrid method of RBF ANN and grey relational analysis able to well predict trihalomethanes levels in tap water. *J. Hydrol.* 591, 125574. <https://doi.org/10.1016/j.jhydrol.2020.125574>
- Hoslett, J., Massara, T.M., Malamis, S., Ahmad, D., Van Den Boogaert, I., Katsou, E., Ahmad, B., Ghazal, H., Simons, S., Wrobel, L., Jouhara, H., 2018. Surface water filtration using granular media and membranes: A review. *Sci. Total Environ.* 639, 1268–1282. <https://doi.org/10.1016/j.scitotenv.2018.05.247>
- Hrudey, S.E., Fawell, J., 2015. 40 years on: what do we know about drinking water disinfection by-products (DBPs) and human health? *Water Supply* 15, 667–674. <https://doi.org/10.2166/ws.2015.036>
- Hu, J., Song, H., Addison, J.W., Karanfil, T., 2010. Halonitromethane formation potentials in drinking waters. *Water Res.* 44, 105–114. <https://doi.org/10.1016/j.watres.2009.09.006>
- Hua, G., Kim, J., Reckhow, D.A., 2014. Disinfection byproduct formation from lignin precursors. *Water Res.* 63, 285–295. <https://doi.org/10.1016/j.watres.2014.06.029>
- Huguet, A., Vacher, L., Relexans, S., Saubusse, S., Froidefond, J.M., Parlanti, E., 2009. Properties of fluorescent dissolved organic matter in the Gironde Estuary. *Org. Geochem.* 40, 706–719. <https://doi.org/10.1016/j.orggeochem.2009.03.002>
- Huang, H., Chen, B.-Y., Zhu, Z.-R., 2017. Formation and speciation of haloacetamides and haloacetonitriles for chlorination, chloramination, and chlorination followed by chloramination. *Chemosphere* 166, 126–134. <https://doi.org/10.1016/j.chemosphere.2016.09.047>
- Hur, J., Lee, B.-M., Lee, S., Shin, J.-K., 2014. Characterization of chromophoric dissolved organic matter and trihalomethane formation potential in a recently constructed reservoir and the surrounding areas – Impoundment effects. *J. Hydrol.* 515, 71–80. <https://doi.org/10.1016/j.jhydrol.2014.04.035>
- Ignatev, A., Tuhkanen, T., 2019. Step-by-step analysis of drinking water treatment trains using size-exclusion chromatography to fingerprint and track protein-like and humic/fulvic-like fractions of dissolved organic matter. *Environ. Sci. Water Res. Technol.* 5, 1568–1581. <https://doi.org/10.1039/C9EW00340A>
- Ioannou, P., Charisiadis, P., Andra, S.S., Makris, K.C., 2016. Occurrence and variability of iodinated trihalomethanes concentrations within two drinking-water distribution networks. *Sci. Total Environ.* 543, 505–513. <https://doi.org/10.1016/j.scitotenv.2015.10.031>

References

- Ireland, A.W., Booth, R.K., Hotchkiss, S.C., Schmitz, J.E., 2012. Drought as a Trigger for Rapid State Shifts in Kettle Ecosystems: Implications for Ecosystem Responses to Climate Change. *Wetlands* 32, 989–1000. <https://doi.org/10.1007/s13157-012-0324-6>
- Islam, M.M., Hasanuzzaman, M., 2020. Introduction to energy and sustainable development, in: *Energy for Sustainable Development*. Elsevier, pp. 1–18. <https://doi.org/10.1016/B978-0-12-814645-3.00001-8>
- Izaguirre, G., Taylor, W.D., 1995. Geosmin and 2-methylisoborneol production in a major aqueduct system.
- Jahn, M., 2015. Economics of extreme weather events: Terminology and regional impact models. *Weather Clim. Extrem.* 10, 29–39. <https://doi.org/10.1016/j.wace.2015.08.005>
- Jane, S.F., Hansen, G.J.A., Kraemer, B.M., Leavitt, P.R., Mincer, J.L., North, R.L., Pilla, R.M., Stetler, J.T., Williamson, C.E., Woolway, R.I., Arvola, L., Chandra, S., DeGasperi, C.L., Diemer, L., Dunalska, J., Erina, O., Flaim, G., Grossart, H.-P., Hambright, K.D., Hein, C., Hejzlar, J., Janus, L.L., Jenny, J.-P., Jones, J.R., Knoll, L.B., Leoni, B., Mackay, E., Matsuzaki, S.-I.S., McBride, C., Müller-Navarra, D.C., Paterson, A.M., Pierson, D., Rogora, M., Rusak, J.A., Sadro, S., Saulnier-Talbot, E., Schmid, M., Sommaruga, R., Thiery, W., Verburg, P., Weathers, K.C., Weyhenmeyer, G.A., Yokota, K., Rose, K.C., 2021. Widespread deoxygenation of temperate lakes. *Nature* 594, 66–70. <https://doi.org/10.1038/s41586-021-03550-y>
- Jennings, E., Jones, S., Arvola, L., Staehr, P.A., Gaiser, E., Jones, I.D., Weathers, K.C., Weyhenmeyer, G.A., Chiu, C.-Y., De Eyto, E., 2012. Effects of weather-related episodic events in lakes: an analysis based on high-frequency data: Episodic events in lakes. *Freshw. Biol.* 57, 589–601. <https://doi.org/10.1111/j.1365-2427.2011.02729.x>
- Jeong, K., Härdle, W.K., Song, S., 2012. A CONSISTENT NONPARAMETRIC TEST FOR CAUSALITY IN QUANTILE. *Econom. Theory* 28, 861–887. <https://doi.org/10.1017/S0266466611000685>
- Jeppesen, E., Brucet, S., Naselli-Flores, L., Papastergiadou, E., Stefanidis, K., Nöges, T., Nöges, P., Attayde, J.L., Zohary, T., Coppens, J., Bucak, T., Menezes, R.F., Freitas, F.R.S., Kernan, M., Søndergaard, M., Beklioglu, M., 2015. Ecological impacts of global warming and water abstraction on lakes and reservoirs due to changes in water level and related changes in salinity. *Hydrobiologia* 750, 201–227. <https://doi.org/10.1007/s10750-014-2169-x>
- Jia, A., Wu, C., Duan, Y., 2016. Precursors and factors affecting formation of haloacetonitriles and chloropicrin during chlor(am)ination of nitrogenous organic compounds in drinking water. *J. Hazard. Mater.* 308, 411–418. <https://doi.org/10.1016/j.jhazmat.2016.01.037>

References

- Jian, Q., Boyer, T.H., Yang, Xiuhong, Xia, B., Yang, Xin, 2016. Characteristics and DBP formation of dissolved organic matter from leachates of fresh and aged leaf litter. *Chemosphere* 152, 335–344. <https://doi.org/10.1016/j.chemosphere.2016.02.107>
- Jöhnk, K.D., Huisman, J., Sharples, J., Sommeijer, B., Visser, P.M., Stroom, J.M., 2008. Summer heatwaves promote blooms of harmful cyanobacteria: HEATWAVES PROMOTE HARMFUL CYANOBACTERIA. *Glob. Change Biol.* 14, 495–512. <https://doi.org/10.1111/j.1365-2486.2007.01510.x>
- Jurado-Sánchez, B., Ballesteros, E., Gallego, M., 2012. Occurrence of aromatic amines and N-nitrosamines in the different steps of a drinking water treatment plant. *Water Res.* 46, 4543–4555. <https://doi.org/10.1016/j.watres.2012.05.039>
- Jutaporn, P., Laolertworakul, W., Armstrong, M.D., Coronell, O., 2019. Fluorescence spectroscopy for assessing trihalomethane precursors removal by MIEX resin. *Water Sci. Technol.* 79, 820–832. <https://doi.org/10.2166/wst.2019.036>
- Kasuga, I., Yuthawong, V., Kurisu, F., Furumai, H., 2020. Molecular-level comparison of dissolved organic matter in 11 major lakes in Japan by Orbitrap mass spectrometry. *Water Supply* 20, 1271–1280. <https://doi.org/10.2166/ws.2020.042>
- Kaushal, S.S., Mayer, P.M., Vidon, P.G., Smith, R.M., Pennino, M.J., Newcomer, T.A., Duan, S., Welty, C., Belt, K.T., 2014. Land Use and Climate Variability Amplify Carbon, Nutrient, and Contaminant Pulses: A Review with Management Implications. *JAWRA J. Am. Water Resour. Assoc.* 50, 585–614. <https://doi.org/10.1111/jawr.12204>
- Kéfi, S., Domínguez-García, V., Donohue, I., Fontaine, C., Thébault, E., Dakos, V., 2019. Advancing our understanding of ecological stability. *Ecol. Lett.* 22, 1349–1356. <https://doi.org/10.1111/ele.13340>
- Kellerman, A.M., Kothawala, D.N., Dittmar, T., Tranvik, L.J., 2015. Persistence of dissolved organic matter in lakes related to its molecular characteristics. *Nat. Geosci.* 8, 454–457. <https://doi.org/10.1038/ngco2440>
- Kermani, F.R., Tugulea, A.-M., Hnatiw, J., Niri, V.H., Pawliszyn, J., 2013. Application of automated solid-phase microextraction to determine haloacetonitriles, halo ketones, and chloropicrin in Canadian drinking water. *Water Qual. Res. J.* 48, 85–98. <https://doi.org/10.2166/wqrjc.2013.012>
- Khan, M.N., Mohammad, F., 2014. Eutrophication: Challenges and Solutions, in: Ansari, A.A., Gill, S.S. (Eds.), *Eutrophication: Causes, Consequences and Control*. Springer Netherlands, Dordrecht, pp. 1–15. https://doi.org/10.1007/978-94-007-7814-6_1

References

- Khorasani, H., Xu, J., Nguyen, T., Kralles, Z., Westerhoff, P., Dai, N., Zhu, Z., 2021. Contribution of wastewater- versus non-wastewater-derived sources to haloacetonitriles formation potential in a wastewater-impacted river. *Sci. Total Environ.* 792, 148355. <https://doi.org/10.1016/j.scitotenv.2021.148355>
- Kimbrough, D.E., 2019. Impact of local climate change on drinking water quality in a distribution system. *Water Qual. Res. J.* 54, 179–192. <https://doi.org/10.2166/wqrj.2019.054>
- King, A.P., Eckersley, R.J., 2019. Inferential Statistics IV: Choosing a Hypothesis Test, in: *Statistics for Biomedical Engineers and Scientists*. Elsevier, pp. 147–171. <https://doi.org/10.1016/B978-0-08-102939-8.00016-5>
- Klante, C., Larson, M., Persson, K.M., 2021. Brownification in Lake Bolmen, Sweden, and its relationship to natural and human-induced changes. *J. Hydrol. Reg. Stud.* 36, 100863. <https://doi.org/10.1016/j.ejrh.2021.100863>
- Klug, J.L., Richardson, D.C., Ewing, H.A., Hargreaves, B.R., Samal, N.R., Vachon, D., Pierson, D.C., Lindsey, A.M., O'Donnell, D.M., Effler, S.W., Weathers, K.C., 2012. Ecosystem Effects of a Tropical Cyclone on a Network of Lakes in Northeastern North America. *Environ. Sci. Technol.* 46, 11693–11701. <https://doi.org/10.1021/es302063v>
- Kohzu, A., Matsuzaki, S.S., Komuro, S., Komatsu, K., Takamura, N., Nakagawa, M., Imai, A., Fukushima, T., 2023. Identifying the true drivers of abrupt changes in ecosystem state with a focus on time lags: Extreme precipitation can determine water quality in shallow lakes. *Sci. Total Environ.* 881, 163097. <https://doi.org/10.1016/j.scitotenv.2023.163097>
- Koks, E.E., Van Ginkel, K.C.H., Van Marle, M.J.E., Lemnitzer, A., 2022. Brief communication: Critical infrastructure impacts of the 2021 mid-July western European flood event. *Nat. Hazards Earth Syst. Sci.* 22, 3831–3838. <https://doi.org/10.5194/nhess-22-3831-2022>
- Kolka, R., Weishampel, P., Fröberg, M., 2008. Measurement and Importance of Dissolved Organic Carbon, in: Hoover, C.M. (Ed.), *Field Measurements for Forest Carbon Monitoring*. Springer Netherlands, Dordrecht, pp. 171–176. https://doi.org/10.1007/978-1-4020-8506-2_13
- Kothawala, D.N., Von Wachenfeldt, E., Koehler, B., Tranvik, L.J., 2012. Selective loss and preservation of lake water dissolved organic matter fluorescence during long-term dark incubations. *Sci. Total Environ.* 433, 238–246. <https://doi.org/10.1016/j.scitotenv.2012.06.029>
- Krasner, S.W., 2009. The formation and control of emerging disinfection by-products of health concern. *Philos. Trans. R. Soc. Math. Phys. Eng. Sci.* 367, 4077–4095. <https://doi.org/10.1098/rsta.2009.0108>

References

- Krasner, S.W., Weinberg, H.S., Richardson, S.D., Pastor, S.J., Chinn, R., Scilimenti, M.J., Onstad, G.D., Thruston, A.D., 2006. Occurrence of a New Generation of Disinfection Byproducts. *Environ. Sci. Technol.* 40, 7175–7185. <https://doi.org/10.1021/es060353j>
- Krasner, S.W., Westerhoff, P., Mitch, W.A., Hanigan, D., McCurry, D.L., Von Gunten, U., 2018. Behavior of NDMA precursors at 21 full-scale water treatment facilities. *Environ. Sci. Water Res. Technol.* 4, 1966–1978. <https://doi.org/10.1039/C8EW00442K>
- Kraus, T.E.C., Bergamaschi, B.A., Hernes, P.J., Doctor, D., Kendall, C., Downing, B.D., Losee, R.F., 2011. How reservoirs alter drinking water quality: Organic matter sources, sinks, and transformations. *Lake Reserv. Manag.* 27, 205–219. <https://doi.org/10.1080/07438141.2011.597283>
- Kumari, M., Gupta, S.K., 2022. Occurrence and Exposure to Trihalomethanes in Drinking Water: A Systematic Review and Meta-analysis. *Expo. Health* 14, 915–939. <https://doi.org/10.1007/s12403-022-00467-3>
- Lakens, D., 2013. Calculating and reporting effect sizes to facilitate cumulative science: a practical primer for t-tests and ANOVAs. *Front. Psychol.* 4. <https://doi.org/10.3389/fpsyg.2013.00863>
- Lavonen, E.E., Gonsior, M., Tranvik, L.J., Schmitt-Kopplin, P., Köhler, S.J., 2013. Selective Chlorination of Natural Organic Matter: Identification of Previously Unknown Disinfection Byproducts. *Environ. Sci. Technol.* 47, 2264–2271. <https://doi.org/10.1021/es304669p>
- Le Moal, M., Gascuel-Oudou, C., Ménesguen, A., Souchon, Y., Étrillard, C., Levain, A., Moatar, F., Pannard, A., Souchu, P., Lefebvre, A., Pinay, G., 2019. Eutrophication: A new wine in an old bottle? *Sci. Total Environ.* 651, 1–11. <https://doi.org/10.1016/j.scitotenv.2018.09.139>
- LeChevallier, M.W., 1999. The case for maintaining a disinfectant residual. *J. AWWA* 91, 86–94. <https://doi.org/10.1002/j.1551-8833.1999.tb08573.x>
- Leenheer, Jerry A., Jean-Philippe Croué, 2003. Peer reviewed: characterizing aquatic dissolved organic matter. *Environmental science & technology* 37, 18A-26A.
- Lehman, J.T., 2014. Understanding the role of induced mixing for management of nuisance algal blooms in an urbanized reservoir. *Lake Reserv. Manag.* 30, 63–71. <https://doi.org/10.1080/10402381.2013.872739>
- Lennox, R.J., Crook, D.A., Moyle, P.B., Struthers, D.P., Cooke, S.J., 2019. Toward a better understanding of freshwater fish responses to an increasingly drought-stricken world. *Rev. Fish Biol. Fish.* 29, 71–92. <https://doi.org/10.1007/s11160-018-09545-9>

References

- Leonard, L.T., Vanzin, G.F., Garayburu-Caruso, V.A., Lau, S.S., Beutler, C.A., Newman, A.W., Mitch, W.A., Stegen, J.C., Williams, K.H., Sharp, J.O., 2022. Disinfection byproducts formed during drinking water treatment reveal an export control point for dissolved organic matter in a subalpine headwater stream. *Water Res.* X 15, 100144. <https://doi.org/10.1016/j.wroa.2022.100144>
- Levy, K., Woster, A.P., Goldstein, R.S., Carlton, E.J., 2016. Untangling the Impacts of Climate Change on Waterborne Diseases: a Systematic Review of Relationships between Diarrheal Diseases and Temperature, Rainfall, Flooding, and Drought. *Environ. Sci. Technol.* 50, 4905–4922. <https://doi.org/10.1021/acs.est.5b06186>
- Li, L., Gao, N., Deng, Y., Yao, J., Zhang, K., 2012. Characterization of intracellular & extracellular algae organic matters (AOM) of *Microcystis aeruginosa* and formation of AOM-associated disinfection byproducts and odor & taste compounds. *Water Res.* 46, 1233–1240. <https://doi.org/10.1016/j.watres.2011.12.026>
- Li, N., Huang, T., Mao, X., Zhang, H., Li, K., Wen, G., Lv, X., Deng, L., 2019. Controlling reduced iron and manganese in a drinking water reservoir by hypolimnetic aeration and artificial destratification. *Sci. Total Environ.* 685, 497–507. <https://doi.org/10.1016/j.scitotenv.2019.05.445>
- Li, R.A., McDonald, J.A., Sathasivan, A., Khan, S.J., 2021. A multivariate Bayesian network analysis of water quality factors influencing trihalomethanes formation in drinking water distribution systems. *Water Res.* 190, 116712. <https://doi.org/10.1016/j.watres.2020.116712>
- Li, S., Bush, R.T., Mao, R., Xiong, L., Ye, C., 2017. Extreme drought causes distinct water acidification and eutrophication in the Lower Lakes (Lakes Alexandrina and Albert), Australia. *J. Hydrol.* 544, 133–146. <https://doi.org/10.1016/j.jhydrol.2016.11.015>
- Li, W., Liang, X., Duan, J., Beecham, S., Mulcahy, D., 2018. Influence of spent filter backwash water recycling on pesticide removal in a conventional drinking water treatment process. *Environ. Sci. Water Res. Technol.* 4, 1057–1067. <https://doi.org/10.1039/C7EW00530J>
- Li, W., Wu, F., Liu, C., Fu, P., Wang, J., Mei, Y., Wang, L., Guo, J., 2008. Temporal and spatial distributions of dissolved organic carbon and nitrogen in two small lakes on the Southwestern China Plateau. *Limnology* 9, 163–171. <https://doi.org/10.1007/s10201-008-0241-9>
- Li, Z., Liu, X., Huang, Z., Hu, S., Wang, J., Qian, Z., Feng, J., Xian, Q., Gong, T., 2019. Occurrence and ecological risk assessment of disinfection byproducts from chlorination of wastewater

References

- effluents in East China. *Water Res.* 157, 247–257.
<https://doi.org/10.1016/j.watres.2019.03.072>
- Lin, H.-C., Tsai, J.-W., Tada, K., Matsumoto, H., Chiu, C.-Y., Nakayama, K., 2022. The impacts of the hydraulic retention effect and typhoon disturbance on the carbon flux in shallow subtropical mountain lakes. *Sci. Total Environ.* 803, 150044.
<https://doi.org/10.1016/j.scitotenv.2021.150044>
- Lin, S.-S., Shen, S.-L., Zhou, A., Lyu, H.-M., 2021. Assessment and management of lake eutrophication: A case study in Lake Erhai, China. *Sci. Total Environ.* 751, 141618.
<https://doi.org/10.1016/j.scitotenv.2020.141618>
- Liew, D., Linge, K.L., Joll, C.A., Heitz, A., Charrois, J.W.A., 2012. Determination of halonitromethanes and haloacetamides: An evaluation of sample preservation and analyte stability in drinking water. *J. Chromatogr. A* 1241, 117–122.
<https://doi.org/10.1016/j.chroma.2012.04.037>
- Linge, K.L., Kristiana, I., Liew, D., Nottle, C.E., Heitz, A., Joll, C.A., 2017. Formation of *N*-Nitrosamines in Drinking Water Sources: Case Studies from Western Australia. *J. AWWA* 109. <https://doi.org/10.5942/jawwa.2017.109.0036>
- Liquete, C., Canals, M., Ludwig, W., Arnau, P., 2009. Sediment discharge of the rivers of Catalonia, NE Spain, and the influence of human impacts. *J. Hydrol.* 366, 76–88.
<https://doi.org/10.1016/j.jhydrol.2008.12.013>
- Liu, B., Gao, J., Xue, M., Lu, B., Ye, C., Liu, J., Yang, J., Qian, J., Xu, X., Wang, W., Tao, Y., Ao, W., 2023. High exogenous humus inhibits greenhouse gas emissions from steppe lakes. *Environ. Pollut.* 319, 120946. <https://doi.org/10.1016/j.envpol.2022.120946>
- Liu, D., Du, Y., Yu, S., Luo, J., Duan, H., 2020. Human activities determine quantity and composition of dissolved organic matter in lakes along the Yangtze River. *Water Res.* 168, 115132. <https://doi.org/10.1016/j.watres.2019.115132>
- Liu, D., Yu, S., Duan, H., 2021. Different storm responses of organic carbon transported to Lake Taihu by the eutrophic Tiaoxi River, China. *Sci. Total Environ.* 782, 146874.
<https://doi.org/10.1016/j.scitotenv.2021.146874>
- Liu, G., Lut, M.C., Verberk, J.Q.J.C., Van Dijk, J.C., 2013. A comparison of additional treatment processes to limit particle accumulation and microbial growth during drinking water distribution. *Water Res.* 47, 2719–2728. <https://doi.org/10.1016/j.watres.2013.02.035>

References

- Liu, J., Jiang, M., Li, G., Xu, L., Xie, M., 2010. Miniaturized salting-out liquid–liquid extraction of sulfonamides from different matrices. *Anal. Chim. Acta* 679, 74–80. <https://doi.org/10.1016/j.aca.2010.09.013>
- Liu, M., Zhang, Yunlin, Shi, K., Zhang, Yibo, Zhou, Y., Zhu, M., Zhu, G., Wu, Z., Liu, Mingliang, 2020. Effects of rainfall on thermal stratification and dissolved oxygen in a deep drinking water reservoir. *Hydrol. Process.* 34, 3387–3399. <https://doi.org/10.1002/hyp.13826>
- Liu, P., Farré, M.J., Keller, J., Gernjak, W., 2016. Reducing natural organic matter and disinfection by-product precursors by alternating oxic and anoxic conditions during engineered short residence time riverbank filtration: A laboratory-scale column study. *Sci. Total Environ.* 565, 616–625. <https://doi.org/10.1016/j.scitotenv.2016.05.061>
- Liu, S., He, Z., Tang, Z., Liu, L., Hou, J., Li, T., Zhang, Y., Shi, Q., Giesy, J.P., Wu, F., 2020. Linking the molecular composition of autochthonous dissolved organic matter to source identification for freshwater lake ecosystems by combination of optical spectroscopy and FT-ICR-MS analysis. *Sci. Total Environ.* 703, 134764. <https://doi.org/10.1016/j.scitotenv.2019.134764>
- Liu, S., Hou, J., Suo, C., Chen, J., Liu, X., Fu, R., Wu, F., 2022. Molecular-level composition of dissolved organic matter in distinct trophic states in Chinese lakes: Implications for eutrophic lake management and the global carbon cycle. *Water Res.* 217, 118438. <https://doi.org/10.1016/j.watres.2022.118438>
- Llasat, M.C., Del Moral, A., Cortès, M., Rigo, T., 2021. Convective precipitation trends in the Spanish Mediterranean region. *Atmospheric Res.* 257, 105581. <https://doi.org/10.1016/j.atmosres.2021.105581>
- López, P., Marcé, R., Armengol, J., 2011. Net heterotrophy and CO₂ evasion from a productive calcareous reservoir: Adding complexity to the metabolism-CO₂ evasion issue. *J. Geophys. Res. Biogeosciences* 116, 1–14. <https://doi.org/10.1029/2010JG001614>
- Lüring, M., Mackay, E., Reitzel, K., Spears, B.M., 2016. Editorial – A critical perspective on geo-engineering for eutrophication management in lakes. *Water Res.* 97, 1–10. <https://doi.org/10.1016/j.watres.2016.03.035>
- Lv, S., Li, X., Wang, R., Wang, Y., Dong, Z., Zhou, T., Liu, Y., Lin, K., Liu, L., 2022. Autochthonous sources and drought conditions drive anomalous oxygen-consuming pollution increase in a sluice-controlled reservoir in eastern China. *Sci. Total Environ.* 841, 156739. <https://doi.org/10.1016/j.scitotenv.2022.156739>

References

- Ly, Q.V., Maqbool, T., Hur, J., 2017. Unique characteristics of algal dissolved organic matter and their association with membrane fouling behavior: a review. *Environ. Sci. Pollut. Res.* 24, 11192–11205. <https://doi.org/10.1007/s11356-017-8683-4>
- Lyle, Z.J., VanBriesen, J.M., Samaras, C., 2023. Drinking Water Utility-Level Understanding of Climate Change Effects to System Reliability.
- Ma, Y.S., 2004. Reaction mechanisms for DBPS reduction in humic acid ozonation. *Ozone-Sci. Eng.* 26, 153–164. <https://doi.org/10.1080/01919510490439429>
- Mac Nally, R., Horrocks, G.F.B., Lada, H., 2017. Anuran responses to pressures from high-amplitude drought–flood–drought sequences under climate change. *Clim. Change* 141, 243–257. <https://doi.org/10.1007/s10584-016-1890-z>
- Maizel, A.C., Li, J., Remucal, C.K., 2017. Relationships Between Dissolved Organic Matter Composition and Photochemistry in Lakes of Diverse Trophic Status. *Environ. Sci. Technol.* 51, 9624–9632. <https://doi.org/10.1021/acs.est.7b01270>
- Manasfi, T., 2021. Ozonation in drinking water treatment: an overview of general and practical aspects, mechanisms, kinetics, and byproduct formation, in: *Comprehensive Analytical Chemistry*. Elsevier, pp. 85–116. <https://doi.org/10.1016/bs.coac.2021.02.003>
- Marcé, R., Armengol, J., 2009. Modeling nutrient in-stream processes at the watershed scale using Nutrient Spiralling metrics. *Hydrol. Earth Syst. Sci.* 13, 953–967. <https://doi.org/10.5194/hess-13-953-2009>
- Marcé, R., Armengol, J., 2009. Water Quality in Reservoirs Under a Changing Climate, in: Sabater, S., Barceló, D. (Eds.), *Water Scarcity in the Mediterranean, The Handbook of Environmental Chemistry*. Springer Berlin Heidelberg, Berlin, Heidelberg, pp. 73–94. https://doi.org/10.1007/698_2009_38
- Marcé, R., Comerma, M., García, J.C., Armengol, J., 2004. A neuro-fuzzy modeling tool to estimate fluvial nutrient loads in watersheds under time-varying human impact. *Limnol. Oceanogr. Methods* 2, 342–355. <https://doi.org/10.4319/lom.2004.2.342>
- Marcé, R., Moreno-Ostos, E., López, P., Armengol, J., 2008. The role of allochthonous inputs of dissolved organic carbon on the hypolimnetic oxygen content of reservoirs. *Ecosystems* 11, 1035–1053. <https://doi.org/10.1007/s10021-008-9177-5>
- Marcé, R., Moreno-Ostos, E., Ordóñez, J., Feijoó, C., Navarro, E., Caputo, L., Armengol, J., 2006. Nutrient fluxes through boundaries in the hypolimnion of Sau reservoir: Expected patterns and unanticipated processes. *Limnetica* 25, 527–540.

References

- Marcé, R., Rodríguez-Arias, M.À., García, J.C., Armengol, J., 2010. El Niño Southern Oscillation and climate trends impact reservoir water quality: CLIMATE PHENOMENA AND RESERVOIR WATER QUALITY. *Glob. Change Biol.* 16, 2857–2865. <https://doi.org/10.1111/j.1365-2486.2010.02163.x>
- Marcé, R., Verdura, L., Leung, N., 2021. Dissolved organic matter spectroscopy reveals a hot spot of organic matter changes at the river–reservoir boundary. *Aquat. Sci.* 83, 67. <https://doi.org/10.1007/s00027-021-00823-6>
- March, H., Saurí, D., 2010. The Suburbanization of Water Scarcity in the Barcelona Metropolitan Region: Sociodemographic and Urban Changes Influencing Domestic Water Consumption. *Prof. Geogr.* 62, 32–45. <https://doi.org/10.1080/00330120903375860>
- Martin-Ortega, J., González-Eguino, M., Markandya, A., 2012. The costs of drought: the 2007/2008 case of Barcelona. *Water Policy* 14, 539–560. <https://doi.org/10.2166/wp.2011.121>
- Mash, C.A., Winston, B.A., Meints Li, D.A., Pifer, A.D., Scott, J.T., Zhang, W., Fairey, J.L., 2014. Assessing trichloromethane formation and control in algal-stimulated waters amended with nitrogen and phosphorus. *Env. Sci Process. Impacts* 16, 1290–1299. <https://doi.org/10.1039/C3EM00634D>
- Mash, H., Westerhoff, P.K., Baker, L.A., Nieman, R.A., Nguyen, M.-L., 2004. Dissolved organic matter in Arizona reservoirs: assessment of carbonaceous sources. *Org. Geochem.* 35, 831–843. <https://doi.org/10.1016/j.orggeochem.2004.03.002>
- Matilla-García, M., Queralt, R., Sanz, P., Vázquez, F.J., 2004. A generalized BDS statistic. *Comput. Econ.* 24, 277–300. <https://doi.org/10.1007/s10614-004-4657-y>
- Maxwell, S.L., Butt, N., Maron, M., McAlpine, C.A., Chapman, S., Ullmann, A., Segan, D.B., Watson, J.E.M., 2019. Conservation implications of ecological responses to extreme weather and climate events. *Divers. Distrib.* 25, 613–625. <https://doi.org/10.1111/ddi.12878>
- Mazhar, M.A., Khan, N.A., Ahmed, S., Khan, A.H., Hussain, A., Rahisuddin, Changani, F., Yousefi, M., Ahmadi, S., Vambol, V., 2020. Chlorination disinfection by-products in municipal drinking water – A review. *J. Clean. Prod.* 273, 123159. <https://doi.org/10.1016/j.jclepro.2020.123159>
- Mazo, D., Alcantud, A., 2012. Water Crisis: Public Management of a Critical Situation, in: Otto-Zimmermann, K. (Ed.), *Resilient Cities 2, Local Sustainability*. Springer Netherlands, Dordrecht, pp. 65–74. https://doi.org/10.1007/978-94-007-4223-9_7

References

- McLaughlin, M.J., Sainani, K.L., 2014. Bonferroni, Holm, and Hochberg Corrections: Fun Names, Serious Changes to *P* Values. *PM&R* 6, 544–546. <https://doi.org/10.1016/j.pmrj.2014.04.006>
- Meerhoff, M., Audet, J., Davidson, T.A., De Meester, L., Hilt, S., Kosten, S., Liu, Z., Mazzeo, N., Paerl, H., Scheffer, M., Jeppesen, E., 2022. Feedback between climate change and eutrophication: revisiting the allied attack concept and how to strike back. *Inland Waters* 12, 187–204. <https://doi.org/10.1080/20442041.2022.2029317>
- Mehmood, H., 2019. *Bibliometrics of Water Research: A Global Snapshot*. United Nations University Institute for Water, Environment and Health. <https://doi.org/10.53328/EYBT8774>
- Melo, L.D.V., Da Costa, E.P., Pinto, C.C., Barroso, G.R., Oliveira, S.C., 2019. Adequacy analysis of drinking water treatment technologies in regard to the parameter turbidity, considering the quality of natural waters treated by large-scale WTPs in Brazil. *Environ. Monit. Assess.* 191, 384. <https://doi.org/10.1007/s10661-019-7526-9>
- Meulemans, C.C.E., 1987. The Basic Principles of UV–Disinfection of Water. *Ozone Sci. Eng.* 9, 299–313. <https://doi.org/10.1080/01919518708552146>
- Mian, H.R., Chhipi-Shrestha, G., Hewage, K., Rodriguez, M.J., Sadiq, R., 2020. Predicting unregulated disinfection by-products in small water distribution networks: an empirical modelling framework. *Environ. Monit. Assess.* 192, 497. <https://doi.org/10.1007/s10661-020-08468-y>
- Miao, S., Lyu, H., Wang, Q., Li, Y., Wu, Z., Du, C., Xu, J., Bi, S., Mu, M., Lei, S., 2019. Estimation of terrestrial humic-like substances in inland lakes based on the optical and fluorescence characteristics of chromophoric dissolved organic matter (CDOM) using OLCI images. *Ecol. Indic.* 101, 399–409. <https://doi.org/10.1016/j.ecolind.2019.01.039>
- Mihaljević, M., Stević, F., Horvatić, J., Hackenberger Kutuzović, B., 2009. Dual impact of the flood pulses on the phytoplankton assemblages in a Danubian floodplain lake (Kopački Rit Nature Park, Croatia). *Hydrobiologia* 618, 77–88. <https://doi.org/10.1007/s10750-008-9550-6>
- Milstead, R.P., Remucal, C.K., 2021. Molecular-Level Insights into the Formation of Traditional and Novel Halogenated Disinfection Byproducts. *ACS EST Water* 1, 1966–1974. <https://doi.org/10.1021/acsestwater.1c00161>
- Minami, K., 2009. Soil and humanity: Culture, civilization, livelihood and health. *Soil Sci. Plant Nutr.* 55, 603–615. <https://doi.org/10.1111/j.1747-0765.2009.00401.x>

References

- Minor, E., Stephens, B., 2008. Dissolved organic matter characteristics within the Lake Superior watershed. *Org. Geochem.* 39, 1489–1501. <https://doi.org/10.1016/j.orggeochem.2008.08.001>
- Minor, E.C., Swenson, M.M., Mattson, B.M., Oyler, A.R., 2014. Structural characterization of dissolved organic matter: a review of current techniques for isolation and analysis. *Env. Sci Process. Impacts* 16, 2064–2079. <https://doi.org/10.1039/C4EM00062E>
- Mishra, A.K., Singh, V.P., 2010. A review of drought concepts. *J. Hydrol.* 391, 202–216. <https://doi.org/10.1016/j.jhydrol.2010.07.012>
- Molina, A., Melgarejo, J., 2016. Water policy in Spain: seeking a balance between transfers, desalination and wastewater reuse. *Int. J. Water Resour. Dev.* 32, 781–798. <https://doi.org/10.1080/07900627.2015.1077103>
- Monteith, D.T., Henrys, P.A., Evans, C.D., Malcolm, I., Shilland, E.M., Pereira, M.G., 2015. Spatial controls on dissolved organic carbon in upland waters inferred from a simple statistical model. *Biogeochemistry* 123, 363–377. <https://doi.org/10.1007/s10533-015-0071-x>
- Mopper, K., Stubbins, A., Ritchie, J.D., Bialk, H.M., Hatcher, P.G., 2007. Advanced Instrumental Approaches for Characterization of Marine Dissolved Organic Matter: Extraction Techniques, Mass Spectrometry, and Nuclear Magnetic Resonance Spectroscopy. *Chem. Rev.* 107, 419–442. <https://doi.org/10.1021/cr050359b>
- Morales-Williams, A.M., Wanamaker, A.D., Williams, C.J., Downing, J.A., 2021. Eutrophication Drives Extreme Seasonal CO₂ Flux in Lake Ecosystems. *Ecosystems* 24, 434–450. <https://doi.org/10.1007/s10021-020-00527-2>
- Morrongiello, J.R., Crook, D.A., King, A.J., Ramsey, D.S.L., Brown, P., 2011. Impacts of drought and predicted effects of climate change on fish growth in temperate Australian lakes: FISH RESPONSES TO ENVIRONMENTAL CHANGE. *Glob. Change Biol.* 17, 745–755. <https://doi.org/10.1111/j.1365-2486.2010.02259.x>
- Mosley, L.M., 2015. Drought impacts on the water quality of freshwater systems; review and integration. *Earth-Sci. Rev.* 140, 203–214. <https://doi.org/10.1016/j.earscirev.2014.11.010>
- Mosley, L.M., Zammit, B., Leyden, E., Heneker, T.M., Hipsey, M.R., Skinner, D., Aldridge, K.T., 2012. The Impact of Extreme Low Flows on the Water Quality of the Lower Murray River and Lakes (South Australia). *Water Resour. Manag.* 26, 3923–3946. <https://doi.org/10.1007/s11269-012-0113-2>
- Mostofa, K.M.G., Liu, C., Mottaleb, M.A., Wan, G., Ogawa, H., Vione, D., Yoshioka, T., Wu, F., 2013a. Dissolved Organic Matter in Natural Waters, in: Mostofa, K.M.G., Yoshioka, T.,

References

- Mottaleb, A., Vione, D. (Eds.), Photobiogeochemistry of Organic Matter, Environmental Science and Engineering. Springer Berlin Heidelberg, Berlin, Heidelberg, pp. 1–137. https://doi.org/10.1007/978-3-642-32223-5_1
- Mostofa, K.M.G., Liu, C., Vione, D., Mottaleb, M.A., Ogawa, H., Tareq, S.M., Yoshioka, T., 2013b. Colored and Chromophoric Dissolved Organic Matter in Natural Waters, in: Mostofa, K.M.G., Yoshioka, T., Mottaleb, A., Vione, D. (Eds.), Photobiogeochemistry of Organic Matter, Environmental Science and Engineering. Springer Berlin Heidelberg, Berlin, Heidelberg, pp. 365–428. https://doi.org/10.1007/978-3-642-32223-5_5
- Mostofa, K.M.G., Liu, C., Yoshioka, T., Vione, D., Zhang, Y., Sakugawa, H., 2013c. Fluorescent Dissolved Organic Matter in Natural Waters, in: Mostofa, K.M.G., Yoshioka, T., Mottaleb, A., Vione, D. (Eds.), Photobiogeochemistry of Organic Matter, Environmental Science and Engineering. Springer Berlin Heidelberg, Berlin, Heidelberg, pp. 429–559. https://doi.org/10.1007/978-3-642-32223-5_6
- Müller, B., Bryant, L.D., Matzinger, A., Wüest, A., 2012. Hypolimnetic Oxygen Depletion in Eutrophic Lakes. Environ. Sci. Technol. 46, 9964–9971. <https://doi.org/10.1021/es301422r>
- Murphy, K.R., Timko, S.A., Gonsior, M., Powers, L.C., Wunsch, U.J., Stedmon, C.A., 2018. Photochemistry Illuminates Ubiquitous Organic Matter Fluorescence Spectra. Environ. Sci. Technol. 52, 11243–11250. <https://doi.org/10.1021/acs.est.8b02648>
- Musikavong, C., Wattanachira, S., 2013. Identification of dissolved organic matter in raw water supply from reservoirs and canals as precursors to trihalomethanes formation. J. Environ. Sci. Health Part -Toxic/Hazardous Subst. Environ. Eng. 48, 760–771. <https://doi.org/10.1080/10934529.2013.744634>
- Na-Phatthalung, W., Musikavong, C., Suttinun, O., 2019. Degradation of N-nitrosodimethylamine and its amine precursors by cumene-induced Rhodococcus sp. strain L4. Biodegradation 30, 375–388. <https://doi.org/10.1007/s10532-019-09876-9>
- Nawrocki, J., Andrzejewski, P., 2011. Nitrosamines and water. J. Hazard. Mater. 189, 1–18. <https://doi.org/10.1016/j.jhazmat.2011.02.005>
- Navarro, T., 2018. Water reuse and desalination in Spain – challenges and opportunities. J. Water Reuse Desalination 8, 153–168. <https://doi.org/10.2166/wrd.2018.043>
- Newcombe, G., Cook, D., 2002. Influences on the removal of tastes and odours by PAC. J. Water Supply Res. Technol.-Aqua 51, 463–474. <https://doi.org/10.2166/aqua.2002.0040>
- Ngwenya, N., Ncube, E.J., Parsons, J., 2013. Recent Advances in Drinking Water Disinfection: Successes and Challenges, in: Whitacre, D.M. (Ed.), Reviews of Environmental

References

- Contamination and Toxicology, Reviews of Environmental Contamination and Toxicology. Springer New York, New York, NY, pp. 111–170. https://doi.org/10.1007/978-1-4614-4717-7_4
- Nimmo, D.G., Mac Nally, R., Cunningham, S.C., Haslem, A., Bennett, A.F., 2015. Vive la résistance: Reviving resistance for 21st century conservation. *Trends Ecol. Evol.* 30, 516–523. <https://doi.org/10.1016/j.tree.2015.07.008>
- Noori, R., Berndtsson, R., Franklin Adamowski, J., Rabiee Abyaneh, M., 2018. Temporal and depth variation of water quality due to thermal stratification in Karkheh Reservoir, Iran. *J. Hydrol. Reg. Stud.* 19, 279–286. <https://doi.org/10.1016/j.ejrh.2018.10.003>
- O'Connor, E.M., Dillon, P.J., Molot, L.A., Creed, I.F., 2009. Modeling dissolved organic carbon mass balances for lakes of the Muskoka River Watershed. *Hydrol. Res.* 40, 273–290. <https://doi.org/10.2166/nh.2009.106>
- Ofori, I., Maddila, S., Lin, J., Jonnalagadda, S.B., 2018. Chlorine dioxide inactivation of *Pseudomonas aeruginosa* and *Staphylococcus aureus* in water: The kinetics and mechanism. *J. Water Process Eng.* 26, 46–54. <https://doi.org/10.1016/j.jwpe.2018.09.001>
- Ofori, I., Maddila, S., Lin, J., Jonnalagadda, S.B., 2017. Chlorine dioxide oxidation of *Escherichia coli* in water – A study of the disinfection kinetics and mechanism. *J. Environ. Sci. Health Part A* 52, 598–606. <https://doi.org/10.1080/10934529.2017.1293993>
- Olds, B.P., Peterson, B.C., Koupal, K.D., Farnsworth-Hoback, K.M., Schoenebeck, C.W., Hoback, W.W., 2011. Water quality parameters of a Nebraska reservoir differ between drought and normal conditions. *Lake Reserv. Manag.* 27, 229–234. <https://doi.org/10.1080/07438141.2011.601401>
- Ogutu-Ohwayo, R., Natugonza, V., Musinguzi, L., Olokotum, M., Naigaga, S., 2016. Implications of climate variability and change for African lake ecosystems, fisheries productivity, and livelihoods. *J. Gt. Lakes Res.* 42, 498–510. <https://doi.org/10.1016/j.jglr.2016.03.004>
- Olds, H.T., Corsi, S.R., Dila, D.K., Halmo, K.M., Bootsma, M.J., McLellan, S.L., 2018. High levels of sewage contamination released from urban areas after storm events: A quantitative survey with sewage specific bacterial indicators. *PLOS Med.* 15, e1002614. <https://doi.org/10.1371/journal.pmed.1002614>
- Olsen, B.K., Chislock, M.F., Wilson, A.E., 2016. Eutrophication mediates a common off-flavor compound, 2-methylisoborneol, in a drinking water reservoir. *Water Res.* 92, 228–234. <https://doi.org/10.1016/j.watres.2016.01.058>

References

- Onstad, G.D., Weinberg, H.S., 2005. Evaluation of the stability and analysis of halogenated furanones in disinfected drinking waters. *Anal. Chim. Acta* 534, 281–292. <https://doi.org/10.1016/j.aca.2004.11.046>
- Ordóñez, J., Armengol, J., Moreno-Ostos, E., Caputo, L., García, J.C., Marcé, R., 2010. On non-Eltonian methods of hunting Cladocera, or impacts of the introduction of planktivorous fish on zooplankton composition and clear-water phase occurrence in a Mediterranean reservoir. *Hydrobiologia* 653, 119–129. <https://doi.org/10.1007/s10750-010-0348-y>
- Osburn, C.L., Anderson, N.J., Stedmon, C.A., Giles, M.E., Whiteford, E.J., McGenity, T.J., Dumbrell, A.J., Underwood, G.J.C., 2017. Shifts in the Source and Composition of Dissolved Organic Matter in Southwest Greenland Lakes Along a Regional Hydro-climatic Gradient: DOM Quality in Greenland Lakes. *J. Geophys. Res. Biogeosciences* 122, 3431–3445. <https://doi.org/10.1002/2017JG003999>
- Paerl, H.W., Paul, V.J., 2012. Climate change: Links to global expansion of harmful cyanobacteria. *Water Res.* 46, 1349–1363. <https://doi.org/10.1016/j.watres.2011.08.002>
- Painter, K.J., Venkiteswaran, J.J., Simon, D.F., Vo Duy, S., Sauvé, S., Baulch, H.M., 2022. Early and late cyanobacterial bloomers in a shallow, eutrophic lake. *Environ. Sci. Process. Impacts* 24, 1212–1227. <https://doi.org/10.1039/D2EM00078D>
- Pakharuddin, N.H., Fazly, M.N., Ahmad Sukari, S.H., Tho, K., Zamri, W.F.H., 2021. Water treatment process using conventional and advanced methods: A comparative study of Malaysia and selected countries. *IOP Conf. Ser. Earth Environ. Sci.* 880, 012017. <https://doi.org/10.1088/1755-1315/880/1/012017>
- Palmstrom, N.S., Carlson, R.E., Cooke, G.D., 1988. Potential Links Between Eutrophication and the Formation of Carcinogens in Drinking Water. *Lake Reserv. Manag.* 4, 1–15. <https://doi.org/10.1080/07438148809354809>
- Pan, R., Huang, Y., Ao, J., Wu, Y., Bu, L., Zhou, S., Deng, L., Shi, Z., 2023. A molecular-level mechanism analysis of PFS coagulation behaviors: Differences in natural organic matter and algal organic matter. *Sep. Purif. Technol.* 314, 123485. <https://doi.org/10.1016/j.seppur.2023.123485>
- Park, J.W., Duong, T.H., Noh, J.H., Chung, S.-Y., Son, H., Prest, E., Oh, S., Maeng, S.K., 2021. Occurrences and changes in bacterial growth-promoting nutrients in drinking water from source to tap: a review. *Environ. Sci. Water Res. Technol.* 7, 2206–2222. <https://doi.org/10.1039/D1EW00514F>

References

- Parparov, A., Gal, G., Zohary, T., 2015. Quantifying the ecological stability of a phytoplankton community: The Lake Kinneret case study. *Ecol. Indic.* 56, 134–144. <https://doi.org/10.1016/j.ecolind.2015.04.002>
- Parparov, A., Gal, G., 2017. Quantifying Ecological Stability: From Community to the Lake Ecosystem. *Ecosystems* 20, 1015–1028. <https://doi.org/10.1007/s10021-016-0090-z>
- Pehlivanoglu-Mantas, E., Sedlak, D.L., 2006. The fate of wastewater-derived NDMA precursors in the aquatic environment. *Water Res.* 40, 1287–1293. <https://doi.org/10.1016/j.watres.2006.01.012>
- Peleato, N.M., 2022. Application of convolutional neural networks for prediction of disinfection by-products. *Sci. Rep.* 12, 612. <https://doi.org/10.1038/s41598-021-03881-w>
- Peleato, N.M., Legge, R.L., Andrews, R.C., 2018. Neural networks for dimensionality reduction of fluorescence spectra and prediction of drinking water disinfection by-products. *Water Res.* 136, 84–94. <https://doi.org/10.1016/j.watres.2018.02.052>
- Pellerin, B.A., Hernes, P.J., Saraceno, J., Spencer, R.G.M., Bergamaschi, B.A., 2010. Microbial Degradation of Plant Leachate Alters Lignin Phenols and Trihalomethane Precursors. *J. Environ. Qual.* 39, 946–954. <https://doi.org/10.2134/jeq2009.0487>
- Peng, J., Huang, H., Zhong, Y., Yin, R., Wu, Q., Shang, C., Yang, X., 2022. Transformation of dissolved organic matter during biological wastewater treatment and relationships with the formation of nitrogenous disinfection byproducts. *Water Res.* 222, 118870. <https://doi.org/10.1016/j.watres.2022.118870>
- Pichel, N., Vivar, M., Fuentes, M., 2019. The problem of drinking water access: A review of disinfection technologies with an emphasis on solar treatment methods. *Chemosphere* 218, 1014–1030. <https://doi.org/10.1016/j.chemosphere.2018.11.205>
- Pietz, D.A., Zeisler-Vralsted, D., 2021. *Water and Human Societies: Historical and Contemporary Perspectives*. Springer International Publishing, Cham. <https://doi.org/10.1007/978-3-030-67692-6>
- Pifer, A.D., Cousins, S.L., Fairey, J.L., 2014. Assessing UV- and fluorescence-based metrics as disinfection byproduct precursor surrogate parameters in a water body influenced by a heavy rainfall event. *J. Water Supply Res. Technol.-Aqua* 63, 200–211. <https://doi.org/10.2166/aqua.2013.122>
- Pikovskoi, I.I., Kosyakov, D.S., 2023. Kendrick mass defect analysis — a tool for high-resolution Orbitrap mass spectrometry of native lignin. *Anal. Bioanal. Chem.* 415, 3525–3534. <https://doi.org/10.1007/s00216-023-04742-3>

References

- Pivokonsky, M., Novotna, K., Petricek, R., Cermakova, L., Prokopova, M., Naceradska, J., 2024. Fundamental chemical aspects of coagulation in drinking water treatment – Back to basics. *J. Water Process Eng.* 57, 104660. <https://doi.org/10.1016/j.jwpe.2023.104660>
- Pokrovsky, O.S., Shirokova, L.S., Kirpotin, S.N., Kulizhsky, S.P., Vorobiev, S.N., 2013. Impact of western Siberia heat wave 2012 on greenhouse gases and trace metal concentration in thaw lakes of discontinuous permafrost zone. *Biogeosciences* 10, 5349–5365. <https://doi.org/10.5194/bg-10-5349-2013>
- Polazzo, F., Roth, S.K., Hermann, M., Mangold-Döring, A., Rico, A., Sobek, A., Van Den Brink, P.J., Jackson, M.C., 2022. Combined effects of heatwaves and micropollutants on freshwater ecosystems: Towards an integrated assessment of extreme events in multiple stressors research. *Glob. Change Biol.* 28, 1248–1267. <https://doi.org/10.1111/gcb.15971>
- Pooja, D., Kumar, P., Singh, P., Patil, S. (Eds.), 2020. *Sensors in Water Pollutants Monitoring: Role of Material, Advanced Functional Materials and Sensors*. Springer Singapore, Singapore. <https://doi.org/10.1007/978-981-15-0671-0>
- Praise, S., Ito, H., Watanabe, K., Sasaki, A., Watanabe, T., 2020. Association of dissolved organic matter characteristics and trace metals in mountainous streams with sabo dams. *Environ. Sci. Pollut. Res.* 27, 456–468. <https://doi.org/10.1007/s11356-019-06911-3>
- Prasert, T., Ishii, Y., Kurisu, F., Musikavong, C., Phungsai, P., 2023. Changes in molecular dissolved organic matter during coagulation/sedimentation and chlorine and chlorine dioxide disinfection by non-target (or unknown) screening analysis. *J. Water Process Eng.* 52, 103528. <https://doi.org/10.1016/j.jwpe.2023.103528>
- Pretty, J.N., Mason, C.F., Nedwell, D.B., Hine, R.E., Leaf, S., Dils, R., 2003. Environmental Costs of Freshwater Eutrophication in England and Wales. *Environ. Sci. Technol.* 37, 201–208. <https://doi.org/10.1021/es020793k>
- Price, D., 1995. Energy and human evolution. *Popul. Environ.* 16, 301–319. <https://doi.org/10.1007/BF02208116>
- Puth, M.-T., Neuhäuser, M., Ruxton, G.D., 2015. Effective use of Spearman’s and Kendall’s correlation coefficients for association between two measured traits. *Anim. Behav.* 102, 77–84. <https://doi.org/10.1016/j.anbehav.2015.01.010>
- Qin, B., Gao, G., Zhu, G., Zhang, Y., Song, Y., Tang, X., Xu, H., Deng, J., 2013. Lake eutrophication and its ecosystem response. *Chin. Sci. Bull.* 58, 961–970. <https://doi.org/10.1007/s11434-012-5560-x>

References

- Raseman, W.J., Kasprzyk, J.R., Rosario-Ortiz, F.L., Stewart, J.R., Livneh, B., 2017. Emerging investigators series: a critical review of decision support systems for water treatment: making the case for incorporating climate change and climate extremes. *Environ. Sci. Water Res. Technol.* 3, 18–36. <https://doi.org/10.1039/C6EW00121A>
- Ratpukdi, T., Sinorak, S., Kiattisaksiri, P., Punyapalakul, P., Siripattanakul-Ratpukdi, S., 2019. Occurrence of trihalomethanes and haloacetonitriles in water distribution networks of Khon Kaen Municipality, Thailand. *Water Supply* 19, 1748–1757. <https://doi.org/10.2166/ws.2019.049>
- Ravichandran, M., 2004. Interactions between mercury and dissolved organic matter—a review. *Chemosphere* 55, 319–331. <https://doi.org/10.1016/j.chemosphere.2003.11.011>
- Raymond, P.A., Saiers, J.E., Sobczak, W.V., 2016. Hydrological and biogeochemical controls on watershed dissolved organic matter transport: pulse-shunt concept. *Ecology* 97, 5–16. <https://doi.org/10.1890/14-1684.1>
- Reckhow, D.A., MacNeill, A.L., Platt, T.L., MacNeill, A.L., McClellan, J.N., 2001. Formation and degradation of dichloroacetonitrile in drinking waters. *J. Water Supply Res. Technol.-Aqua* 50, 1–13. <https://doi.org/10.2166/aqua.2001.0001>
- Reid, E., Igou, T., Zhao, Y., Crittenden, J., Huang, C.-H., Westerhoff, P., Rittmann, B., Drewes, J.E., Chen, Y., 2023. The Minus Approach Can Redefine the Standard of Practice of Drinking Water Treatment. *Environ. Sci. Technol.* 57, 7150–7161. <https://doi.org/10.1021/acs.est.2c09389>
- Ribatet, M., 2011. A User ' s Guide to the POT Package (Version 1 . 4) An Introduction to the EVT The univariate case 1–31.
- Riise, G., Haaland, S.L., Xiao, Y., 2023. Coupling of iron and dissolved organic matter in lakes—selective retention of different size fractions. *Aquat. Sci.* 85, 57. <https://doi.org/10.1007/s00027-023-00956-w>
- Ringnér, M., 2008. What is principal component analysis? *Nat. Biotechnol.* 26, 303–304. <https://doi.org/10.1038/nbt0308-303>
- Rooney, G.G., Van Lipzig, N., Thiery, W., 2018. Estimating the effect of rainfall on the surface temperature of a tropical lake. *Hydrol. Earth Syst. Sci.* 22, 6357–6369. <https://doi.org/10.5194/hess-22-6357-2018>
- Rosario-Ortiz, F.L., Korak, J.A., 2017. Oversimplification of Dissolved Organic Matter Fluorescence Analysis: Potential Pitfalls of Current Methods. *Environ. Sci. Technol.* 51, 759–761. <https://doi.org/10.1021/acs.est.6b06133>

References

- Ross, S.R.P. -J., Suzuki, Y., Kondoh, M., Suzuki, K., Villa Martín, P., Dornelas, M., 2021. Illuminating the intrinsic and extrinsic drivers of ecological stability across scales. *Ecol. Res.* 36, 364–378. <https://doi.org/10.1111/1440-1703.12214>
- Runge, J., Bathiany, S., Bollt, E., Camps-Valls, G., Coumou, D., Deyle, E., Glymour, C., Kretschmer, M., Mahecha, M.D., Muñoz-Marí, J., Van Nes, E.H., Peters, J., Quax, R., Reichstein, M., Scheffer, M., Schölkopf, B., Spirtes, P., Sugihara, G., Sun, J., Zhang, K., Zscheischler, J., 2019. Inferring causation from time series in Earth system sciences. *Nat. Commun.* 10, 2553. <https://doi.org/10.1038/s41467-019-10105-3>
- Russo, S., Sillmann, J., Fischer, E.M., 2015. Top ten European heatwaves since 1950 and their occurrence in the coming decades. *Environ. Res. Lett.* 10. <https://doi.org/10.1088/1748-9326/10/12/124003>
- Sadiq, R., Rodriguez, M., 2004. Disinfection by-products (DBPs) in drinking water and predictive models for their occurrence: a review. *Sci. Total Environ.* 321, 21–46. <https://doi.org/10.1016/j.scitotenv.2003.05.001>
- Sadro, S., Melack, J.M., 2012. The Effect of an Extreme Rain Event on the Biogeochemistry and Ecosystem Metabolism of an Oligotrophic High-Elevation Lake. *Arct. Antarct. Alp. Res.* 44, 222–231. <https://doi.org/10.1657/1938-4246-44.2.222>
- Saleem, M., Bachmann, R.T., 2019. A contemporary review on plant-based coagulants for applications in water treatment. *J. Ind. Eng. Chem.* 72, 281–297. <https://doi.org/10.1016/j.jiec.2018.12.029>
- Sanuy, M., Rigo, T., Jiménez, J.A., Llasat, M.C., 2021. Classifying compound coastal storm and heavy rainfall events in the north-western Spanish Mediterranean. *Hydrol. Earth Syst. Sci.* 25, 3759–3781. <https://doi.org/10.5194/hess-25-3759-2021>
- Sanchez, N.P., Skeriotis, A.T., Miller, C.M., 2013. Assessment of dissolved organic matter fluorescence PARAFAC components before and after coagulation–filtration in a full scale water treatment plant. *Water Res.* 47, 1679–1690. <https://doi.org/10.1016/j.watres.2012.12.032>
- Sanchís, J., Gernjak, W., Munné, A., Catalán, N., Petrovic, M., Farré, M.J., 2021. Fate of N-nitrosodimethylamine and its precursors during a wastewater reuse trial in the Llobregat River (Spain). *J. Hazard. Mater.* 407. <https://doi.org/10.1016/j.jhazmat.2020.124346>
- Schwarzenbach, R.P., Egli, T., Hofstetter, T.B., Von Gunten, U., Wehrli, B., 2010. Global Water Pollution and Human Health. *Annu. Rev. Environ. Resour.* 35, 109–136. <https://doi.org/10.1146/annurev-environ-100809-125342>

References

- Selkimäki, M., González-Olabarria, J.R., 2017. Assessing Gully Erosion Occurrence in Forest Lands in Catalonia (Spain). *Land Degrad. Dev.* 28, 616–627. <https://doi.org/10.1002/ldr.2533>
- Slavik, I., Uhl, W., 2009. Analysing water quality changes due to reservoir management and climate change for optimization of drinking water treatment. *Water Sci.*
- Shammas, N.K., Kumar, I.J., Chang, S.-Y., Hung, Y.-T., 2005. *Sedimentation*. Springer.
- Sharma, S., Bhattacharya, A., 2017. Drinking water contamination and treatment techniques. *Appl. Water Sci.* 7, 1043–1067. <https://doi.org/10.1007/s13201-016-0455-7>
- Sommer, F., Anderson, J.M., Bharti, R., Raes, J., Rosenstiel, P., 2017. The resilience of the intestinal microbiota influences health and disease. *Nat. Rev. Microbiol.* 15, 630–638. <https://doi.org/10.1038/nrmicro.2017.58>
- Staben, N., Nahrstedt, A., Merkel, W., 2015. Securing safe drinking water supply under climate change conditions. *Water Supply* 15, 1334–1342. <https://doi.org/10.2166/ws.2015.099>
- Savory, A., 1994. Will we be able to sustain civilization? *Popul. Environ.* 16, 139–147. <https://doi.org/10.1007/BF02208780>
- Scheff, S.W., 2016. Nonparametric Statistics, in: *Fundamental Statistical Principles for the Neurobiologist*. Elsevier, pp. 157–182. <https://doi.org/10.1016/B978-0-12-804753-8.00008-7>
- Schindler, D.W., Curtis, P.J., Bayley, S.E., Parker, B.R., Beaty, K.G., Stainton, M.P., 1997. Climate-induced changes in the dissolved organic carbon budgets of boreal lakes. *Biogeochemistry* 36, 9–28.
- Sgroi, M., Vagliasindi, F.G.A., Snyder, S.A., Roccaro, P., 2018. N-Nitrosodimethylamine (NDMA) and its precursors in water and wastewater: A review on formation and removal. *Chemosphere* 191, 685–703. <https://doi.org/10.1016/j.chemosphere.2017.10.089>
- Shah, A.D., Mitch, W.A., 2012. Halonitroalkanes, Halonitriles, Haloamides, and N-Nitrosamines: A Critical Review of Nitrogenous Disinfection Byproduct Formation Pathways. *Environ. Sci. Technol.* 46, 119–131. <https://doi.org/10.1021/es203312s>
- Shahi, N.K., Maeng, M., Dockko, S., 2020. Models for predicting carbonaceous disinfection by-products formation in drinking water treatment plants: a case study of South Korea. *Environ. Sci. Pollut. Res.* 27, 24594–24603. <https://doi.org/10.1007/s11356-019-05490-7>
- Shang, Y., Wen, Z., Song, K., Liu, G., Lai, F., Lyu, L., Li, S., Tao, H., Hou, J., Fang, C., He, C., Shi, Q., He, D., 2022. Natural versus anthropogenic controls on the dissolved organic

References

- matter chemistry in lakes across China: Insights from optical and molecular level analyses. *Water Res.* 221, 118779. <https://doi.org/10.1016/j.watres.2022.118779>
- Shao, L., Zhang, H., Chen, J., Zhu, X., 2021. Effect of oil price uncertainty on clean energy metal stocks in China: Evidence from a nonparametric causality-in-quantiles approach. *Int. Rev. Econ. Finance* 73, 407–419. <https://doi.org/10.1016/j.iref.2021.01.009>
- Sharp, J.O., Wood, T.K., Alvarez-Cohen, L., 2005. Aerobic biodegradation of N-nitrosodimethylamine (NDMA) by axenic bacterial strains. *Biotechnol. Bioeng.* 89, 608–618. <https://doi.org/10.1002/bit.20405>
- Shi, P., Zhu, M., You, R., Li, H., Zou, W., Xu, H., Xiao, M., Zhu, G., 2023. Rainstorm events trigger algal blooms in a large oligotrophic reservoir. *J. Hydrol.* 622, 129711. <https://doi.org/10.1016/j.jhydrol.2023.129711>
- Shi, W., Zhuang, W.-E., Hur, J., Yang, L., 2021. Monitoring dissolved organic matter in wastewater and drinking water treatments using spectroscopic analysis and ultra-high resolution mass spectrometry. *Water Res.* 188, 116406. <https://doi.org/10.1016/j.watres.2020.116406>
- Shutova, Y., Baker, A., Bridgeman, J., Henderson, R.K., 2014. Spectroscopic characterisation of dissolved organic matter changes in drinking water treatment: From PARAFAC analysis to online monitoring wavelengths. *Water Res.* 54, 159–169. <https://doi.org/10.1016/j.watres.2014.01.053>
- Sikder, R., Zhang, T., Ye, T., 2023. Predicting THM Formation and Revealing Its Contributors in Drinking Water Treatment Using Machine Learning. *ACS EST Water* acsestwater.3c00020. <https://doi.org/10.1021/acsestwater.3c00020>
- Sillanpää, M., Ncibi, M.C., Matilainen, A., Vepsäläinen, M., 2018. Removal of natural organic matter in drinking water treatment by coagulation: A comprehensive review. *Chemosphere* 190, 54–71. <https://doi.org/10.1016/j.chemosphere.2017.09.113>
- Sillmann, J., Thorarindottir, T., Keenlyside, N., Schaller, N., Alexander, L.V., Hegerl, G., Seneviratne, S.I., Vautard, R., Zhang, X., Zwiers, F.W., 2017. Understanding, modeling and predicting weather and climate extremes: Challenges and opportunities. *Weather Clim. Extrem.* 18, 65–74. <https://doi.org/10.1016/j.wace.2017.10.003>
- Silva, F.N., Vega-Oliveros, D.A., Yan, X., Flammini, A., Menczer, F., Radicchi, F., Kravitz, B., Fortunato, S., 2021. Detecting Climate Teleconnections With Granger Causality. *Geophys. Res. Lett.* 48. <https://doi.org/10.1029/2021GL094707>

References

- Simard, A., Pelletier, G., Rodriguez, M., 2011. Water residence time in a distribution system and its impact on disinfectant residuals and trihalomethanes. *J. Water Supply Res. Technol.-Aqua* 60, 375–390. <https://doi.org/10.2166/aqua.2011.019>
- Sleighter, R.L., Hatcher, P.G., 2007. The application of electrospray ionization coupled to ultrahigh resolution mass spectrometry for the molecular characterization of natural organic matter. *J. Mass Spectrom.* 42, 559–574. <https://doi.org/10.1002/jms.1221>
- Smeets, P.W.M.H., Medema, G.J., Van Dijk, J.C., 2009. The Dutch secret: how to provide safe drinking water without chlorine in the Netherlands. *Drink. Water Eng. Sci.* 2, 1–14. <https://doi.org/10.5194/dwes-2-1-2009>
- Smith, M.D., 2011. An ecological perspective on extreme climatic events: a synthetic definition and framework to guide future research: Defining extreme climate events. *J. Ecol.* 99, 656–663. <https://doi.org/10.1111/j.1365-2745.2011.01798.x>
- Smith, V.H., Tilman, G.D., Nekola, J.C., 1999. Eutrophication: impacts of excess nutrient inputs on freshwater, marine, and terrestrial ecosystems. *Environ. Pollut.* 100, 179–196. [https://doi.org/10.1016/S0269-7491\(99\)00091-3](https://doi.org/10.1016/S0269-7491(99)00091-3)
- Smyth, M.P., Dunning, N.P., Weaver, E.M., van Beynen, P., Zapata, D.O., 2017. The perfect storm: climate change and ancient Maya response in the Puuc Hills region of Yucatán. *Antiquity* 91, 490–509. <https://doi.org/10.15184/aqy.2016.266>
- Sohn, J., Amy, G., Cho, J., Lee, Y., Yoon, Y., 2004. Disinfectant decay and disinfection by-products formation model development: chlorination and ozonation by-products. *Water Res.* 38, 2461–2478. <https://doi.org/10.1016/j.watres.2004.03.009>
- Solomon, C.T., Jones, S.E., Weidel, B.C., Buffam, I., Fork, M.L., Karlsson, J., Larsen, S., Lennon, J.T., Read, J.S., Sadro, S., Saros, J.E., 2015. Ecosystem Consequences of Changing Inputs of Terrestrial Dissolved Organic Matter to Lakes: Current Knowledge and Future Challenges. *Ecosystems* 18, 376–389. <https://doi.org/10.1007/s10021-015-9848-y>
- Song, Y., Chen, M., Li, J., Zhang, L., Deng, Y., Chen, J., 2023. Can selective withdrawal control algal blooms in reservoirs? The underlying hydrodynamic mechanism. *J. Clean. Prod.* 394, 136358. <https://doi.org/10.1016/j.jclepro.2023.136358>
- Sossou, S.K., Gbedenu, D.K., Konate, Y., Sawadogo, B., Ameyapoh, Y., Maiga, A.H., Funamizu, N., 2016. Damage mechanisms of pathogenic bacteria in drinking water during chlorine and solar disinfection. *Int. J. Biol. Chem. Sci.* 10, 519. <https://doi.org/10.4314/ijbcs.v10i2.6>
- Soto Cárdenas, C., Gereá, M., García, P.E., Pérez, G.L., Diéguez, M.C., Rapacioli, R., Reissig, M., Queimaliños, C., 2017. Interplay between climate and hydrogeomorphic features and their

References

- effect on the seasonal variation of dissolved organic matter in shallow temperate lakes of the Southern Andes (Patagonia, Argentina): a field study based on optical properties. *Ecohydrology* 10, e1872. <https://doi.org/10.1002/eco.1872>
- Stadler, M., Ejarque, E., Kainz, M.J., 2020. In-lake transformations of dissolved organic matter composition in a subalpine lake do not change its biodegradability. *Limnol. Oceanogr.* 65, 1554–1572. <https://doi.org/10.1002/lno.11406>
- Stedmon, C.A., Markager, S., 2005. Tracing the production and degradation of autochthonous fractions of dissolved organic matter by fluorescence analysis. *Limnol. Oceanogr.* 50, 1415–1426. <https://doi.org/10.4319/lo.2005.50.5.1415>
- Stepczuk, C., Martin, A.B., Effler, S.W., Bloomfield, J.A., Auer, M.T., 1998a. Spatial and temporal patterns of THM precursors in a eutrophic reservoir. *Lake Reserv. Manag.* 14, 356–366. <https://doi.org/10.1080/07438149809354343>
- Stepczuk, C., Owens, E.M., Effler, S.W., Auer, M.T., Bloomfield, J.A., 1998b. A modeling analysis of THM precursors for a eutrophic reservoir. *Lake Reserv. Manag.* 14, 367–378. <https://doi.org/10.1080/07438149809354344>
- Stockwell, J.D., Doubek, J.P., Adrian, R., Anneville, O., Carey, C.C., Carvalho, L., Senerpont, L.N.D., Gaël, D., Grossart, M.A.F.H., Ibelings, B.W., Lajeunesse, M.J., Rinke, K., Rudstam, L.G., Rusak, J.A., Salmaso, N., 2020. Storm impacts on phytoplankton community dynamics in lakes 1–27. <https://doi.org/10.1111/gcb.15033>
- Su, M., Jia, D., Yu, J., Vogt, R.D., Wang, J., An, W., Yang, M., 2017. Reducing production of taste and odor by deep-living cyanobacteria in drinking water reservoirs by regulation of water level. *Sci. Total Environ.* 574, 1477–1483. <https://doi.org/10.1016/j.scitotenv.2016.08.134>
- Summerhayes, R.J., Morgan, G.G., Lincoln, D., Edwards, H.P., Earnest, A., Rahman, Md.B., Byleveld, P., Cowie, C.T., Beard, J.R., 2011. Spatio-temporal variation in trihalomethanes in New South Wales. *Water Res.* 45, 5715–5726. <https://doi.org/10.1016/j.watres.2011.08.045>
- Summers, R.S., Kim, S.M., Shimabuku, K., Chae, S.-H., Corwin, C.J., 2013. Granular activated carbon adsorption of MIB in the presence of dissolved organic matter. *Water Res.* 47, 3507–3513. <https://doi.org/10.1016/j.watres.2013.03.054>
- Sun, W., Zhang, Y., Lu, Z., Ke, Y., Wang, X., Wu, J., 2023. Fate of Naturally Dissolved Organic Matter and Synthetic Organic Compounds Subjected to Drinking Water Treatment Using

References

- Membrane, Activated Carbon, and UV/H₂O₂ Technologies. *Environ. Sci. Technol.* 57, 5558–5568. <https://doi.org/10.1021/acs.est.2c06727>
- Szkokan-Emilson, E.J., Kielstra, B.W., Arnott, S.E., Watmough, S.A., Gunn, J.M., Tanentzap, A.J., 2017. Dry conditions disrupt terrestrial–aquatic linkages in northern catchments. *Glob. Change Biol.* 23, 117–126. <https://doi.org/10.1111/gcb.13361>
- Tak, S., Vellanki, B.P., 2018. Natural organic matter as precursor to disinfection byproducts and its removal using conventional and advanced processes: state of the art review. *J. Water Health* 16, 681–703. <https://doi.org/10.2166/wh.2018.032>
- Takkouk, S., Casamitjana, X., 2016. Application of the DYRESM–CAEDYM model to the Sau Reservoir situated in Catalonia, Spain. *Desalination Water Treat.* 57, 12453–12466. <https://doi.org/10.1080/19443994.2015.1053530>
- Tang, H.L., Chen, Y.-C., Regan, J.M., Xie, Y.F., 2012. Disinfection by-product formation potentials in wastewater effluents and their reductions in a wastewater treatment plant. *J. Environ. Monit.* 14, 1515. <https://doi.org/10.1039/c2em00015f>
- Tang, Y., Long, X., Wu, M., Yang, S., Gao, N., Xu, B., Dutta, S., 2020. Bibliometric review of research trends on disinfection by-products in drinking water during 1975–2018. *Sep. Purif. Technol.* 241, 116741. <https://doi.org/10.1016/j.seppur.2020.116741>
- Thayne, M.W., Kraemer, B.M., Mesman, J.P., Ibelings, B.W., Adrian, R., 2021. Antecedent lake conditions shape resistance and resilience of a shallow lake ecosystem following extreme wind storms. *Limnol. Oceanogr.* 1–20. <https://doi.org/10.1002/lno.11859>
- Thibault, K.M., Brown, J.H., 2008. Impact of an extreme climatic event on community assembly. *Proc. Natl. Acad. Sci.* 105, 3410–3415. <https://doi.org/10.1073/pnas.0712282105>
- Thompson, B., 2007. Effect sizes, confidence intervals, and confidence intervals for effect sizes. *Psychol. Sch.* 44, 423–432. <https://doi.org/10.1002/pits.20234>
- Tiwari, T., Sponseller, R.A., Laudon, H., 2022. The emerging role of drought as a regulator of dissolved organic carbon in boreal landscapes. *Nat. Commun.* 13, 5125. <https://doi.org/10.1038/s41467-022-32839-3>
- Toming, K., Kotta, J., Uemaa, E., Sobek, S., Kutser, T., Tranvik, L.J., 2020. Predicting lake dissolved organic carbon at a global scale. *Sci. Rep.* 10, 8471. <https://doi.org/10.1038/s41598-020-65010-3>
- Toming, K., Kutser, T., Tuvikene, L., Viik, M., Nöges, T., 2016. Dissolved organic carbon and its potential predictors in eutrophic lakes. *Water Res.* 102, 32–40. <https://doi.org/10.1016/j.watres.2016.06.012>

References

- Tomlinson, A., Drikas, M., Brookes, J.D., 2016. The role of phytoplankton as pre-cursors for disinfection by-product formation upon chlorination. *Water Res.* 102, 229–240. <https://doi.org/10.1016/j.watres.2016.06.024>
- Tranvik, L.J., Von Wachenfeldt, E., 2014. Interactions of Dissolved Organic Matter and Humic Substances in Freshwater Systems☆, in: Reference Module in Earth Systems and Environmental Sciences. Elsevier, p. B9780124095489093957. <https://doi.org/10.1016/B978-0-12-409548-9.09395-7>
- Trueman, B.F., MacIsaac, S.A., Stoddart, A.K., Gagnon, G.A., 2016. Prediction of disinfection by-product formation in drinking water via fluorescence spectroscopy. *Environ. Sci. Water Res. Technol.* 2, 383–389. <https://doi.org/10.1039/C5EW00285K>
- Tye, S.P., Siepielski, A.M., Bray, A., Rypel, A.L., Phelps, N.B.D., Fey, S.B., 2022. Climate warming amplifies the frequency of fish mass mortality events across north temperate lakes. *Limnol. Oceanogr. Lett.* 7, 510–519. <https://doi.org/10.1002/lol2.10274>
- Ummenhofer, C.C., Meehl, G.A., 2017. Extreme weather and climate events with ecological relevance: a review. *Philos. Trans. R. Soc. B Biol. Sci.* 372, 20160135–20160135. <https://doi.org/10.1098/rstb.2016.0135>
- Uyak, V., Ozdemir, K., Toroz, I., 2008. Seasonal variations of disinfection by-product precursors profile and their removal through surface water treatment plants. *Sci. Total Environ.* 390, 417–424. <https://doi.org/10.1016/j.scitotenv.2007.09.046>
- Uzun, H., Kim, D., Karanfil, T., 2014. ScienceDirect Seasonal and temporal patterns of NDMA formation potentials in surface waters. *Water Res.* 69, 162–172. <https://doi.org/10.1016/j.watres.2014.11.017>
- Vachon, D., Del Giorgio, P.A., 2014. Whole-Lake CO₂ Dynamics in Response to Storm Events in Two Morphologically Different Lakes. *Ecosystems* 17, 1338–1353. <https://doi.org/10.1007/s10021-014-9799-8>
- Valdiviezo Gonzales, L.G., García Ávila, F.F., Cabello Torres, R.J., Castañeda Olivera, C.A., Alfaro Paredes, E.A., 2021. Scientometric study of drinking water treatments technologies: Present and future challenges. *Cogent Eng.* 8, 1929046. <https://doi.org/10.1080/23311916.2021.1929046>
- Van Der Hoek, J.P., Bertelkamp, C., Verliefde, A.R.D., Singhal, N., 2014. Drinking water treatment technologies in Europe: state of the art – challenges – research needs. *J. Water Supply Res. Technol.-Aqua* 63, 124–130. <https://doi.org/10.2166/aqua.2013.007>

References

- van de Pol, M., Jenouvrier, S., Cornelissen, J.H.C., Visser, M.E., 2017. Behavioural, ecological and evolutionary responses to extreme climatic events: challenges and directions. *Philos. Trans. R. Soc. B Biol. Sci.* 372, 20160134–20160134. <https://doi.org/10.1098/rstb.2016.0134>
- Van Der Walt, A.J., Fitchett, J.M., 2022. Extreme Temperature Events (ETEs) in South Africa: a review. *South Afr. Geogr. J.* 104, 70–88. <https://doi.org/10.1080/03736245.2021.1907219>
- Van Meerbeek, K., Jucker, T., Svenning, J., 2021. Unifying the concepts of stability and resilience in ecology. *J. Ecol.* 109, 3114–3132. <https://doi.org/10.1111/1365-2745.13651>
- Vanderley, R.F., Ger, K.A., Becker, V., Bezerra, M.G.T.A., Panosso, R., 2021. Abiotic factors driving cyanobacterial biomass and composition under perennial bloom conditions in tropical latitudes. *Hydrobiologia* 848, 943–960. <https://doi.org/10.1007/s10750-020-04504-7>
- Verma, S., Daverey, A., Sharma, A., 2017. Slow sand filtration for water and wastewater treatment – a review. *Environ. Technol. Rev.* 6, 47–58. <https://doi.org/10.1080/21622515.2016.1278278>
- Vidal Celma, A., Om Tubau, J., 1993. The eutrophication process in Sau Reservoir (NE Spain): A long term study. *SIL Proc.* 1922-2010 25, 1247–1256. <https://doi.org/10.1080/03680770.1992.11900367>
- Vidal, J., Marcé, R., Serra, T., Colomer, J., Rueda, F., Casamitjana, X., 2012. Localized algal blooms induced by river inflows in a canyon type reservoir. *Aquat. Sci.* 74, 315–327. <https://doi.org/10.1007/s00027-011-0223-6>
- Villanueva, C.M., Garfí, M., Milà, C., Olmos, S., Ferrer, I., Tonne, C., 2021. Health and environmental impacts of drinking water choices in Barcelona, Spain: A modelling study. *Sci. Total Environ.* 795, 148884. <https://doi.org/10.1016/j.scitotenv.2021.148884>
- Vione, D., Minero, C., Carena, L., 2021. Fluorophores in surface freshwaters: importance, likely structures, and possible impacts of climate change. *Environ. Sci. Process. Impacts* 23, 1429–1442. <https://doi.org/10.1039/D1EM00273B>
- Von Gunten, U., 2003. Ozonation of drinking water: Part II. Disinfection and by-product formation in presence of bromide, iodide or chlorine. *Water Res.* 37, 1469–1487. [https://doi.org/10.1016/S0043-1354\(02\)00458-X](https://doi.org/10.1016/S0043-1354(02)00458-X)
- Wagner, S., Riedel, T., Niggemann, J., Vähätalo, A.V., Dittmar, T., Jaffé, R., 2015. Linking the Molecular Signature of Heteroatomic Dissolved Organic Matter to Watershed Characteristics in World Rivers. *Environ. Sci. Technol.* 49, 13798–13806. <https://doi.org/10.1021/acs.est.5b00525>

References

- Walker, B., Holling, C.S., Carpenter, S.R., Kinzig, A.P., 2004. Resilience, Adaptability and Transformability in Social-ecological Systems. *Ecol. Soc.* 9, art5. <https://doi.org/10.5751/ES-00650-090205>
- Walters, M., Scholes, R.J. (Eds.), 2017. *The GEO Handbook on Biodiversity Observation Networks*. Springer International Publishing, Cham. <https://doi.org/10.1007/978-3-319-27288-7>
- Wang, H., He, G., 2022. Rivers: Linking nature, life, and civilization. *River* 1, 25–36. <https://doi.org/10.1002/rvr2.7>
- Wang, H., Li, T., Zhu, J., Liu, Z., Yang, J.R., 2022. Effects of extreme water levels on nutrient dynamics in a large shallow eutrophic lake (Changhu Lake, China). *J. Freshw. Ecol.* 37, 131–143. <https://doi.org/10.1080/02705060.2021.2023053>
- Wang, J.-J., Dahlgren, R.A., Erşan, M.S., Karanfil, T., Chow, A.T., 2015. Wildfire Altering Terrestrial Precursors of Disinfection Byproducts in Forest Detritus. *Environ. Sci. Technol.* 49, 5921–5929. <https://doi.org/10.1021/es505836m>
- Wang, K., Pang, Y., Yi, Y., Yang, S., Wang, Y., He, C., Shi, Q., He, D., 2023. Response of dissolved organic matter chemistry to flood control of a large river reservoir during an extreme storm event. *Water Res.* 230, 119565. <https://doi.org/10.1016/j.watres.2023.119565>
- Wang, L., Li, Y., Shang, X., Shen, J., 2014. Occurrence and removal of N-nitrosodimethylamine and its precursors in wastewater treatment plants in and around Shanghai. *Front. Environ. Sci. Eng.* 8, 519–530. <https://doi.org/10.1007/s11783-013-0610-4>
- Wang, L., Zhang, Q., Chen, B., Bu, Y., Chen, Y., Ma, J., Rosario-Ortiz, F.L., 2020. Photolysis and photocatalysis of haloacetic acids in water: A review of kinetics, influencing factors, products, pathways, and mechanisms. *J. Hazard. Mater.* 391, 122143. <https://doi.org/10.1016/j.jhazmat.2020.122143>
- Wang, S., Loreau, M., Arnoldi, J.-F., Fang, J., Rahman, K.Abd., Tao, S., De Mazancourt, C., 2017. An invariability-area relationship sheds new light on the spatial scaling of ecological stability. *Nat. Commun.* 8, 15211. <https://doi.org/10.1038/ncomms15211>
- Wang, X., Mao, Y., Tang, S., Yang, H., Xie, Y.F., 2015. Disinfection byproducts in drinking water and regulatory compliance: A critical review. *Front. Environ. Sci. Eng.* 9, 3–15. <https://doi.org/10.1007/s11783-014-0734-1>
- Wang, X., Zhang, H., Zhang, Y., Shi, Q., Wang, J., Yu, J., Yang, M., 2017. New Insights into Trihalomethane and Haloacetic Acid Formation Potentials: Correlation with the Molecular Composition of Natural Organic Matter in Source Water. *Environ. Sci. Technol.* 51, 2015–2021. <https://doi.org/10.1021/acs.est.6b04817>

References

- Wang, X., Wang, Xuelin, Mi, J., Du, Q., Wang, Y., Chen, W., Sun, D., Song, W., Shao, M., Jia, R., 2023. UV/H₂O₂/O₃ removal efficiency and characterization of algae-derived organic matter and odorous substances. *J. Environ. Chem. Eng.* 11, 109128. <https://doi.org/10.1016/j.jece.2022.109128>
- Wang, Y., Hu, Y., Yang, C., Wang, Q., Jiang, D., 2019. Variations of DOM quantity and compositions along WWTPs-river-lake continuum: Implications for watershed environmental management. *Chemosphere* 218, 468–476. <https://doi.org/10.1016/j.chemosphere.2018.11.037>
- Weber, M., Rinke, K., Hipsey, M.R., Boehrer, B., 2017. Optimizing withdrawal from drinking water reservoirs to reduce downstream temperature pollution and reservoir hypoxia. *J. Environ. Manage.* 197, 96–105. <https://doi.org/10.1016/j.jenvman.2017.03.020>
- Wei, M., Huang, S., Zhang, T., Li, M., Li, L., Akram, W., Gao, R., Ge, Z., Sun, Y., 2022. DOM stratification and characteristics versus thermal stratification – A case study in the Panjiakou Reservoir, China. *J. Hydrol. Reg. Stud.* 42, 101160. <https://doi.org/10.1016/j.ejrh.2022.101160>
- Wen, Z., 2022. Composition of dissolved organic matter (DOM) in lakes responds to the trophic state and phytoplankton community succession. *Water Res.*
- Westerhoff, P., Rodriguez-Hernandez, M., Baker, L., Sommerfeld, M., 2005. Seasonal occurrence and degradation of 2-methylisoborneol in water supply reservoirs. *Water Res.* 39, 4899–4912. <https://doi.org/10.1016/j.watres.2005.06.038>
- Weston, S.L., Scheili, A., Behmel, S., Rodriguez, M.J., 2022. Water quality in drinking water distribution systems: research trends through the 21st century. *Environ. Sci. Water Res. Technol.* 8, 3054–3064. <https://doi.org/10.1039/D2EW00491G>
- Wilhelm, S., Adrian, R., 2007. Impact of summer warming on the thermal characteristics of a polymictic lake and consequences for oxygen, nutrients and phytoplankton. *Freshw. Biol.* 0, 071004210218001-??? <https://doi.org/10.1111/j.1365-2427.2007.01887.x>
- Williamson, J., Evans, C., Spears, B., Pickard, A., Chapman, P.J., Feuchtmayr, H., Leith, F., Waldron, S., Monteith, D., 2023. Reviews and syntheses: Understanding the impacts of peatland catchment management on dissolved organic matter concentration and treatability. *Biogeosciences* 20, 3751–3766. <https://doi.org/10.5194/bg-20-3751-2023>
- Winn, N., Williamson, C.E., Abbitt, R., Rose, K., Renwick, W., Henry, M., Saros, J., 2009. Modeling dissolved organic carbon in subalpine and alpine lakes with GIS and remote sensing. *Landsc. Ecol.* 24, 807–816. <https://doi.org/10.1007/s10980-009-9359-3>

References

- Wlostowski, A.N., Jennings, K.S., Bash, R.E., Burkhardt, J., Wobus, C.W., Aggett, G., 2022. Dry landscapes and parched economies: A review of how drought impacts nonagricultural socioeconomic sectors in the US Intermountain West. *WIREs Water* 9, e1571. <https://doi.org/10.1002/wat2.1571>
- Wolfe, R.L., 1990. Ultraviolet disinfection of potable water. *Environ. Sci. Technol.* 24, 768–773. <https://doi.org/10.1021/es00076a001>
- Woods, G.C., Dickenson, E.R.V., 2016. Natural attenuation of NDMA precursors in an urban, wastewater-dominated wash. *Water Res.* 89, 293–300. <https://doi.org/10.1016/j.watres.2015.11.058>
- Woods, G.C., Trenholm, R.A., Hale, B., Campbell, Z., Dickenson, E.R.V., 2015. Seasonal and spatial variability of nitrosamines and their precursor sources at a large-scale urban drinking water system. *Sci. Total Environ.* 520, 120–126. <https://doi.org/10.1016/j.scitotenv.2015.03.012>
- Woolway, R.I., Sharma, S., Smol, J.P., 2022a. Lakes in Hot Water: The Impacts of a Changing Climate on Aquatic Ecosystems. *BioScience* 72, 1050–1061. <https://doi.org/10.1093/biosci/biac052>
- Worrall, F., Burt, T., 2004. Time series analysis of long-term river dissolved organic carbon records. *Hydrol. Process.* 18, 893–911. <https://doi.org/10.1002/hyp.1321>
- Wright, B., Stanford, B., Weiss, J., Debroux, J., Routt, J., Khan, S., 2013. Climate Change how does Weather Affect Surface Water Quality? *Opflow* 39, 10–15. <https://doi.org/10.5991/OPF.2013.39.0001>
- Wright, B., Stanford, B.D., Reinert, A., Routt, J.C., Khan, S.J., Debroux, J.F., 2014. Managing water quality impacts from drought on drinking water supplies. *J. Water Supply Res. Technol. - AQUA* 63, 179–188. <https://doi.org/10.2166/aqua.2013.123>
- Wu, J., Yao, H., 2022. Simulating dissolved organic carbon during dryness/wetness periods based on hydrological characteristics under multiple timescales. *J. Hydrol.* 614, 128534. <https://doi.org/10.1016/j.jhydrol.2022.128534>
- Wu, J., Yao, H., Chen, Xiaohong, Chen, Xingwei, 2023. Dynamics of dissolved organic carbon during drought and flood events: A phase-by-stages perspective. *Sci. Total Environ.* 871, 162158. <https://doi.org/10.1016/j.scitotenv.2023.162158>
- Wu, T., Wang, Z., Niu, C., Zhang, Y., Li, B., Li, P., 2015. The effect of intense hydrodynamic disturbance on chromophoric dissolved organic matter in a shallow eutrophic lake. *J. Freshw. Ecol.* 30, 143–156. <https://doi.org/10.1080/02705060.2014.961043>

References

- Xenopoulos, M.A., Barnes, R.T., Boodoo, K.S., Butman, D., Catalán, N., D'Amario, S.C., Fasching, C., Kothawala, D.N., Pisani, O., Solomon, C.T., Spencer, R.G.M., Williams, C.J., Wilson, H.F., 2021. How humans alter dissolved organic matter composition in freshwater: relevance for the Earth's biogeochemistry. *Biogeochemistry* 154, 323–348. <https://doi.org/10.1007/s10533-021-00753-3>
- Xu, J., Kralles, Z.T., Hart, C.H., Dai, N., 2020. Effects of Sunlight on the Formation Potential of Dichloroacetonitrile and Bromochloroacetonitrile from Wastewater Effluents. *Environ. Sci. Technol.* 54, 3245–3255. <https://doi.org/10.1021/acs.est.9b06526>
- Xu, X., Kang, J., Shen, J., Zhao, S., Wang, B., Yan, P., Fu, Q., Chen, Z., 2022. Formation pathway of disinfection by-products of lignin monomers in raw water during disinfection. *Sci. Total Environ.* 825, 153706. <https://doi.org/10.1016/j.scitotenv.2022.153706>
- Xu, Z., Shen, J., Qu, Y., Chen, H., Zhou, X., Hong, H., Sun, H., Lin, H., Deng, W., Wu, F., 2022. Using simple and easy water quality parameters to predict trihalomethane occurrence in tap water. *Chemosphere* 286, 131586. <https://doi.org/10.1016/j.chemosphere.2021.131586>
- Xue, S., Jin, W., Zhang, Z., Liu, H., 2017. Reductions of dissolved organic matter and disinfection by-product precursors in full-scale wastewater treatment plants in winter. *Chemosphere* 179, 395–404. <https://doi.org/10.1016/j.chemosphere.2017.02.106>
- Yang, L., Chen, X., She, Q., Cao, G., Liu, Y., Chang, V.W.-C., Tang, C.Y., 2018. Regulation, formation, exposure, and treatment of disinfection by-products (DBPs) in swimming pool waters: A critical review. *Environ. Int.* 121, 1039–1057. <https://doi.org/10.1016/j.envint.2018.10.024>
- Yang, M., Zhang, X., 2016. Current trends in the analysis and identification of emerging disinfection byproducts. *Trends Environ. Anal. Chem.* 10, 24–34. <https://doi.org/10.1016/j.teac.2016.03.002>
- Yang, Q., Fowler, M.S., Jackson, A.L., Donohue, I., 2019. The predictability of ecological stability in a noisy world. *Nat. Ecol. Evol.* 3, 251–259. <https://doi.org/10.1038/s41559-018-0794-x>
- Yang, X., Shang, C., Westerhoff, P., 2007. Factors affecting formation of haloacetonitriles, halo ketones, chloropicrin and cyanogen halides during chloramination. *Water Res.* 41, 1193–1200. <https://doi.org/10.1016/j.watres.2006.12.004>

References

- Yang, X., Rosario-Ortiz, F.L., Lei, Y., Pan, Y., Lei, X., Westerhoff, P., 2022. Multiple Roles of Dissolved Organic Matter in Advanced Oxidation Processes. *Environ. Sci. Technol.* 56, 11111–11131. <https://doi.org/10.1021/acs.est.2c01017>
- Yang, X., Wu, X., Hao, H., He, Z., 2008. Mechanisms and assessment of water eutrophication. *J. Zhejiang Univ. Sci. B* 9, 197–209. <https://doi.org/10.1631/jzus.B0710626>
- Yang, Z., Zhang, M., Shi, X., Kong, F., Ma, R., Yu, Y., 2016. Nutrient reduction magnifies the impact of extreme weather on cyanobacterial bloom formation in large shallow Lake Taihu (China). *Water Res.* 103, 302–310. <https://doi.org/10.1016/j.watres.2016.07.047>
- Yaseen, T., Bhat, S.U., 2021. Assessing the Nutrient Dynamics in a Himalayan Warm Monomictic Lake. *Water. Air. Soil Pollut.* 232, 111. <https://doi.org/10.1007/s11270-021-05054-x>
- Yoon, B., Raymond, P.A., 2012. Dissolved organic matter export from a forested watershed during Hurricane Irene: DOM EXPORT DURING HURRICANE IRENE. *Geophys. Res. Lett.* 39. <https://doi.org/10.1029/2012GL052785>
- Yu, Y., Reckhow, D.A., 2015. Kinetic Analysis of Haloacetonitrile Stability in Drinking Waters. *Environ. Sci. Technol.* 49, 11028–11036. <https://doi.org/10.1021/acs.est.5b02772>
- Zargar, A., Sadiq, R., Naser, B., Khan, F.I., 2011. A review of drought indices. *Environ. Rev.* 19, 333–349. <https://doi.org/10.1139/a11-013>
- Zaw, M., Chiswell, B., 1999. Iron and manganese dynamics in lake water. *Water Res.* 33, 1900–1910. [https://doi.org/10.1016/S0043-1354\(98\)00360-1](https://doi.org/10.1016/S0043-1354(98)00360-1)
- Zeng, T., Glover, C.M., Marti, E.J., Woods-Chabane, G.C., Karanfil, T., Mitch, W.A., Dickenson, E.R.V., 2016. Relative Importance of Different Water Categories as Sources of N - Nitrosamine Precursors. *Environ. Sci. Technol.* 50, 13239–13248. <https://doi.org/10.1021/acs.est.6b04650>
- Zhang, H., Zheng, Y., Wang, X.C., Wang, Y., Dzakpasu, M., 2021. Characterization and biogeochemical implications of dissolved organic matter in aquatic environments. *J. Environ. Manage.* 294, 113041. <https://doi.org/10.1016/j.jenvman.2021.113041>
- Zhang, Jie, Mostofa, K.M.G., Yang, X., Mohinuzzaman, M., Liu, C.-Q., Senesi, N., Senesi, G.S., Sparks, D.L., Teng, H.H., Li, L., Yuan, J., Li, S.-L., 2023. Isolation of dissolved organic matter from aqueous solution by precipitation with FeCl₃: mechanisms and significance in environmental perspectives. *Sci. Rep.* 13, 4531. <https://doi.org/10.1038/s41598-023-31831-1>
- Zhang, Jianzhen, Ye, D., Fu, Q., Chen, M., Lin, H., Zhou, X., Deng, W., Xu, Z., Sun, H., Hong, H., 2023. The combination of multiple linear regression and adaptive neuro-fuzzy inference system can accurately predict trihalomethane levels in tap water with fewer water

References

- quality parameters. *Sci. Total Environ.* 896, 165269.
<https://doi.org/10.1016/j.scitotenv.2023.165269>
- Zhang, Q., Kuang, W. fang, Liu, L. ying, Li, K., Wong, K. hang, Chow, A.T., Wong, P. keung, 2009. Trihalomethane, haloacetonitrile, and chloral hydrate formation potentials of organic carbon fractions from sub-tropical forest soils. *J. Hazard. Mater.* 172, 880–887.
<https://doi.org/10.1016/j.jhazmat.2009.07.068>
- Zhang, R., Wang, F., Chu, W., Fang, C., Wang, H., Hou, M., Xiao, R., Ji, G., 2019. Microbial degradation of typical amino acids and its impact on the formation of trihalomethanes, haloacetonitriles and haloacetamides during chlor(am)ination. *Water Res.* 159, 55–64.
<https://doi.org/10.1016/j.watres.2019.04.032>
- Zhang, T.-Y., Lin, Y.-L., Xu, B., Cheng, T., Xia, S.-J., Chu, W.-H., Gao, N.-Y., 2016. Formation of organic chloramines during chlor(am)ination and UV/chlor(am)ination of algae organic matter in drinking water. *Water Res.* 103, 189–196.
<https://doi.org/10.1016/j.watres.2016.07.036>
- Zhang, X., Yang, H., Wang, X., Fu, J., Xie, Y.F., 2013. Formation of disinfection by-products: Effect of temperature and kinetic modeling. *Chemosphere* 90, 634–639.
<https://doi.org/10.1016/j.chemosphere.2012.08.060>
- Zhang, Y., Van Dijk, M.A., Liu, M., Zhu, G., Qin, B., 2009. The contribution of phytoplankton degradation to chromophoric dissolved organic matter (CDOM) in eutrophic shallow lakes: Field and experimental evidence. *Water Res.* 43, 4685–4697.
<https://doi.org/10.1016/j.watres.2009.07.024>
- Zhang, Y., Zhang, E., Yin, Y., Van Dijk, M.A., Feng, L., Shi, Z., Liu, M., Qina, B., 2010. Characteristics and sources of chromophoric dissolved organic matter in lakes of the Yungui Plateau, China, differing in trophic state and altitude. *Limnol. Oceanogr.* 55, 2645–2659. <https://doi.org/10.4319/lo.2010.55.6.2645>
- Zhang, Y., Zhao, X., Zhang, X., Peng, S., 2015. A review of different drinking water treatments for natural organic matter removal. *Water Supply* 15, 442–455.
<https://doi.org/10.2166/ws.2015.011>
- Zhang, Y., Zhou, L., Zhou, Y., Zhang, L., Yao, X., Shi, K., Jeppesen, E., Yu, Q., Zhu, W., 2021. Chromophoric dissolved organic matter in inland waters: Present knowledge and future challenges. *Sci. Total Environ.* 759, 143550.
<https://doi.org/10.1016/j.scitotenv.2020.143550>
- Zhao, B., Nakada, N., Itai, S., Hanamoto, S., Okumura, K., Tanaka, H., 2020. Diurnal patterns of N-nitrosodimethylamine and formaldehyde behaviors in different seasons in surface water

References

- influenced by effluent from sewage treatment plants. *J. Hazard. Mater.* 383, 121155–121155. <https://doi.org/10.1016/j.jhazmat.2019.121155>
- Zheng, L., Diamond, J.M., Denton, D.L., 2013. Evaluation of whole effluent toxicity data characteristics and use of Welch's *T*-test in the test of significant toxicity analysis. *Environ. Toxicol. Chem.* 32, 468–474. <https://doi.org/10.1002/etc.2075>
- Zhou, Q., Sun, H., Jia, L., Wu, W., Wang, J., 2022. Simultaneous biological removal of nitrogen and phosphorus from secondary effluent of wastewater treatment plants by advanced treatment: A review. *Chemosphere* 296, 134054. <https://doi.org/10.1016/j.chemosphere.2022.134054>
- Zhou, X.R., Lin, Y.L., Zhang, T.Y., Xu, B., Chu, W.H., Cao, T.C., Zhu, W.Q., 2019. Speciation and seasonal variation of various disinfection by-products in a full-scale drinking water treatment plant in East China. *Water Sci. Technol. Water Supply* 19, 1579–1586. <https://doi.org/10.2166/ws.2019.026>
- Zhou, Y., Davidson, T.A., Yao, X., Zhang, Y., Jeppesen, E., De Souza, J.G., Wu, H., Shi, K., Qin, B., 2018a. How autochthonous dissolved organic matter responds to eutrophication and climate warming: Evidence from a cross-continental data analysis and experiments. *Earth-Sci. Rev.* 185, 928–937. <https://doi.org/10.1016/j.earscirev.2018.08.013>
- Zhou, Y., Liu, Miao, Zhou, L., Jang, K.-S., Xu, H., Shi, K., Zhu, G., Liu, Mingliang, Deng, J., Zhang, Y., Spencer, R.G.M., Kothawala, D.N., Jeppesen, E., Wu, F., 2020. Rainstorm events shift the molecular composition and export of dissolved organic matter in a large drinking water reservoir in China: High frequency buoys and field observations. *Water Res.* 187, 116471. <https://doi.org/10.1016/j.watres.2020.116471>
- Zhou, Yuntao, Michalak, A.M., Beletsky, D., Rao, Y.R., Richards, R.P., 2015. Record-Breaking Lake Erie Hypoxia during 2012 Drought. *Environ. Sci. Technol.* 49, 800–807. <https://doi.org/10.1021/es503981n>
- Zhou, Y., Xiao, Q., Yao, X., Zhang, Y., Zhang, M., Shi, K., Lee, X., Podgorski, D.C., Qin, B., Spencer, R.G.M., Jeppesen, E., 2018b. Accumulation of Terrestrial Dissolved Organic Matter Potentially Enhances Dissolved Methane Levels in Eutrophic Lake Taihu, China. *Environ. Sci. Technol.* 52, 10297–10306. <https://doi.org/10.1021/acs.est.8b02163>
- Zhou, Yongqiang, Zhang, Y., Shi, K., Niu, C., Liu, X., Duan, H., 2015. Lake Taihu, a large, shallow and eutrophic aquatic ecosystem in China serves as a sink for chromophoric dissolved organic matter. *J. Gt. Lakes Res.* 41, 597–606. <https://doi.org/10.1016/j.jglr.2015.03.027>

References

- Zohary, T., Ostrovsky, I., 2011. Ecological impacts of excessive water level fluctuations in stratified freshwater lakes. *Inland Waters* 1, 47–59. <https://doi.org/10.5268/IW-1.1.406>
- Zou, X.-Y., Peng, X.-Y., Zhao, X.-X., Chang, C.-P., 2023. The impact of extreme weather events on water quality: international evidence. *Nat. Hazards* 115, 1–21. <https://doi.org/10.1007/s11069-022-05548-9>
- Zwart, J.A., Sebestyen, S.D., Solomon, C.T., Jones, S.E., 2017. The Influence of Hydrologic Residence Time on Lake Carbon Cycling Dynamics Following Extreme Precipitation Events. *Ecosystems* 20, 1000–1014. <https://doi.org/10.1007/s10021-016-0088-6>

Acknowledgements

8 Acknowledgements.

A million thanks go out to Advisors of this thesis, **Dr Rafael Marcé** and **Professor Lisette de Senerpont Domis**, for their unwavering support throughout the elongated period this thesis took to get completed. Your faith in my abilities kept me going throughout the course, including dark moments of research uncertainties and personal circumstances. I can't thank you enough, Drs, for sticking around to steer this thesis, through rough seas, to completion. Your names and faces are forever imprinted in my heart. Sincere appreciation to you Rafael and your family for being my Spanish family throughout all the years I lived in Catalunya. It all began in your house in that summer of 2017 and ended in your house too the day before I left Spain, in the summer of 2020, amidst the Covid pandemic. Also, thank you for translating the abstract of this thesis into Catalan and Spanish languages. I will forever be grateful for the warm reception towards an unknown foreigner. To you Lisette, I had a seamless research stay in Wageningen because of you. I consider NIOO-KNAW my "home" because of the experience I had under you. I wish you nothing short of the best and an extension of this kind of welcome and openness to other international researchers you might be receiving in future.

A huge "thank you" deservedly goes out to **Dr Maria José Farré** for your technical guidance and supervisory role on research activities on disinfection by-products, that culminated into publication of **Papers II** and **III** of this thesis. You literally gave me the practical experience in this research domain, which will go a long way in my professional trajectory. You will forever live in my memory for your kindness to assume leadership on those two papers!

The majority of research that culminated into this thesis happened at the Institut Català de Recerca de l'Aigua (ICRA), which was my host institute from 2017 through 2020. Fate brought me into an institute, whose staff, both indigenous and international, were quite warm-hearted to new additions to the research flock, providing an appropriate environment for integration of new entrants. Colleagues that I joined in the Resource and Ecosystems Group were extremely supportive in my integration. I have fond memories of seniors such as **Sergi Sabater, Josep Mas-Plà, Vicenç Acuña, Nuria Catalan, Carme Font, Didac Capdevilla, Julio Lopez, Elisabet Tornés and Anna Freixa** who always provided that much needed critical voice and support during the research process and a family-like set up to folks like me who had no immediate families in

Acknowledgements

Catalonia. And then I had “un caballero” **Daniel Mercado!** What a fine lad! Daniel deserves a special mention for being quite handy and a run-to person whenever I was stuck with R programming. Daniel, you have been a huge pillar in this journey and will forever remain imprinted in my memory! Outside the research arena, I interacted with a bunch of other staff and fellow graduate students: I will forever be grateful to the generosity of **Luisa Morales**, who fed me cookies right from the day of my arrival and departure from ICRA. Luisa has a golden heart, she always spoke to me even though she knew that I understood very little Spanish but her persistent conversations were a light in those dark moments when research took a huge toll on my mental health, something I will always appreciate because it reinforced my survival; had great companionship with fellow researchers in training such **Nikoletta Tsiarta, Juan Davide Gonzalez, Federico Ferrari, Esther Mendoza and Giannis-Florjan Norra**, that mostly made evening dinner dates too irresistible to stay away from. You live on in my memories, lads, wherever you are! Special mention to all administrative staff at ICRA, for your efforts in making my stay less painful in managing documents, employment contracts and travel logistics.

I had a memorable mandatory six-month research stay at the Netherlands Institute of Ecology (NIOO-KNAW) in Wageningen, in 2019, under the kind supervision of Professor **Lisette de Senerpont Domis** and companionship of **Maggie Margaret Armstrong**. My immersion in the AKWA research group was seamless. The free coffee machines installed all over NIOO-KNAW literally turned me into a coffee addict and simplified the rather intensive research atmosphere in the building and the phase I was going through at that time. Random disruptions for a chat over coffee from Maggie turned out as appropriate breathing vents from research pressure.

Earlier on, in 2017, I undertook a month long industrial placement at the Ens d'Abastament d'Aigua Ter-Llobregat, a public drinking water supply company servicing the Metropolitan City of Barcelona, under the supervision of **Juan Carlos Garcia**, who I would like to sincerely appreciate for providing me with a primer on the context of municipal water supply operations in Barcelona, which gave me an appropriate footing and data that became fundamental in this thesis. Thanks, Juan Carlos, for making my stay at ATL worthwhile and the human connections that made subsequent field sampling trips seamless.

Acknowledgements

This thesis documents research activities that were part of the larger **MANTEL** (Management of Climatic Extreme Events in Lakes and Reservoirs for the Protection of Ecosystem Services) programme, a European Joint Doctorate Innovative Training Network (ITN). The network comprised eight beneficiary universities and research institutes, supported by ten partner organisations across Europe and funded by the European Union's Horizon 2020 research and innovation programme under the Marie Skłodowska-Curie Grant Agreement No. 722518. It's aim was to research, through training of twelve early career researchers, on impacts of climate extremes on aquatic ecosystems and translating the outcomes to management decisions of the water sector. I sincerely appreciate Professor **Eleanor Jennings** who led this consortium and the supervisory board, made up of seasoned researchers in the beneficiary institutions, that steered each of these twelve doctoral research projects.

The ITN attracted early career researchers from Asia, Africa, North and South America and Europe, forming a cohort enriched with a diversity of both professional and cultural backgrounds. Physical meetings in network-wide training schools and international conferences were quite remarkable with fun-filled social events that left us yearning for the next available opportunity. In particular, I had the pleasure of hanging out a lot with **Hares** in Barcelona, he is a great lad with amazing hosting and cooking skills! Then I had a great encounter with Persian philosophy with **Nasime**! She is a lovely lady who will, randomly, engage you in some deep philosophical discussions that are always captivating and funny! I had the pleasure of “hosting” **Maggie** at ICRA twice, with the last period curtailed by the covid pandemic! Maggie is an amazing chap, who would randomly pop up to disrupt you in the middle of head splitting research thoughts, for a brief chat over coffee! Besides, she played a great host during my research stay in Wageningen, at the NIOO-KNAW, together with another amazing lad, **Qing**! Qing would encourage me to go out and play social football with him in Wageningen, not forgetting to showing me a nice Chinese eatery nearby that turned out to be my favorite spot throughout my six months stay. I also had loads of fun with a chap from London, **Harriet**, a joyful girl whom never runs short of stories! Our last walk on the beach at Rottneest Island in Perth, December 2018, is imprinted in my memory! It was also a pleasure to hang out with **Ana**, my buddy from Granada! Ana is super calm but with a huge sense of humor whenever she is relaxed! I really enjoyed her company whenever we physically met. Then there was **Julio**, What a lad! It was a pleasure having you around in Wageningen, in 2019. Even though the perturbation experiments had you by the neck almost all the time, I enjoyed our walks in the streets of Wageningen. Your philosophical takes on the future

Acknowledgements

of ecological resilience were quite intriguing in as much as they were controversial! Hopefully we meet again one day to live your dream of doing science and living on a boat for life! I also had interesting times and conversations with **Ewan, Cleo, Truls, Mike, Jorrit** and **Alexa**. This account, by no means expresses all the sentiments I hold about you guys but limitations of space means that I can only say this little about the three years we worked together as a cohort. Our last physical meeting in Estonia, in October 2019, brings strong emotions, considering that it may have been the last we will ever have met! Keep safe y'all and prosper!

Curriculum Vitae



CONTACTS

Email: elias.munthali@gmail.com

Mobile: +265999376637

LinkedIn: [elias.munthali](#)

Orcid: <https://orcid.org/0000-0001-6681-4371>

SKILLS

Classical & Instrumental analytical techniques. Liquid and Solid phase extraction techniques. Quality Management Systems development & Audits. Data analysis. Statistical Modeling. Spatial Analyses. Statistical computing.

VISION

Modernize water resources management in Malawi through strategies that enhance data collection, analysis and modelling by applying global best practices, in order to promote sustainability and resilience of national water resources against pressures such as population growth, anthropogenic pollution and climate change.

WORK EXPERIENCE

- Senior Water Quality and Environmental Officer | Northern Region Water Board | 2008-08-11- present

Managing water treatment and quality control processes in 5 supply districts. Championing implementation of ISO 9000 series QMS across NRW. Implementing basin-wide water resource quality monitoring to track pollution evolution.

- Staff Associate | University of Malawi-The Polytechnic | September 2007-July 2008

Taught, examined and assessed undergraduates in Energy Technology & Industry, Electronic Instrumentation and Applied Nuclear Physics.

Curriculum Vitae

EDUCATION

- PhD (Water Science & Technology) | pending 2024 | Universitat de Girona (UdG) + Wageningen University & Research (WUR)
- Master of Science (Water and Environmental Engineering) | February 2015 | University of Surrey (UK)
- Bachelor of Science (Environmental Science & Technology) | June 2006 | University of Malawi-The Polytechnic.

PUBLICATIONS

- **Munthali E**, de Senerpont Domis LN, Marcé R. Drastic reduction of nutrient loading to a reservoir alters its resistance to impacts of extreme climatic events. *Environ Res Lett.* 2022 Aug 1;17(8):084007.
- Sanchís J, Jaén-Gil A, Gago-Ferrero P, **Munthali E**, Farré MJ. Characterization of organic matter by HRMS in surface waters: Effects of chlorination on molecular fingerprints and correlation with DBP formation potential. *Water Res.* 2020;176.
- **Munthali E**, Marcé R, Farré MJ. Drivers of variability in disinfection by-product formation potential in a chain of thermally stratified drinking water reservoirs. *Env Sci Water Res Technol.* 2022;8(5):968–80.
- Armstrong M, Zhan Q, **Munthali E**, Jin H, Teurlincx S, Peters P, et al. Stressors in a bottle: A microcosm study on phytoplankton assemblage response to extreme precipitation events under climate warming. *Freshw Biol.* 2023 Jun;fwb.14109.
- Cianci-Gaskill, J. A.; Klug, J. L.; Merrell, K. C.; Millar, E. E.; Wain, D. J.; Kramer, L.; van Wijk, D.; Paule-Mercado, M. C. A.; Finlay, K.; Glines, M. R.; **Munthali, E. M.**; Teurlincx, S.; Borre, L.; Yan, N. D. A Lake Management Framework for Global Application: Monitoring, Restoring, and Protecting Lakes through Community Engagement. *Lake Reserv. Manag.* 2024, 1–27. <https://doi.org/10.1080/10402381.2023.2299868>.
- Wander, H. L.; Farruggia, M. J.; La Fuente, S.; Korver, M. C.; Chapina, R. J.; Robinson, J.; Bah, A.; **Munthali, E.**; Ghosh, R.; Stachelek, J.; Khandelwal, A.; Hanson, P. C.; Weathers, K. C. Using Knowledge-Guided Machine Learning To Assess Patterns of Areal Change in Waterbodies across the Contiguous United States. *Environ. Sci. Technol.* 2024, acs.est.3c05784. <https://doi.org/10.1021/acs.est.3c05784>.

REFERENCES

- Dr. Rafael Marcé, Principal Researcher (Scientist), Blanes Centre for Advanced Studies, Cala St. Francesc, 14 Blanes - Girona - 17300 (España). Email: rmarce@ceab.csic.es
- Prof. Lisette de Senerpont Domis, Netherlands Institute of Ecology, Droevendaalsesteeg 10, 6708 PB Wageningen, NL. Email: L.deSenerpontDomis@nioo.knaw.nl